



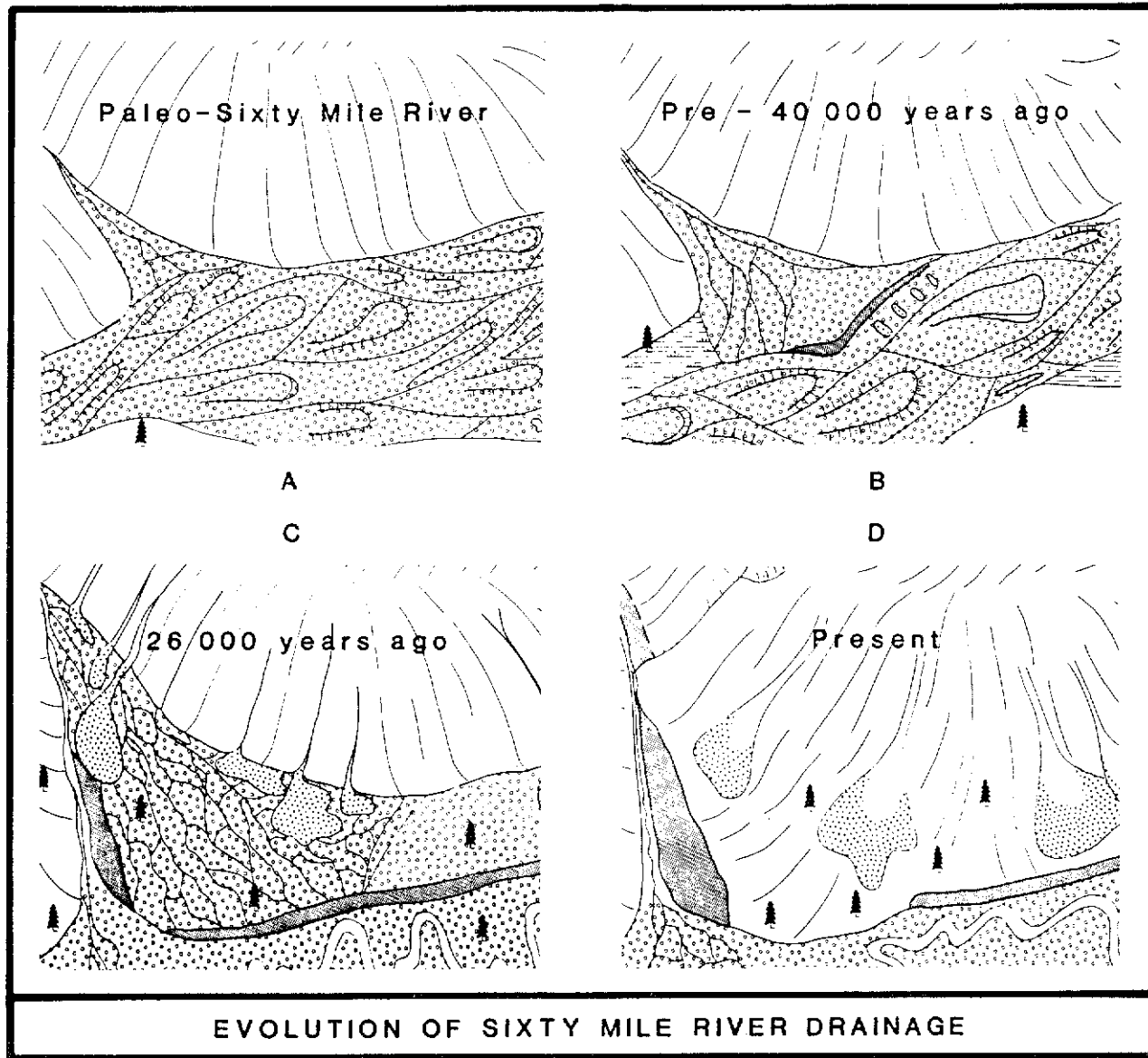
Indian and Northern
Affairs Canada

Affaires indiennes
et du Nord Canada

GC-1
\$10.00

YUKON GEOLOGY

Volume 1



Canada

COVER: Placer gold was discovered in the Sixty Mile River area in 1892. Since that time, the district has significantly contributed to Yukon placer gold production. Sedimentologic studies show that there are at least four distinct fluvial settings (pre-fan aggradation, fan aggradation, terrace development, post-terrace development) which played important roles in the development of these Quaternary placer deposits. These settings are discussed by R.L. Hughes et al. in this volume on pages 50-55.

Exploration and Geological Services Division of Northern Affairs Program invites readers to write and inform us of their language preference with respect to Yukon Exploration and Geology Reports and other geo-technical reports prepared by the Division. Please write to:

Exploration and Geological Services Division
Northern Affairs Program
200 Range Road
Whitehorse, Yukon
Y1A 3V1

YUKON GEOLOGY

Volume 1

**Exploration and Geological Services Division
Mineral Resources Directorate
Northern Affairs Program, Yukon
Indian and Northern Affairs Canada**

Edited by J.A. Morin and D.S. Emond

Published under the authority of the
Hon. Bill McKnight, P.C., M.P.,
Minister of Indian Affairs and
Northern Development,
Whitehorse, 1986.

QS-Y036-000-EE-A1
Catalogue No. R71-40/1E
ISBN 0-662-15041-4

PREFACE

This volume of Yukon Geology is the first of a series that will report on geology of the Yukon, especially those studies with an economic aspect. It is an outgrowth of the Yukon Exploration and Geology series, containing the material that made up the first half of the book. That material forming the second half of the book (summaries of mine production, current mineral exploration work and description of mineral showings) is now published in the Yukon Exploration series.

Papers suitable for Yukon Geology are invited from all workers in the field, be it industry, university, or government. Most of the papers in this volume represent work of geologists involved in graduate thesis work that was supported in varying degrees by Exploration and Geological Services Division of the Mineral Resources Directorate, Northern Affairs Program, Department of Indian Affairs and Northern Development, Yukon. Other papers represent work of geologists with the Division involved in conducting economic geology investigations in Yukon, and geologists from mining companies and other government agencies such as the Geological Survey of Canada and the Alaska Division of Geological and Geophysical Surveys. In addition, two contributions were funded by the Canada-Yukon Economic Development Agreement (EDA).

J.A. Morin
Chief Geologist
Exploration and Geological
Services Division

YUKON GEOLOGY VOLUME 1
LOCATION INDEX OF PAPERS



TABLE OF CONTENTS

	PAGE NO.
RÉSUMÉ	1
ECONOMIC GEOLOGY	
Gold, Silver	
1. B.W.R. McDONALD and C.I. GODWIN: Geology of the Main Zone at Mt. Skukum, Wheaton River area, southern Yukon	6
2. B.W.R. McDONALD, C.I. GODWIN and E.B. STEWART: Exploration geology of the Mt. Skukum epithermal gold deposit, southwestern Yukon	11
3. L.D. MEINERT: Gold in skarns of the Whitehorse Copper Belt	19
4. M.B. DUFRESNE, S.R. MORISON and B.E. NESBITT: Evidence of hydrothermal alteration in White Channel sediments and bedrock of the Klondike area, west-central Yukon	44
5. R.L. HUGHES and S.R. MORISON: Placer gravels of Miller Creek, Sixtymile River area, 116 B, C	50
6. J.G. ABBOTT: Epigenetic mineral deposits of the Ketza-Seagull district, Yukon	56
7. L. WALTON: Textural characteristics of the Venus vein and implications for ore shoot distribution	67
8. J.L. DUKE and C.I. GODWIN: Geology and alteration of the Grew Creek epithermal gold-silver prospect, south-central Yukon	72
Silver, Base Metals	
9. K.W. WATSON: Silver-lead-zinc deposits of the Keno Hill-Galena Hill area, central Yukon	83
10. G. LYNCH: Mineral zoning in the Keno Hill Ag-Pb-Zn mining district, Yukon	89
11. J.P. FRANZEN: Metal-ratio zonation in the Keno Hill District, central Yukon	98
12. J.G. ABBOTT: Geology of the PLATA-INCA property, Yukon	109
Tin, Tungsten	
13. D.S. EMOND: Tin and tungsten veins and skarns in the McQuesten River area, central Yukon	113
REGIONAL GEOLOGY	
14. V.L. HANSEN: Preliminary structural and kinematic analysis of mylonitic rocks of the Teslin Suture Zone, 105 E, Yukon	119
15. V.L. HANSEN: Petrotectonic study of the Teslin Suture Zone, Yukon: a progress report	125
16. D.T. OSBORNE, G.M. NARBONNE and J. CARRICK: Stratigraphy and economic potential of Precambrian - Cambrian boundary strata, Wernecke Mountains, east-central Yukon	131
17. L.E. JACKSON, S.P. GORDEY, R.L. ARMSTRONG and J.E. HARAKAL: Bimodal Paleogene volcanics near Tintina Fault, east-central Yukon and their possible relationship to placer gold	139
18. M.J. PRIDE: Description of the Mount Skukum Volcanic Complex, southern Yukon	148
19. T. SKULSKI and D. FRANCIS: On the geology of the Tertiary Wrangell Lavas in the St. Clare Province, St. Elias Mountains, Yukon	161
20. M.D. ALBANESE, T.E. SMITH, M.S. ROBINSON and T.K. BUNDTZEN: Summary of DGGS investigations at Livengood, Alaska: Geology, mineral potential and regional correlations with east-central Yukon	171

RÉSUMÉ

GÉOLOGIE ÉCONOMIQUE Or, Argent

McDonald décrit la zone principale des gisements aurifères du mont Skukum comme des filons de quartz et carbonate presque verticaux qui recoupent des andésites subhorizontales, et contiennent de l'électrum et donc de l'or, et des concentrations très faibles de minéraux sulfurés. Ces filons minéralisés représentent le second stade de formation des filons après l'apparition de veinules de calcédoine.

Dans un article ultérieur sur le même thème, rédigé par **McDonald, Stewart et Godwin**, sont décrits les filons de quartz et calcite, aurifères et argentifères, à faible teneur en sulfures, de gisement du mont Skukum; ces auteurs les décrivent comme des filons de niveau élevé, qui ont pu se former dans un milieu de "type source thermale," à proximité de la surface, à quelques centaines de mètres de l'ancienne surface.

La stratigraphie volcanique de la région du gisement est caractérisée par quatre cycles d'activité volcanique, dont chacun correspond à un différent style éruptif et à une différente composition des roches éruptives. Dans la région des gisements, d'abondantes failles normales fortement inclinées, de direction générale nord nord-est, dissèquent les roches volcaniques relativement horizontales. Des filons du Cirque principal (Main Cirque) sont contenus dans ces grandes zones de failles normales qui limitent les compartiments affaissés d'une structure d'effondrement.

Les deux stades de formation des filons (filon de calcédoine et filon minéralisé) se répètent. Les filons de quartz et carbonate du second stade paraissent en équilibre avec une altération propylitique destructive. Dans certains cas, on observe une altération phyllique plus intense.

L'information obtenue indique que les gisements du mont Skukum se sont formés à basse température dans un milieu rapproché de la surface, en présence d'eaux météoriques circulant dans un système hydrothermal alimenté par une source de chaleur associée aux dykes fessiliques de cette région. L'écoulement des fluides était probablement régi par des failles perméables, des corps bréchiformes, des surfaces d'écoulement bréchoïdes, et des lits de tufs. Les fluides, durant leur circulation, ont peut-être lessivé l'or des roches volcaniques andésitiques environnantes durant l'étape de propylitisation, et l'ont précipité aux points de sortie qu'offraient les zones de failles fortement perméables.

L'étude de **Meinert** porte sur les skarns de la zone cuprifère de Whitehorse (Whitehorse Copper Belt). On rencontre ces skarns à la fois dans des roches carbonatées, dolomitiques et calcitiques, près des contacts avec la phase de contact dioritique du batholite de Whitehorse. Les skarns sont semblables, du point de vue de leur minéralogie et de leur composition, à des skarns cuprifères typiques (Einaudi et al., 1981). Les principaux minéraux progrades du skarn sont des grenats du type de l'andradite et des pyroxènes du type du diopside; les roches dolomitiques minéralisées contiennent des quantités significatives d'olivine du type de la forstérite. Localement, une intense altération rétrograde a converti le grenat en epidote \pm chlorite \pm hématite, le pyroxène en actinolite \pm chlorite, et l'olivine en serpentine \pm chlorite \pm magnétite. La couleur, la composition et la minéralogie des minéraux progrades et rétrogrades des skarns reflètent la composition du protolith.

Dans son ensemble, la minéralisation sulfurée est associée à l'altération rétrograde. La chalcopyrite et la pyrite sont associées de façon préférentielle à l'actinolite et à la chlorite, la bornite et la chalcocite à l'épidote et localement à la serpentine. L'autre minéral cuprifère important, la vallériite, se limite aux roches magnésiennes, et se trouve fréquemment associé à la phlogopite, à la serpentine et à la chlorite. Dans l'ensemble, le système de Whitehorse est riche en cuivre et pauvre en soufre; les sulfures de fer ne sont pas abondants.

On a extrait des quantités significatives d'or et d'argent des skarns de Whitehorse. L'or se présente sous forme d'électrum de titre moyen 890. Lors de la présente étude, on a observé de l'or visible se présentant en grains grossiers dans une carotte de sondage, mais ceci n'est pas fréquent. L'or se présente aussi en quantités accessoires, mais économiquement importantes, dans une partie de la chalcopyrite et de la vallériite. L'association de la chalcopyrite à l'altération rétrograde du pyroxène en actinolite peut constituer une indication utile de ce second type de venue aurifère. On rencontre aussi de l'argent dans l'électrum, mais celui-ci est probablement plus abondant sous forme de constituant accessoire de la chalcocite et de la bornite. L'association de la chalcocite et de la bornite à l'épidote pseudomorphe du grenat, et à la serpentine pseudomorphe de l'olivine et du diopside, peut être un indicateur utile de ce type de venue argentifère. On pourrait sans doute déterminer les zones contenant des quantités significatives de métaux précieux, en cartographiant la minéralogie des skarns progrades et rétrogrades.

On peut employer les taux de Cu, Ag et Au déterminés lors de l'analyse d'essais sur échantillons prélevés dans un ensemble, pour distinguer les divers types de skarns de Whitehorse. Les gisements qui se sont formés dans un calcaire relativement pur semblent caractérisés par des taux faibles de métaux précieux. Les gisements formés dans des protolithes de caractère plus magnésien semblent être riches en argent. Les gisements caractérisés par les plus forts taux d'or semblent s'être formés dans des roches mixtes composées de calcaire et de dolomie détritique. Les taux métalliques sur lesquels porte la production totale du district sont semblables à la moyenne de ceux des gisements de Little Chief et War Eagle, les deux plus grands producteurs de ce district. De plus, le gisement de Little Chief est caractérisé par le plus fort taux moyen d'or de tous les gisements étudiés.

La corrélation générale entre les taux de cuivre et de métaux précieux suggère que les précédents programmes d'exploration ont probablement permis de situer les gisements de type skarn du district, qui présentent le meilleur potentiel de production de métaux précieux. Les corrélations entre les taux de métaux précieux et la minéralogie des skarns, décrites dans la présente étude, pourraient servir d'indicateurs pour explorer de nouveaux gisements et réévaluer les gisements connus. Le fait que l'on ait exploité à grande échelle le skarn de Little Chief, qui est le plus grand gisement et le plus riche en or de la zone cuprifère de Whitehorse, suggère que l'on doit à l'avenir axer l'exploration sur les skarns similaires des districts périphériques tels que Jackson Lake. On doit tout particulièrement étudier la minéralogie des skarns et la composition du protolith.

Dufresne, Morison et Nesbitt ont étudié l'altération hydrothermale des sédiments de White Channel et du sous-basement du district du Klondike dans la partie ouest-centrale du Yukon.

Des relations établies *in situ* pour les sédiments supérieurs blanchis et kaolinisés de White Channel, que l'on trouve sur la colline Dago, suggèrent que l'altération ultérieure à la phase de sédimentation n'était due ni à l'action des agents atmosphériques ni à celle de processus supergénés. Dans les 2 à 3 mètres inférieurs du gravier altéré à taches ferrugineuses que l'on rencontre sur le site de la colline Dago, une kaolinite secondaire bien cristallisée, de l'illite (mica de 10 Å) et des hydroxydes de fer présents dans la matrice du gravier, suggèrent que dans cette zone, l'altération a une origine hydrothermale. La présence d'adulaire dans les galets de rhyolite altérée est probablement le résultat de l'altération hydrothermale à basse température des feldspaths potassiques. De même, la goethite, la muscovite et l'adulaire secondaires qui cimentent le gravier de la colline Nugget sont probablement le résultat d'une altération hydrothermale *in situ*. L'altération généralisée de l'argile se prolonge souvent de 2 à 5 mètres dans la roche de fond au-dessous du contact

avec le gravier de White Channel, et elle est ultérieure à la phase de sédimentation. De la kaolinite bien cristallisée et soit de l'illite et de la smectite, ou de la chlorite et de la smectite interstratifiées sont les produits d'altération. De minces filons de quartz (10 cm) et de carbonate de fer semblent génétiquement associés à la roche de fond altérée de façon généralisée au-dessous des sédiments altérés de White Channel. La minéralogie et la morphologie de ces filons suggèrent que leur mise en place a eu lieu durant l'altération hydrothermale de la roche de fond et des sédiments sus-jacents de White Channel. Les relations observées *in situ*, la minéralogie et la texture du gravier altéré, de la roche de fond altérée et des filons associés ne peuvent s'expliquer par l'action des éléments atmosphériques ou d'autres processus supergénèses apparentés. Par conséquent, on suggère l'hypothèse suivant laquelle des processus hydrothermaux ont causé l'altération des sédiments de White Channel et de la roche de fond sous-jacente, et le dépôt des filons associés que l'on trouve dans les régions de Hunker et de Last Chance Creek.

Les travaux qu'a effectués **Hughes** à Miller Creek dans la région de la rivière Sixty Mile, dans la partie ouest-centrale du Yukon, ont permis de déterminer que des sédiments graveleux aurifères transportés par l'ancien ruisseau Miller, se sont déposés dans deux milieux principaux de formation des placers. Il s'agit de séquences formées dans des cours d'eau anastomosés précédant la formation d'un cône alluvial, et de séquences graveleuses typiques de ravins. Les dépôts de ravins sont constitués de sédiments graveleux, faiblement triés, anguleux, où s'est concentré l'or alluvial durant le creusement de ces ravins. Les sédiments graveleux transportés par des cours d'eau anastomosés se sont déposés durant une période d'élargissement de la vallée, avant la phase d'aggravation d'un cône alluvial. L'or alluvial s'est concentré dans l'environnement des cours d'eau anastomosés durant le remaniement du filon exploitable initialement présent dans des ravins; ainsi se sont formées des poches discontinues avec concentration de minéraux lourds, au-dessous des séquences moyennes et distales des cônes alluviaux. Il est aussi possible que des restes du filon exploitable initialement présent dans les ravins, existent actuellement près du thalweg de l'ancienne vallée, au-dessous des séquences proximales des cônes alluviaux.

La distribution et les concentrations d'or alluvial dans les sédiments graveleux de Miller Creek sont le résultat de processus sédimentaires et de l'évolution géomorphique du terrain. Ainsi, pour interpréter de façon crédible les programmes d'exploration ou les programmes globaux d'essais, il est nécessaire de comprendre ces facteurs sous leur aspect technique.

Abbott résume les caractéristiques des manifestations épigénétiques de minerai aurifère et argentifère, dans les monts Pelly du Yukon central, à l'intérieur du district de Ketza-Seagull, et montre que celles-ci sont liées à un soulèvement en forme de dôme (arche de Ketza-Seagull), et à une ou plusieurs intrusions souterraines.

Walton décrit le filon aurifère de Venus situé sur le mont Montana, comme un filon de fort pendage, contenant l'ensemble quartz-arsénopyrite-pyrène-sphalerite-galène, et présentant une structure rubanée, des textures en crête de coq, et des parois ondulantes. Les caractéristiques du filon indiquent sa formation par des solutions hydrothermales, qui ont à la fois comblé les espaces interstitiels et remplacé les minéraux le long des surfaces courbes et aplaniées des failles. L'emplacement des passes minéralisées est sans doute le résultat des conditions physico-chimiques.

Duke et Godwin traitent du gîte possible, aurifère et épithermal, de Grew Creek, dans la partie sud-centrale du Yukon. Ce gîte possible se situe à proximité et au sud-ouest de la route principale Robert Campbell, et à mi-chemin entre les communautés de Ross River et de Faro. Le gîte se trouve à l'intérieur du sillon de Tintina qui, du Crétacé supérieur au Tertiaire, a été le siège d'un grand mouvement de décrochement dextre, qui a juxtaposé les ardoises cambriennes et ordoviennes et les phyllites de la plate-forme de Pelly.

Cassiar (au sud-ouest) aux roches de l'alluvion d'Anvil (au nord-est).

Les roches de Grew Creek sont d'âge Éocène moyen, d'après la datation par la méthode K-Ar du basalte, qui a donné pour résultats $51,4 \pm 1,8$ Ma et $50,7 \pm 1,8$ Ma; la datation de grains de pollen présents dans des roches volcanoclastiques a indiqué un âge de 56 à 46 Ma. Les roches volcaniques felsiques et les roches volcanoclastiques ont été recouvertes par une séquence de sédiments clastiques grossiers interstratifiés, de coulées de basaltes et de roches volcanoclastiques de caractère basaltique. Les épisodes de soulèvement et de faillage survenus au Tertiaire supérieur ont favorisé la conservation des roches d'âge Éocène dans un graben de structure complexe, limité au sud par la faille de Grew Creek et au nord par la faille de Danger Creek.

À Grew Creek, la minéralisation s'est produite à la pointe d'un prisme orienté vers l'ouest, principalement composé d'un congolomérat felsique et volcanique à lapilli dans une matrice fine. La zone de dépôt des métaux précieux est tronquée au nord-est par des sédiments clastiques de fort pendage, et au sud-ouest par la faille de Grew Creek. On a identifié la présence d'or, d'électrum, de pyrite et de séléniure d'argent dans un échantillon de forte teneur provenant de l'affleurement où l'on a découvert le gîte.

À Grew Creek, l'altération est à la fois superficielle et hydrothermale. L'altération superficielle est fréquente, généralisée, et caractérisée par la présence d'argiles à couches mixtes et de carbonates. L'altération hydrothermale, qui a permis la minéralisation en or et argent, est étroitement associée à la présence de dykes rhyolitiques et se présente sous trois formes: silicique, sulfatée acide, et à la fois sulfatée acide et argilique. La datation par la méthode K-Ar de la séricite indique que l'altération hydrothermale date de l'Éocène moyen ($51,5 \pm 1,8$ Ma et $47 \pm 1,7$ Ma), et qu'elle est synchrone avec le dépôt des roches volcaniques.

Le quartz associé à la minéralisation de Grew Creek est enrichi en isotopes lourds de l'oxygène. L'une des explications de cet enrichissement est la présence d'une source magmatique profonde, d'où seraient venus les fluides minéralisants.

Argent, Plomb, Zinc

Watson présente une image générale du type de minéralisation de la région de Keno Hill, et l'historique de l'exploitation minière. Il traite en particulier des deux plus grandes mines actuellement exploitées qui se trouvent sur la même structure filonienne, à savoir Husky et Husky Southwest. La minéralogie des filons et les métaux prédominants sont différents dans les deux gisements: le filon Husky contient une gangue de sidérite, à laquelle est principalement associée de la galène argentifère; ce filon est semblable à la plupart des filons exploités de la région, tandis que les gisements de Husky Southwest contiennent principalement une gangue de quartz, à laquelle sont associés de l'argent natif, de faibles concentrations de plomb et de zinc, mais des concentrations élevées d'or.

Lynch présente son étude sur la zonation des minéraux du district minier de Keno Hill-Galena Hill dans le centre du Yukon. Les corps minéralisés typiques sont de vastes réseaux filonians contenant de la sidérite, du quartz, de la pyrite, de la galène, de la sphalerite et de la freibergite en combinaisons diverses. Les filons se limitent à des zones faillées de fort pendage SE, principalement confinées dans une unité à quartzite graphitique fragile, et dans quelques corps concordants composés de roches vertes. Les principaux filons argentifères constituent une étroite zone d'orientation est-ouest, de 25 km de long; on leur a attribué un âge Crétacé moyen, ainsi qu'à des corps granitiques proches et à leurs minéralisations associées en Sn-W.

Cette étude des minéraux filonians indique que des groupes de gisements adjacents contiennent des assemblages minéraux caractéristiques, qui les distinguent d'autres groupes; ceux-ci constituent divers faciès sur toute la longueur de la zone. On peut ainsi résumer les principaux faciès minéralogiques d'ouest en est: (1) pyrargyrite dans des filons de quartz-sidérite contenant un peu d'argent natif,

de polybasite, de stéphanite et d'acanthite, surtout à l'ouest. (2) On rencontre de la sidérite, de la galène, de la sphalérite et de la freibergite dans la plupart des gisements, mais ces minéraux apparaissent sans les autres minéraux caractéristiques au sommet de Galena Hill. (3) On rencontre la pyrrhotine et l'arsénopyrite dans des affleurements de veines profondes, à l'intérieur de la vallée comprise entre les collines Galena Hill et Keno Hill. (4) On rencontre aussi de la calcite dans les veines profondes qui jouxtent le flanc est de Galena Hill, mais ce minéral se prolonge à l'est jusqu'à sur la colline Keno Hill. (5) Dans l'extrême est du district, des tronçons de veines contenant de la boulangérite-jamesonite et des quantités abondantes de quartz et d'arsénopyrite, chevauchent la zone calcitique. On a noté des teneurs aurifères élevées dans les zones (1), (3) et (5).

Les variations des faciès minéralogiques indiquent que le milieu où s'est produit le dépôt de minéraux a évolué à l'intérieur d'un réseau filonien continu, hydrothermal, de 25 km de long. On estime que les gisements situés à l'ouest correspondent aux équivalents de plus haut niveau ou latéralement situés en "aval" des gisements situés à l'est.

Cette séquence zonée est typique, et clairement définie dans d'autres régions du monde. On sait que de tels réseaux minéralisés progressent vers le bas dans des filons de quartz aurifère, avant d'atteindre les zones minéralisées en Sn-W et les corps granitiques associés.

Franzen traite des configurations du rapport métallique, dans le district de Keno Hill, où pendant presque 70 ans, on a exploité des failles contenant d'étroits filons. Durant cette période, 3,9 millions de tonnes métriques (4,3 millions de tonnes courtes) de minerai ont donné 5 754 millions de grammes (185 millions d'onces) d'argent. Toute cette production venait de passes minéralisées sous-affleurantes; l'enrichissement supergène n'est pas un facteur important dans la plupart des gisements. On a observé dans d'autres champs filoniers de la Cordillère le parallélisme de la zone minéralisée avec la surface actuelle, mais malgré des efforts de recherche considérables, les exploitants de ces zones ont rarement réussi à trouver des passes minéralisées aveugles.

On peut étudier, en rapport avec la zonation des rapports métalliques, les possibilités de rencontrer le minerai aveugle dans le district de Keno Hill. Une reconstruction approximative du réseau original de fractures dans ce district, et la définition du rapport métallique caractérisant un système hydrothermal actif à l'intérieur de ces fractures, suggèrent que certaines passes minéralisées ont été érodées, et que certaines d'entre elles sont exposées à la surface actuelle, tandis que d'autres restent conservées en profondeur.

Abbott présente de façon résumée la géologie de filons argentifères de la propriété de Plata-Inca, dans la partie nord-centrale du Yukon. Les strates de la toute fin du Protérozoïque et du tout début du Cambrien, présentes dans le sous-sol de la propriété, sont plissées et recoupées par des failles de chevauchement plus anciennes que les failles normales et filons de fort pendage, et sans rapport avec ces derniers. On rencontre les filons le long des failles normales prononcées et bien définies; la plupart contiennent de la galène, de la sphalérite et de la tétraédrite dans une gangue de sidérite et de quartz, avec un peu de barytine et de calcite. Une zonation systématique n'est pas apparente dans les filons individuels. La présence de failles normales de direction générale est indique qu'il y a peut-être eu un mouvement tardif du chevauchement de Plata, qui aurait favorisé la minéralisation.

Il existe une lentille de barytine à l'emplacement du chevauchement de Plata; ceci démontre qu'il serait possible de trouver des gisements stratifiés de barytine, et peut-être de barytine métallifère à l'ouest des gisements connus qui se situent au niveau de la transition, située entre le Paléozoïque inférieur et le Paléozoïque moyen, des argiles liées aux carbonates.

Étain, Tungstène

Emond a étudié les filons et skarns contenant de l'étain et du tungstène dans la région de la rivière McQuesten, dans le centre du Yukon. Ces gisements se trouvent dans les zones de contact d'amas intrusifs, culots et dykes granitiques, à biotite et gros cristaux de feldspath. La plupart des manifestations se trouvent dans l'exocontact de plutons, dans les roches encaissant métasédimentaires fragiles que l'on connaît sous le nom d'unités du grès grossier, d'âge Précamalien supérieur à Cambrien inférieur. On rencontre la cassiterite (+/- argent) dans des brèches à matrice de chlorite, tourmaline et quartz, contenant des fragments de quarzite, de schistes, et de matériaux de remplissage des filons avec une gangue peu abondante de chlorite, tourmaline ou quartz; dans des filonnets minces avec une gangue peu abondante de tourmaline, feldspath potassique, ou muscovite; et dans un skarn avec actinolite-quartz-épidote-axinite-grenat (+/- pyrrhotine, pyrite et chalcocrite). La scheelite est principalement disséminée dans un exoskarn à grain fin, avec diopside-quartz, ou actinolite-quartz (+/- pyrrhotine), qui est interstratifié avec un skarn à wollastonite blanche - quartz. La scheelite (+/- molybdénite) existe aussi dans des filons stratifiés de quartz (+/- feldspath) à la fois dans les régions d'endocontact et d'exocontact des deux amas de granite porphyroïde avec cristaux de feldspath. L'étain et le tungstène coexistent rarement; toutefois on a rencontré dans quelques manifestations de tungstène de faibles concentrations d'étain, et vice-versa. Le tungstène se trouve plus près de l'intrusion associée que l'étain.

GÉOLOGIE RÉGIONALE

Hanson, dans deux articles, traite de son étude sur la zone de suture de Teslin.

La zone de suture de Teslin (TSZ) constitue la limite fondamentale entre les roches déposées le long de l'ancienne marge de l'Amérique du Nord et les terrains allochtones à l'ouest. À la fois les roches du continent nord-américain et les roches allochtones ont été soumises à une déformation ductile et simultanément métamorphisées dans les conditions du faciès supérieur des schistes verts au faciès des amphibolites, à des températures comprises entre 450 et 650 °C, et sous des pressions supérieures ou égales à 6 kbars, probablement durant une période allant du Trias supérieur au Jurassique moyen. La schistosité de direction nord-nord-ouest présente un fort pendage dans la partie ouest de la zone TSZ, mais à l'est, dans les roches autochtones nord-américaines, se rapproche de l'horizontale.

Dans le secteur de carte combinant l'est de Laberge et l'ouest du lac Quiet, la zone TSZ se subdivise en trois domaines structuraux distincts et allongés, parallèles à la zone TSZ de direction NNW. On identifie les domaines suivant la distribution des linéations étendues Le1 et Le2, différemment orientées, qui sont apparues durant la déformation ductile non coaxiale, et suivant la distribution de leurs "plans de mouvement" associés. Le1 a une direction générale ouest et plonge suivant le pendage, tandis que Le2 a une orientation générale NNW-SSE et plonge faiblement. Le1 et Le2 sont associées aux mêmes assemblages minéraux et se sont formées dans des conditions de métamorphisme similaires. Les assemblages de minéraux silicatés indiquent des températures ayant atteint 625 °C, et des pressions allant jusqu'à 8 kbars; les assemblages carbonatés indiquent des températures de l'ordre de 350-500 °C. Les différences de température suggérées par ces assemblages peuvent refléter des températures plus basses de fluage et de recristallisation dans les roches carbonatées.

Les domaines de Le1 allongés en forme de lentille sont séparés l'un de l'autre par les zones plus étroites de Le2 de direction générale NNW, qui forment une zone de cisaillement anastomosée à l'échelle régionale. Deux domaines ouest de Le1 sont principalement composés de roches allochtones, ou de roches d'affinités incertaines;

toutefois, le domaine est comprend des roches autochtones nord-américaines, que l'on considérait auparavant comme non modifiées par le métamorphisme et la déformation de la zone TSZ.

À l'échelle macroscopique et microscopique, les indicateurs cinématiques ont continuellement enregistré un mouvement de décrochement dextre, avec extrémité supérieure dirigée vers le nord, parallèle à Le2. La cinématique associée à Le1 est plus complexe. À l'ouest, les indicateurs cinématiques ont enregistré un mouvement (normal) parallèle à Le1 et dont le côté ouest est dirigé vers le bas; ailleurs, à la fois un mouvement inverse et un mouvement normal ont été enregistrés. Les relations observées in situ suggèrent que Le1 a commencé à se former avant Le2, puis qu'à la fois Le1 et Le2 se sont constitués, et enfin qu'il s'est produit un mouvement parallèle seulement à Le2. Ces géométries et étapes de mouvement indiquent que les roches de la zone TSZ et les roches autochtones qui leur sont structurellement associées ont enregistré la succession des transpressions suivies de décrochements dextres le long de cette partie de la marge du continent nord-américain, durant le Trias et le Jurassique. Le mouvement s'est d'abord traduit par une compression tectonique initiale, à un fort angle par rapport à l'ancienne marge, puis par une phase de translation latérale dextre approximativement parallèle à la marge mésozoïque de la partie ouest de l'Amérique du Nord.

Osborne, Narbone et Carrick décrivent les aspects lithostratigraphiques, biostratigraphiques et lithologiques des strates de la limite du Précambrien et du Cambrien des monts Werneck, en particulier des unités les plus hautes du Protérozoïque et les plus basses du Cambrien (formation de Vampire). Les roches les plus hautes du Protérozoïque sont constituées de strates moyennes à épaisseur de dolomie, avec un peu de microgrès, de calcaire et de brèche dolomitique près du sommet.

Des indices suggèrent que la sédimentation a eu lieu sur une plate-forme carbonatée peu profonde, et que la face supérieure de cette unité constitue une importante discordance. On n'a observé de minéralisation associée, plombifère et zincifère, que dans les coupes situées le plus au sud, où les argiles litées déposées dans les eaux adjacentes plus profondes ont pu servir de source d'ions métalliques.

La formation de Vampire est principalement constituée de grès, de microgrès et d'argiles litées, et se laisse subdiviser en six lithofaciès: un faciès à argile litée/dolomie, un faciès dégradé vers le haut, un faciès à hématite, un faciès à microgrès/grauwacke, un faciès à microgrès/arénite, et un faciès à microgrès. La portion inférieure de cette unité représente un milieu de sédimentation pro-deltaïque, ou de sédimentation sur la pente supérieure d'un bassin, tandis que la portion supérieure montre les lithotypes et structures sédimentaires typiques des milieux peu profonds de plate-forme continentale. On rencontre un lit de calcaire phosphate à la base de la formation de Vampire, dans la coupe D.

Une minéralisation en sulfures apparaît sporadiquement dans ce faciès basal. Les accumulations significatives d'hématite détritique se limitent au faciès à hématite.

Jackson, Gordey, Armstrong et Harakal présentent les résultats de récentes analyses de datation isotopique et analyses chimiques d'une série volcanique bimodale d'intrusions et coulées rhyolitiques, et d'un basalte columnaire à olivine, d'un tuf basaltique et d'une brèche volcanique pyroclastique, que l'on rencontre le long et immédiatement au nord de la faille de Tintina, près de Faro. La géochronométrie de la portion nord de cette zone confirme l'âge des roches volcaniques rhyolitiques comme allant du Paléocène supérieur à l'Éocène, et celui du basalte, autrefois considéré comme Quaternaire, comme correspondant aussi à l'Éocène. La concordance d'âge des roches volcaniques mafiques et felsiques indique qu'il existe une seule province volcanique bimodale d'âge Paléogène, que l'on peut lier à l'extension de la croûte terrestre et à la formation de failles normales (Ewart, 1979). Dans ces conditions, elle est probablement associée à un décrochement

survenu le long de la faille de Tintina.

Les recherches effectuées *in situ*, au nord-est et à l'est de la région décrite par Tempelman-Kluit (1972), ont permis de délimiter deux corps volcaniques felsiques supplémentaires, qui d'après la datation par la méthode K-Ar de la roche totale, sont aussi d'âge Éocène. La similarité de composition entre ces deux manifestations datées et des roches volcaniques felsiques plus rapprochées de la faille de Tintina, suggère fortement que ces dernières sont d'âge Éocène; inversement, l'association récente de l'or à des roches volcaniques felsiques proches de la faille de Tintina à Grew Creek suggère que les deux corps datés sont peut-être minéralisés en or. Les indices géologiques indiquent que les basaltes nouvellement datés, situés au nord-est de la faille de Tintina, semblent situés dans des bassins limités par des failles, qui ont subi des déports horizontaux considérables. La séparation verticale suggère que depuis l'Éocène, a eu lieu une érosion différentielle de bassins adjacents séparés et limités par des failles, ou bien qu'il y a eu fragmentation d'un bassin initialement plus grand.

On n'a pu déterminer en fin de compte l'origine de l'or alluvial présent dans la partie supérieure du bassin de la rivière Pelly, mais la concordance entre les limites des roches volcaniques paléogènes et les placers et certains détails géologiques de surface, suggère qu'il existe un lien.

Pride subdivise la géologie du complexe volcanique du mont Skukum en 5 formations principales et plusieurs épisodes (présentés ici successivement): 1) des dépôts alluviaux grossiers résultant d'un épisode initial de soulèvement et de faillage; 2) le dépôt de roches volcaniques et andésitiques; 3) l'éruption de coulées de laves andésitiques provenant de cheminées volcaniques proches; 4) des éruptions catastrophiques de type plinien, avec coulées pyroclastiques de caractère felsique; et 5) des failles ou bien des éruptions pyroclastiques ayant donné des brèches hétérolithiques. Ensuite, ont eu lieu d'autres éruptions, la formation d'un cratère, l'intrusion d'un culot rhyolitique, et la mise en place d'un réseau de fractures de direction générale nord-nord-est, événements qui ont tous contribué à la formation ultérieure de gîtes aurifères hydrothermaux.

Skulski et Francis ont rapporté les résultats d'une étude sur les laves de Wrangell, dans la province de St-Clare, dans le sud-ouest du Yukon. Ces laves font partie de la vaste zone volcanique de Wrangell, qui a manifesté de l'activité durant tout le Cénozoïque supérieur; leur éruption a eu lieu dans un milieu tectonique transitionnel qui reflète la transpression régionale suivant le réseau de failles (failles transformantes de Queen Charlotte — failles de Fairweather — Totschunda), ainsi que la subduction de la plaque de Farallon au-dessous de l'Amérique du Nord. La province volcanique est composée de basaltes subalcalins (31%), d'andésites basaltiques (30%), d'andésites (21%), de dacites (2%) et de basaltes normatifs à néphéline (16%). Les basaltes normatifs à hypersthène contiennent (suivant l'ordre d'apparition) de gros cristaux de spinelle - olivine-plagioclase +/- oxydes de Fe-Ti +/- clinopyroxène, tandis que les andésites contiennent des phénocristaux de plagioclase, d'oxydes de Fe-Ti, de clinopyroxène, +/- orthopyroxène, et les dacites et latites intrusives contiennent des phénocristaux de plagioclase, +/- clinopyroxène, hornblende, +/- biotite, +/- sanidine. Les roches normatives à néphéline, lorsqu'elles sont porphyriques, contiennent des phénocristaux d'olivine, de plagioclase et de hornblende. Dans la partie centrale du secteur de carte, les coulées les plus basses sont des basaltes normatifs à néphéline interstratifiés avec des sédiments clastiques, et recouverts par des andésites basaltiques, des andésites et des conglomérats volcaniques. Cette succession est recouverte par des basaltes interstratifiés avec des roches sédimentaires clastiques et des roches pyroclastiques. Dans la partie sud du secteur de carte, on rencontre des basaltes alcalins à ce niveau stratigraphique. La partie sommitale des laves de Wrangell est de nature andésitique, et interstratifiée avec de petites quantités de roches volcanoclastiques. Les laves normatives à hypersthène de la province de St-Clare sont transitionnelles, du point de vue de leur rapport

$\text{Na}_2\text{O} + \text{K}_2\text{O}/\text{SiO}_2$, entre les séries magmatiques alcalines et subalcalines, et du point de vue de leur rapport FeO^*/MgO en fonction de SiO_2 , entre les séries tholéïtiques et calco-alcalines. La composition chimique de ces roches reflète le cadre tectonique exceptionnel dans lequel on les trouve.

Albanese et al décrivent la stratigraphie de la région de Livengood en Alaska, que l'on peut corrélérer avec l'unité des grès grossiers d'âge Précamalien supérieur à Cambrien inférieur, unité qui recouvre la formation de Road River et d'autres unités stratigraphiques au Yukon.

GEOLOGY OF MAIN ZONE AT MT. SKUKUM, WHEATON RIVER AREA, SOUTHERN YUKON

Bruce W.R. McDonald and Colin I. Godwin
Department of Geological Sciences
University of British Columbia
Vancouver, B.C.

McDONALD, B.W.R. and GODWIN, C.I., 1986. Geology of Main Zone at Mt. Skukum, Wheaton River area, southern Yukon; in Yukon Geology, Vol. 1; Exploration and Geological Services Division, Yukon, Indian and Northern Affairs Canada, p. 6-10.

INTRODUCTION

The Main Zone of the Mt. Skukum gold-silver deposit, 65 km southwest of Whitehorse, Yukon ($60^{\circ}12'$ north and $135^{\circ}28'$ west; NTS map sheet 105 D; elevation 1,675 m), occurs in Main Cirque which forms the headwaters of Butte Creek in the southwestern part of the Mt. Skukum Volcanic Complex (Fig. 1). The deposit consists of low sulphide, gold-silver bearing quartz-calcite veins which crosscut a sequence of nearly flat-lying andesitic volcanic rocks.

The deposit was discovered in 1980 by Agip Canada Ltd. of Calgary, Alberta, during follow-up of geochemical anomalies found in stream sediment samples during regional exploration (Doherty et al., 1983). Diamond drilling, trenching and sampling, conducted from 1981 to 1984, led to the discovery of many zones of economic significance. Main Zone is presently perceived to be the most important. Erickson Gold Mines Ltd. of Vancouver, B.C., current operators on the property, completed a production adit to the Main Zone in late July, 1984. Proven reserves of the Main Zone (R. Somerville, 1985, pers. comm.) are 148,980 tonnes (164,222 tons) of ore with an average grade of 24.98 g/t gold and 20.5 g/t silver.

EXPLORATION HISTORY

Mt. Skukum occurs in Sloko volcanic rocks within the Coast Crystalline Belt (Fig. 1). Similar volcanics occur in the Bennett Lake Caldera Complex, and possibly at Montana Mountain. Both of these areas host precious metal occurrences (Doherty et al., 1983). Montana Mountain is perhaps the best known, nearby area of mineralization at which a number of gold-bearing quartz-sulphide veins have been mined at various times since early this century (Tempelman-Kluit, 1981). The Wheaton River district first became known in 1893 with the discovery of precious metal and antimony veins in the area. Since that time, a number of vein occurrences of galena, sphalerite and minor gold and silver have been found within the Berney Creek fracture which forms the southern boundary of the Mt. Skukum Volcanic Complex. Nevertheless, only limited metal production has come from deposits in the area. Since the beginning of this century, very little mineral exploration has taken place in the Mt. Skukum area. At nearby Chieftain Hill, 5.5 km east of Mt. Skukum, Yukon Antimony Corporation undertook a diamond drilling program for porphyry copper mineralization during 1967 and 1968. However, no recorded exploration or staking had occurred in the central area of the Mt. Skukum Volcanic Complex prior to the 1980 activities of Agip Canada Ltd. (Doherty et al., 1983).

GENERAL GEOLOGY

The Mt. Skukum deposits are hosted in andesitic rocks of the Mt. Skukum Volcanic Complex which unconformably overlie Precambrian schist and marble of the Yukon Group (Wheeler, 1961; Smith, 1983; Pride, 1985 — this volume), and granitic intrusive rocks of the Coast Crystalline Complex. An Early Eocene age of 51.6 ± 1.8 Ma for the andesitic volcanic rocks enclosing the deposit is indicated by the average of two K-Ar dates on whole rock (Table 1).

Mt. Skukum Volcanic Complex covers an area of about 140 square km, is fault-bounded, and has been intruded in places by felsic dykes and stocks. The complex is divided into two sections by a major north-trending fault. The western part includes a lower

interlayered sedimentary-volcanic sequence and a thick upper sequence of andesitic volcanic rocks. The eastern part includes an 800 m thick sequence of felsic pyroclastic flows and brecciated, flow-layered and spherulitic felsic lava flows, felsic lapilli tuff and densely welded felsic tuffs (Pride, 1986 — this volume).

The Mt. Skukum deposits occur in the southwestern portion of the volcanic complex where they are enclosed in the upper sequence of andesites estimated at 500 m thick (Fig. 2) are extensively dissected by north-trending faults and many late rhyolitic, dacitic and andesitic dykes which have a similar orientation. Several late

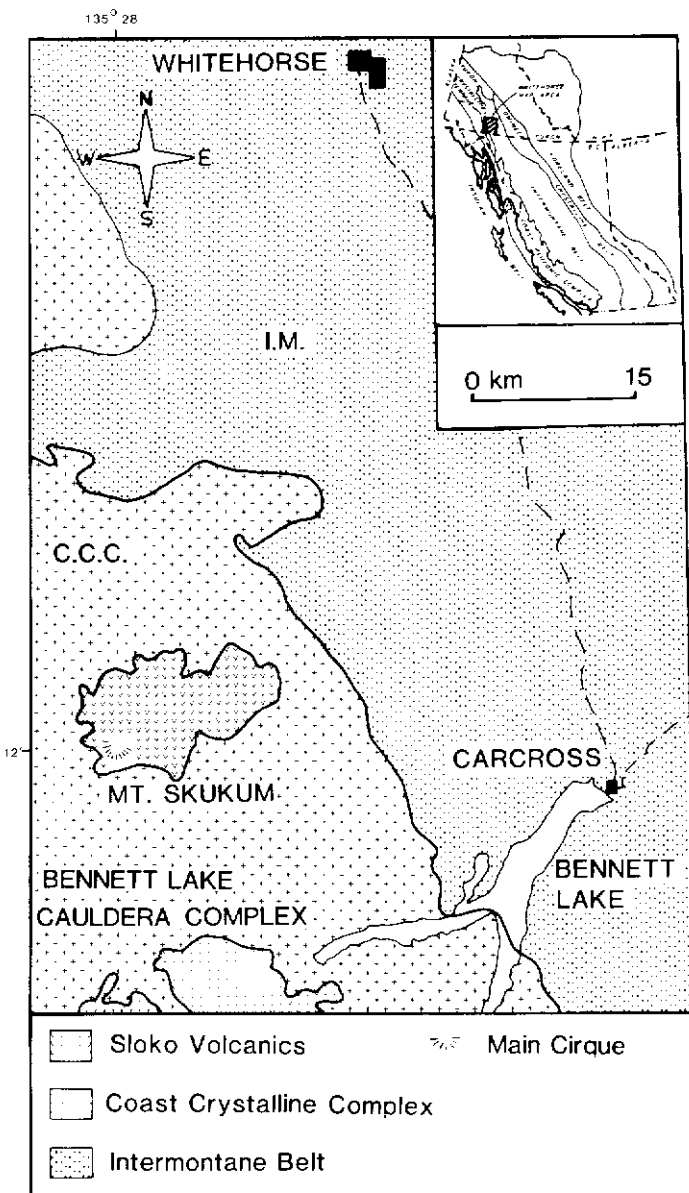


Figure 1. Location map of Mt. Skukum Volcanic Complex and Bennett Lake complex within the Coast Crystalline Complex.

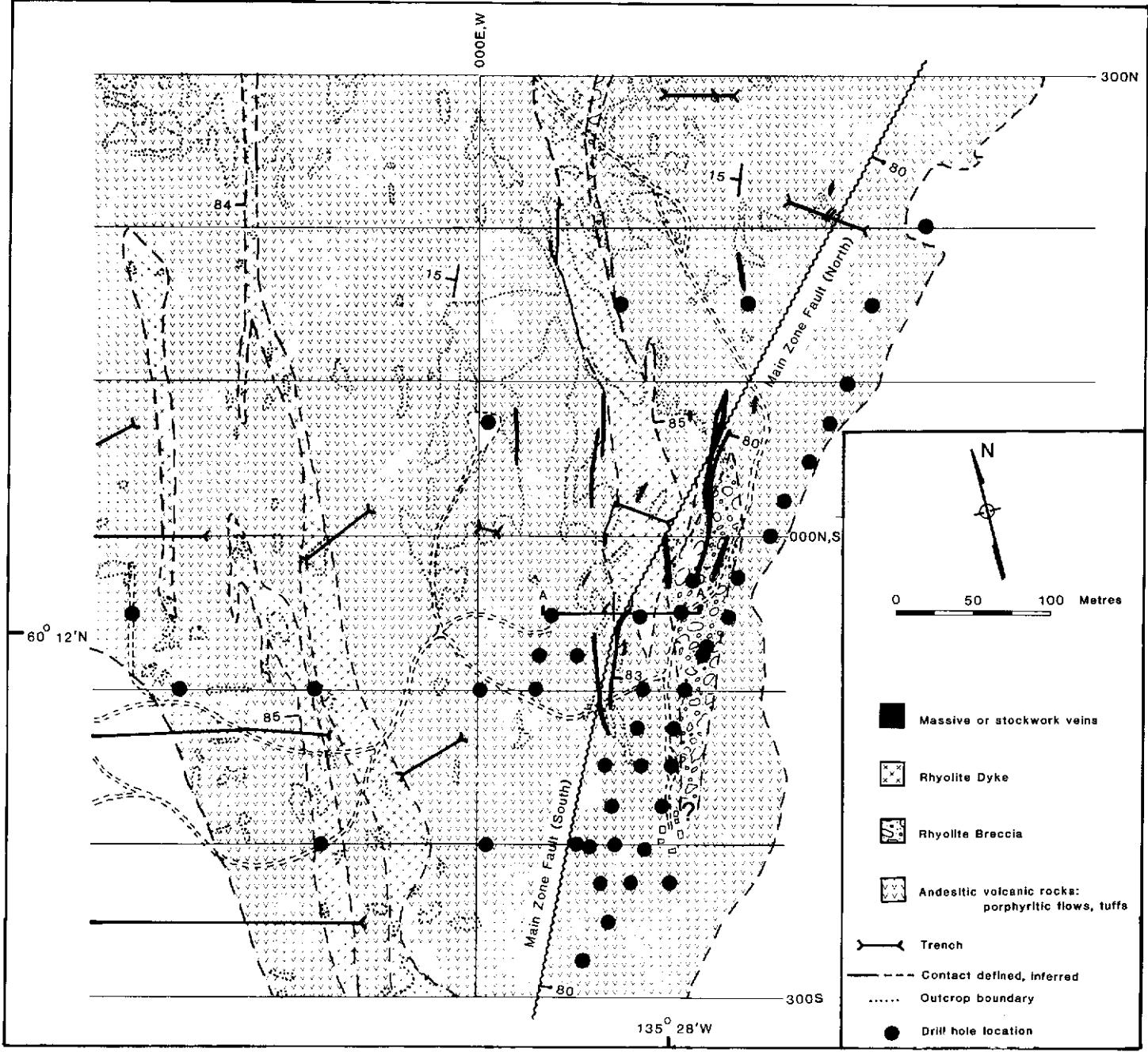


Figure 2. Geology of the Main Zone, Mt. Skukum gold vein deposit (cross-section A-A' is in Fig. 3).

quartz-feldspar porphyry bodies outcrop near the deposit, the closest being a small plug located on cliffs immediately northeast of the Main Cirque (Doherty et al., 1982).

GEOLOGY OF THE MAIN ZONE

The Main Zone occurs in Main Cirque at the northeastern foot of Mt. Skukum, at an elevation of 1675 m. It is one of three major quartz-carbonate vein systems within the Main Cirque which trend NNE and bisect the enclosing volcanic rocks at high angles. Each of these vein systems (Main Zone, Brandy Zone, and Lake Zone), all within 300 m of each other, host gold and silver mineralization with only trace amounts of sulphide minerals. Enclosing volcanic rocks (Fig. 2) dip gently to the southwest and consist of porphyritic andesite flows with vesiculated flow tops and brecciated flow bottoms as well as andesitic lapilli tuffs with minor bedded tuff layers. In the vicinity of the deposit, these rocks have undergone magnetite and plagioclase destructive alteration and characteristically display abundant chlorite, calcite and epidote. Alteration occurs in alternating layers of fresh or propylitized

andesites which are clearly visible as bands of pale-altered or dark-fresh rock in cliff exposures. Altered layers tend to encompass the interfaces between individual flow units which, through their higher permeability, may have been preferentially altered relative to the more massive flow centres (Fig. 4).

A major fault zone (the Main Fault Zone) bisects the Main Cirque and may have acted as a conduit for hydrothermal fluids during formation of the Main Zone vein. The fault zone ranges from 20 to 30 m across, and consists of two or three major faults and associated heavy fracturing. The Main Fault Zone can be divided into two parts according to its orientation (Fig. 2): the southern part which trends 030° and dips 80° east. Faults are poorly expressed on surface, but occur in drill core as gouge ranging from 10 cm to 3 m or more in width. The Main Fault Zone is the easternmost of several subparallel vein fault systems which are current exploration targets on the property. The others lie immediately to the west of the map area. The operator has indicated that mineable ore exists in the Brandy Zone whereas the others have yet to be defined (R. Somerville, 1985, pers. comm.).

A second major fault occurs along the eastern wall of the

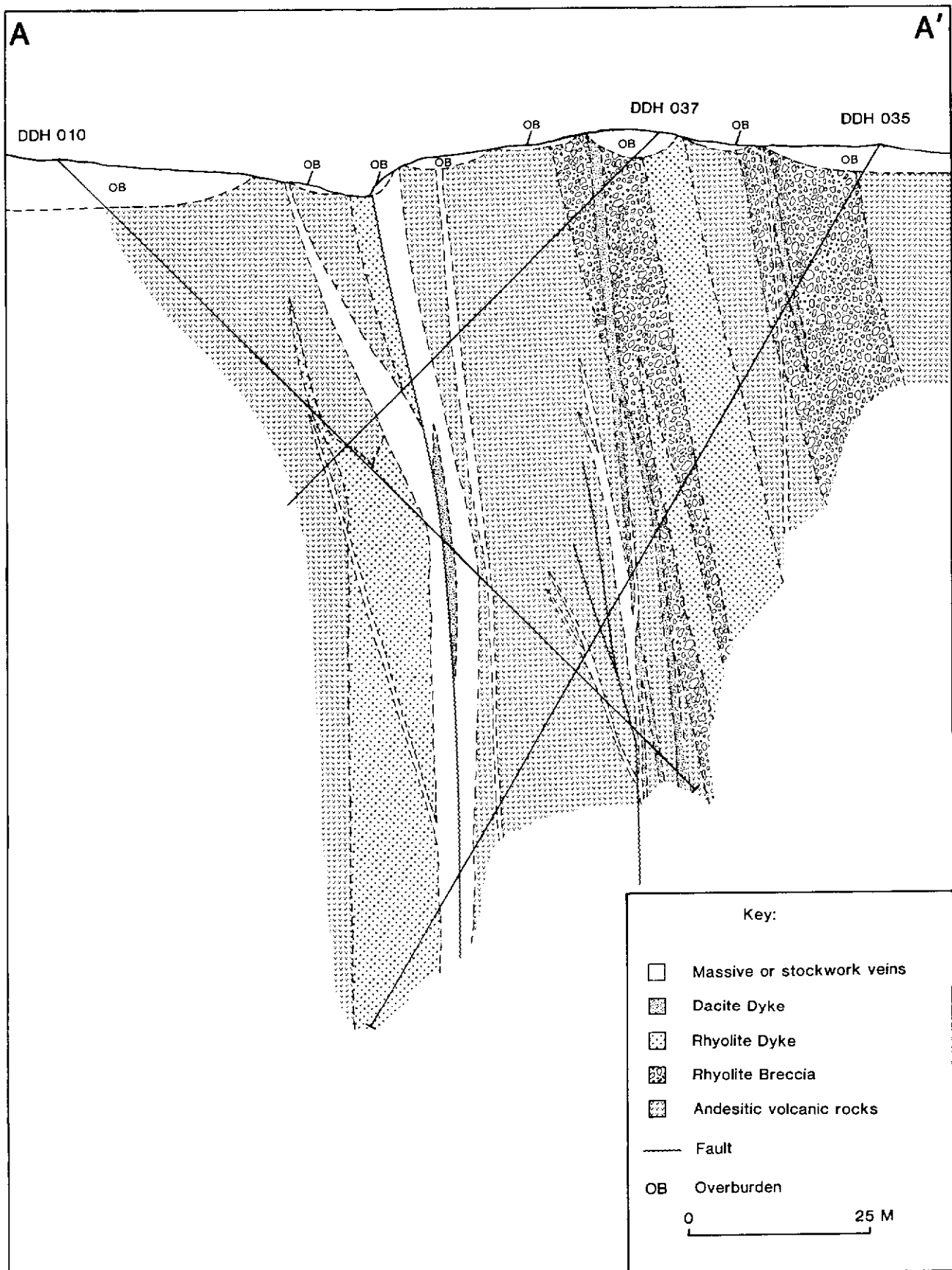


Figure 3. Cross-section A-A', at 0+ 50 m south, through the Main Zone, Mt. Skukum gold vein deposit (Fig. 2).

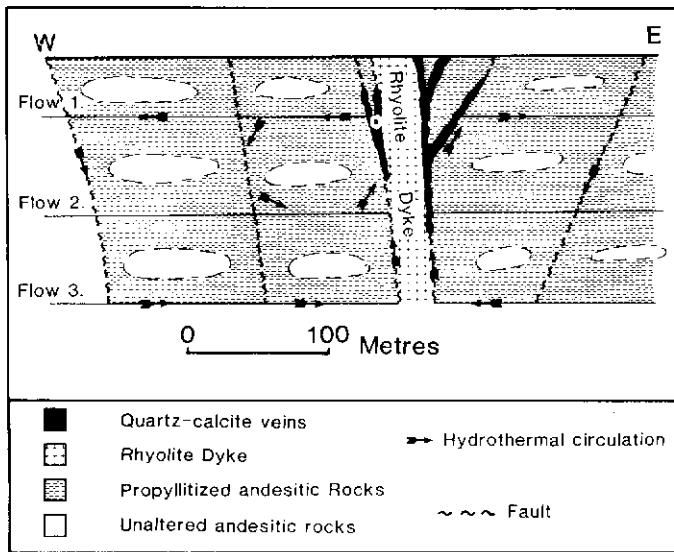


Figure 4. Schematic cross-section of hydrothermal system causing regional propylitic alteration of source area for precious metals, and deposition of gold-silver bearing, quartz calcite vein zones at Mt. Skukum. Vertical scale is diagrammatic.

Main Cirque and also has a northeasterly trend. This fault forms the eastern contact between the andesites of the Main Cirque and the stratigraphically overlying felsic extrusives (Pride, 1986 — this volume). In these felsic extrusive rocks, 1100 m south of the Main Zone, a localized zone of pale, recessive and locally limonitic, intensely altered rock is apparent in a cliff exposure. X-ray diffraction analysis of a specimen taken from higher elevations of this altered zone showed it to contain abundant alunite and pyrophyllite.

Numerous felsic to intermediate dykes parallel the Main Zone Fault and are most abundant in its immediate vicinity (Figs. 2 and 3). A prominent felsic dyke, up to 30 m thick, occurs immediately adjacent to mineralized vein material in the southern end of the Main Zone structure. This dyke is one of three which are crosscut by narrower, but equally extensive andesitic and dacitic dykes. All dykes have subsequently been crosscut by the veins.

Several extensive tabular breccia bodies crosscut the volcanic strata at high angles throughout the Main Cirque and are parallel to dominant local fractures. The largest, immediately east of the Main Zone structure, consists exclusively of a highly siliceous matrix enclosing angular rhyolitic and/or andesitic fragments that range up to 10 cm in diameter. This body is at most about 10 m thick and closely parallels the eastern rhyolitic dyke along most of its length (Fig. 3). Several small breccia bodies, rarely over 1 m across, are scattered throughout the area surrounding the Main Cirque. Unlike their larger counterpart, these bodies are composed of a range of clastic components including granitic, rhyolitic, andesitic, schist, and marble fragments. All fragments are angular to subrounded and are enclosed in a siliceous matrix.

Two stages of vein formation occur in rocks of the Main Zone. The first is marked by blue-grey chalcedonic veinlets rarely more than 2 mm thick. These veinlets usually display pyritic selvages and envelopes, and are associated with extensive wall-rock alteration ranging from pervasive silicification to phyllitic alteration characterized by abundant muscovite, quartz and pyrite. Locally, these first stage veinlets form dense stockworks (up to 60 veinlets/m in drill core) associated with intense alteration and pyritization. Throughout the Main Cirque area, these stockworks are marked by heavily iron-stained gossans which bear no relation to the economic veins. First stage veinlets have not been found with significant gold or silver mineralization.

The second stage of veins, in contrast to the first, contains most known gold mineralization and contains no sulphides. These veins, found throughout the Main Cirque area, are concentrated in and around the Main Fault Zone structure. Megascopically, second stage veins are white and consist exclusively of a quartz-calcite assemblage. Characteristic textures range from a sugary massive appearance to a vuggy texture with abundant wallrock breccia

fragments and well developed cockade structures. Calcite commonly appears as coarse, bladed crystals up to 1.5 cm intergrown with quartz.

An "ore" shoot has been defined in the Main Zone occurring over a section of the second stage veins south of the flexure in the Main Fault Zone. This "ore" shoot, as defined by drill holes, is 200 m long with an average width of 5 m and a vertical extent of about 80 m (Doherty *et al.*, 1983). The ore zone vein which is up to 10 m thick branches at shallow depths into smaller, closely spaced, discontinuous veins that parallel the Main Fault Zone. A 1983 petrographic study by Bacon, Donaldson and Associates Ltd., Vancouver, B.C., of a limited number of specimens of vein material showed that gold (more correctly electrum) occurs as fine flakes between 15 and 20 microns in diameter. Within the vein, electrum is contained only in quartz, although assay values are highest in veins with at least equal amounts of quartz and calcite. The 1.2:1 ratio between gold and silver assay values (R. Somerville, 1985, pers. comm.) shows no systematic variation with vertical position in the deposit. The ratio between gold and silver combined with the lack of observed native silver or possible silver-bearing phases indicates that both gold and silver occur as electrum. Values for gold and silver drop abruptly in wallrock adjacent to the veins. Precious metal content also appears to be low in veins distant from the rhyolite dyke.

Alteration associated with second stage veins is poorly developed. Veins 1 and 2 m in width can have phyllitic alteration envelopes which extend up to 2 cm into the wallrock; more commonly, alteration envelopes are absent.

CONCLUSIONS

Gold mineralization at the Mt. Skukum deposit occurs in nearly vertical quartz-carbonate veins which crosscut flat-lying andesites with a NNE trend. The mineralized veins represent the second stage of a two stage hydrothermal system, the first of which resulted in emplacement of thin chalcedonic veinlets. These two stages of veins are probably indicative of an evolving hydrothermal fluid rather than being representative of two separate events, although consistent crosscutting relationships clearly show that the first stage predates the second. Vein emplacement is one of the latest of a series of events which began with volcanism, producing felsic and andesitic volcanic rocks which overlie basement in this area. Subsequent periods of tectonism related to extrusion of the most recent rhyolitic rocks and possibly to depletion of magma chambers at depth, produced large faults along which rhyolitic dykes were emplaced. Continued tectonism resulted in reactivation of old faults along which andesitic and dacitic dykes were injected, crosscutting rhyolite dykes in many cases. As volcanic activity waned, the faults remained active, leaving zones of high permeability which acted as conduits for the still active hydrothermal circulation. The area of intense alteration south of the Main Zone contains alunite-pyrophyllite and cryptocrystalline silica which may represent a near-surface expression of a hydrothermal vent that possibly was active during formation of the Main Zone.

Veins appear to have been emplaced at low temperature in a circulating hydrothermal system driven by a heat source at depth associated with dykes present in the area (Fig. 4). Circulating hydrothermal fluids may have leached gold from the surrounding andesitic volcanics during propylitization (Roslyakova and Rozlyakov, 1975). Permeability may have been controlled by faulting, brecciated flow tops and bottoms, and lapilli tuff horizons. Gold was precipitated in highly permeable conduits, such as the Main Fault Zone and breccia bodies.

ACKNOWLEDGEMENTS

This project has been funded by the Exploration and Geological Services Division of the Department of Indian Affairs and Northern Development. Many thanks go to J. Morin who initiated this study and arranged funding for most of the presented research. Thanks also are extended to Agip Canada Ltd., R.A. Doherty, M. Balog, R. Robertson, E. Stewart and the Mt. Skukum field crew who made their field facilities available and gave a great deal of guidance to this project. We also acknowledge the cooperation and support from Erickson Gold Mines Ltd., particularly R. Somerville and R. Basnett.

REFERENCES

- DOHERTY, R.A., BALOG, M., ROBERTSON, R., 1982. Mount Skukum Project: 1982 Exploration Activities; Unpublished Assessment Report, Agip Canada Ltd.
- DOHERTY, R.A., BALOG, M., ROBERTSON, R., 1983. Mount Skukum Project: 1983 Exploration Activities; Unpublished Assessment Report, Agip Canada Ltd.
- HARLAND, W.B., COX, A.V., LLEWELLYN, P.G., PICKTON, C.A.G., SMITH, A.G., and WALTERS, R., 1982. A Geologic Time Scale; Cambridge Earth Science Series, Cambridge University Press, 131 p.
- MCDONALD, B.W.R. and C.I. GODWIN, 1985. Epithermal gold veins of the Main Zone at Mt. Skukum, southwest Yukon Territory; Unpublished manuscript, University of British Columbia, Vancouver, Presented at Cordilleran Roundup, B.C. and Yukon Chamber of Mines, Vancouver, January.
- PRIDE, M.J., 1986. Interlayered sedimentary-volcanic Sequence, Mt. Skukum Volcanic Complex; in Yukon Geology 1984-85, Dept. Ind. Aff. Nor. Dev., Whitehorse, Yukon, this volume.
- ROSLYAKOVA, N.V. and N.A. ROZLYAKOV, 1975. Gold deposit endogenic halos; Academy of Sciences of the USSR Siberian Section, Vol. 182, p. 4-130, translated by Energy Mines and Resources, Canada, Translation Bureau No. 751465.
- SMITH, M.J., 1983. The Skukum volcanic complex, 105 D SW: Geology and comparison to the Bennett Lake cauldron complex; Yukon Exploration and Geology 1982, Dept. Ind. Aff. Nor. Dev., Whitehorse, Yukon, p. 94-104.
- STEIGER, R.H. and E. JAGER, 1977. Subcommission on geochronology: Convention on the use of decay constants in geo- and cosmochronology; Earth and Planetary Science Letters, Vol. 36, p. 67-71.
- TEMPELMAN-KLUIT, D.J., 1981. Geology and mineral deposits of southern Yukon: in Yukon Geology and Exploration 1979-80, Dept. Ind. Aff. Nor. Dev., Whitehorse, Yukon, p. 7-31.
- WHEELER, J.O., 1961. Whitehorse map-area, Yukon Territory, 105 D; Geol. Surv. Can., Memoir 312.

TABLE 1

**POTASSIUM-ARGON DATA FROM WHOLE ROCK ANALYSES OF ANDESITE FROM THE MT. SKUKUM PROPERTY,
MAIN ZONE AREA, YUKON**

Sample number	Location		Rock description	% K (\pm)	$\frac{^{40}\text{Ar}^*}{^{40}\text{Ar}_{\text{total}}} - 2$	$\frac{^{40}\text{Ar}^*}{10^{-5} \text{ cm}^3 \text{ STP/g}} - 2$	Apparent age (Ma) ³	Time ⁴
	lat($^{\circ}$ N)	long($^{\circ}$ W)						
ASTN-13WR DDH83-63: 57.61M	60°20'	135°47'	Fine grained andesite with pervasive propylitic alteration	2.71 0.01	0.674	0.5416	50.7 \pm 1.8	Tertiary Early Eocene
ASTN-14WR DDH83-63: 59.19M	60°20'	135°47'	Fine grained, fresh andesite	2.18 0.04	0.938	0.4574	53.2 \pm 1.8	Tertiary Early Eocene

1. Argon analyses are by J. Harakal and potassium analyses are by K. Scott; all analyses were done at the Geochronology Laboratory, The University of British Columbia

2. Ar* indicates radiogenic argon

3. Constants used are from Steiger and Jager (1977): $\lambda_{\text{K}} = 0.581 \times 10^{-10} \text{ yr}^{-1}$; $\lambda_{\text{Ar}} = 4.962 \times 10^{-10} \text{ yr}^{-1}$; $^{40}\text{K}/\text{K} = 1.167 \times 10^{-4}$

4. Time designation is from Harland *et al.* (1982).

EXPLORATION GEOLOGY OF THE MT. SKUKUM EPITHERMAL GOLD DEPOSIT, SOUTHWESTERN YUKON

Bruce W.R. McDonald and Colin I. Godwin
Department of Geological Sciences
University of British Columbia
Vancouver, B.C.

and

Elmer B. Stewart
Agip Canada Ltd.
Calgary, Alberta

McDONALD, B.W.R., STEWART, E.B. and GODWIN, C.I., 1986. Exploration geology of the Mt. Skukum epithermal gold deposit, southwestern Yukon; in Yukon Geology, Vol. 1; Exploration and Geological Services Division, Yukon, Indian and Northern Affairs Canada, p. 11-18.

INTRODUCTION

The Mt. Skukum gold-silver deposit, 65 km southwest of Whitehorse, (60°12' N, 135°28' W; elevation 1800m a.s.l.; Fig. 1), occurs in Main Cirque which forms the headwaters of Butte Creek (Fig. 2) in the southwestern part of the Tertiary Mt. Skukum Volcanic Complex, immediately northwest of the Wheaton River. The deposit consists of low sulphide, high-level, gold-silver bearing quartz-calcite veins which may have formed in a near surface "hot-spring type" environment within several hundred meters of paleo-surface. Mineral and alteration assemblages resemble those described as adularia-sericite epithermal systems (Berger, oral. comm., 1986), however, adularia commonly associated with this type of mineralization does not appear to be present. The deposit represents the most recent mine brought into production in the Yukon Territory. With an average grade of approximately 25 g/t Au it is one of the richest gold mines in Canada. It is easily accessible from Whitehorse using a newly upgraded road.

EXPLORATION HISTORY

Exploration for silver and gold lodes in Yukon Territory began following the Klondike Gold Rush with attention focussed in the Wheaton district on several occasions. Precious metal and antimony veins were first discovered in the Wheaton River district in 1893 (Cairnes, 1912, 1916), but only limited production has come from these deposits. The Montana Mountain camp, 45 km to the east, is the best known precious metal area close to Mt. Skukum. The Venus Mine, on the southeastern part of Montana Mountain produced gold from a quartz-sulphide vein on several occasions, most recently in 1981.

During 1979 and 1980, Agip Canada Ltd. of Calgary conducted reconnaissance exploration in two areas of Skukum Group volcanic rocks, the Bennett Lake Caldera Complex and the Mt. Skukum Volcanic Complex. Geological mapping by the Geological Survey of Canada combined with reconnaissance work indicated that these areas had excellent potential for volcanic-hosted epithermal mineralization.

The 1980 reconnaissance program consisted of preliminary prospecting, mapping and sampling including an extensive stream sediment geochemistry program. Evaluation of geochemical data indicated anomalous concentrations of gold and arsenic in sediment from Butte Creek in the Mt. Skukum Volcanic Complex. Sediments in this creek contained up to 630 ppb Au and 192 ppm As. In all, nine samples containing values in excess of 85 ppb Au against a background of 5 ppb Au were defined in the headwaters of Butte Creek and were considered to be a significant exploration target. On the basis of this exploration, 48 claims were staked in May 1981 to cover the geochemical anomaly in Butte Creek and the gossanous zones in Main Cirque. Prior to this, very little modern, detailed exploration had occurred in the central area of the Mt. Skukum Volcanic Complex and no record of previous staking of the area exists.

REGIONAL GEOLOGY AND TECTONIC SETTING

The Mt. Skukum gold-silver deposit occurs in an early

Eocene age (51.6 ± 1.8 Ma) volcanic complex on the border of the Coast Plutonic Complex and the Yukon Crystalline Terrane, approximately 27 km north-northwest of the Bennett Lake Caldera Complex (Fig. 3). Both volcanic centers are of a similar early Tertiary age, but the Bennett Lake Caldera Complex consists of a relatively higher proportion of felsic volcanic rocks and displays a well

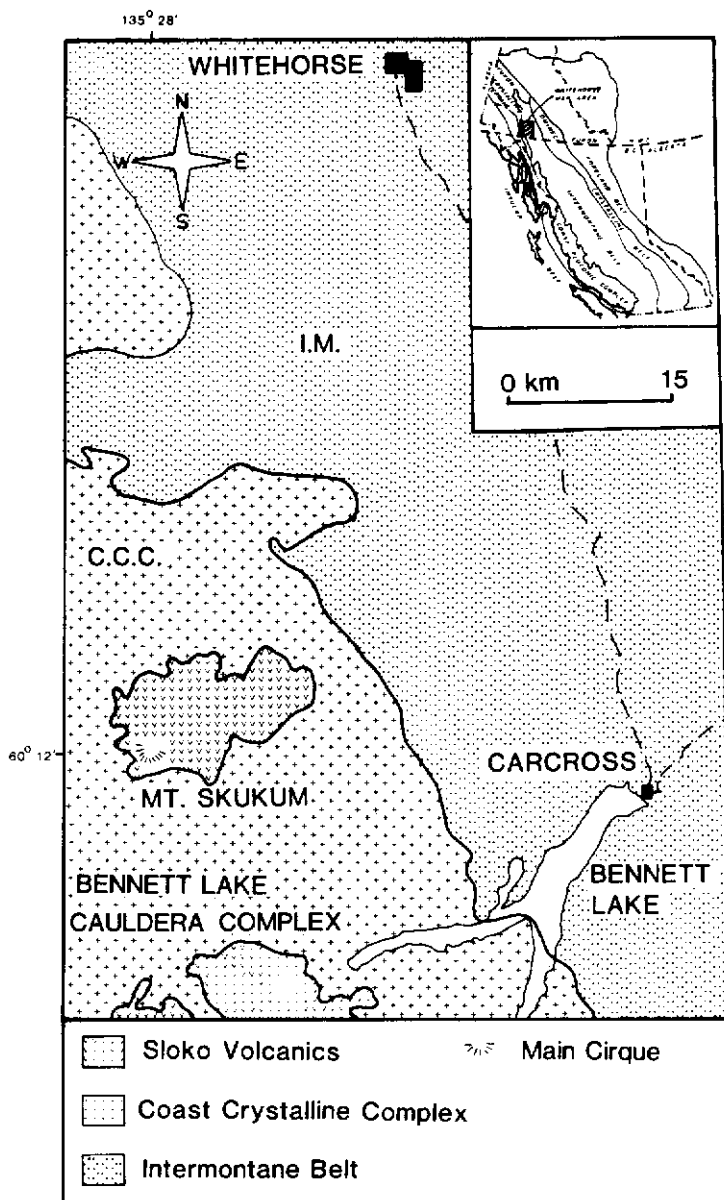


Figure 1. Location of the Mt. Skukum Volcanic Complex

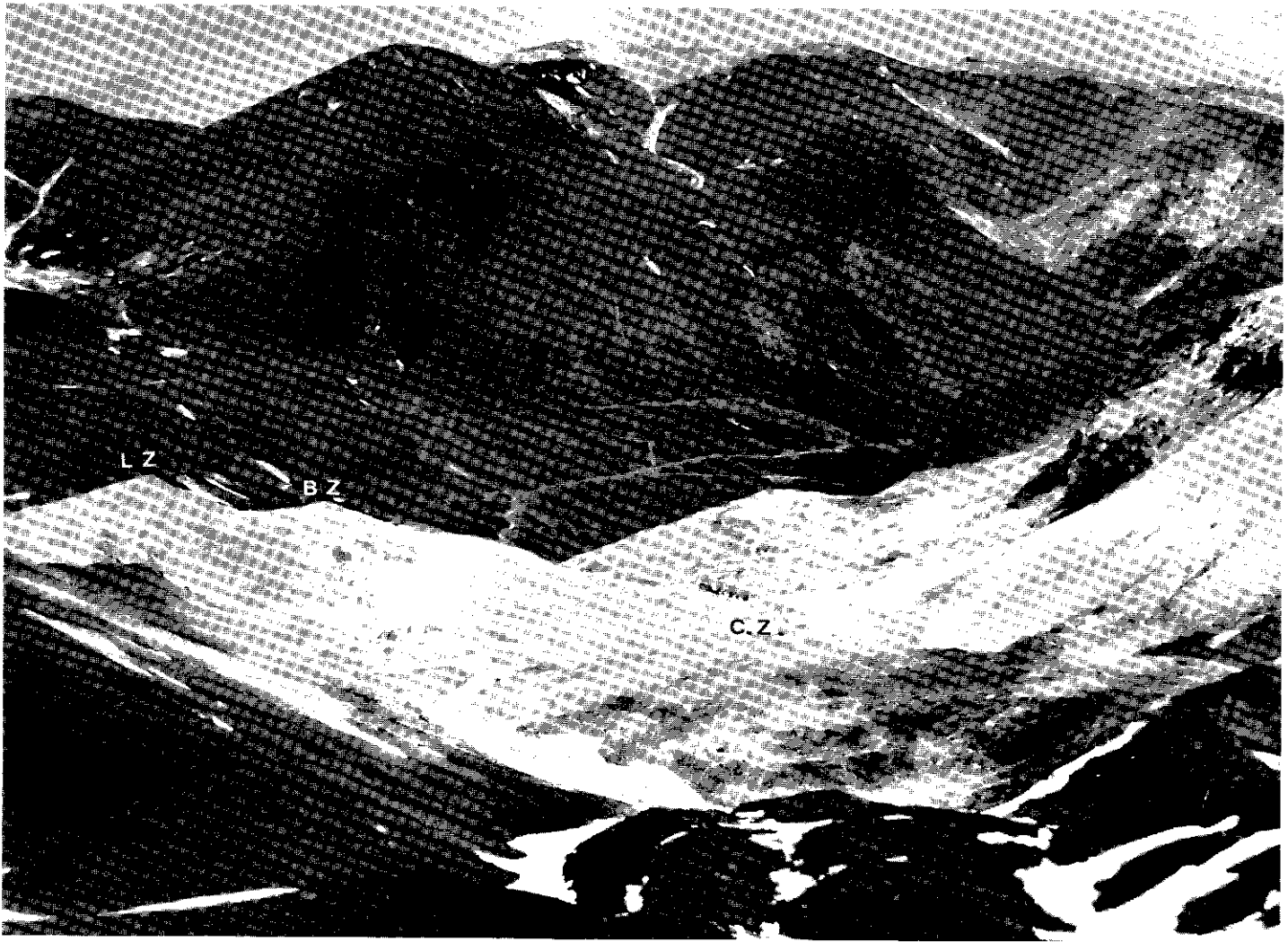


Figure 2. View of Main Cirque looking due north with the Butte Creek valley in the background. L.Z. = Lake Zone, B.Z. = Brandy Zone, C.Z. = Cirque Zone.

defined felsic ring dyke partially surrounding it. The Mt. Skukum Volcanic Complex contains both andesitic and felsic volcanic rocks and is surrounded by many small, high-level rhyolitic to dacitic intrusions which may represent late associated ring fracture intrusions related to a caldera event. Lithogeochemical evidence, however, indicates that peripheral intrusions surrounding the two volcanic complexes originated from different magma chambers (Smith, 1982).

Each of these volcanic systems are interpreted by Smith (1983) to represent distinctive structural and volcanic settings rather than being two erosional remnants of the same volcanic system. Both were formed during a time of crustal extension accompanied by block faulting, tilting and local folding throughout the western Cordillera (Lambert, 1974). It was also a time of widespread granitic intrusion in the Cassiar and Coast Crystalline Belts that was accompanied by volcanic activity in the southern Yukon and central British Columbia (Souther, 1970). Volcanic activity gave rise to three large volcanic provinces, the Sloko Province, Ootsa Lake Province, and Kamloops-Midway Province, all of which consist mainly of rhyolitic and dacitic rocks (Lambert, 1974). The Mt. Skukum Volcanic Complex forms the northernmost extent of the Sloko Volcanic Province which, in Yukon Territory, has been correlated with Skukum Group volcanic rocks ranging in age from 50 to 60 Ma (Nelson, 1985).

The Mt. Skukum Volcanic Complex (Fig. 4) consists of a 140 km², subrounded remnant of fault-bounded Tertiary andesitic and felsic volcanic rocks which have been intruded by small, late-stage rhyolitic stocks and dykes (Pride, 1986 — this volume). The volcanic complex has been down-dropped along its eastern and part of its southern margins into underlying basement rocks. Basement unconformably underlies the Skukum Group volcanic rocks and

consists of Cretaceous granitic rocks of the Coast Crystalline Complex and upper Precambrian to lower Paleozoic marbles, schists and gneisses of the Yukon Group, all of which are aligned in a NNW trending belt.

LOCAL GEOLOGY

The Mt. Skukum gold-silver deposits are located in the southwestern portion of the Mt. Skukum Volcanic Complex in a north-facing cirque at the foot of Mt. Skukum. They consist of three major and many minor N to NE trending quartz-carbonate vein-fault systems which cross-cut the volcanic stratigraphy with steep to vertical dips (Fig. 5).

Volcanic stratigraphy in the deposit area consists of four cycles of volcanic activity, each representing different eruptive styles and compositions. Cycle I, deposited during initiation of volcanic activity, produced lower conglomerates and débris flows followed by pyroclastic flows, airfall tuff deposits, and locally water-lain tuffaceous sediments. This cycle is characterized by the abundance of basement fragments in all rock types and by the intimate interbedding of pyroclastic and epiclastic deposits. Composition of most of the pyroclastic debris is rhyolitic to dacitic, especially towards the bottom of the sequence, with a trend upwards to rocks of andesitic composition.

Cycle II volcanic rocks immediately overlie cycle I and represent a change in the style of volcanism in the area from one of violent pyroclastic eruption to slightly more quiescent eruption of andesitic lava flows interspersed with pyroclastic eruptive debris. Rocks of cycle II form a stratigraphic pile up to 800 m thick that can be subdivided into two packages.

The lower package of cycle II consists of individual porphy-

ritic andesite flows generally between 1.5 and 4 m thick displaying a highly variable porphyritic character. Flow rocks are commonly interspersed with variable thicknesses of andesitic ash and lapilli tuffs and debris flows, as well as andesitic pyroclastic flows which display a slight degree of welding. Flow units in this lower package also tend to display a low MgO content relative to the upper package which typically contains in excess of 2.1% MgO (Pride, pers. comm., 1985).

The upper package of cycle II volcanics is much more uniform, consisting of greater thicknesses of andesitic flow rocks formed by many successive eruptive episodes closely related in time. Individual flow units in the upper package are themselves very similar in appearance and are often only distinguishable by their characteristic flow top and flow bottom breccias marking the boundaries between each flow. Pyroclastic rocks are much less frequent in the upper package of cycle II, but where present, they consist of lithology similar to the lower package.

Cycle III rocks unconformably overlie porphyritic andesite flow rocks of cycle II in the area of the deposits and represent a return to felsic volcanism. Rock types range from rhyolitic to dacitic and consist mainly of rhyolite flows and pyroclastics with a minor amount of debris flow material predominantly in the lower levels of the cycle. Two rock types dominate cycle III. The first is a maroon flow banded rhyolite which is slightly porphyritic and commonly contains abundant spherulites, 2 to 6 cm in diameter, in bands which parallel the flow bands. This unit occurs at high elevations throughout the volcanic complex and, in the vicinity of the deposits, occurs high (elevation 2000 m) on the eastern wall of Main Cirque. It appears to be related to a similar circular dome-like intrusion of maroon, flow banded, autobrecciated rhyolite which occurs at the southernmost end of Main Cirque and may have been a feeder to the rhyolite flow.

The second dominant rock type comprising cycle III rocks in the area of the deposits is a densely welded felsic tuff. This rock type occurs at the highest elevations (2100 m) on the eastern wall of Main Cirque, and is limited to an unusual rounded, bowl-shaped depression carved deeply into the flow-banded rhyolite (Fig. 6). The rock is brown in colour with abundant cognate and crystal fragments as well as elongate juvenile fragments with well

developed flambé structures. The unit is several hundred meters thick and displays a well developed columnar jointing throughout. It is interpreted to represent an eruptive crater infilled by its own eruptive product. This is supported by the presence of a megabreccia unit which partially surrounds the welded tuff. This megabreccia may have formed on the edges of the crater during slumping and collapse of material from the crater margins. It consists of enormous rotated blocks of flow banded rhyolite, andesite and rocks resembling those of cycle I. Some of these blocks attain sizes several times that of a large house and all occur in a matrix of finer breccia material.

Cycle IV volcanic rocks are stratigraphically highest and represent a return to andesitic volcanism. These rocks occur in the south and west of Main Cirque and the entire peak of Mt. Skukum is composed of this material. Cycle IV volcanic rocks consist of a very thick and extensive porphyritic andesite eruption breccia composed of unsorted, rounded to sub-rounded fragments of porphyritic andesite up to several meters across in a partially silicified matrix of finer fragments of the same material. These rocks are intruded at irregular intervals by dykes and sills of columnar jointed porphyritic andesite.

STRUCTURE

The entire volcanic complex is highly dissected by faults and is divided in two by a major N-trending fault. The western section includes felsic and andesitic rocks mainly of cycles I and II with cycles III and IV only preserved at the highest elevations. The eastern section preserves an abundance of felsic rocks of cycle III because it has been significantly down-dropped.

In the area of the deposits, abundant high angle normal faults dissect the volcanic rocks and display a dominant NNE trend. The morphology of Main Cirque, which hosts the gold-silver deposits is largely controlled by several of these faults. It appears to be composed of at least three down-dropped blocks. The down-

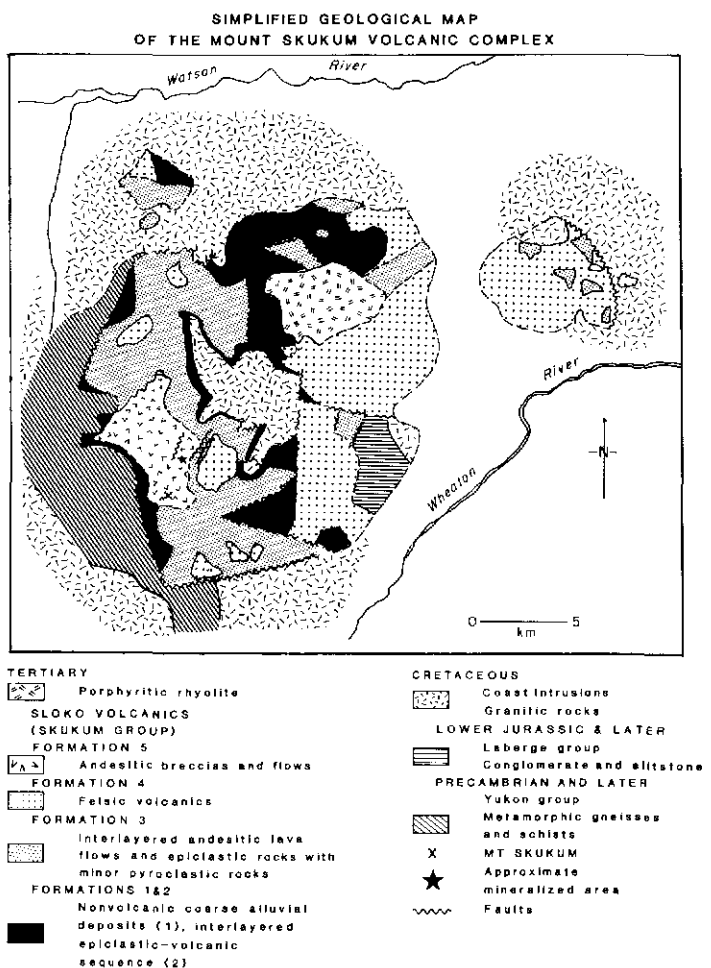
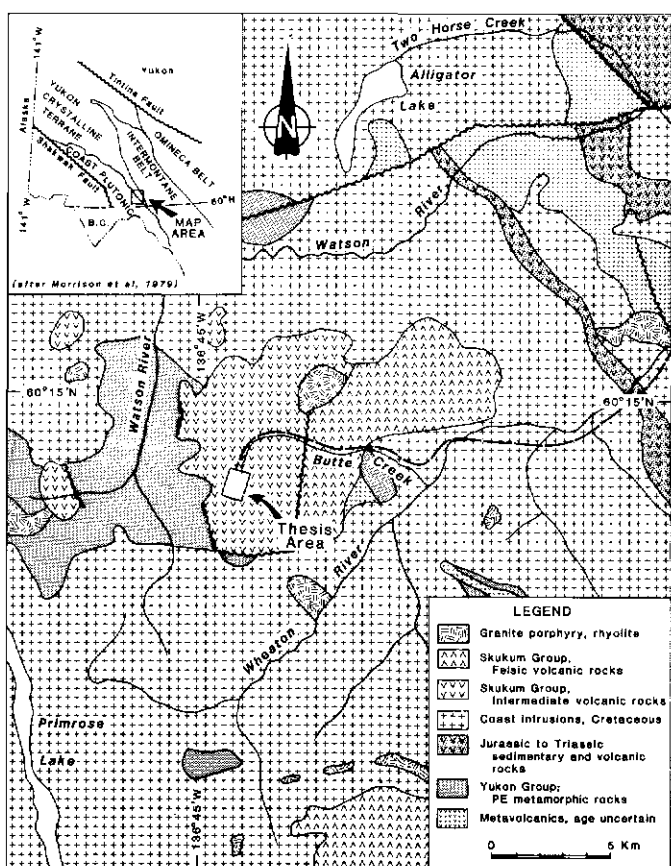
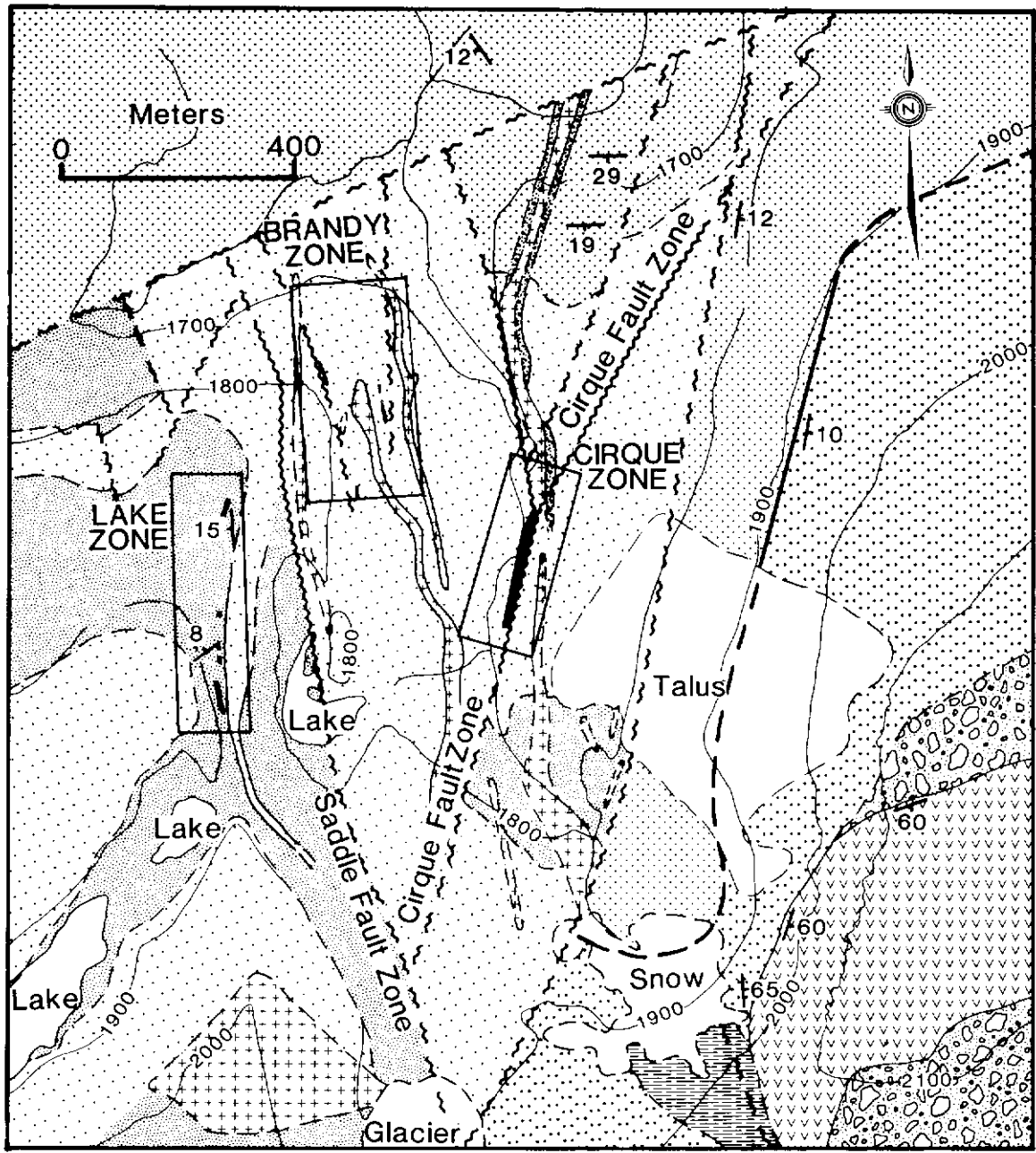


Figure 3. Regional geology of Mt. Skukum area modified after Wheeler (1960) and Pride (1985).

Figure 4. Distribution of major rock types in the Mt. Skukum Volcanic Complex from Pride (1985).



- | | |
|--|---|
| ■ Quartz-carbonate veins and stockwork | ■ Rhyolite dykes |
| ■ Alunite-pyrophyllite clay altered zone | ■ Breccia body |
| ■ Densely-welded felsic tuff (cycle 3) | ■ Andesitic lapilli and ash tuff (cycle 2) |
| ■ Felsic megabreccia (cycle 3) | ■ Porphyritic andesite flows (cycle 2) |
| ■ Flow-banded rhyolite (cycle 3) | ■ Andesitic flows and fragmentals (cycle 1) |
| ~~~ Fault | — Angular unconformity |

Figure 5. Geology of Main Cirque.

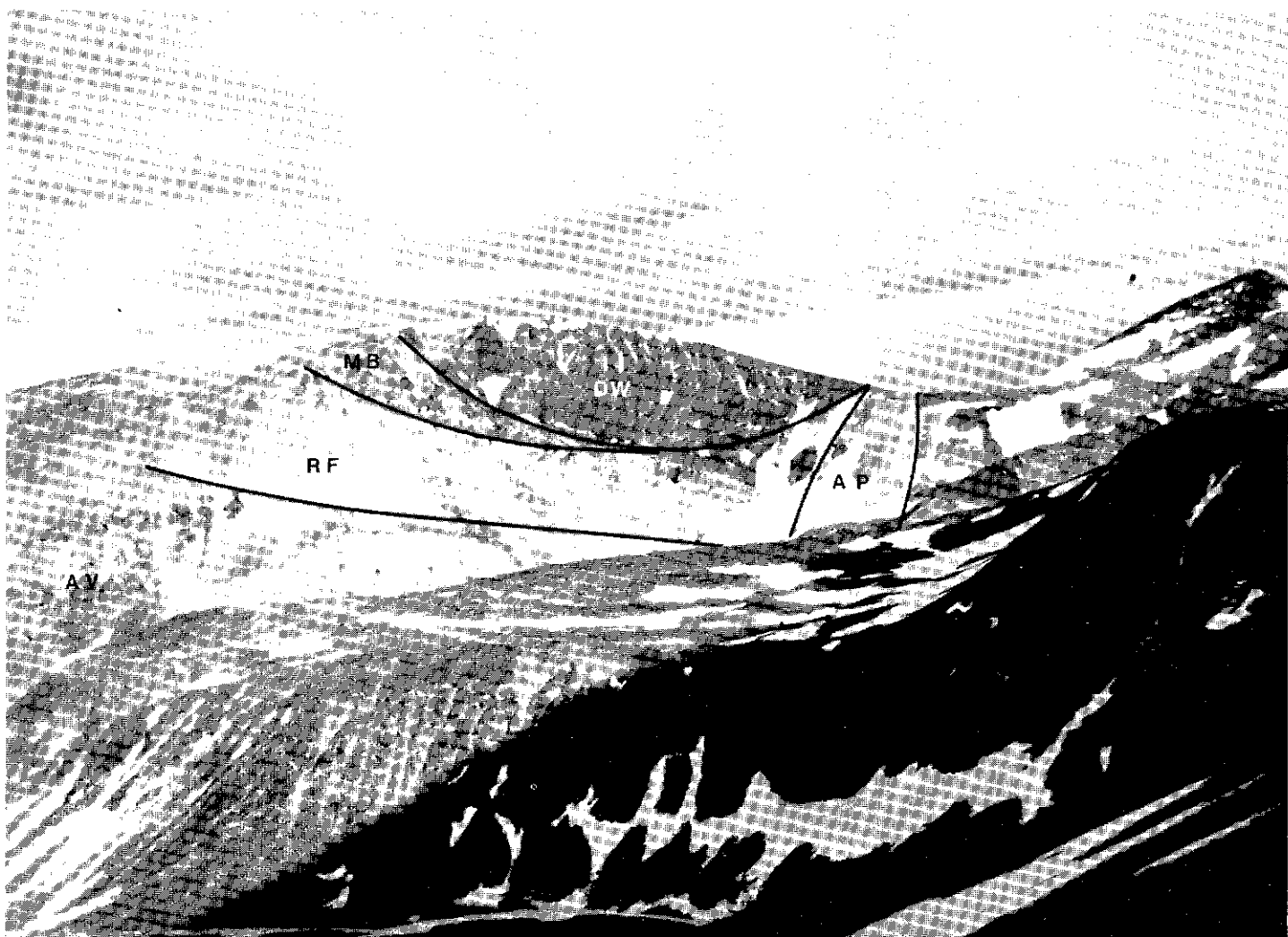


Figure 6. View of east wall of Main Cirque showing:

- 1) Densely-welded felsic tuff (DW)
- 2) Megabreccia (MB)

- 3) Rhyolite flow (RF)
- 4) Andesitic volcanics (AV)
- 5) Alunite-pyrophyllite altered zone (AP).

ward displacement of each appears to increase progressively to the east, resulting in a step-like topography downward from west to east. Each block is bounded by normal faults and the eastern and western walls of the cirque are fault scarps marking the edges of this collapse feature.

Attitudes of volcanic strata in and around Main Cirque tends to be flat lying with dips rarely more than 20° . Attitudes of strata vary from one down-dropped block to another; however, dips in the eastern and western wall of the cirque show a systematic divergence. Stratigraphy in the western cliffs of the cirque dip gently (8° to 12°) but dips in the eastern cliffs are of equal magnitude to the east. These divergent attitudes may reflect the original topography surrounding an eruptive center or may indicate a doming of the area during insurgence of the high level rhyolitic intrusives and deposition of cycle III volcanic rocks. This would be analogous to resurgent doming seen in other areas of volcanism.

MINERALIZATION

Gold occurs as finely disseminated electrum hosted in quartz-carbonate-sericite vein-fault systems which formed within the bounding faults between down-dropped blocks in Main Cirque. Many mineralized veins have been found, all localized within faults. The best known of these vein systems are the Cirque Zone, Brandy Zone and Lake Zone which form three sub-parallel N and NE trending zones in Main Cirque. The Cirque Zone, which is currently in production, measures 200 m long, 80 m deep and averages 5 m wide. It contains proven reserves of approximately 149,000 tonnes of ore grading about 25 g/t Au and 20.5 g/t Ag. The Brandy Zone, about 350 m west of the Cirque Zone contains

proven reserves in excess of 27,500 tonnes of ore averaging about 17 g/t Au and 13 g/t Ag (R. Somerville, pers. comm., 1985). Reserves in the Lake Zone are yet to be defined.

Two stages of vein formation have been defined in Main Cirque. The early stage is marked by blue-grey chalcedonic veinlets rarely more than 2 mm thick. These veinlets occur sporadically throughout the Cirque Zone but are ubiquitous in the Lake Zone and are characterized by abundant pyrite selvages and envelopes with traces of pyrrhotite, sphalerite and chalcopyrite. Locally, these first stage veinlets form dense stockworks associated with intense argillite alteration including abundant kaolinite and quartz. Due to the high pyrite content, these areas form small, heavily iron stained gossans. However, first stage veinlets do not host significant gold or silver mineralization.

In contrast, the second stage of vein formation hosts more of the gold mineralization. Second stage veins characteristically consist of quartz with variable amounts of calcite, minor sericite and trace amounts of albite and potassium feldspar; they contain no sulphides. Textures in these veins range from a sugary massive appearance to a vuggy texture with abundant wallrock breccia fragments (Fig. 7) and well developed cockade structures. Calcite locally displays a bladed habit (Fig. 8) with large, elongate crystals up to 4 cm long intergrown with quartz. This texture has also been noted in other epithermal gold districts such as the Bodie district in northern California where it is associated with high grade ore (Silberman, pers. comm., 1985). Microscope investigation shows that electrum occurs within, or interstitial to, quartz grains in the veins; however, gold values tend to occur in veins with at least equal amounts of quartz and calcite.



Figure 7. Photo taken underground in a sub-drift in the Cirque Ore Zone showing abundance and distribution of wallrock breccia fragments (dark) in the quartz-carbonate vein material (light).

ALTERATION

Alteration in the area surrounding Main Cirque is widespread, but only locally intense. It consists primarily of plagioclase and magnetite destructive propylitic alteration characterized by the breakdown of plagioclase to epidote and calcite. Second stage quartz-carbonate veins commonly appear to have been in equilibrium with this alteration assemblage. In some cases however, a more intense alteration halo consisting of a moderate intensity of phyllitic alteration including minor pyrite extends up to 10 cm from the veins. This alteration consists mainly of the breakdown of plagioclase to sericite and minor epidote, invariably accompanied by the development of minute disseminated grains of pyrite and commonly associated with minor silicification. A similar form of phyllitic alteration is found surrounding rhyolite dykes found in Main Cirque, however, alteration halos surrounding these dykes tend to be slightly more intense and wider, up to 1.5 m across.

Two other zones of unusual alteration occur in the walls surrounding Main Cirque. One zone on the western cirque wall consists of a broad area of bright orange-brown staining which covers a rhyolite plug. The bright colour is developed only in the soil horizon covering the intrusion and is probably caused by hematite formed by oxidation of disseminated pyrite in the rhyolitic intrusion.

A second area of brightly coloured orange-brown iron stained soil occurs in the southeast wall of the cirque. It occurs over an area of intense kaolinitic alteration marked by rocks that have been intensely and completely altered to soft white kaolinitic clays retaining only ghosted remnants of primary textures (Fig. 6). X-ray diffraction analysis of rocks from this area showed that they contained

in order of decreasing abundance, pyrophyllite, alunite and quartz. The hematitic iron staining in this area may be the result of either the initial alteration or oxidation of disseminated pyrite.

EXPLORATION METHODS

Exploration on the Mt. Skukum property since its initial staking in May 1981 has included mapping, prospecting, trenching and a variety of geophysical surveys. At the outset of exploration, emphasis was placed on examination of the highly coloured gossanous zones scattered throughout Main Cirque. However, during the course of the first year of exploration, it was noted that none of the anomalous gold in soil values were associated with these gossans, but rather with macroscopically unmineralized quartz-carbonate veins. In addition, a prominent linear gold in soil anomaly was defined along the east side of the creek which drains Main Cirque. The anomaly was 110 m long and 30 m wide and contained values ranging from 300 to 800 ppb Au. This anomaly occurs over what is today known as the Cirque Ore Zone. Rock chip sampling also produced promising results from several areas; most notably, the Lake Zone returned values as high as 20.5 g/t Au over 5.0 m. By the end of the 1981 exploration season, emphasis had switched from the gossanous zones to the quartz-carbonate veins and an additional 354 claims had been staked.

In 1982, the first detailed exploration program was begun within Main Cirque with the objective of extending the existing soil geochemistry and geophysics grids and carrying out more detailed prospecting on the property. Soil geochemistry proved to be one of the most successful exploration methods and several strong anomalies were found. Most notable was one located about 300 m west of the Cirque Zone which contained gold in soil values of



Figure 8. Bladed calcite crystals in a quartz-carbonate vein.

3845 ppb. This anomaly was subsequently trenched to reveal the vein system known today as the Brandy Ore Zone. Prospecting was also successful with the discovery of four additional zones by the end of the season. Geophysical surveys completed over the area included magnetometer, EM-31, EM-34 and IP-resistivity. Overall they proved to be of only limited success, with both EM surveys returning inconclusive results. Magnetic survey data picked up the Cirque Zone and Brandy Zone quartz-carbonate vein systems as linear NE trending magnetic lows. IP-resistivity showed a general correlation with zones of low magnetic signature, however, the response of these two geophysical techniques is not completely dependent on the presence of mineralized quartz-carbonate veins. It is likely that the magnetometer low and corresponding IP-resistivity anomalies are produced at least in part by areas of alteration and disseminated pyrite surrounding fault zones, quartz-carbonate veins and rhyolite dykes, all of which commonly occur together throughout Main Cirque. Moreover, the presence of a rhyolite dyke in andesitic stratigraphy would produce a magnetic low even without associated mineralized veins. Geophysical surveys generally identify the presence of fault zones and/or rhyolite dykes. Since quartz-carbonate veins are commonly

in faults or adjacent to dykes, geophysics is a useful tool in finding favourable environments of deposition for mineralized vein material.

Soil geochemistry for gold and silver in conjunction with prospecting have proven to be the most useful exploration techniques and have been used to discover the nine known mineralized zones. Use of trace pathfinder elements such as arsenic and mercury is difficult, because although they do occur in anomalous quantities, their distribution is erratic, and other pathfinders such as antimony are not present in anomalous amounts. Geophysics, including IP-resistivity and magnetometer surveys, may continue to define favourable structures at depth, in areas where soil geochemistry anomalies cannot be traced to a source in outcrop.

CONCLUSION

The vein systems at Mt. Skukum and most other epithermal systems are closely dependent on a pre-existing structure. Consequently, understanding of the structure and geology of the property is essential to exploration. Veins in Main Cirque are hosted in major normal fault zones bounding down-dropped blocks to depletion of a magma chamber below the adjacent eruptive center. Residual heat within the exhausted magma chamber or perhaps a slight resurgence of intrusive material may have driven the hydrothermal circulation which resulted in regional alteration and deposition of the quartz-carbonate veins. Due to the close relationship of these factors, the identification of further eruptive chambers within the volcanic complex as well as any associated collapse features is critical to future exploration. Identification of additional faults associated with the collapse feature represented by Main Cirque is also important because these faults potentially host additional ore.

Gold-silver veins at Mt. Skukum display many of the classic characteristics of a relatively low temperature epithermal system similar to those described by Bonham (1986) and many others as a low-sulphide adularia-sericite system. Although adularia has not been identified in thin section, abundant sericite commonly replaces feldspar grains that may represent original adularia.

Vein formation probably occurred within several hundred meters of the paleosurface which may be represented by the intense kaolinitic alteration zone and the crater on the southeastern wall of Main Cirque. Intense kaolinitic alteration such as this is commonly found at the top of many epithermal systems in the oxidized area above the paleo-watertable in or near the hot-spring environment.

Evidence indicates that the Mt. Skukum deposits formed at low temperature in a near surface environment by circulating meteoric waters in a hydrothermal system driven by a heat source associated with felsic dykes present in the area. Fluid flow was probably controlled by permeable faults, breccia bodies as well as brecciated flow surfaces and tuff beds, all of which are found to host significant gold values. Circulating fluids may have leached gold from surrounding andesitic volcanic rocks during propylitization and precipitated it in outlet areas provided by highly permeable fault zones forming the vein-fault systems which host most of the gold mineralization.

Exploration to date has proven the economic merits of the Cirque and Brandy Ore Zones. However, the relatively short time between initial discovery and production has left a tremendous amount of exploration to be done on the many remaining mineralized zones.

REFERENCES

- BONHAM, H.F., 1986. Models for volcanic-hosted epithermal precious metal deposits: a review; in Proc. of Symposium 5: Volcanism, Hydrothermal Systems and Related Mineralization, University of Auckland, N.Z.
- CAIRNES, D.D., 1912. Wheaton District, Yukon Territory; Geol. Surv. Can., Mem. 31.
- CAIRNES, D.D., 1916. Wheaton District, Yukon Territory; Geol. Surv. Can., Supplement to Sum. Rept. for 1915, p. 36-49.
- DOHERTY, R.A., BALOG, M., ROBERTSON, R., 1982. Mount Skukum project: 1982 exploration activities; Unpublished company report, Agip Canada Ltd.

- DOHERTY, R.A., BALOG, M., ROBERTSON, R., 1983. Mount Skukum project: 1983 exploration activities; Unpublished company report, Agip Canada Ltd.
- HARLAND, W.B., COX, A.V., LLEWELLYN, P.G., PICKTON, C.A.G., SMITH, A.G., and WALTERS, R., 1982. A Geologic Time Scale; Cambridge Earth Science Series, Cambridge University Press, 131 p.
- LAMBERT, M.B., 1974. The Bennett Lake cauldron subsidence complex, British Columbia and Yukon Territory; *Geol. Surv. Can. Bull.* 227, 213 p.
- McDONALD, B.W.R. and GODWIN, C.I., 1985. Epithermal gold veins of the Main Zone at Mt. Skukum, southwest Yukon Territory; *Unpubl. manuscript of oral presentation at B.C. and Yukon Chamber of Mines Cordilleran Roundup*, Vancouver.
- McDONALD, B.W.R. and GODWIN, C.I., 1986. Geology of Main Zone at Mt. Skukum, Wheaton River area, southern Yukon; *in Yukon Geology, Vol. 1; Exploration and Geological Services Division, Yukon, Indian and Northern Affairs Canada*.
- NELSON, J., 1985. Cretaceous and Paleogene history of the western Canada Cordillera; *Geol. Surv. Can. Open File 1162*, 37 p. and 2 maps.
- PRIDE, M.J., 1985. Interlayered sedimentary-volcanic sequence, Mt. Skukum Volcanic Complex; p. 94-104 *in Yukon Exploration and Geology 1983*, Exploration and Geological Services Division, Yukon, Indian and Northern Affairs Canada, 317 pp.
- ROSLYAKOVA, N.V. and ROZLYAKOV, N.A., 1975. Gold deposit endogenic halos; *Academy of Sciences of the U.S.S.R. Siberian Section, Vol. 182*, p. 4-130 (translated by Energy, Mines and Resources, Canada, Translation Bureau No. 751465).
- SMITH, M.J., 1983. The Skukum Volcanic Complex, 105 D SW: Geology and comparison to the Bennett Lake cauldron complex; p. 68-72 *in Yukon Exploration and Geology 1982*, Exploration and Geological Services Division, Indian and Northern Affairs Canada, 259 pp.
- SMITH, M.J., 1982. Petrology and geology of high-level rhyolite intrusives of the Skukum area, 105 D SW, Yukon Territory; p. 62-73 *in Yukon Exploration and Geology 1981*, Exploration and Geological Services Division, Indian and Northern Affairs Canada, 281 pp.
- SOUTHER, J.G., 1970. Volcanism and its relationship to recent crustal movements in the Canadian Cordillera; *Can. Jour. Earth. Sci.*, Vol. 7, p. 553-568.
- TEMPELMAN-KLUIT, D.J., 1981. Geology and mineral deposits of southern Yukon: p. 7-31 *in Yukon Geology 1979-80*, Exploration and Geological Services Division, Indian and Northern Affairs Canada, 364 pp.
- WHEELER, J.O., 1961. Whitehorse map-area, Yukon Territory, 105 D; *Geol. Surv. Can., Mem. 312*.

GOLD IN SKARNS OF THE WHITEHORSE COPPER BELT SOUTHERN YUKON

(This study was partly funded by Program I, Mineral Resources Sub-agreement of the Canada-Yukon Economic Development Agreement.)

Lawrence D. Meinert
Department of Geology
Washington State University
Pullman, WA 99164-2812

MEINERT, L.D., 1986. Gold in skarns of the Whitehorse Copper Belt, southern Yukon; in Yukon Geology, Vol. 1, Exploration and Geological Services Division, Yukon, Indian and Northern Affairs Canada, p. 19-43.

INTRODUCTION

Skarns in the Whitehorse Copper Belt have produced 121,600 tonnes of copper, 97,000 kg of silver, and 7,700 kg of gold from 10 million tonnes of ore between 1967 and 1982 (Tenny, 1981; Watson, 1984). By the end of mining activities in 1982, gold and silver contributed a significant proportion of the ore value, thus sparking a renewed interest in the occurrence of gold in the Whitehorse skarns. A calculated gold grade (assuming 100% recovery) of 0.7 g/t Au for the Whitehorse deposits is probably too low, but neither exploration nor production drill holes were routinely assayed for gold. Hureau (1985) estimated that the 9 million tonnes of tailings from the Whitehorse deposits contain about 1,500 kg of gold and Tenny (1981) reported that tailings assays ranged up to 250 g/t Au near the tailings decant. It appears likely that not all the gold was recovered from Whitehorse skarn ore, that the calculated average gold grade for the deposit is too low, and that further gold-silver potential in the district may exist.

Worldwide, about 1.5×10^9 grams of gold have been produced from skarn deposits. The majority of this production has come as a by-product of large scale mining of skarns associated with porphyry copper deposits (Meinert, 1986). Most skarns in porphyry copper districts contain less than 0.5 g/t Au, although some deposits (e.g. Bingham, Utah, Cameron and Garmoe, 1983) contain local zones with grades up to 70 g/t Au. Little is known about the distribution of gold within these skarns or about possible correlations of skarn mineralogy or alteration stage with gold grade. In terms of gold grade, the Whitehorse skarns appear to contain more gold than most porphyry copper skarns and thus represent a unique opportunity to study the distribution of gold within a large copper skarn system. The present paper reports the results of a reconnaissance study of alteration, gold distribution, and mineralogy of skarns in the Whitehorse Copper Belt.

Scope of Study

More than 32 mines and prospects occur within the Whitehorse Copper Belt (Kindle, 1964; Tenney, 1981). Similar skarns occur in the surrounding area (e.g. the Jackson Lake prospect 16 km northwest of Whitehorse at $60^{\circ}41'N$, $135^{\circ}22'W$). Nine skarn deposits (Fig. 1) within the Whitehorse Copper Belt were chosen for a comparative study to address the following three questions: 1) What is the skarn mineralogy and how does it compare to other types of skarn deposits (e.g. Einaudi et al., 1982)? 2) What is the distribution of gold in the various deposits? and 3) Can the gold content be correlated with the skarn mineralogy or alteration type?

In an attempt to answer these questions, selected drill core from each deposit was relogged and available mine workings were inspected. For each of the nine studied deposits, samples were collected for Cu, Ag, and Au assay from diamond drill core and where available, from mine workings or surface outcrops. Each sample was also studied petrographically and, where appropriate, individual skarn mineral grains were analyzed with an electron microprobe.

GEOLOGIC SETTING

The Whitehorse Copper Belt is a northwest trending zone of Cu-Fe-Mo-Au-Ag skarns about 30 km long located 5 km west of Whitehorse, Yukon (Fig. 1). Skarn is localized along the irregular west margin of the mid-Cretaceous Whitehorse Batholith (Table 1), a composite biotite-hornblende granodiorite pluton with a horn-

blende diorite margin (Morrison, 1981). The Whitehorse Batholith is one of a suite of calc-alkaline intrusions (Coast Plutonic Complex) which were emplaced during formation and probable accretion of a Permian to Jurassic island arc terrane (the Intermontane Belt). Although the main mass of the Whitehorse Batholith is relatively unaltered, Morrison (1981) describes quartz-kspar-bornite-chalcopyrite veins which locally cut the diorite margin of the batholith.

Skarn has formed dominantly in the Upper Triassic Lewes River Group which consists of both clastic and carbonate rocks. The clastic rocks are largely arkose and graywacke (70% plagioclase, 15% augite, 10% oxides, and minor quartz; Grabher, 1974), which in hand specimen have a salt and pepper texture very similar to the diorite. Carbonate rocks include limestone, carbonaceous limestone, dolomitic limestone, and dolostone (based upon staining tests reported in Grabher, 1974). Detailed descriptions and chemical compositions of the sedimentary units are given in Grabher (1974) and Morrison (1981). The dominant skarn protoliths (as deduced from the skarn mineralogy) for each of the deposits studied are listed in Table 2.

SKARN MINERALOGY

The skarn mineralogy of the Whitehorse skarns is fairly typical of the copper skarns summarized by Einaudi et al. (1981), Einaudi (1982), and Einaudi and Burt (1982). As noted by Morrison (1981), the silicate mineralogy of individual skarn deposits in the Whitehorse Copper Belt is largely a function of the skarn protolith.

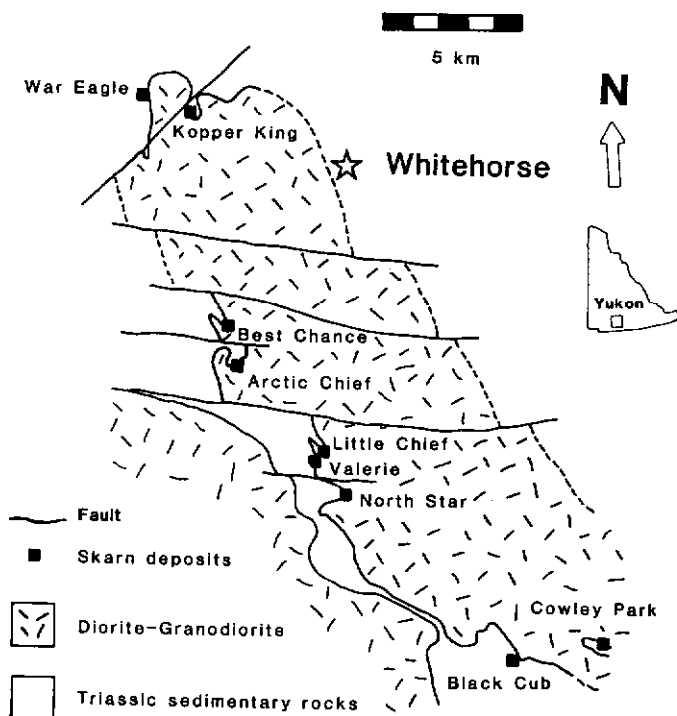


Figure 1. Simplified regional geology map of Whitehorse Copper Belt showing principle skarn deposits (after Tenney, 1981).

Skarns with a limestone protolith (e.g. Best Chance, Cowley Park, and Kopper King, Table 2) contain abundant garnet, pyroxene, and wollastonite with variable actinolite, epidote, and chlorite. Skarns with a more dolomitic protolith (e.g. Arctic Chief and Little Chief, Table 2) contain abundant magnesian minerals such as diopside, olivine, phlogopite, and serpentine.

Pyroxene, the most abundant calc-silicate mineral in the Whitehorse Copper Belt, occurs in skarn formed from both dolomitic and non-dolomitic carbonate rocks and from siltstone. Pyroxene formed from a dolomitic protolith is very magnesium-rich, (usually pure diopside, Table 3) and ranges from fine-grained hornfels to coarse-grained (up to 2 cm) euhedral crystals. Pyroxene formed from limestone is more iron-rich (up to 37 mole % hedenbergite, Table 3) and typically is coarse-grained. Skarn formed in siltstone has more aluminous pyroxene than skarn formed in carbonate rock. All the pyroxenes analyzed in this study fall within the field defined by typical copper skarn pyroxenes (Fig. 2).

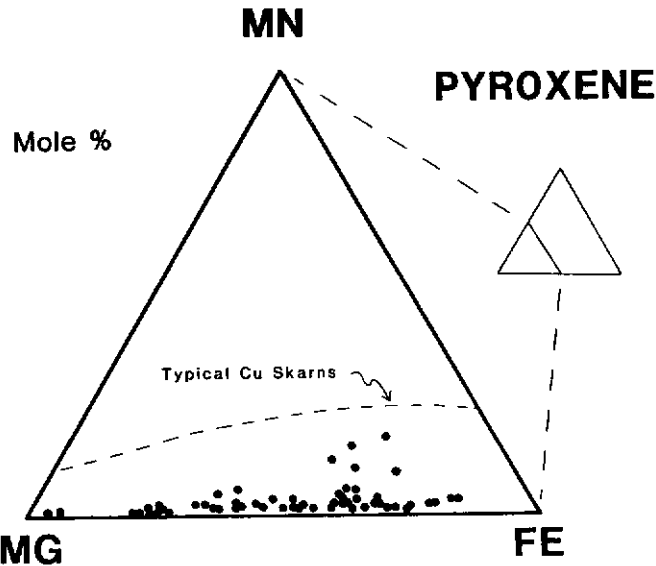


Figure 2. Triangular plot of pyroxene electron microprobe compositions.

Garnet also occurs in both calcic and magnesian skarn, but is far more abundant in the former. In skarn formed from limestone, garnet is typically yellowish-tan to dark brown in hand specimen, whereas in skarn formed from dolostone, garnet is reddish brown. In both types of skarn, garnet varies from fine-grained hornfels to large (up to 4 cm) euhedral crystals, although garnet in calcic skarn tends to be coarser-grained. All the garnets analyzed in this study are andraditic (Table 4) and fall well within the field of typical copper skarn garnets (Fig. 3).

Olivine only occurs in skarn formed from dolostone. It is typically a distinctive yellow-green colour and ranges from massive skarn to isolated 0.1 to 1 cm euhedral crystals in dolostone. Most olivine is magnesium-rich (nearly pure forsterite, e.g. AC-53-1496, Table 5) and has altered to hydrous magnesium-silicate minerals such as brucite, phlogopite, serpentine, and/or talc. Although most serpentine in the Whitehorse skarns is an alteration product of olivine, some serpentine (with magnetite) occurs as veins and patches directly replacing dolostone. Massive magnetite and phlogopite may also directly replace dolostone, although Grabher (1974) describes local olivine pseudomorphs within the massive magnetite.

In contrast to olivine, the minerals idocrase and wollastonite apparently occur only in skarn formed from a non-dolomitic protolith. In most cases, the occurrence of olivine, idocrase, or wollastonite along with the colour and composition of garnet and pyroxene can be used to identify the nature of the carbonate protolith. This relationship can be useful where poor exposures (or closed mines!) prevent detailed stratigraphic investigations.

All other minerals in the Whitehorse skarns are interpreted to have replaced, at least in part, previously formed silicate minerals. In some cases, these minerals have compositions similar to the replaced mineral(s), and thus can be used to help decipher the original stratigraphy. Additionally, relative to the prograde

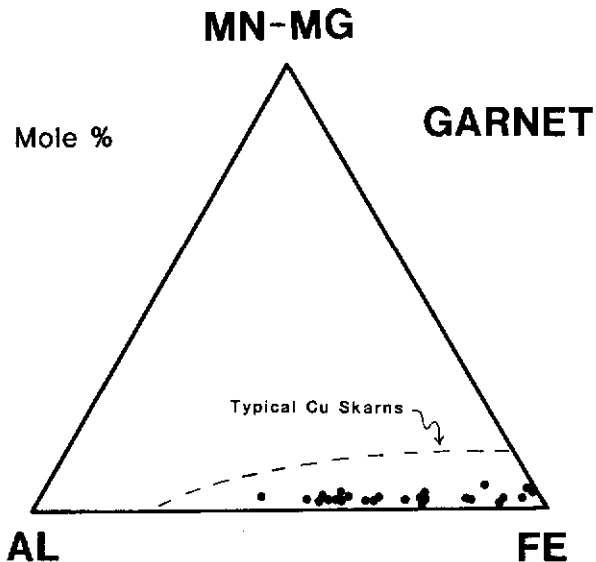


Figure 3. Triangular plot of garnet electron microprobe compositions.

minerals, some of the later minerals are stable under lower temperature or more hydrous conditions and thus can be considered to result from retrograde alteration.

Amphibole is the main alteration product of pyroxene and also occurs with massive sulphide replacement (mainly chalcopyrite and pyrite) of skarn (Fig. 4a). Most of the amphibole is actinolitic (Table 6), but locally (in more aluminous rocks?) hornblende is abundant. Amphibole in the Whitehorse skarns falls within the typical field of copper skarn amphiboles (Fig. 5). Other minerals associated with amphibole alteration of pyroxene include chlorite (Table 7), muscovite, apatite, and locally serpentine. Where amphibole has replaced garnet-pyroxene skarn, kspar (Table 5) is locally present in the alteration assemblage.

Epidote (Table 8) is the main alteration product of garnet and typically is intergrown with amphibole and chlorite where the replaced skarn contained both garnet and pyroxene. Epidote is commonly associated with the introduction of sulphides (especially bornite-chalcocite, Fig. 4b). The systematic association of epidote with bornite-chalcocite and amphibole with chalcopyrite may reflect the more oxidized environment of the former and a more reduced environment for the latter. A similar oxidation control on sulphide mineralogy was proposed by Morrison (1981).

Several unusual minerals occur in minor to trace amounts in the Whitehorse skarn deposits. Valleriite ($\text{Cu}_{1.20}\text{Fe}_{0.80}\text{S}_{2.00} \cdot 1.67(\text{Mg}_{0.73}\text{Al}_{0.06}\text{Fe}_{0.21})(\text{OH})_2$), Petruck et al., 1971; Harada et al., 1973) is a rare micaceous mineral with alternating sheets of Cu-Fe-S and brucite which occurs in magnesium-rich rocks. In the Whitehorse skarns, valleriite occurs in magnetite and sulphide-rich skarn replacing dolomite. Locally, valleriite is coarse-grained and constitutes 20-30% of the rock. Associated with the valleriite in some occurrences is a zinc-bearing spinel similar to gahnite. Other minor minerals described by Grabher (1974) and Morrison (1981) but not observed in the present study include: scapolite, digenite, djurleite, tennantite-tetrahedrite, carrollite ($\text{Cu}_2\text{Co}_3\text{S}_4$), wittichenite ($\text{Cu}_3\text{Bi}_2\text{S}_3$), tellurobismuthite (Bi_2Te_3), and stutzite (Ag_5Te_3).

DISTRIBUTION OF PRECIOUS METALS IN WHITEHORSE SKARNs

To assess the distribution of precious metals in the Whitehorse skarns, 144 spot samples were collected from diamond drill core, sawn in half with a diamond saw, and cleaned vigorously with soapy water and a nylon brush. One half of each sample was assayed for Cu, Ag, and Au, (Table 9) while the other half was saved for petrographic examination. The assayed samples typically were about 50 grams in size and were chosen to illustrate specific rock, skarn mineralogy, mineralization, and alteration types; they should not be construed as bulk samples indicative of average deposit grades. All samples were analyzed by fire assay and atomic absorption methods by Bondar-Clegg & Company Ltd. (Vancouver

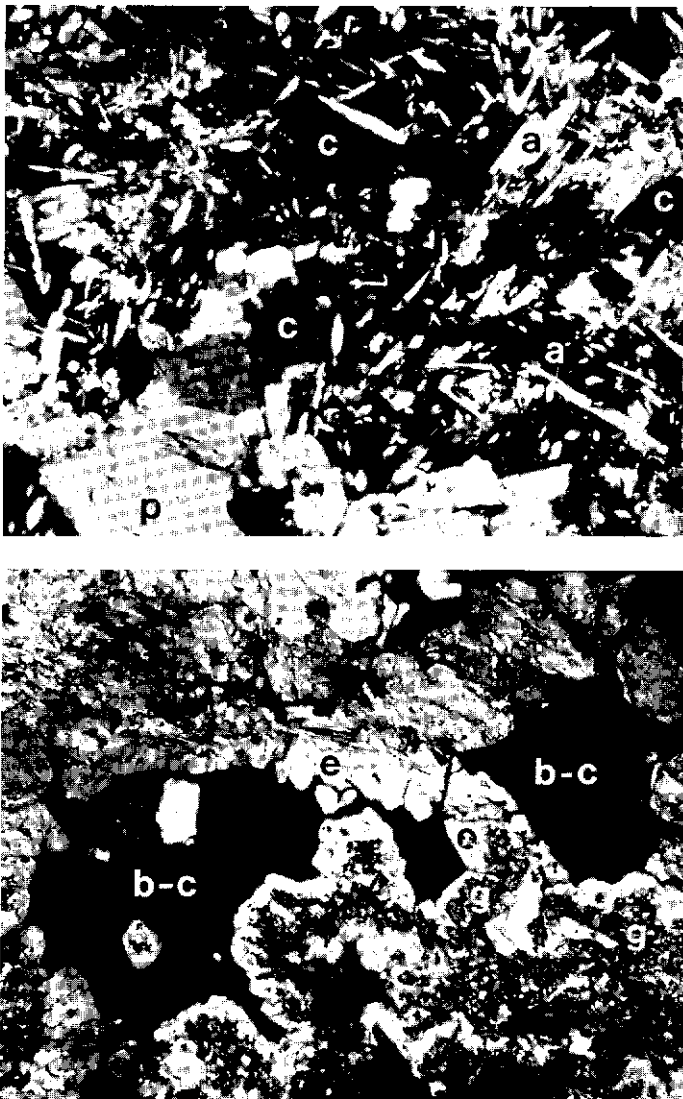


Figure 4. Photomicrographs of associated retrograde alteration of sulphide mineralization: a) actinolite-chalcopyrite replacement of pyroxene, Sample AC-53-352 b) epidote-chalcocite, replacement of garnet, Sample AC-51-269. a = actinolite, b-c = bornite-chalcocite, cp = chalcopyrite, e = epidote, g = garnet, p = pyroxene.

office). Minimum detection limits were: Cu = 1 ppm, Ag = 50 ppb, and Au = 1 ppb. Additionally, 23 ore grade samples were assayed for platinum and palladium to check the reported occurrence of these elements by Kindle (1964); all Pt assays were less than or equal to 50 ppb and all Pd were less than or equal to 70 ppb.

When all 144 samples are plotted as a group (Fig. 6 a-c), there is a moderate correlation between Cu and Au, a moderately strong correlation between Cu and Ag, and a strong correlation between Ag and Au. Similar correlations were noted by Tenney (1981) for composite drill core samples from the Little Chief Mine. The plot of Cu versus Au (Fig. 6a) shows significant scatter, but several generalizations can be made: 1) all samples with high gold contain significant copper (e.g. all samples with more than 1 ppm Au contain more than 5,000 ppm Cu), 2) samples with high copper do not necessarily contain significant gold (e.g. samples with greater than or equal to 5000 ppm Cu range from 1 to 80,000 ppb Au). These generalizations suggest that gold is only deposited in a restricted zone or time of copper mineralization and that gold does not occur in solid solution or as systematic inclusions within copper sulphide minerals. In contrast, the stronger correlation of Cu and Ag values (Fig. 6b), suggests that silver may occur in solid solution or as mineral intergrowths with copper sulphide minerals and that silver is probably deposited throughout the period of copper mineralization. The plot of Ag versus Au (Fig. 6c) further disting-

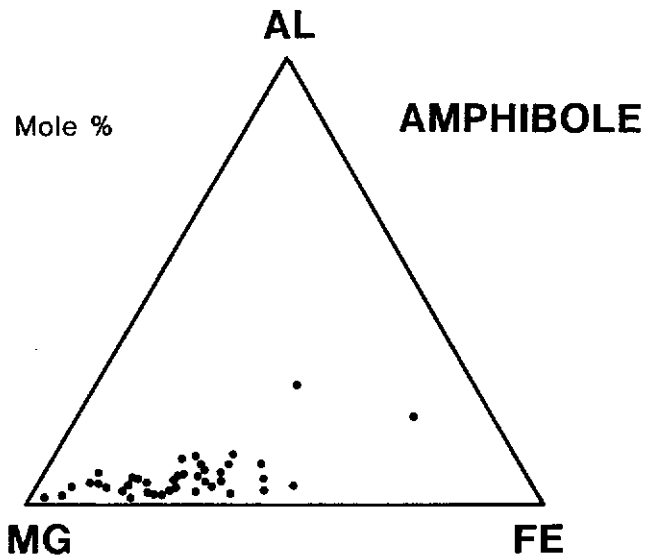


Figure 5. Triangular plot of amphibole electron microprobe compositions.

ishes the occurrence of gold and silver. All of the analyses in Figure 6c are more silver-rich than the average fineness (890, Table 10) of electrum which occurs in Whitehorse skarns and the trend of these analyses is subparallel to the average electrum fineness. Thus, silver must occur in other mineral phases in addition to electrum, whereas electrum could be the only gold mineral present in the Whitehorse skarns.

Individual mineral phases were analysed for the presence of gold, silver, and tellurium (Table 10). Pyrite and all the silicate minerals tested (garnet, pyroxene, olivine, amphibole, phlogopite, epidote, chlorite, and serpentine) were at or below the limit of detection (about 100 ppm) for all three elements on the electron microprobe. Additionally, there does not appear to be any correlation between major element composition of these minerals and the precious metal assays of the enclosing rock (Tables 3-8).

Silver was detectable in chalcocite, bornite and vallerite and was highest (2.44 wt. %) in chalcocite surrounded by electrum. It is not known whether this silver is present in solid solution or as a separate mineral phase smaller than the 1 μm microprobe beam diameter. Chalcocite and bornite commonly contain significant silver (Elsing, 1930) and they are probably the main silver hosts in the Whitehorse skarn deposits. Gold was detected in some chalcopyrite, bornite, and vallerite, although many samples of each contained no detectable gold. The highest gold values occur in chalcopyrite (up to 0.20 wt. %). Significant tellurium was only detected in one sulphide sample (AC-51-269, chalcocite, this sample also contained electrum). In general, the amount of tellurium does not correlate with the amount of gold or silver in a given mineral, suggesting that the gold and silver are probably not present as telluride minerals.

In summary, gold in the Whitehorse skarns occurs mainly as electrum, but the minor and erratic occurrence of gold in chalcopyrite and vallerite may have been an important contribution to the historic district gold production. In contrast, although silver also occurs in electrum, the bulk of silver was probably recovered from chalcocite and to a lesser extent, bornite.

The distribution of copper, gold, and silver among the various Whitehorse skarn deposits is difficult to assess without bulk assay or production data. The samples assayed for the present study represent a variety of rock and alteration types, so direct correlation of metal grades by deposit is not appropriate. However, a limited comparison can be made based upon metal ratios of Cu, Ag, and Au (Fig. 7). This is supported by the fact that the production average for the entire Whitehorse district plots close to the spot assay average for the Little Chief and War Eagle deposits, which together constitute more than 90% of district production. Three deposits (Cowley Park, Best Chance, and Kopper King) have low precious metal ratios. These deposits occur mainly in limestone protoliths (Table 2). Two deposits (Arctic Chief and North Star) have relatively copper-poor, silver-rich ratios and were formed largely from dolostone. The remaining four deposits (Little Chief,

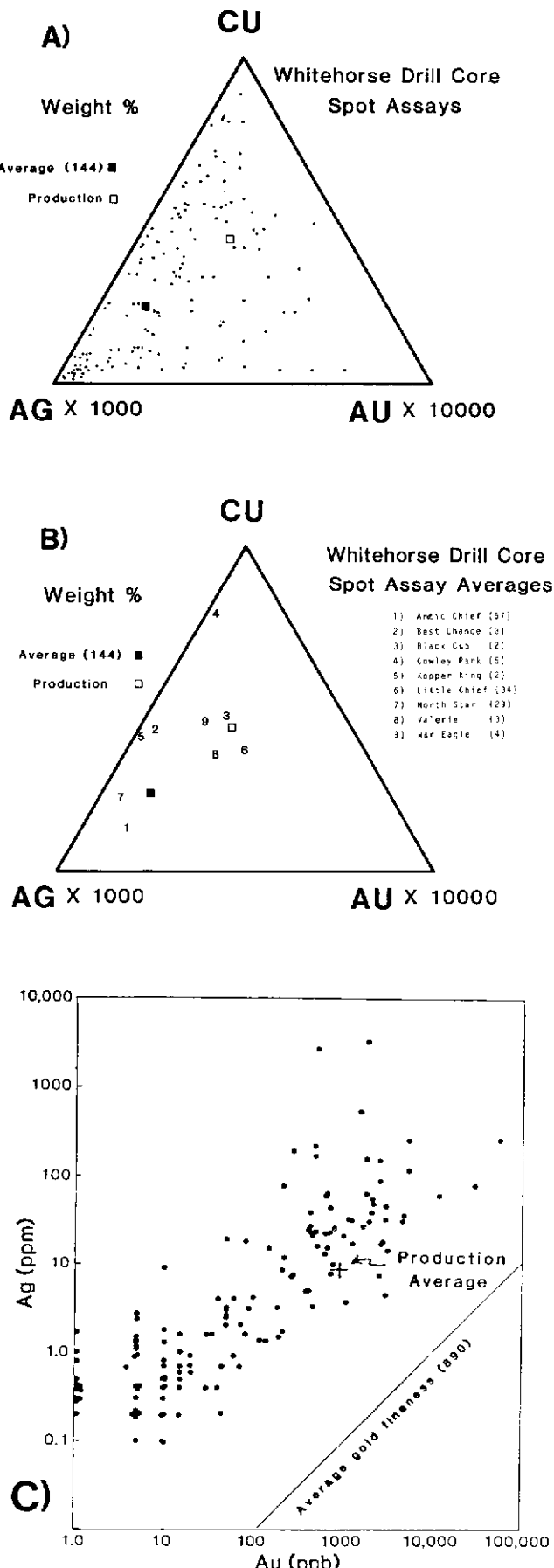


Figure 6. Spot drill core assays of samples from Whitehorse Copper Belt.

Valerie, Black Cub, and War Eagle) have relatively high gold ratios and formed from mixed limestone-dolostone protoliths.

To assess the distribution of Cu, Ag, and Au in various protoliths and alteration types, the spot samples were subdivided into six groups: 1) relatively unaltered diorite, 2) relatively unaltered limestone and dolostone, 3) skarn with little retrograde alteration or sulphide mineralization, 4) skarn with abundant retrograde alteration, 5) skarn with abundant sulphide mineralization, and 6) skarn with both abundant retrograde alteration and sulphide mineralization. The unaltered carbonate protolith is very low in Cu, Ag, and Au and would not be a good source rock for any of these elements (Fig. 8). Other sedimentary rocks in the local stratigraphic section do not contain significantly more of these elements, although Morrison (1981) concluded that the pyritic siltstone unit might be an important source for copper.

The Cu, Ag, and Au in the diorite (Fig. 8) are about average for typical mafic igneous rocks (Krauskopf, 1967) and are slightly higher than the values reported by Morrison (1981). If the Whitehorse pluton (approximately 500 km³) was the source of the ore elements in skarn the total production from the Whitehorse district would require an average depletion in the pluton of about 100 ppb Cu, 0.1 ppb Ag, and 0.01 ppb Au. This level of depletion would be undetectable in the present study. However, it is unknown how much, if any, of the Whitehorse pluton generated or interacted with the skarn-forming liquids.

Relative to the diorite pluton and carbonate protolith, skarn that has not been affected by significant retrograde alteration or sulphide mineralization is slightly enriched in Cu and Au, but not Ag (Fig. 8). This type of skarn is not ore grade and, importantly, is distinguishable in thin section and hand specimen from higher grade skarn material. As would be expected, sulphide-rich skarn has high average Cu, Ag, and Au grades (Fig. 8). Skarn that has strong retrograde alteration also is typically ore grade (Fig. 8). Some of the skarn samples with strong retrograde alteration have high Au-Ag assays even though sulphides are minor or not visible in hand specimen. The highest average Ag and Au grades occur in skarn that is both sulphide-rich and has abundant retrograde alteration.

SUMMARY AND CONCLUSIONS

Skarns in the Whitehorse Copper Belt occur in both dolomitic and calcareous carbonate rocks near contacts with the diorite contact phase of the Whitehorse Batholith. The skarns are mineralogically and compositionally similar to typical copper skarns (Einaudi et al., 1981). The main prograde skarn minerals are andraditic garnet and diopsidic pyroxene, with significant forsteritic olivine in dolomitic host rocks. Locally, intense retrograde alteration has converted garnet to epidote ± chlorite ± hematite, pyroxene to actinolite ± chlorite, and olivine to serpentine ± chlorite ± magnetite. The colour, composition, and mineralogy of prograde and retrograde skarn minerals reflect the protolith composition.

The bulk of sulphide mineralization is associated with retrograde alteration. Chalcocite and pyrite are preferentially associated with actinolite and chlorite, whereas bornite and chalcocite are preferentially associated with epidote and locally serpentine. The other important copper mineral, vallerite, is restricted to magnesian rocks and is commonly associated with phlogopite, serpentine, and chlorite. Overall, the Whitehorse system is copper-rich and sulphur-poor; iron sulphide minerals are not abundant.

Significant amounts of gold and silver have been recovered from the Whitehorse skarns. Gold occurs as electrum with an average fineness of 890. Coarse-grained visible gold was observed in drill core in the present study but is not common. Gold also occurs in minor, but economically important, amounts in some chalcopyrite and vallerite. The association of chalcopyrite with actinolitic retrograde alteration of pyroxene may be a useful guide to this latter occurrence of gold. Silver also occurs in electrum, but probably is more abundant as a minor constituent of chalcocite and bornite. The association of chalcocite and bornite with epidote after garnet and serpentine after olivine and diopside, may be a useful guide to this occurrence of silver. It may be possible to locate zones with significant precious metals by mapping prograde and retrograde skarn mineralogy.

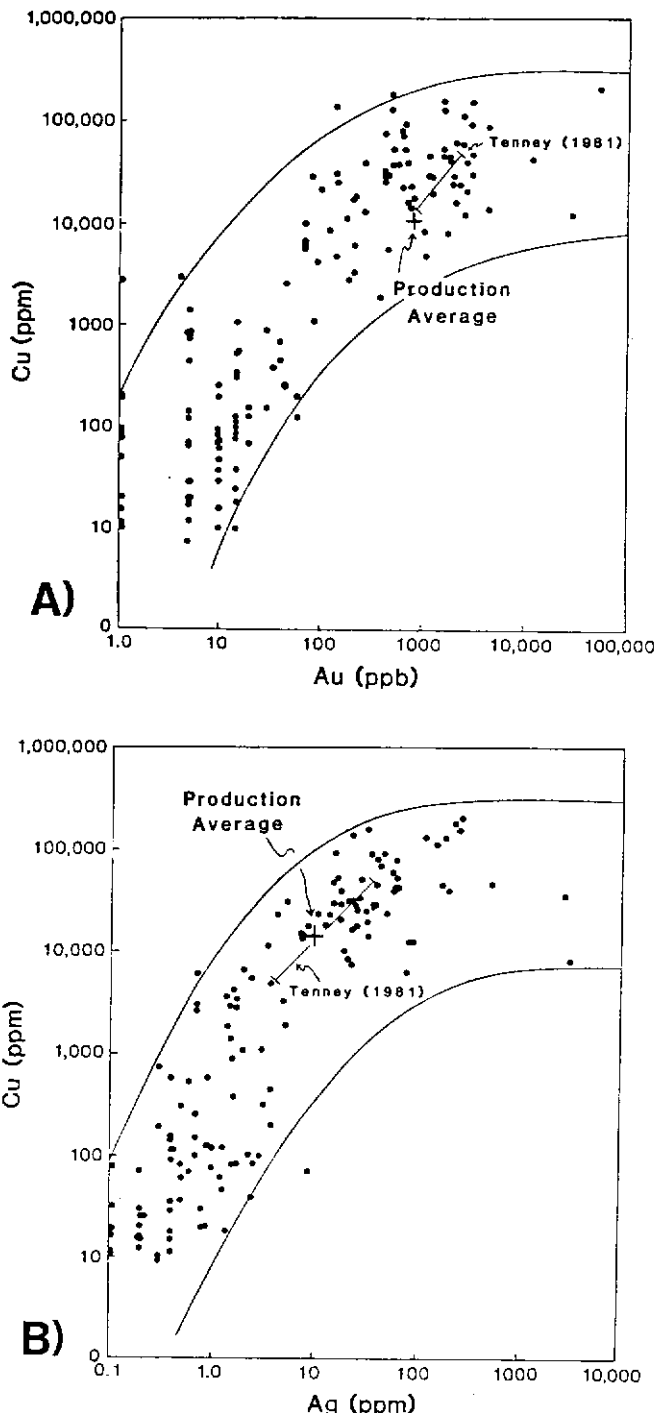


Figure 7. Cu, Ag, and Au metal ratios for spot samples from Whitehorse Copper Belt.

Cu, Ag, and Au metal ratios of spot sample assays can be used to discriminate among the different Whitehorse skarns. Deposits formed from relatively pure limestone appear to have low precious metal ratios. Deposits formed from more magnesian protoliths appear to be silver-rich. Deposits with the highest gold ratios appear to have formed from mixed limestone-dolostone lithology. The metal ratio for total district production is similar to the average for the Little Chief and War Eagle deposits, the two largest producers in the district. Furthermore, the Little Chief deposit has the highest average gold metal ratio of the deposits studied.

The general correlation between copper and precious metal grades suggests that past exploration programs probably located the skarn deposits in the district with the most potential for precious metal production. The correlations between precious metal content and skarn mineralogy outlined in the present study can be used to guide exploration for new deposits and reevaluation of known deposits. The fact that the Little Chief skarn, the largest deposit with the highest gold metal ratio in the Whitehorse Copper Belt, has been extensively mined, suggests that future exploration should focus on similar skarns in peripheral districts such as Jackson Lake. Particular attention should be paid to skarn mineralogy and protolith composition.

ACKNOWLEDGEMENTS

This project was partly funded by Program I, Mineral Resources Sub-agreement of the Canada-Yukon Economic Development Agreement. Co-operation and assistance of Hudson Bay Exploration and Development Company Ltd. with access to information and funding of the geochemical analyses is appreciated. Competent field assistance of M. Cosec is also acknowledged.

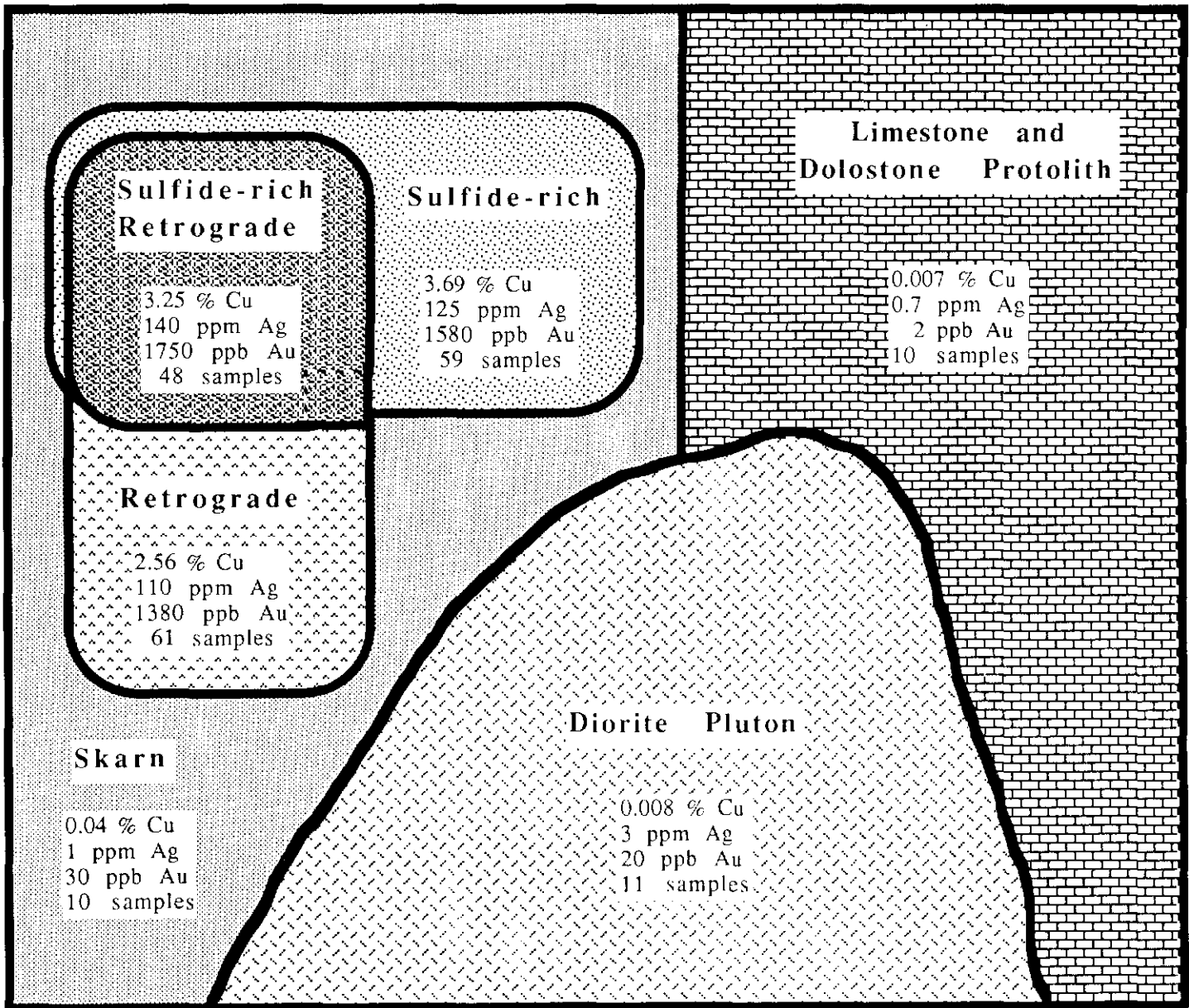


Figure 8. Cartoon illustrating distribution of Cu, Ag, and Au in rock and alteration types in the Whitehorse Copper Belt.

REFERENCES

- CAMERON, D.E., and GARMOE, W.J., 1983. Distribution of gold in skarn ores in the Carr Fork Mine, Toole, Utah: Geol. Soc. America, Abstr. w. Programs, Vol. 15, p. 299.
- EINAUDI, M.T., MEINERT, L.D., and NEWBERRY, R.J., 1981. Skarn deposits: Econ. Geol. 75th ANNIV. VOL., p. 317-391.
- EINAUDI, M.T., 1982. Descriptions of skarns associated with porphyry copper plutons, southwestern North America, in Titley, S.R. (ed.), Advances in geology of the porphyry copper deposits, southwestern North America: Univ. Arizona Press, p. 139-184.
- EINAUDI, M.T., and BURT, D.M., 1982. Introduction — Terminology, classification, and composition of skarn deposits: Econ. Geol., Vol. 77, p. 745-754.
- ELSING, M.J., Secondary enrichment at Cananea: Engr. and Mining Journal, Vol. 130, p. 285-288.
- GRABHER, D.E., 1974. Skarn ore relationships in a contact metasomatic Cu-Fe deposit Little Chief Mine, Whitehorse, Yukon Territory: unpub. MSc thesis, Univ. Wisconsin, Madison, 103 p.
- HARADA, K., NAKAO, K., and NACASHIMA, K., 1973. Valleriite from Little Chief Mine, Whitehorse Copper Belt, Yukon, Canada: Mineralogical Journal, Vol. 7, p. 221-227.
- HURREAU, A., 1985. Potential for gold exploration, Whitehorse Copper Belt, Yukon: unpublished report, Hudson Bay Exploration and Development Co. Ltd., Whitehorse, Yukon, 12 p.

- KINDLE, K.B., 1979. *Introduction to Geochemistry*: McGraw-Hill, New York, 721 p.
- KRAUSKOPF, K.B., 1979. *Introduction to Geochemistry*: McGraw-Hill, New York, 721 p.
- MEINERT, L.D., 1986. *Precious metals in skarn deposits*: Geol. Soc. America, Abstr. w. Programs, Vol. 19.
- MORRISON, G.W., 1981. *Setting and origin of skarn deposits in the Whitehorse Copper Belt, Yukon*: unpub. PhD thesis, Univ. Western Ontario, London, 306 p.
- PETRUK, W., HARRIS, D.C., and MURRAY, E.J., 1970. An occurrence of valleriite from New Imperial Mine, Yukon: Canada Dept. Energy Mines Resources — Mines Branch, Division Report MS PP 70-1, 6 p.
- TENNEY, D., 1981. *The Whitehorse Copper Belt: Mining, exploration, and geology (1967-1980)*: Dept. Indian and Northern Affairs, Geology Section, Yukon, Bulletin 1, 29 p.
- WATSON, P.H., 1984. *The Whitehorse Copper Belt — A compilation; Exploration and Geological Services Division — Yukon, Indian and Northern Affairs, Canada, Open File, 1:25,000 scale map with marginal notes*.

Table 1 Average* igneous whole rock composition

SiO ₂	58.27
TiO ₂	0.62
Al ₂ O ₃	15.65
Fe ₂ O ₃ (T)	5.39
MnO	0.08
MgO	3.43
CaO	6.97
Na ₂ O	4.12
K ₂ O	1.54
P ₂ O ₅	0.23
LOI	1.54
 Cu (ppm)	61
Ag (ppm)	0.7
Au (ppb)	6
 Norms	
Q	9.77
Or	9.3
Ab	37.79
An	39.27

* Average of specimens (G25H, Pb1, Pb11, 75-50, Pb13A, Pb13B, ACNOR1, G26, GR21, Pb4) from near skarn in the Whitehorse mining district (Morrison, 1981, Appendix 2)

Table 2 Skarn Protoliths

Deposit	Abv.	Protolith	Main Silicate Skarn Minerals
Arctic Chief	AC	dolostone >> limestone	pyx>sp>act=gar=phl>ep>ol
Best Chance	BC	limestone > dolostone	gar>pyx>wo
Black Cub	BLC	limestone > dolostone	gar=pyx=act=ep
Cowley Park	CP	limestone >> dolostone	gar=pyx>wo
Kopper King	KK	limestone	gar>act=pyx
Little Chief	LC	dolostone > limestone > siltstone	pyx>gar=phl=sp=ol>act
North Star	NS	dolostone = limestone	gar=pyx>ep
Valerie	V	limestone = dolostone	pyx=gar
War Eagle	WE	limestone > dolostone	gar>pyx>wo

TABLE 3 ELECTRON MICROPROBE ANALYSES OF PYROXENE

Sample #	AC-21-153	AC-21-180	AC-21-180	AC-21-185	AC-21-215	AC-21-215	AC-51-268	AC-51-268	AC-51-269	AC-51-290	AC-51-290	AC-51-320
SiO ₂	53.63	53.98	53.52	54.50	54.66	53.48	53.59	52.91	53.98	52.82	54.32	52.51
TiO ₂	0.11	0.11	0.02	0.01	0.02	0.05	0.05	0.16	0.06	0.07	0.06	0.09
Al ₂ O ₃	1.82	0.40	0.73	0.36	0.34	0.81	0.51	0.70	0.79	1.51	0.42	1.49
FeO	1.73	2.52	1.85	2.09	1.63	2.37	4.47	4.61	4.53	6.38	1.52	4.84
MgO	16.90	16.75	17.45	17.15	17.58	16.75	15.20	15.01	15.24	14.56	17.69	15.25
MnO	0.19	0.09	0.06	0.28	0.13	0.12	0.29	0.40	0.26	0.11	0.12	0.08
CaO	25.76	25.97	26.04	26.09	26.33	25.69	25.13	25.57	25.15	24.75	25.60	25.22
Na ₂ O	0.00	0.04	0.11	0.05	0.03	0.05	0.23	0.22	0.28	0.25	0.06	0.20
K ₂ O	0.00	0.01	0.00	0.00	0.01	0.00	0.00	0.00	0.00	0.00	0.01	0.00
Total	100.14	99.87	99.78	100.53	100.73	99.32	99.47	99.58	100.29	100.45	99.80	99.68
Cations Based on 6 Oxygens												
Si	1.949	1.976	1.958	1.979	1.977	1.968	1.985	1.966	1.982	1.953	1.979	1.947
Ti	0.003	0.003	0.001	0.000	0.000	0.001	0.001	0.005	0.002	0.002	0.002	0.003
Al	0.078	0.017	0.032	0.016	0.015	0.035	0.022	0.031	0.034	0.066	0.018	0.065
Fe	0.053	0.077	0.057	0.063	0.049	0.073	0.138	0.143	0.139	0.197	0.046	0.150
Mg	0.916	0.914	0.952	0.928	0.948	0.919	0.839	0.831	0.834	0.802	0.961	0.843
Mn	0.006	0.003	0.002	0.009	0.004	0.004	0.009	0.013	0.008	0.003	0.004	0.002
Ca	1.003	1.019	1.021	1.015	1.021	1.013	0.997	1.018	0.990	0.980	0.999	1.002
Na	0.000	0.003	0.008	0.004	0.002	0.004	0.017	0.016	0.020	0.018	0.004	0.014
K	0.000	0.001	0.000	0.000	0.001	0.000	0.000	0.000	0.000	0.000	0.000	0.000
Sum	4.008	4.014	4.029	4.014	4.016	4.015	4.010	4.022	4.009	4.021	4.013	4.025
Mole %												
Di	94.0	91.9	94.2	92.8	94.7	92.3	85.0	84.2	85.0	80.0	95.0	84.7
Hd	5.4	7.8	5.6	6.3	4.9	7.3	14.0	14.5	14.2	19.7	4.6	15.1
Jo	0.6	0.3	0.2	0.9	0.4	0.4	0.9	1.3	0.8	0.3	0.4	0.2
Assay												
Cu (ppm)	200	72	72	18	70	70	10000	10000	12400	15	15	11
Ag (ppm)	3.9	9.0	9.0	0.4	0.6	0.6	18.8	18.8	80.2	0.2	0.2	0.4
Au (ppb)	60	10	10	15	20	20	70	70	28490	1	1	1

TABLE 3 ELECTRON MICROPROBE ANALYSES OF PYROXENE

Sample #	AC-51-320	AC-51-339	AC-51-339	AC-51-351	AC-51-490	AC-51-490	AC-51-498	AC-51-498	AC-51-498	AC-51-503	AC-51-503	AC-53-349
SiO ₂	52.80	50.46	53.41	52.58	54.62	55.13	53.94	53.37	55.34	54.16	53.87	55.28
TiO ₂	0.06	0.36	0.07	0.00	0.15	0.05	0.00	0.00	0.07	0.00	0.04	0.01
Al ₂ O ₃	1.36	3.65	1.15	1.49	1.10	0.24	0.73	0.43	0.12	0.48	0.91	0.00
FeO	4.63	6.65	4.39	4.73	1.19	0.97	6.01	9.47	1.11	2.08	2.08	0.90
MgO	15.16	13.95	15.64	15.58	17.95	17.84	15.19	13.06	17.93	17.04	17.12	18.06
MnO	0.20	0.18	0.15	0.17	0.01	0.00	0.25	0.29	0.00	0.07	0.14	0.02
CaO	25.05	25.06	25.23	25.40	25.88	26.04	25.12	23.56	25.57	25.89	25.95	26.22
Na ₂ O	0.18	0.28	0.14	0.14	0.09	0.06	0.21	0.35	0.04	0.03	0.07	0.01
K ₂ O	0.00	0.02	0.00	0.01	0.00	0.00	0.00	0.00	0.00	0.01	0.00	0.01
Total	99.44	100.61	100.18	100.10	100.99	100.33	101.45	100.53	100.18	99.76	100.18	100.51
Cations Based on 6 Oxygens												
Si	1.959	1.874	1.963	1.942	1.962	1.991	1.971	1.992	1.999	1.980	1.963	1.994
Ti	0.002	0.010	0.002	0.000	0.004	0.001	0.000	0.000	0.002	0.000	0.001	0.000
Al	0.060	0.160	0.050	0.065	0.047	0.010	0.032	0.019	0.005	0.021	0.039	0.000
Fe	0.144	0.207	0.135	0.146	0.036	0.029	0.184	0.296	0.033	0.064	0.064	0.027
Mg	0.838	0.772	0.857	0.857	0.961	0.960	0.827	0.727	0.966	0.928	0.930	0.971
Mn	0.006	0.006	0.005	0.005	0.000	0.000	0.008	0.009	0.000	0.002	0.004	0.001
Ca	0.995	0.997	0.994	1.005	0.996	1.008	0.984	0.942	0.990	1.014	1.013	1.013
Na	0.013	0.020	0.010	0.010	0.007	0.004	0.015	0.026	0.003	0.002	0.005	0.001
K	0.000	0.001	0.000	0.000	0.000	0.000	0.000	0.000	0.000	0.000	0.000	0.000
Sum	4.016	4.046	4.015	4.031	4.013	4.004	4.020	4.011	3.998	4.011	4.019	4.006
Mole %												
Di	84.8	78.4	86.0	85.0	96.4	97.0	81.2	70.4	96.7	93.4	93.2	97.2
Hd	14.5	21.0	13.5	14.5	3.6	3.0	18.0	28.7	3.3	6.4	6.4	2.7
Jo	0.6	0.6	0.5	0.5	0.0	0.0	0.7	0.9	0.0	0.2	0.4	0.1
Assay												
Cu (ppm)	11	29	29	20	14200	14200	29000	29000	29000	101	101	18000
Ag (ppm)	0.4	0.1	0.1	0.2	33.2	33.2	17.5	17.5	17.5	3.0	3.0	25.0
Au (ppb)	1	10	10	5	4380	4380	1230	1230	1230	15	15	800

TABLE 3 ELECTRON MICROPROBE ANALYSES OF PYROXENE

Sample #	AC-53-349	AC-53-420	AC-53-420	LC-111-847	LC-111-847	NS-15-1378	NS-15-1393	NS-15-1393	NS-15-1404	NS-15-1404	NS-15-1404	NS-15-1407
SiO ₂	53.54	52.31	52.69	54.87	54.69	54.80	54.62	53.08	54.28	54.66	54.33	53.97
TiO ₂	0.00	0.00	0.03	0.00	0.07	0.03	0.00	0.04	0.05	0.03	0.02	0.00
Al ₂ O ₃	1.06	0.35	0.24	0.10	0.40	0.26	0.14	0.90	0.20	0.21	0.30	0.60
FeO	2.47	11.64	11.10	2.20	1.06	1.32	2.76	4.15	2.95	0.98	4.99	3.29
MgO	16.62	10.57	11.11	17.70	17.98	17.86	16.76	15.68	16.47	18.21	14.43	16.27
MnO	0.06	0.47	0.50	0.10	0.09	0.00	0.22	0.13	0.08	0.07	0.85	0.10
CaO	25.79	24.51	24.40	25.52	25.95	26.35	26.02	25.71	25.66	26.29	25.57	25.55
Na ₂ O	0.06	0.20	0.12	0.06	0.02	0.06	0.02	0.19	0.18	0.02	0.22	0.13
K ₂ O	0.00	0.00	0.00	0.02	0.00	0.03	0.02	0.00	0.02	0.01	0.03	0.00
Total	99.60	100.05	100.19	100.57	100.26	100.71	100.56	99.88	99.89	100.48	100.74	99.91
Cations Based on 6 Oxygens												
Si	1.964	1.992	1.996	1.987	1.979	1.979	1.988	1.960	1.989	1.976	1.997	1.979
Ti	0.000	0.000	0.001	0.000	0.002	0.001	0.000	0.001	0.001	0.001	0.001	0.000
Al	0.046	0.016	0.011	0.004	0.017	0.011	0.006	0.039	0.008	0.009	0.013	0.026
Fe	0.076	0.371	0.352	0.067	0.032	0.040	0.084	0.128	0.090	0.030	0.154	0.101
Mg	0.909	0.600	0.628	0.956	0.970	0.962	0.909	0.863	0.899	0.981	0.790	0.890
Mn	0.002	0.015	0.016	0.003	0.003	0.000	0.007	0.004	0.003	0.002	0.026	0.003
Ca	1.014	1.000	0.990	0.991	1.006	1.020	1.015	1.017	1.007	1.018	1.007	1.004
Na	0.004	0.015	0.009	0.004	0.002	0.004	0.002	0.014	0.013	0.001	0.016	0.010
K	0.000	0.000	0.000	0.001	0.000	0.002	0.001	0.000	0.001	0.000	0.001	0.000
Sum	4.014	4.008	4.002	4.013	4.011	4.017	4.010	4.026	4.012	4.019	4.004	4.012
Mole %												
Di	92.1	60.9	63.1	93.2	96.5	96.0	90.9	86.7	90.6	96.9	81.5	89.5
Hd	7.7	37.6	35.3	6.5	3.2	4.0	8.4	12.9	9.1	2.9	15.8	10.1
Jo	0.2	1.6	1.6	0.3	0.3	0.0	0.7	0.4	0.3	0.2	2.7	0.3
Assay												
Cu (ppm)	18000	195	195	40000	40000	156000	184000	184000	29500	29500	29500	18700
Ag (ppm)	25.0	0.3	0.3	56.5	56.5	249.7	219.2	219.2	24.0	24.0	24.0	12.7
Au (ppb)	800	10	10	680	680	1510	480	480	410	410	410	210

TABLE 3 ELECTRON MICROPROBE ANALYSES OF PYROXENE

Sample #	NS-15-1407	NS-15-1415	NS-15-1415	NS-15-1415	NS-15-1422
SiO ₂	54.25	54.46	54.04	53.75	53.04
TiO ₂	0.05	0.21	0.00	0.02	0.03
Al ₂ O ₃	0.21	1.04	0.15	0.16	0.68
FeO	1.79	0.13	7.12	5.12	6.05
MgO	17.68	18.78	13.23	14.49	14.58
MnO	0.09	0.00	1.02	1.43	0.29
CaO	25.88	25.88	25.02	25.07	25.25
Na ₂ O	0.02	0.11	0.25	0.04	0.22
K ₂ O	0.00	0.01	0.00	0.01	0.00
Total	99.97	100.62	100.83	100.09	100.14
Cations Based on 6 Oxygens					
Si	1.977	1.956	2.002	1.993	1.969
Ti	0.001	0.006	0.000	0.001	0.001
Al	0.009	0.044	0.007	0.007	0.030
Fe	0.055	0.004	0.221	0.159	0.188
Mg	0.960	1.006	0.731	0.801	0.806
Mn	0.003	0.000	0.032	0.045	0.009
Ca	1.010	0.996	0.993	0.996	1.004
Na	0.001	0.007	0.018	0.003	0.016
K	0.000	0.000	0.000	0.001	0.000
Sum	4.017	4.019	4.003	4.004	4.023
Mole %					
Di	94.4	99.6	74.3	79.7	80.4
Hd	5.4	0.4	22.4	15.8	18.7
Jo	0.3	0.0	3.2	4.5	0.9
Assay					
Cu (ppm)	18700	33000	33000	33000	94000
Ag (ppm)	12.7	4.4	4.4	4.4	15.4
Au (ppb)	210	2950	2950	2950	650

TABLE 4 ELECTRON MICROPROBE ANALYSES OF GARNET

Sample #	AC-21-153	AC-21-180	AC-21-180	AC-21-185	AC-21-189	AC-21-241	AC-51-268	AC-51-268	AC-51-269	AC-51-269	AC-51-338
SiO ₂	36.24	35.71	35.49	36.67	36.34	36.25	36.50	36.85	38.63	38.15	37.00
TiO ₂	0.99	0.06	0.02	0.15	0.00	0.00	2.41	2.34	1.08	0.74	0.12
Al ₂ O ₃	4.72	0.17	0.74	4.71	4.76	2.91	9.27	10.18	14.09	13.94	7.24
Fe ₂ O ₃	24.28	31.13	30.41	24.85	24.46	27.14	16.40	15.86	11.31	11.55	21.23
MgO	0.20	0.12	0.12	0.10	0.09	0.08	0.24	0.14	0.22	0.10	0.12
MnO	0.24	0.18	0.16	0.25	0.16	0.28	0.33	0.36	0.51	0.51	0.31
CaO	34.43	33.04	33.28	34.41	34.40	33.46	34.48	34.71	35.17	35.22	34.44
Na ₂ O	0.00	0.04	0.01	0.10	0.08	0.00	0.14	0.03	0.03	0.03	0.09
K ₂ O	0.00	0.00	0.00	0.01	0.00	0.00	0.03	0.01	0.00	0.00	0.00
Total	101.10	100.45	100.23	101.25	100.29	100.12	99.80	100.48	101.04	100.24	100.55
Cations based on 16 Oxygens											
Si	5.913	6.004	5.971	5.976	5.977	6.021	5.874	5.874	5.984	5.969	5.984
Ti	0.121	0.008	0.003	0.018	0.000	0.000	0.291	0.281	0.126	0.087	0.015
Al	0.907	0.034	0.147	0.904	0.923	0.569	1.757	1.913	2.572	2.570	1.381
Fe	2.982	3.939	3.850	3.047	3.027	3.392	1.985	1.903	1.319	1.360	2.583
Mg	0.048	0.030	0.031	0.023	0.022	0.020	0.058	0.033	0.051	0.023	0.030
Mn	0.033	0.025	0.024	0.034	0.022	0.039	0.045	0.048	0.066	0.067	0.043
Ca	6.019	5.952	5.999	6.008	6.062	5.955	5.945	5.929	5.837	5.905	5.968
Na	0.000	0.014	0.002	0.031	0.024	0.001	0.042	0.008	0.008	0.010	0.029
K	0.000	0.000	0.000	0.002	0.000	0.000	0.005	0.002	0.000	0.000	0.000
Sum	16.022	16.006	16.026	16.044	16.058	15.997	16.002	15.990	15.961	15.991	16.032
Mole %											
Pyralspite	2.0	1.4	1.3	1.4	1.1	1.5	2.5	1.9	2.9	2.3	1.8
Andradite	75.8	97.8	95.0	76.1	75.8	84.4	55.0	52.3	64.2	63.9	65.8
Grossularite	22.2	0.8	3.6	22.5	23.1	14.1	42.5	45.8	32.9	33.8	32.4
Assay											
Cu (ppm)	200	72	72	18	46000	124000	10000	10000	12400	12400	530
Ag (ppm)	3.9	9.0	9.0	0.4	507.5	88.4	18.8	18.8	80.2	80.2	0.6
Au (ppb)	60	10	10	15	1510	2530	70	70	28490	28490	15

TABLE 4 ELECTRON MICROPROBE ANALYSES OF GARNET

Sample #	AC-51-338	AC-51-358	AC-51-503	AC-53-420	NS-15-1384	NS-15-1384	NS-15-1384	NS-15-1393	NS-15-1415	NS-15-1415
SiO ₂	37.45	36.99	36.14	35.85	35.93	35.56	37.23	35.78	37.92	36.06
TiO ₂	0.14	0.12	0.26	2.04	0.08	0.08	0.09	0.09	0.26	0.03
Al ₂ O ₃	9.71	6.92	2.87	6.92	1.52	0.03	8.46	0.72	12.42	1.94
Fe ₂ O ₃	18.68	21.92	27.36	20.39	28.75	31.50	19.91	30.30	15.13	27.42
MgO	0.14	0.14	0.06	0.26	0.09	0.08	0.10	0.13	0.03	0.00
MnO	0.34	0.28	0.25	0.38	0.17	0.18	0.39	0.18	0.67	1.19
CaO	34.35	34.32	34.14	34.04	33.55	32.95	33.66	33.54	35.05	32.81
Na ₂ O	0.07	0.06	0.02	0.04	0.05	0.05	0.01	0.00	0.06	0.05
K ₂ O	0.00	0.01	0.00	0.00	0.00	0.01	0.00	0.00	0.00	0.00
	100.88	100.76	101.10	99.92	100.14	100.44	99.85	100.74	101.54	99.50
Cations based on 16 Oxygens										
Si	5.972	5.981	5.960	5.853	6.014	5.990	6.020	5.986	5.941	6.061
Ti	0.017	0.014	0.032	0.250	0.010	0.010	0.011	0.011	0.030	0.004
Al	1.825	1.318	0.558	1.331	0.299	0.007	1.613	0.142	2.293	0.385
Fe	2.242	2.667	3.395	2.505	3.621	3.992	2.423	3.814	1.784	3.469
Mg	0.034	0.034	0.016	0.064	0.024	0.020	0.023	0.032	0.008	0.000
Mn	0.046	0.038	0.035	0.052	0.024	0.026	0.054	0.025	0.088	0.169
Ca	5.869	5.946	6.031	5.955	6.016	5.947	5.832	6.012	5.884	5.909
Na	0.021	0.200	0.007	0.013	0.015	0.016	0.003	0.000	0.017	0.017
K	0.000	0.002	0.000	0.001	0.000	0.003	0.000	0.006	0.000	0.000
Sum	16.025	16.021	16.033	16.024	16.022	16.011	15.977	16.023	16.045	16.014
<u>Mole %</u>										
Pyrospite	1.9	1.8	1.2	2.8	1.2	1.1	1.9	1.4	2.3	4.2
Grossularite	54.3	65.8	84.9	65.6	91.3	98.7	59.0	95.1	43.2	86.2
Andradite	43.8	32.4	13.8	31.7	7.5	0.2	39.1	3.5	54.6	9.6
Assay										
Cu (ppm)	530	30	101	195	117000	117000	117000	184100	33000	33000
Ag (ppm)	0.6	0.8	3.0	0.3	149.7	149.7	149.7	219.2	4.5	4.5
Au (ppb)	15	10	15	10	2470	2470	2470	480	2950	2950

TABLE 5 ELECTRON MICROPROBE ANALYSES OF MISCELLANEOUS SILICATE MINERALS

Sample #	AC-51-498	AC-51-498	AC-53-420	AC-53-420	AC-53-149	AC-53-149	AC-51-268	AC-51-268	AC-51-351	AC-51-269	AC-51-282	AC-51-282	AC-51-503
	Feldspar	Feldspar	Feldspar	Feldspar	Olivine	Olivine	Muscovite	Muscovite	Muscovite	Phlogopite	Phlogopite	Phlogopite	Phlogopite
SiO ₂	65.80	66.41	64.29	64.39	42.43	42.57	47.26	47.33	46.76	37.46	40.40	43.01	40.78
TiO ₂	0.03	0.02	0.02	0.00	0.00	0.00	0.00	0.01	0.01	0.19	0.04	0.02	0.05
Al ₂ O ₃	19.28	19.15	18.33	18.46	0.06	0.02	38.13	38.73	36.44	17.71	10.51	11.86	14.07
Feo/Fe ₂ O ₃	0.04	0.04	0.00	0.09	0.42	0.41	0.25	0.24	1.70	8.43	3.85	2.82	1.67
MgO	0.00	0.01	0.01	0.02	56.79	57.13	0.37	0.25	0.41	22.38	29.91	28.14	26.77
MnO	0.00	0.00	0.04	0.00	0.03	0.00	0.00	0.03	0.07	0.27	0.06	0.00	0.00
CaO	0.00	0.03	0.07	0.07	0.02	0.05	0.07	0.07	0.05	0.07	0.03	0.04	0.00
Na ₂ O	0.27	0.28	0.26	0.36	0.04	0.00	0.02	0.02	0.17	0.00	0.01	0.04	0.14
K ₂ O	16.07	15.34	15.43	16.10	0.01	0.01	10.70	10.85	10.49	8.07	6.21	9.84	10.77
Total	101.49	101.28	98.45	99.49	99.80	100.19	96.80	97.53	96.10	94.58	91.02	95.77	94.25
# Oxygens	8	8	8	8	4	4	24	24	24	24	24	24	24
Si	2.986	2.993	3.014	2.991	0.998	0.997	6.129	6.098	6.162	5.408	5.874	6.001	5.795
Ti	0.001	0.001	0.001	0.000	0.000	0.000	0.000	0.001	0.001	0.021	0.004	0.002	0.005
Al	1.031	1.017	1.013	1.011	0.002	0.001	5.829	5.881	5.660	3.013	1.801	1.950	2.356
Fe	0.001	0.002	0.000	0.004	0.008	0.008	0.027	0.026	0.187	1.018	0.468	0.329	0.199
Mg	0.000	0.001	0.001	0.001	1.991	1.995	0.072	0.048	0.080	4.816	6.482	5.852	5.671
Mn	0.000	0.000	0.002	0.000	0.001	0.000	0.000	0.003	0.008	0.033	0.008	0.000	0.000
Ca	0.000	0.002	0.003	0.004	0.001	0.001	0.009	0.009	0.007	0.011	0.005	0.005	0.000
Na	0.024	0.025	0.023	0.032	0.002	0.000	0.006	0.005	0.042	0.000	0.004	0.012	0.039
K	0.930	0.940	0.863	0.954	0.000	0.000	1.770	1.783	1.763	1.487	1.153	1.751	1.952
Sum	4.974	4.979	4.921	4.996	3.002	3.002	13.842	13.854	13.909	15.806	15.798	15.902	16.016
Assay													
Cu (ppm)	29000	29000	195	195	156	156	10000	10000	20	12400	30000	30000	101
Ag (ppm)	17.5	17.5	0.3	0.3	0.7	0.7	18.8	18.8	0.2	80.2	36.3	36.3	3.0
Au (ppb)	1230	1230	10	10	20	20	70	70	5	28490	1160	1160	15

TABLE 5 ELECTRON MICROPROBE ANALYSES OF MISCELLANEOUS SILICATE MINERALS

Sample #	AC-51-503	LC-111-774	LC-111-847	AC-53-348
	Phlogopite	Phlogopite	Phlogopite	Serpentine
SiO ₂	41.62	39.56	37.98	43.60
TiO ₂	0.07	0.33	0.36	0.02
Al ₂ O ₃	13.07	14.52	15.50	0.09
Feo/Fe ₂ O ₃	1.39	1.24	1.52	1.77
MgO	27.01	28.95	28.85	40.63
MnO	0.00	0.01	0.05	0.00
CaO	0.00	0.04	0.03	0.03
Na ₂ O	0.16	0.11	0.07	0.03
K ₂ O	10.77	7.97	7.02	0.01
Total	94.09	92.73	91.38	86.18
# Oxygens	24	24	24	36
Si	5.911	5.624	5.468	8.166
Ti	0.008	0.036	0.039	0.003
Al	2.187	2.433	2.630	0.020
Fe	0.166	0.148	0.184	0.277
Mg	5.717	6.315	6.191	11.342
Mn	0.000	0.002	0.006	0.000
Ca	0.000	0.007	0.005	0.005
Na	0.043	0.031	0.020	0.011
K	1.952	1.445	1.290	0.002
Sum	15.984	16.040	15.831	19.826
Assay				
Cu (ppm)	101	11500	40000	21200
Ag (ppm)	3.0	3.4	56.5	17.5
Au (ppb)	15	180	7	2600

TABLE 6 ELECTRON MICROPROBE ANALYSES OF AMPHIBOLES

Sample #	AC-21-180	AC-21-241	AC-21-246	AC-21-246	AC-21-191	AC-51-290	AC-51-290	AC-51-320	AC-51-339	AC-51-351	AC-51-490
SiO ₂	52.27	51.87	54.80	56.01	54.37	55.18	55.32	55.12	55.19	52.26	54.71
TiO ₂	0.04	0.01	0.04	0.05	0.04	0.06	0.18	0.18	0.10	0.06	0.06
Al ₂ O ₃	1.59	2.79	1.30	0.78	1.89	0.65	1.61	1.61	0.69	3.32	0.84
FeO	18.25	13.33	11.35	9.55	11.92	13.46	8.34	7.77	10.96	12.24	11.85
MgO	12.30	15.33	16.58	18.67	16.60	15.89	19.27	18.68	16.94	15.74	16.56
MnO	0.38	0.60	0.28	0.22	0.11	0.38	0.17	0.18	0.19	0.27	0.13
CaO	12.18	11.70	12.53	12.66	12.60	12.62	13.00	13.13	12.88	12.80	12.84
Na ₂ O	0.33	0.31	0.24	0.16	0.30	0.25	0.36	0.24	0.14	0.21	0.11
K ₂ O	0.08	0.10	0.05	0.03	0.06	0.02	0.03	0.07	0.01	0.12	0.01
Total	97.42	96.04	97.17	98.13	97.89	98.51	98.28	96.98	97.10	97.02	97.11
Cations Based on 23 Oxygens											
Si	7.768	7.642	7.872	7.893	7.778	7.900	7.763	7.816	7.920	7.588	7.885
Ti	0.005	0.002	0.004	0.005	0.004	0.007	0.019	0.020	0.010	0.007	0.006
Al	0.279	0.485	0.220	0.130	0.318	0.109	0.267	0.269	0.117	0.568	0.144
Fe	2.268	1.642	1.364	1.126	1.427	1.612	0.979	0.921	1.315	1.487	1.429
Mg	2.725	3.367	3.551	3.921	3.540	3.391	4.030	3.947	3.623	3.407	3.558
Mn	0.048	0.075	0.034	0.026	0.013	0.046	0.020	0.021	0.024	0.033	0.016
Ca	1.939	1.847	1.929	1.911	1.931	1.936	1.955	1.995	1.980	1.991	1.983
Na	0.095	0.088	0.068	0.042	0.083	0.070	0.099	0.065	0.039	0.060	0.030
K	0.015	0.018	0.009	0.006	0.011	0.004	0.005	0.013	0.002	0.022	0.002
Sum	15.142	15.166	15.051	15.060	15.105	15.075	15.136	15.068	15.030	15.161	15.051
Mole %											
Fe/Fe+Mg+Mn	45.0	32.3	27.6	22.2	28.6	31.9	19.5	18.8	26.5	30.2	28.6
Mg/Fe+Mg+Mn	54.0	66.2	71.8	77.3	71.1	67.2	80.1	80.7	73.0	69.2	71.1
Mn/Fe+Mg+Mn	1.0	1.5	0.7	0.5	0.3	0.9	0.4	0.4	0.5	0.7	0.3
Assay											
Cu (ppm)	72	124000	90000	90000	1900	15	15	11	29	20	14200
Ag (ppm)	9.0	88.4	35.3	35.3	5.1	0.2	0.2	0.4	0.1	0.2	33.2
Au (ppb)	10	2530	4280	4280	380	1	1	1	10	5	4380

TABLE 6 ELECTRON MICROPROBE ANALYSES OF AMPHIBOLES

Sample #	AC-51-490	AC-51-498	AC-51-498	AC-51-503	AC-51-503	AC-51-503	AC-53-349	AC-53-349	AC-53-420	LC-111-847	NS-15-1384
SiO ₂	52.19	54.64	53.73	51.53	55.16	57.73	53.42	55.70	52.97	56.28	54.19
TiO ₂	0.20	0.08	0.03	0.10	0.08	0.14	0.11	0.03	0.00	0.05	0.02
Al ₂ O ₃	2.57	1.03	1.23	3.46	2.02	0.45	2.48	1.03	1.86	0.89	0.50
FeO	14.77	14.38	15.13	15.47	4.98	2.35	12.77	7.28	14.76	7.45	16.18
MgO	13.65	15.02	14.51	14.01	21.56	23.44	15.14	19.02	14.17	19.56	14.15
MnO	0.25	0.21	0.36	0.21	0.24	0.03	0.30	0.15	0.36	0.23	0.95
CaO	12.35	12.69	12.42	12.75	12.73	13.66	12.43	13.34	12.83	13.29	11.43
Na ₂ O	0.38	0.18	0.23	0.49	0.40	0.15	0.31	0.19	0.21	0.10	0.38
K ₂ O	0.11	0.02	0.10	0.11	0.08	0.04	0.13	0.00	0.05	0.00	0.05
Total	96.47	98.25	97.74	98.13	97.25	97.99	97.09	96.74	97.21	97.85	97.85
Cations Based on 23 Oxygens											
Si	7.703	7.873	7.828	7.523	7.708	7.894	7.747	7.892	7.760	7.887	7.920
Ti	0.023	0.008	0.004	0.011	0.009	0.014	0.012	0.003	0.000	0.005	0.002
Al	0.447	0.176	0.211	0.596	0.332	0.072	0.423	0.172	0.322	0.147	0.086
Fe	1.824	1.733	1.843	1.889	0.582	0.269	1.548	0.863	1.808	0.873	1.978
Mg	3.004	3.227	3.150	3.049	4.489	4.778	3.273	4.018	3.094	4.086	3.083
Mn	0.031	0.025	0.044	0.026	0.028	0.004	0.037	0.018	0.045	0.027	0.117
Ca	1.953	1.959	1.939	1.995	1.906	2.001	1.932	2.025	2.014	1.996	1.790
Na	0.109	0.051	0.065	0.138	0.109	0.041	0.088	0.052	0.058	0.027	0.106
K	0.020	0.004	0.018	0.020	0.014	0.007	0.025	0.000	0.010	0.000	0.010
Sum	15.114	15.057	15.103	15.246	15.177	15.079	15.085	15.043	15.111	15.047	15.092
Mole %											
Fe/Fe+Mg+Mn	37.5	34.8	36.6	38.1	11.4	5.3	31.9	17.6	36.5	17.5	38.2
Mg/Fe+Mg+Mn	61.8	64.7	62.5	61.4	88.0	94.6	67.4	82.0	62.5	82.0	59.5
Mn/Fe+Mg+Mn	0.6	0.5	0.9	0.5	0.5	0.1	0.8	0.4	0.9	0.5	2.3
Assay											
Cu (ppm)	14200	29000	29000	101	101	101	18000	18000	195	40000	117000
Ag (ppm)	33.2	17.5	17.5	3.0	3.0	3.0	25.0	25.0	0.3	56.5	149.7
Au (ppb)	4380	1230	1230	15	15	15	800	800	10	680	2470

TABLE 6 ELECTRON MICROPROBE ANALYSES OF AMPHIBOLES

Sample #	NS-15-1384	NS-15-1407	NS-15-1415	NS-15-1727
SiO ₂	45.42	55.35	56.38	58.08
TiO ₂	0.13	0.06	0.00	0.11
Al ₂ O ₃	9.28	0.34	0.20	0.24
FeO	19.80	10.54	8.06	1.17
MgO	9.69	17.48	18.95	23.86
MnO	0.21	0.49	0.42	0.04
CaO	12.41	12.59	13.31	13.65
Na ₂ O	1.27	0.26	0.09	0.14
K ₂ O	0.15	0.06	0.01	0.15
Total	98.36	97.17	97.42	97.44
Cations Based on 23 Oxygens				
Si	6.817	7.934	7.964	7.942
Ti	0.015	0.006	0.000	0.012
Al	1.641	0.057	0.034	0.039
Fe	2.486	1.263	0.953	0.134
Mg	2.167	3.735	3.991	4.864
Mn	0.026	0.060	0.050	0.005
Ca	1.995	1.933	2.014	1.999
Na	0.370	0.072	0.025	0.037
K	0.029	0.012	0.002	0.026
Sum	15.546	15.073	15.032	15.057
Mole %				
Fe/Fe+Mg+Mn	53.1	25.0	19.1	2.7
Mg/Fe+Mg+Mn	46.3	73.8	79.9	97.2
Mn/Fe+Mg+Mn	0.6	1.2	1.0	0.1
Assay				
Cu (ppm)	117000	18700	33000	43100
Ag (ppm)	149.7	12.7	4.5	63.7
Au (ppb)	2470	210	2950	1780

TABLE 7 ELECTRON MICROPROBE ANALYSES OF CHLORITE

Sample #	AC-21-241	AC-51-269	AC-51-331	AC-51-351	LC-111-774	NS-15-1422
SiO ₂	30.98	30.73	28.36	31.61	36.71	30.65
TiO ₂	0.03	0.06	0.03	0.01	0.06	0.05
Al ₂ O ₃	16.46	17.31	17.79	16.53	11.84	15.38
FeO	14.65	8.33	20.09	14.46	2.95	14.71
MgO	23.27	28.03	20.09	24.70	31.45	24.08
MnO	1.77	0.34	0.46	0.15	0.02	0.38
CaO	0.21	0.04	0.13	0.18	0.09	0.33
Na ₂ O	0.00	0.00	0.00	0.01	0.05	0.00
K ₂ O	0.02	0.04	0.02	0.04	3.57	0.05
Total	87.39	84.88	86.97	87.69	86.74	85.63
Si	4.433	4.351	4.186	4.461	5.020	4.459
Ti	0.003	0.006	0.004	0.001	0.007	0.006
Al	2.775	2.888	3.095	2.749	1.909	2.637
Fe	1.753	0.987	2.479	1.707	0.338	1.790
Mg	4.963	5.915	4.419	5.195	6.411	5.222
Mn	0.214	0.041	0.057	0.019	0.003	0.046
Ca	0.032	0.006	0.021	0.027	0.013	0.052
Na	0.000	0.000	0.000	0.004	0.012	0.000
K	0.004	0.008	0.004	0.006	0.623	0.009
Sum	14.177	14.201	14.265	14.168	14.335	14.220
Mole %						
Fe/Fe+Mg+Mn	25.3	14.2	35.6	24.7	5.0	25.4
Mg/Fe+Mg+Mn	71.6	85.2	63.5	75.1	95.0	74.0
Mn/Fe+Mg+Mn	3.1	0.6	0.8	0.3	0.0	0.7
Assay						
Cu (ppm)	124000	12400	155	20	11500	94000
Ag (ppm)	88.4	80.2	0.4	0.2	3.4	15.4
Au (ppb)	2530	28490	30	5	180	650

TABLE 8. ELECTRON MICROPROBE ANALYSES OF EPIDOTE

Sample #	AC-21-153	AC-21-185	AC-21-189	AC-51-238	AC-51-269	AC-51-269	AC-51-331	AC-51-331	AC-51-338	AC-51-490	AC-51-490	AC-53-420
SiO ₂	37.90	37.55	37.65	37.53	38.26	38.87	37.30	37.37	37.42	37.88	37.30	37.24
TiO ₂	0.18	0.08	0.19	0.12	0.00	0.03	0.00	0.15	0.03	0.01	0.34	0.03
Al ₂ O ₃	24.12	22.12	22.69	21.67	24.61	28.86	23.18	23.34	21.16	21.74	21.45	21.17
Fe ₂ O ₃	11.17	13.46	12.61	13.97	9.71	5.89	12.69	11.93	14.53	13.36	13.39	14.04
MgO	0.08	0.02	0.03	0.00	0.04	0.03	0.60	0.13	0.08	0.04	0.08	0.00
MnO	0.07	0.16	0.11	0.03	0.00	0.02	0.11	0.46	0.17	0.03	0.00	0.10
CaO	23.78	23.24	23.55	23.69	23.59	24.35	23.13	23.25	23.25	23.15	23.55	23.07
Na ₂ O	0.00	0.01	0.05	0.04	0.00	0.03	0.05	0.03	0.00	0.03	0.00	0.03
K ₂ O	0.00	0.00	0.00	0.00	0.00	0.00	0.00	0.00	0.00	0.00	0.00	0.01
Total	97.30	96.64	96.88	97.05	96.21	98.08	97.06	96.66	96.64	96.24	96.11	95.69
Cations Based on 13 Oxygens												
Si	2.605	2.633	2.622	2.631	2.633	2.568	2.605	2.601	2.642	2.662	2.634	2.648
Ti	0.009	0.004	0.010	0.007	0.000	0.002	0.000	0.008	0.002	0.001	0.018	0.002
Al	1.953	1.827	1.862	1.790	1.996	2.247	1.908	1.915	1.760	1.801	1.785	1.774
Fe	0.642	0.789	0.734	0.819	0.559	0.325	0.741	0.695	0.858	0.785	0.791	0.835
Mg	0.008	0.002	0.004	0.000	0.004	0.003	0.007	0.014	0.008	0.004	0.008	0.000
Mn	0.004	0.010	0.006	0.002	0.000	0.001	0.007	0.027	0.010	0.002	0.000	0.006
Ca	1.751	1.746	1.757	1.779	1.739	1.723	1.731	1.734	1.758	1.743	1.781	1.758
Na	0.000	0.001	0.007	0.005	0.000	0.003	0.007	0.004	0.000	0.004	0.000	0.004
K	0.000	0.000	0.000	0.000	0.000	0.000	0.000	0.000	0.000	0.000	0.000	0.001
Sum	6.972	7.012	7.002	7.032	6.931	6.871	7.006	6.997	7.038	7.001	7.017	7.027
Assays												
Cu (ppm)	200	18	46000	530	12400	12400	155	155	530	14200	14200	195
Ag (ppm)	19.0	0.4	507.5	0.6	80.2	80.2	0.4	0.4	0.6	33.2	33.2	0.3
Au (ppb)	15	15	1510	15	28490	28490	30	30	15	4380	4380	10

Table 9 Hand sample descriptions of assayed samples

Sample #	Cu(ppm)	Ag(ppm)	Au(ppb)	Hand Sample Description
AC-21-120	77	19.00	15	Diorite endoskarn (gar<pyx).
AC-21-153	200	3.90	60	Ep-act patch in gar-pyx endoskarn.
AC-21-160	39	2.50	15	Pale gar-pyx endoskarn.
AC-21-180	72	9.00	10	Banded gar-pyx skarn with qtz-mt vugs.
AC-21-185	18	0.40	15	C.g. pyx-mt skarn, no sulfides.
AC-21-189	46000	507.53	1510	Qtz-ep-cp retrograde vein in gar skarn.
AC-21-191	1900	5.14	380	Py vein of pyx-mt skarn.
AC-21-192	7100	22.26	620	Pyx skarn cut by qtz-gar-mt vein with cp-py env.
AC-21-193	53000	27.40	1640	Pyx skarn with (mt-cp-py)=20%.
AC-21-215	70	0.60	20	Pyx=mt skarn with no sulfides.
AC-21-223	45000	156.52	1780	C.g. brown garnet skarn with 3-5% cp stringers minor mt fringe.
AC-21-241	124000	88.37	2530	Gar-pyx-cp vein cutting mt>pyx skarn.
AC-21-245	48100	14.39	3010	C.g. pyx (1-2cm) with interstitial cp and mt.
AC-21-246	90000	35.28	4280	Ca-qtz vein with cp env cutting mt>pyx skarn.
AC-21-262	5700	3.43	450	Pale gar>pyx skarn with cp vugs.
AC-21-265	35	0.40	5	Dolostone at marble front.
AC-21-288	37	0.50	10	Dolostone 24ft. from skarn.
AC-51-115	29	0.20	5	Gray dolostone.
AC-51-262	12	0.20	5	Pure white dolostone.
AC-51-268	10000	18.84	70	Pale gar-pyx skarn with bn±cc clumps.
AC-51-269	12400	80.15	28490	Pale gar-pyx skarn with ep retrograde and bn±cc clumps.
AC-51-272	8100	3014.00	1780	Mt-phi skarn with bn-cc.
AC-51-282	30000	36.31	1160	Mt-pyx skarn with bn-cp.
AC-51-290	15	0.20	1	Mottled f.g. pyx skarn.
AC-51-320	11	0.40	1	Pyx hornfels
AC-51-325	10	0.10	10	Phi-olv-pyx skarn, no mt.
AC-51-331	155	0.40	30	Qtz-ep-act-py vein-vug retrograde.
AC-51-338	530	0.60	15	Massive red brown garnet skarn.
AC-51-339	29	0.10	10	Qtz-ep-mt vug in garnet skarn.
AC-51-351	20	0.20	5	Pyx skarn with <5% garnet.
AC-51-358	30	0.80	10	Pyx skarn cut by planar qtz-act veins.
AC-51-400	8500	21.00	1000	Diorite endoskarn wth gar-pyx± ep-py.
AC-51-445	129	0.90	20	"Fresh" diorite with mafic xenoliths.
AC-51-490	14200	33.22	4380	Py-cp-ep retrograde of pyx skarn at diorite contact.
AC-51-498	29000	17.47	1230	Cp-act- retrograde of pyx skarn.
AC-51-503	101	3.00	15	Gar-pyx skarn in small pendent-xenolith in diorite.
AC-51-645	85	1.60	15	Fresh diorite.
AC-53-135	15	0.20	10	Br specks in white dolostone.
AC-53-149	156	0.70	20	Fringe serpentine vein with env. of br specks
AC-53-167	25	0.20	45	Wavy convoluted contact between diorite endoskarn (gar-ep) and 10cm green sp-phi-br skarn.
AC-53-185	124	1.00	15	C.g. spinel, possible gahnite.
AC-53-340	22800	4.11	100	Contact of dolostone with massive mt-cp-olv(sp) skarn.
AC-53-342	70	0.10	10	Possibe fresh olv. in fringe zone of skarn.
AC-53-345	43000	57.88	10170	Massive mt-bn-valleriite?skarn.
AC-53-348	21200	17.47	2600	Massive mt-valleriite ol.(sp) skarn.
AC-53-349	18000	25.00	800	Zonation sequence of dol to olv (sp) to pyx-py to gar skarn.
AC-53-352	153200	32.54	2910	10% cp disseminated in pyx with act retrograde.
AC-53-353	94.00	0.40	10	Garnet skarn.
AC-53-363	3000	0.69	4	1% cp in pyx±mt near gar vein.
AC-53-383	13000	7.54	270	Pyx skarn with cp veinlets near diorite dike.
AC-53-387	2600	0.70	45	Pyx skarn wiht cp veinlets near diorite dike.
AC-53-411	70	0.20	5	Gar-pyx skarn cut by qtz-ep vein (1mm).
AC-53-420	195	0.30	10	Gar- dark pyx skarn with qtz-chl-py fractures.
AC-53-453	17	0.10	5	Dark pyx skarn.
AC-53-515	6100	79.12	210	Gar-pyx-cp.

<u>Sample #</u>	<u>Cu(ppm)</u>	<u>Ag(ppm)</u>	<u>Au(ppb)</u>	<u>Hand Sample Description</u>
AC-53-604	25	0.20	15	C.g. olv-talc.
AC-53-607	16	0.20	10	Olv-br at diorite contact.
BC22-96	6600	2.06	70	Skarn.
BC-39-517	20	0.90	5	Pure CaCO ₃ limestone.
BC-39-570	585	0.90	5	C.g. 2 cm blue-green pxy-lim.
BC-39-591	325	3.30	15	Gar-tan pyx(Mn?) -hm.
BC-39-602	85	1.80	10	Dark green pxy-gar-hm.
BC-39-616	10	0.30	1	Fresh diorite.
BC-46-263	2800	1.70	1	Skarn.
BC-46-265	855	2.60	5	Skarn.
Black Cub South	70000	43.84	2360	Gar<pyx go to ep-act-cp.
BLC-46-543	4900	3.80	1050	Skarn.
CP-115-272	3700	1.37	140	Skarn.
CP-115-292	1100	2.00	15	Skarn.
CP-115-297	18000	8.56	210	Skarn.
CP-115-335	139300	22.61	140	Pyx-ep-cc-cp.
CP-70-250	735	0.30	5	Gar>pyx skarn; Tr ace mo-py.
KK-5-477	84	0.50	1	Skarn.
KK-5-515	1400	1.50	5	Skarn.
LC-111-769	104	2.40	5	Dolostone <1ft. from skarn.
LC-111-773	28300	37.00	80	Gar-pyx skarn with mt band.
LC-111-774	11500	3.40	180	Mt>pyx skarn±cp.
LC-111-775	131000	172.28	480	Skarn.
LC-111-776	31200	5.14	140	Mt-phi skarn with cp-bn in phi-rich bands.
LC-111-778	5600	2.40	70	Qtz-ca-wollastonite? zone with cp blebs.
LC-111-782	119	0.40	1	Biotitized siltstone with vertical qtz-py fractures.
LC-111-788	145	0.40	5	Biotitized siltstone with vertical qtz-py fractures.
LC-111-790	63	1.20	5	Biotitized siltstone with vertical qtz-py fractures.
LC-111-813	119	0.40	1	Strongly biotitized siltstone, no sulfides.
LC-111-829	47	1.30	10	Pale green siltstone with qtz-py veins.
LC-111-847	40000	56.51	680	Pyx-cp skarn at contact with siltstone.
LC-111-882	6000	0.69	70	Mt-cp±sp.
LC-111-887	23800	13.36	620	Mt-cp-bn and ca veins.
LC-114-914	25600	15.07	140	Diorite fractured with qtz-cp-feldspar flooding.
LC-111-947	450	3.80	40	Mudstone skarnoid (gar-pyx-ep) with py>cp.
LC-111-977	79	1.00	1	Salt-pepper graywacke.
LC-96-137	15	0.40	1	C.g. gar-pyx skarn no sulfides.
LC-96-150	124	1.30	5	Diorite with green pyx laths replacing hbd.
LC-96-45	29	0.40	5	C.g. pale grossularite gar with interstitial blue-green pyx.
LC-96-700	18	1.40	5	Typical gar-pyx of copper skarn.
LC-96-710	1870	1.40	120	Gar-pyx-ep endoskarn of diorite.
LC-96-750	71500	39.39	410	1/2 mt-phi-bn, 1/2 mt-dark sp.
LC-96-760	80000	60.28	620	Mt>bn>pyx (1mm laths 5%).
LC-96-770	212400	255.16	53240	1-2cm euhedral pyx crystals with 2% 1mm brown gar and 10% bn.
LC-96-780	33600	26.37	410	Mt-sp-phi skarn with 5% bn patches.
LC-96-820	60900	55.83	2050	Felted 1-5mm green pyx-mt skarn with 1% bn.
LC-96-835	134300	116.11	1510	1cm euhedral green pyx-phi-mt with 5% bn.
LC-96-840	32800	23.29	480	Pyx>sp>mt>phi 1% bn skarn.
LC-96-845	54000	16.44	510	Sp-cp skarn.
LC-96-855	15600	7.54	2050	Mt-olv goes to sp-valleriite skarn.
LC-96-86	7	1.10	5	Buff pyx hornfels with 5mm green pyx eyes and stockwork act fractures.
LC-96-930	14100	7.88	750	Mt>sp>cp skarn.
LC-96-800	32000	21.58	450	Banded mt-sp-bn.
NS-15-1375	100	0.70	15	Pale green pyx, no sulfides.
NS-15-1378	156000	249.68	1510	Retrograde pyx to clay 10% cp.

<u>Sample #</u>	<u>Cu(ppm)</u>	<u>Ag(ppm)</u>	<u>Au(ppb)</u>	<u>Hand Sample Description</u>
NS-15-1384	117000	149.67	2470	2cm euhedral gar-ep with interstitial 20% bn, 2% cp.
NS-15-1385	16700	22.00	700	2cm euhedral gar with vugs of specular hm-ca-qtz. <1% cp+bn.
NS-15-1393	184100	219.20	480	Gar-pyx skarn goes to ep-act with 20% cp, 2% bn.
NS-15-1398	92000	45.55	2810	C.g. fresh pale pyx with 5% cp, <1% bn.
NS-15-1400	380	1.60	35	C.g white dolostone cut by mt vein.
NS-15-1404	29500	23.98	410	C.g. fresh pale pyx with 25% c.g. cp.
NS-15-1407	18700	12.67	210	Pale pyx rosettes with 25% c.g. cp.
NS-15-1409	24000	30.48	1880	Strong clay retrograde of pyx skarn, little sulfide.
NS-15-1415	33000	4.45	2950	Pyx>gar skarn with 10% cp 1% bn and minor qtz. vein.
NS-15-1422	94000	15.41	650	Clay retrograde pyx skarn with vugs of ca - specular hm, minor cp and bn.
NS-15-W1-1098	25600	25.00	410	C.g. olv in mt-cp skarn.
NS-15-W1-1102	20	0.80	1	C.g. white dolomitic marble.
NS-15-W1-1110	29000	39.73	1990	Contact of mt-cp skarn with mt-ca-cp vein.
NS-15-W1-1112	260	0.70	10	Gray peppery dolomitic limestone.
NS-15-W1-1116	23600	10.62	750	Mt-olv-tr-bn in middle of skarn.
NS-15-W2-1694	890	1.60	30	Green olv to sp, with isolated 1cm phl rosettes.
NS-15-W2-1700	38500	2071.10	550	Dark green-black olv-sp skarn 5% cp, 2% mt.
NS-15-W2-1705	46200	39.05	1160	Mt goes to pyx skarn 5% cp, 3% bn.
NS-15-W2-1710	39000	191.46	270	Mt>pyx-tr skarn with 5% cp.
NS-15-W2-1718	10	0.10	15	Dark diabase-diorite dike with 1 cm ep clots.
NS-15-W2-1727	43100	63.71	1780	Tr>phl-mt 1% bn.
NS-15-W2-1742	24000	48.29	2230	OI to sp-mt skarn 5% valleriite, 3% bn, 1% cp.
NS-15-W2-1746	315	0.50	15	Olv-mt-gar skarn.
NS-15-W2-1758	9	0.30	1	Diorite.
NS-15-W2-1764	128	0.90	60	Ep endoskarn.
NS-17-26	61	0.50	10	Skarn.
NS-17-41	19200	30.83	1200	Retrograde skarn.
V-19-400	580	0.40	40	Skarn.
V-19-403	1100	3.20	85	Skarn.
V-19-405	2900	1.50	190	Skarn.
WE-54-182	53000	62.34	650	Pale gar>pyx with 5% bn 1 cm patches.
WE-8-250	3400	1.71	210	Gar-pyx>ep sk wtih 2% cp.
WE-D2-280	40000	17.47	2640	Pyx-skarn cut by cp-act veins 3% cp.
WE-D8-30	4200	1.60	90	Gar=pyx>ep-ca skarn 1% cp.

Abbreviations used in table:

act=actinolite, bn=bornite, br=brucite, ca=calcite, cc=chalcocite, c.g.=coarse-grained, chl=chlorite, cp=chalcocite, do=dolomite, env=envelope, ep=epidote, f.g.=fine-grained, gar=garnet, hbd=hornblende, hm=hematite, lim=limonite, mt=magnetite, olv=olivine, phl=phlogopite, py=pyrite, pyx=pyroxene, qtz=quartz, sp=serpentine, tr=tremolite.

Table 10 Electron microprobe analyses of opaque minerals

Sample # Mineral	AC-51-269 Bn	CP-115-292 Bn	CP-115-292 Bn	NS-15-1393 Bn	NS-15-1393 Bn	V-19-405 Bn	WE-D2-280 Bn	WE-D2-280 Bn	WE-D2-280 Bn	AC-51-269 Cc	AC-51-269 Cc
Cu	63.23	63.02	62.98	62.43	62.67	61.70	63.04	61.15	57.06	78.44	78.95
Fe	10.81	11.56	11.57	11.49	11.10	11.59	11.36	12.24	14.39	0.15	0.36
S	24.86	26.22	26	25.12	25.34	25.88	25.51	25.76	28.04	20.53	20.21
Ag	0.16	0.13	0.22	0.17	0.34	0.01	0.27	0.23	0.10	0.86	0.08
Au	0.04	0.04	0	0.06	0.00	0.05	0.00	0.00	0.10	0	0
Te	0.03	0	0.07	0.02	0.04	0.05	0.03	0.00	0.10	0.54	0.07
Total	99.13	100.97	100.84	99.29	99.49	99.28	100.21	99.38	99.79	100.52	99.67

Sample # Mineral	AC-51-269 Cc in gold	AC-51-269 Cc in gold	AC-21-189 Cp	AC-21-241 Cp	AC-53-352 Cp	AC-53-352 Cp	AC-53-515 Cp	AC-53-515 Cp	Black Cub South Cp	Black Cub South Cp	BLC-46-549 Cp
Cu	76.95	76.6	33.97	34.25	34.27	34.49	34.47	34.79	34.19	34.42	34.23
Fe	0.15	0.69	30.25	30.64	30.25	30.11	29.86	29.88	29.96	29.87	30.05
S	20.42	20.68	34.23	34.18	34.96	35.04	34.53	34.65	34.53	34.80	34.47
Ag	2.44	1.69	0.08	0.09	0.00	0.03	0.18	0.11	0.05	0.00	0.06
Au	0.04	0.04	0	0.18	0.20	0.08	0.01	0.09	0.00	0.00	0
Te	0.04	0.01	0.06	0	0.00	0.00	0.02	0.00	0.04	0.00	0.01
Total	100.04	99.71	98.59	99.34	99.68	99.75	99.07	99.52	98.77	99.09	98.82

Table 10 Electron microprobe analyses of opaque minerals

Sample # Mineral	KK-5-515 O _p	KK-5-515 O _p	NS-15-1393 O _p	NS-15-1710 O _p	V-19-405 O _p	WE-54-182 O _p	CP-115-292 O _p adj. to Bn	BC-46-265 O _p in Bn-Cc	AC-51-269 Gold	AC-51-269 Gold	AC-51-269 Gold	AC-51-269 Gold
Cu	34.38	34.27	34.60	34.42	34.75	34.26	34.82	33.43	0.21	0.25	0.40	0.22
Fe	30.5	30.38	29.98	30.30	30.27	29.92	30.39	30.45	0.02	0.10	0.01	0.04
S	34.94	34.72	34.32	34.01	35.22	34.22	35.01	33.81	0.01	0.01	0.03	0.03
Ag	0	0	0.07	0.07	0.00	0.09	0.03	0.06	10.42	11.52	7.40	9.83
Au	0.08	0	0.00	0.00	0.00	0.03	0	0.03	88.02	87.76	92.95	89.18
Te	0.02	0	0.03	0.00	0.08	0.06	0.02	0.02	0.08	0.08	0.11	0.11
Total	99.92	99.37	99.00	98.80	100.32	98.58	100.27	97.80	98.76	99.72	100.90	99.41

Sample # Mineral	AC-21-189 Magnetite	AC-21-241 Magnetite	AC-51-269 Magnetite	NS-15-1710 Magnetite	AC-21-246 Py	NS-15-1107A Valleriite
Cu	0.01	0	0.00	0.00	0	22.47
Fe	64.76	67.86	65.44	66.50	45.74	13.86
S	0.03	0	0.00	0.00	52.58	19.04
Ag	0	0	0.07	0.00	0	0.14
Au	0	0.01	0.00	0.08	0	0.05
Te	0	0	0.05	0.02	0	0.00
Total	64.8	67.87	65.56	66.60	98.32	55.56

EVIDENCE OF HYDROTHERMAL ALTERATION IN WHITE CHANNEL SEDIMENTS AND BEDROCK OF THE KLONDIKE AREA, WEST-CENTRAL YUKON

M.B. Dufresne

Department of Geology
University of Alberta
Edmonton, Alberta

S.R. Morison

Exploration and Geological Services Division
Indian and Northern Affairs Canada
Whitehorse, Yukon

B.E. Nesbitt

Department of Geology
University of Alberta
Edmonton, Alberta

DUFRESNE, M.B., MORISON, S.R. and NESBITT, B.E., 1986. Evidence of hydrothermal alteration in White Channel sediments and bedrock of the Klondike area, west-central Yukon; in Yukon Geology, Vol. 1, Exploration and Geological Services Division, Yukon, Indian and Northern Affairs Canada, p. 44-49.

INTRODUCTION

The stratigraphy and sedimentology of the Pliocene to early Pleistocene White Channel gravelly deposit in the Klondike area was first described by R.G. McConnell (1905, 1907) and has been subsequently described by Milner (1976), Naldrett (1981), Dufresne and Morison (1985) and Morison (1985). Alteration in White Channel sediments and underlying bedrock on Dago Hill has been described by Tempelman-Kluit (1982), Dufresne and Morison (1985) and Dufresne (1986).

Field mapping during the 1984-85 field season has shown that three distinct alteration zones are present in White Channel sediments and underlying bedrock on hills such as Dago, Preido, Paradise, and Nugget (Fig. 1). In addition, low temperature hydrothermal veins are present in altered bedrock below altered White Channel sediments on these hills. The field relationships, mineralogy and chemistry of the alteration zones and associated veins suggest that they are the result of Pliocene to early Pleistocene hydrothermal processes. This report outlines evidence supporting hydrothermal alteration of White Channel sediments and bedrock in the lower Hunker Creek drainage basin (Fig. 1).

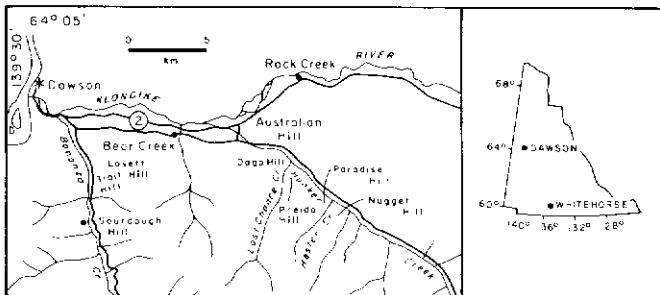


Figure 1. Location map of lower Hunker and Bonanza Creeks, Klondike area.

ALTERATION

High level terraces in the Klondike area contain White Channel alluvium which ranges in thickness from a few metres to over 35 metres. Within White Channel sediment is a distinct post-depositional alteration product which varies from 20 to 25 m in thickness and extends 5 to 10 m into the underlying bedrock. Alteration is characterized by the development of secondary clay minerals, and is divided into 3 zones termed the Bleached Zone, the Iron Zone and the Footwall Zone.

Unaltered Sediments and Bleached Zone

An iron-stained fluvial gravel unit which unconformably

overlies White Channel alluvium (Fig. 2) lacks significant clay alteration except at the surface within the soil profile. Surface clay alteration and iron-staining of this upper fluvial gravel unit is probably the result of weathering and seepage of meteoric fluids since the pre-Reid glacial interval (Rutter et al., 1978). Unaltered White Channel gravelly sediments are generally yellow to light brown with lithofacies relationships and sedimentary structures clearly distinguishable (Dufresne and Morison, 1985). Felsic porphyry and mica schist gravel clasts are usually competent to friable and commonly iron-stained, and the gravel matrix has little secondary clay development (Dufresne and Morison, 1985). The mineralogy of the unaltered gravel matrix (determined by X-ray diffraction) consists of quartz, muscovite (10 Å mica), potassium feldspar and plagioclase (Fig. 2). A trace amount of clay minerals (less than 1 wt.%) occurs within the gravel matrix in the less than 2 µm size fraction, and consists of approximately equal amounts of smectite, illite (10 Å mica) and kaolinite (Fig. 2). Poorly developed diffractometer patterns for these clay minerals indicate low crystallinities. The Hinckley (1963) crystallinity index (HCl) of kaolinite in the less than 2 µm size fraction for primary unaltered gravel matrix is generally less than 0.3 which is characteristic of poorly crystallized kaolinite.

Unaltered White Channel sediments are underlain by intensely altered Bleached Zone sediments with a sharp, thin (20 to 50 cm thick), brown to purple alteration boundary separating the two units (Fig. 2). The alteration boundary follows and cuts across lithofacies contacts and sedimentary structures, indicating that alteration processes were post-depositional (Dufresne and Morison, 1985; Morison, 1985). Alteration of White Channel alluvium is completely isolated from the iron-stained fluvial gravel unit and the surface weathering zone, with exceptions such as at the north end of the Dago Hill exposure (Dufresne and Morison, 1985). At that point, the iron-stained fluvial gravel unit truncates altered White Channel overbank silty-clay sediments. This demonstrates that alteration processes predate sedimentation of the iron-stained gravel unit.

White Channel sediments cut by the Bleached Zone have a characteristic white to grey colour. The zone generally extends downward to within 2 to 4 m of the bedrock contact. Within the Bleached Zone, schist and porphyry gravel clasts are soft and have been replaced by secondary clay minerals (Tempelman-Kluit, 1982; Dufresne and Morison, 1985). Lithofacies characteristics have been masked or destroyed due to volume changes associated with pervasive secondary clay development within the gravel matrix (Dufresne and Morison, 1985).

Gravelly matrix samples from the Bleached Zone usually contain 10 to 15 wt.% secondary clay minerals in the less than 2 µm size fraction. Mineralogy of the matrix is dominantly quartz, muscovite and kaolinite with minor illite and trace feldspars (Fig. 2). Kaolinite is the dominant secondary mineral phase in the Bleached Zone. The HCl of kaolinite in this zone generally ranges

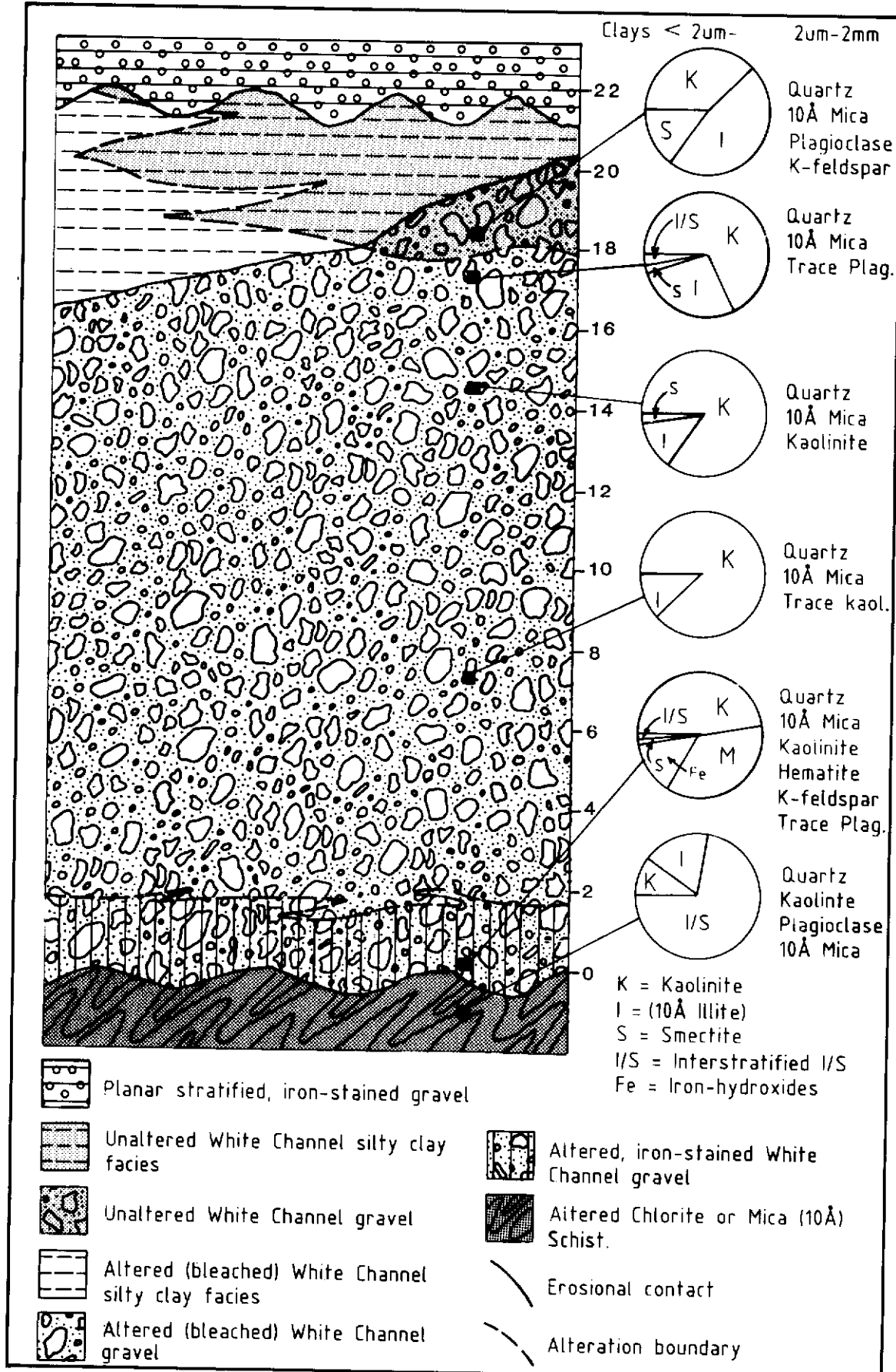


Figure 2. Idealized section of alteration at Dago Hill showing the distribution of clay minerals in the less than $2\mu\text{m}$ size fraction and mineralogy of the $2\mu\text{m}-2\text{mm}$ size fractions.

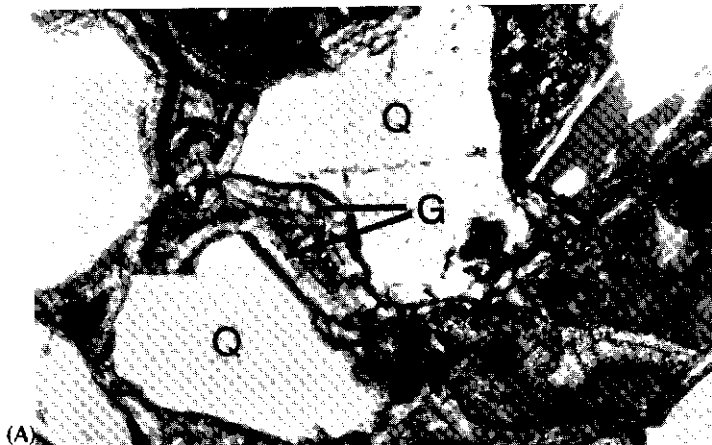
from less than 0.3 to 0.6.

Chemical analyses indicate that the Bleached Zone gravel is depleted in Mg, Ca, Na and K relative to unaltered White Channel gravel, whereas little or no change occurs in the concentration of Fe, P, S, Ba, Mn and As (Dufresne, 1986).

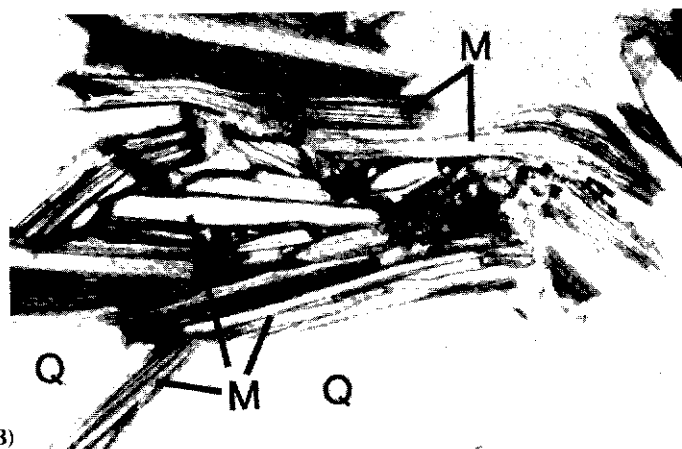
Iron Zone

On Dago Hill, a 2 to 4 m horizon of altered and iron-stained White Channel gravel immediately above bedrock is termed the Iron Zone (Fig. 2). Gravel matrix within this zone contains abundant quartz, muscovite and feldspar with varying amounts of kaolinite, illite, smectite, hematite, lepidocrocite and goethite (Fig. 2). Hematite occurs as a post-depositional cement in several outcrops of Iron Zone gravel on Dago Hill. However, as in the Bleached Zone gravel, a large percentage of the Iron Zone gravelly matrix (i.e. 5 to 15 wt.%) is present in the less than 2 μm size fraction. This size fraction is dominantly composed of kaolinite, illite, lepidocrocite and goethite with minor smectite. The HCl of kaolinite in this zone is generally high, ranging from 1.0 to 1.6, and is indicative of well-crystallized kaolinite. In addition, illite, goethite and lepidocrocite exhibit sharp and symmetric peaks on their diffractogram patterns, which also indicates well-crystallized and ordered minerals.

On Nugget Hill, (Fig. 1), a similar zone of alteration and iron-staining occurs in the lower 2 and 3 m of altered White Channel gravel and upper 2 m of bedrock. Intense iron addition has resulted in the cementation of the gravel by iron-hydroxides. In this zone, the gravel matrix contains trace to low amounts of secondary clay minerals in the less than 2 μm size fraction. In the less than 2 μm size fraction, quartz, goethite and adularia are abundant, with only trace amounts of illite and kaolinite. In the coarser size fractions, quartz is the dominant mineral with minor muscovite, goethite, illite and trace amounts of plagioclase and adularia.



(A)



(B)

The abundance of adularia in the less than 2 μm size fraction and its absence in the coarser size fractions may indicate a secondary origin. Botryoidal goethite (Fig. 3a), and coarse secondary muscovite (1 to 2 mm in size, Fig. 3b) are also visible in thin section. Goethite appears to cement clasts and matrix, but muscovite is a minor cement, commonly occurring as rims on clasts and intergrowths with goethite (Fig. 3c). Although only trace amounts of clay minerals are present in the 2 to 3 m zone of iron-stained and cemented White Channel gravel on Nugget Hill, the higher Bleached Zone gravel is intensely clay altered.

Altered rhyolite porphyry gravel clasts within the Iron Zone of Dago Hill contain greater than 30 wt.% clay in the less than 2 μm size fraction. This size fraction is dominantly composed of quartz, adularia and kaolinite, with minor illite. Kaolinite and adularia are the dominant secondary minerals; HCl of kaolinite in the clasts ranges from less than 0.3 to 1.3. Unaltered cobbles or rhyolite bedrock contain little or no kaolinite and adularia.

Chemical analyses of matrix samples from both the Dago Hill and Nugget Hill Iron Zone gravels (Dufresne, 1986), indicate that concentrations of Fe are enriched, but the concentrations of Mg, Ca, Na and K are unchanged relative to primary unaltered White Channel gravel. In addition, the concentrations of P, S, Ba, Mn and As are higher by an order of magnitude in the Iron Zone gravel relative to unaltered gravel. Significant amounts of Sb, Hg and Co have also been detected in the Iron Zone gravel.

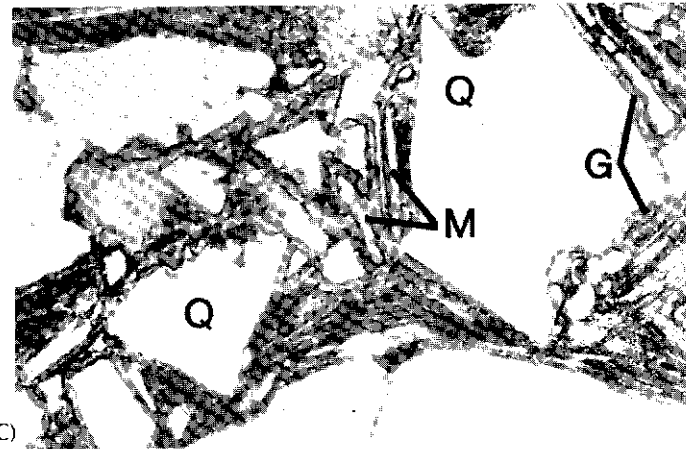
Footwall Zone

Intense alteration in bedrock often extends 5 to 10 m into bedrock below the gravel contact. Below this, alteration is commonly restricted to zones of highly fractured bedrock. Altered schist typically contains 10-15 wt.% material in the less than 2 μm size fraction, compared to less than 1 wt.% for unaltered schist. Mica and/or chlorite schist bedrock show a progressive alteration in the less than 2 μm size fraction to a secondary clay mineral assemblage of kaolinite, illite and either interstratified illite/smectite or interstratified chlorite/smectite respectively (Fig. 2). One sample of mica schist from Dago Hill contained secondary kaolinite with an HCl of 1.03, indicative of well-crystallized kaolinite. The interstratified clay minerals result from the incomplete alteration of primary metamorphic mica or chlorite to ilite in the schists.

Veins associated with Footwall Zone Alteration

Spatially associated with altered bedrock below White Channel gravel in the Hunker and lower Bonanza Creek valleys are thin, post-metamorphic hydrothermal veins. These veins are divided into three types based upon their textures, mineralogy and morphology. Field relationships indicate that these veins were emplaced during the alteration of the Footwall Zone rocks and the overlying White Channel sediments.

Type 1 veins consist dominantly of quartz and chalcedony, with minor kaolinite, dickite, illite, Fe-hydroxides, hematite, Fe-carbonate and pyrite. These veins are generally less than 2-3 cm in



(C)

Figure 3. Photomicrographs of iron-stained and cemented White Channel gravel on Nugget Hill showing: (A) Botryoidal goethite cementing detrital quartz grains; (B) Coarse muscovite (10 Å mica 1-2 mm in length) rimming detrital quartz grains; (C) Intergrown goethite and muscovite (10 Å mica) cementing the matrix of the iron-stained gravel. Q = quartz, M = muscovite and G = goethite.

thickness (in places 10-20 cm thick) and lack iron-stain. Characteristic of type 1 veins are vugs with euhedral quartz, and banding, cockscomb, cockade and crustiform textures. Type 2 veins are dominantly composed of siderite and quartz, with minor amounts of ankerite, calcite, goethite, hematite, gypsum, pyrite and clay minerals. Type 2 veins are intensely iron-stained and are generally less than 1-2 cm thick; however, associated concretions are 10 to 30 cm thick. Common textures exhibited by type 2 veins include botryoidal growth structures, replacement banding and vugs. Type 3 veins, minor in occurrence, consist of microfractures containing either the smectite group minerals and goethite, or amorphous silicates and goethite. Lussatite (a variety of opal) is present in several veins from the Trail Hill Footwall Zone. Type 3 veins are generally less than 1-2 cm in thickness, and show few textures.

Fluid inclusion analyses of these veins indicates that they were deposited from low temperature (approx. 125°C), dilute hydrothermal fluids. Also, the veins contain anomalously high concentrations of trace elements such as S, Ba, As, Sb and Au.

Types 1, 2 and 3 veins cross-cut all structural fabrics in the Klondike Schist. Types 1 and 2 veins in places contain fragments of partially clay altered and visibly bleached Footwall Zone rocks. In addition, siderite and quartz concretions related to type 2 veins contain various stages of replacement of clay altered schist and diabase on Jackson Hill. These relationships indicate that cementation and/or replacement of partially or completely clay altered bedrock must have occurred during clay alteration. In addition, there is a positive correlation between increased alteration and abundance of the veins, further suggesting that types 1, 2 and 3 veins were emplaced during alteration of the Footwall Zone rocks.

DISCUSSION

The field relationships, mineralogy and chemistry of alteration in White Channel gravelly sediments contrasts with the observed features of surface weathering horizons and residual kaolin deposits. Bleached Zone alteration in the White Channel sediments is completely isolated from the surface weathering zone. In addition, the relationship of unaltered sediments overlying altered sediments (with a sharp boundary separating the two units) is zoned contrary to what would be expected in a surface weathering environment. Alteration from the percolation of surface fluids should result in a gradational change from altered to unaltered material with increasing depth below the surface.

In some respects, the intense kaolinization of Bleached Zone White Channel sediments is similar to the lower zones of laterites developed during weathering in locations such as the Tertiary sediments of South Carolina and Georgia (Harder, 1952; Hassanipak and Eslinger, 1985) and the Ordovician sandstones of the Chateaubriant area of Brittany (Esteoule-Choux, 1983). In lateritic type deposits, kaolinization is accompanied by the development of ironstone pisoliths or concretions consisting of kaolinite, iron-oxides, iron-hydroxides and occasionally iron-carbonates. The entire kaolinite zone of laterites is usually pervasively iron-stained due to residual enrichment and oxidation of iron. These features develop during surface weathering, from either downward-percolating meteoric fluids or a fluctuating water table (Loughnan and Bayliss, 1961). In contrast, however, the kaolinized White Channel sediments appear to be bleached and show no evidence of enrichment and oxidation of iron relative to unaltered sediments, except in a 2 to 3 m horizon of altered gravel at the bedrock contact. This further suggests that alteration of the White Channel sediments was not the product of surface weathering processes.

The mineralogy of the Bleached, Iron and Footwall Zones shows surface differences with that of residual deposits in the surface weathering zone. For example, residual kaolin deposits, laterites and bauxites are usually characterized by the presence of minerals such as kaolinite, diasporite, gibbsite, iron-oxides and iron-hydroxides. The crystallinity of these minerals is generally poor, with minerals such as kaolinite and the iron-hydroxides exhibiting broad, ill-defined peaks on their X-ray patterns. Kaolinite produced from the supergene alteration of clastic sediments in Devon, England (Vincent, 1983); Chateaubriant, Brittany (Esteoule-Choux, 1983; Keller, 1976a) and South Carolina and Georgia (Hassanipak and Eslinger, 1985; Hinckley, 1963; Keller, 1976b) is characterized by low crystallinities with Hinckley (1963) crystallinity indexes generally less than 0.3.

In contrast to the above residual deposits, secondary kaolinite from the Iron and Footwall Zones generally has an HCl of greater than 1.0. In addition, well crystallized illite and iron-hydroxides are also present in the Iron and Footwall Zones. The high crystallinity index of kaolinite is very similar to that of hydrothermally produced kaolinite from Japan (Keller, 1977), Mexico (Hanson et al., 1981; Keller and Hanson, 1968, 1969) and England (Bristow, 1977; Vincent, 1983). The high crystallinity of lepidocrocite is similar to the well crystallized hydrothermal lepidocrocite reported at the Enfield Bell Mine of Nevada (Birak and Hawkins, 1985). Interstratified illite/smectite or chlorite/smectite, present in the Iron and Footwall Zones, has also been reported in the hydrothermal alteration zones of northeast Japan (Inoue et al., 1983; Inoue and Utada, 1983; Matsuda et al., 1981a, 1981b). Adularia, present in the Iron Zone and altered rhyolite cobbles, is commonly reported as a hydrothermal phase often associated with muscovite and kaolinite in hydrothermal vein deposits and the upper levels of alteration halos associated with geothermal hot-spring deposits (Berger, 1985; Buchanan, 1980, 1981). Thus, White Channel alteration contrasts to what one would expect in a surface weathering environment, and bears a distinct resemblance to hydrothermal alteration zones associated with vein deposits and geothermal systems.

Trace element concentrations of the Iron Zone gravel are similar to the chemical signatures of many epithermal vein deposits and geothermal systems. The near-surface geothermal environment, including sinters, hot-spring pools and argillic alteration halos, typically contains high levels of Au, As, Sb, Hg, Ti, Fe, Mn, Ba, Co, P, S and F (Weissberg et al., 1979; White, 1981, 1985). Precious metal vein deposits contain a similar enrichment of these trace elements in veins and alteration halos formed near the paleosurface and at low temperatures (less than 200°C) (Berger, 1985; Buchanan, 1980, 1981). Within the Iron Zone gravel, anomalous concentrations of Fe, Mn, As, Sb, Hg, Co, Ba and S were introduced during alteration. The similarities of this trace element enrichment to the trace element suite commonly found in the near-surface hydrothermal environments described above also suggests that similar hydrothermal processes were responsible for the alteration of the White Channel gravels.

The presence of types 1, 2 and 3 veins in the Footwall Zone lends further support to a hydrothermal origin for alteration of the White Channel gravels. Replacement textures, incorporated clay altered bedrock and their spatial relationship to Footwall Zone rocks suggest that the veins were emplaced during alteration of the footwall rocks and the overlying sediments. In addition, the presence of chalcedony and/or opal, and banding, cockscomb, cockade and crustiform textures is characteristic of veins and associated alteration halos formed by low temperature hydrothermal fluids within 100-200 m of the surface (Berger, 1985; Buchanan, 1980, 1981; Hedenquist and Henley, 1985). Consequently, types 1, 2 and 3 veins were deposited by low temperature (less than 200°C) hydrothermal fluids during the post-depositional alteration of the White Channel gravels and underlying footwall rocks.

SUMMARY

A post-depositional hydrothermal alteration product in White Channel sediments and underlying bedrock is divided into 3 zones. These zones termed the Bleached Zone, the Iron Zone, and the Footwall Zone are characterized by the development of secondary clay minerals with moderate to high crystallinities. Trace element concentrations of Fe, Mn, As, Sb, Hg, Co, Ba and S are anomalously high in the Iron and Footwall zones. Three types of low temperature, post-metamorphic veins appear to be spatially related to both the distribution and intensity of alteration. Field relationships of altered and unaltered White Channel sediment show zoning patterns which cannot be explained by surface weathering and percolation of meteoric surface fluids.

Economic implications of the alteration of White Channel alluvium are that there may be a hydrothermal style of gold mineralization, in addition to gold which was initially deposited in a placer environment. Testing and exploration of altered White Channel alluvium should be done with this in mind, particularly for extremely fine-grained gold which may accompany the alteration product.

REFERENCES

- BERGER, B.R., 1985. Geological-geochemical features of hot-spring precious-metal deposits; in *Geologic characteristics of sediment- and volcanic-hosted disseminated gold deposits — search for an occurrence model*; Tooker, E.W. (ed.), U.S.G.S. Bulletin 1646, p. 47-54.
- BRISTOW, C.M., 1977. A review of the evidence for the origin of kaolin deposits of S.W. England; in *Proceedings of the 8th Int. Kaolin Symp. Mtg. Alunite, Madrid, Rome*, p. 1-19.
- BUCHANAN, L.J., 1980. Ore controls of vertically stacked deposits, Guanajuato, Mexico; Society of Mining Engineers of A.I.M.E., Preprint no. 80-82, 16 p.
- BUCHANAN, L.J., 1981. Precious metal deposits associated with volcanic environments in the southwest; in *Relationships of tectonics to ore deposits in the southern Cordillera*; W.R. Dickinson and W.D. Payne, (eds.), Arizona Geological Society Digest Vol. XIV, Tucson, Arizona, p. 237-262.
- BURAK, D.J. and HAWKINS, R.J., 1985. The geology of the Enfield Bell mine and the Jerritt Canyon district, Elko County, Nevada; in *Geologic characteristics of sediment- and volcanic-hosted disseminated gold deposits — Search for an occurrence model*; Tooker, E.W. (ed.), U.S.G.S. Bulletin 1646, p. 95-106.
- DUFRESNE, M.B., 1986. Origin of gold in the White Channel sediments of the Klondike region, Yukon Territory; Unpublished MSc thesis, University of Alberta, Edmonton, Alberta.
- DUFRESNE, M.B. and MORISON, S.R., 1985. Stratigraphy and alteration of the White Channel gravel at Dago Hill, a progress report, Klondike area, Yukon; in *Yukon Exploration and Geology 1983*; Exploration and Geological Services Division, D.I.A.N.D., Yukon, p. 55-59.
- ESTEOULE-CHOUX, J., 1983. Kaolinitic weathering profiles in Brittany: genesis and economic importance; in *Residual deposits: surface related weathering processes and materials*; Geol. Soc. Spec. Pub., No. 11, Wilson, P.C.L. (ed.), Blackwell Science Publications, p. 33-38.
- HANSON, R.F., ZAMORA, R., and KELLER, W.D., 1981. Nacrite, dickite and kaolinite in one deposit in Nayarit, Mexico; *Clays and Clay Minerals*, Vol. 29, No. 6, p. 451-453.
- HARDER, E.C., 1952. Examples of bauxite deposits illustrating variations in origin; in *Problems of clay and laterite genesis*; Symposium at Ann. Meet. of Am. Inst. of Min. and Met. Eng., St. Louis, Missouri, 1951, Pub. by A.I.M.E., p. 35-64.
- HASSANIPAK, A.A. and ESLINGER, E., 1985. Mineralogy, crystallinity, O¹⁸/O¹⁶ and D/H of Georgia kaolins; in *Clays and Clay Minerals*, Vol. 33, No. 2, p. 99-106.
- HEDENQUIST, J.W. and HENLEY, R.W., 1985. Hydrothermal eruptions in the Waiotapu geothermal system, New Zealand: Their origin, associated breccias, and relation to precious metal mineralization; *Econ. Geol.*, Vol. 80, p. 1640-1668.
- HINCKLEY, D.N., 1963. Variability in "crystallinity" values among the kaolin deposits of the coastal plain of Georgia and South Carolina; in *Clays and Clay Minerals*, Mono. 13, Proc. 11th Natl. Conf., Ottawa, Ont., 1962; Perg. Press, N.Y., p. 229-235.
- HUGHES, O.L., RAMPTON, V.N. and RUTTER, N.W., 1972. Quaternary geology and geomorphology, Southern and Central Yukon (Northern Canada); XXIV International Geological Congress, Montreal, 1972; Excursion A11, p. 30-34.
- INOUE, A., MINATO, H. and UTADA, M., 1983. Mineralogical properties and occurrence of illite/montmorillonite mixed layer minerals formed from Miocene volcanic glass in Wagga-Omono district; *Clay Science*, Vol. 5, p. 123-136.
- INOUE, A. and UTADA, M., 1983. Further investigations of a conversion series of dioctahedral mica/smectites in the Shinzan hydrothermal area, Northeast Japan; in *Clay and Clay Minerals*, Vol. 31, No. 6, p. 401-412.
- KELLER, W.D. and HANSON, R.F., 1968. Hydrothermal alteration of a rhyolite flow breccia near San Luis Potosi, Mexico to refractory kaolin; in *Clays and Clay Minerals*, Vol. 16, p. 223-229.
- KELLER, W.D. and HANSON, R.F., 1969. Hydrothermal argillation volcanic pipes in limestone, Mexico; in *Clays and Clay Minerals*, Vol. 17, p. 9-12.
- KELLER, W.D., 1976a. Scan electron micrographs of kaolins collected from diverse environments of origin- I; in *Clays and Clay Minerals*, Vol. 24, p. 107-113.
- KELLER, W.D., 1976b. Scan electron micrographs of kaolins collected from diverse environments of origin- II; in *Clays and Clay Minerals*, Vol. 24, p. 114-117.
- KELLER, W.D., 1977. Scan electron micrographs of kaolins collected from diverse environments of origin- V. Kaolins collected in Australia and Japan on field trips of the sixth and seventh clay conferences; in *Clays and Clay Minerals*, Vol. 25, p. 347-364.
- LOUGHNAN, F.C. and BAYLISS, P., 1961. The mineralogy of the bauxite deposits near Weipa, Queensland; *American Mineralogist*, Vol. 46, p. 209-217.
- MATSUDA, T., HENMI, K., NAGASAWA, K. and HONDA, S., 1981a. Chemical composition and X-ray properties of regularly interstratified mica/smectites; *Journ. Miner. Soc. of Japan, Spec. Iss.*, Vol. 15, p. 96-106.
- MATSUDA, T., NAGASAWA, K., TSUZUKI, Y. and HENMI, K., 1981b. Regularly interstratified dioctahedral mica/smectite from Roseki deposits in Japan; *Clay Minerals*, Vol. 16, p. 91-102.

- McCONNELL, R.G., 1905. Report on the Klondike gold fields; in Ann. Report for 1901, Vol. XIV, pt.B, Geol. Surv. Can. Pub., No. 884, p. 1-71.
- McCONNELL, R.G., 1907. Report on the gold values in the Klondike high level gravels; Geol. Surv. Can. Pub., No. 979, 34 p.
- MILNER, M.W., 1976. Geomorphology of the Klondike placer goldfields; Final report, Contract OSV 5-0047, D.I.A.N.D., Exploration and Geological Services Division, Yukon, 157 p.
- MORISON, S.R., 1985. Sedimentology of White Channel placer deposits, Klondike area, West-Central Yukon; Unpublished MSc Thesis, University of Alberta, Edmonton, Alberta, 149 p.
- NALDRETT, D.L., 1981. Aspects of the surficial geology and permafrost conditions, Klondike goldfields and Dawson City, Yukon Territory; Unpublished MSc Thesis, University of Ottawa, Ottawa, Ontario. 150 p.
- RUTTER, N.W., FOSCOLOS, A.E. and HUGHES, O.L., 1978. Climatic trends during the Quaternary in central Yukon based upon pedological and geomorphological evidence; in Quaternary soils, reprinted from the Third York Quaternary Symposium, Pub. by Geol. Abs., Norwich, England, p. 309-359.
- TEMPELMAN-KLUIT, D.J., 1982. White Channel gravel of the Klondike; in Yukon Exploration and Geology, 1981; D.I.A.N.D., Exploration and Geological Services Division, Yukon, p. 74-79.
- VINCENT, A., 1983. The origin and occurrence of Devon ball clays; in Residual deposits: surface related weathering and materials; Geol. Soc. Spec. Pub. No. 11, Wilson, R.C.L. (ed.), Blackwell Science Pub., p. 39-45.
- WEISSBERG, B.C., BROWN, P.R.L. and SEWARD, T.M., 1979. Ore metals in active geothermal systems; in Geochemistry of hydrothermal ore deposits, Barnes, H.L. (ed.), John Wiley and Sons Inc., p. 738-780.
- WHITE, D.E., 1981. Active geothermal systems and hydrothermal ore deposits; in Seventy-fifth anniversary volume, 1905-1980; Skinner, B.J. (ed.), Econ. Geol. Publishing Co., El Paso, Texas, p. 392-423.
- WHITE, D.E., 1985. Summary of Steamboat Springs geothermal area, Nevada, with attached road-log commentary; in Geologic characteristics of sediment- and volcanic-hosted disseminated gold deposits-Search for an occurrence model; Tooker, E.W. (ed.), U.S.G.S. Bulletin 1646, p. 79-88.

PLACER GRAVELS OF MILLER CREEK, SIXTYSILE RIVER AREA, 116 B,C

Rhys L. Hughes
Department of Geology
University of Alberta
Edmonton, Alberta

S.R. Morison
Exploration and Geological Services Division
Indian and Northern Affairs Canada
Whitehorse, Yukon

and

F.J. Hein
Department of Geology
University of Alberta
Edmonton, Alberta

HUGHES, R.L., MORISON, S.R. and HEIN, F.J., 1986. Placer gravels of Miller Creek, Sixtymile River Area, 116 B,C; in Yukon Geology, Vol. 1; Exploration and Geological Services Division, Yukon, Indian and Northern Affairs Canada, p. 50-55.

MEMORIAL

Rhys Hughes died in a tragic accident during the summer of 1986. Rhys worked for the Geology Division for three summers studying the geology of placer deposits in the Klondike, Sixtymile and Big Creek areas. He completed a Master of Science thesis on placer deposits in the Sixtymile area, and as a result has produced new insights to alluvial sedimentation and placer deposit information in unglaciated areas in Yukon Territory. He was a diligent and reliable worker who was well liked by his colleagues at Northern Affairs and by the placer miners whom he worked with. He will be missed.

INTRODUCTION

Miller Creek and four other small tributaries of the Sixtymile River drainage basin (Fig. 1) were the sites of rich placer discoveries in 1892 (Gilbert, 1983). The first important geological report on the Sixtymile River was by Cockfield (1921) who described regional geology, stratigraphy and location and value of placer gold recovered by the early miners. At that time, total gold production by hand mining and a small dredge operation was 50 million U.S. dollars, at \$30.00 per ounce.

The distribution of gold-bearing gravelly sediments in the Sixtymile area is related to geomorphic history, gravel stratigraphy and fluvial sedimentology. This report relates the distribution of placer gold to Quaternary depositional environments of gravelly sediments in the Miller Creek area. It is hoped that this report will enhance results and interpretations from exploration and testing programs in the Sixtymile River placer area.

PREVIOUS WORK

In the Sixtymile River area, Cockfield (1921) provided notes on general stratigraphy of the gravel exposures in pits and shafts. Debicki (1983) described the locations, mining methods and general stratigraphy of active placer mining properties in the Sixtymile River area. Glasmacher (1984) and Glasmacher and Friedrich (1985) described the bedrock geology, petrology, mineralization, general placer settings and heavy minerals suites.

GENERAL GEOLOGY AND STRATIGRAPHY

The study area is within Yukon Cataclastic Complex, which is comprised of three assemblages of highly sheared and metamorphosed rocks that are thrust over less deformed strata of the Nasina Shelf and Cassiar Platform (Tempelman-Kluit, 1981).

The Pelly Gneiss (a foliated muscovite-biotite granodiorite of assumed Paleozoic age), and the Klondike Schist (a chlorite-muscovite schist) outcrop immediately south of the study area. In the Sixtymile River area, metamorphosed Nasina Series basement rocks are not dated, but elsewhere are traceable into the Lower Ordovician to possibly Mississippian sedimentary rocks of the

Cassiar Platform (Tempelman-Kluit, 1981).

Nasina Series rocks are overlain by volcanic rocks of the Carmacks Group (Tempelman-Kluit, 1974) of late Cretaceous age (Nelson, 1985). These andesites, dacites and tuffs underlie gravelly sediments at Sections 3 to 7 in the Sixtymile River valley, and Section 8 in the Glacier Creek valley (Fig. 1). Locally along the Sixtymile River, sandstone, shale and conglomerates underlie and are interbedded with Carmacks volcanic rocks (Tempelman-Kluit, 1973; Lowey, 1982). Carmacks volcanics are overlain by flat-lying alkali-olivine flow basalts of the Quaternary Selkirk Group.

PHYSIOGRAPHY, QUATERNARY DEPOSITS AND LANDFORMS

The Sixtymile placer area is in the unglaciated portion of the western Yukon Plateau or the Klondike Plateau (Bostock, 1948). This rolling upland landscape formed during the Tertiary after deposition of the Carmacks Group volcanics and before the onset of White Channel valley-fill deposition (Bostock, 1948, Cockfield, 1921). The general physiography of the Sixtymile River area is an accordant surface with elevations up to 1,300 metres that has been deeply dissected by stream erosion (Cockfield, 1921). Tempelman-Kluit (1980) suggests that this plateau surface was incised and eroded after the Eocene and before the Pliocene. Prior to the Pliocene, the Sixtymile River was a tributary of the paleo-Yukon River system which drained southerly. Drainage diversions to the north began with differential uplift of the Yukon Plateau, and were completed during the Pleistocene as a result of glacial advances and ice-damming (Tempelman-Kluit, 1980).

Quaternary deposits of the Sixtymile River drainage basin include valley bottom alluvial plains and terraces, gulch alluvium, colluvial veneers and blankets, and scattered debris flows (Fig. 1). The youngest Quaternary deposits include active colluvium, valley bottom gulch alluvium and the broad alluvial plain in the Sixtymile River valley. Older alluvial deposits include the higher terrace levels in the upper reaches of Miller and Glacier Creeks, the second terrace level in the lower reaches of Miller Creek, and the broad terrace found on the north side of the Sixtymile River valley, both upstream and downstream from Miller Creek (Fig. 1).

Miller Creek and Glacier Creek are both in asymmetric valleys which contain high level terraces on the northeast side (looking upstream) of the valley slope (Fig. 1). In the upper reaches of these creeks, narrow terraces are found approximately 20 metres above the valley floor. These terraces are underlain by alluvial-fill sequences up to 10 metres thick. In the lower reaches of Miller Creek, a second terrace level is contained by a bedrock topographic high, and is underlain by 20 metres of alluvium (Fig. 2). This tributary terrace system was deposited as a confined alluvial fan which prograded into the main Sixtymile valley. Only an eroded remnant of a similar terrace exists in the lower part of Glacier Creek. The third, and largest terrace within the study area is found on the north side of the Sixtymile River valley (Fig. 1). The main Sixtymile terrace system was initially deposited as a braidplain sequence before incision. Hughes (1970) suggests that inci-

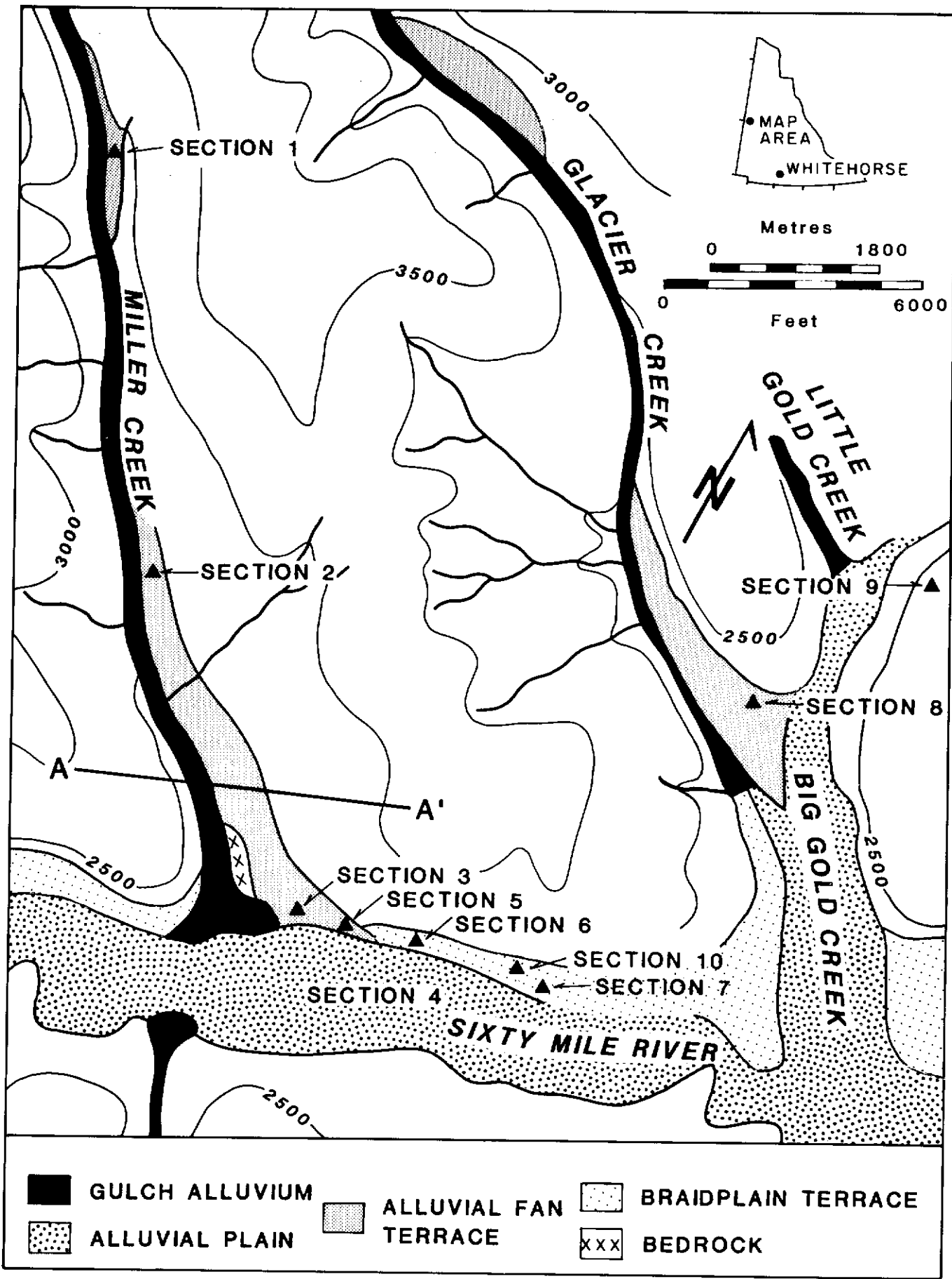


Figure 1. Location map for study area, showing section locations and types of placer deposits.

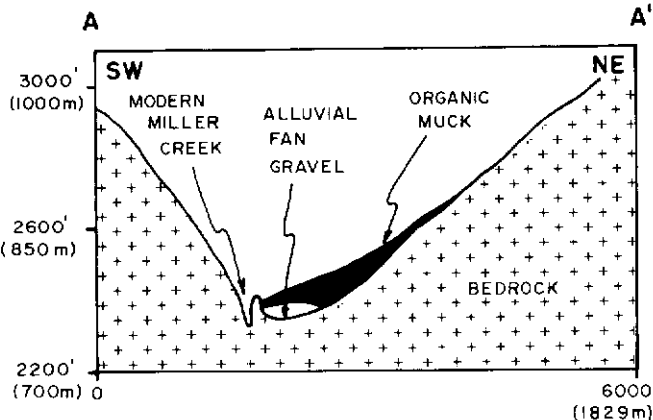


Figure 2. Cross-section A-A' of lower Miller Creek showing relative position of the modern channel to the alluvial fan terrace gravel and the colluvial blanket of organic muck.

sion and preservation of these terraces is the result of Pliocene-Pleistocene uplift in the Klondike area.

CHRONOLOGICAL HISTORY OF INCISION AND VALLEY-FILL AGGRADATION AT MILLER CREEK

After reaching a local base level, paleo-Miller Creek underwent a period of valley widening through the initiation of alluvial fan sedimentation (Fig. 3a). This widening resulted in the deposition of discontinuous placer concentrations over a broad paleo-Miller Creek valley bottom. Within the main Sixtymile River valley, braided river alluvium was also depositing discontinuous concentrations of placer minerals. Lateral widening of the main Sixtymile River valley was accompanied by headward migration of the paleo-Miller Creek alluvial fan. Aggradation of the paleo-Miller Creek alluvial fan was accompanied by progradation into the Sixtymile River valley (Fig. 3b). At the confluence of the broad Sixtymile braidplain and paleo-Miller Creek valley, erosion of distal Miller Creek fan gravel by Sixtymile braided alluvium may have signif-

icantly contributed to point sources of placer gold in Sixtymile alluvium. This may explain placer gold enrichment on bedrock in this location (M. Brisbois, pers. comm.).

Radiocarbon dates from *in situ* wood interbedded within Miller Creek fan gravel (GSC-4032), and *in situ* peat above upper fan gravel (GSC-3934) indicates that Miller Creek fan sedimentation was complete before 40,000 years ago.

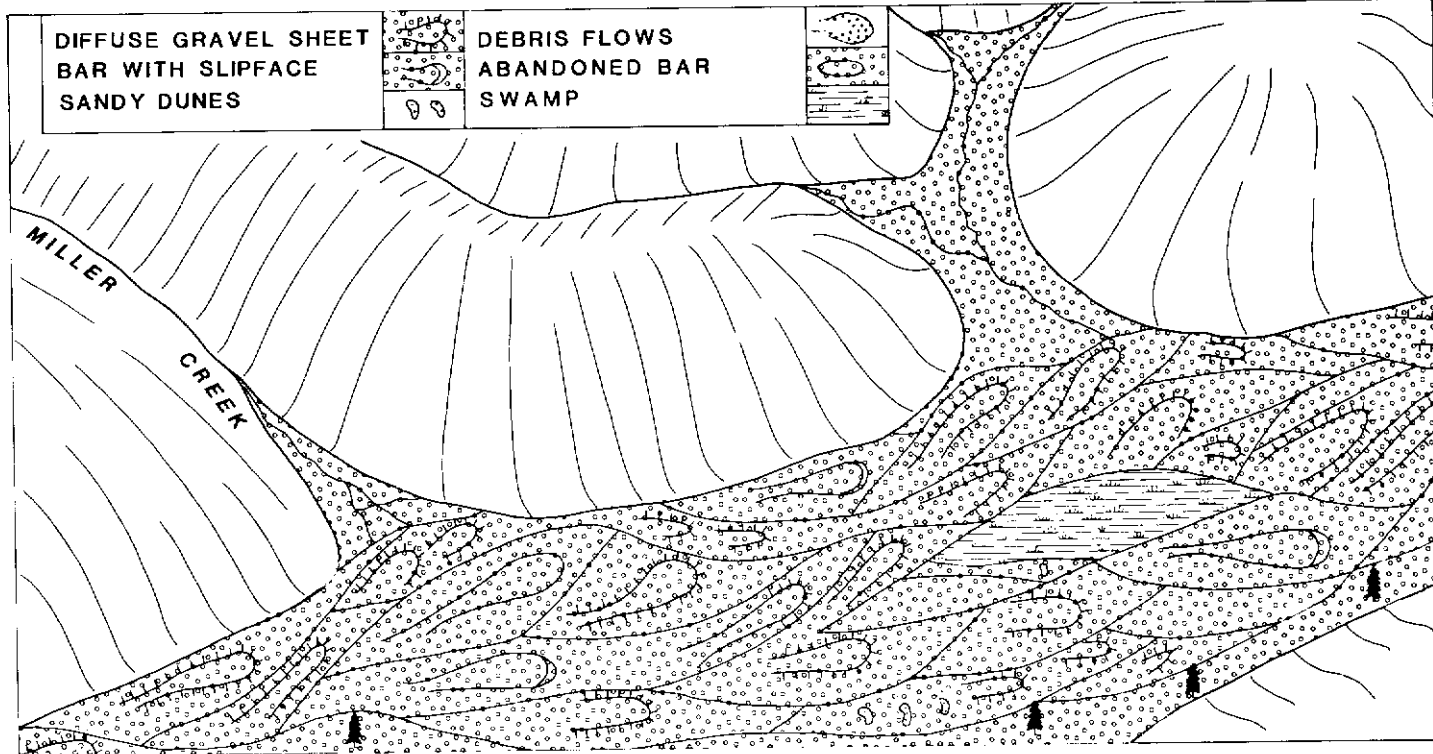
A radiocarbon date (Beta-13870) from wood in muddy sediments (Section 7; Fig. 1) indicates that by 26,000 years ago, surficial processes were dominated by debris flow sedimentation. Also, during this time Miller Creek alluvial fan and Sixtymile braidplain aggradation was complete and active incision with terrace development was occurring. During incision of the Sixtymile braidplain, the stream environment changed to a single channel meandering system (Fig. 3c). Timing for the incision and formation of the modern channel of Miller Creek is difficult to judge, but may have occurred concurrently with the change in the channel pattern of the Sixtymile River.

After terrace development in the Sixtymile drainage basin, continued debris-flow and loess sedimentation dominated surficial processes (Fig. 3d). Minor vertical aggradation of stream gravel and valley widening in the modern Miller Creek channel occurred during the Holocene.

REGIONAL DISTRIBUTION OF PLACER GOLD

Based on the historical records provided by Cockfield (1921) and samples collected during the field season, the highest concentrations of placer gold appear to be in the tributary terrace levels of Miller and Glacier Creeks (Fig. 4). Lode sources for placer gold include structurally controlled vein systems and Tertiary epithermal mineralization (Glasmacher, 1984; Glasmacher and Friedrich, 1985).

Historical records (Cockfield, 1921) indicate the presence of a poorly defined paystreak at the base of the upper terrace level at Miller Creek (Fig. 4). This paystreak is found in massive, angular gravels which have a preferred a-axis upstream imbrication type (Sections 1,2; Fig. 1). These characteristics suggest local gravelly sedimentation in the form of hyperconcentrated flood flows. In contrast, gravelly beds interpreted as proximal talus and colluvium at the same sites are barren of gold. The associated hydrodynamics



SW

NE

Figure 3a. Sketch showing sedimentary environments of the Sixtymile River and Miller Creek prior to fan aggradation. Note the initiation of tributary valley widening and braidplain environment of the main valley which has a stream flow direction from left to right.

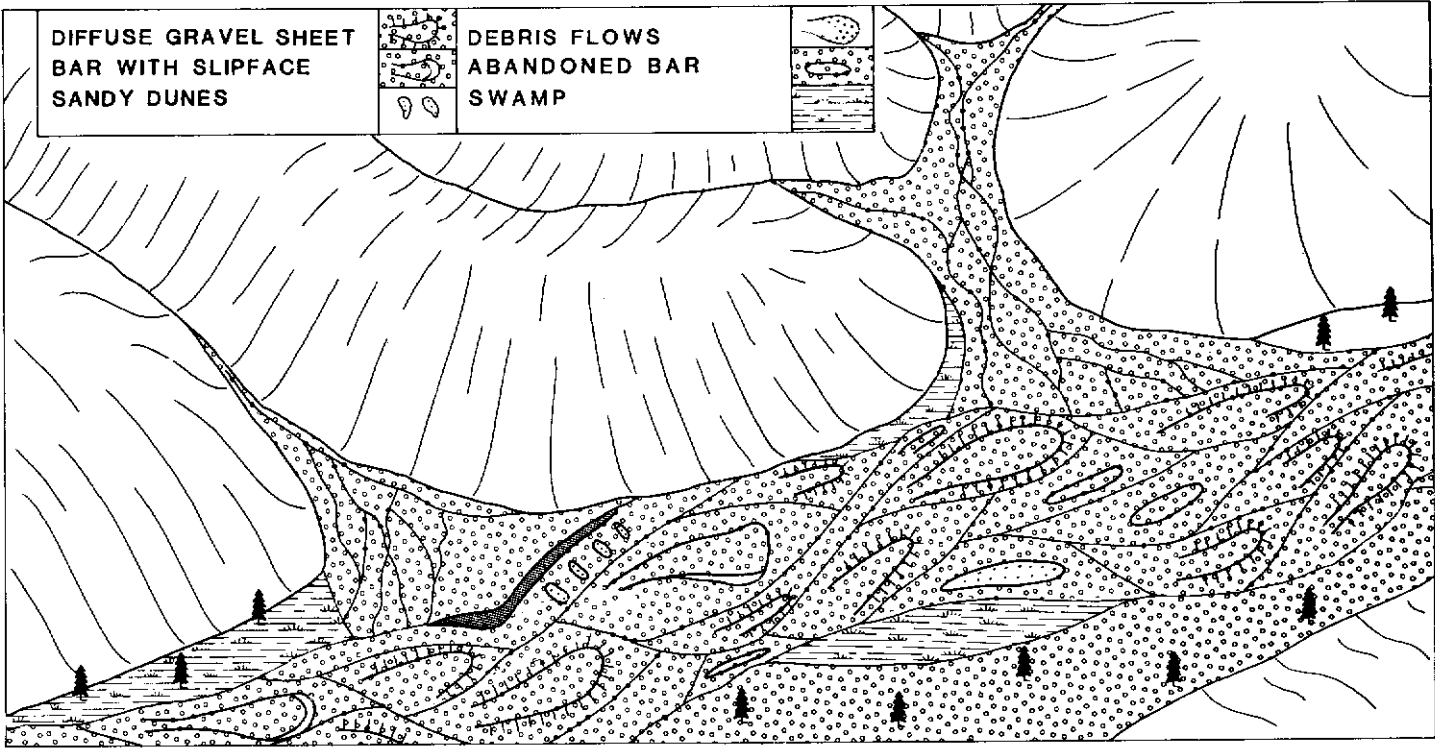


Figure 3b. Sketch showing aggradation of Miller Creek alluvial fan. Fan aggradation was complete before 40,000 years ago; and note the erosion of distal fan sediments by the Sixymile River.

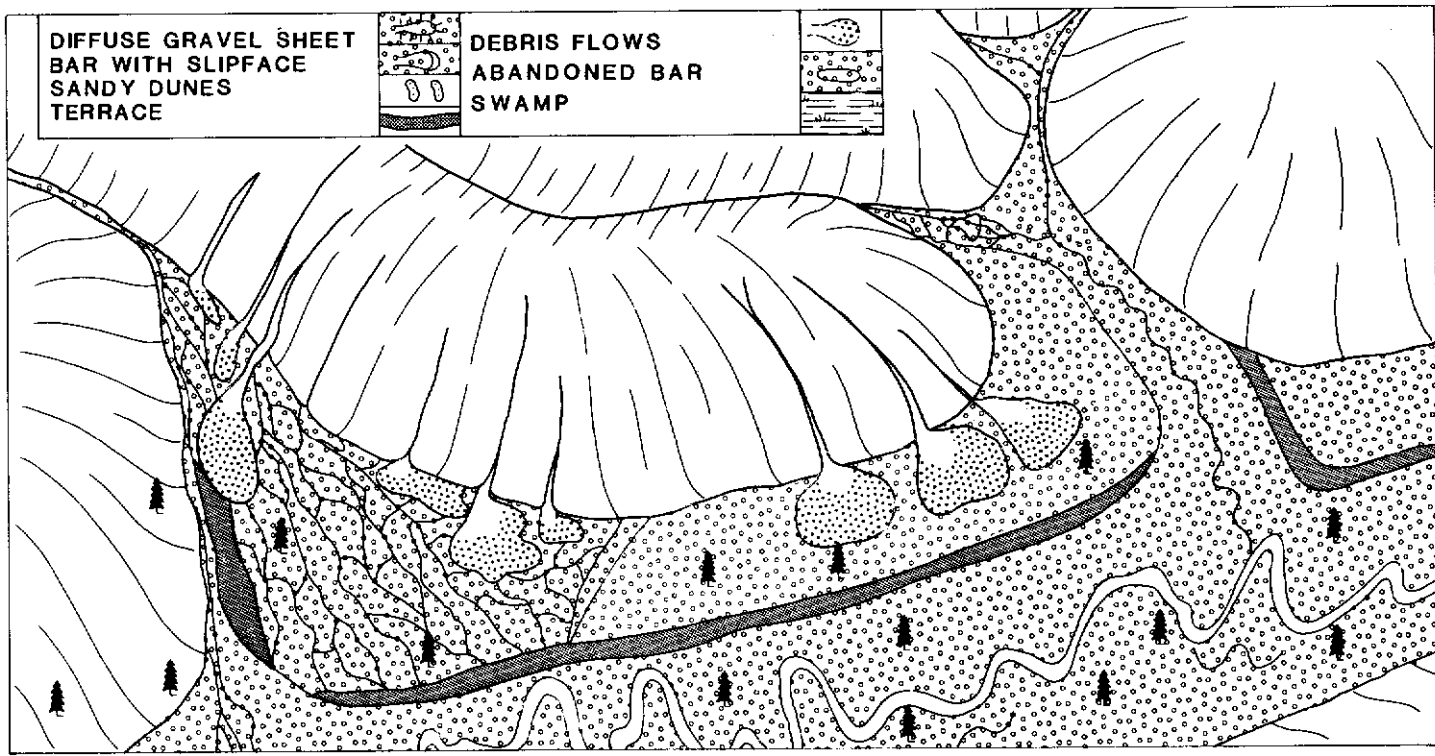


Figure 3c. Sketch showing debris flow sedimentation and terrace development 26,000 years ago. Note Miller Creek is being diverted to the SW side of the valley and is beginning to incise a new channel, and the Sixymile River has changed channel pattern from braided to meandering.

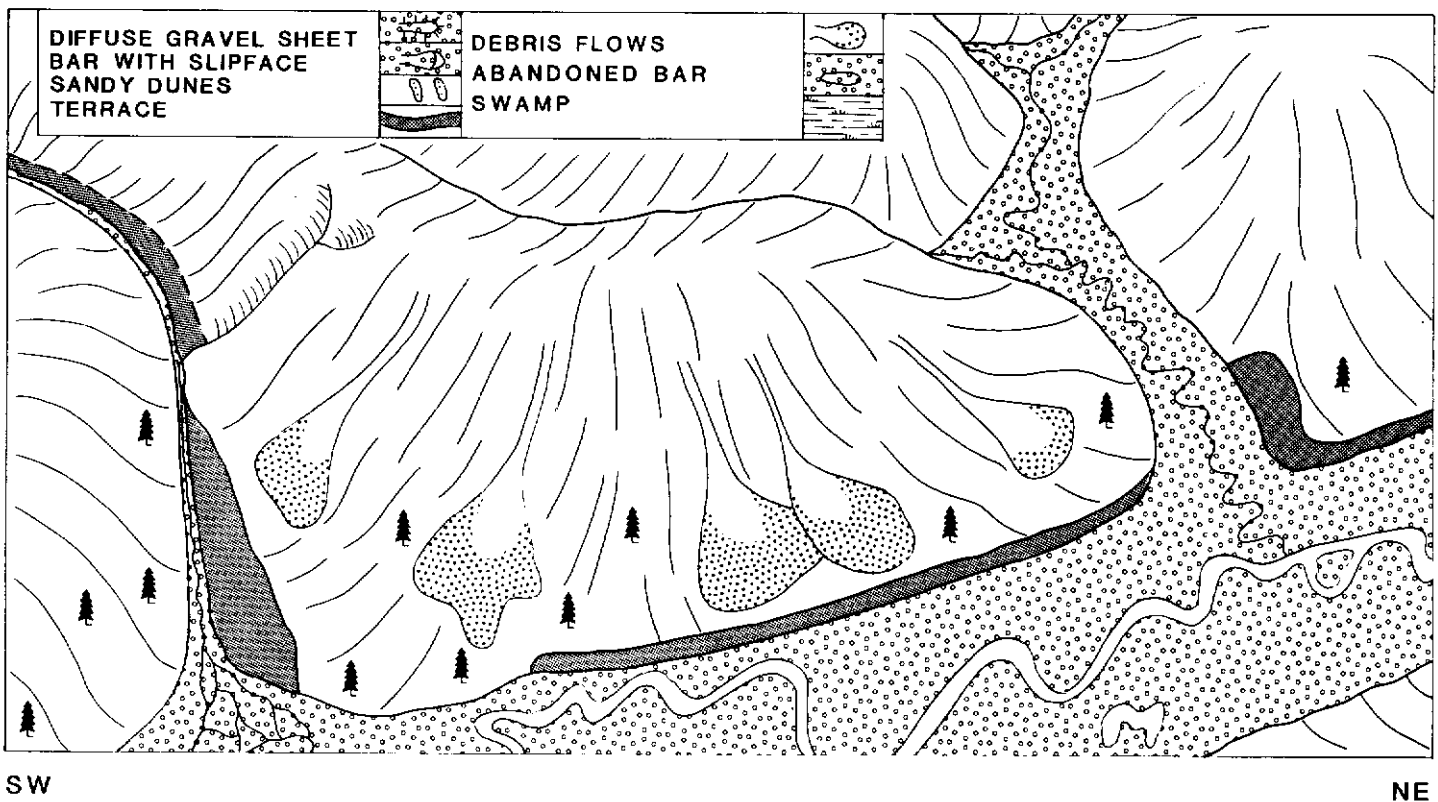
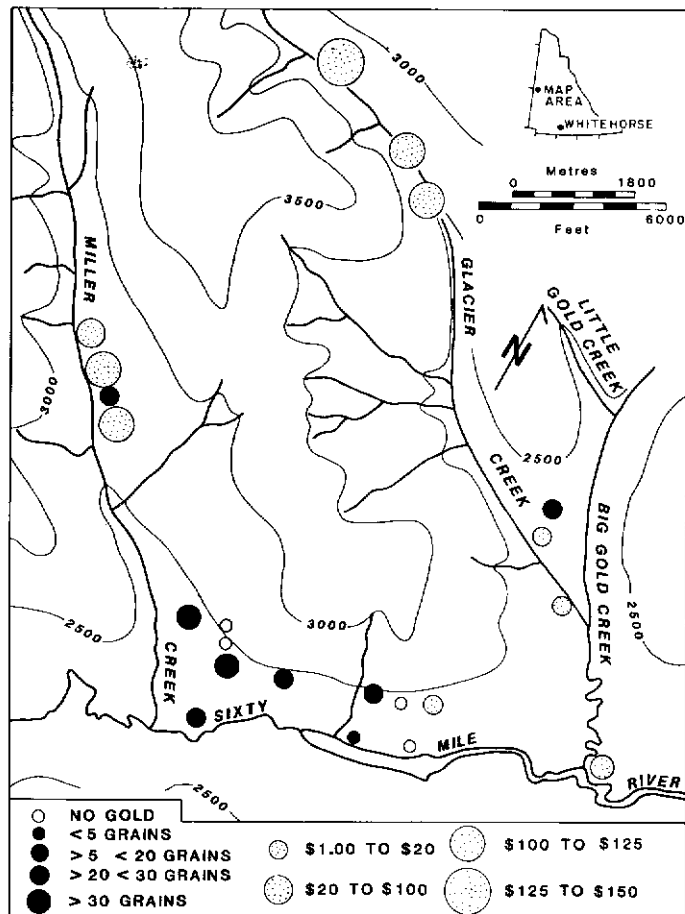


Figure 3d. Sketch showing post-terrace development with active debris flow sedimentation and valley widening at the mouth of Miller Creek.

of flood flow gravelly sediments suggests they are not favourable sites for heavy mineral concentration. However, rich accumulations of placer gold do occur in this setting, and thus point to the presence of local bedrock point sources.



Distal terrace levels in Miller Creek valley (Sections 3,5; Fig. 1) contain aggraded sequences of massive gravel sheets. The distinct lack of sedimentary structures and the poorly sorted nature of these distal gravelly sediments indicates lack of convergent or concentrating stream flow. However, limited sampling and historical records have shown that economic concentrations of placer gold are found at the bedrock surface (Fig. 4). It is also interesting to note that gold concentration levels appear to decrease distally in the Miller Creek fan sequence (Fig. 4). The above observations suggest a local gold provenance, which was depleted during aggradation of the fan. In a general sense, the preferred site of placer formation in Miller Creek fan gravel is at the bedrock surface where coarse-grained, massive lag gravel trapped gold particles.

The Sixymile River terrace gravels (Fig. 1) are interpreted to be the product of a medial braidplain sequence. Economic gold concentrations are scattered (Fig. 4) and are typical for a braided environment where local point sources are discontinuous and stream flow patterns are variable (Smith and Minter, 1980).

None of the bulk samples from Sixymile alluvial plain gravel (Fig. 4) contained an appreciable enrichment of placer gold, although there was an abundance of other heavy minerals in massive gravels found in contact with the bedrock surface. Possible explanations for the lower concentrations of gold in this setting include "flushing" of the heavy minerals (Adams et al., 1978) or change of gravel source areas during incision of the Sixymile River to its present level.

SUMMARY

Within the Sixymile River drainage basin, Quaternary placer deposits include tributary valley bottom gulch gravel, a broad main valley alluvial plain, and high level terrace systems in both tributary and main valley settings. After downcutting, paleo-Miller Creek underwent valley widening during alluvial fan erosion and sedimentation. During this time, the main Sixymile River valley was

Figure 4. Distribution of placer gold in study area. Solid circles are samples collected by authors and patterned circles are values reported by Cockfield (1921). Cockfield's estimates refer to the amount of gold (at \$20.67 U.S. per fine ounce) present in one sluice box length which is equivalent to 12 square feet.

also being laterally eroded during braidplain aggradation. Terrace development and incision through both fan and braidplain sediments coincided with significant debris flow sedimentation. The Sixtymile River changed from a braided environment to single channel meandering environment during terrace development. Incision of Miller Creek through the fan surface to present levels probably coincided with downcutting of the Sixtymile River. Economic concentrations of placer gold are found in: 1) the upper Miller Creek terrace where coarse-grained, massive and angular

flood flow gravel forms a crude pay streak above the bedrock surface; 2) the distal Miller Creek terrace where discontinuous concentrations of gold were formed over a broad paleo-surface of lag gravel prior to fan aggradation; 3) laterally discontinuous pockets in the main Sixtymile valley terrace which was originally part of an aggraded braidplain sequence; and 4) lower, but still economic placer concentrations in gravels of the alluvial plain in the main Sixtymile valley.

REFERENCES

- ADAMS, J., ZIMPFER, G.L., and McLANE, C.F., 1978. *Basin dynamics, channel processes, and other placer formation: a model study*; Econ. Geol., Vol. 73, p. 416-426.
- BOSTOCK, H.S., 1948. *Physiography of the Canadian Cordillera, with special reference to the area north of the fifty-fifth parallel*; Geol. Surv. Canada, Memoir 247, p. 101.
- CHENEY, E.S., and PATTON, T.C., 1967. *Origin of the bedrock values of placer deposits*; Econ. Geol., Vol. 62, p. 852-860.
- COCKFIELD, W.E., 1921. *Sixtymile and Ladue River area, Yukon*; Geol. Surv. Canada, Memoir 123.
- DEBICKI, R.L., 1983. *Yukon placer mining industry, 1978-1982*; Exploration and Geological Services Division, D.I.A.N.D., Yukon, p. 100-108.
- GILBERT, G.W., 1983. *A brief history of placer mining in the Yukon*; Mining and Engineering Division, D.I.A.N.D., Yukon, 16 p.
- GLASMACHER, U., 1984. *Geology, petrography and mineralization in the Sixtymile River area, Yukon Territory, Canada*; (unpub. MSc thesis), Institut of Mineralogy and Economic Geology, Aachen, Germany.
- GLASMACHER, U., and FRIEDRICH, G., 1985. *Placer gold in the Sixtymile River area, Yukon Territory*. Proceedings of the seventh annual conference on Alaska placer mining; Alaskan Prospecting Publishing, Fairbanks, Alaska, p. 53-57.
- HUGHES, O.L., 1970. *Incidental observations on Quaternary crustal movements, central Yukon Territory*; Can. Jour. Earth Sci., Vol. 7, p. 569.
- LOWEY, G., 1982. *Report of 1982 field work on early Tertiary clastics, west-central Yukon*; Yukon Exploration and Geology 1982; Exploration and Geological Services Division, D.I.A.N.D., Yukon, p. 34-37.
- NELSON, J., 1985. *Cretaceous and Paleogene history of the western Canada Cordillera*; Geol. Surv. Can. Open File 1162.
- SMITH, N.D., and MINTER, W.E.L., 1980. *Sedimentologic controls of gold and uranium in two Witwatersrand paleoplacers*; Econ. Geol., Vol. 75, p. 1-14.
- TEMPELMAN-KLUIT, D.J., 1973. *Reconnaissance geology of Aishihik Lake, Snag and part of Stewart River map-areas, west-central Yukon*; Geol. Surv. Canada, Open File 161.
- TEMPELMAN-KLUIT, D.J., 1974. *Reconnaissance geology of Aishihik Lake, Snag and part of Stewart River map-areas, west-central Yukon Territory*; Geol. Surv. Canada, Bulletin 208, p. 73.
- TEMPELMAN-KLUIT, D.J., 1980. *Evolution of physiography and drainage in southern Yukon*, Can. Jour. Earth Sci., Vol. 17, p. 1189-1203.
- TEMPELMAN-KLUIT, D.J., 1981. *Geology and mineral deposits of southern Yukon*; Yukon Exploration and Geology 1979-1980, Exploration and Geological Services Division, D.I.A.N.D., Yukon, p. 7-31.

EPIGENETIC MINERAL DEPOSITS OF THE KETZA-SEAGULL DISTRICT, YUKON

Grant Abbott
Exploration and Geological Services Division
Indian and Northern Affairs Canada
Whitehorse, Yukon

ABBOTT, J.G., 1986. Epigenetic mineral deposits of the Ketza-Seagull district, Yukon; in Yukon Geology, Vol. 1, Exploration and Geological Services Division, Yukon, Indian and Northern Affairs Canada, p. 56-66.

INTRODUCTION

Most epigenetic occurrences of gold and silver in the Pelly Mountains of central Yukon form two adjacent clusters at the headwaters of the Ketza River and Seagull Creek, which together, occupy a region about 45 km long and 15 km wide, that is here named the Ketza-Seagull district. The origin of these deposits has never been clear because they have been scarcely studied. Many are in Mississippian volcanic and intrusive rocks to which some have been attributed, and none are clearly associated with Mesozoic intrusions. This paper summarizes the characteristics of those deposits (Table 1) which are certainly, or probably, epigenetic, and presents evidence that they are related to a domal uplift here named the Ketza-Seagull Arch (Figure 1), and to one or more buried Cretaceous intrusions.

The writer spent about six weeks in the district in 1985. Descriptions in Table 1 also include information from assessment reports summarized in D.I.A.N.D. publications; Yukon Exploration and Geology or the Mineral Industry Report - Yukon Territory, from Geological Survey of Canada papers entitled The Mineral Industry of Yukon Territory and Southwestern District of Mackenzie, or from the National Mineral Inventory. Archer, Cathro and Associates kindly provided some information from the Northern Cordillera Mineral Inventory. Only the latter source, which is not readily available to the public, is referenced.

Steve Parry with Canamax Resources, Jeff Rowe, Mike Stammers, and Ed Balon with Cordilleran Engineering, and Ian Patterson with Cominco kindly gave the writer informative tours of their properties, were generous with information, and provided stimulating discussion. This study was possible because Cordilleran Engineering allowed the writer to charter their helicopter. Comments by S.R. Morison and D. Tempelman-Kluit improved the manuscript, and are appreciated.

REGIONAL GEOLOGY

The Ketza-Seagull District and surrounding area (Fig. 1) is underlain by Late Proterozoic to Triassic, miogeoclinal clastic, volcanic, and carbonate rocks that were deformed during Mesozoic arc-continent collision, and by mid-Cretaceous intrusions of intermediate composition (Tempelman-Kluit, 1977, 1979). The map units used in this paper are those of Tempelman-Kluit (1977, 1979, in press), and are not described here.

The structural framework is dominated by a few large thrust faults, mainly the McConnell, Porcupine-Seagull-Pass Peak, Cloutier, and St. Cyr, (Tempelman-Kluit, in press) and by the Ketza-Seagull Arch (Fig. 1). The Cloutier thrust sheet is bounded below by the St. Cyr thrust sheet, and above by the Porcupine-Seagull thrust sheet. The Ketza-Seagull Arch is a broad window in which strata in the Cloutier Thrust sheet are exposed beneath the Porcupine-Seagull Thrust. The Ketza Uplift and Seagull Uplift are two parts of the Ketza-Seagull Arch. Shortening on the Porcupine-Seagull-Pass Peak Thrust alone must be at least 30 km. Displacement on the others is probably less, but in the same order of

magnitude. Right lateral, Late Cretaceous and Early Tertiary movement on the Tintina Fault is at least 450 km (Gabrielse, 1985).

KETZA-SEAGULL ARCH

Ketza-Seagull Arch is introduced here as a revision of Ketza Uplift, a term used by Tempelman-Kluit (in press) for a small domal structure centered about the headwaters of the Ketza River. The writer interprets the Ketza-Seagull Arch to include a second dome, called the Seagull Uplift, which together with the Ketza Uplift, forms a window in the Porcupine-Seagull Thrust. The origin of that window is not certain, but is probably, wholly, or in part, related to uplift about one or more buried Cretaceous intrusions. The basis for this revision is some detailed mapping by the writer between Seagull and Groundhog Creeks (Fig. 2) and relatively insignificant reinterpretations of Tempelman-Kluit's (1977, in press) mapping near Ketza River (Fig. 1).

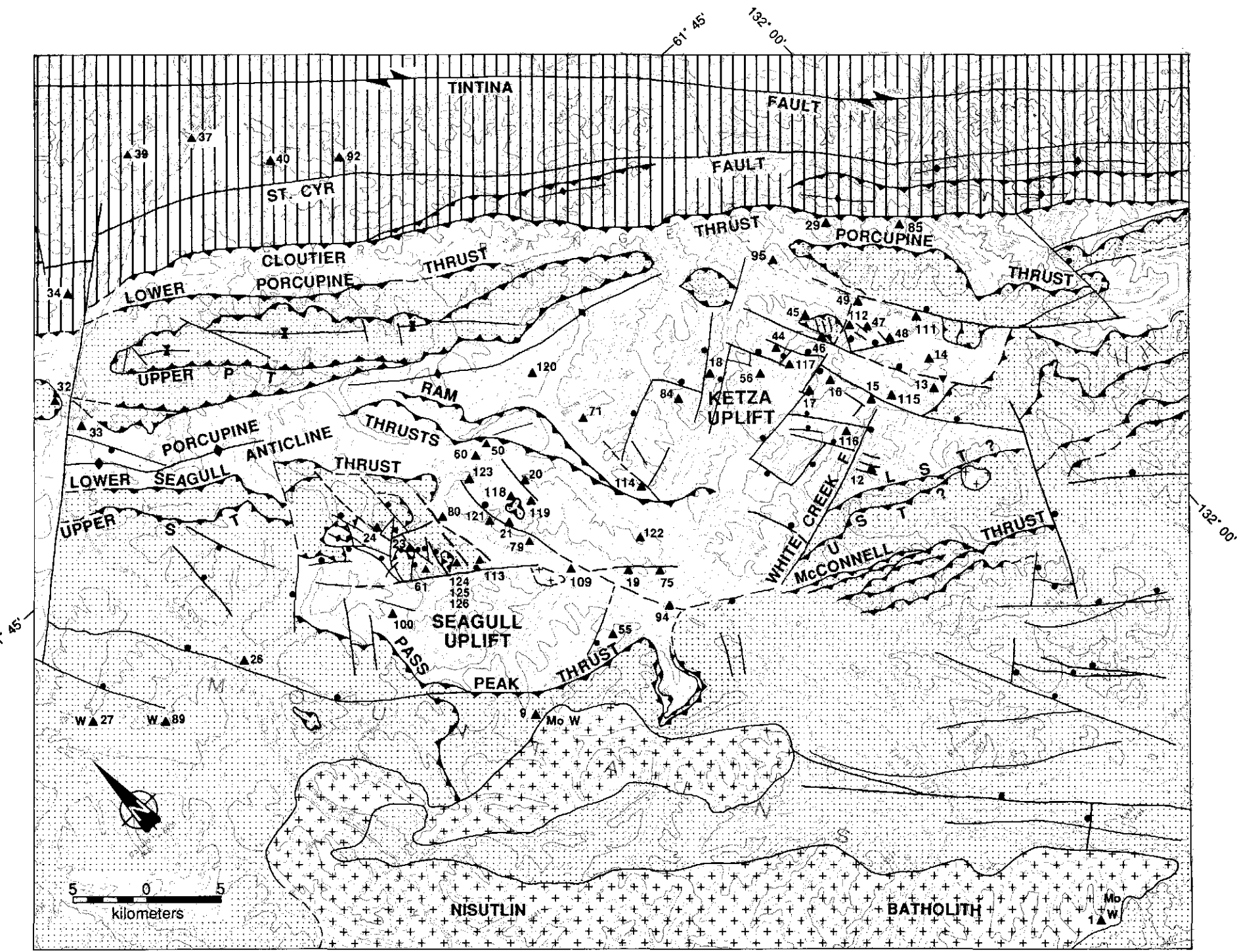
Difference between the Ketza Uplift of Tempelman-Kluit and Ketza-Seagull Arch reflect differences in the way the Seagull Thrust is mapped and correlated. Tempelman-Kluit (1977, in press) interprets the Upper and Lower Seagull Thrusts to extend eastward along Seagull Creek to the White Creek Fault, where they are offset to the east. In this interpretation, the Pass Peak and McConnell Thrusts are equivalent to one another, but separate from and structurally higher than the Seagull Thrusts. The writer (Fig. 1) interprets the Seagull Thrusts to be equivalent to the Pass Peak Thrust, with only the McConnell Thrust separate from, and structurally higher than the Seagull Thrusts.

New mapping, west of Seagull Creek, (Fig. 2) reveals how the Seagull Thrusts and the Pass Peak Thrust may be the equivalent, and form the northern and southern flanks of a complexly faulted arch, the Seagull Uplift. This interpretation assumes that the Lower Seagull Thrust places Siluro-Devonian carbonate onto Devono-Mississippian shale and volcanics, and that the Upper Seagull Thrust places Cambro-Ordovician phyllite onto Devono-Mississippian shale. The two splays may merge in the northwest part of the area, where only the Upper Seagull Thrust has been recognized. Many normal faults with a variety of orientations are superimposed on the Upper and Lower Seagull Thrusts. In most fault-bounded blocks, strata can only be assigned with confidence to one of the three possible structural levels defined by the thrusts, if a thrust is exposed in that block.

Although it is open to interpretation, Figures 1 and 2 show that it is difficult to run the Seagull Thrusts the full length of Seagull Creek because their trailing edges are brought to surface far to the west. In another interpretation, the fragments of thrust faults seen west of Seagull Lakes might belong to the Pass Peak Thrust, and be separate from the Seagull Thrust. However, if the Seagull Thrusts are not equivalent to the Pass Peak Thrust, then the latter terminates abruptly to the northwest, with no explanation.

The pattern of faulting and uplift documented in Figure 2 resembles that seen in the Ketza Uplift (Fig. 1) where fault orientations and overall sense of movement indicates local doming centered a short distance west of the KETZA RIVER deposit (17).

Figure 1. Structural setting of epigenetic mineral occurrences in the central Pelly Mountains. Most occurrences are associated with two domal structures, the Ketza and Seagull Uplifts, which together form Ketza-Seagull Arch. Ketza-Seagull Arch is a window through the Seagull-Porcupine-Pass Peak Thrust, and includes the unpatterned area southwest of the Porcupine Thrust, and southeast of the Porcupine Anticline. The Arch and Uplifts are defined by the window, by the pattern of normal faults in it, and by the distribution of map units, which are not shown here (see Tempelman-Kluit, 1977). Abbreviations include Lower Seagull Thrust (LST), Upper Seagull Thrust (UST), Porcupine Thrust (PT). See Figure 2 for explanation of other symbols and Table 1 for deposit descriptions.



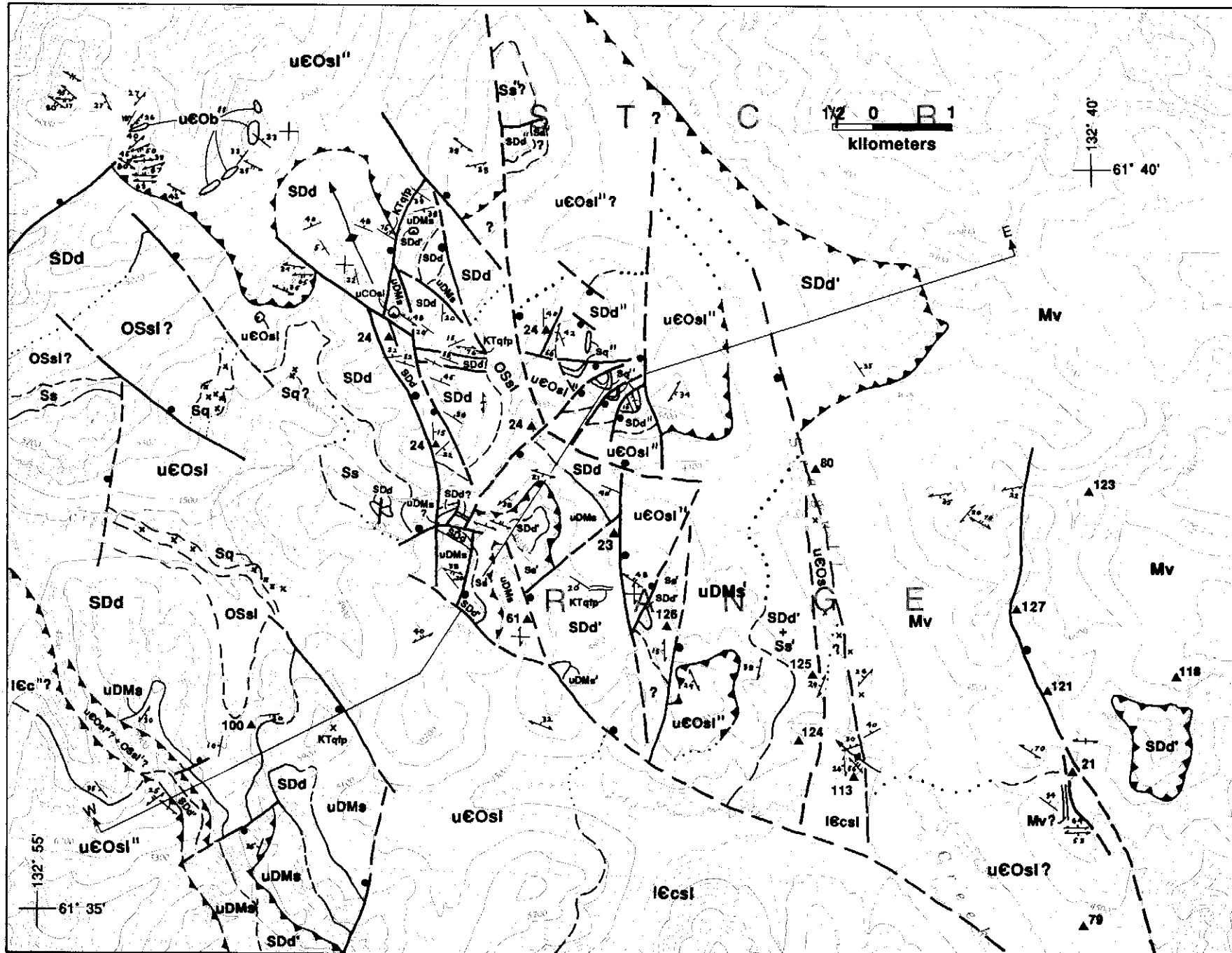


Figure 2. Geological map of the Seagull Uplift at the western end of Ketza-Seagull Arch. This map and cross-section show the evidence that the Pass Peak and Seagull Thrusts are equivalent, and probably domed about a buried intrusion.

Strata in the cores of both uplifts are Lower Cambrian, but are as young as Mississippian in between (Tempelman-Kluit, 1977), where there is less uplift. There are also few normal faults in the central part of the Ketza-Seagull Arch, but the White Creek Fault, along the southern margin could account for most of the uplift.

Other structures possibly related to the Ketza-Seagull Arch include the Ram Thrusts and the Porcupine Thrust sheet, probably as a splay of the underlying Cloutier Thrust. They were not examined by the writer, but appear to be relatively small, with little bearing on the configuration of Ketza-Seagull Arch. The Porcupine Anticline merges with the northwest end of the Ketza-Seagull Arch, may continue east along the Cloutier Thrust (Fig. 3), and may be a passive fold that developed above a step in the Cloutier Thrust. The relationship, if any, to the Ketza-Seagull Arch is unknown.

A small undated stock is near the core of the Seagull Uplift (Fig. 1). The metamorphic grade of adjacent Lower Cambrian schist and marble is noticeably higher than that seen elsewhere, and drill core at mineral locality 109 is reported to contain skarn. An intrusion such as the one shown hypothetically in Figure 2 may therefore underlie much of the area. In the core of the Ketza Uplift, just east of the Ketza River deposits, a small hornfels suggests the presence of an intrusion at depth. Mafic dykes are widespread and fairly common, but it is not known if they are confined to the Ketza-Seagull Arch. A radiometric age of 112 Ma has been obtained from one of these dykes (Tempelman-Kluit, in press).

MINERAL DEPOSITS

Figure 1 shows, and Table 1 describes all known and suspected epigenetic mineral occurrences both in and around the Ketza-Seagull Arch. These demonstrate the empirical, and presumed genetic relationship between the two. Suspected volcanogenic occurrences are excluded, and only epigenetic occurrences in the Ketza-Seagull Arch are discussed here.

Most mineral occurrences are veins of galena, sphalerite, quartz, and siderite, \pm pyrite, pyrrhotite, arsenopyrite, chalcopyrite, and tetrahedrite. Mantos consisting of pyrrhotite, pyrite, \pm arsenopyrite, siderite, galena, and sphalerite are found only on the KETZA RIVER (17) (Canamax), SONNY (12), and OXO (15) properties. Precious metal content varies widely. Most deposits contain silver in association with galena and tetrahedrite. Silver content reaches 7714 g/t in the SOUTH FAULT Zone (111), but generally ranges from 300 to 700 g/t, with ratios of about 340 g/t Ag to 1% Pb. Some, but not all deposits rich in arsenopyrite, pyrite, and pyrrhotite contain gold. Only the GRAYLING (20), KETZA RIVER (17), LP (109), and HOEY (47) are significant. Grab samples from the GRAYLING occurrence has reached 155.3 g/t Au, but the average grade of 12.36 g/t Au in the PEEL and RIDGE Zone of Canamax's Ketza River property is more typical.

Most veins are pods or lenses along strong, well-defined faults with apparent displacements that are small. In many places, vein materials are crushed and brecciated, or cut by slickensided faults, as if faulting was intermittently active during mineralization. Few veins exceed a meter in width, and the largest reserves are on the STUMP Vein (A1) (48) where 36,280 tonnes of proven reserves grade 353 g/t Ag and 8.4% Pb.

Mantos are near faults, and form tubelike lenses along the contact between Lower Cambrian limestone and overlying shale. The PEEL and RIDGE Zones on Canamax's Ketza River property, with estimated reserves of 861,840 tonnes grading 12.36 g/t Au, demonstrate that although mantos are rare, they are attractive exploration targets. Siluro-Devonian dolomite and limestone underlies much of the Seagull Area, and may also contain mantos, although none have yet been recognized in those rocks.

Mineral occurrences form two clusters, the Ketza and Seagull areas, which are spatially associated with Ketza and Seagull Uplifts. In the Ketza area, deposits are zoned about the center of the Ketza Uplift. Gold-bearing, pyrrhotite- and arsenopyrite-rich mantos, chimneys and secondary oxides are in the core (KETZA RIVER DEPOSITS, 17, OXO), silver- and galena-rich veins are in the eastern and northern flanks, and barren pyrrhotite and siderite-rich mantos (SONNY 12) are on the southeast margin. In the Seagull area, occurrences on the west, north, and east peripheries (BOX 19, GROUNDHOG 24, TAKU 60, FOX 71, GULL 75, LORNE 100, ROWE 114, FALCON 120, GOAT 122) tend to be sphalerite- and galena-rich, while most of the others contain

more pyrrhotite, pyrite, and arsenopyrite. In the south-center, the LP (109) occurrence comprises gold-bearing pyrite and pyrrhotite in association with skarn. With more work, an accurate zonation related to the Seagull Uplift may be established.

During the mid 1970's, many geologists were in the district exploring for massive sulphide deposits in Mississippian volcanic rocks. Some interpreted the above deposits to be either volcanogenic, or veins related to Mississippian intrusions (Morin, 1977, 1981). Some may be, but most of those examined by the writer are in faults that cut sharply across Mesozoic metamorphic fabrics, none are foliated, and their mineral ratios and general character resemble those of Mesozoic veins in other parts of the northern Cordillera. Near Seagull Creek (Fig. 2), veins are in different Mesozoic thrust sheets, along normal faults that cut those thrusts. If the thrusts, with many kilometers of displacement, are younger than the veins, the present juxtaposition of veins is more than fortuitous. Descriptions of most deposits not visited by the writer resemble those that were seen. In the writer's opinion, only the GUANO (59), NOKLUIT (58), MM (10), BNOB (96), CHZERPNOUGH (77), and CPA (11) occurrences (not shown on Fig. 1) might be volcanogenic.

ORIGIN OF THE KETZA-SEAGULL ARCH

The spacial association of epigenetic mineral deposits to the Ketza-Seagull Arch suggests that the two are genetically related. Mineral zoning appears to coincide with the smaller Ketza and Seagull Uplifts, which respectively contain hornfels and schist in their cores. The Ketza-Seagull Arch may therefore reflect doming and uplift about a buried Cretaceous intrusion, with apophyses beneath the Ketza and Seagull Uplifts.

The only obvious alternative is the possibility that the Ketza-Seagull Arch wholly or partially reflects a step in an underlying thrust fault (Fig. 3c). The miogeoclinal assemblage that underlies the Ketza-Seagull District was detached from basement and compressed and transported eastward or northeastward during deformation that probably lasted from late Jurassic to Early Tertiary time (Tempelman-Kluit, 1979). Generally, deformation migrated eastward and deeper with time, such that movement probably occurred first on the McConnell Thrust, then the Pass Peak-Seagull-Porcupine Thrust, then the Cloutier Thrust, and finally the St. Cyr Thrust before changing to dextral strike-slip on the Tintina Fault. If a thrust cut abruptly upward across strata, then as it continued to move, the thicker strata in the hangingwall would passively form an arch or anticline (Boyer and Elliott, 1982; Dahlstrom, 1969). The Porcupine Anticline along the northern margin of Ketza-Seagull Arch may be such a feature (Fig. 3a). The presence of abnormally thick Mississippian volcanic rocks in the Ketza-Seagull Arch and the probability that they are associated with complex Paleozoic faults at depth suggests that Mesozoic thrust faults in this region developed irregularities or steps. Perhaps the Porcupine Anticline is part of a larger step that encompasses all of the Ketza-Seagull Arch. However, if the Ketza-Seagull Arch is solely related to passive folding, the empirical association with epigenetic veins is difficult to explain. There could only be a connection if the thickness of strata carried above the step is so much greater than elsewhere that tectonic thickening resulted in high heat flow, and (?) the generation of some small intrusions by partial melting. The mechanism has been used by Tempelman-Kluit (1979) to explain the origin of mid-Cretaceous intrusions in the region. He argued that tectonic thickening of the Cordilleran thrust and fold belt as a whole resulted in anatexitic melting at the base of the continental crust. No correlation between single intrusions and areas of unusual tectonic thickening has been demonstrated.

Perhaps the Ketza-Seagull Arch is a composite feature that reflects both doming about an intrusion, and arching above a step. In this interpretation, a step may define the configuration of the whole arch, and two relatively small intrusions, the Ketza and Seagull Uplifts. It is possible but unlikely that such a step is younger than mid-Cretaceous (Fig. 3b). Late Cretaceous and (?) Early Tertiary strata at the leading edge of the Rocky Mountain Thrust and Fold Belt, far to the east of the Ketza-Seagull District (Stott, D.F., 1982), are deformed, and therefore detached from basement. The basal detachment must continue west beneath the Ketza-Seagull District, to the suture zone. This step would have to be in the basal detachment somewhere beneath the Cloutier Thrust (Tempelman-

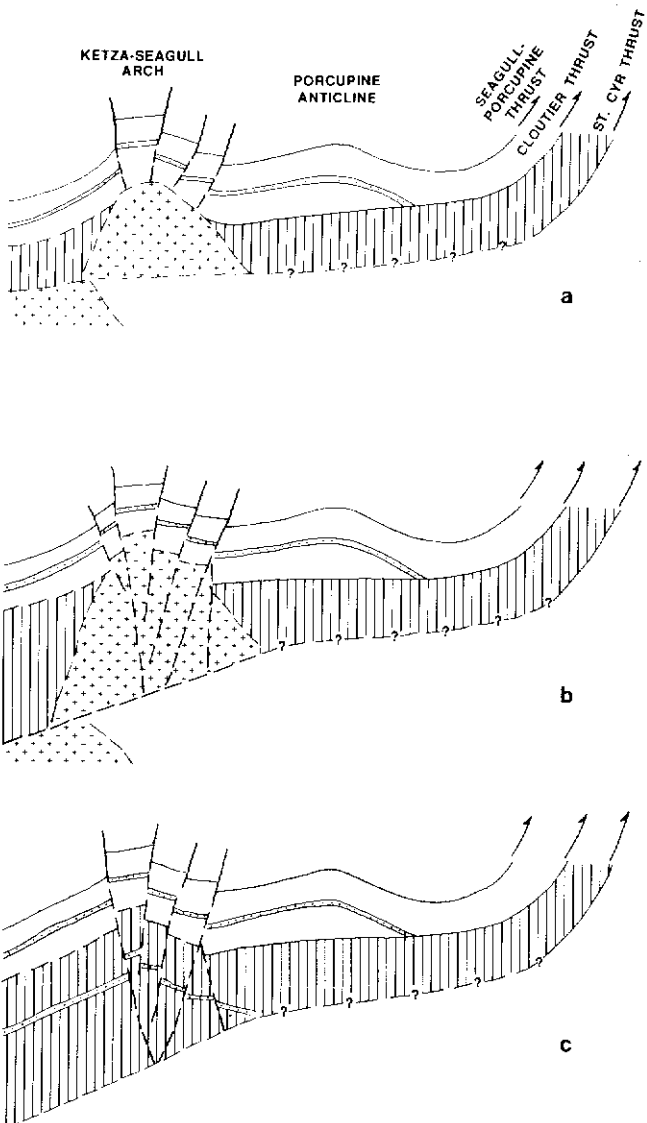


Figure 3. At least three explanations for the origin of Ketza-Seagull Arch are possible, the first (a) is most likely. (a) Domining about an intrusion, which may be truncated by a younger thrust. (b) Combination of domining about an intrusion, and uplift above a step in a younger (or older) thrust fault. (c) Anomalous heating as a result of tectonic thickening above a step, with no large intrusion. A step is the abrupt change in stratigraphic level of a thrust fault which results in a change in thickness and arching or passive folding of the overlying thrust sheet. The Porcupine Thrust may be such a feature.

Kluit, in press).

The above discussion shows that any explanation of the setting of epigenetic mineral deposits in the Ketza-Seagull District must not only consider their relationship to intrusions, but also to

their regional tectonic setting. Mineralization occurred during the waning stages of deformation and transportation of supracrustal rocks above a passive basement, and faults associated with the Ketza-Seagull Arch may reflect a long and complex history. Normal faults may be related to buried intrusions, to the Porcupine-Seagull-Pass Peak Thrust, or to younger and deeper thrust faults that were active before and after (?) emplacement of mid-Cretaceous intrusions. Normal faults containing veins are younger than the Porcupine-Seagull-Pass Peak Thrust, and most likely reflect uplift about one or more buried intrusions.

COMPARISONS WITH THE SETTINGS OF VEINS IN OTHER AREAS

Many silver- and gold-bearing veins and mantos in central Yukon resemble those in the Ketza-Seagull District, but the local tectonic setting of some is different. This brief summary of the more important districts emphasizes that no consistent pattern of faulting has yet been identified with this type of deposit, and no area should be excluded from exploration on that basis. However, the deposits are all confined to that part of the Yukon underlain by deformed migeocinal strata, and mid-Cretaceous to Early Tertiary intrusions. They are in or near late faults that cut regional folds and thrusts, and penetrative fabrics, and are mid-Cretaceous to Early Tertiary in age, but are commonly not near an intrusion. The Mt. Hundere deposits, north of Watson Lake, replace lower Cambrian limestone in the core of a small domal uplift over a buried intrusion (Abbott, 1977, 1981). Veins in the Plata Camp (Abbott, this volume) are fault controlled, a small undated porphyry dyke is near some veins, but not others, and there is no evidence of doming. The veins cut earliest (?) Cambrian limestone, but show no tendency to form mantos. The McMillan (Quartz Lake) deposit, located east of Watson Lake, was briefly visited by the writer who agrees with Morin's (1981) interpretation that it is a manto in (?) Earliest Cambrian limestone. The deposit and other small zones of veining and hydrothermal alteration underlie an area about 5 km x 5 km, but there is no exposed intrusion, or doming, although outcrop is scarce. The Keno Hill District is a belt about 25 km long, on the southern flank of the McQuesten Anticline (Boyle 1965). Most veins are along NE-trending faults with sinistral movement that are cut by NW-trending-faults with dextral movement. Displacements are in the order of 100 m or less (Lynch, this volume). Small Cretaceous intrusions are nearby, but no consistent relationship has been demonstrated to them. The McQuesten Anticline plunges southwest to form a partial window through the Robert Service Thrust that is about the same size as the Ketza-Seagull Arch. Abo (1963, 1964) proposed that vein and faults in the Keno Hill district are related to the development of the McQuesten Anticline, and indirectly to the nearby intrusions.

In the Rancheria District (Abbott, 1985), deposits are associated with many widespread Late Cretaceous and Early Tertiary dykes and small intrusions. Veins are along faults that display a systematic pattern indicative of a regional tectonic control that probably results from movement on large strike-slip faults such as the Tintina. The exact nature of this relationship is not yet clear. The small secondary faults could be riedel shears as suggested by Abbott (1985), although the writer now favours a broad zone of crustal extension that would have resulted in abnormally high heat flow, and partial crustal melting.

REFERENCES

- ABBOTT, J.G., 1977. *Structure and stratigraphy of the Mt. Hundere area, southeastern Yukon*; unpublished MSc thesis, Queen's University, 111 p.
- ABBOTT, J.G., 1981. A new geological map of Mt. Hundere and the area north; in *Yukon Geology and Exploration, 1979-80*, D.I.A.N.D., p. 45-50.
- ABBOTT, J.G., 1985. Silver-bearing veins and replacement deposits of the Rancheria District; in *Yukon Exploration and Geology, 1983*, p. 34-44.
- AHO, AARO E., 1963. Silver in the Yukon; C.I.M., Bull., Vol. 56, No. 611, p. 232-239.
- AHO, AARO E., Mineral potential of the Mayo District; *Western Miner*, Vol. 39, No. 4, p. 127-148.

- BOYER, STEPHEN E., and ELLIOTT, DAVID, 1982. Thrust systems; A.A.P.G. Bull., Vol. 66, p. 1196-1230.
- BOYLE, 1965. Geology, geochemistry, and origin of the lead-zinc-silver-deposits of the Keno Hill-Galena Hill area, Yukon Territory; Geol. Surv. Can., Bull. 111, 302 p.
- DAHLSTROM, C.D.A., 1969. Balanced cross-sections; Can. Jour. Earth Sci., Vol. 6, p. 743-757.
- GABRIELSE, H., 1985. Major transcurrent displacements along the northern Rocky Mountain trench and related lineaments in north-central British Columbia; Geol. Soc. of Am. Bull., Vol. 96, p. 1-14.
- LYNCH, G., 1986. Mineral zoning in the Keno Hill District, central Yukon; in Yukon Geology, Vol. 1, Exploration and Geological Services Division, Yukon, Indian and Northern Affairs, Canada.
- MORIN, J.A., 1976. Ag-Pb-Zn Mineralization in the MM Deposit and Associated Mississippian Felsic Volcanic Rocks in the St. Cyr Range, Pelly Mountains; in D.I.A.N.D., Mineral Industry Report 1976, Yukon Territory, EGS 1977-1, p. 83-97.
- MORIN, J.A., 1981. Model of mineralization related to cauldron facies syenite in the Pelly Mountains; in D.I.A.N.D., Yukon Geology and Exploration; 1979-80, p. 88-90.
- MORIN, J.A., 1981. The McMillan deposit - a stratabound lead-zinc-silver-deposit in sedimentary rocks of Upper Proterozoic age; in D.I.A.N.D., Yukon Geology and Exploration 1979-80, p. 105-109.
- STOTT, D.F., 1982. Lower Cretaceous Fort St. John Group and Upper Cretaceous Dunvegan Formation of the foothills and plains of Alberta, British Columbia, District of Mackenzie and Yukon Territory; Geol. Surv. Can., Bull. 328, 124 p.
- TEMPELMAN-KLUIT, D.J., 1977. Geology of Quiet Lake and Finlayson Lake map areas, Yukon Territory (105 F and G); Geol. Surv. Can., Open File 486.
- TEMPELMAN-KLUIT, D.J., 1979. Transported ophiolite, cataclastic, and granodiorite in Yukon: evidence of arc-continent collision; Geol. Surv. Can., Paper 79-14, 27 p.
- TEMPELMAN-KLUIT, D.J., in press. Geology of Quiet Lake (105 F) and Finlayson Lake map areas, Yukon Territory; Geol. Surv. Can., Mem.

TABLE 1

NAME (YEX Ref. No. (105 F))	TYPE	HOST ROCK	ASSOCIATED INTRUSIONS	DESCRIPTION
MOLLY (1)	Skarn Mo, W	Siluro-Devonian dolomite	Cretaceous Nisutlin Batholith	Diopside-garnet and wollastonite-garnet skarn contains molybdenite, pyrrhotite, chalcopyrite, and fluorite over a strike length of about 200 m and narrow widths. The best drill intersection assayed 1.08% MoS ₂ across 4 m. Endoskarn about 1 km to the north contains powellite.
STORMY (9)	Skarn Mo, W	Lower Cambrian limestone	Cretaceous Nisutlin Batholith	Molybdenite and minor scheelite occur in skarn and in granodiorite at the contact between the Nisutlin Batholith and Lower Cambrian limestone. Probable reserves are 17,000 tons grading 1.05% MoS ₂ .
★ SONNY (12)	Manto	Lower Cambrian limestone	Cretaceous Mafic dyke	Three mantos, comprised mainly of siderite and pyrrhotite and some pyrite and quartz, are exposed over a strike-length of about a kilometer. The largest and westernmost of the three is exposed for a length of about 75 m and a width of 2 or 3 m. The deposits are probably tubelike, but their orientation is unknown.
KAY (13)	Vein	Siluro-Devonian dolomite, limestone	?	Galena, sphalerite, chalcopyrite, and tetrahedrite, with lesser amounts of pyrite, pyrrhotite, and manganeseiferous siderite and minor quartz and barite form veins and breccias along fractures and faults or replace limestone (NCMI).
SHARON (14)	Vein	Cambro-Ordovician phyllite	?	Two north-trending, weakly mineralized quartz veins, about 450 m apart, assayed as high as 476.6 g/t Ag and 20% Pb across 1.75 m.
★ OXO (15)	Manto	Lower Cambrian	—	A lens of pyrrhotite, galena, sphalerite, and pyrite is exposed over 15 m x 30 m at the contact between Lower Cambrian limestone and overlying black shale. A 4 m chip sample assayed 349.7 g/t Au, 12.7% Pb, 0.03% Cu, 0.4% Zn, and 0.68 g/t Au. Next to the massive sulphides, in the same position, a quartz vein up to 2 m wide and 50 m long contains some chalcopyrite and pyrite.
KOPINEC (16)	Vein	Lower Cambrian phyllite	?	A vein of massive pyrrhotite, pyrite, and chalcopyrite assayed as high as 0.15% Cu over an undisclosed width (NCMI). Recent exploration has failed to find this occurrence.
★ KETZA RIVER (17) (WOODCOCK, BOOM, KON)	Mantos, chimneys	Lower Cambrian limestone	Cretaceous hornfels	The TARN, PEEL, RIDGE, PENGUIN, CREEK, and FLINT Zones are all localized along a steep east-trending fault known as the 080 fault. The RIDGE Zone is a chimney; the rest are mantos. The first three contain gold and are rich in arsenopyrite as well as pyrrhotite and pyrite. The PEEL and RIDGE Zones contain an estimated 861,840 tonnes grading 12.36 g/t Au. Most of these reserves are oxides. The other zones are barren and consist mainly of ankerite and pyrite.
★ BOX (JD) (19)	Vein	Mississippian volcanics, shale	—	A southeast-trending, southwest-dipping fault contains massive galena, pyrite, arsenopyrite, and crushed vein quartz, in a lens about 50 m long and up to 1 m wide. Grab samples have assayed as high as 1584.6 g/t Ag, 21% Pb, 1.03 g/t Au, and 0.25% Zn.
★ GRAYLING (20)	Vein	Mississippian volcanics	—	Two lenses of massive sulphides at least 2 m thick and of unknown length replace very coarse calcite along a steep north-trending fault. Pyrrhotite, pyrite, black sphalerite, galena, and minor chalcopyrite and arsenopyrite are the main sulphides. Talus fragments of manganeseiferous siderite, calcite, and quartz are associated with the sulphides. A chip sample across the Upper Zone averaged 21.28% Pb, 1.69% Zn, 522.5 g/t Ag, and 6.0 g/t Au across 6.2 m. A chip sample across the Lower Zone assayed 27.25% Pb, 2.23% Zn, 620 g/t Ag, across 1.6 m.
★ COXALL (SUN) (21)	Vein?	Mississippian volcanics	—	Only one small siderite veinlet with a small amount of sphalerite was seen by the writer.
★ TYRO (22)	Vein?	Mississippian volcanics	Mississippian syenite	Small faults contain quartz, carbonate, ± pyrite veins up to 30 cm across. In felsic volcanics, near lineaments that may reflect young faults, rusty irregular zones up to a meter or two wide contain disseminated pyrite and pyrrhotite.
★ HAYDN (23)	Vein	Siluro-Devonian dolomite	Cretaceous mafic dykes	Partially oxidized float boulders up to 1 m across contain pyrite, galena, and minor chalcopyrite, sphalerite, and tetrahedrite in a siderite and quartz matrix.

TABLE 1 (cont.)

NAME (YEX Ref. No. (105 F))	TYPE	HOST ROCK	ASSOCIATED INTRUSIONS	DESCRIPTION
★ GROUNDHOG (24)	Vein	Siluro-Devonian dolomite	Cretaceous mafic dykes	Four sets of veins consisting of galena and variable amounts of tetrahedrite in massive white quartz and lesser siderite are scattered over an area 1 km x 1 km. Reserves of 2558 tonnes grading 695 g/t Ag, and 42.5% Pb were established in 1969 on the largest vein (NCMI).
★ PONY (26)	Vein	Cambro-Ordovician phyllite	—	A vein containing a little galena, jamesonite, and arsenopyrite assayed 0.17 g/t Au, 52.8 g/t Ag, and 3.82% Pb.
★ HAM (27)	Skarn	Lower Cambrian schist and limestone	Cretaceous batholith	Scheelite (?) has been traced over a strike length of 300 m and widths of 3 to 4 m. Assays of grab samples ranged from 0.71% to 4.06% WO ₃ .
AMBROSE (29)	Vein	Siluro-Devonian dolomite	?	A quartz vein up to 2.5 m wide and more than 1 km long contains pyrite and lesser amounts of chalcopyrite (NCMI).
BARITE MOUNTAIN (32)	Vein	Siluro-Devonian dolomite	Cretaceous (?) mafic dykes	Several northeast striking faults contain barren veins, 0.6 - 3.5 m wide.
McNEE (33)	Vein	Siluro-Devonian dolomite	—	A few, small barite veins contain a little galena, pyrite, and copper stain.
CANUSA (34)	Vein	Siluro-Devonian dolomite	—	A northwest-trending fault contains a quartz, pyrite, and galena vein up to 1 meter wide. A chip sample across the vein assayed 0.34 g/t Au, 45.94 g/t Ag and 5.19% Pb.
LAPIE (37)	Vein	Ordovician-Silurian phyllite	—	A quartz vein contains some pyrite and galena.
DANGER (39)	Disseminated(?) stratabound(?)	Devonian sooty limestone	—	Five scattered exposures, containing no visible sulphides, assayed as high as 6% zinc.
MT. MISERY (44)	Vein	Siluro-Devonian dolomite	?	A northeast-trending, brecciated fault zone contains lenses of galena and siderite that assayed up to 332.6 g/t Ag, 18.2% Pb, and 0.68 g/t Au across 5 m (NCMI).
★ KEY 3 (45)	Vein	Devono-Mississippi shale	—	A vein up to 1 m wide, in a steep north-trending fault, contains quartz, siderite, galena, and minor sphalerite, tetrahedrite, and pyrite. A bulk sample averaged 1114.3 g/t Ag, 4.8% Pb, and 0.35% Cu.
★ LAP 10 (46)	Vein	Devono-Mississippi shale	—	A northeast-trending fault zone about 1.5 m wide contains several pods of massive galena up to 30 cm across as well as smaller lenses and stringers of galena and quartz. Channel samples indicated a grade of 1200 g/t Ag, and 38.5% Pb over a width of 1 m and a strike length of 137 m (NCMI).
★ HOEY (F2, F3) (47)	Vein	Silurian quartzite	—	Several veins include two that are important. The eastern (F3) vein is in a northwest-trending fault that juxtaposes Ordovician-Silurian black shale against Siluro-Devonian dolomite, and consists of siderite, galena, sphalerite and pyrite. Nearby, galena also occurs in veinlets and replaces dolomite. The western (F2) vein is in a steep north-trending fault zone. The vein is about 2 m wide, and contains mainly quartz, with some pyrite, siderite, and a little galena. Surface exposures contain silver, but underground workings intersected a zone that assayed 23.3 g/t Au, but no Ag across 0.73 m, and a length of 9.1 m (NCMI).
★ STUMP (A1) (48)	Vein	Cambro-Ordovician phyllite	—	A steep, north-trending vein more than 200 m long and up to 1 m wide consists mainly of variable amounts of siderite, quartz, galena, and pyrite. Proven reserves in 1975 were 36,280 tonnes grading 8.4% Pb, and 353 g/t Ag (NCMI).
★ KETZA KEY (49) (K18-b)	Vein	Cambro-Ordovician phyllite	—	Galena and pyrite with minor tetrahedrite and sphalerite in a gangue of quartz and siderite form a north-trending pod about 1.5 m wide and 32 m long that cuts across foliation at a shallow angle. Proven and possible reserves in 1975 were 10,702 tonnes grading 545.1 g/t Ag and 12.15% Pb (NCMI).
GYR (50)	Replacement	Siluro-Devonian dolomite	?	Irregular masses of sphalerite replace dolomite. A grab sample assayed 29.64% Zn and 33.94 g/t Ag.
CONNELL (55)	?	Siluro-Devonian dolomite	?	Tetrahedrite occurs in veinlets (NCMI).

TABLE 1 (cont.)

NAME (YEX Ref. No. (105 F))	TYPE	HOST ROCK	ASSOCIATED INTRUSIONS	DESCRIPTION
FURY (56)	Vein	Lower Cambrian carbonate	?	Quartz veins containing chalcopyrite and tetrahedrite are 0.1 to 1.4 m wide and at least 100 m long. The best chip sample assayed 3.2% Cu and 10.3 g/t Ag across 1.4 m. A selected specimen assayed 7.8% Cu, 1559.9 g/t Ag, and 15.1 g/t Au (NCMI).
TAKU (60)	Vein	Mississippian volcanics, shale	?	Veinlets of galena and sphalerite are reflected in a local geochemical anomaly.
★ H(PEAK)(61)	Vein	Siluro-Devonian carbonates	Cretaceous mafic dykes	Boulders of arsenopyrite, pyrite, quartz, and pyrrhotite, up to 30 cm across, are exposed for 30 m along a creek bank.
★ FOX (71)	Vein	Siluro-Devonian dolomite	Cretaceous mafic dykes	Brown carbonate, black sphalerite, and minor galena form diffuse veinlets.
★ GULL (75)	Vein	Mississippian volcanics	—	Several narrow veins of massive white quartz, 6-10 cm across, contain small amounts of galena and sphalerite and are associated with an intermittent zone of clay alteration and chalcedonic veining.
★ ANISE (80)	Float	—	—	Glacial till in the valley of Seagull Creek contains fragments, up to 30 cm across, of vein quartz, pyrite, and arsenopyrite. Other fragments consist of massive arsenopyrite, with calcite and galena.
DROC (84)	?	Cambro-Ordovician phyllite	?	Chalcopyrite with traces of galena and sphalerite occur in a zone rich in quartz, pyrite and siderite (NCMI).
★ HOWRU (85)	Diagenetic? Disseminated	Siluro-Devonian quartzite	—	Ovoid disseminations of galena, 1 mm to 1 cm across, are scattered through thick beds of quartzite over a stratigraphic thickness of about 100 m and an unknown strike length.
★ LAP (89)	Skarn Vein	Lower Cambrian schist, limestone	Cretaceous porphyritic granodiorite	Chalcopyrite-bearing pods of massive pyrrhotite, and scheelite, are sporadically distributed in quartz-chlorite-actinolite skarn, and quartz-pyroxene-pyrrhotite skarn, respectively. Narrow quartz veins contain pyrite, galena, ± boulangerite, ± sphalerite, ± calcite.
★ ANGIE (92)	Diagenetic? Disseminated	Devonian sooty limestone	—	Sphalerite, smithsonite, and native silver form pelletoidal disseminations that are concentrated in bands parallel to bedding and as secondary replacement and vein fillings. The largest zone is 280 m long, lenticular, and erratic. Higher grade portions assayed 5.8% Zn and 122.5 g/t Ag across 3.2 m.
GRAY (94)	Float	Overburden	?	Float boulders along the south side of Grayling Lake contain minor pyrrhotite, pyrite, chalcopyrite, and galena.
IGLE (95)	Diagenetic? galena Disseminated?	Siluro-Devonian quartzite	?	Galena and sphalerite are disseminated(?) in quartzite, much like the HOWRU occurrence.
★ LORNE (100)	Vein	Siluro-Devonian dolomite	Cretaceous mafic dykes	Galena occurs in boulders of massive sulphide float up to 30 cm across, in narrow fracture fillings, and as blebs up to 3 cm across in dolomite.
★ LP (109)	Float	Lower Cambrian schist, limestone	Cretaceous granite	Boulders of quartz, pyrrhotite, and pyrite bearing schist found along the Seagull Creek road have returned assays between 2 and 27 g/t Au. Five drill holes intersected similar material. Most were low grade, but one returned an intersection containing 2.8 g/t Au across 4.5 m. Garnet skarn, and granitic sills or dykes are associated with the sulphides.
SOUTH FAULT (111) (F4, F6)	Vein	Cambro-Ordovician phyllite	?	The F-4 occurrence consists of small lenses and pods of galena with lesser amounts of sphalerite and traces of tetrahedrite along a steep east-trending fault. Selected specimens ranged from 2228.5 to 7714.1 g/t Ag. The F-6 occurrence, located 1 km farther south consists of galena float assaying 4967.9 g/t Ag, 71.4% Pb, and 0.17 g/t Au (NCMI).
★ K33 (112)	Vein	Cambro-Ordovician phyllite	—	A steeply dipping south southeast-trending vein up to 1.5 m wide and of unknown length contains siderite, quartz, pyrite, arsenopyrite and galena.
★ TROUT (113)	Vein	Lower Cambrian? phyllite	—	A steeply dipping north-trending quartz vein about 1.5 m across and an unknown length contains variable amounts of pyrite and arsenopyrite. A grab sample assayed 35 g/t Ag, 0.07 g/t Au, 0.15% Pb, and 0.07% Zn.

TABLE 1 (cont.)

NAME (YEX Ref. No. (105 F))	TYPE	HOST ROCK	ASSOCIATED INTRUSIONS	DESCRIPTION
★ ROWE (114)	Vein, Replacement	Siluro-Devonian carbonate	Cretaceous mafic dykes	A gossan about 50 m x 75 m contains clots and lumps of zinc and iron oxides in vuggy dolomite. Galena veins up to 4 cm across occur nearby. Chip samples assayed as high as 5.35% Zn across 22 m.
CARL (115)	Vein	Lower Cambrian limestone Siluro-Devonian dolomite	?	A 30 m wide zone of narrow quartz veins contains galena and sphalerite. A selected sample assayed 16.0% Pb, 506.4 g/t Ag, 7.73% Zn, and 0.1% Cu. About 1.5 km to the northwest, coarse-grained galena and black sphalerite occur in rubble below cliffs of Lower Cambrian carbonate. A selected grab sample assayed 42.8% Pb, 1230.1 g/t Ag, and 4.76% Zn.
WHITE (116)	Vein	Lower Cambrian carbonate, phyllite	?	A lens of massive pyrrhotite and arsenopyrite about 7 m long and up to 0.5 m wide, and a sheared east-northeast trending quartz vein about 0.5 to 0.77 m wide, are along a phyllite-carbonate contact. A selected sample of the sulphides assayed 15.4 g/t Ag, 0.03 g/t Au, 0.48% Pb, and 0.12% Cu.
QUILL (117)	Vein? Replacement? float	Lower Cambrian quartzite, phyllite	?	Boulders of massive pyrrhotite with variable amounts of arsenopyrite and minor pyrite returned assays as high as 2.8 g/t Au, 2.3 g/t Ag, and 32.83% As. The sulphides are associated with a stockwork of narrow, vuggy quartz veins containing pyrite and arsenopyrite.
PIKA (118)	Vein float	Mississippian volcanics	Mississippian syenite	Several closely spaced float occurrences of vein material contain semi-massive galena, sphalerite, pyrite, ± chalcopyrite, ± arsenopyrite. A typical grab sample assayed 242.4 g/t Ag, 0.14 g/t Au, 8.00% Pb, and 4.25% Zn.
LOON (119)	Vein	Mississippian volcanics	?	Several small, widely spaced veins with low silver, gold, zinc and lead contents include one containing arsenopyrite, pyrrhotite, pyrite, and chalcopyrite, and several others containing galena, barite, and tetrahedrite in quartz-carbonate gangue.
FALCON (120)	Vein float	Mississippian volcanics	?	Boulders of massive barite ± galena assayed as high as 63.5% Pb, 605.8 g/t Ag, 0.07 g/t Au.
BEAR (121)	Vein	Mississippian volcanics	Cretaceous ? mafic dykes Mississippian syenite	Grab samples from small veins containing disseminated arsenopyrite and pyrite, assayed as high as 125.8 g/t Ag and 1.6 g/t Au.
GOAT (122)	Vein	Mississippian syenite	?	Sparse float of coarse grained galena, and quartz-carbonate containing disseminations and blebs of sphalerite assayed 1136.9 g/t Ag and 0.068 g/t Au.
LEAPER (123)	Vein	Mississippian syenite	?	Galena, quartz, and calcite veins, and massive galena veins include one as wide as 0.45 m and one that assayed as high as 360.7 g/t Ag, 0.34 g/t Au, and 80.5% Pb.
RAVEN (124)	Vein, replacement suboutcrop	Siluro-Devonian dolomite	?	Small veins and replacement zones of disseminated galena and iron oxides are associated with a large, north-trending geochemical soil anomaly. A selected grab sample assayed 782.0 g/t Ag, 4.8 g/t Au, and 22.4% Pb.
VOLE (125)	Vein, replacement suboutcrop	Siluro-Devonian dolomite, sandstone	?	Small amounts of galena and pyrite occur in oxidized carbonate veins, and replace dolomite.
LYNX (126)	Vein	Devono-Mississippian shale; Cambro-Ord. phyllite	?	Two closely spaced float occurrences consist of sphalerite, galena, and pyrite in a fine grained quartz, barite matrix; and iron oxides with quartz veins and breccia containing galena. A grab sample from the latter occurrence assayed 1024.1 g/t Ag, 20.9 g/t Au, and 54.6% Pb.
BID (127)	Vein	Mississippian volcanics	—	A few fragments of float in a creek bed consist of either massive galena with a little chalcopyrite or massive milled pyrite and quartz with angular pieces of arsenopyrite and pyrite and quartz.

★ Visited by writer

TEXTURAL CHARACTERISTICS OF THE VENUS VEIN AND IMPLICATIONS FOR ORE SHOOT DISTRIBUTION

Lori Walton

Department of Geology
University of Alberta
Edmonton, Alberta

WALTON, L., 1986. *Textural characteristics of the Venus Vein and implications for ore shoot distribution; in Yukon Geology, Vol. 1; Exploration and Geological Services Division, Yukon, Indian and Northern Affairs Canada, p. 67-71.*

INTRODUCTION

The Venus Mine is a gold-silver-lead-zinc quartz vein, 120 km south of Whitehorse, in Upper Cretaceous volcanic rocks known as the Montana Mountain volcanic complex (Roots, 1982).

Gold at Venus is concentrated in steeply pitching ore shoots of varying size, shape and continuity. The purpose of this study is to develop a model explaining the distribution of gold by determining the paragenetic sequence of events and physio-chemical controls operating during ore deposition.

This paper is based on field observations made during a six week period of systematic sampling along each of the five levels in the mine. The emphasis is on describing various mineralogical, textual and structural features, and discussing their controls on ore shoot distribution.

The mine is situated on a steep, southeast facing slope overlooking Windy Arm of Tagish Lake, at latitude 60°01'N and longitude 134°37'W on N.T.S. mapsheet 105 D 2 (Fig. 1). The volcanic complex encompasses an elevated region roughly 8 by 12 km in area, containing both gently dipping plateaus and severe topography. Access to the mine is by Klondike Highway 2.

Intermittent mining and exploration of the deposit has been carried out since the early 1900's, when mineralized quartz veins were first discovered on Montana Mountain. In 1912, mining operations shut down, and since then exploration and development of Venus has been sporadic. The current owner is United Keno Hill Mines Ltd., who conducted an extensive underground and surface exploration program during the summer of 1984. Ore reserve figures for Venus indicate 70,460 tonnes (77,600 tons) of 9.3 g/t Au (0.27 oz/ton), 246.8 g/t Ag (7.20 oz/ton), 2.11% Pb and 1.38% Zn. These figures have not yet been updated using 1984 exploration results.

The Whitehorse map sheet was mapped by Wheeler (1961). C. Roots (1981) described the geological setting of gold-silver veins on Montana Mountain and the geology of Montana Mountain (1982). K. Ralfs (1975) from U.B.C. did a BSc thesis on Venus, and J. Morin included Venus in his study of element zoning in Yukon gold-silver veins (1981). T. Stubens from U.B.C. is currently studying the geostatistics of the Venus vein system.

For the purpose of this study, "Venus Vein" will refer only to that portion of the vein sampled underground, unless specified otherwise.

REGIONAL GEOLOGY

The Venus Mine is located between the western dip of the Whitehorse Trough and the eastern edge of the Coast Crystalline Complex (Fig. 1). The Montana Mountain volcanic complex was probably generated during the late stages of a Mesozoic collision between the North American craton and allochthonous island arc derived volcanic and sedimentary rocks (Roots, 1982).

LOCAL GEOLOGY

The geology of Montana Mountain was mapped by C. Roots (1982). A simplified version of his geology map is shown in Figure 1.

Upper Paleozoic Cache Creek Group rocks border the northeast part of the complex and outcrop across Windy Arm. They consist of amphibolites interlayered with chert and limestone.

Lower Jurassic Laberge Group sedimentary rocks occur along the west boundary of the volcanic complex and separate older Cache Creek Group rocks from younger granites on the east

side of the complex.

Volcanic rocks on Montana Mountain are now considered by Roots (1982) to be equivalent to Mt. Nansen Group volcanic rocks in south central Yukon. Mt. Nansen Group volcanic rocks belong to the Sloko province of Late Cretaceous to Early Tertiary volcanic rocks distributed over 500 km along the border between the Coast Crystalline Complex and the Intermontane Belt.

The Montana Mountain volcanic complex consists of lower greenschist facies, andesitic to dacitic flows, and breccias. Detailed descriptions of the various volcanic units are given by Roots (1982). In the vicinity of the mine, a felsic orange weathering quartz latite to trachyte dyke intrudes and crosscuts the gently deformed succession of volcanic flow rocks.

Granitic to granodioritic plutons intrude the north part of the complex. Since erosion has exposed the pluton in this area, it is inferred to lie at shallow depths below the rest of the complex (Roots, 1982).

Roots (1982), studied the structural relations of the various units and suggested that upwards arching of the volcanic rocks caused by intrusion of granitic magma opened fissures and faults in a semi-radial pattern. Felsic dykes then intruded and filled these openings. Venus partially follows a zone of structural weakness marked by one of these dykes.

Venus has a known strike length on surface of 2 km, with a strike orientation of N20°E, which changes to N65°E in the southern part of the mine. It has an average dip of 30-35°NW into the hill and a known vertical depth of 390 m. It has an average width of 0.8 m to 1.0 m, but can vary up to 3.0 m. The five main levels in the mine follow the vein at elevations 2600, 2650, 2700, 2800 and 2850 feet (792, 808, 823, 853, and 869 metres).

FIELD OBSERVATIONS

Physical characteristics of Venus resemble those of a fissure opened up by movement along slightly curved planar surfaces. The undulatory nature of the vein reflects this movement. Due to the absence of marker beds, it is difficult to determine how much movement has taken place.

The vein exhibits both open space filling and replacement textures. It is frequently separated from the hanging wall and footwall by a pervasive layer of clay gouge. In other places, the vein-wallrock boundary is poorly defined due to replacement of wall-rock by vein material. In the southern part of the mine, parallel, quartz-filled veins interbanded with altered host rock are common in the hanging wall and footwall of the main vein. The veins are commonly connected by a network of barren quartz stringers.

The gangue material in the vein is quartz, which ranges from milky white grains 1 mm in size, up to well-developed euhedral crystals 15 cm long. The larger crystals are frequently developed in single and multiple layers of comb structures, and in vugs located near the center of the vein. Vein quartz is slightly finer grained on upper levels than on lower levels.

The ore assemblage is relatively simple. Four sulphides comprise over 95% of the ore minerals. In order of decreasing abundance, these are arsenopyrite, pyrite, galena and sphalerite. Arsenopyrite-pyrite-quartz is the most common assemblage.

Pyrrhotite, tetrahedrite, realgar and orpiment are locally visible underground. Chalcopyrite, diaphorite, jameisonite and electrum have been reported in polished section (K. Ralfs, 1975, D. Prince, pers. comm.).

Limonite, yukonite, scorodite and covellite are found in the supergene weathering zone and on surface. Galena and arsenopyrite are the most common sulphides found in surface exposures

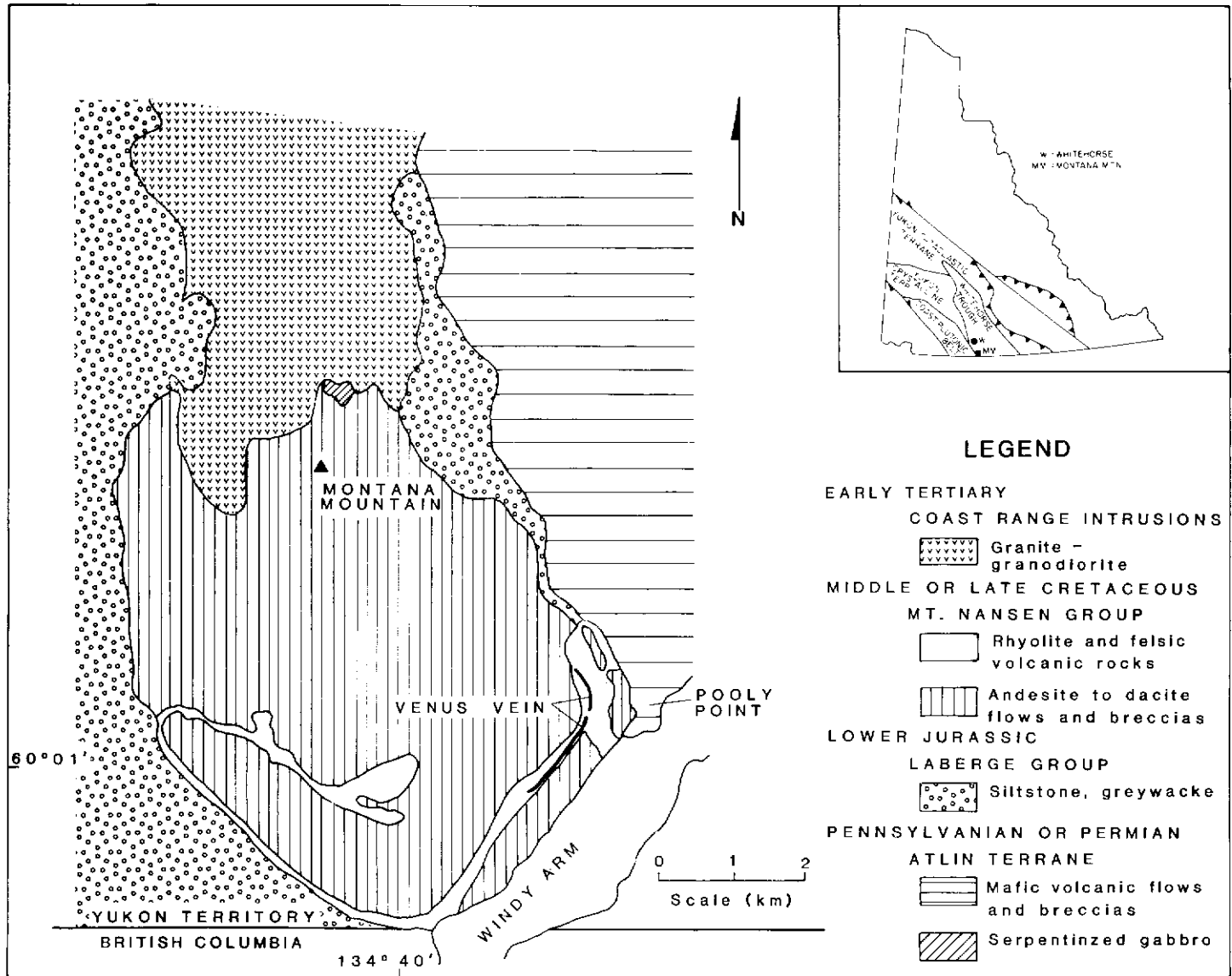


Figure 1. Location map and geology of Montana Mountain (after Roots, 1982).

of the vein.

Crude bands of arsenopyrite and pyrite concentrated on outer edges of the vein are prevalent. In some places, it is the center of the vein which is sulphide rich, with barren quartz concentrated on outer edges. Sulphide bands range in width from 1 cm to over 1 m, and can be monomineralic or consist of narrow alternating bands of arsenopyrite and pyrite. On upper levels, arsenopyrite has developed locally into comb structures, with long bladed crystals growing perpendicular to the walls. Single grains, and disseminations of arsenopyrite and pyrite are common in altered host rock near the vein.

Galena and sphalerite also occur in bands, but more frequently fill interstitial spaces between euhedral quartz crystals towards the center of the vein, and locally replace arsenopyrite and pyrite.

Thick sulphide bands are more common on upper levels where sulphides constitute 30 to 60% of the vein material, as opposed to lower levels which usually contain less than 15% sulphides. Most banding in the vein is crude and massive, except for thin streaks of sulphides (usually arsenopyrite) or host rock smeared out in ribbon textures, concentrated towards the center of the vein. Large scale banding is usually asymmetrical. Crustiform mirror image banding is more common on a smaller scale in individual bands, thin stringers or veinlets.

Crosscutting bands generated by multiple fluid phases and replacement processes, indicate sphalerite and galena were deposited later than arsenopyrite and pyrite. Some parts of the vein contain all four major sulphides but lack evidence of multiple fluid

injections.

Venus has many features which suggest there has been repeated movement along the vein system. These features include:

- 1) slickensides on vein walls;
- 2) clay gouge separating the vein from the hanging wall and footwall;
- 3) asymmetric banding;
- 4) multiple layers of comb quartz;
- 5) one-sided comb structures;
- 6) quartz filled sulphide fractures; and
- 7) ribbon textures in the vein walls.

Intercalated wallrock in the vein, either as bands or unsupported angular fragments, is common. Where the bands of host rock are thin and clayey, it is possible that reopening of the fissure tore loose slabs of wallrock which were incorporated into the vein and smeared by later movement. Thick banding between wallrock and quartz could be caused by replacement of wallrock or by secondary quartz filled fissures close to the main vein.

Many of the features described above are illustrated in Figures 2, 3 and 4.

ORE SHOOTS

Ore shoots at Venus are defined solely on the basis of assay information, since the gold is microscopic. For mining purposes, the assay information is taken to a 1.5 m (5 ft) mining width, re-worked, then plotted as mineral blocks. Each block is assigned an average grade, tonnage and value. Correlation between blocks of

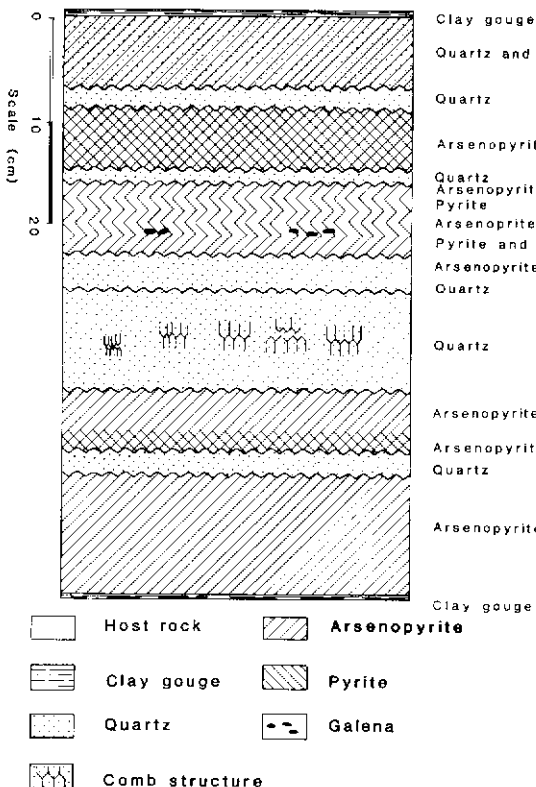


Figure 2. Section of vein from 2850 level showing asymmetrical sulphide bands concentrated on the outer edges of the vein.

equal value roughly outline ore shoot location.

Like many other deposits of this type, ore shoots at Venus are concentrated in columnar, steeply-pitching bodies of varying size, shape and continuity. The shoots comprise 20% of the vein system and have a dip length to strike length ratio of 10:1 to 5:1. Some of the more persistent shoots extend through all five levels in the mine. They are more regularly spaced in the northern part of the mine than in the south.

Many shoots are associated with wide portions of the vein. These shoots typically contain a high percentage of all four major sulphides. If a vein section displays massive bands of arsenopyrite-pyrite and later injections of galena-sphalerite, there is a good possibility it contains high grade ore. However, sections of vein displaying typical quartz-arsenopyrite-pyrite could also be high grade, and look identical to low grade portions on either side.

Assay information across vein segments show a distinct correlation between gold, arsenopyrite and pyrite. This is illustrated in Figure 4. Silver is carried mainly by galena. Gold increases with elevation, which is reflected in the greater amount of massive arsenopyrite-pyrite mineralization relative to quartz gangue on the upper levels.

DISCUSSION

Underground observations indicate Venus formed from hydrothermal solutions by both open space filling and replacement processes. Quartz deposition was ubiquitous throughout the sequence. Arsenopyrite and pyrite occur underground in bands near outer edges of the vein, implying early precipitation.

Repeated movement along curved planar surfaces opened more space for sulphide deposition. Wallrock slabs and fragments occasionally dropped from the wall to be incorporated in the vein and smeared as a result of later movement. As mineral precipitation continued, galena and sphalerite replaced arsenopyrite and pyrite, and precipitated in open spaces and vugs. At some point in the sequence, gold was introduced and deposited in the wider portions of the vein and in other areas.

Although precipitation of gold was probably controlled by physio-chemical conditions operating during ore deposition, the mechanism for concentration of gold into ore shoots is unknown.

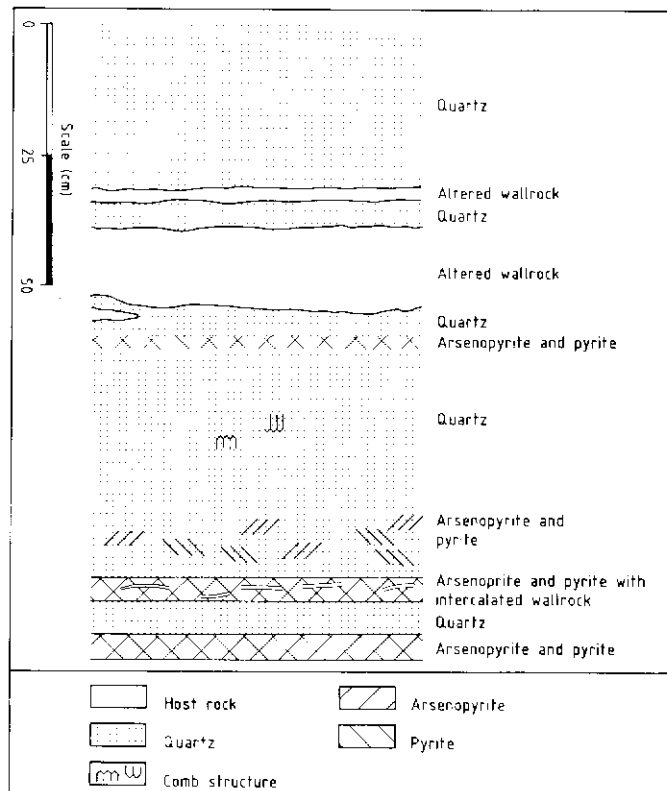


Figure 3. Section of vein from 2700 level showing a quartz core with bands of sulphides and altered wallrock.

In many vein systems of this type, there is no known structural control for occurrence of ore shoots along the vein. The presence of other features may complicate attempts to develop a model for ore shoot distribution based solely on structure. For instance, intense clay alteration is associated with a strong ore shoot in the northern part of the mine, and is found locally in other areas along the vein.

Recurrent opening and closing of the fissure along warped planar surfaces generated available open spaces for movement of gold-rich fluid. The larger the opening, the easier was fluid movement. Many ore shoots are contained in wider sections of the vein. Thinner portions of the vein would fill quickly and block fluid movement, creating localized stagnant areas. There may be a relation between dip and gold grade at Venus (D. Prince, pers. comm.). In this case, it is possible that normal or reverse faulting would create steep or flat open spaces (depending on fault type) which would localize gold-rich fluids.

If there is a structural control on ore shoot occurrence at Venus, it is most likely that the ore is concentrated in shoots by physical fluid behavior and available open space during deposition of gold-bearing fluids.

FUTURE WORK

Field study provided valuable information on the mineralogy, texture, structure and alteration of the Venus deposit. Current laboratory work includes fluid inclusion research, polished and thin section petrography and X-ray diffraction analysis of wallrock alteration. Consolidation of research data should generate a useful model defining controls on gold distribution in the Venus Vein and other similar vein systems.

ACKNOWLEDGEMENTS

This project was supported by Exploration and Geological Services Division, Department of Indian Affairs and Northern Development in Whitehorse, Yukon. I am grateful to J. Morin for suggesting the topic. I am especially grateful to Dennis Prince and the rest of the United Keno Hill Mines Ltd. staff who provided addi-

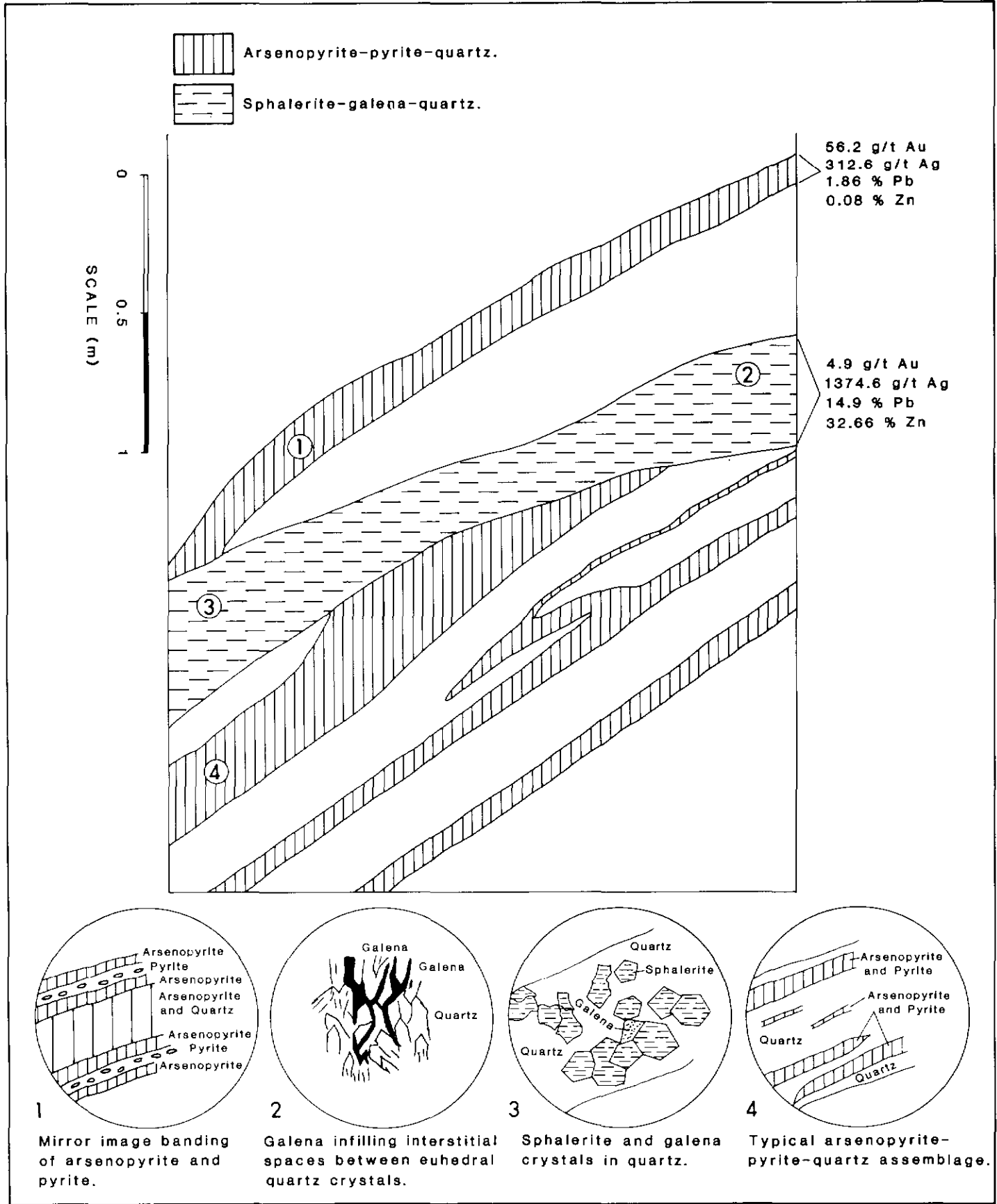


Figure 4. 2850 level north face. Section of vein in high grade ore shoot showing arsenopyrite-pyrite and sphalerite-galena rich phases.

tional support, encouragement and access to the mine. I would also like to thank Teresa Potter and Donna Hudgeon for their assistance in the field. The author is a graduate student at the

University of Alberta under the supervision of Dr. B. Nesbitt.

REFERENCES

- MORIN, J., 1981. Element distribution in Yukon gold-silver deposits; *in* Yukon Geology and Exploration 1979-80, Dept. Ind. Aff. Nor. Dev., Whitehorse, Yukon, p. 68-84.
- RALFS, K., 1975. A study of the mineralogy, paragenesis, zoning and wallrock alteration, Venus Vein, Montana Mountain, southwest Yukon; *Unpublished BSc Thesis*, University of British Columbia, Vancouver, B.C., 48 p.
- ROOTS, C.F., 1981. Geological setting of gold-silver veins on Montana Mountain; *in* Yukon Geology and Exploration 1979-80; Dept. Ind. Aff. Nor. Dev., Whitehorse, Yukon, p. 116-122.
- ROOTS, CLF., 1982. Geology of the Montana Mountain Area, Yukon; *Unpublished MSc Thesis*, Carleton University, Ottawa, Ont., 127 p.
- WHEELER, J.O., 1961. Whitehorse map-area, Yukon Territory; *Geol. Surv. Can., Memoir 312*, 156 p.

GEOLOGY AND ALTERATION OF THE GREW CREEK EPITHERMAL GOLD-SILVER PROSPECT, SOUTH-CENTRAL YUKON

Jesse L. Duke and Colin I. Godwin
Department of Geological Sciences
University of British Columbia
Vancouver, British Columbia

DUKE, J.L., and GODWIN, C.I., 1986. Geology and alteration of the Grew Creek epithermal gold-silver prospect, south-central Yukon; in Yukon Geology, Vol. 1; Exploration and Geological Services Division, Yukon, Indian and Northern Affairs Canada, p. 72-82.

ABSTRACT

Grew Creek epithermal gold prospect, in south-central Yukon Territory, is adjacent to and southwest of the Robert Campbell Highway, halfway between the communities of Ross River and Faro. The prospect is within the Tintina Trench, which from Late Cretaceous to Tertiary time was a zone of major right lateral movement that juxtaposed Cambrian and Ordovician slates and phyllites of the Pelly-Cassiar Platform (to the southwest) against rocks of the Anvil Allochthon (to the northeast).

Grew Creek rocks are mid-Eocene based on K-Ar dates of basalt of 51.4 ± 1.8 Ma and 50.7 ± 1.8 Ma, and pollen spores in volcaniclastic rock dated at 56 to 46 Ma. Felsic volcanic and volcaniclastic rocks were overlain by a sequence of interbedded coarse clastic sediments, basaltic flows, and basaltic volcaniclastic rock. Late Tertiary uplift and faulting resulted in graben formation and consequent preservation of Eocene rocks in a structurally complex graben bounded to the south by the Grew Creek fault and to the north by the Danger Creek fault.

Mineralization at Grew Creek occurs at the tip of a westwardly pointing wedge of dominantly felsic, crystal lithic lapilli tuff. The zone of precious metal deposition is truncated to the northeast by steeply dipping clastic sediments and to the southwest by the Grew Creek Fault. Gold, electrum, pyrite, and silver selenide were identified in a high grade sample from the discovery outcrop.

Alteration at Grew Creek is both surficial and hydrothermal. Surficial alteration is ubiquitous, pervasive, and characterized by mixed-layer clays and carbonates. Hydrothermal alteration, responsible for the gold-silver mineralization is closely associated with rhyolitic dykes and is of three types: silicic, acid sulphate, and argillic acid sulphate. K-Ar dating of sericite indicates hydrothermal alteration is mid-Eocene (51.5 ± 1.8 Ma and 47.0 ± 1.7 Ma) and synchronous with deposition of the volcanics.

Quartz associated with mineralization at Grew Creek is enriched in heavy oxygen isotopes. A deep magmatic source for the mineralized fluids is one explanation for this enrichment.

INTRODUCTION

The Grew Creek epithermal gold-silver prospect lies near Grew Creek about 1 km west of the Robert Campbell Highway, halfway between the communities of Ross River and Faro in south-central Yukon Territory. The Canyon claim block covering the zone of mineralization is on the western flank of a broad valley which marks the Tintina Trench. This valley was scoured by Pleistocene glacial ice and is extensively covered by till, drumlins and a few small lakes.

Sparse jackpine, spruce, and fir with willow and buckbrush characterize the claim area. Summer weather tends to be cool with daily highs ranging between 15° and 25°C ; rainfall is frequent. The Canyon property, owned by Al Carlos of Whitehorse, Yukon Territory, was optioned in 1984 by Hudson Bay Exploration and Development Company Ltd., Toronto, Ontario, who subsequently have conducted an exploration program involving trenching, diamond drilling, geochemical sampling and geophysics.

The Grew Creek discovery is significant as the first reported Tertiary volcanic-hosted epithermal gold showing in the Tintina Trench. This report examines the geology at Grew Creek with special emphasis on the alteration associated with the mineralization.

REGIONAL GEOLOGY

At Grew Creek, epithermal gold-silver mineralization lies within Eocene felsic volcaniclastic rocks in the Tintina Trench. During the Late Cretaceous, major right-lateral movement along the trench caused at least 450 km of displacement (Rodick, 1967; Tempelman-Kluit, 1979). In the Grew Creek area, this resulted in the juxtaposition of the Pelly-Cassiar Platform against rocks of the Anvil Allochthon.

The area southwest of Grew Creek consists of rocks of the Pelly-Cassiar Platform, early Paleozoic pale green phyllite, argillite, and laminated chert of the Kechika Group (Fig. 1, Unit 1). The area northeast of the Tintina Fault zone adjacent to Grew Creek is part

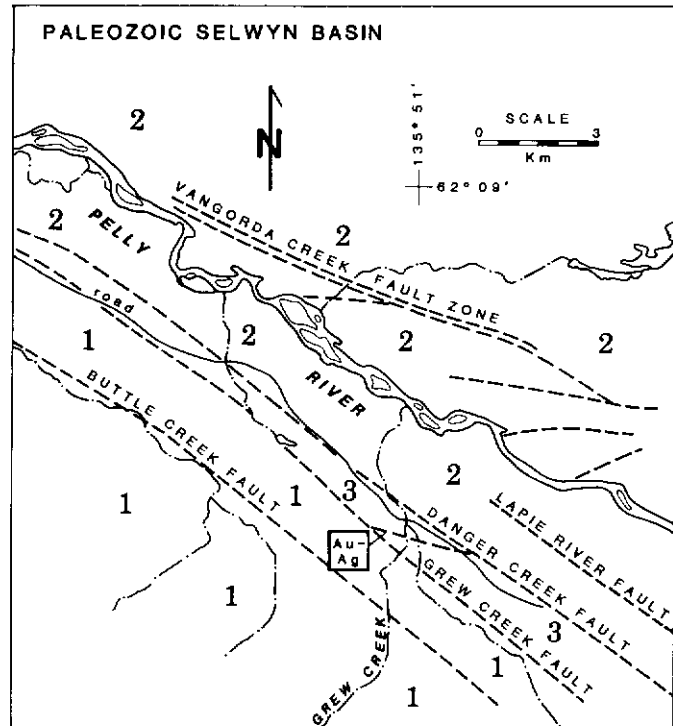


Figure 1. Grew Creek regional geological setting. 1 = unit 1, early Paleozoic Pelly-Cassiar Platform phyllite and chert. 2 = unit 2, Anvil Allochthon metabasalt and marble. 3 = unit 3, Eocene volcanic, volcaniclastic, and fluvial clastics. Grew Creek is marked as Au-Ag occurrence.

of the Anvil Allochthon (Fig. 1, Unit 2), which represent eugeoclinal equivalents of the Selwyn Fold Belt that were thrust northeastward during the Mesozoic (Tempelman-Kluit, 1979; Gorday, 1983).

Balsaltic to rhyolitic volcanism during the Eocene produced the rocks hosting the Grew Creek prospect. The graben created in the Tintina Fault zone during the late Miocene or Pliocene (Tempelman-Kluit, 1980) provided the complex structural setting at Grew Creek. Thus, the Eocene volcanic, volcaniclastic, and fluvial clastic sequence at Grew Creek (Fig. 1, Unit 3) is preserved in a graben sandwiched between these major tectonic elements.

LOCAL GEOLOGY

The Grew Creek prospect area, adjacent to the southwestern margin of the Tintina Trench, is cut by five major northwesterly trending fault zones (Fig. 1). Significant strike-slip and dip-slip motion may have occurred along these steeply dipping faults (Tempelman-Kluit, 1972). Interpretation of the geology at Grew

Creek is hampered by very poor exposure and extensive fault disruption. The only good outcrop of the Eocene rocks is along Grew and Rat Creeks and at the discovery outcrop (Fig. 3). Nevertheless, three distinct lithologic units were recognized. They are numbered from oldest to youngest in Figures 1 to 3, and are described in detail below.

Unit 1

Phyllite, argillite, and chert (Fig. 3: PHYL), early Paleozoic in age (Roddick, 1961), form tan weathered outcrop in large cliffs and canyons southwest of the Grew Creek fault. Phyllite is pale green or grey, argillite is dark grey, and chert is grey and laminated.

Unit 2

Metabasalt forms large, green cliffs (Fig. 2). Thin sections show this unit to be schistose and composed of dark green, very fine grained chlorite and carbonate (60%), swirls and clots of feldspars (35%), and anhedral quartz (5%). Marble occurs throughout the metabasalt as white cliffs of cream and pale grey medium-grained massive recrystallized limestone.

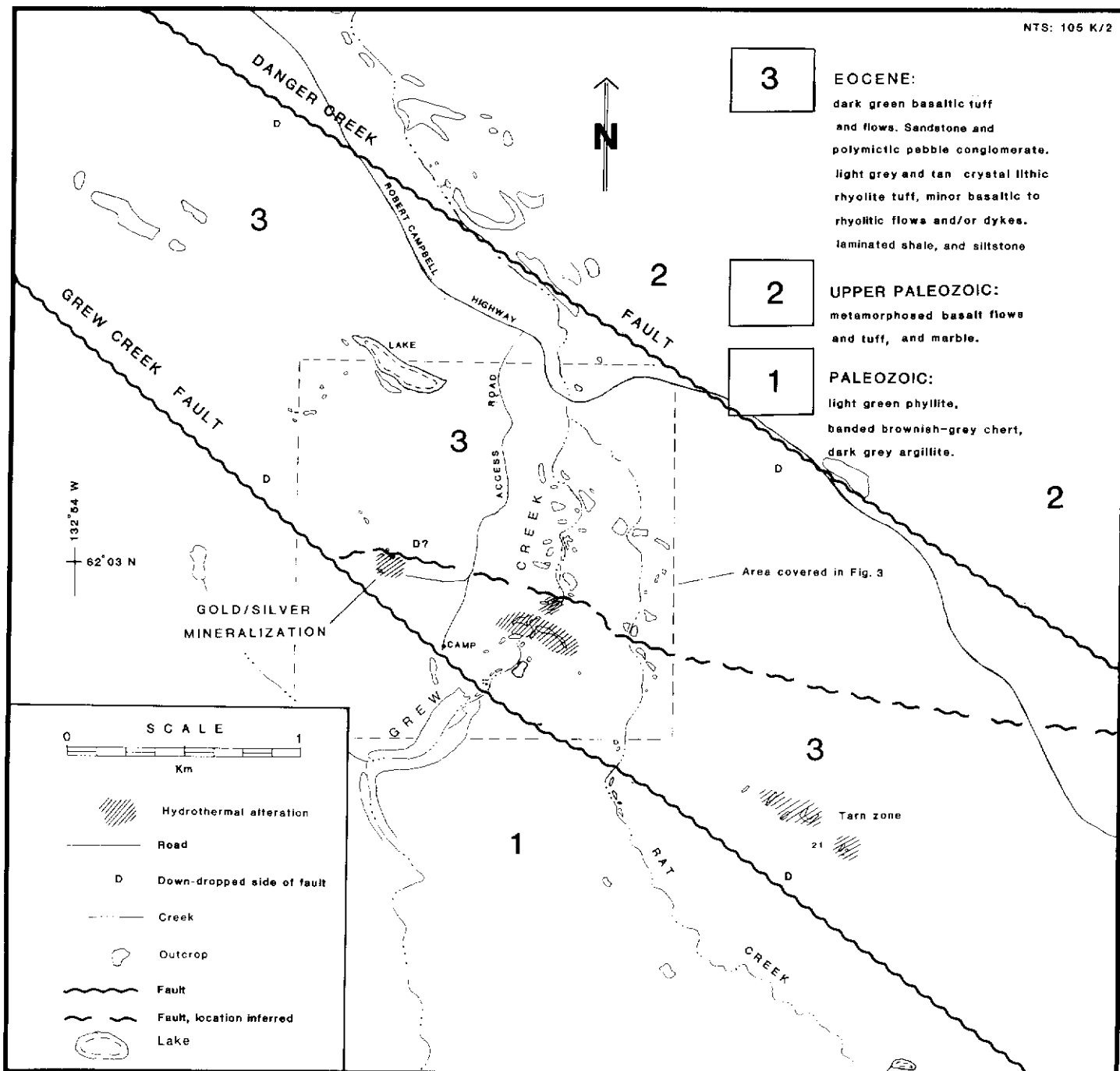


Figure 2. Grew Creek general geology.

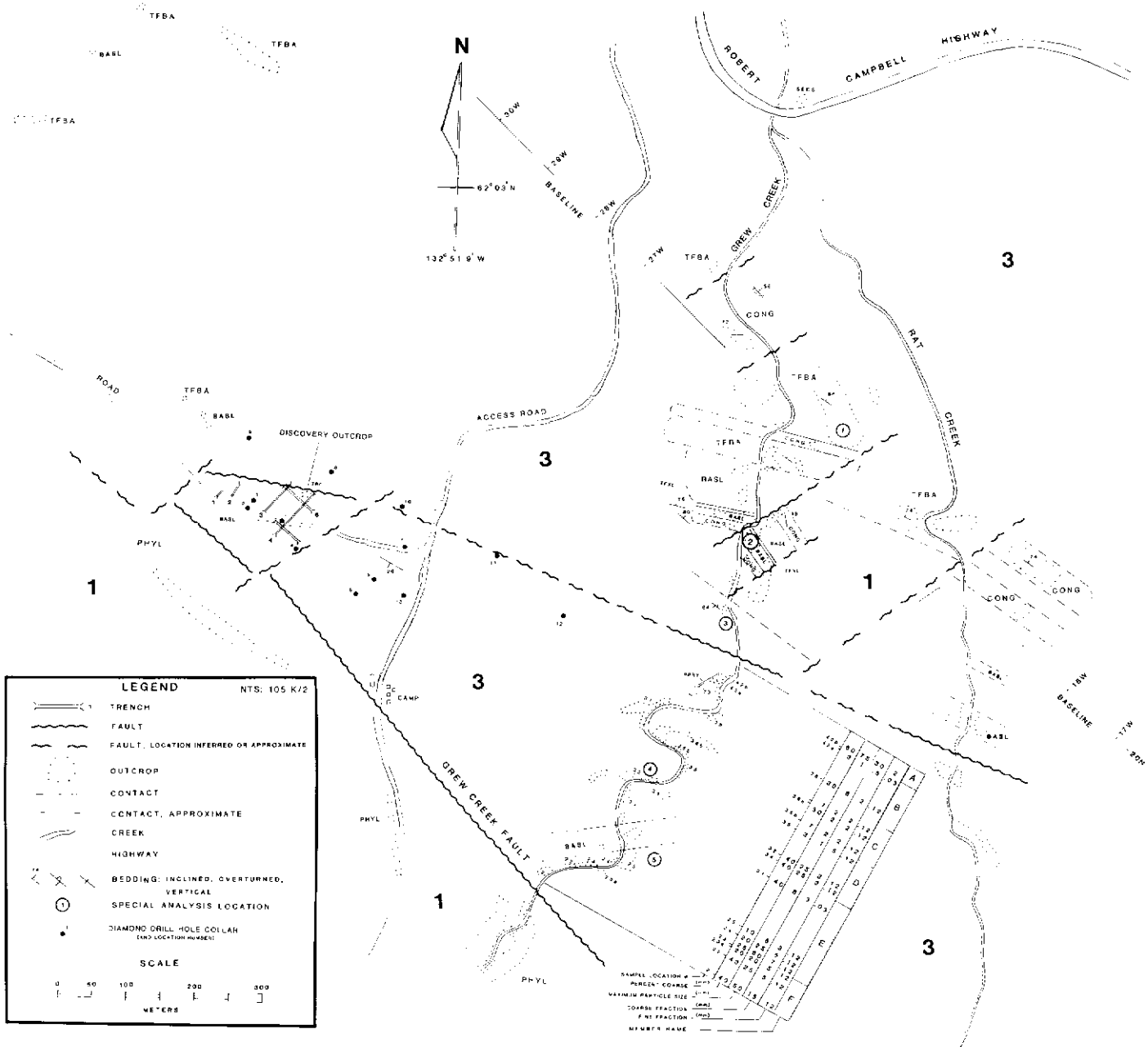
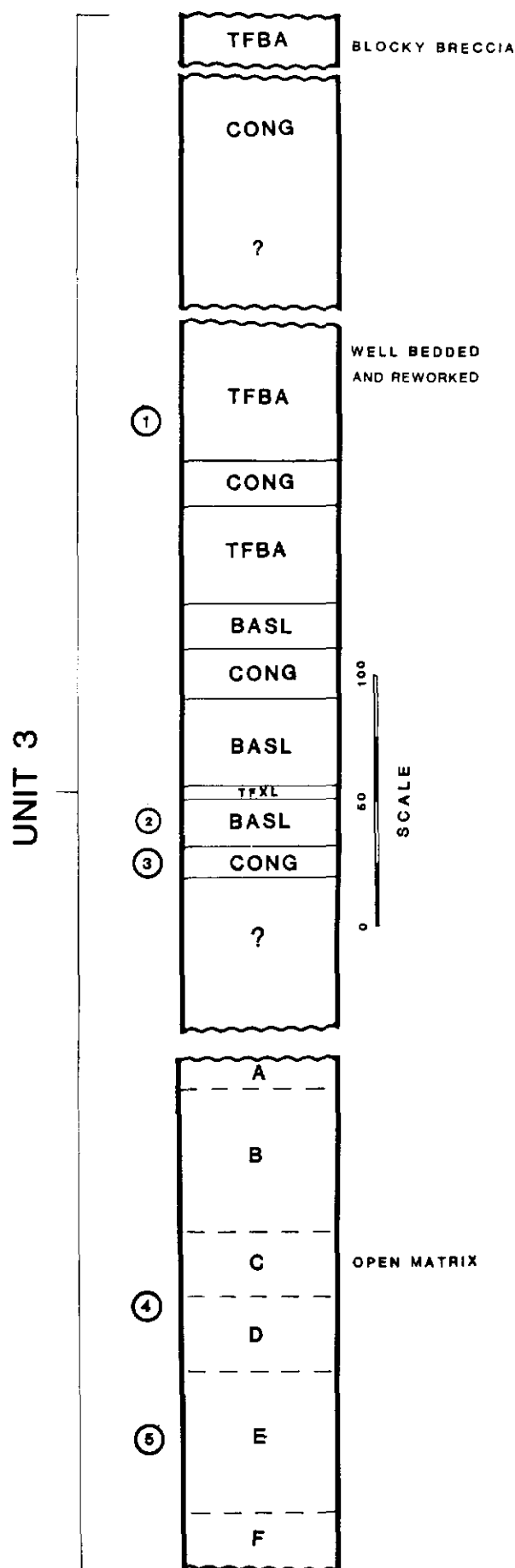


Figure 3. Sample and drill hole location map of the Grew Creek area. Circled numbers indicate special analysis was performed on samples from that location as follows: **1)** Sample D-52, basalt bomb in a well-bedded tuff. Prominent epidote alteration. Whole-rock K-Ar date: 51.4 ± 1.8 Ma. **2)** Sample D-6, porphyritic basalt (BASL). Whole-rock K-Ar date: 50.7 ± 1.8 Ma. **3)** Sample D-43, poorly sorted conglomerate (CONG) clast lithology listed in Table 1. **4)** Sample D-32, TXFL, Unit 3, Member C, strong sericitic alteration. Whole-rock K-Ar date: 51.5 ± 1.8 Ma. **5)** Sample D-25c, crystal lithic lapilli tuff (TXFL), Unit 3, Member B, strong sericitic alteration. Whole-rock K-Ar date: 36.0 Ma (± 1.3 Ma).

DRILL HOLE INFORMATION:

HOLE NUMBER	ANGLE	DIRECTION	DEPTH
1	-50°	az = 045°	103.6m
2	-50°	045°	96.6m
3	-50°	225°	137.8m
4	-50°	225°	112.5m
5	-50°	045°	125.0m
6	-50°	045°	122.2m
7	-50°	045°	111.2m
8	-50°	225°	136.8m
9	-50°	225°	144.2m
10	-50°	225°	177.4m
11	-50°	225°	164.6m
12	-60°	225°	142.0m
13	-50°	225°	137.8m

GREW CREEK SECTION



Unit 3

This unit has been divided as illustrated in Figure 4. It consists of Eocene rocks in a graben defined by the Grew Creek fault to the southwest, and the Danger Creek fault to the northeast (Figs. 2 and 3). Figure 4 is a cross-section through the Eocene volcanic and sedimentary sequence of Unit 3 at Grew Creek. Subdivisions within this unit are described below.

Crystal lithic lapilli tuff (Fig. 3, TFXL) is the dominant lithology in Unit 3. This tuff is pale grey and weathers recessively to a pale yellow-tan. Good exposures are restricted to the walls of Grew Creek. Grain size is variable and texture is clast supported. Clasts consist of felsic volcanics and variable amounts of subrounded to angular locally derived shale, and phyllite. Some fragments show weakly developed flow banding. Thin sections of felsic fragments show most feldspar crystals pervasively altered to green, white, and grey clays. Quartz occurs both as scattered subrounded "eyes" and as angular fragments. Patches of carbonate and opaque minerals also are common.

Grain size variations in the exposure of tuff along Grew Creek are documented in Figure 3. Grain size tends to be bimodal with a fine fraction of about 0.1 mm (coarse ash) and a coarse fraction of 2 to 6 mm (small lapilli). Six distinct depositional events are evident based on normally graded variations in the maximum particle size and the coarse fraction of the lapilli and blocks. Fragments up to 75 cm in diameter occur, indicating that the volcanic activity may have been proximal and explosive. Changes in grain size over short distances suggest at least a moderately dipping sequence striking easterly. However, the nearest structural data from core near the discovery outcrop about 300 m to the northwest (Fig. 3) indicates gently dipping bedding at that location. A sericitically altered sample (Fig. 3: outcrop 32) yielded a whole rock K-Ar date of 51.5 ± 1.8 Ma (Table 5).

Porphyritic rhyolite (Fig. 3: PPRY) forms small reddish brown weathering outcrops that probably represent dykes within the felsic volcaniclastic rocks. Rhyolite is also found in drill core as green flow-like units up to 2 m thick. It is a competent grey rock with a trachytic texture. A thin section shows the rock to consist of 40% euhedral, sub-parallel plagioclase phenocrysts to 4 mm in size, and 5% altered relict opaque minerals within a very fine-grained to aphanitic matrix (55%) rich in opaques, clay, and K-feldspar.

Volcaniclastic sediments form thin distinctive beds found only in drill core. They are matrix-supported, poorly lithified black volcaniclastic debris flows or laharls that contain fragments of altered and silicified felsic volcanics in a soft carbon-rich muddy matrix. These rocks are interbedded with felsic volcanic flows, mudstone, and sandstone, and are spatially associated with the conglomerate and sandstone described below.

Conglomerate and sandstone (Fig. 3: CONG) occur as isolated small outcrops along Grew Creek that are steeply dipping and poorly lithified. They are pale grey, clast-supported, have a cleanly washed appearance, and are variably sorted with normal and reversely graded bedding with frequent channel scours, and occasional carbonized plant debris. Cementing is largely carbonate. Clast lithology is in Table 1.

Figure 4. Grew Creek section. Circled numbers indicate special analysis was performed on samples from that location as follows: 1) Sample D-52, basalt bomb in a well-bedded tuff. Prominent epidote alteration. Whole-rock K-Ar date: 51.4 ± 1.8 Ma. 2) Sample D-6, porphyritic basalt (BASL). Whole-rock K-Ar date: 50.7 ± 1.8 Ma. 3) Sample D-43, poorly sorted conglomerate (CONG) clast lithology listed in Table 1. 4) Sample D-32, TFXL, Unit 3, Member C, strong sericitic alteration. Whole-rock K-Ar date: 51.5 ± 1.8 Ma. 5) Sample D-25c, crystal lithic lapilli tuff (TFXL), Unit 3, Member B, strong sericitic alteration. Whole-rock K-Ar date: 36.0 ± 1.3 Ma.

TABLE 1
Clast description from conglomerate in Unit 3 (CONG; from outcrop 43, special sample location 3; Figs. 3 and 4).

45%	thinly laminated dark-grey muscovite-quartz schist with frequent limonite stained patches and streaks.
16%	pale green, laminated (0.5 mm layers) muscovite-feldspar-quartz schist with limonite stained spots.
15%	white (vein?) quartz.
13%	crumbly pale grey volcanic clasts (TFXL).
6%	pale-green to pale-grey medium-grained sucrosic muscovite-feldspar schist.
3%	banded black and grey carbonaceous chert.
2%	equigranular coarse-grained (0.5 to 1 mm in diameter) quartzite.

The altered felsic volcanic fragments indicate felsic tuff (Fig. 3, TFXL) from the same unit as a probable source. This suggests the conglomerate and associated basalt post-date the felsic rocks. However, one small bed of felsic crystal tuff with vesicular fragments does occur upsection adjacent to a basalt flow.

Porphyritic basalt (Figs. 3 and 4, BASL) occurs throughout the map area as flows conformable to bedding and as dykes and/or sills. It forms prominent outcrops, commonly cliffs, and is brown weathering. The matrix is grey and fine-grained. Plagioclase (An_{95}) occurs as anhedral phenocrysts up to 3 mm in diameter and as smaller euhedral crystals. Thin sections show the rock consists of 50% plagioclase, 20% opaques, 20% indeterminant matrix altered to carbonate, 5% relict oxyhornblende, and 5% relict olivine. A weakly altered sample (Fig. 3: Outcrop 6) yielded a whole rock K-Ar date of 50.7 ± 1.8 Ma (Table 5). Whole rock chemical analyses, shown in Table 2, indicate a relatively unaltered and subalkaline (de Rosen-Spence, 1976), high to very high K (Gill, 1981), tholeiitic basalt (Miyashiro, 1974).

Basaltic volcaniclastics (Figs. 3 and 4, TFBA) are throughout the map area. They are dark green, extremely variable rocks, breccias, and ash to block tuff with variable amounts of rock fragments, mostly shale and dark coloured volcanic clasts. Rocks include well-bedded, reworked tuff deposits with sub-rounded sand-sized quartz grains, massive, chaotic, clast-supported, extremely angular breccia dominated by schist and shale fragments, and medium-green, vesicular basalt flows with small carbonate and quartz amygdules and drusy cavities. Mineral assemblage and major element abundance (Table 2) of a bomb in the well-bedded member of TFBA (Figs. 3 and 4, Special Sample Location 1) is almost identical to that of a basalt flow (Fig. 3: Special Sample Location 2). This suggests a similar magmatic source and the probability of periodic basaltic volcanism during rapid sedimentation of the felsic volcanic pile. A K-Ar date of 51.4 ± 1.8 Ma was obtained from this bomb (Table 5).

Muddy sediments (Fig. 3: SEDS) occur north of the highway as scattered exposures along Grew Creek. They are grey to pale purple weathering rocks consisting of interbedded conglomerate, sandstone, mudstone, and shale. The conglomerate is very poorly sorted with a clay or silt matrix. Conglomerate beds include numerous channel scours filled with silt. The bedded sediments range from arkosic, well-sorted fine-grained sandstone up to 30 cm thick with variable amounts of plant debris, to thinly bedded, fissile, micaceous, carbonaceous and silty shale. These rocks are separated from the rest of the Eocene sequence by a gap of several hundred meters that obscures any relationship with the Grew Creek section and precludes their inclusion in Figure 4.

ALTERATION

Analytical methods

Both general and detailed studies of alteration were done. Ninety-four sample locations in Unit 3 (Fig. 3) were examined by X-ray diffraction on oriented water mounts (Carroll, 1970). This data was compared to standard runs of minerals of known composition using the same preparation technique, and to tabulated X-ray diffraction data (Joint Committee on Powder Diffraction Standards, 1980). All mineral assemblages in Table 3, Figure 5, and in the text are listed in order of decreasing diffraction peak intensity. Peak intensity was used as a qualitative measure of relative

TABLE 2
Chemical compositions (oxides, weight %)¹, actual and normalized for basaltic rocks from Grew Creek, Yukon. Samples D52 (basaltic bomb, TFBA) and D6 (porphyritic basalt, BASL) are from Unit 3 (Fig. 3).

	— Sample D52 —		— Sample D6 —	
	Composition	Normalized	Composition	Normalized
SiO ₂	47.34	49.05	47.88	50.62
TiO ₂	2.42	2.51	2.26	2.39
Al ₂ O ₃	16.10	16.68	16.13	17.05
Fe ₂ O ₃	3.92	4.06	3.76	3.98
FeO	6.25	6.48	6.43	6.80
MgO	5.02	5.20	3.94	4.17
CaO	7.75	10.10	7.64	8.08
Na ₂ O	3.38	3.50	3.84	4.06
K ₂ O	1.32	1.37	1.94	2.05
P ₂ O ₅	0.52	0.54	0.63	0.67
MnO	0.50	0.52	0.13	0.14
LOI	2.59		4.34	
TOTAL	99.82	100.01	98.92	100.01

1. Weight % oxides calculated by Midland Earth Science Associates, Conway House, Conway Street, Long Eaton, Nottingham, U.K.
LOI = loss on ignition.

amounts of each phase present. Surficial and hydrothermal alteration types were identified, as described below.

Surficial alteration

Warm subtropical conditions that existed during the Eocene (Hopkins, 1974; Rouse, 1977; Wolfe, 1978), in conjunction with heavy rainfall (over 1,800 mm/year, Rouse, pers. comm., 1986), the high permeability of the host rock, and a fluvial sedimentary environment contributed to a deep weathering profile at Grew Creek. Pleistocene glaciation and erosional processes removed most exposures of the Eocene rocks. Only exposures along Grew Creek and isolated outcrops elsewhere remain (Fig. 3).

Felsic volcanic rock in outcrop is friable. Feldspar crystals are altered to a waxy white and grey material and the matrix to a grey material with a resinous lustre. The characteristic alteration assemblage consists of mixed-layer smectite/illite + quartz + various feldspars + iron rich carbonates. These alteration minerals are attributed to surficial weathering processes.

Surficial alteration is superimposed on all hydrothermal alteration facies. Although surficial alteration can be pervasive and intense, it lacks acid sulphates and the abundant secondary K-feldspar characteristic of the hydrothermal alteration discussed below.

Hydrothermal alteration

Areas of intense hydrothermal alteration are shown by diagonal hatching in Figure 2. Hydrothermal alteration is subdivided into the following facies based on mineralogy: silicic, acid sulphate, and argillic acid sulphate.

Silicic alteration, represented in the felsic lapilli tuff of Unit 2 (Fig. 3) forms resistant, rounded knobs in outcrop. Original pyroclastic textures are obscured and altered rocks are a darker grey compared to unsilicified specimens. The mineral assemblage is dominated by quartz ± K-feldspar ± mixed-layer smectite/illite ± albite ± Fe-rich carbonate. This assemblage is associated closely with anomalously high precious metal values and gold-silver-rich chalcedonic quartz plus K-feldspar veins up to several cm thick.

Acid sulphate alteration occurs along Grew Creek in several places near altered felsic dykes. The presence of an acid sulphate mineral, jarosite or alunite, as determined by X-ray diffraction, distinguished this facies.

Argillic acid sulphate alteration, recognized only in trenches and core because weathers recessively, is characterized by crumbly rock that is pale grey or white when dry. Strong alteration totally obliterates original textures. The associated mineral assemblage is dominated by smectite ± mixed-layer smectite/illite, + carbonate ± jarosite ± alunite ± sericite ± kaolinite ± K-feldspar (primary?) ± plagioclase (primary?) ± iron-oxides ± quartz (partly primary?). Either one or the other of the acid

TABLE 3
Detailed lithological and alteration features of Trench 4
from 0 to 84 meters. (Fig. 3)

METERS	LITHOLOGY ¹	QUARTZ % ²	CLAY % ²	VEIN ³ STRIKE/DIP	AU ⁴	AG ⁴	AS ⁴ PPM	HG ⁴ PPB	ALTERATION ⁵
1	TFXL								
2	TFXL								
3	TFXL	50							
4	TFXL	20							QZ ML OR si
5	TFXL		20			2			
6	TFXL		30						
7	TFXL	40							
8	TFXL	40							
9	TFXL	40							
10	TFXL		20		1	2	500	220	
11	ROTN		20						ML sm ms il or
12	ROTN		20						
13	TFXL	70			1	1	300	115	
14	TFXL	70			1	2	210	200	
15	ROTN		20	093/-	1	1	30	110	
16	ROTN		20						QZ ML fs
17	TFXL	70							QZ ML OR ca si al
18.5	TFXL	70			1	1	90	300	
19	ANDS								
20	ANDS								
21	ANDS								
22.5	ROTN		30		—	1	33	220	
23.5	TFXL	10	10		1	1	85	330	ML fs qz ka
24.3	TFXL	20							
25.2	TFXL	70			1	1	240	120	ML AB ka
26	TFXL	10			1	1	330	155	
27	TFXL	10			2	2	190	360	QZ ml or ca
28	TFXL	10							
29	TFXL	10							
30	TFXL	10							
31	TFXL	10							
32.3	TFXL	10							
33	ROTN		20						
34	ROTN		20						
35	ROTN		20		1	2	75	295	
36	TFXL	40							
36.5	ROTN				1	1	100	500	QZ ml or pl ca si
38	TFXL	40			1	2	62	295	
39	TFXL	40							
40	TFXL								
41	TFXL								
42	TFXL								
43	TFXL	20			—	2	115	160	
44	TFXL	20			—	1	90	60	
45	TFXL	20					100	125	
46	TFXL	20			1	1	170	110	
47	TFXL	20							
48	TFXL	20			1	1	200	650	
49	TFXL	20							
50	TFXL	20							QZ OR al ja ca
51	TFXL	70							
52	TFXL	70							
53	TFXL	70			1	2			
54	TFXL	70		280/66	\$	\$			
55	TFXL	70			\$	\$			
56	TFXL	70		150/90	\$	\$			QZ OR ja al ml si cb
57	TFXL	70			\$	\$			
58	TFXL	70			\$	\$			

TABLE 3 (cont.)

METERS	LITHOLOGY ¹	QUARTZ% ²	CLAY% ²	VEIN ³ STRIKE/DIP	AU ⁴	AG ⁴	AS ⁴ PPM	HG ⁴ PPB	ALTERATIONS ⁵
59	TFXL	70			\$	\$			
60	TFXL	70			\$	\$			
61	TFXL	70			\$	\$			
62	TFXL	70			\$	\$			
63	TFXL	70		140/90	\$	\$			
64	TFXL	70			\$	\$			
65	TFXL	70		084/83	\$	\$			
66	TFXL	70		154/90	\$	\$			
67	TFXL	70			\$	\$			
68	TFXL	70			\$	\$			
69	TFXL	70			1	1	300	120	QZ OR al ja ca si
70	TFXL	70							
71	TFXL	70							
72	TFXL	70			1	1	100	110	
73	TFXL	70							
74	TFXL	70			1	2	270	140	
75	TFXL	70							
76	TFXL	70							
77	TFXL	70			1	2	150	240	
78	TFXL	70							
79	TFXL	20			1	1	75	60	
80	TFXL	20			1	2	140	310	
81	TFXL	20							
82	TFXL	20							
83	TFXL	20							
84	TFXL	20							
85	TFXL	20							

1. LITHOLOGY: TFXL = rhyolitic, crysal lithic lapilli tuff; ROTN = totally disaggregated rock material, probably TFXL. BASL = porphyritic basalt. See unit descriptions in text for complete description.
2. QUARTZ% = estimated total percentage of secondary quartz present. CLAY% = estimated total percentage of clay minerals present.
3. VEIN STRIKE/DIP = the strike and dip (to the right of strike direction) of major chalcedonic quartz and quartz-feldspar veins.
4. Au, Ag: - = not detected, much less than 2g/tonne; 1 = less than 2g/tonne; 2 = 2-7g/tonne; 3 = less than 7g/tonne; \$ = high values (pers. comm., Hudson Bay geologists) but no data available); black space = no data available.
5. Alteration is coded so that upper case indicates dominant phases, lower case indicates relatively smaller quantities as determined by weaker XRD peaks. QZ = quartz, ML = Mixed-layer clays dominated by smectite and illite, OR = K-feldspar, CA = calcite, SI = siderite, AL = alunite, JA = jarosite, CB = carbonate.

Trench strikes 045° (azimuth) and is inclined -5° in this direction. O meters is at 1334.00N, 2804.00E on property grid (Fig. 3).

sulphates is always present in this facies. Anomalous concentrations of heavy metals also occur with these assemblages.

Dykes are a feature common to all zones where increased alteration is evident in outcrop. This increased alteration may reflect local hydrothermal effects from the emplacement of hot dyke material into the porous lithic tuff. On the other hand, the emplacement of the impermeable dyke material may restrict and channel the flow of groundwater along the dyke margins, causing increased alteration associated with the locally higher flux of water.

Intense hydrothermal alteration occurs between Outcrop 25 and 31 within and proximal to the basalt dyke (Fig. 3). The basalt is completely altered to a cream, brown, and green spotted clay at one place (Fig. 3, Outcrop 25) that masks the original texture and mineralogy of the rock. K-feldspar and albite are the dominant alteration phases in some exposures. Kaolinite and epidote are also present in the altered basaltic material.

At the discovery outcrop (Fig. 3), the largest silicic alteration zone has an assemblage of quartz, K-feldspar and precious metals. Jarosite, alunite, and Fe-rich carbonate occur as a later episode of veining around brecciated fragments of strongly silicified tuff. Steeply dipping, commonly brecciated, chalcedonic quartz and K-feldspar veins with very strong precious metal values are prominent in this zone. Immediately adjacent to this silicic alteration, a rhyolite dyke is intensely altered to a soft, friable smectite.

Outcrop 42 (Fig. 3) has minor alunite in an otherwise dominantly surficial assemblage. This acid sulphate occurrence is ad-

jacent to a porphyritic rhyolite dyke with extensive pervasive alteration and minor disseminated pyrite. The dyke crosses Outcrop 37 (Fig. 3) near the acid sulphate and silicic alteration found in Outcrop 36b; it is too small to show at the scale of Figure 3.

Trench 4 alteration

A detailed analysis of part of a wall in Trench 4 is shown in Figure 5. This part of the trench provided clean exposure of the different facies of alteration associated with the mineralization. Samples were taken to represent each visually and texturally distinct alteration type. Silicic alteration represented by Samples 5, 6, 7, and 8 is dominated by quartz and K-feldspar. Mineralization also appears to be favoured in this zone, although the correlation based on these few samples is erratic and may be affected by cross-cutting quartz-feldspar-precious metal rich veins. There is an abrupt change in Samples 2, 3, and 4 which represent a zone of pervasive argillic acid sulphate alteration characterized by a mixed-layer illite/smectite and a diverse assemblage that includes the sulphates jarosite and alunite. A hematite stained zone of the argillic acid sulphate facies appears to be associated with the margin of the silicic facies. This juxtaposition of argillic and silicic facies is repeated seven times along Trench 4. Detailed features of Trench 4 are reported in Table 3.

TRENCH 4

X-SECTION

(0 TO 8m)

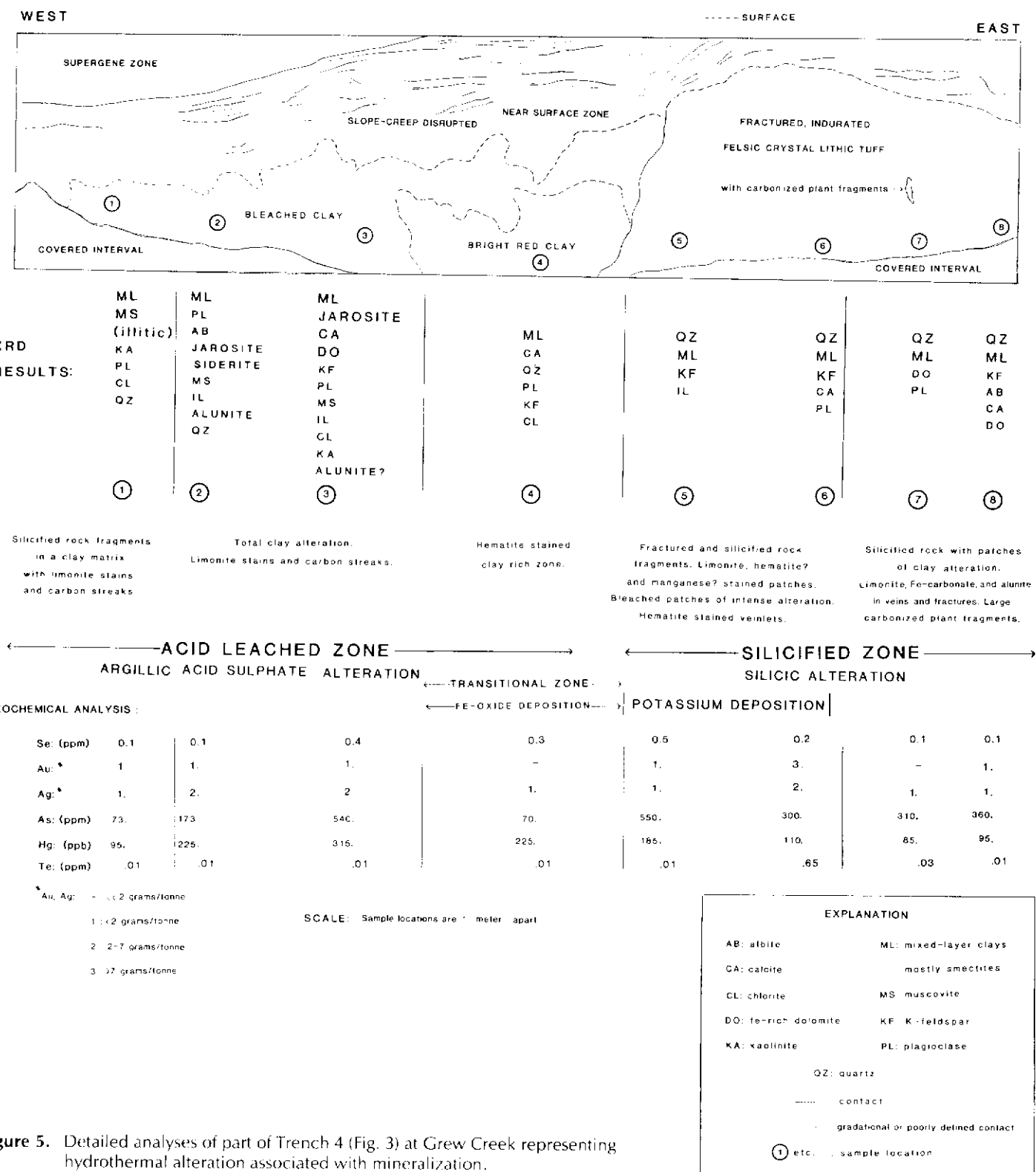


Figure 5. Detailed analyses of part of Trench 4 (Fig. 3) at Grew Creek representing hydrothermal alteration associated with mineralization.

MINERALIZATION

High-grade gold-silver mineralization occurs in the discovery outcrop, adjacent trenches and drill holes. It is associated with the silicic alteration; chalcedonic quartz and K-feldspar veins in silicified material contain the highest values of precious metals.

Gold, electrum, pyrite, and silver selenide, occur as disseminated specks in and adjacent to quartz-potassium feldspar veins. Figure 6 is a backscattered electron photomicrograph of a sample from the discovery outcrop (Fig. 3: Outcrop 76c) showing two grains of gold (white colour), one located in a vein hosted by crystal tuff (TFXL) and the other in an iron-oxide and alunite vein (distinguished by a paler grey shade, Fig. 6). The host rock has

been strongly silicified and has patches of K-feldspar. The pale grey mesh-like network in Figure 6 indicates areas of higher iron content. Gold in the iron-oxide and alunite vein (Fig. 6) may represent an inclusion from the silicified wall rock because all other precious metal grains were found in the silicic host.

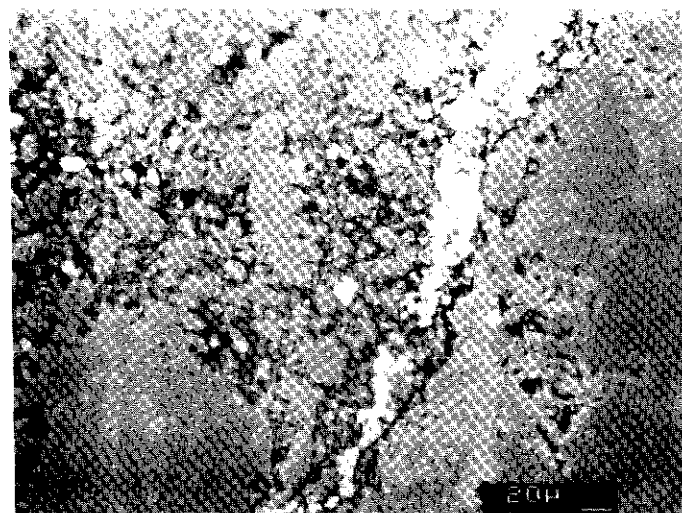


Figure 6. Scanning electron micrograph of gold associated with silicic alteration at Grew Creek (Fig. 3, discovery outcrop). Pale vein hosting one of the gold grains consists of iron oxides and alunite.

SAMPLE D-76c Z 00
PR 100S 100SEC 334184 INT
V 16K H 40KEV 1:1H AQ 40KEV 1H

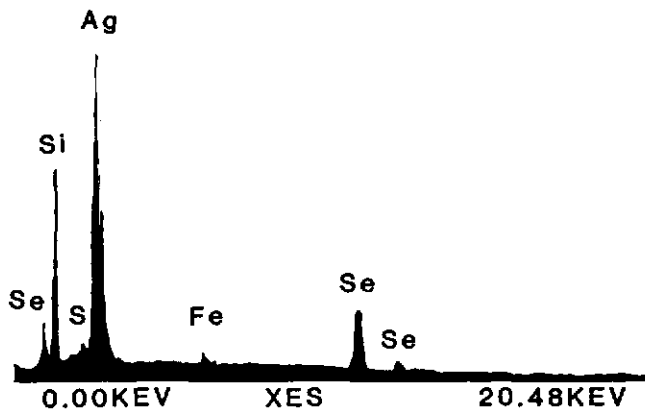


Figure 7. Energy dispersive spectrograph of a silver selenide mineral in the discovery outcrop (Fig. 3) at Grew Creek. Iron and sulphur may indicate pyrite in which case the silver-selenium peaks may represent haumannite, Ag_2Se or aguilarite, Ag_4SeS . The silica peak reflects the silicic alteration associated with mineralization in the discovery outcrop (Fig. 3).

The occurrence of precious metals with different gangue phases may indicate repeated mineralization events. The association of silica with mineralization and prominent vein layering suggests episodic deposition from the same hydrothermal fluid. The high gold and silver content of the argillic facies (Fig. 6) may represent remobilization of metals during a later stage acid leaching of the silicified rock.

Silver selenide is defined by Figure 7 which shows a graph of the energy dispersive spectrum for a grain in Sample 76c (Fig. 3). Peaks corresponding to characteristic energy levels for silver, selenium, sulphur, and iron are labelled in Figure 7. The iron and

sulphur may indicate a separate pyritic phase. If so, a silver selenide such as haumannite, Ag_2Se , or aguilarite, Ag_4SeS is indicated. Assays for selenium in Trench 4 are shown in Figure 5; values are not unusual relative to other precious metal deposits (Boyle, 1979).

The proximal location of the two alteration facies in Trench 4 (Fig. 5: silicic with the K-feldspar, argillic with the alunite and jarosite) indicates two incompatible pH conditions — a low pH assemblage superimposed upon a near neutral pH regime. A possible explanation for this association involves the evolution of carbon dioxide and hydrogen sulphide from a rising solution which results in a rise in the pH of the residual solution that causes precipitation of silica, feldspar, gold, silver, silver selenide, and iron sulphide. Carbon dioxide and hydrogen sulphide react under oxidizing surface conditions to form strong acids, and these leach the host rock adjacent to the silicified zone, leaving clays and other phases such as alunite and jarosite that are stable under such acid conditions (Rose, et al., 1979).

OXYGEN ISOTOPES

Analyses of four quartz-carbonate vein samples for stable heavy oxygen isotopes are in Table 4.

TABLE 4
Oxygen isotope results from Grew Creek, Yukon.

SAMPLE NO.	MINERAL	$\delta^{18}\text{O}$	(SMOW) ¹
10-1-95	quartz	6.8	
10-2-95	carbonate	6.9	
10-1-143	quartz	5.5	
10-2-143	carbonate	11.0	
10-1-152	quartz	5.6	
10-2-152	carbonate	11.0	
12-1-119	quartz	2.1	
12-2-119	carbonate	7.7	

1. All analyses by K. Mullenbachs, University of Alberta, Edmonton, Alta.

Laboratory results show $\delta^{18}\text{O}$ values ranging between 2.1 and 7.7 for quartz and between 5.6 and 11 for carbonate. A comparison of these values with results obtained in other similar systems described as epithermal (Nesbitt, et al., 1986) show the Grew Creek veins to be considerably enriched in $\delta^{18}\text{O}$. This enrichment is intermediate between the values often seen in epithermal deposits ($\delta^{18}\text{O} = -5$ to +2 per mil) and those found in mesothermal deposits ($\delta^{18}\text{O} = +15$ to +18 per mil).

Heavy isotope enrichment of a brine is commonly a result of one of three main processes: 1) a primary magmatic source for the brine in which the isotopic composition is in equilibrium with an ^{18}O enriched magma, 2) an isotopic exchange with an extremely enriched sedimentary host rock, and 3) extensive reaction with a moderately enriched host rock under conditions of low water/rock ratios. Any combination of these factors may be operating in a geothermal system.

The most probable explanation for the heavy isotope enrichment at Grew Creek is a primary magmatic source for the ore-forming fluids. This seems especially reasonable in view of the position of Grew Creek in a zone of deep crustal fracturing and major associated intrusive activity. However, other factors may be important. The Grew Creek deposit lies very close to metasediments of Unit 1 and these types of rocks are highly enriched in heavy oxygen isotopes (Taylor, 1974). However, it does not seem likely that there would be a significant exchange of oxygen occurring with this highly indurated rock. Epithermal systems regionally associated with clastic carbonates tend to have relatively enriched ^{18}O values (Taylor, 1974; White, 1974). About 1.5 km to the north, the nearest limestone crops out just across the Danger Creek Fault (Fig. 1). Extensive faulting that has occurred since the Eocene increases the possibility that blocks of ^{18}O -rich limestone may be near Grew Creek, and may have reacted with heated circulating groundwater.

The relatively high porosities of the tuffaceous rock that hosts the deposit and adjacent sandstones indicate a probable high water/rock ratio in the geothermal system, precluding extensive

isotopic exchanges with a moderately enriched rhyolitic host rock.

The large difference in $\delta^{18}\text{O}$ values between the quartz and carbonate in the veins reflects disequilibrium conditions. Cross cutting relations show the carbonate deposition was clearly a later event. $\delta^{18}\text{O}$ enhancement in the carbonate may be due to the easier exchange of heavy oxygen isotopes with the carbonate relative to the quartz.

AGE DATING

Potassium-argon

Five specimens from Unit 3 were chosen for whole-rock age dating. Results are in Table 5. Samples 6 and 52 date whole rocks, but Samples 25c and 32 date strong sericitic alteration. Sample 21 shows only partial sericitic alteration. Field locations are in Figures 2, 3, and 4. Detailed descriptions of analysed samples are in Duke (1986).

Palynology

Two samples from Diamond Drill Hole 9 (Fig. 3) at 32.5 m (mudstone) and 115.5 m (TFXL) contained 11 varieties of palynomorphs listed in Table 6. A middle Eocene assemblage, estimated as representing 56 to 46 Ma was found. The following combination of palynomorphs was the diagnostic criteria (Glen E. Rouse, pers. comm., 1986): *Pistillipollenites macgregorii* (late Paleocene to mid-Eocene), *Tilia vescipites* (early to late Eocene), *Fusiformisporites - B* (mid to late Eocene), *Tetracellaesporites - 1* (restricted to mid-Eocene), and over 10 specimens of *Granatisporites cotalus* (which peaks in the mid-Eocene).

The plant material examined was very heavily carbonized, indicating that it was subjected to temperatures of at least 270°C and probably over 300°C (Rouse, pers. comm., 1986).

TABLE 5

Potassium-argon data for volcanic rocks from Grew Creek area, south-central Yukon

Sample number	Location lat($^{\circ}$ N) long($^{\circ}$ W)	Rock unit and rock name	% K (\pm) (n = 2)	$\frac{{}^{40}\text{Ar}^*}{{}^{40}\text{Ar}_{\text{total}}}$	$\frac{{}^{40}\text{Ar}^*}{10^{-5} \text{ cm}^3 \text{ STP/g}}$	Apparent age (Ma) ³	Time ⁴	
D-25c	62.05	132.87	Lapilli tuff breccia, unit 3 (TFXL)	2.23 0.02	0.653	3.152	36.0 ± 1.3	Eocene-Oligocene border
D-21	62.05	132.87	Felsic tuff, unit 3 (TFXL), sericitized	4.62 0.03	0.925	8.552	47.0 ± 1.7	Eocene
D-32	62.05	132.87	Felsic lapilli tuff, unit 3 (TFXL), sericitized	4.29 0.03	0.856	8.705	51.5 ± 1.8	Eocene
D-6	62.05	132.87	Basalt flow, unit 3 (BASL)	1.73 0.00	0.709	3.458	50.7 ± 1.8	Eocene
D-52	62.05	132.87	Basaltic bomb, unit 3 (TFBA), epidotized	1.16 0.01	0.911	2.350	51.4 ± 1.8	Eocene

1. Argon analyses are by J. Harakal and potassium analyses are by K. Scott; all analyses were done at the Geochronology Laboratory, The University of British Columbia.

2. Ar* indicates radiogenic argon.

3. Constants used are from Steiger and Jager (1977): $\lambda_e = 0.581 \times 10^{-10} \text{ yr}^{-1}$; $\lambda = 4.962 \times 10^{-10} \text{ yr}^{-1}$; ${}^{40}\text{K}/\text{K} = 1.167 \times 10^{-4}$.

4. Time designation is from Harland et al. (1982).

TABLE 6

Palynology¹ of Grew Creek samples from Drill Hole 9 (Fig. 3), 32.5m (mudstone), and 115.5m (crystal lithic lapilli tuff).

NAME	AGE RANGE
Spores and pollen	
<i>Pistillipollenites macgregorii</i>	late Paleocene to mid-Eocene
<i>Tilia vescipites</i>	early to late Eocene
Fungal spores	
<i>Circulosporites - 1</i>	mid-Eocene
<i>Tetracellaesporites - 1</i>	mid-Eocene
<i>Fusiformisporites - B</i>	mid to late Eocene
<i>Disporisporites sp.</i>	early to mid-Eocene
<i>Granatisporites cotalus</i>	peak in mid-Eocene
<i>Pesavis</i>	late Paleocene to late Eocene
Recycled	
<i>Cicatricosporites cf. hughesii</i>	Albian to Maastrichtian
<i>cf. Palaeoperidinum pyrophorum</i>	Upper Cretaceous to Paleocene
<i>Triporopollenites mullensis</i>	Paleocene

1: All analyses by Glen E. Rouse, Department of Geological Sciences, The University of British Columbia, Vancouver, B.C.

CONCLUSIONS

Rocks preserved in a graben in Tintina Trench at Grew Creek are part of a sequence that represent proximal explosive felsic volcanism followed by interspersed rapid fluvial sedimentation and basaltic volcanism. K-Ar dates on unaltered whole rocks agree closely with palynology and indicate an age of mid-Eocene.

K-Ar whole rock dates on sericitically altered samples suggest hydrothermal alteration occurred from the time of deposition and may have continued at least until the end of the Eocene. Hydrothermal alteration appears to be spatially related to rhyolite dykes. Gold and silver mineralization is found with silicic and argillic alteration associated with a rhyolite dyke and acid sulphate minerals. It is characterized by multiple episodes of precious metal-rich chalcedonic quartz veining and brecciation of the felsic tuff host. Mineralization at the discovery outcrop is offset by faults that probably formed during creation of Tintina Trench in late Miocene or Pliocene. This suggests the mineralization pre-dates that event. Heavy oxygen isotopes in chalcedonic quartz veins suggest a deep, hot, magmatic source for the mineralized fluid.

ACKNOWLEDGEMENTS

The writers extend special thanks to Tom Garagan who helped our understanding of the geology at Grew Creek and contributed a great deal to this project. We also thank Hudson Bay Exploration and Development Company Ltd. for field support. Glen Rouse, John Knight, and Joe Harakal extended technical support at The University of British Columbia. Analyses of oxygen isotopes by

Karlis Mullenbachs at the University of Alberta also are gratefully acknowledged. This project was funded mainly by Exploration and Geological Services Division of the Northern Affairs Program in Whitehorse, under the direction of J.A. Morin. Support from The University of British Columbia and from research grants to C.I. Godwin are also acknowledged.

REFERENCES

- BOYLE, R.W., 1979. *The Geochemistry of Gold and its Deposits*; Geological Survey of Canada, Bulletin 280, 584 p.
- CARROLL, Dorothy, 1970. *Clay minerals: a guide to their X-ray identification*; Geological Society of America, Special Paper 126, 80 p.
- DE ROSEN-SPENCE, A.F., 1976. *Stratigraphy, development and petrogenesis of the Central Noranda Volcanic Pile*, Noranda, Quebec; Unpub. PhD thesis, University of Toronto.
- DUKE, J.L., 1986. *The geology and alteration of the Grew Creek epithermal gold-silver occurrence in south-central Yukon Territory (105 K 2)*; Unpub. BSc thesis, The University of British Columbia, 65 p.
- GILL, J.D., 1981. *Orogenic andesites and plate tectonics*; published by Springer-Verlag, New York, 390 p.
- GORDEY, S.P., 1983. *Thrust faults in the Anvil Range and a new look at the Anvil Range group, south-central Yukon Territory*; in *Current Research, Part A, Geological Survey of Canada, Paper 83-1A*, p. 225-227.
- HARLAND, et al, 1982. *A Geologic Time Scale*; Cambridge University Press.
- HOPKINS, W.S., JR, and NORRIS, D.K., 1974. An occurrence of Paleogene sediments in the Old Crow structural depression, northern Yukon Territory; in *Report of Activities, Part A, Geological Survey of Canada, Paper 74-1A*, p. 315-316.
- HUGHES, J.D., LONG, D.G.F., 1980. *Geology and coal resource potential of early Tertiary strata along Tintina Trench, Yukon Territory*; Geological Survey of Canada, Paper 79-32, 21 p.
- KUNO, H., 1966. Lateral variation of basalt and magma types across continental margins and island arcs; *Volc. Bull.*, Vol. 29, p. 195-222.
- MIYASHIRO, A., 1974. *Volcanic rock series in island arcs and active continental margins*; American Journal of Science, Vol. 274, p. 321-355.
- NESBITT, Bruce E., MUROWCHICK, James B., MUEHLENBACHS, Karlis, 1986. Dual origins of lode gold deposits in the Canadian Cordillera; *Geology*, in press.
- RODDICK, J.A. and GREEN, L.H., 1961. Tay River, Yukon Territory, NTS: 105 K; Geological Survey of Canada Preliminary Series, Map 13-1961.
- RODDICK, J.A., 1967. Tintina Trench; *Journal of Geology*, Vol. 75, no. 1, p. 23-33.
- ROSE, Arthur W., BURT, Donald, M., 1979. Hydrothermal alteration; p. 173-235 in Barnes, H.L., ed., *Geochemistry of Hydrothermal Ore Deposits*, second edition, John Wiley & Sons, New York, 797 p.
- ROUSE, Glen E., 1977. Paleogene palynomorph ranges in western and northern Canada; in Elsik, W.C., ed., *Contributions of Stratigraphic Palynology*, Vol. 1, *Cenozoic Palynology*, Amer. Assoc. Stratigraphic Palynologists, Contr. Ser., No. 5A, p. 48-65.
- SEWARD, T.M., 1973. Thiocomplexes of gold and the transport of gold in hydrothermal ore solutions; *Geochimica et Cosmochimica Acta*, Vol. 37, p. 379-399.
- STEIGER and JAGER, 1977. Subcommission on geochronology: convention on the use of decay constants in geo- and cosmochronology; *Earth and Planetary Science Letters*, Vol. 36, p. 359-362.
- TAYLOR, HUGHES P. JR., 1974. The application of oxygen and hydrogen isotope studies to problems of hydrothermal alteration and ore deposition; *Economic Geology*, Vol. 69, p. 843-883.
- TEMPELMAN-KLUIT, D.J., 1972. Geology and origin of the Faro, Vangorda, and Swim concordant zinc-lead deposits, central Yukon Territory; *Geological Survey of Canada, Bulletin 208*, 73 p.
- TEMPELMAN-KLUIT, D.J., 1976. The Yukon Crystalline Terrane: enigma in the Canadian cordillera; *Geological society of America Bulletin Vol. 87*, p. 1343-1357, doc. no. 60917. September.
- TEMPELMAN-KLUIT, D.J., 1979. Five occurrences of transported synorogenic clastic rocks in Yukon Territory; *Geological Society of Canada, Paper 79-1A*, p. 1-12.
- TEMPELMAN-KLUIT, D.J., 1980. Evolution of physiography and drainage in southern Yukon; *Canadian Journal of Earth Sciences*, Vol. 17, No. 9, p. 1189-1203.
- WHITE, Donald E., 1974. Diverse origins of hydrothermal ore fluids; *Economic Geology*, Vol. 69, p. 954-973.
- WOLFE, J.A., 1978. A Paleozoic interpretation of Tertiary climates in the northern hemisphere; *American Scientist*, Vol. 66, p. 694-703.

SILVER-LEAD-ZINC DEPOSITS OF THE KENO HILL - GALENA HILL AREA, CENTRAL YUKON

Ken W. Watson
United Keno Hill Mines Limited
Elsa, Yukon

WATSON, K.W., 1986. Silver-lead-zinc deposits of the Keno Hill - Galena Hill area, central Yukon; in Yukon Geology, Vol. 1; Exploration and Geological Services Division, Yukon, Indian and Northern Affairs Canada, p. 83-88.

INTRODUCTION

This paper is intended as a review of the silver lode deposits of the Keno Hill - Galena Hill area.

Two deposits, Husky and Husky S.W., are briefly described; they are among 30 silver-lead-zinc past and present producers in the district. The Husky Mine is currently United Keno Hill Mines Limited's single largest producer of silver. Husky S.W. is United Keno's most recently developed under-ground deposit and may represent a type of mineralization new to the district.

The Keno Hill - Galena Hill area is located in central Yukon, 354 kilometres (220 miles) due north of Whitehorse (Fig. 1). Mining has taken place in the district for the last 70 years, with mine head production to date (March, 1985) totalling 6.407 billion grams (206 million ounces) of silver.

The Sadie, Ladue and Lucky Queen mines were the main silver producers during the 1920's. By 1929, most of the favourable ground on both Keno Hill and Galena Hill had been staked, and was being actively prospected and mined by numerous companies and individuals.

The Wernecke mill was shut down in 1931, and in 1936 a 136 tonne (150 ton) per day mill commenced operation in Elsa, on Galena Hill. The main suppliers of ore for this mill were the Elsa, Silver King, Hector and Calumet mines, all located on Galena Hill.

The sudden death of Livingston Wernecke in 1941, coupled with low silver prices, led to a cessation of virtually all organized mining in the district by 1942.

In 1945, Keno Hill Mining Company Limited acquired all former Treadwell Yukon Company Limited's interests. This company was reorganized as United Keno Hill Mines Limited (U.K.H.M.) in 1946.

The first U.K.H.M. production came from the Hector-Calumet vein system in 1947. In 1949, the mill in Elsa burned down and was rebuilt with a 228 tonne (250 ton) per day capacity. This capacity was increased in 1951 to 450 tonnes (500 tons) per day. By 1958, U.K.H.M. had acquired most of the significant claims in the Keno Hill - Galena Hill area. Production at this time was coming from several underground mines on both Keno Hill and Galena Hill.

The single largest producing mine throughout the 1950's and 1960's was the Hector-Calumet Mine on Galena Hill. Underground mining in the Hector-Calumet Mine ended in 1972 as primary production from the Husky Mine came on-line. Husky Mine has remained the single largest underground producer since that time.

Mining in the Keno Hill - Galena Hill area, from 1913 to present, has produced 4.54 million tonnes (5.0 million tons) of ore with an average grade of 1412 g/t Ag (41.20 oz/ton Ag), 6.84% Pb and 4.60% Zn. Since 1947, U.K.H.M. has produced revenue shipments of some 4.417 billion g (142 million oz) silver, 214 million kg (473 million lb) lead, 150 million kg (330 million lb) zinc and 1.8 million kg (4 million lb) cadmium. Total mine head silver production by all operators in the Keno Hill - Galena Hill area since 1913 has exceeded 6.4 billion g (206 million oz) silver. U.K.H.M. has been the only significant operator in the area since 1958.

GENERAL GEOLOGY

The Keno Hill - Galena Hill area is underlain by Yukon Group metasedimentary rocks (Boyle, 1965).

These rocks include various types of argillite, phyllite, slate, schist and quartzite. Conformable greenstone (altered diorite/gabbro) lenses and sills occur in places and few narrow lamprophyre and quartz-feldspar porphyry dykes occur locally. Granitic bodies have intruded the metasedimentary - greenstone package at several places to the north and south of the Keno Hill - Galena Hill area.

The metasedimentary rocks have been divided locally into three formations; Upper Schist, Central Quartzite and Lower Schist. The Upper Schist consists of quartz-mica schist, quartzite, graphitic schist and minor limestone. The Central Quartzite contains thick- and thin-bedded quartzite, massive quartzite, graphitic phyllite, graphitic schist and calcareous schist. This unit is approximately 700 m (2300 ft) thick and hosts most of the major silver deposits in the area. The Lower Schist includes graphitic schist, argillite, thin-bedded quartzite, calcareous schist, phyllite, slate, sericite schist and minor thick-bedded quartzite.

These metasedimentary sequences trend east-west and dip 20 to 30 degrees south. In the Keno Hill - Galena Hill area, they



Figure 1. Location map of Keno Hill - Galena Hill area.

History

Prospecting for placer gold began in the Keno Hill - Galena Hill area in the late 1890's.

The first silver vein discovery in the district was in 1906, when the Silver King vein was located on Galena Creek near the base of Galena Hill (Fig. 2). Small scale silver production from the Silver King vein began in 1913.

In 1919, silver vein discoveries were made on Keno Hill and this precipitated a staking rush in the area. Treadwell Yukon Company Limited initiated large scale development on Keno Hill in 1921, under the management of Mr. Livingston Wernecke. In 1925, the company built a 113 tonne (125 ton) per day mill at Wernecke Camp on Keno Hill.

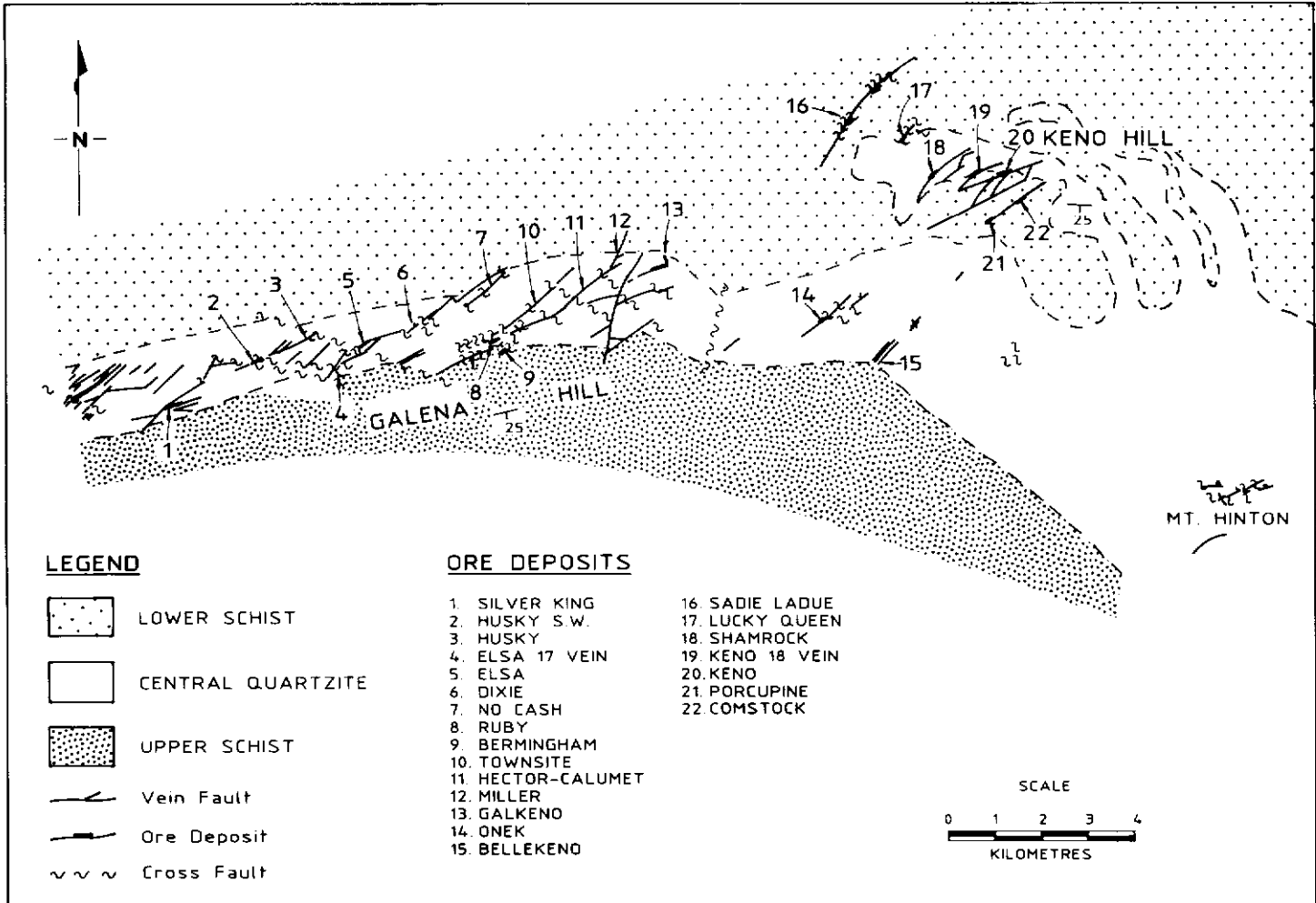


Figure 2. Geology and location of ore deposits in the Keno Hill - Galena Hill area.

form the southern flank of the McQuesten anticline.

A series of faults, striking northeast and dipping steeply southeast, host the silver-lead-zinc lode deposits. These vein faults exhibit left lateral movement, commonly offsetting the surrounding metasedimentary sequences by over 150 m (500 ft). Vein faults range in width from 0.3 m to over 30 m (1 to 100 ft).

The vein faults are offset in places by two types of unmineralized faults. The first type, known as cross faults, strike northwest and dip 40 to 60 degrees southwest. These cross faults are typically normal, right lateral faults with apparent horizontal movements ranging from 1 to 610 m (3 to 2000 ft). The second type of unmineralized faults are bedding plane thrust faults which exhibit movements ranging from 1 to 30 m (3 to 100 ft). Both cross faults and bedding plane faults show indications of post-ore movement. Several ore zones within the area have been offset by cross faulting. Some limited post-ore movement is also evident within the vein faults.

ORE DEPOSITS

In excess of 65 ore deposits and prospects have been identified within the district. These deposits are contained within vein faults with a combined total strike length in excess of 160 km (100 mi). All the economically mineable silver lodes located to date have been contained within an area of 26 km (16 mi) long by 1.6 to 6.4 km (1 to 4 mi) wide.

The principal lode deposits occur within the Central Quartzite in areas where brittle failure of the competent quartzite has allowed open areas conducive to ore deposition. Where the vein faults pass into schistose units, they generally become narrow and normally contain little or no ore. Ore zones are also known to occur in the Lower Schist where a competent unit, such as a greenstone lens, forms one or two of the walls of the vein fault. Most

ore zones (ore shoots) in this area have had their shape and size boundaries defined on a greater than 515 g/t Ag (15 oz/ton) basis.

Principal ore minerals are argentiferous galena, freibergite (argentiferous tetrahedrite - "greycopper"), and pyrargyrite ("ruby silver"). Polybasite, stephanite, argentite and native silver occur locally in minor amounts. The principal gangue mineral is siderite.

Vein faults can take the form of 'simple' veins, breccia zones and sheeted zones.

'Simple' veins consist of a gangue of siderite, commonly with some quartz. Mineralization consists of discontinuous bands and lenses of silver-bearing sulphides. Some brecciation is always present with fragments of country rock included in the vein.

Breccia zones consist of generally angular rock fragments (quartzite, phyllite, greenstone) in a matrix of siderite, commonly with some quartz. In some areas, the breccia fragments have been rounded or ground into a clay or sandy gouge. Breccia fragments normally account for 20 to 50% of the vein but may exceed 80% in places.

Sheeted zones consists of rectilinear slabs of quartzite or greenstone separated by narrow (1-10 cm; 0.5-4 in) breccia or gouge filled fractures. The breccia fragments and rectilinear slabs are cemented by siderite, sulphides and some quartz within the ore shoots. The fractures are barren or contain only a few carbonate minerals outside of ore shoots. Vein faults may grade from breccia to sheeted zones.

Several vein fault systems consist of two or more distinct, parallel to sub-parallel, vein faults. The inter-vein material between these vein faults in some locations consists of country rock shot with narrow mineralized fractures. In areas where the density of the mineralized fractures is sufficient this inter-vein material may produce ore.

Vein faults are typically made up of a series of slips or fault planes. Slickensides are common on wall rock, siderite and

sphalerite along these fault planes.

The transition from an ore shoot to a barren section of vein fault typically exhibits no changes in vein appearance other than a decrease in silver-bearing minerals.

Ore shoots range from 0.3 to 30 m (1 to 100 ft) in thickness. Strike length and dip extension of individual ore shoots range from 30 to 335 m (100 to 1100 ft). Several ore shoots commonly occur in a single vein fault.

Ten deposits in the Keno Hill - Galena Hill area have had documented silver production in excess of 31.1 million g (1,000,000 oz), eight more deposits have produced from 3.1 to 31.1 million g (100,000 to 1,000,000 oz) and a further seven have produced in excess of 311,000 g (10,000 oz).

The largest single producer is the Hector-Calumet Mine which has produced 2,383,543 tonnes (2,627,406 tons) of ore with an average grade of 1237 g/t Ag (36.09 oz/ton Ag).

Two stages of vein mineralization are distinguished in the area. The first stage deposited quartz, pyrite, some arsenopyrite, trace gold and some sulphosalts in the vein faults. Following movement on the vein faults, a second stage of mineralization deposited siderite, galena, sphalerite, pyrite, freibergite, and pyrargyrite. Most of the economically mineable ore deposits to date have been stage two types. Supergene enrichment has occurred, but is not believed to have been an important ore forming process. The oxidation zone extends from a few metres to 150 metres (10 - 500 ft) below surface. Within this zone, minerals such as limonite, pyrolusite, cerussite, and anglesite are common. Native silver, argentite and jarosite may occur locally.

Ore zones, within vein faults in the Central Quartzite, appear to be spatially associated with some or all of the following features: a) adjacent to and in the footwall of cross faults; b) the junction of two or more veins; c) cymoid loops; d) areas where the vein fault changes dip; e) directly beneath the contact with the Upper Schist. The ore deposits are believed to be of hydrothermal origin and the listed features have produced areas of lower pressure and temperature within the vein faults, conducive to ore deposition.

The origins of the Keno Hill - Galena Hill mineralized vein faults are still a subject of much debate. K-Ar dating has returned an age of .90 Ma for the mineralized vein faults (Sinclair et al., 1980). Granitic intrusions occur to the north and south of the district and are of similar age to the vein mineralization. It is assumed that these granitic intrusions, or a buried intrusion below the district, acted as a heat pump for the hydrothermal systems. Temperature of formation of the deposits has not been clearly determined.

All deposits known to date have been located in a near surface environment. This may be due in part to exploration techniques which have been directed towards shallow lying deposits. One current theory is that deeper, buried deposits may be present, but have yet to be found.

Most deposits mined to date have been mined to a depth of 90 to 150 m (300 to 500 ft) below surface. A notable exception has been the Hector-Calumet Mine which was mined to a depth of 336 m (1200 ft) below surface. Part of the apparent depth limitation is man-made, with contributing factors such as the topographic location of adits and the predetermined depth of shafts. Several mines appear to have ore zones continuing below the lowermost level of the mine.

Metal zonation has been difficult to establish. There appears to be a trend towards a regional lateral zonation of silver and gold. Silver is predominant within the central lode deposits of the district. Gold has never been an important economic constituent within these lodes. Outside the central core are several gold and gold-silver lodes such as those on Mt. Hinton and in the Dublin Gulch area. Most of these are hosted by quartz-rich veins. Even within the central core, elevated gold values have been noted at the extremities, in the Husky S.W. and Silver King vein systems, the Moth vein and some of the Keno Hill vein systems. The significance of this zonation, if any, has yet to be determined.

Vertical zonation within individual deposits is also a matter of some debate. An overriding theory in this area, developed in the 1920's, maintains that all deposits bottom out in zinc. This has been a self-fulfilling theory in some mines with decisions made to bottom a mine based on elevated zinc values rather than on a lack of silver values. The depth of oxidation, when compared to the

depth of the workings in many mines, may be significant. Zinc depletion within this oxidation zone may be a contributing factor to the apparent zonation which indicates a significant increase in zinc with depth.

There does not appear to be any well defined trace element zonation within or around individual ore shoots. A workable exploration technique utilizing trace elements has yet to be developed.

Alteration haloes surrounding vein faults are commonly not distinct. Alteration within the sedimentary sequences may take the form of minor pyritization, some small chemical changes and irregular carbonate leaching. The leached zone may extend up to 4.6 m (15 ft) away from the vein zone. Other alteration rarely extends more than 15 m (50 ft) from the vein fault.

A fracture zone, consisting of small stringers of siderite with sulphides, is common in all types of country rock, for distances up to 7.6 m (25 ft) away from the main vein fault.

Alteration haloes are distinct, but narrow where the vein faults cut greenstone. The alteration zone commonly extends only a few centimetres away from the vein fault. It consists of a carbonate + sericite zone adjacent to the vein fault grading to a carbonate + chlorite zone grading to unaltered greenstone.

The origin of the silver lodes located within vein faults of the Keno Hill - Galena Hill area is still an enigma. More studies are required to fully define the genesis of these deposits.

HUSKY DEPOSIT

Husky Mine, which was discovered by rotary percussion drilling in the mid 1960's, is currently the main underground producer. The Husky Mine is located near the base of Galena Hill, a half mile downslope from the Elsa townsite. Ore production from Husky to December 31, 1984 has totalled 359,450 tonnes (396,230 tons) grading 1450 g/t Ag (42.32 oz/ton). This production figure includes some recent production from the Husky S.W. Deposit which is currently serviced by the Husky shaft.

Husky is serviced by a 129 m (423 ft) deep, three compartment shaft. Three levels, the 125, 250 and 375 foot levels were developed from the shaft. In 1977, a decline was driven to develop a 450 foot level for the mine.

The Husky Deposit has a strike length of 520 m (1700 ft) and has been mined to a depth of 140 m (460 ft) below surface. The deposit is still open below the lowermost mining level. The deepest ore intersection to date has been an 8468 g/t Ag (247.0 oz/ton) intersection over a 0.64 m (2.1 ft) vein width, located 170 m (560 ft) below surface.

There are two principal veins in the Husky Mine, the #1 and #2 veins. These veins vary from 'simple' veins to highly brecciated zones. Vein widths are from 1 to 4.5 m (3 to 15 ft). These two veins are separated by 4.5 to 9.0 m (15 to 50 ft) of country rock, normally quartzite. This inter-vein quartzite is commonly moderately to highly fractured with siderite infillings.

Ramifying structures in some areas have produced up to four parallel to sub-parallel vein or fracture/breccia structures. The fractured inter-vein material between the #1 and #2 veins contains 34 to 1715 g/t Ag (1 to 50 oz/ton). The main ore mineral in Husky is argentiferous galena. In a few areas, pyrargyrite is the primary ore mineral. Stephanite and polybasite occur locally in minor amounts. The host rock for the Husky vein faults is quartzite with interbedded graphitic and micaceous schist and some greenstone sills. The primary gangue mineral in the veins is siderite with some quartz. Calcite and barite occur locally in minor amounts within the vein faults.

The lead and zinc content within Husky Deposit averages 3.96% and 0.27% Zn. The 10.7:1 silver to lead ratio (ounces silver to percent lead) in the Husky Deposit is the third highest among the district's major silver producers (Lucky Queen = 12.8:1 and Elsa = 12.6:1). Zinc content is significantly lower than any other major deposit of the district (district average = 4.6% Zn). The low zinc content is also unusual in light of the fact that the Husky Deposit exhibits very little evidence of oxidation.

HUSKY S.W. DEPOSIT

The Husky S.W. deposit is located, 1400 m (4600 ft) southwest of the Husky shaft. This deposit occurs on the primary Husky

Silver King structure, but is separate, both spatially and mineralogically, from either of those deposits.

Husky S.W. was found by overburden drilling in the early 1970's and later follow-up diamond drilling in the late 1970's. Current exploration sub-drilling has revealed a strong vein structure, varying in width from 1.5 to 12 m (5 to 40 ft), carrying excellent silver grades. The first stope level on ore above the 250 level has now been mined and returned an average grade of 1584 g/t Ag (46.2 oz/ton) over a 5.2 m (17.1 ft) width and a 38.7 m (127 ft) strike length.

The Husky S.W. vein zone is a highly fractured breccia structure with a quartz-rich gangue. Mineralization occurs as native silver with some argentite (acanthite) and stephanite within fracture veinlets with a pyrite/graphite matrix. Some native silver also occurs as microscopic wires within the quartz gangue. The ore is completely non-visual; barren portions of the vein are identical in appearance to mineralized sections.

There are two distinct veins on the 250 level separated by 3 to 6 m (10 to 20 ft) of country rock. Diamond drilling has indicated only one vein below the 250 level, but further work will be required to confirm this.

The ore shoot does not occupy the full width of the vein. The #1 vein (hanging wall) is 6.1 m (20 ft) wide just above the 250 level and the ore shoot varies from 3.6 to 5.5 m (12 to 18 ft) wide. The ore shoot in the #2 vein (footwall) in this area is 1.8 m (6 ft) wide. The width of the #2 vein is not currently known.

Below the 250 level, the average diamond drill indicated true width is 10.7 m (35 ft). The widest vein intersection is 22.2 m (73 ft), located 140 m (460 ft) below surface. The ore shoot, below the 250 level, has an average width of 3 m (10 ft).

Underground diamond drilling has indicated that the Husky S.W. ore shoot lengthens along strike to 76 m (250 ft) at a depth of 122 m (400 ft) below surface. This drilling has also indicated that the Husky S.W. deposit is still open at a depth of 183 m (600 ft) below surface.

The amount of lead and zinc within the Husky S.W. deposit is very low (0.2% Pb and 0.03% Zn). The galena in Husky S.W. has a silver to lead ratio of 1:1. Gold occurs in this deposit and appears to be tied closely to silver. The silver:gold ratio varies from 1200:1 in the upper portions of the deposit to 300:1 in the lower portions. These ratios are preliminary; further work is required to develop a statistically valid data base.

Husky S.W. is anomalous in many respects when compared to the other silver deposits of the district. The silver to lead ratio of 195:1 in this deposit is an order of magnitude higher than in any deposit ever mined in the area (district average is 6:1). The zinc content in Husky S.W. is an order of magnitude lower than in any deposit ever mined in the district. There is almost no siderite associated with Husky S.W. The Husky S.W. deposit contains more gold than any other silver lode deposit on Galena Hill or Keno Hill.

It may be that Husky S.W. is a silver-rich stage 1 type deposit or an unusual combination (for this district) between stage 1 and stage 2 type mineralization. Mining in Husky S.W. began in 1984 and the data base is still too small to be able to draw any significant conclusions regarding this deposit.

A second ore shoot, very similar in appearance to Husky S.W., is located 200 m (655 ft) northeast of Husky S.W. on the same vein (between Husky and Husky S.W.). This ore shoot, known as the Husky Central Zone, appears to be slightly more pyritic than Husky S.W. Little is known about this zone since only limited exploration has been conducted on it.

Recent exploration work has indicated a good possibility that further ore shoots, with similar geological characteristics to Husky S.W., may exist on other veins in this area.

MINING AND MILLING

The mineralized vein faults in the area vary from 0.3 to 30 m (1 to 100 ft) in width with a steep (70°) dip. The host rocks range from competent quartzite to incompetent schist and crushed fault zones. Due to the presence of the incompetent schist and the amount of fracturing and faulting, ground conditions in the mines can be described as "heavy."

All the underground mines operated by U.K.H.M. are tracked mines using small electric locomotives and 1.4 to 2.7 tonne (1.5 to 3 ton) ore cars to tram the ore. Most of the underground mining

requires the extensive use of timber for ground support. In most mines, square set timber mining is employed which allows a 1.5 to 1.7 m (5.0 to 5.5 ft) minimum mining width. Open stoping is employed in a few areas with competent host rock. Some mines which contain narrow veins use round timber stoping, which allows a 1.2 to 1.4 m (4.0 to 4.5 ft) minimum mining width.

Due to the topographic relief in the area, most of the underground mines have adit access. The Husky Mine is the only operating mine with shaft access.

Open pit mining was introduced as an integral part of the operation in 1977. Most of the open pits mined to date have produced 9000 to 18,000 tonnes (10,000 to 20,000 tons) of ore. The Birmingham Pit was an exception, producing in excess of 145,000 tonnes (160,000 tons) of ore. Mining initially takes place to the hanging wall of the vein. All waste is removed, leaving the vein untouched. A bulldozer is then used to peel off the vein to the footwall. The use of a bulldozer permits very selective mining. Dilution in the open pits can be kept very low. The use of a backhoe allows the recovery of an additional 7.6 m (25 ft) of ore below the floor of an open pit. A backhoe has also been used in areas where narrow vein widths have precluded the economic operation of a formal open pit.

The mill in Elsa has a capacity of 450 tonnes (500 tons) per day. Standard flotation is used to produce a lead concentrate containing an average of 8570 g/t Ag (250 oz/ton). Some 18 to 23 tonnes (20 to 25 tons) of concentrate are produced each day. Current mill recoveries are 85% for silver and 70% for lead. The mill has a cyanide circuit, however it is not being used at the present time. A small smelter, located near the mill, can be used to smelt the cyanide precipitate when available.

Current mill feed tonnage is split 3:2 between open pit production (including stockpiled pit ore) and underground production ore.

EXPLORATION TECHNIQUES

The exploration targets in the Keno Hill - Galena Hill area are small ore shoots located on vein fault structures.

The Keno Hill - Galena Hill area has from 2 to 5% surface outcrop exposure. Surface prospecting in the 1920's identified many of the vein structures within the district. The hand panning of overburden samples to identify galena and the use of ground sluicing served to locate several more veins. By the mid 1930's, most of the veins structures in the area had been identified. Exploration for ore shoots along these vein faults was by surface hand trenching or the use of small prospect adits and shafts.

In the 1960's to the early 1970's, extensive geochemical and geophysical surveys were conducted, with some limited success. When compared to most vein systems in Yukon, ore shoots in the vein faults of this area have poor soil geochemical expressions. Many known ore deposits exhibit very poor geochemical responses. The 3 to 30 m (10 to 100 ft) of overburden cover on the lower portions of the slopes, commonly consisting of glacial till and glacio-fluvial deposits, has contributed to this lack of geochemical response. Much of the area was covered by soil sampling grids in the mid 1960's and very little soil geochemistry has been conducted since that time.

Most geophysical methods, from electromagnetic to gravity surveys, were run in the 1960's and early 1970's. These methods met with limited success. Some of the vein faults produced anomalies, but a combination of graphitic schist horizons which occur in abundance within the Central Quartzite, conductive clays and pyrite within fault zones, and the high density of structural features within the area made interpretation of results very difficult. No new ore zones were located. Ground VLF EM-16 and horizontal loop EM-17 surveys were conducted over a few targets in 1984. In addition to this work, a DIGHEM III survey was flown over all the property in 1984. Preliminary results indicate good success in locating vein faults; however, these methods may not be able to locate ore shoots within the vein faults.

In 1963, the rotary percussion drill was introduced as a exploration tool. The drill was originally used to drill vertical holes to penetrate overburden and take samples just above the bedrock surface. These samples were analysed for lead and zinc and the results were used to try to identify veins and ore shoots on veins. Due to this work, the rotary percussion drill is locally referred to as

an overburden drill.

In the mid 1960's, it was found that the overburden drill was successful in penetrating up to 61 m (200 ft) into bedrock. The mast of the drill was angled to be able to drill -60° holes and the drill was used to drill bedrock for vein intersections.

This drill has been the most successful surface exploration tool in recent years. It has been credited with the discovery of the Husky, Husky S.W. and Ruby ore deposits. It has also served to define most of the open pits.

Drill cuttings from every 1.5 m (5 ft) drilled are routinely assayed for silver, lead and zinc. The drill cuttings are examined under a binocular microscope and a drill log is compiled from this work. Grade and tonnage calculations based solely on rotary percussion drill results have been found to be very accurate.

Within the fractured, abrasive quartzite of this district, the percussion drill has been found to have four times the penetration rate of a diamond drill for less than one-fifth of the cost per unit drilled. Vein recovery is excellent, except in some areas containing wet vein (the drill employs an air flush system). This is often better than diamond drill recoveries which can be as low as 5% in some vein intersections.

The limitation of the rotary percussion drill is depth. Holes in excess of 61 m (200 ft) in length are rare. The deepest hole ever drilled with the rotary percussion drill was 122 m (400 ft) in length. It is, however, an excellent tool for locating ore in the near surface environment.

The drill is used by U.K.H.M. as a penetrating tool. Drill fences are run across areas of suspected veins. If vein intersections are made, the grid is tightened up and drill patterns are concentrated over vein locations indicated by the drill fences. The lack of outcrop and poor geochemical and geophysical responses of ore shoots in this area have made the percussion drill an invaluable primary exploration tool. A total of 566,198 metres (1,857,604 ft) of rotary percussion drilling has been done by U.K.H.M. in this area.

Diamond drilling cannot be used as a prospecting tool due to its high cost and slow rate of drilling. Diamond drilling is used as a follow-up tool to test percussion drill indicated ore zones at depth and to test geological, geochemical or geophysical anomalies in areas where the percussion drill has not proven effective. Although a drill log is compiled using percussion drill cuttings, diamond drilling must occasionally be used to clarify the geology of an area.

Bulldozer stripping has proven effective in many areas with less than 6.1 m (20 ft) of overburden cover. In the past, the bulldozer was used to cut trenches across an area of suspected mineralization. It has been found in recent years that stripping is almost as cost effective as trenching and it allows a much more accurate interpretation of bedrock geology. In areas that prove to contain economic mineralization, the exploration stripping turns into the initial stages of pit preparation.

Backhoe slot trenching is beginning to be used as an exploration tool in this area. The ability of a backhoe to rapidly cut deep trenches is very useful in the initial evaluation of an area. Interpretation of bedrock geology between trenches, in areas of faulting and discontinuous vein structures, is often difficult, but the backhoe trenches allow an initial interpretation of bedrock geology and mineralization.

It is believed that much more remains to be located in the Keno Hill - Galena Hill area. Due to the nature of the mineralization, exploration is very difficult. The Silver King - Husky vein system is a good example, with 70 years separating the discovery of the first ore deposit on this system and the most recently discovered deposit. Some mines have been in operation for more than 50 years and new ore is still being located within the ore zone.

Since 1947, U.K.H.M. has maintained an average of three years of documented ore reserves. Surface exploration techniques, primarily rotary percussion drilling, are being used to locate and delineate potential open pits and indicate the presence of larger ore shoots that will require underground mining. For the potential underground deposits, underground exploration and development is required to locate the ore and develop reserves, a very slow process. Given a healthy precious metal market, it is expected that U.K.H.M. will still have three years of ore reserves by the turn of the century.

ACKNOWLEDGEMENTS

I would like to thank the management of United Keno Hill Mines Limited for permission to publish this paper. Background information was aided by discussions with U.K.H.M. geological staff including Jim McFaull, Senior Exploration Geologist and Michael Dufresne, Senior Mine Geologist. This paper has benefited from a thorough review by Pat Watson.

REFERENCES

- AHO, A.E., 1963. *Silver in the Yukon*; CIM Bulletin, Vol. 56, No. 611.
- BLUSSON, S.L., 1978. Regional geologic setting of lead-zinc deposits in Selwyn Basin, Yukon; in *Current Research, Part A, Geol. Surv. Can.*, Paper 78-1A.
- BOYLE, R.W., 1957. Lead-zinc-silver lodes of the Keno Hill - Galena Hill area, Yukon; in *Structural Geology of Canadian Ore Deposits*, Vol. II, C.I.M.M. Geology Division.
- BOYLE, R.W., 1965. Geology, geochemistry, and origin of the lead-zinc-silver deposits of the Keno Hill - Galena Hill area, Yukon Territory. *Geo. Surv. Can.*, Bulletin 111, 302 p.
- CARMICHAEL, A.D. Jr., 1957. United Keno Hill Mines; in *Structural Geology of Canadian Ore Deposits*, Vol. II, C.I.M.M. Geology Division.
- FRANZEN, J.P., 1978. Cross fault ore control model; *United Keno Hill Mines Limited report*, unpublished.
- FRANZEN, J.P., 1984. Metal-ratio zonation in the Keno Hill District; unpublished.
- GREEN, L.H., 1971. Geology of Mayo Lake, Scougale Creek and McQuesten Lake map-areas, Yukon Territory; *Geol. Surv. Can.*, Memoir 357, 72 p.
- KINDLE, E.D., 1955. Keno Hill, Yukon Territory (map with marginal notes); *Geol. Surv. Can.*, Paper 55-12.
- McTAGGART, K.C., 1960. The Geology of Keno and Galena Hills, Yukon Territory. *Geol. Surv. Can.*, Bulletin 58.
- SINCLAIR, A.J., TESSARI, O.J., HARAKAL, J.E., 1980. Age of silver-lead-zinc mineralization, Keno Hill - Galena Hill area, Yukon Territory; *Canadian Journal of Earth Sciences*, Vol. 17, No. 8.
- THE STAFF, 1961. Current operation of United Keno; *CIM Bulletin*, Vol. 54, No. 594.
- TEMPELMAN-KLUIT, D.J., 1970. Stratigraphy and structural geology of the "Keno Hill Quartzite" in Tombstone River - Upper Klondike River map-areas. *Geol. Surv. Can.*, Bulletin 180, 102 p.

TREADWELL YUKON COMPANY LIMITED, 1921-1941. Staff reports; unpublished.

UNITED KENO HILL MINES LIMITED, 1947-1984. Staff reports; unpublished.

VAN TASSELL, R.E., 1969. Exploration by overburden drilling at Keno Hill Mines Limited; *Quarterly of the Colorado School of Mines - International Exploration Symposium*, 64.

MINERAL ZONING IN THE KENO HILL SILVER-LEAD-ZINC MINING DISTRICT, YUKON

(This study was partly funded by Program 1, Mineral Resources Sub-agreement of the Canada-Yukon Economic Development Agreement.)

G. Lynch
Department of Geology
University of Alberta
Edmonton, Alberta

LYNCH, G., 1986. Mineral zoning in the Keno Hill silver-lead-zinc mining district, Yukon; in Yukon Geology, Vol. 1, Exploration and Geological Services Division, Yukon, Indian and Northern Affairs Canada, p. 89-97.

ABSTRACT

The Keno Hill — Galena Hill mining district of central Yukon has been a prolific silver-lead-zinc producer since the early part of the century. Typical orebodies are extensive vein systems with a mineralogy consisting of siderite, quartz, pyrite, galena, sphalerite, and freibergite in varying combinations. The veins are restricted to steep SE-dipping fault zones principally contained within a brittle graphitic quartzite unit and some concordant greenstone bodies. The main silver lodes form a narrow east-west belt, 25 km long, and have been assigned a mid-Cretaceous age as have nearby granitic bodies and their associated tin and tungsten mineralization.

This study of the vein minerals indicates that groups of adjacent deposits have characteristic mineral assemblages distinguishing them from other groups; these form zones along the entire length of the belt. The following summarizes the principal mineralogical zones from west to east: (1) Pyrargyrite in quartz-siderite veins with some native silver, polybasite, stephanite, and acanthite are mainly in the west. (2) Siderite, galena, sphalerite, and freibergite occur in most deposits but are found without the other index minerals on top of Galena Hill. (3) Pyrrhotite and arsenopyrite are in deep vein exposures in the valley between Galena Hill and Keno Hill. (4) Calcite is also in the deep veins along the eastern flank of Galena Hill but extends to the east onto Keno Hill. (5) Boulangerite-jamesonite and abundant quartz-arsenopyrite rich fractions of veins at the eastern end of the district overlap with the calcite zone. Higher gold values are recorded in zones (1), (3) and (5).

The changing mineralogical facies record an evolving environment of deposition in a continuous, 25 km long hydrothermal vein system. The western deposits are thought to be higher level, or laterally "downstream" equivalents of the eastern deposits.

This zoning sequence is typical and is well established in other regions of the world. Such systems are known to progress further downwards, into gold-quartz veins before attaining tin and tungsten mineralization and associated granitic bodies.

INTRODUCTION

The Keno Hill — Galena Hill mining district is located in central Yukon, 354 km north of Whitehorse and 45 km northeast of Mayo (Fig. 1). Since 1913, five million tons of ore have been recovered at an average grade of 41 oz/ton Ag, 6.8% Pb, and 4.0% Zn (Watson, this issue).

This paper presents evidence for district-wide mineral zoning in the veins. Ten weeks were spent in the area by the writer describing and documenting vein mineralogy from underground exposures, open pit workings, and surface trenches. The zones are based on the occurrence of specific hypogene index minerals, as established in the field during vein mapping. These mineral facies, or zones, are thought to mark changing precipitation conditions and fluid chemistry across the 25 km long mineralized belt — a scale not often recognized for single continuous hydrothermal systems.

The most extensive geological work completed on the veins is by Boyle (1965). Zoning however was only vaguely inferred in the original work, with particular reference to the increase in abundance of arsenopyrite on Keno Hill relative to Galena Hill. Further patterns were not established, possibly due to the fact that two key deposits (Husky in the west, Mt. Hinton in the east) were not yet discovered, and seemingly because of some confusion between distinguishing hypogene from supergene mineralogy. A geochemical study, involving sulphur isotope ratios of some of the vein minerals, was later completed by Boyle et al. (1970); the veins were shown to be clearly zoned on a regional scale in their isotopic signatures, however the significance of this was greatly down played by the writers. A contour map of the sulphur data is included in this report for comparison with the mineralogical zoning.

Further work of significance came in the establishment of corresponding mid-Cretaceous ages for the veins and local felsic plutons, implying a likely genetic link between the two (Sinclair and Tessari, 1980; Godwin et al., 1982).

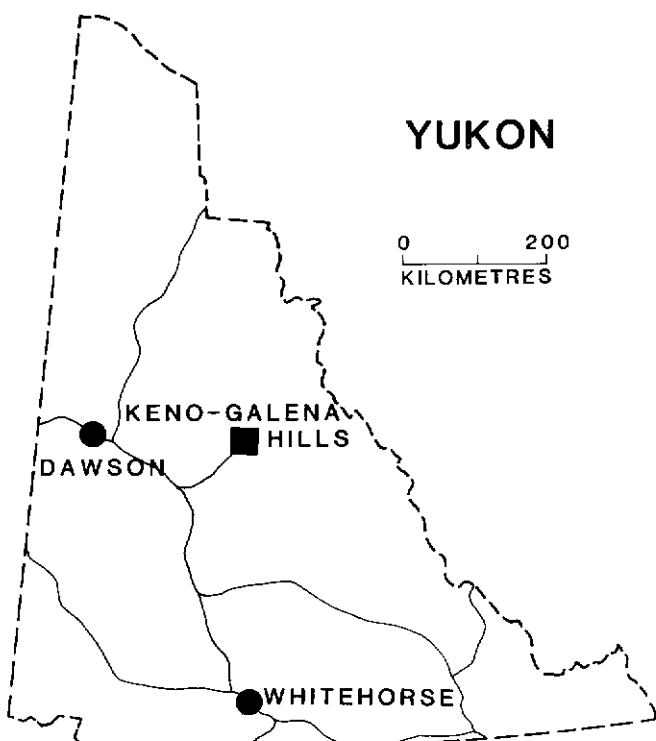


Figure 1. Location of the Keno Hill - Galena Hill Mining District in central Yukon.

LOCAL GEOLOGY

Most veins are contained within the Central Quartzite, which is also known as the Keno Hill Quartzite (Tempelman-Kluit, 1970). It dips moderately to the south and extends east and west well beyond the mining district (Fig. 2). The exposed width or apparent thickness at the surface in the local area is up to 7-8 km. The lithology consists of thin and thick sections of dark graphitic quartzite, with interlayers of black graphitic schist, some massive white quartz segregations and lesser quartz-muscovite schist. To the north below the Central Quartzite lies the Lower Schist consisting of quartz-mica, graphite, and chlorite schists. The Upper Schist, above and to the south of the Central Quartzite, resembles the Lower Schist but contains some crystalline limestone (McTaggart, 1960). Thick concordant greenstone lenses are dispersed throughout the three units. The greenstones are gabbroic, and have been metamorphosed to various combinations of chlorite, zoisite, albite, quartz, and actinolite (McTaggart, 1960). The greenstones may also host the silver-lead-zinc veins.

Small and medium scale isoclinal folds are seen throughout the sequence and are well exposed in the open pit workings (Fig. 3). Axial planes are parallel to lithological layering. Fold axes are horizontal to shallowly plunging and trend east-west. An upright crenulation, superimposed on the isoclinal fabric, forms southeast plunging lineations on the layering. These lineations are parallel to regional fold axes. Hook refold interference patterns are sometimes seen (Fig. 3b). Such observations agree well with the structural reports of McTaggart (1960). Because of the intense isoclinal deformation the "Upper Schist," "Central Quartzite," and "Lower Schist" may be structurally transposed and not in normal stratigraphic sequence. Furthermore recent maps (Tempelman-Kluit, 1970; Green, 1971) show the south dipping Robert Service Thrust Fault to separate the Upper Schist from the Central Quartzite. Ages of the units are currently being revised by other workers and are not presently known to the writer.

Granitic bodies and dykes are common in the surrounding region, some have associated tin-tungsten mineralization (Fig. 2). They crosscut the sedimentary sequence and postdate deformation. Radiometric dating has established a mid-Cretaceous age for the intrusions, for the tin-tungsten mineralization, and for the silver-lead-zinc veins of Keno Hill - Galena Hill (Sinclair and Tessari, 1980; Godwin et al., 1982; W.D. Sinclair written comm. 1985). Lamprophyre dykes of uncertain age are also found.

Vein faults which host the orebodies form an en echelon set which strike northeast, diagonally through the quartzite and dip steeply to the southeast (Fig. 4 and 5). Movement has been relatively small, in most cases less than a few tens of metres, with movement of the hangingwall downwards and across towards the northeast (McTaggart, 1960). Many of the vein faults and orebodies are terminated by later steeply dipping northwest striking faults, which have apparent right-lateral offsets of up to 900 metres along gouge clogged surfaces.

In a few exposures, altered quartz-porphyry dykes can be observed to have intruded along the northeast striking faults and have in turn been crosscut by the silver-lead-zinc veins.

MINERALIZATION AND MINERAL ZONING

The principal hypogene minerals in the deposits are siderite, quartz, pyrite, galena, and sphalerite with lesser to minor freibergite, pyrargyrite (ruby silver), arsenopyrite, chalcopyrite, pyrrhotite, jamesonite, boulangerite, polybasite, stephanite, calcite, and barite among others. The dominant minerals are generally medium to coarse grained and massive. Some veins are variably banded (Boyle, 1965), or can change in mineralogy along strike from quartz-rich to carbonate and/or sulfide rich fractions. Mineralized faults are sharp planar veins up to 50 cm wide or may be extensive stockwork, sheeted vein, and breccia zones greater than 15 metres in width. Systems such as the Hector-Calumet and the Sadie-Ladue veins are each continuous along strike for over

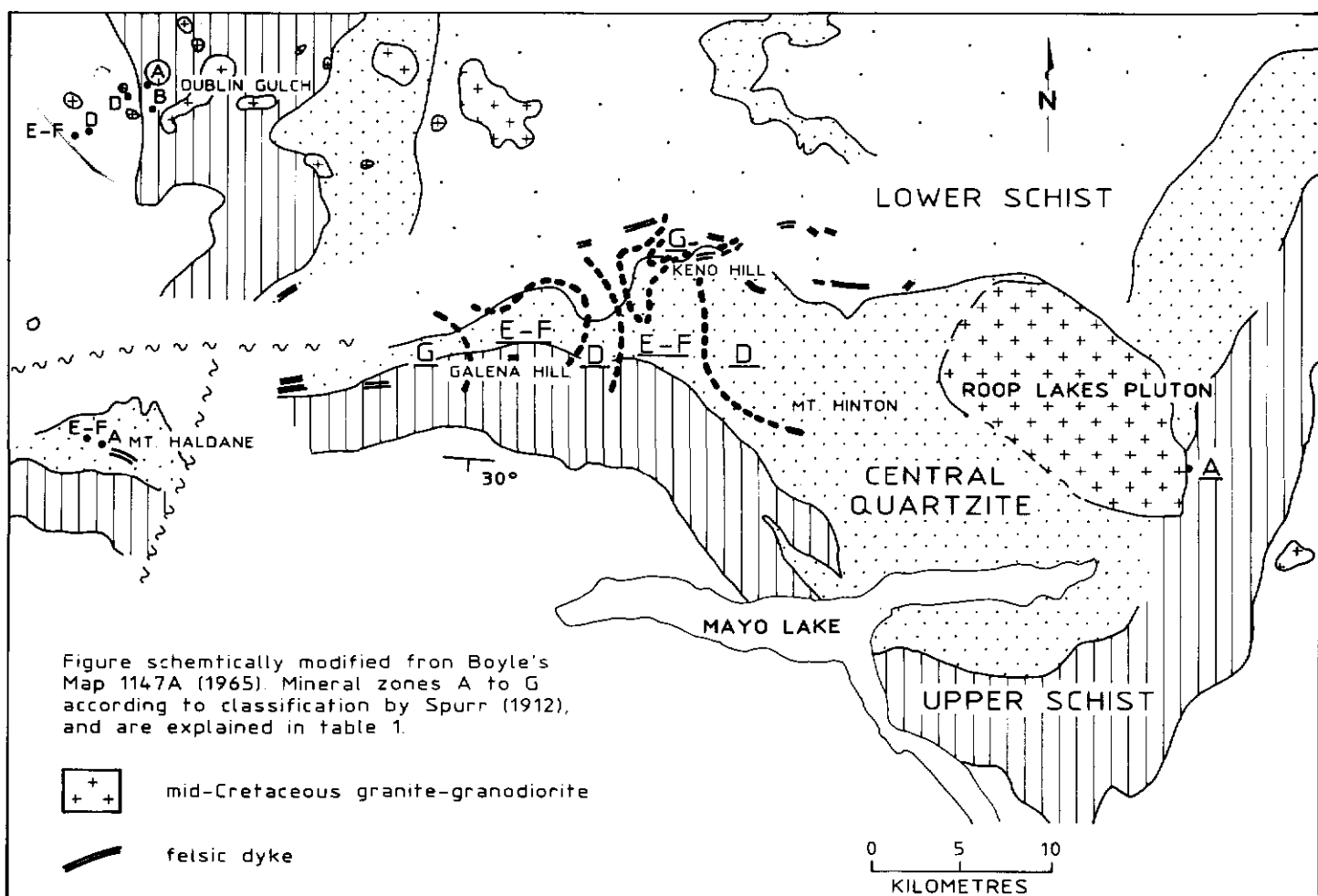


Figure 2. Map showing position of Upper Schist, Central Quartzite, Lower Schist, intrusive bodies, and areas of mineralization.



Figure 3a. Typical small scale isoclinal fold within the host units.

two kilometres.

On a detailed scale paragenetic and textural relationships can be complicated and variable, showing considerable overlap and repetition. Such complications are possibly due to advancing and retreating hydrothermal fronts, as well as by continued movement and brecciation along the faults during mineralization. However, on a broader scale zoning patterns defined by specific vein minerals become clear; these are illustrated in the maps of Figures 6, 7 and 8. Three veining stages are often recognized. The earliest is principally a quartz veinlet stockwork with lesser pyrite and arsenopyrite and occasional feldspar. Minor boulangerite, some galena and sphalerite are reported by Boyle (1965). Boyle stresses that arsenopyrite is a typical mineral of this stage on Keno Hill but is absent or present in only small amounts in the veins of Galena Hill. The second stage consists of carbonate-sulfide-sulphosalt veins crosscutting the early quartz stockworks (Fig. 9); this includes the bulk of the ore material. A third stage of veining and vug encrustations consists of quartz and pyrite and has a sparse distribution (Fig. 10).

Alteration of host rocks is generally weak, however, pyrite disseminated through the wallrock along the veins is common and is accompanied by silicification/recrystallization. Bleaching of the dark graphitic host to lighter colours is also seen, especially in sections of the quartz-pyrite rich Husky S.W. deposit. The greenstones in contact with the veins are variably sericitized and chloritized.

The deposits at the western end of the district, such as the Husky, Husky S.W., Elsa, and Silver King Mines, as well as the Lucky Queen Mine in the east, are distinguished by the presence of pyrargyrite (Fig. 11). It occurs as fine grained stringers in association with typical hypogene minerals such as quartz, siderite, and pyrite. It was not firmly established in the past whether pyrargyrite is of a supergene or hypogene origin, however the occurrence of pyrargyrite in deep exposures of the Husky Mine apparently untouched by surface processes, such as rust staining, indicates a likely hypogene nature. In general pyrargyrite is known to be more likely hypogene than supergene (Guilbert and Park, 1986, p. 818). Other index minerals of the veins in this zone are polybasite, stephanite, acanthite, and wire native silver (Fig. 12). Very coarse grained world class samples of polybasite and stephanite have been collected from the Husky Mine — supergene processes rarely produce such coarse textures. Further evidence of a hypogene origin is the fact that deposits of this zone are situated almost entirely in the west whereas all deposits, east and west, have been exposed to the same supergene conditions after erosion and exposure and therefore should have developed the same supergene assemblages. Lastly, the frigid Yukon climate does not promote extensive supergene activity.

Along the eastern flank of Galena Hill, deep vein exposures at low altitudes contain pyrrhotite. It is typically fine grained and a minor component; however, in the Flame and Moth as well as the Duncan Creek veins it is present in considerable quantity. Arsenopyrite within these carbonate-quartz-pyrrhotite veins is

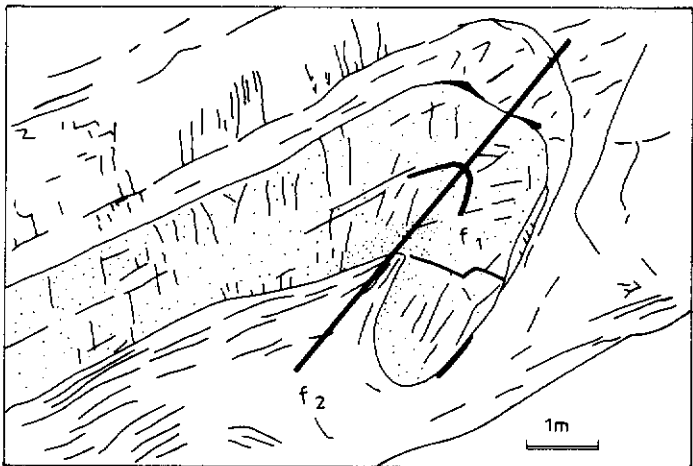
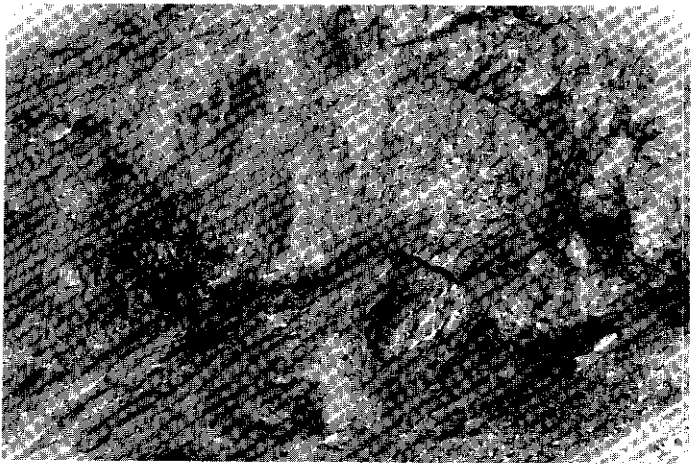


Figure 3b. Medium scale isoclinal fold refolded into hook pattern, exposure from Birmingham open pit.

another indicator for this zone. Chalcopyrite and sphalerite appear to be more abundant here as well.

Calcite (Fig. 13 and 14) is in the deep veins of the valley between Galena and Keno Hills but also extends east onto Keno Hill and beyond. Along the eastern side of Galena Hill, calcite, siderite, arsenopyrite and pyrrhotite bearing veins reach up to 900 meters in altitude, whereas siderite veining without calcite, arsenopyrite or pyrrhotite, extends upwards above 1300 metres altitude. The trio calcite, arsenopyrite and pyrrhotite appear to be markers for relatively deeper vein exposures.

At the eastern end of the district, the Keno, Homestake, and Mt. Hinton deposits are characterized by jamesonite-boulangerite. They are associated with abundant quartz, arsenopyrite, pyrite, and light reddish-brown sphalerite (Fig. 15). Carbonate is typically absent from these portions of the veins, though they appear to extend laterally into siderite and/or calcite rich fractions. Jamesonite is characteristic of splay faults extending off of the principal vein faults (Boyle, 1965).

Presently the smelter is crediting the mines with some gold recovery. The Husky S.W. deposits in the west accounts for much of this (K. Watson, writt. comm., 1986). In general, gold appears to be within quartz-rich fractions of the western deposits such as the Husky S.W. orebody, or to the east in association with arsenopyrite, pyrrhotite, or jamesonite bearing veins such as at the Mt. Hinton, Flame and Moth, and Homestake deposits. The area on Galena Hill intermediate to these two extremes is lower in its gold values.

DISCUSSION OF MINERAL ZONING

Individual orebodies do not in general appear to be zoned in any obvious or systematic manner. However, zonation is clearly developed on a district wide scale. Consequently the district may be viewed as a large singular deposit, formed from one continuous

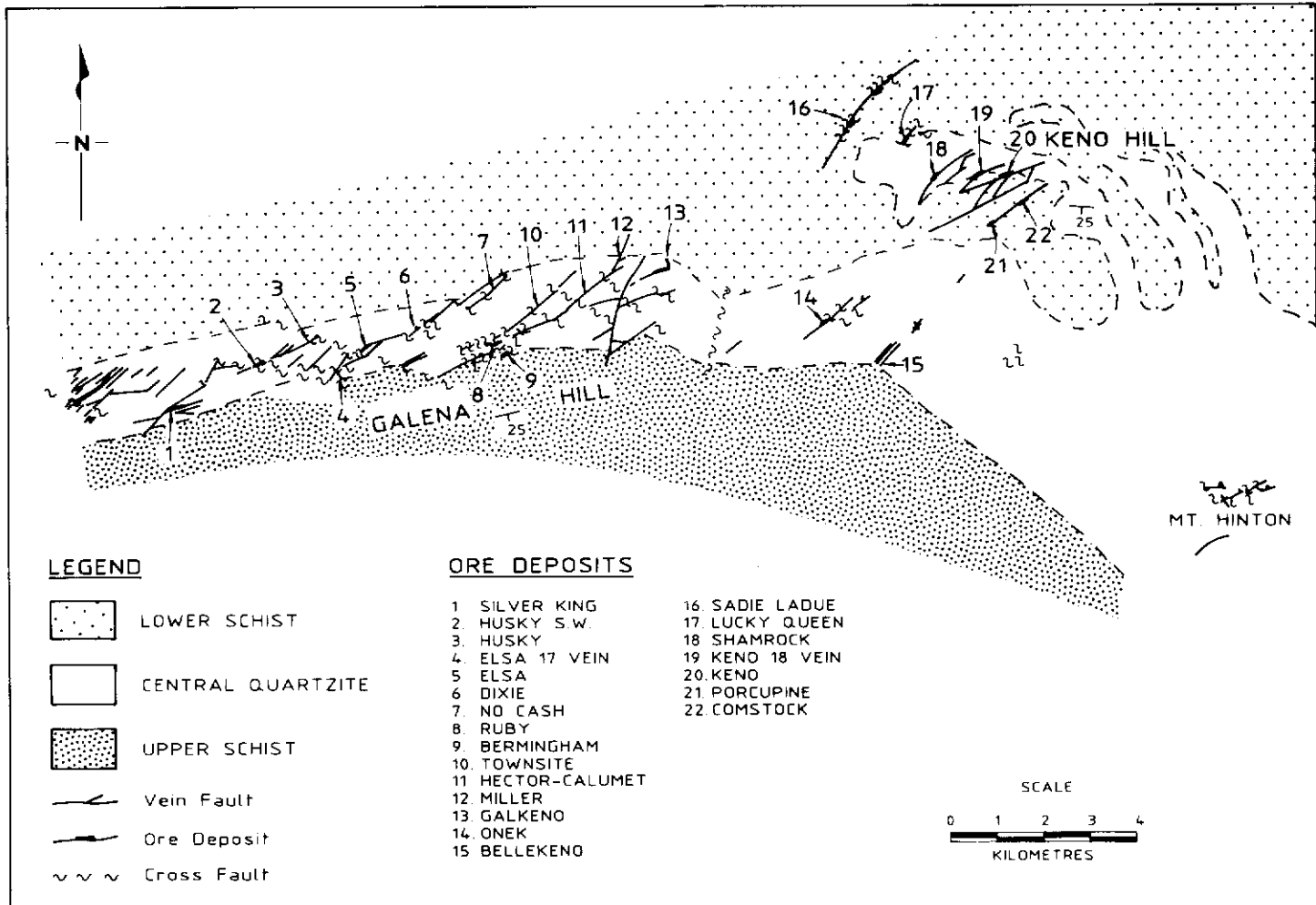


Figure 4. Map showing host rock units, distribution of mines, and vein fault attitudes as well as cross faults (taken from Watson this volume, modified from Boyle 1965, 1970).



Figure 5. Planar fault surface scraped clean of its mineralization, exposure from Hector open pit.

hydrothermal system. The zonation seen here is typical of felsic intrusive related cordilleran-type vein deposits, of which several idealized zoning models are known. The models are pieced together from various deposits and districts (Spurr 1907, 1912; Emmons, 1924, 1936; Guilbert and Park, 1986, p. 219). The version that most closely matches the observed sequence from Keno Hill-Galena Hill is by Spurr (1912), and is presented in Table 1 for comparison. A few deposits from the surrounding region are included to complete the model. The western deposits would be the most distal from the source area as they contain primary polybasite, stephanite, argentiferous tetrahedrite (freibergite), and acanthite among others, with high gold values. The deposits of Galena Hill are in a relatively intermediate position making up the main galena-sphalerite zone. The eastern deposits are more proximal to the source as characterized by pyrrhotite, auriferous arsenopyrite, and jamesonite-boulangerite. Not directly contained within the Keno Hill-Galena Hill fault systems, but found in the local region, are possible analogues of the deeper zones. An equivalent to Spurr's (1912) deep gold-auriferous pyrite zone with coarse quartz gangue is found in the immediate area to the north at Dublin Gulch (Fig. 2). It is in close spatial association with felsic intrusive rocks and related tin-tungsten mineralization, and has been classified as a "mesothermal" gold deposit (Morin, 1981). Application of Spurr's model in this fashion would indicate potential for gold mineralization to the east of and/or below Keno Hill -Galena Hill, as well as tin-tungsten potential.

Another zoning model, based on theoretical grounds from mineral stability, metal solubility, and aqueous sulphide complex considerations put forth by Barnes (1975) is also useful. In it



Figure 6. Map showing separate distribution of index minerals in veins throughout the district.

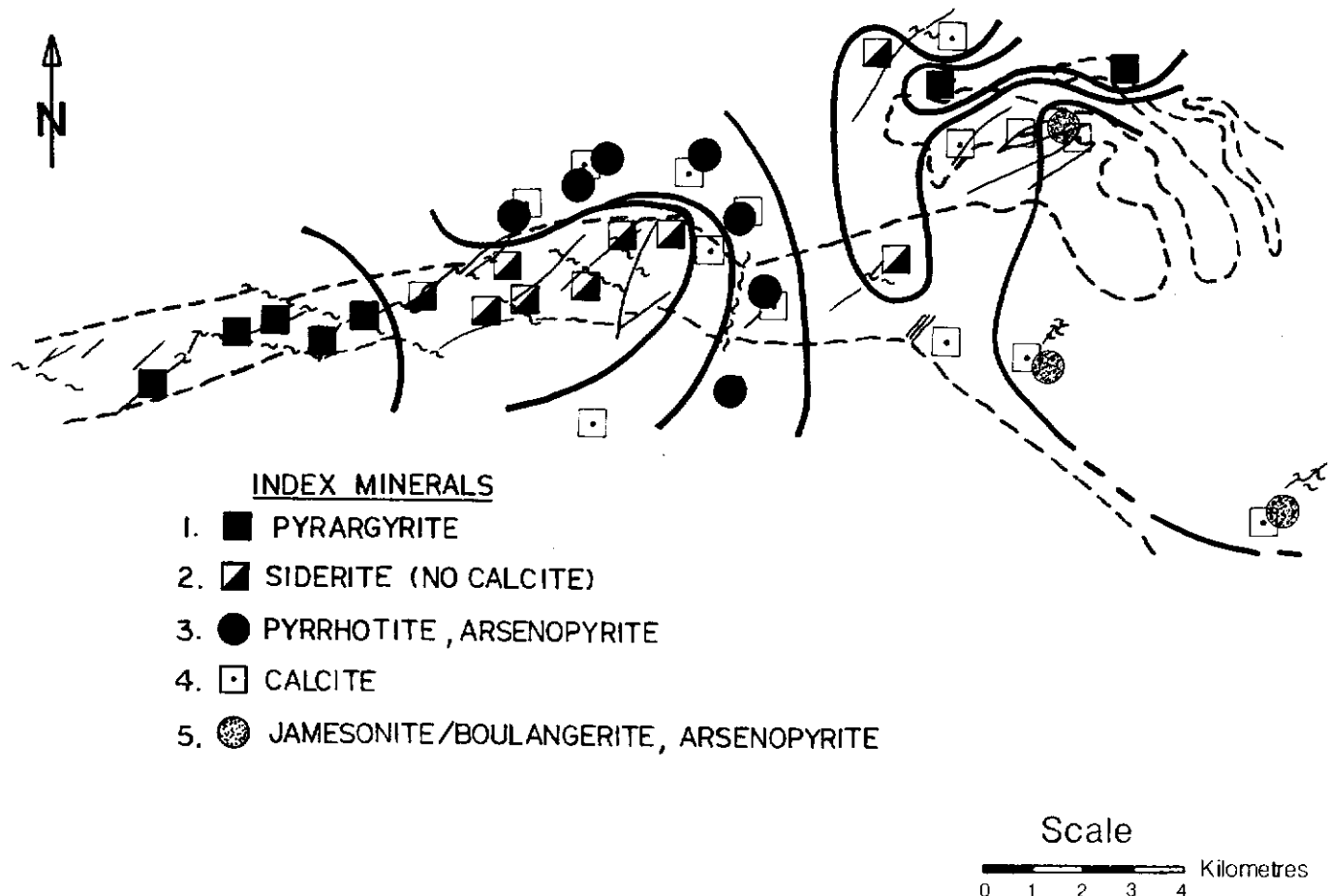


Figure 7. Mineral zoning map according to position of index minerals in veins for the Keno Hill - Galena Hill mining district.

TABLE 1

Table shows the mineral zones which are present at Keno Hill-Galena Hill and surrounding area, and how they correspond to equivalent zones of a general model established by Spurr (1912) for typical vein deposits.

	A	B	C	D	E F	G
Idealized mineral zoning sequence for vein deposits, by Spurr (1912). Minerals in parenthesis added by writer.	Quartz-feldspar Tourmaline, Sn-W-Mo	Gold-quartz-pyrite Veining (Arseno-pyrite)	Cu-pyrite Zone	Pyrrhotite Arsenopyrite Jamesonite Boulangerite	Sphalerite-galena	Polybasite Stephanite Acanthite Freibergite Gold (Pyrargyrite) (Native-Ag)
Deposits in the Keno Hill-Galena Hill District corresponding to the above zones. Areas in parenthesis are located in the district but are not contained in Keno Fault system, they are likely analogous but separate isolated systems.	Roop Lakes (Dublin Gulch) (Mt. Haldane) (Kalzas, see Lynch, 1985)	(Dublin Gulch)	None Distinct	Mt. Hinton Homestake Keno Flame & Moth Duncan (Dublin Gulch)	Keno Hill-Galena Hill	Husky Silver-King Elsa Lucky Queen
MAIN OREBODIES						
PROXIMAL TO FELSIC PLUTONIC BODIES				→ DISTAL TO FELSIC PLUTONIC BODIES		

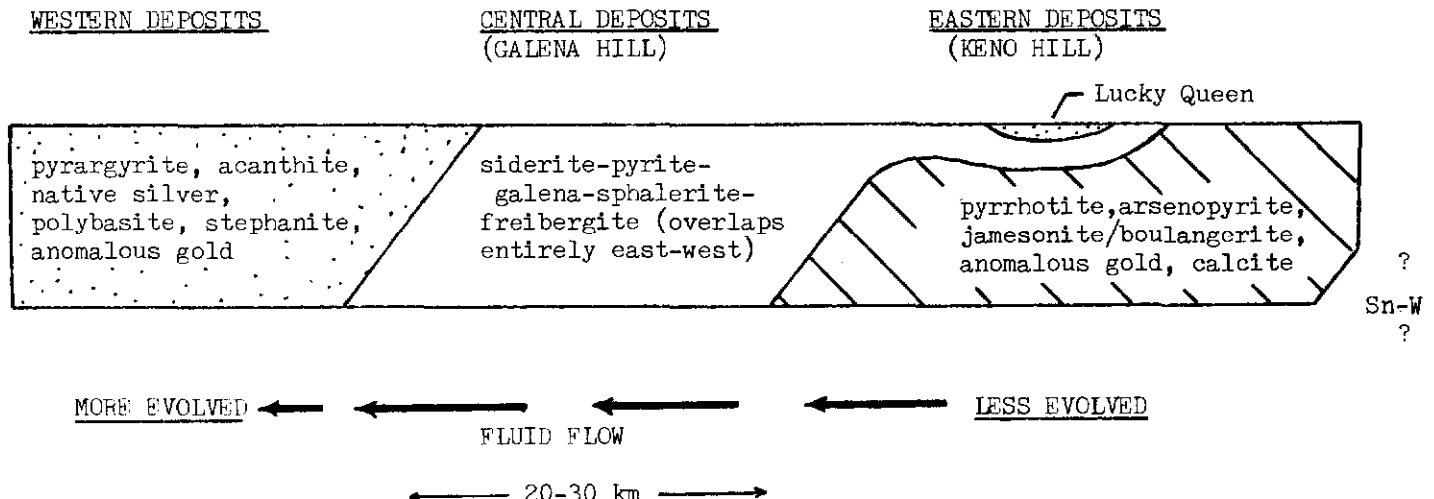


Figure 8. Schematic east-west cross-section through the area which summarizes and idealizes the mineral zoning sequence within the veins.

arsenopyrite and pyrrhotite are deeper or less evolved, sphalerite-tetrahedrite-galena are intermediate, acanthite and associated minerals plus gold are more evolved or distal. Barnes (1975) points out that such zoning is not dominantly caused by temperature gradients, as commonly assumed.

Zoning of vein deposits is generally perpendicular to the direction of fluid flow of the mineralizing solutions. And, in contradiction to normal belief, vertical zoning is usually much less well developed than lateral zoning (Turneaure and Welker, 1947; Barnes, 1975). To illustrate, base metal depositing hydrothermal fluids monitored in active geothermal systems rarely if ever discharge at the earth's surface; their higher densities hold them to greater depths (White, 1981) at which level their flow is predominantly lateral if in contact with permeable fault planes. At depth, thermal and chemical equilibrium of the fluids with the host rocks (as indicated by the general lack of wallrock alteration at Keno) could conceivably allow for great travel distances to be covered by the mineralizing solutions before deposition. These features, and the mineral distribution in the project area, argue for a lateral component of migration from east to west for the mineralizing fluids along the semi-continuous fault system during deposition. The indications are such that the large pluton at the eastern end of the district (Fig. 2) may have been responsible for the hydrothermal system which deposited the orebodies.

COMPARISON OF SULPHUR ISOTOPE DATA WITH MINERAL ZONING PATTERN

Boyle *et al.* (1970) conducted an extensive study on sulphur isotope ratios of host rock and vein sulphides from the Keno Hill-Galena Hill district. Tabulated data for vein galena was plotted on a map here (Fig. 16) and contoured for comparison with the mineral zoning map (Fig. 7). A strong correlation is observed; galena from the eastern deposits is relatively enriched in the heavy isotope with values close to 0 (zero parts per mil), whereas galena from the western deposits is depleted having values down to -10. The transition from one end to the other is strikingly systematic and gradational. A 900 foot vertical section in the Calumet Mine was sampled and analyzed with no regular pattern in this dimension observable at this scale. The geochemical study demonstrates very well the unidirectional nature of the zoning and lends confidence to the established mineral zoning pattern through independent means.

Even large variations in temperature will not generally cause changes in the sulphur isotope value of individual sulphide minerals by ten parts per mil. On the other hand, an increase in pH and/or in the oxidation fugacity of the fluids under hydrothermal conditions can easily account for a decrease of 10 per mil in galena (Ohmoto, 1977; Rye and Ohmoto, 1974) and possibly occurred from east to west here.

Generally sulphides in igneous rocks have average $\delta^{34}\text{S}$ close to 0 per mil (Ohmoto, 1979). Sedimentary sulphides have a

wide range, but are typically depleted in the heavy isotope. Boyle *et al.* (1970) have shown that pyrite from the host rocks here average near 0 per mil. Thus a host rock source or an igneous source for the sulphur cannot be distinguished in this case, if it is assumed that the ratios from the eastern deposits (near 0 per mil) are more representative of the source area. In any case the interpretation of the isotopic data is not stressed and is open for further debate; but rather the strong zonal distribution is underlined, and in the absence of index minerals sulphur isotopes from galena can be used to give relative position in the system.

ACKNOWLEDGEMENTS

Funding for this project was received through a contract with the Yukon Economic Development Agreement, for which I am grateful. Further help and accommodation was received from United Keno Hill Mines Ltd., who allowed full access to their underground workings, drill core, maps and geological files. Guidance and advice was generously extended from the geological staff of United Keno Hill Mines in Elsa, to whom I am very thankful, namely: Ken Watson, Jim McFaull, Mike Dufresne, Neil O'Brien, and Pat Watson.

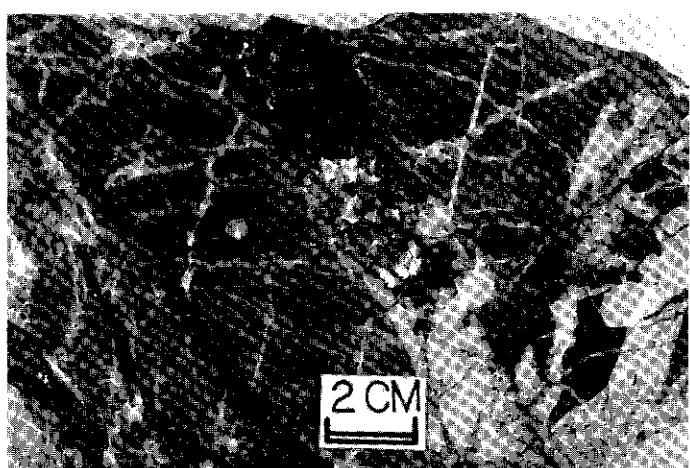


Figure 9. Photograph showing siderite-pyrite-galena vein cutting quartz veinlet stockwork.

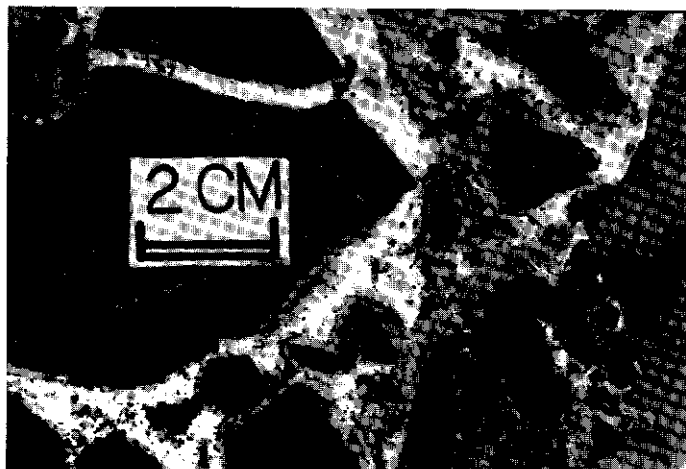


Figure 10. Late quartz encrustations over carbonate filling vugs in fault breccia.



Figure 13. Calcite-quartz-arsenopyrite vein from the lower slope on the northern side of Galena Hill.

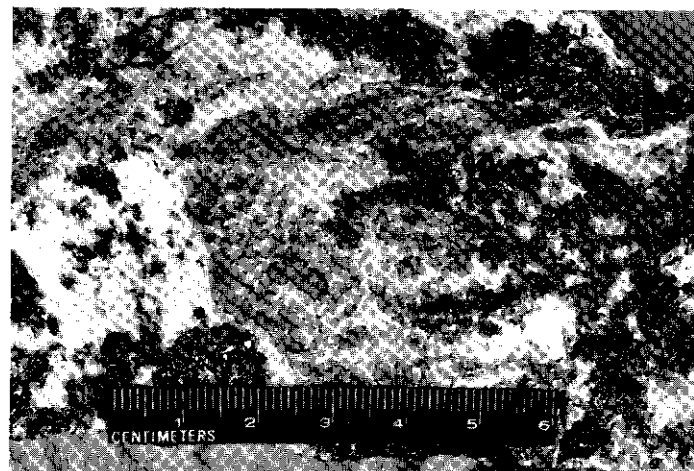


Figure 11. Siderite-quartz-pyrrhotite, veinlets with some galena and pyrite (Husky mine, raise 224).

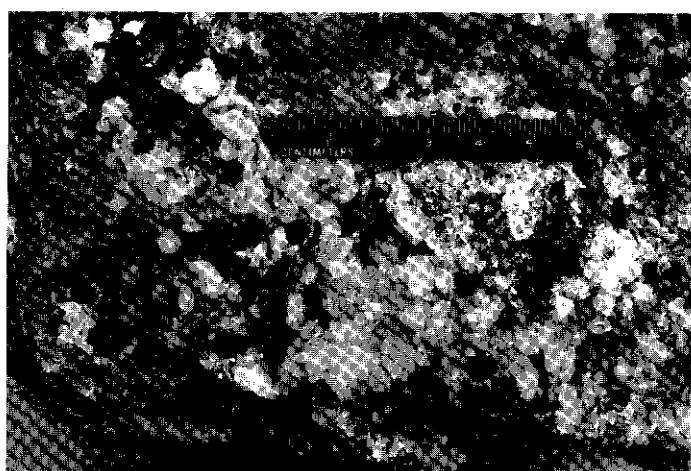


Figure 14. Calcite and galena growing into open vug.

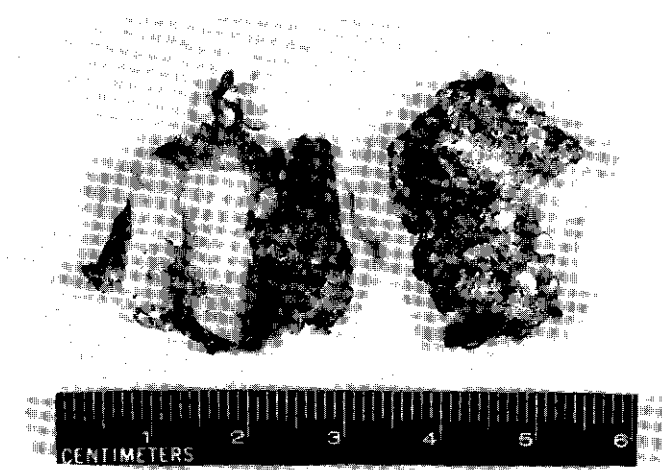


Figure 12. Native silver wires from the Silver King mine.

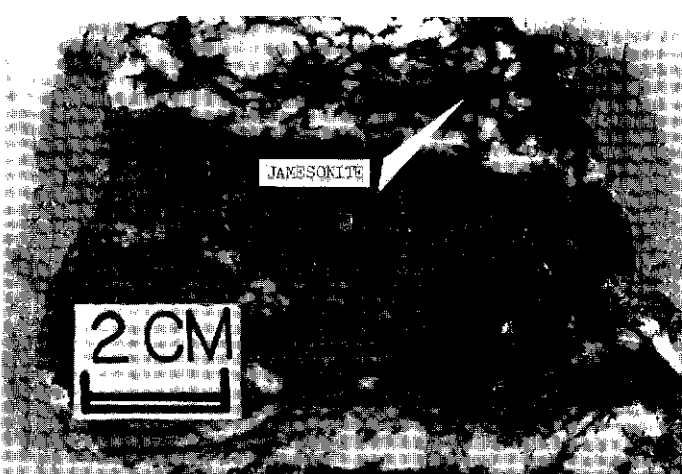


Figure 15. Jamesonite/boulangerite with quartz, sphalerite, pyrite and arsenopyrite from the Homestake deposit at the eastern end of the district.

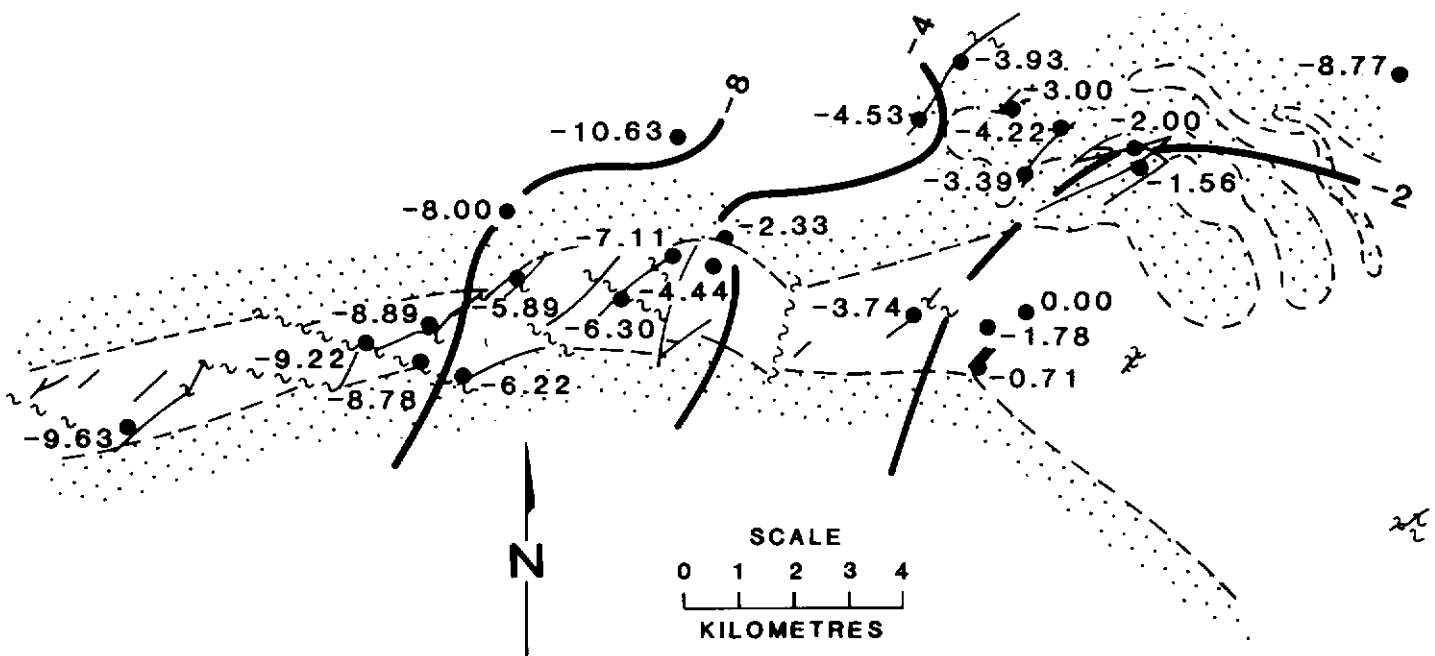


Figure 16. Map showing general decrease of sulphur isotope ratios in galena from east to west creating a pattern which roughly mimics the mineral zoning. Values for map taken from tabulated data of Boyle et al. (1970).

REFERENCES

- BARNES, H.L., 1975. Zoning of ore deposits: types and causes; *Trans. Roy. Soc. Edinburgh*, Vol. 69, p. 295-311.
- BOYLE, R.W., 1965. Geology, geochemistry, and origin of the lead-zinc-silver deposits of the Keno Hill - Galena Hill area, Yukon Territory; *Geo. Surv. Can., Bulletin 111*, 302 p.
- BOYLE, R.W., WANLESS, R.K., STEVENS, R.D., 1970. Sulphur isotope investigation of the lead-zinc-silver-cadmium deposits of the Keno Hill - Galena Hill area, Yukon, Canada; *Econ. Geol.*, Vol. 65, p. 1-10.
- EMMONS, W.H., 1936. Hypogene zoning in metalliferous lodes; *16th Int. Geol. Congr. Rept.*, pt. 1, p. 417-432.
- EMMONS, W.H., 1924. Primary downward changes in ore deposits; *AlME trans.*, Vol. 70, p. 964-997.
- GREEN, H.L., 1971. Geology of Mayo Lake, Scougale Creek and McQuesten Lake map-areas, Yukon Territory; *Geol. Surv. Can., Memoir 357*, 72 p.
- GUILBERT, J.M., PARK, C.F.Jr., 1986. *The Geology of Ore Deposits*; W.H. Freeman and Co., 985 p.
- GODWIN, C.I., SINCLAIR, A.J., RYAN, B.D., 1982. Lead isotope models for the genesis of carbonate hosted Ba-Zn-Pb, and silver-rich deposits in the Northern Canadian Cordillera; *Econ. Geol.*, Vol. 77, p. 82-94.
- LYNCH, G.V., 1985. Mineralization and alteration zonation of the Kalzas wolframite vein-deposit, Yukon Territory; *MSc thesis, Washington State University, Pullman, Washington*, 123 p.
- McTAGGART, K.C., 1960. The Geology of Keno and Galena Hills, Yukon Territory; *Geol. Surv. Can., Bulletin 58*.
- MORIN, J.A., 1981. Element distribution in Yukon gold-silver deposits; *in Yukon Geology and Exploration 1979-80, Dept. Ind. Aff. Nor. Dev., Whitehorse, Yukon*, p. 68.
- OHMOTO, H., RYE, R.O., 1979. Isotopes of sulphur and carbon; *in Barnes, H.L., ed, Geochemistry and Hydrothermal Ore Deposits*; New York, John Wiley and Sons, p. 509-567.
- RYE, R.O., OHMOTO, H., 1974. Sulfur and carbon isotopes and ore genesis; a review; *Econ. Geol.*, Vol. 69, p. 826-842.
- SINCLAIR, A.J., TESSARI, O.J., HARAKAL, J.E., 1980. Age of silver-lead-zinc mineralization, Keno Hill - Galena Hill area, Yukon Territory; *Can. J. Earth Sci.*, Vol. 17, p. 1100-1103.
- SPURR, J.E., 1907. A theory of ore deposition; *Econ. Geol.*, Vol. 2, p. 781-795.
- SPURR, J.E., 1912. Theory of ore deposition; *Econ. Geol.*, Vol. 7, p. 485-492.
- TEMPELMAN-KLUIT, D.J., 1970. Stratigraphy and structure of the "Keno Hill Quartzite" in Tombstone River-Upper Klondike River map areas; *Geol. Surv. Can., Bulletin 180*, 102 p.
- TURNEAURE, F.S., WELKER, K.K., 1947. The ore deposits of the Eastern Andes of Bolivia; Vol. 42, p. 595-625.
- WHITE, D.E., 1981. Active geothermal systems and hydrothermal ore deposits; *Economic Geology 75th Anniversary Volume, B.J. Skinner (editor)*, p. 392-423.

METAL-RATIO ZONATION IN THE KENO HILL DISTRICT, CENTRAL YUKON

J.P. Franzen
North Vancouver, B.C.

FRANZEN, J.P., 1986. Metal-ratio zonation in the Keno Hill district, central Yukon; in *Yukon Geology, Vol. 1; Exploration and Geological Services Division, Yukon, Indian and Northern Affairs Canada*, p. 98-108.

ABSTRACT

Silver has been won from narrow vein faults in the Keno Hill district for nearly 70 years. During this period, 3.9 million tonnes (4.3 million tons) of ore have yielded 5754 million grams (185 million ounces) of silver. All of this production has come from sub-cropping ore shoots; supergene enrichment is not an important factor in most deposits. Parallelism of the ore zone with the present surface has been seen in other Cordilleran vein camps, but despite considerable effort, operators in these camps have met with little success in their search for blind ore shoots.

The potential for blind ore in the Keno Hill district is examined from the perspective of metal-ratio zonation. An approximate reconstruction of the original fracture pattern in the district and the metal-ratio definition of a hydrothermal system acting within these fractures suggest that some ore shoots have been eroded, some are exposed at the present surface, and others remain preserved at depth.

INTRODUCTION

The Keno Hill district, 354 km north of Whitehorse, Y.T. and 274 km east of the Alaska-Yukon border (Fig. 1), has been a prolific silver producer for nearly 70 years. During this period, 14 significant deposits, each containing more than 7.8 million g (250,000 oz) of silver have yielded a total of 5754 million tonnes (4.3 million tons) of ore mined. The historical silver ore production grade has averaged 1475 g/t Ag (43.0 oz/ton), 7.2% Pb and 4.7% Zn. By way of comparison, the Slocan district produced 1711 million g (55 million oz) of silver, the Cobalt district 11,353 million g (365 million oz) of silver and the Coeur d'Alene district is approaching 31,103 million g (1 billion oz) of silver production.

All of the known significant Keno Hill district deposits subcrop. In 11 of these mines, the ore shoot(s) dies out 91 m (300 ft) to 152 m (500 ft) vertically below subcrop, even though the enclosing vein fault structure remains strong at depth. The Hector-Calumet mine, the deepest in the district, has been mined to 366 vertical metres beneath the outcrop, yielding just over one half the total district silver production. If this mine is excluded, the 0 to 122 m vertical depth zone of the remaining 13 significant mines account for 90 percent of the combined silver production. Supergene enrichment is not an important factor in most deposits. The elevation difference between the top of the highest deposit and bottom of the lowest deposit is 1036 metres. Most deposits show an increase in sphalerite and decrease in argentiferous galena with depth. In exploration for new deposits, the apparent parallelism of the ore to the present surface is an important consideration. If it is real, there is little likelihood of finding deep or blind ore in the district.

United Keno Hill Mines Limited has been operating in the Keno Hill district since 1947. Successful exploration programs, both underground in the operating mines and on surface using rotary percussion drilling on a grid pattern (Van Tassell, 1969; Franzen and Van Tassell, 1981), have enabled the company to maintain mining operations. Completion of 15,000 grid rotary percussion holes, at an average depth of 37 metres per hole, has tested many of the known shallow targets in the district. The long term future of the district may depend on the discovery of deep and blind ore shoots.

This paper describes metal-ratio zonation in the Keno Hill district. The potential for deep ore is considered in terms of a large, metal-ratio defined hydrothermal system.

Previous Work

Detailed descriptions of geology, mineral deposits and mining operations in the Keno Hill district have been given in various publications. McTaggart (1960) and Green (1971) established the fundamental stratigraphy and structural geology, whereas Aho (1963) and Boyle (1965) considered the geology of the silver deposits. Tempelman-Kluit (1970) described the regional geology of the Keno Hill Quartzite. More recently, Sinclair et al. (1980), and Sinclair and Tessari (1981) have reported on vein geochemistry

of individual deposits and K-Ar age dates of vein mineralization. Mining operations are described by The Staff (1961). The reader is referred to the above mentioned papers for detailed background information.

KENO HILL DISTRICT GEOLOGY

The Keno Hill district is 29 km long in an east-west direction and 6.5 km wide (Fig. 2). Within it, some 70 vein deposits are known along sub-parallel vein fault structures, with a total strike length of 56 km. The steeply south-dipping vein faults are for the most part confined to the structurally favorable Central Quartzite Unit of probable Lower Cretaceous age. This unit has an apparent structural thickness of 914 to 1829 m (3000 to 6000 ft) and consists of variably-bedded orthoquartzite with interbeds of graphitic phyllite and less common greenstone sills. Compositional layering dips moderately to the south and the rocks are strongly foliated parallel to it. The geology of the district is complex and not fully understood. Small isoclinal folds with axial planes parallel to the foliation are common and the apparent thickness of rock units and the stratigraphic succession may be the result of large-scale isoclinal folding or thrusting.

The Central Quartzite Unit is underlain by the Lower Schist Unit of probable Jurassic age and overlain by the Upper Schist Unit of uncertain age. Both consist of thin-bedded quartzite, phyllitic quartzite and sericitic to graphitic phyllite. In addition, the Lower Unit contains numerous greenstone sills and on Keno Hill, the No. 9 Quartzite Member near the top of the unit. Greenstone and quartzite of the Lower Schist Unit contain mineralized vein structures. Cretaceous granitic stocks intrude the structural succession, although there are no known occurrences of granite in the vicinity of the mine workings.

In the Keno Hill district, open folding outlined by rocks of the Central Quartzite Unit has been superimposed on earlier, complex structures. Most important is the McQuesten anticline, an open, upright structure that plunges gently to the west (Fig. 3). Near the summit of Keno Hill, the strike of the rocks swings to the southeast on the flank of another open structure, the Mayo Lake anticline. The vein faults strike more or less parallel to the axial plane of the anticline, their orientation and spatial distribution suggesting that the structure has controlled their development. On the south limb, much of the Central Quartzite Unit has been eroded, while other portions remain buried beneath the rocks of the Upper Schist Unit. It seems logical to assume that some portions of the accompanying vein faults have been eroded, while others remain buried, the present erosional surface cutting obliquely through the original Keno Hill district fracture pattern.

At the west end of the structure, the Central Quartzite Unit outcrops close to the anticlinal crest (Fig. 4 - Point A). Traversing easterly along the quartzite outcrop one moves obliquely down the limb of the anticline (Fig. 4 - Point B). In effect, at the present erosion level one sees an en echelon view of isolated portions of individual vein faults rather than a true section across the original

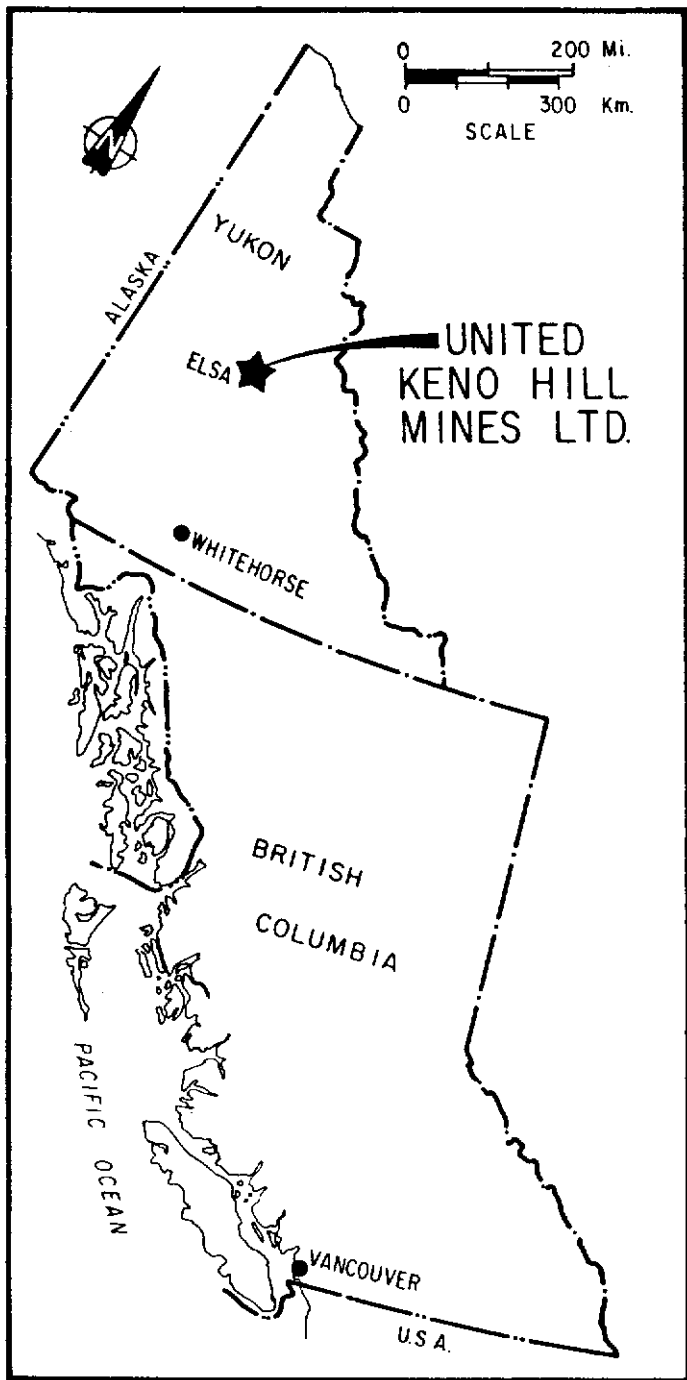


Figure 1. Location map of Keno Hill district.

fracture pattern. Before examining metal-ratio zonation between and within these vein faults, it is important to know what this original fracture pattern looked like. Figure 5 is a generalized cross-sectional reconstruction, normal to the anticline hinge line, of the original fracture pattern on the south limb of the McQuesten anticline. This cross section was constructed by compressing the en echelon known portions of individual vein faults (Fig. 4) onto a common or composite cross section. Construction of such a section requires a horizontal and vertical coordinate for each vein fault in the district. The horizontal position of individual vein faults was determined by measuring, in plan, the normal distance between a reference line parallel to the surface trace of the axial plane and the location of the vein fault. The vertical position of individual vein faults is simply the stratigraphic position of the vein fault in the structural succession. Constructing a district composite or generalized cross section in this manner avoids strike variation problems inherent in actually projecting individual veins to a common section line. Figure 5 shows that vein faults occur in an 8 kilometre wide zone on the south limb of the anticline. The rare

vein faults on the unproductive north limb of the anticline dip in the opposite direction.

VEIN FAULT STRUCTURE AND MINERALIZATION

Deposits in the Keno Hill district share a common structural style, but differ markedly in the character of their mineralization. The vein faults are breccia zones or sheeted zones or transitions between these two types. Drag along vein fault wallrocks indicates that the last sense of movement along these zones was of the normal type. Vein fault widths vary between 0.6 and 30 m, but are most commonly in the 1.5 to 4.6 m range. Individual ore shoots vary in size from tens of metres to a few hundreds of metres vertically and laterally. These ore shoots commonly occur in or near structurally complicated zones within the vein fault where cymoid loops, junction zones, and cross faults make for difficult mining conditions.

Many of the Keno Hill deposits are mineralogically distinctive. Visual inspection of a hand size sample will often allow the geologist to identify the mine and stope source of the material. Gangue mineralization typically consists of variable amounts of quartz, calcite and manganese siderite. The latter generally predominates in the ore zones. The main ore minerals are argentiferous galena, freibergite and sphalerite. Primary pyrargyrite, stephanite and polybasite sulphosalts mineralization accompany the normal argentiferous galena-freibergite association at the rich Husky Mine. In some of the mines the oxidation zone extends to a depth of approximately 152 m. In this zone, cerussite and anglesite are common; native silver and argentiferous jarosites may also occur. For a detailed account of the structural geology and mineralization in individual deposits, the reader is referred to Boyle (1965).

DISTRICT METAL-RATIO ZONATION

Like many other high-grade, narrow vein deposits mined elsewhere in the world, those of the Keno Hill district have required careful geology and grade control. It is a 70 year accumulation of documented geological and grade information that forms the basis of this metal-ratio zonation study.

There is a wide range in the size of significant deposits in the Keno Hill district. Table 1 summarizes production data to September 1979 for the 14 significant deposits considered in this study. Hector-Calumet Mine is in a class by itself. This deposit has produced 2955 million g (95 million oz) of silver from 2.4 million tonnes (2.6 million tons) of ore. Structural arguments and mineralogical considerations (Franzen, 1978) suggest that the Elsa and Husky Mines were originally a single deposit, now separated by cross-faulting. This combined deposit has produced 1120 million g (36 million oz) of silver from 523, 666 tonnes (577,297 tons) of ore and continues to operate. Consequently, the Hector-Calumet and Husky-Elsa deposits account for 70 percent of the silver production in the district. Most of the remaining significant deposits fall into the range of 31 to 467 million g (1 to 15 million oz) of silver and 27,213 to 272,130 tonnes (30,000 to 300,000 tons) of ore. In general, a deposit containing in excess of 311 million g (10 million oz) of silver is considered to be a major deposit in the district. On a reconstructed cross section (Fig. 6), major deposits, with the exception of Keno 9, are confined to a 1.8 km wide zone that is close to, but dipping away from, the axial plane of the McQuesten anticline (Fig. 6). The apparent vertical or up-dip continuity of these major deposits is noteworthy. Minor producers and deposits with important mineralization are scattered across the reconstructed section. This distribution of known deposits indicates that mineralizing solutions were either more readily available adjacent to the anticline axial plane or that proximity to the axial plane is a prerequisite for effective tapping and localization of mineralizing solutions. In either case, the general distribution of silver suggests a decreasing production potential, with increasing distance from the zone of major producers.

The ore mineralogy of vein faults does not vary systematically with the position in the structural succession. However, total ore production metal ratios from the significant deposits show a definite zonation in reconstructed cross section. These structural and metal-ratio reconstructions assume that production metal ratios from known deposits are representative of eroded and

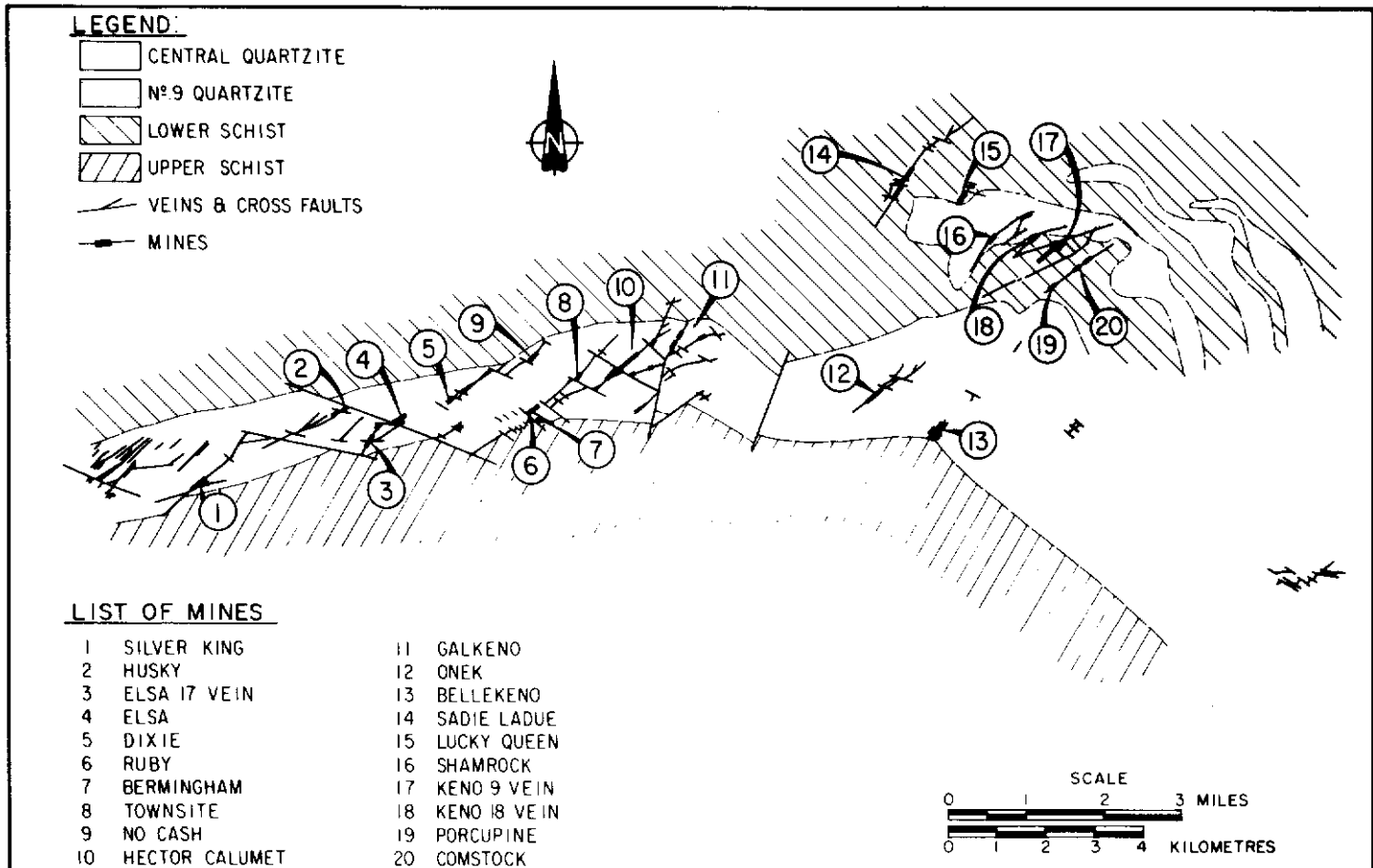


Figure 2. Mines and fault structures on Galena and Keno Hills.

buried along-strike portions of the vein faults. Metal-ratio contours for Ag/Pb, Pb/Zn and Ag/Zn (Figs. 7, 8 and 9 respectively) show a dominant and regular, concave-up pattern deep in the structural succession. The axis of this concave-up pattern is coincident for Ag/Pb and Ag/Zn values; the Pb/Zn axis shows a shift to the south. For all three ratios, the axis of the concave-up pattern is approximately parallel to the dip of vein faults in the camp. Higher in the structural succession, Ag/Pb and Pb/Zn values define a variant, subordinate metal-ratio trend whose axis parallels compositional layering. The large and high-grade Husky-Elsa deposit is at the centre of this. Studies within individual veins in other mining districts (Goodell and Petersen, 1974) have shown that the shape of metal-ratio contours can outline zones of maximum permeability and, as a result, indicate the direction of flow of mineralizing solutions. The dominant and deep-seated metal-ratio dome indicated for Keno Hill district suggests that mineralizing solutions moved up through the structural succession along the centre of a pervasively fractured zone on the south limb of the McQuesten anticline. The Lucky Queen and Hector-Calumet vein systems have been the site of major flows of mineralizing solutions. Deposits in the Lower Schist and No. 9 Quartzite are tight and generally lack textures indicative of open space filling. The relatively gentle metal-ratio gradients of these deposits suggest that they were relatively deep-seated at their time of formation; Pb/Zn values are typically low. Deposits in the Central Quartzite commonly show open space vein filling textures. The steep metal-ratio gradients of these deposits suggest that they were relatively shallow at their time of formation. In them, deposition of metals from ore solutions appears to have been rapid, perhaps in response to marked temperature-pressure fluctuations in a high level environment; Pb/Zn values are generally high. This district variation in Pb/Zn values has also been noted on an individual deposit scale, with many of the mines showing an increase in zinc relative to lead with depth. In the author's opinion, the deposits mined to date in the Lower Schist and Central Quartzite Units carry the distinctive signature or fingerprint of an eroded, metal-ratio defined hydrothermal system. This metal-ratio signature varies with vein fault

position in the hydrothermal system and in the structural succession.

Testing of District Metal-Ratio Zonation

The concept of a district metal-ratio pattern that defines the "fossil" hydrothermal system presents some problems. The base of the metal-ratio dome in Figures 7, 8 and 9 is well established with five metal-ratio control points. Unfortunately, erosion has removed structurally favorable rocks higher in the dome and, as a result, there are no control points directly below the Central Quartzite Unit; metal-ratio contours are, at best, speculative in this area. It could be argued that positioning alone of certain Central Quartzite-hosted deposits has generated a dome shape that would not otherwise exist. The representativeness of district metal-ratio contours was examined in an independent test.

Detailed Deposit Metal-Ratios

To assign metal-ratio values to a particular deposit, production from that entire deposit was considered (Table 1). The resulting metal-ratio value, in conjunction with other deposit metal-ratios, was used to establish contour lines of the reconstructed cross section (Figs. 7, 8 and 9). If these district contours are meaningful, one must expect some correspondence with depth variations in metal-ratios in individual deposits. Figures 10 and 11 show detailed level by level metal-ratio profiles in six deposits, for which there are sufficient data. A comparison of these detailed down-dip mine profiles with the down-dip trends, as observed and interpolated in district contours, shows the two trends to be in general agreement. Ag/Pb values show the best correlation between detailed and district trends. This probably reflects the fact that the bulk of mining activity has concentrated on silver- and lead-rich, and zinc-poor zones in the deposits. These observations support the suggestion of a metal-ratio zonation in the district.

Regional Considerations

In the author's opinion, the metal-ratio zonation in the Keno Hill district suggests that we are looking at an eroded root zone of a

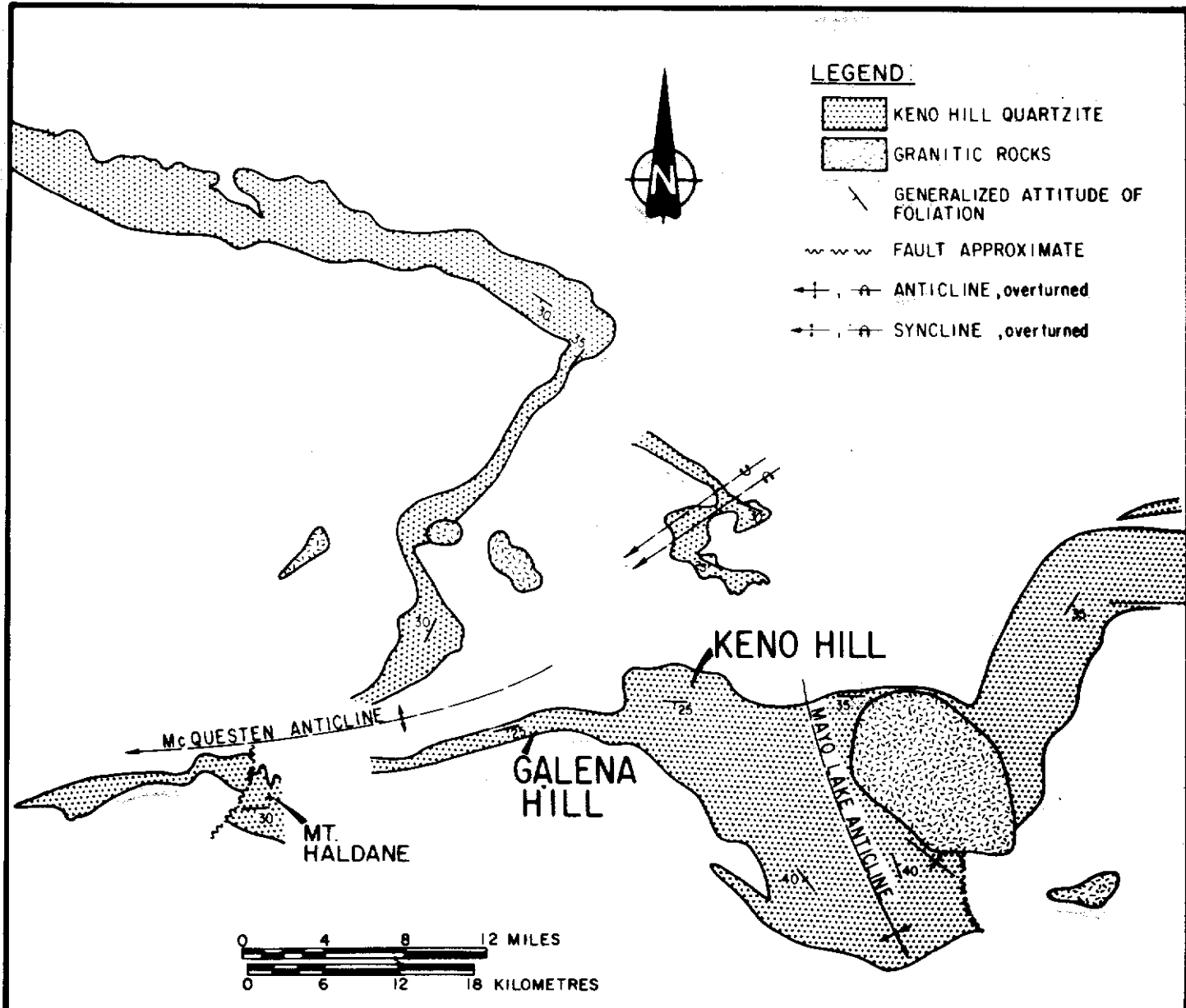


Figure 3. Structural elements in the Keno Hill district (after Green, 1971).

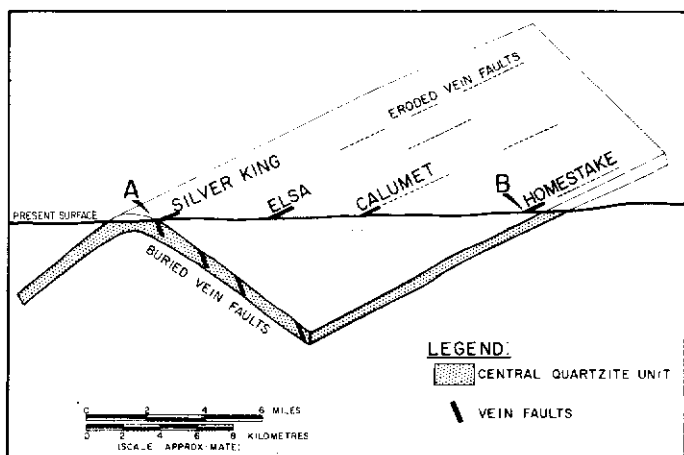


Figure 4. Schematic diagram of the south limb of the McQuesten Anticline showing the positioning of the anticline and vein faults relative to the present surface.

hydrothermal system at the eastern end and the top of a system at the western end, with much of the latter buried beneath cover rocks of the Upper Schist Unit (Figs. 12a and b respectively). The overall shape and orientation of the system appear to be similar to that of the vein fault-controlling McQuesten anticline. Additional mining and the discovery of new deposits may change this shape.

Considering the vein faults in terms of stratigraphic position or original depth, rather than viewing them solely as near surface features, can be supported by an examination of stratigraphic Ag/Pb zonation in the region. The average Ag/Pb value for deposits in Keno Hill district proper is 6/1; the average Ag/Pb value for three small deposits (Rambler, Foley and Paul) in the Lower Schist Unit in the core of the McQuesten anticline is 1/1 (Fig. 12b). This difference is significant and indicates that deposits in low stratigraphic positions have been deposited from relatively silver-deficient mineralizing solutions. If one considers the Lower Schist Unit as the source of the ore fluid (Boyle, 1965), then at least two explanations can account for this systematic Ag/Pb variability:

1. Low level deposits with low Ag/Pb ratios have been generated by hydrothermal solutions that have experienced limited upward migration through Lower Schist source rocks prior to reaching structurally favorable host rocks. Mineralizing solu-

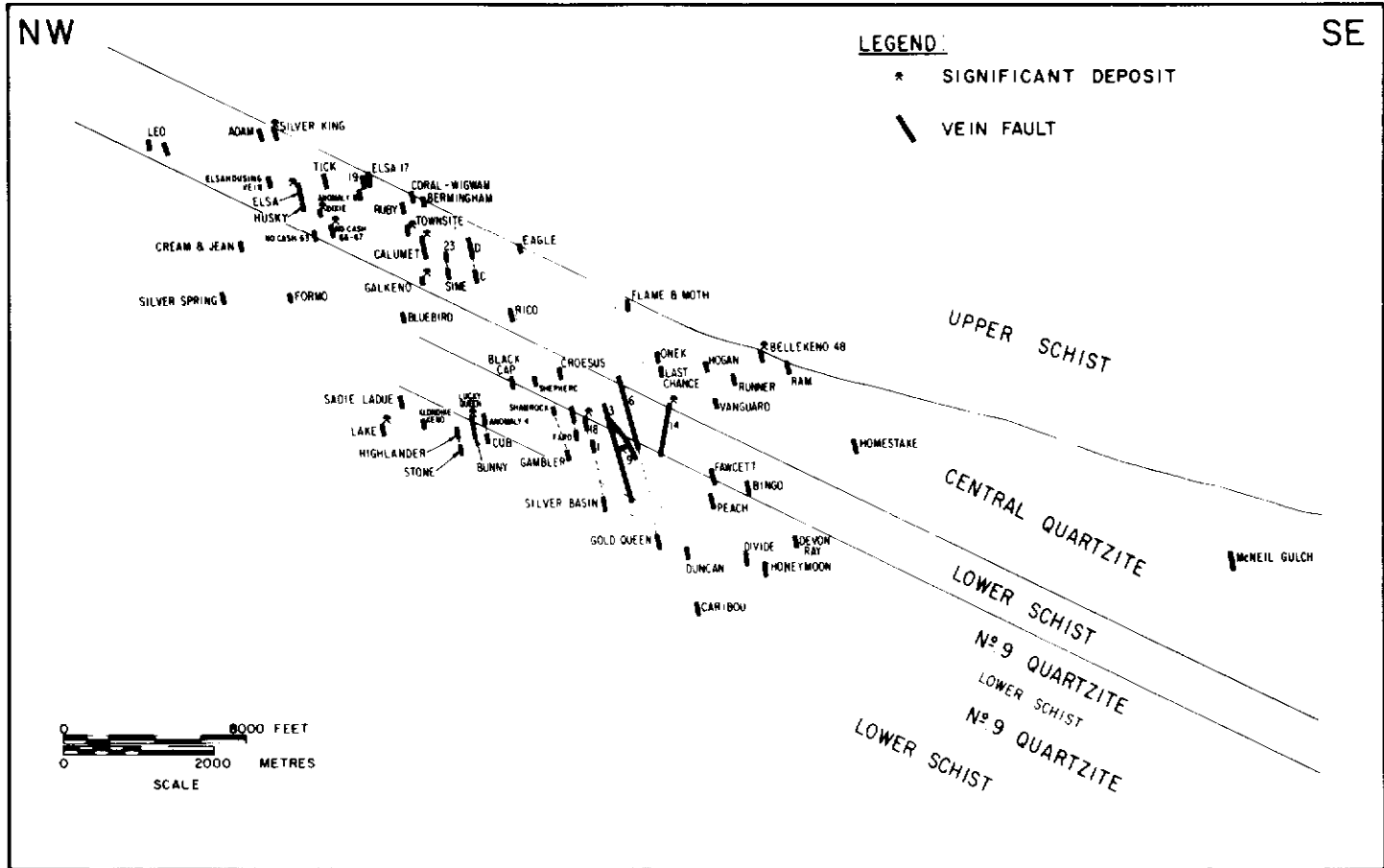


Figure 5. Approximate composite cross section reconstruction of the original fracture pattern on the south limb of the McQuesten Anticline.

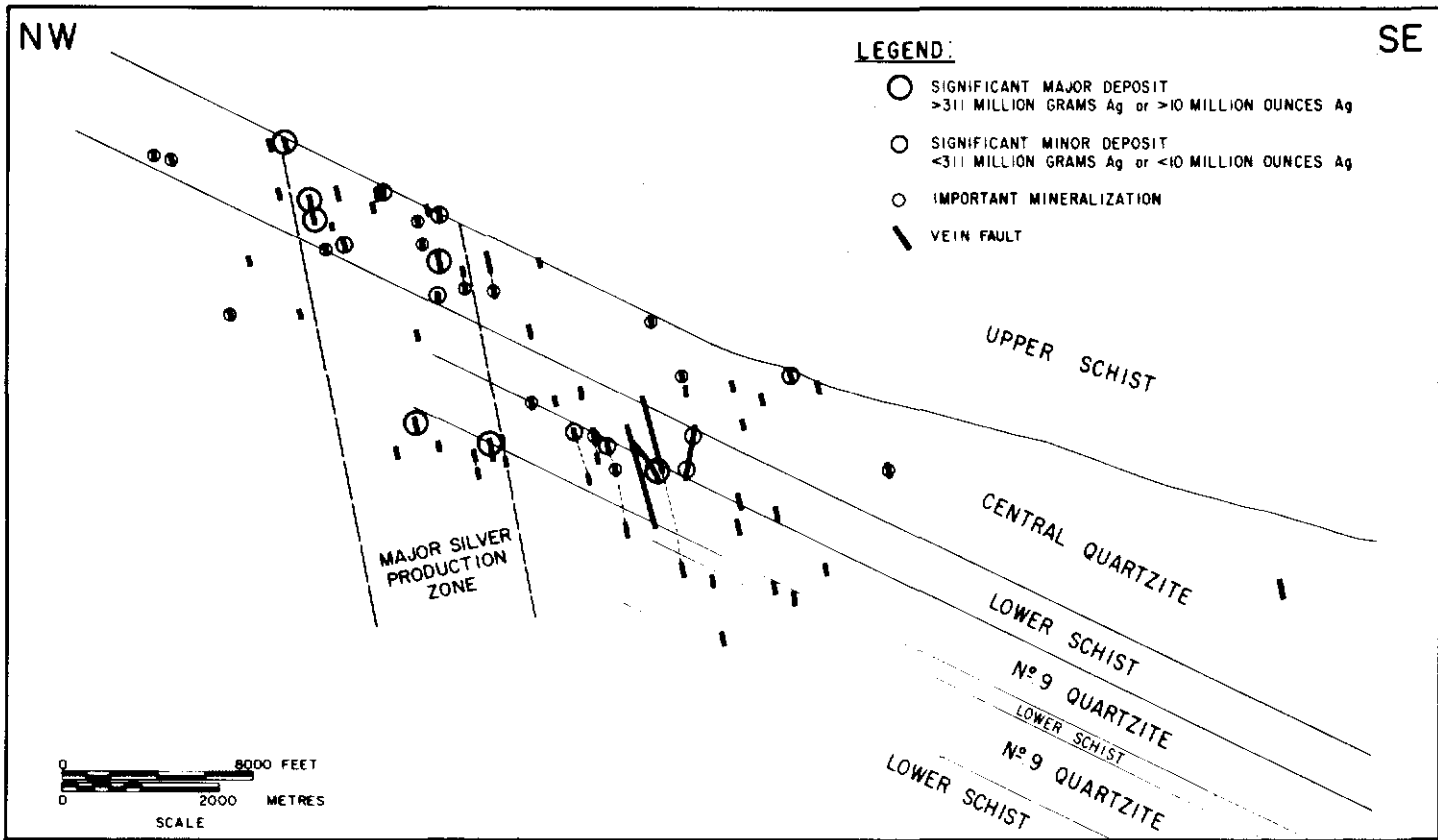


Figure 6. Approximate composite cross section reconstruction of the original fracture pattern showing silver production from significant deposits in the Keno Hill district.

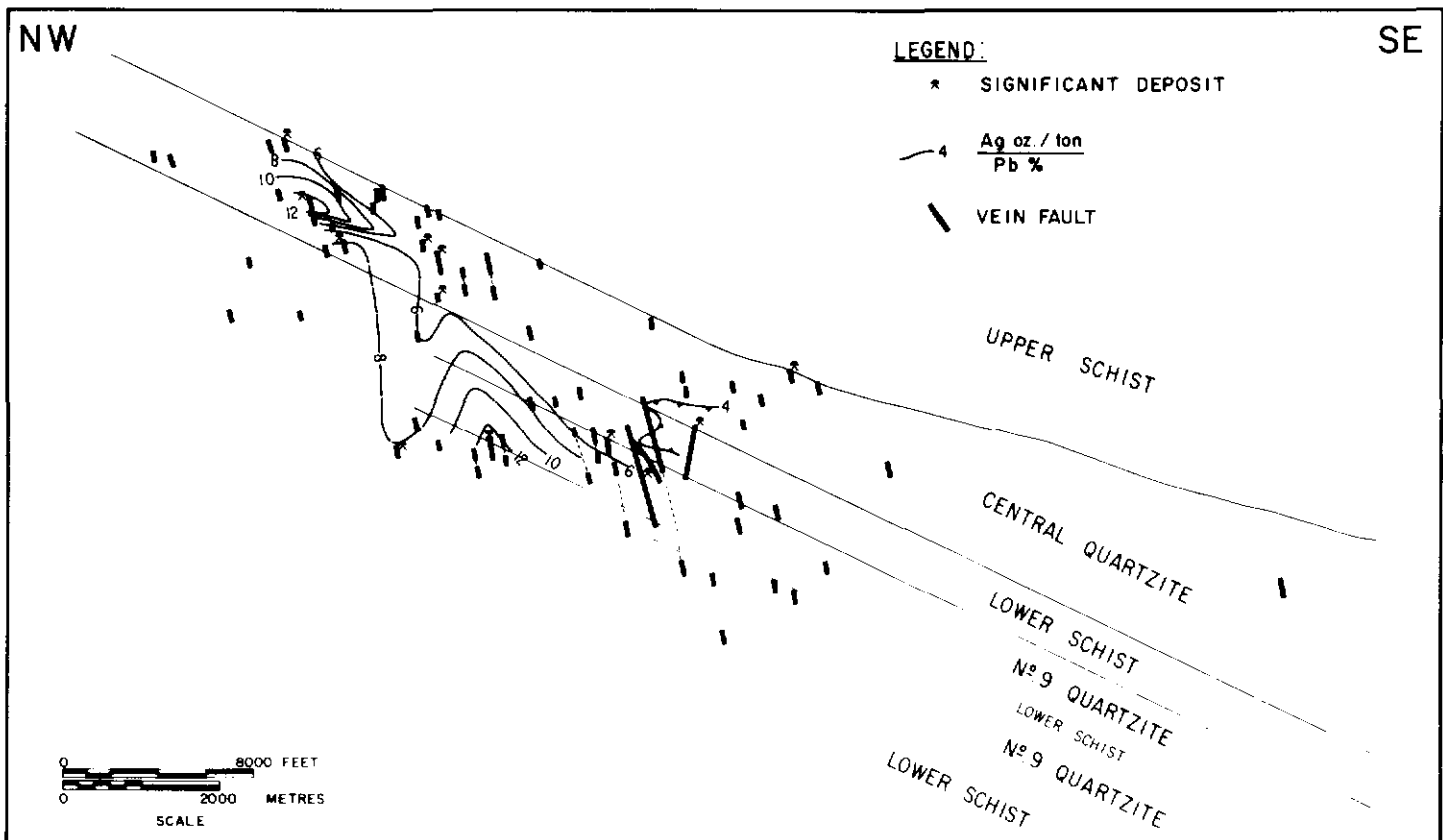


Figure 7. Approximate composite cross section reconstruction of the original fracture pattern showing the zonation of Ag (oz/ton)/Pb (%) values between significant deposits in the Keno Hill district.

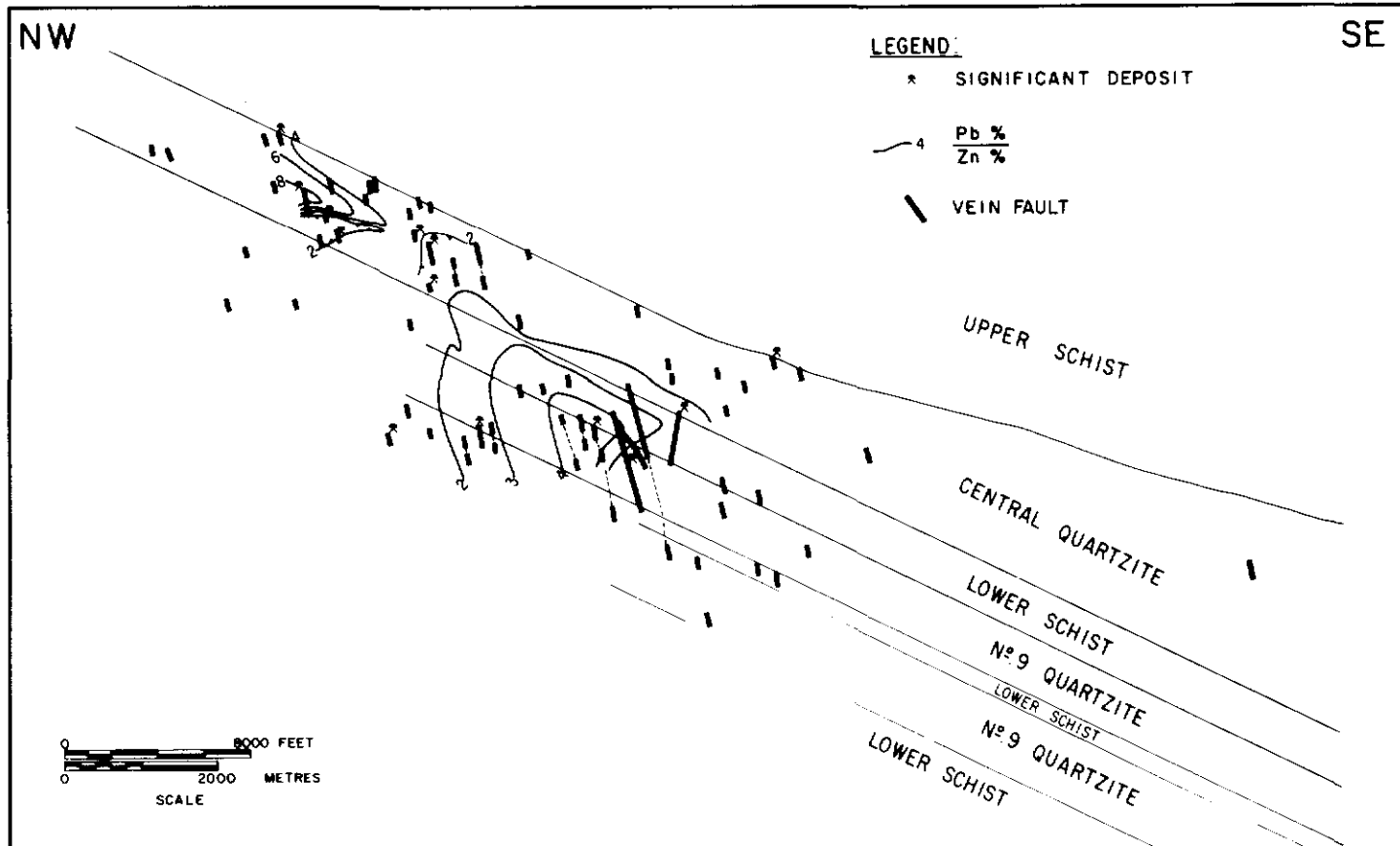


Figure 8. Approximate composite cross section reconstruction of the original fracture pattern showing the zonation of Pb(%) / Zn(%) values between significant deposits in the Keno Hill district.

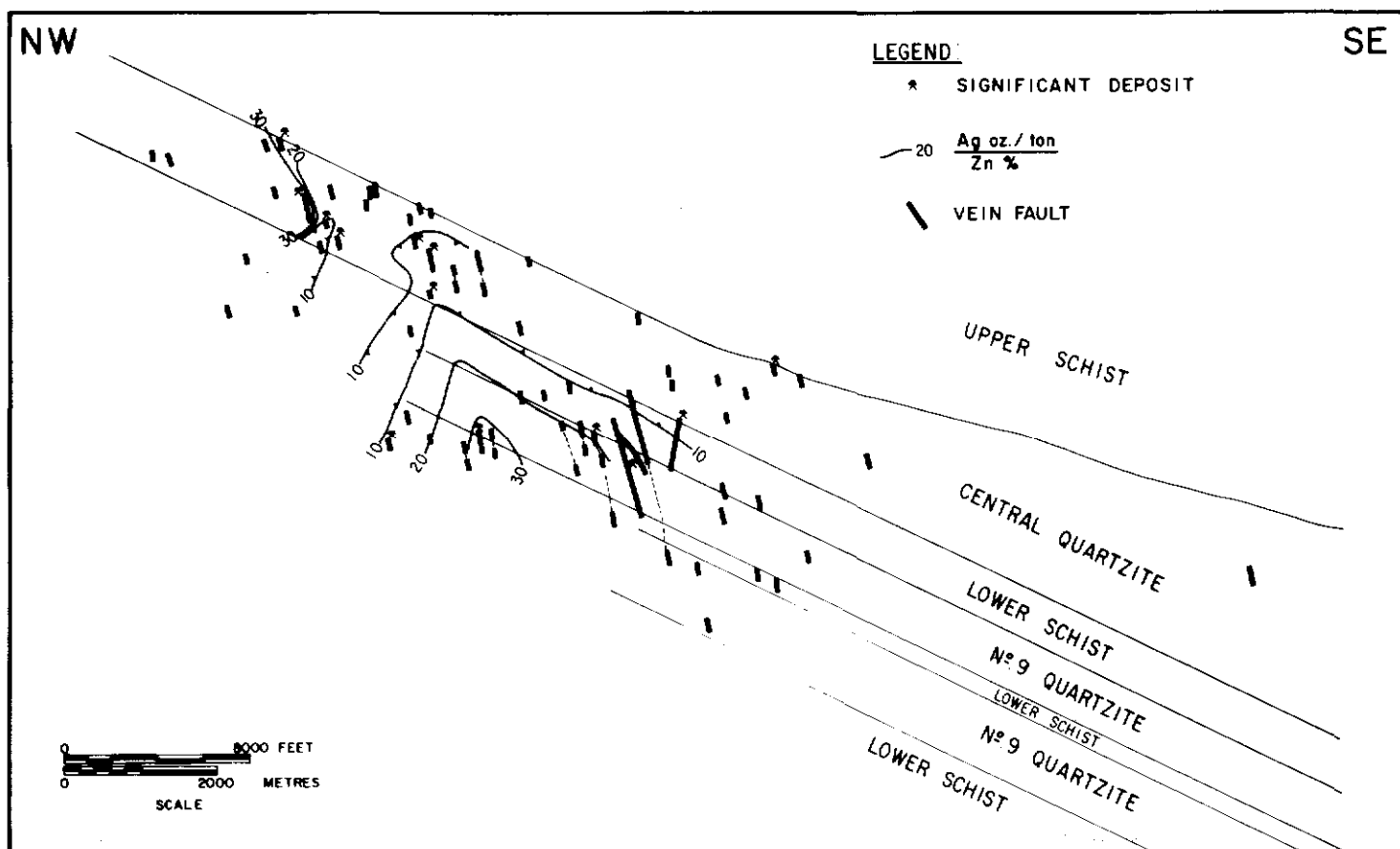


Figure 9. Approximate composite cross section reconstruction of the original fracture pattern showing Ag (oz/ton)/Zn (%) values between significant deposits in the Keno Hill district.

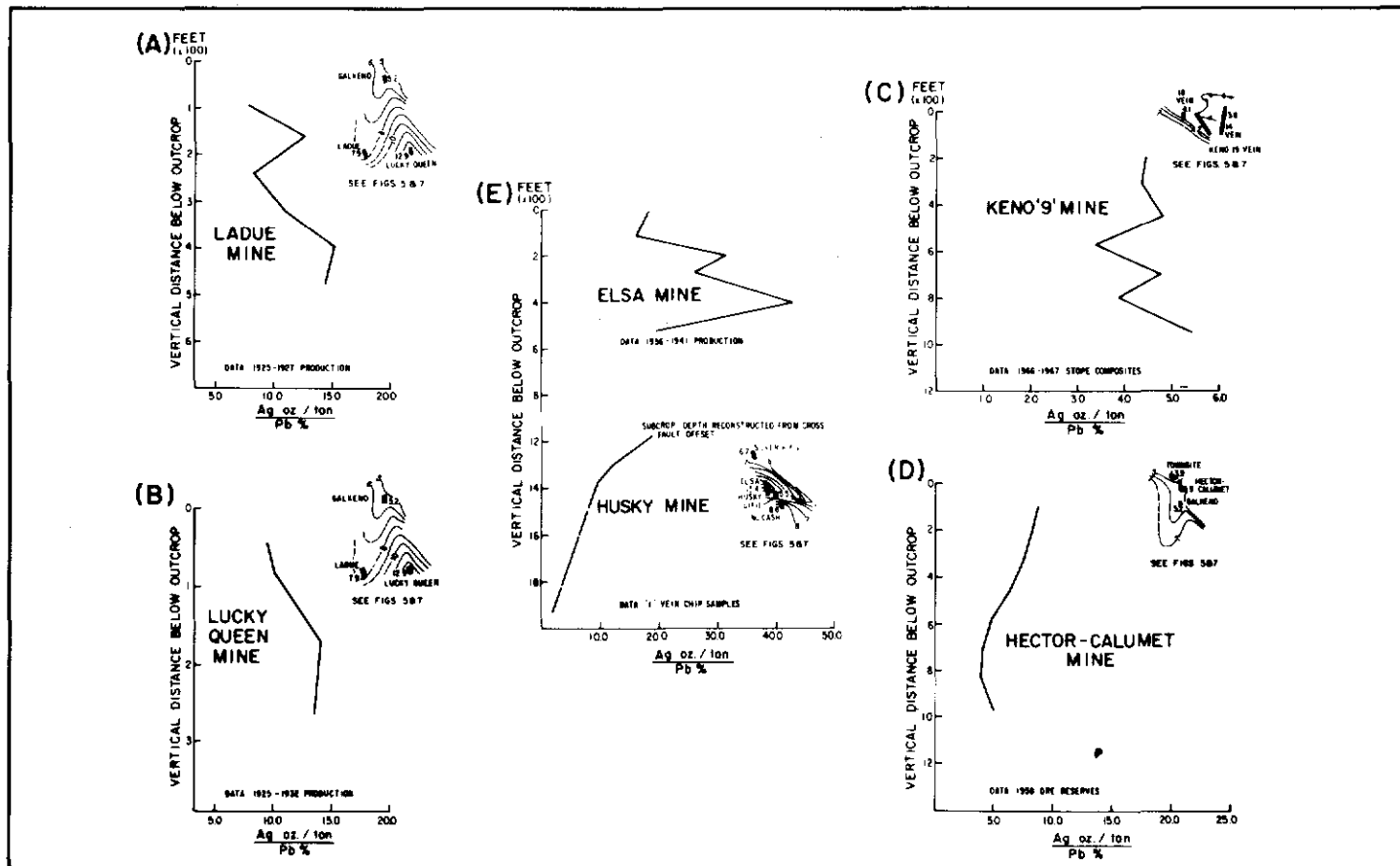


Figure 10. Level by level Ag/Pb metal-ratio profiles for (a) Ladue Mine (b) Lucky Queen Mine (c) Keno '9' Mine (d) Hector-Calumet Mine (e) Elsa-Husky Mines.

tions have been unable to scavenge sufficient metals. In contrast, high level deposits are the result of mineralizing solutions that have extracted metals from the entire Lower Schist section before deposition in structurally favorable host rocks. These latter fluids were silver-rich. Success in metal extraction may be related to the relative solubilities of silver and lead in the mineralizing solution. In early or "immature" low level deposits, "equal" amounts of silver and lead were extracted. As mineralizing solutions moved up-section to high level or "mature" positions, silver was being extracted from source rocks at a rate much greater than lead. Hence resulting high level mineralizing solutions were enriched in silver, relative to the low level deposits.

2). Alternatively, a horizon geochemically rich in silver may occur in a high stratigraphic position in the Lower Schist Unit. Low level mineralizing solutions have been unable to accumulate metals from this horizon and are, in effect, stranded. In contrast, mineralizing solutions that have reached high level stratigraphic positions have extracted and up-graded ore shoots accordingly. Blusson (1978) has postulated such a metal-rich source bed for the Keno Hill deposits, but, if present, it has yet to be found.

Sinclair et al. (1980) have demonstrated that the mineralizing solutions flowed through some of the vein faults in the district about 90 million years ago. Indicated Pb isotope model ages for carbonate-hosted lead-zinc mineralization in the Kathleen Lakes area (80 km northeast of Keno Hill) and the Keno Hill district are consistent with a common age of mineralization in the two districts (Godwin, Sinclair and Ryan, 1982). Because granitic stocks in the district have similar ages, Sinclair et al. (1981) suggest that vein mineralization is related to a hydrothermal system driven by thermal energy from these granitic intrusions. During the subsequent 90 million years, it would be possible to remove some 3000 m of the structural succession at normal rates of erosion. These observations suggest that parallelism of ore with the present surface in the district is fortuitous and is primarily a function of shallow explora-

tion and mining programs.

SUMMARY AND CONCLUSIONS

Parallelism of ore zones with the present surface topography is a recurring problem encountered in many Cordilleran vein deposits. In the Keno Hill district, records covering seventy years of mining provide an opportunity to examine this relationship. Productive vein faults in the Keno Hill district are associated with and are sub-parallel to the McQuesten anticline. An approximate cross sectional reconstruction of this pattern indicates that the south limb of the McQuesten anticline has been pervasively fractured and that the present erosional surface cuts obliquely through this fracture pattern. Production metal-ratios from deposits within these fractures show a definite zonation. Detailed metal-ratio studies within individual deposits support the suggestion that production metal-ratio zonation outlines the movement path of mineralizing solutions in the district. The deposits mined to date carry the signature of this hydrothermal system. The present surface, with about 1000 metres of relief, cuts across it, exposing deposits at different levels within it and at different positions in the stratigraphic succession. In the author's opinion, the data suggest that parallelism of the ore with the surface topography is fortuitous. Rather, some deposits have been eroded, others are exposed at the present surface and still others remain preserved, as yet undiscovered at depth.

ACKNOWLEDGEMENTS

This paper was presented in 1979 at the Seventh Geoscience Forum, Whitehorse, Y.T. when the writer was employed as Chief Geologist, United Keno Hill Mines Limited. The writer thanks the management of United Keno Hill Mines Limited for permission to publish. The manuscript benefited from review by A.J. Sinclair and L.H. Green. Funding for drafting work was provided by Billiton Canada Ltd.

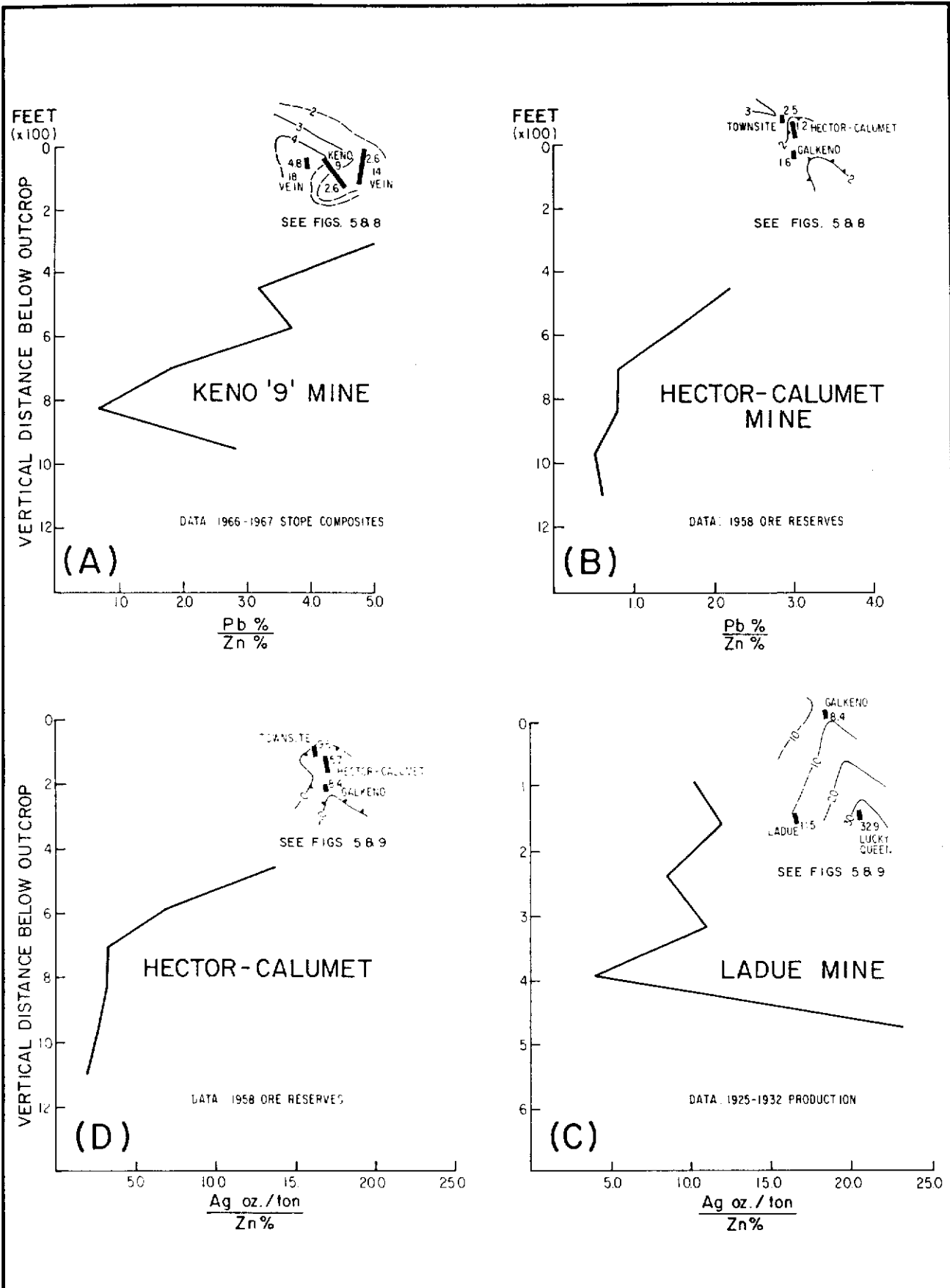


Figure 11. Level by level Pb/Zn metal-ratio profiles for (a) Keno '9' Mine (b) Hector-Calumet Mine. Level by level Ag/Zn metal-ratio profiles for (c) Ladue Mine (d) Hector-Calumet Mine.

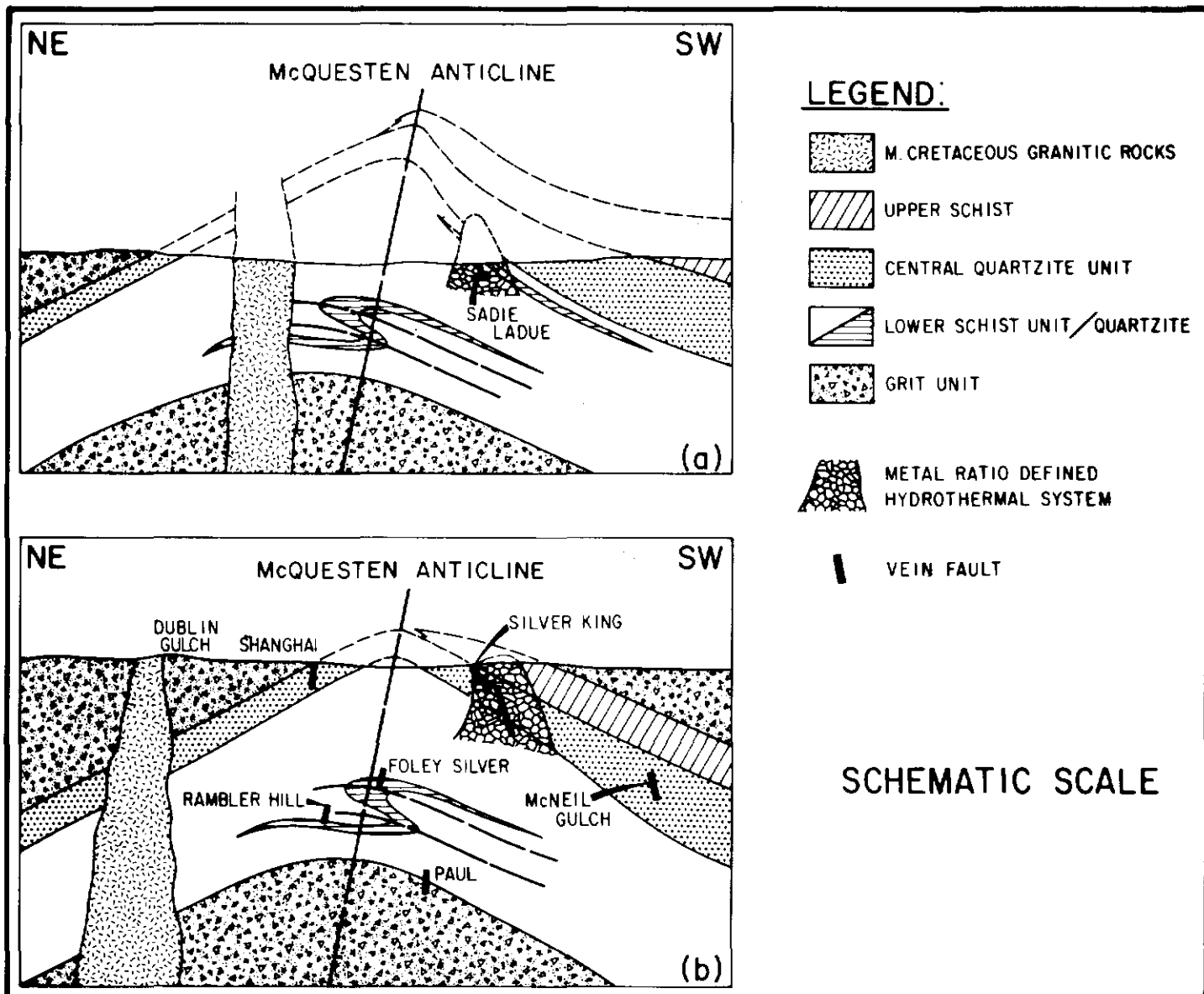


Figure 12. Regional cross sections normal to the McQuesten Anticline. Section (a) is at the eastern end of the district and contains the Ladue Mine. Section (b) is at the western end of the district and contains the Silver King Mine. See Figure 2 for the approximate location of section lines.

REFERENCES

- AHO, A.E. 1963. Silver in the Yukon; CIM Bulletin, Vol. 56, No. 611, p. 232-239.
- BLUSSON, S.L., 1978. Regional geologic setting of lead-zinc deposits in Selwyn Basin, Yukon; Current Research, Part A, Geol. Surv. Can., Paper 78-1A, p. 77-80.
- BOYLE, R.W. 1965. Geology, geochemistry and origin of the lead-zinc-silver deposits of the Keno Hill - Galena Hill area, Yukon Territory; Geol. Surv. Can., Bulletin 111, 302 p.
- FRANZEN, J.P., 1978. Cross fault ore control model; Unpublished United Keno Hill Mines Limited report, 27 p.
- FRANZEN, J.P. and VAN TASSELL, R.E., 1981. Grid rotary percussion drilling — a bedrock geochemical approach to silver vein exploration at United Keno Hill Mines Limited, Elsa, Yukon; Presented at Precious Metals in Geochemical Exploration Vancouver.
- GODWIN, C.I., SINCLAIR, A.J. and RYAN, B.D., 1982. Lead isotope models for the genesis of carbonate-hosted Zn-Pb, shale-hosted Ba-Zn-Pb and silver-rich deposits in the northern Canadian Cordillera; Economic Geology, Vol. 77, No. 1, p 82-94.
- GOODELL, P.C. and PETERSON, U., 1974. Julcani Mining District, Peru. A study of metal ratios; Economic Geology, Vol. 69, No. 3, p. 347-361.
- GREEN, L.H., 1971. Geology of Mayo Lake, Scougale Creek and McQuesten Lake map-areas, Yukon Territory; Geol. Surv. Can., Memoir 357, 72 p.

- McTAGGART, K.C., 1960. *The geology of Keno and Galena Hills, Yukon Territory*; Geol. Surv. Can., Bulletin 58, 37 p.
- SINCLAIR, A.J., TESSARI, O.J. and HARAKAL, J.E., 1980. Age of Ag-Pb-Zn mineralization, Keno Hill - Galena Hill area, Yukon Territory; Canadian Journal of Earth Sciences, Vol. 17, No. 8, p. 1100-1103.
- SINCLAIR, A.J. and TESSARI, O.J., 1981. Vein geochemistry, an exploration tool in the Keno Hill Camp, Yukon Territory, Canada; Journal of Geochemical Exploration, Vol. 14, No. 1, p. 1-24.
- THE STAFF, 1961. Current Operations of United Keno; CIM Bulletin, Vol. 54, No. 594, p. 722-739.
- TEMPELMAN-KLUIT, D.I., 1970. Stratigraphy and structure of the "Keno Hill Quartzite" in Tombstone River - Upper Klondike River map-areas; Geol. Surv. Can., Bulletin 180, 102 p.
- VAN TASSELL, R.E., 1969. Exploration by overburden drilling at Keno Hill Mines Limited; Quarterly of the School of Mines — International Exploration Symposium, Vol. 64, p. 457-478.

GEOLOGY OF THE PLATA-INCA GOLD-SILVER VEINS, YUKON

Grant Abbott
Exploration and Geological Services Division
Indian and Northern Affairs Canada
Whitehorse, Yukon

ABBOTT, J.G., 1986. Geology of the Plata-Inca property, Yukon; in Yukon Geology, Vol. 1; Exploration and Geological Services Division, Yukon, Indian and Northern Affairs Canada, p. 109-112.

INTRODUCTION

This note summarizes the geology of silver bearing veins on the Plata-Inca property, located in north-central Yukon (Lansing map sheet, 105 N), 160 km north of Ross River. It is based on a five day visit by the writer in August 1985, and assessment reports by W. Roberts. These assessment reports and others are also summarized by Morin et al. (1977, p. 111-114), Sinclair et al. (1975, p. 17, 18), and Sinclair and Gilbert (1975, p. 17-19). Dawson Eldorado Gold Explorations Ltd. kindly gave permission to visit the property. John James and Dave Knight were generous with their hospitality, time, and information.

In 1976, 1983, 1984, and 1985, a total of about 2800 tonnes of ore with grades ranging from 60-70% Pb, and 2995-9599 g/t Ag have been mined from the PLATA #1, #2, and #6 and INCA #7, #10, and #12 Veins. This included 90 tonnes averaging 70% Pb, and 7314.1 g/t Ag in 1976, 599 tonnes grading 62.5% Pb, and 4251.0 g/t Ag in 1983, 1270 tonnes grading 60% Pb, and 4241.0 g/t Ag in 1984, 816 tonnes grading 72% Pb and 3995.0 g/t Ag in 1985. Ore was excavated from surface pits, hand sorted, flown by helicopter to an airstrip 10 km to the south, ferried by fixed wing aircraft to the Canol Road either at Twin Creeks or Ross River, 100 and 160 km to the southeast and south, respectively, and then trucked to a smelter in Montana or to Vancouver for shipment to a smelter in France.

Reserves suitable for highgrading are almost exhausted, and the possibility of finding more is uncertain, although the potential for other reserves remains high. Exploration to date has included geochemical surveys, and bulldozer trenching and some diamond drilling on the main showings. In the winter of 1984-85, an adit about 205 m long was collared about 100 m below the Plata #2 vein. The vein was intersected, but barren.

GENERAL GEOLOGY

Latest (?) Proterozoic to Earliest Cambrian, and Devonian to (?) Mississippian strata, and a Cretaceous or Early Tertiary porphyry dyke underlie the Plata-Inca property (Fig. 1). The sedimentary rocks are part of the dominantly clastic assemblage that makes up the other part of the northern Cordilleran miogeocline (Abbott et al., in press). The dyke is probably part of the Selwyn Plutonic Suite (Anderson, 1983), a group of mid-Cretaceous, post-tectonic intrusions that underlie much of central Yukon.

Figure 2 shows the apparent stratigraphic succession. Although broad sedimentary units can be easily mapped, most small units cannot be traced more than a short distance, and appear to be disrupted by shearing and thrust faulting. Known thrust faults place Proterozoic strata on Devonian strata, and others are possible, but cannot be proven because few fossils have been recovered. True thicknesses are unknown, and the stratigraphy of the Devonian rocks, especially, is uncertain.

The Latest Proterozoic-Earliest Cambrian strata include four divisions that are grouped into unit ICps on the map. At least 200 m of massive, resistant quartz sandstone and quartz feldspar grit form the base of the unit in the southern thrust sheet, but are probably much thicker. Elsewhere in central Yukon, these grits form sequences several thousand meters thick (Abbott et al., in press). The coarse clastic rocks grade upwards into about 200 m of maroon, green, and buff weathering shale, in no consistent stratigraphic order. About 50 m of grey to buff weathering, thick bedded limestone, orange weathering sandy limestone, and grey quartz sandstone are intercalated with the varicoloured shales. Shales above and below the carbonate are identical, except those above contain the trace fossil "Oldhamia" (M. Cecile, pers. comm., 1985).

Unconformably overlying the Earliest Cambrian strata is a thick sequence of Devonian and Mississippian shale and chert. Two relatively thin members of blue weathering chert and siliceous shale (Dt 1 and 2) are apparently separated by a thick sequence of dull brown weathering grey shale and siltstone with minor sandstone and at least one discrete, thin interval of chert (Dt). South of the Plata thrust, white, light grey, and black chert (Dt) forms a discrete interval about 30 m thick. North of the Plata unit Dt comprises dark brown weathering dark siliceous argillite and chert at least 100 m thick.

The upper blue siliceous shale member (Dt2) contains a lens of finely laminated dark grey barite up to 4 m thick and at least 0.5 km long.

These rocks are part of the Earn Group, an assemblage of coarse and fine clastic strata of Middle Devonian to mid-Mississippian age that is widespread in central Yukon and northeastern British Columbia (Abbott et al., in press). The Earn Group probably represents an episode of rifting and wrench faulting that interrupted passive margin sedimentation in the Cordilleran miogeocline. Chert pebble conglomerate and other coarse clastic rocks that typify the assemblage elsewhere are absent on the property. Also, in most other areas, Silurian and/or Devonian strata are preserved beneath the Earn Group.

A pale, siliceous, quartz, feldspar porphyry dyke or sill as wide as 4 m and more than 2 km long intrudes Devonian shale in the northwest part of the map area. It may be discontinuous and is subparallel to cleavage and bedding. The dyke is undated, but is most likely mid-Cretaceous because that is the age of nearby intrusions of equigranular, biotite quartz monzonite that belong to the Selwyn Plutonic Suite. An Early Tertiary age is also possible, but no intrusions of that age are known to occur nearby.

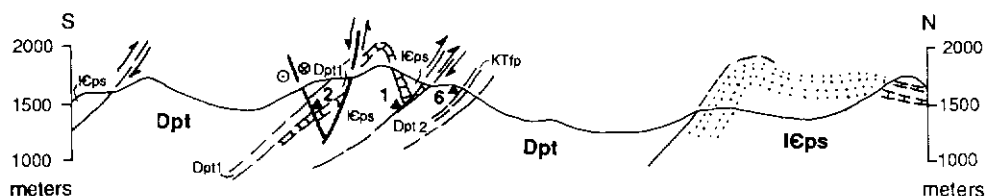
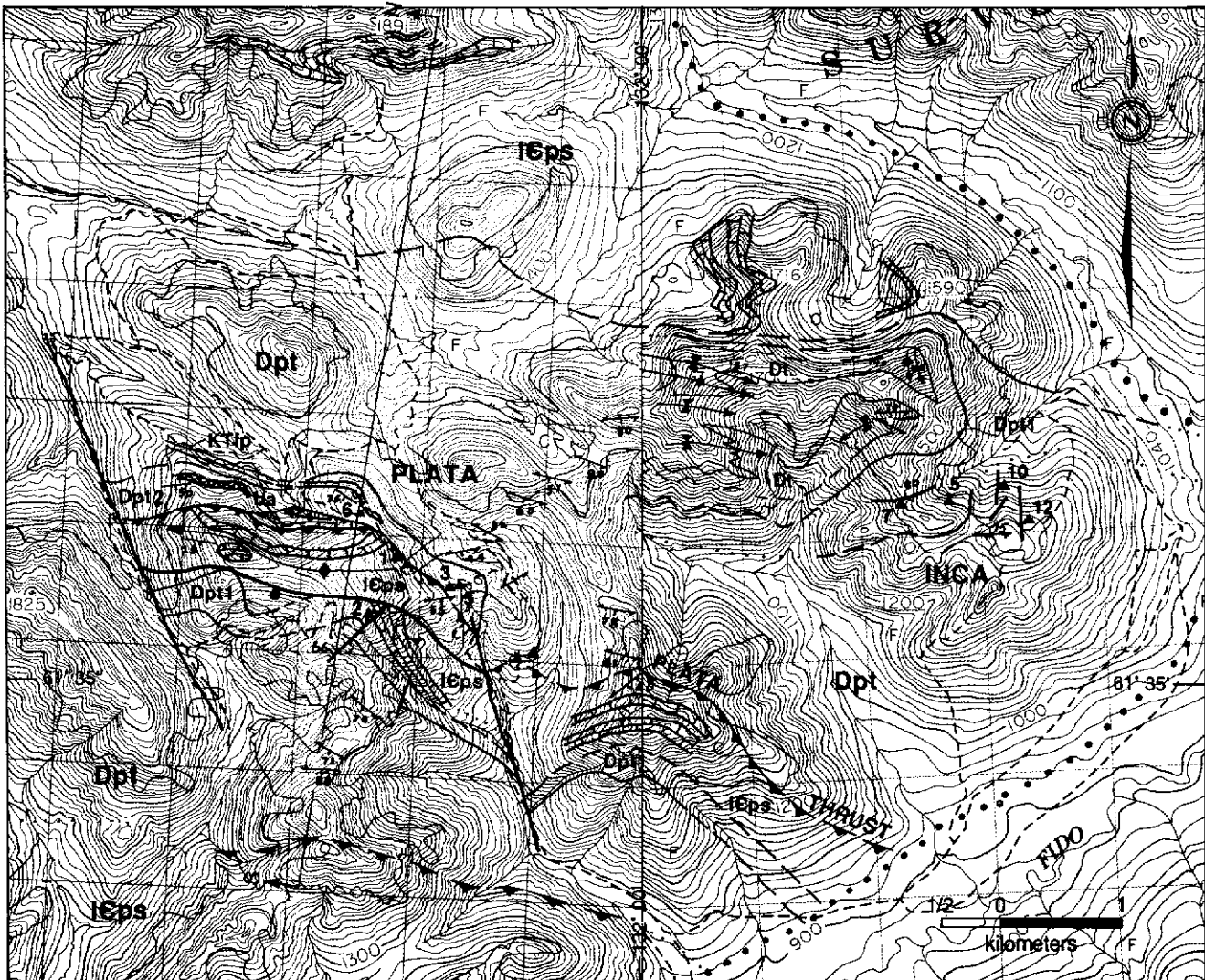
STRUCTURE

The sedimentary rocks are folded and cut by thrust faults and younger (?) normal faults. Only two thrusts have been recognized; one is here called the Plata thrust, the other is unnamed. The amount of displacement is unknown, but both place Latest Proterozoic strata onto Devonian-Mississippian strata and have a stratigraphic throw of about one kilometer. Both thrusts dip moderately south, at an angle slightly more shallow than well developed cleavage with a roughly parallel strike and a steep dip. Axial planar to the cleavage are large, tight folds. Other folds in the northeast corner of the property with steep southerly plunging axes may be younger.

The internal structure may be more complex than is apparent in Figure 1. Detailed sedimentary units cannot be traced for any distance and other thrusts may be present, but remain unrecognized because there are few markers.

Steep normal faults with a variety of orientations cut all other structures. These faults host most of the veins and are well exposed in the mine workings. Most appear to have displacements of a few meters or tens of meters, although no offsets have been measured. Roberts (1974a) reports NE-trending faults with left-lateral offset, NE-trending faults with right lateral offset, and N-trending joints. The E-trending faults shown on Figure 1 are not reported by Roberts and show normal displacement.

Roberts (1974 a, b) suggested that the NE- and NW-trending faults define a conjugate set, which together with subsidiary N-trending joints, are related to the E-trending thrusts and folds. The evidence allows, but does not prove this possibility, and the faults could also be younger than, and unrelated to the thrusts. The writer prefers the second alternative because the faults are sharp, well-defined, "brittle" features that sharply cut both the thrusts and the more ductile penetrative fabric which is likely related to



EXPLANATION

CRETACEOUS

KTqfp Aphanitic, quartz feldspar porphyry.

DEVONIAN

Dpt, Brown weathering shale, sandstone, and chert (includes Dt)

Dpt1,2 Blue weathering shale and chert

Dt Brown weathering chert and shale

LOWER CAMBRIAN AND (?) PROTEROZOIC

Icps Maroon, green, and buff weathering shale; resistant, dark grey weathering quartz sandstone and grit

Thick bedded grey limestone

- | | |
|--|--|
| Geological contact; defined, approx..... | |
| Fault; sense of movement unknown..... | |
| Normal fault..... | |
| Thrust fault..... | |
| Anticline, syncline..... | |
| Bedding..... | |
| Foliation; inclined, vertical..... | |
| Limit of mapping..... | |
| Vein..... | |

Figure 1. Geology of the Plata-Inca property.

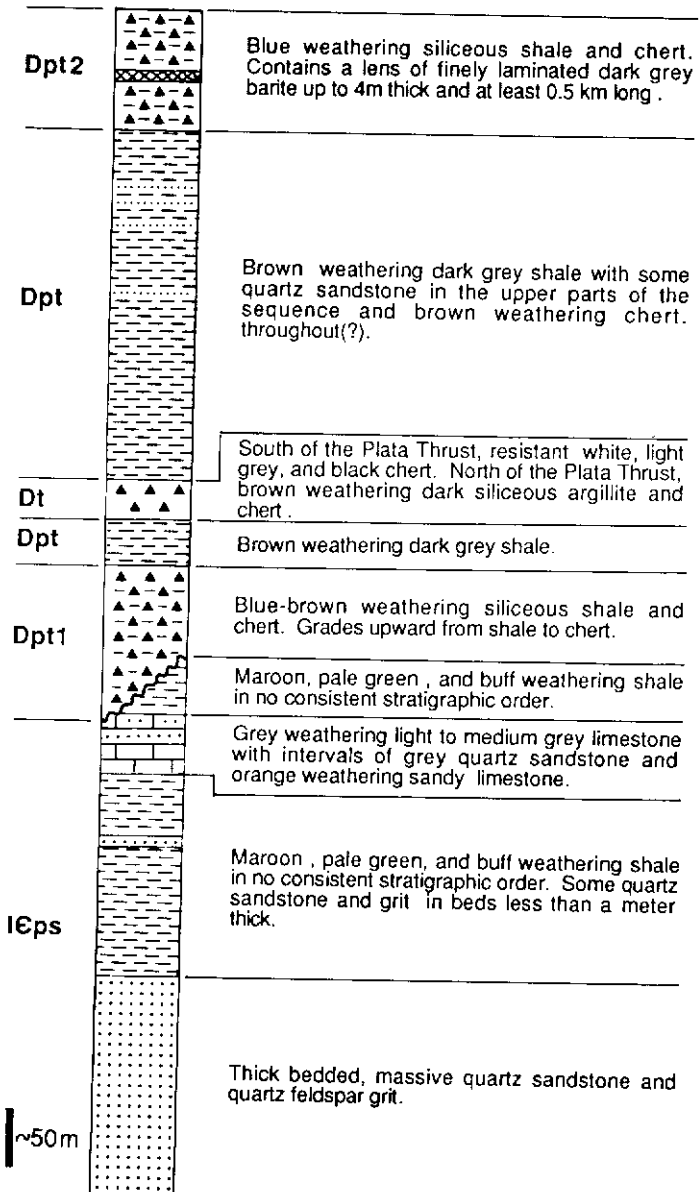


Figure 2. Composite stratigraphic column for the Plata-Inca property. Thicknesses are estimated, and thrust faults may repeat parts of the sequence.

the thrusts. The presence of E-trending normal faults suggests that the pattern of normal faulting is more complex than that proposed by Roberts.

VEINS

The veins form two clusters about 5 km apart. Thirty one are reported in the Plata area and thirteen in the Inca area. The ten most significant are listed in Table 1. Most veins are along strong, well defined normal faults, but the Plata #3 and #4 veins appear to be in the Plata thrust (Roberts, 1974a). Most are small pods less than 0.3 m across, but a few reach widths of 1.5 m.

Most veins contain galena, sphalerite, and tetrahedrite in a gangue of siderite and quartz with minor barite and calcite. Silver-lead ratios determined from the grade of ore shipments range from 55.5 g/t Ag: 1% Pb to 137.1 g/t Ag: 1% Pb. Unlike the rest, the Plata #3 and #4 veins contain arsenopyrite and pyrite, with minor

galena, tetrahedrite, sphalerite, and boulangerite in a quartz gangue. These veins may be an attractive exploration target because they contain gold, and appear to be more consistent laterally than the galena-and sphalerite-rich veins. Some veins are cut by parallel faults and contain brecciated and cemented quartz gangue, which suggests that faulting was active during mineralization.

Systematic zonation in individual veins is not apparent. Changes from galena-rich zones to sphalerite-rich zones or to sulphide-poor zones appear to be erratic and to occur over distances of a few meters. It is unlikely that these changes reflect a fundamental zonation of the whole vein system. Therefore the possibility of finding galena-rich zones below or laterally to others should not be discounted. For example, the #2 vein is barren where intersected underground, but there is no evidence to discount the possibility that a galena-rich zone may be nearby, in any direction. The veins display no preference for one type of host rock, and occur in shale, chert, quartz sandstone, and dolomite. There is little indication of the presence of mantos along shale-carbonate contacts like those recently recognized near Ketza River, Mt. Hundere, and at Midway, although this possibility cannot be discounted. The #2 zone appears to widen slightly along the contact between Early Cambrian sandstone and dolomite, and overlying Devonian shale with the widest part of the vein in shale just above the contact. Roberts (1974a) reports that galena and sphalerite replace limestone in a few places.

The #3 and #4 veins, however, are consistently rich in pyrite and arsenopyrite, and are separate from other veins. In the Ketza-Seagull and Keno Hill Districts (Abbott, this volume; Lynch, this volume), this mineral assemblage has been interpreted to be nearer to a heat source than nearby galena- and sphalerite-rich veins. This would suggest that fluids migrated from the southeast to northwest, in the Plata area. The porphyry dyke at the north end of the Plata area is closer to galena- and sphalerite-rich veins than to the "hotter" mineral assemblages, and may only suggest the presence of a nearby intrusion, but not have been directly involved in mineralization.

DISCUSSION

The age and origin of the veins in the Plata-Inca camp is unclear. They are most likely related to a buried intrusion, although the only evidence for one is the small porphyry dyke at the northwest end of the property. There are no other intrusions nearby, but the deposits are at the northern margin of the belt of mid-Cretaceous intrusions that belong to the Selwyn Plutonic Suite (Anderson, 1983). Roberts (1974a) reasoned that the thrusts, normal faults, and veins are coeval and genetically related because normal faults form a conjugate set that indicate a direction of maximum stress parallel to the direction of thrusting, and the #3 and #4 veins are in the Plata thrust and are sheared. However, regional deformation and metamorphism in the Selwyn Fold Belt predates the emplacement of mid-Cretaceous plutons. If Roberts is right, either the veins are older than, and unrelated to mid-Cretaceous or younger intrusions, or thrusting is mid-Cretaceous or younger.

The writer prefers the alternative possibility that the thrusts are older than, and unrelated to the normal faults and veins. Near the #3 and #4 veins, an east-trending normal fault, overlooked by Roberts, strikes parallel to and intersects the Plata thrust. Its orientation is incompatible with the conjugate set proposed by Roberts. The fault strikes parallel to the Plata thrust, suggesting the possibility of late normal movement on the Plata thrust that may be related to mineralization. If the normal faults are younger than the thrusts, they might be related to a buried Cretaceous intrusion, although there is no indication of doming or uplift.

REFERENCES

- ABBOTT, J.C., GORDEY, S.P., and TEMPELMAN-KLUIT, D.J., in press. Setting of stratiform, sediment-hosted lead, zinc deposits in Yukon and northeastern British Columbia; in Morin, J.A., ed. *Mineral Deposits of Northern Cordillera*, C.I.M. Spec. Vol.

- ANDERSON, R.G., 1983. Selwyn plutonic suite and its relationship to tungsten skarn mineralization, south-eastern Yukon and District of Mackenzie; in *Current Research, Part A, Geol. Surv. Can.*, Paper 83-1A, p. 151-163.
- MORIN, J.A., 1977. Mineral industry report 1976; Yukon Territory; D.I.A.N.D., EGS 1977-1, 264 p.
- ROBERTS, W., 1974a. Geochemical, geological, cat trenching, and engineering evaluation report on the Plata Group; D.I.A.N.D. assessment report #061092, 25 p.
- ROBERTS, W., 1974b. Geochemical, geological, cat trenching, and engineering evaluation report on the Plata Group; D.I.A.N.D. assessment report #061152.
- SINCLAIR, W.D., and GILBERT, G.W., 1975. Mineral Industry report 1976, Yukon Territory. D.I.A.N.D., EGS 1975-7, 177 p.
- SINCLAIR, W.D., MALONEY, J.M., and CRAIG, D.B., 1975. Mineral industry report 1974, Yukon Territory. D.I.A.N.D., EGS 1975-9, 216 p.

TABLE 1

NAME	DESCRIPTION
PLATA #1	A lens about 15 m long, 0.6 - 1.2 m wide, and 6 m deep, contained massive galena and tetrahedrite. Only float boulders of manganeseiferous siderite containing coarse blobs of galena and sphalerite remain.
PLATA #2	A lens about 55 m long, 0.6 - 1.5 m wide, and an unknown depth was in a fault striking 30° and dipping 55°-70°NW. Remnants of the veins are up to a meter wide and consist of galena and sphalerite in a siderite matrix. The ratio of sulphides to gangue varies widely, and sphalerite and galena tend to be separate. The vein appears to widen along the contact between Lower Cambrian sandstones and quartzite, and overlying Devonian shale. An adit driven 100 m below the surface exposures intersected the same fault where it contains siderite with only a little sphalerite and galena. There the vein is in Lower Cambrian strata.
PLATA #3	An intensely shattered quartz vein up to 1.5 m wide and at least 275 m long in (?) the Plata thrust and dips moderately south. The vein contains banded pyrite and arsenopyrite with minor galena, tetrahedrite, sphalerite, and boulangerite, and assayed 67.1 g/t Ag and 20.5 g/t Au.
PLATA #4	A quartz vein 0.15 - 1.5 m thick containing banded pyrite and arsenopyrite with minor galena, tetrahedrite, sphalerite, and boulangerite in (?) the Plata thrust. It is exposed for a strike length of about 100 m and dips moderately south. Assays range from 6.8 - 4070.1 g/t Ag and 3.4 - 8.5 g/t Au. Not mined.
PLATA #5	A narrow fault zone up to 0.76 m wide contains fragments of massive galena, with tetrahedrite, in a silver-rich gouge. Siderite boulders are nearby.
PLATA #6	Massive galena and tetrahedrite float, and oxidized siderite containing galena occur near a graphic fault zone striking north and dipping 65°W. The vein terminates to the north against a quartz feldspar porphyry dyke. Only a single outcrop about 1m ² is preserved.
INCA #5	Oxidized sulphide float is in a large gossan. The source has not been found.
INCA #7	Three subparallel faults that trend from 75 - 110° and dip 75 - 80°N form a zone 15 m wide. Most of a lens of massive galena at least 21 m long, 11 m deep, and 0.6 - 1.2 m wide was mined, but 50 m to the east, on the same structure, was also mined. The remnant of this zone is a single fault which contains a galena-bearing quartz vein about 0.3 m wide.
INCA #10	Veins are in two subparallel fault zones about 25 m apart. One strikes 28 - 45°NE and dips steeply northwest. The other strikes about 0° and dips steeply west. The first vein is mined out and now consists of a diffuse zone, 0.5 - 5 m wide, of brecciated and faulted quartz veins that contain a little massive galena and tetrahedrite. The second zone contains a pod of massive galena and tetrahedrite up to 0.5 m wide. A splay connecting the two faults also contains another pod of massive galena up to 30 cm wide.
INCA #12	A lens of massive, coarse-grained galena and tetrahedrite at least 40 m long, 29 m deep, and 0.3 - 0.9 m wide was in a fault striking 25° and dipping 60°W.

TIN AND TUNGSTEN VEINS AND SKARNS IN THE McQUESTEN RIVER AREA, CENTRAL YUKON

D.S. Emond
Exploration and Geological Services Division
Indian and Northern Affairs Canada
Whitehorse, Yukon

EMOND, D.S., 1986. Tin and tungsten veins and skarns in the McQuesten River area, central Yukon: in Yukon Geology, Vol. 1; Exploration and Geological Services Division, Yukon, Indian and Northern Affairs Canada, p. 113-118.

ABSTRACT

Tin and tungsten veins and skarns in the McQuesten River area occur in the contact zones of Cretaceous feldspar-porphyritic biotite granite stocks, plugs, and dykes. Most occurrences are located in the exocontact of plutons, in the brittle metasedimentary country rocks known as the Grit Unit of Upper Precambrian to Lower Cambrian age. Cassiterite (+/- silver) occurs in chlorite-, tourmaline-, and quartz-matrix breccias with fragments of quartzite, schist, and vein material of chlorite, tourmaline or quartz; in thin veinlets with little gangue of tourmaline, K-feldspar, or muscovite; and in actinolite-quartz-epidote-axinite-garnet skarn (+/- pyrrhotite, pyrite and chalcopyrite). Scheelite is mainly disseminated in fine-grained, diopside-quartz, or actinolite-quartz (+/- pyrrhotite) exoskarn which is interlayered with white wollastonite-quartz skarn. Scheelite (+/- molybdenite) also occurs in sheeted quartz (+/- feldspar) veins in both the endo- and exocontact regions of two feldspar-porphyritic granite stocks. Rarely do tin and tungsten occur together, however some low tin values are found in some tungsten occurrences; and vice versa. Tungsten occurs closer to the associated intrusion than tin.

INTRODUCTION

The McQuesten River is located about 30 km northwest of Mayo, traversing an area approximately 65 x 40 km containing occurrences of tin and tungsten (Fig. 1). Aside from exploration companies' assessment reports, very little is documented on the nature of this mineralization. The purpose of this report is to concisely describe and compare the tin and tungsten occurrences and give some guidance in further exploration. This study is based on property visits carried out in July and August, 1985 and a review of assessment reports.

History and Previous Work

Placer gold was discovered in the McQuesten and Mayo areas soon after the start of the Klondike gold rush, and mining still takes place mainly on Higher, Johnson, Duncan and Haggart Creeks (Bostock, 1957). Placer scheelite was also recovered from 1976 to 1978 at Dublin Gulch, on Haggart Creek (Debicki, 1983). Abundant placer cassiterite is also noted to occur in this creek (Mulligan, 1974).

A few kilometres northeast of the study area lies the Keno Hill-Galena Hill district where silver-lead veins cutting quartzite have been mined intermittently since the early 1900's (Tempelman-Kluit, 1970; Boyle, 1965; Franzen, 1986, Lynch, 1986, and Watson, 1986 - all this volume).

The McQuesten River area has been prospected for lode deposits since the early 1900's. Lode gold was soon found at Dublin Gulch (MacLean, 1914). Lode tin was found at Dublin Gulch in 1943, and tungsten, at Scheelite Dome in 1945 (Mulligan, 1974). Some work was done in the area in the 1960's and early 1970's, but more intensive exploration for tin and tungsten was carried out from 1978 to 1982, mainly by CCH Resources, INCO and Billiton Canada Ltd. of the Cortin Joint Venture, Cominco Ltd. and Canada Tungsten Mining Corporation. Reconnaissance stream sediment geochemistry, followed by more detailed geochemistry and geological mapping were the exploration methods employed. SCHEELITE DOME, OLIVER CREEK (EPD), and SUNSHINE CREEK (SP) are among the few properties that were trenched and drilled.

A detailed report is available on the TIN DOME (SHEPPARD) tin-bearing vein (and breccia) at Dublin Gulch by Thompson (1945). Recently, two properties in the Mayo and McQuesten area have been the subject of Master of Science theses. One thesis is on the KALZAS tungsten-tin-molybdenum porphyry located approximately 70 km southeast of Mayo, by Lynch (summarized in Lynch, 1985), the other is on the OLIVER CREEK (EPD) tin-silver-bearing breccia/vein deposit, by the author (Emond, 1985), which followed up a less detailed BSc thesis by Noble (1980).

REGIONAL GEOLOGY

The McQuesten area is in the northwestern Selwyn Basin and is underlain mainly by Upper Precambrian to Lower Cambrian metasedimentary rocks of the 'Grit Unit' (Fritz et al., 1983) (Fig. 2). To the north, these rocks are thrust on to by Ordovician to Devonian Road River Formation sedimentary rocks. Numerous small, high level, acid intrusions and some coeval volcanic rocks, in the southeast part of the area are Cretaceous (83-103 Ma age for

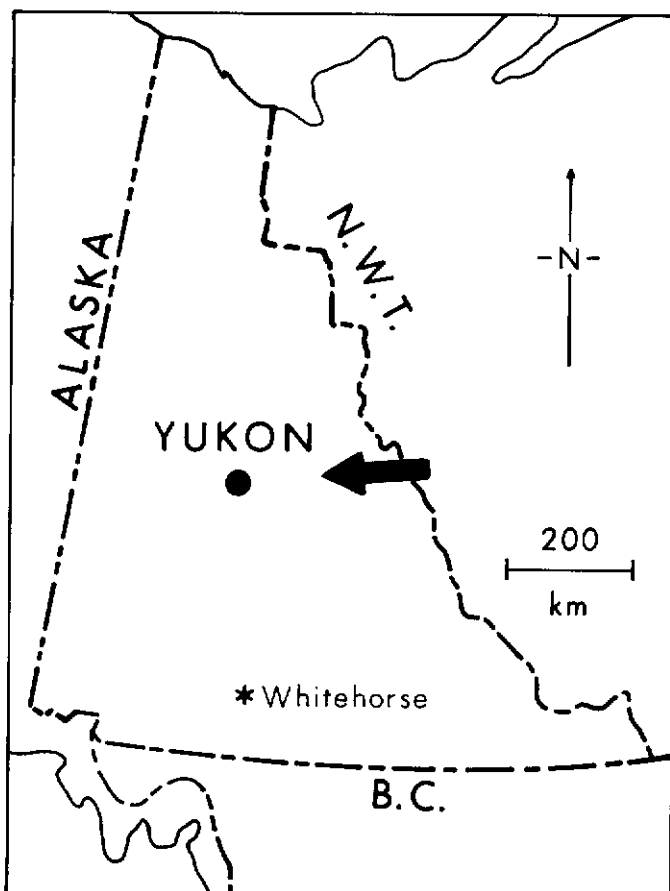


Figure 1. Location map of McQuesten River area.

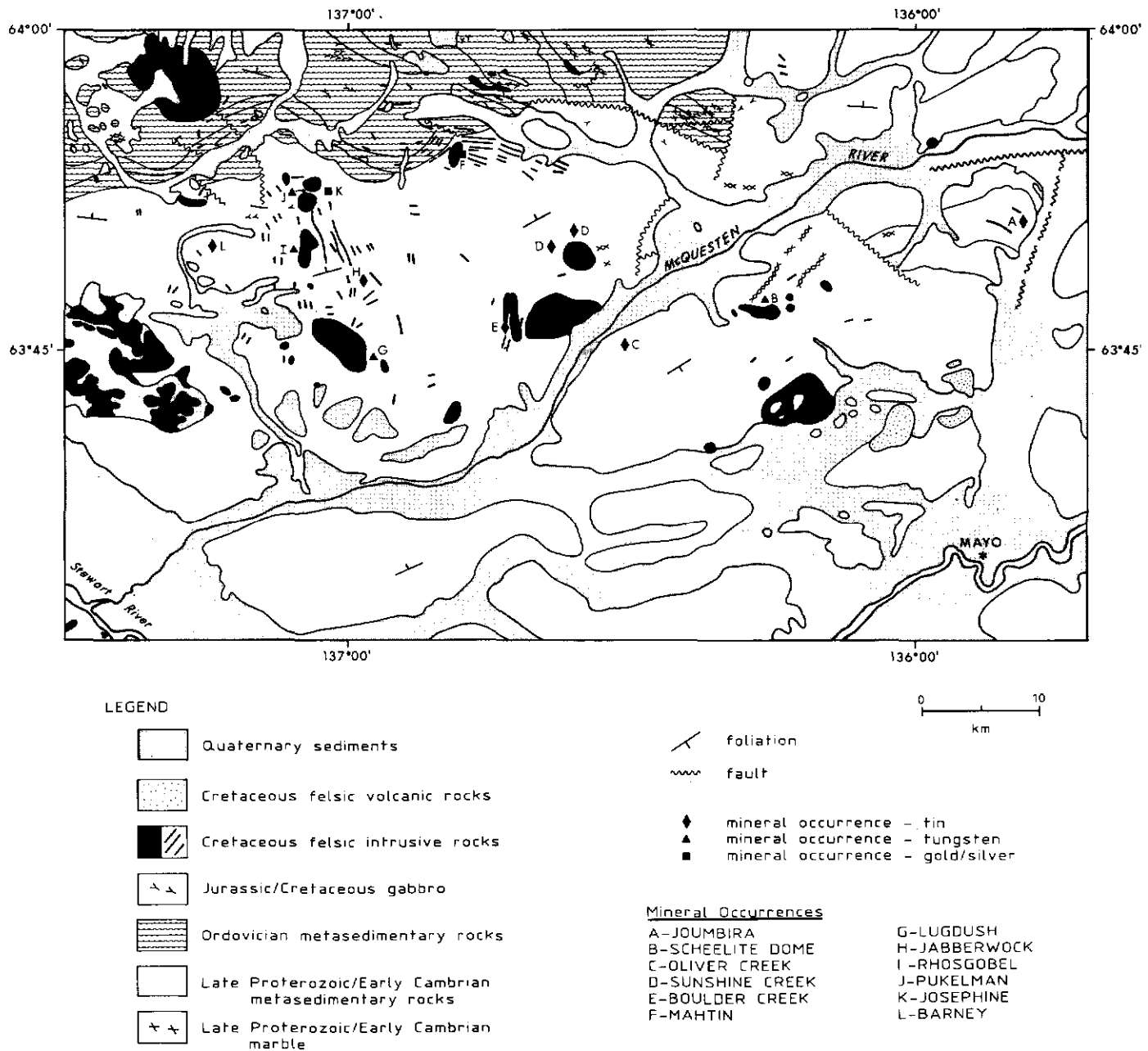


Figure 2. Geology and mineral occurrence map of the McQuesten River area.

granites, K/Ar on biotite, Stevens et al., 1982a; 89 Ma age for volcanic flow rock, K/Ar on biotite, Stevens et al., 1982b).

GEOLOGY

The Grit Unit is a homogenous, thick, blocky grey-weathering unit consisting of highly deformed, greenschist facies metamorphosed quartzite, quartz-mica schist and phyllite with minor intercalated limestone, dolomite and amphibolite. A large NE-trending anticline, the "McQuesten Anticline" (Mulligan, 1974), traverses through the area, just north of the McQuesten River. Foliation dips shallowly northwest to the north, and shallowly southeast to the south of the anticline.

Cretaceous intrusions vary from syenite in the north to granite and quartz monzonite in the south and centre. Most are stocks, plugs and dykes; the latter are locally sheeted. These intrusive rocks are grey- to orange-weathering and predominantly feldspar-, or feldspar-quartz porphyries. Feldspar phenocrysts are up to 10 cm in length, but more commonly 0.5 to 2 cm. Biotite is the dominant mafic mineral, and commonly makes up 5 to 10% of the rock. Hornblende occurs with biotite in the syenite. Creamy

weathering aplite dykes are found in the contact zones of many stocks and plugs.

Vertically columnar-jointed, grey-weathering, porphyritic hornblende rhyolite flows located just southeast of Mayo Lake, likely represent a down-faulted remnant of flows coeval with the Cretaceous intrusions.

STYLES OF TIN AND TUNGSTEN MINERALIZATION

Characteristics of the mineral occurrences are summarized in Table 1 and properties are located on the map in Figure 2. Veins, breccia-veins, sheeted veins and skarns containing tin and tungsten are near the margins of plutons and dykes in both country rocks (exocontact), and in intrusive rocks (endocontact).

Veins

Veins bearing tin are on the JOUMBIRA (on Mt. Haldane) and the JABBERWOCK (central West Ridge) properties, in the exocontact of dykes and/or stocks. They are mostly controlled by joints in the country rock, and thus tend to occur in steeply-dipping to vertical sets. The veins are generally less than 5 mm

TABLE 1
Description of tin and tungsten occurrences in the McQuesten River area.

IDENTITY	PROPERTY NAME (CLAIMS)	N.T.S.	STYLE OF MINERALIZATION	HOST ROCK	ASSOCIATED INTRUSION	DESCRIPTION
A	JOUMBIRA	105 N 13	1) VEIN SN 2) VEIN SN 3) VEIN AG	1) QZIT (GRIT U.) 2) PPQZ DYKE 3) QZIT (GRIT U.)	SMALL PPQF GRANITE STOCK, SEVERAL PPQF & PPQZ DYKES	1) TO (+CT) IN NEAR VERTICAL JOINTS, QZ-TO VEINS 2) QZ-TO (+CT) VEINLETS & TO IN JOINTS 3) QZ-TO (+ASP-GL-SL) & QZ-MU VEINS
B	SCHEELITE DOME (SUN, GLOW)	115 P 16	SKARN W, AU	QZIT, SHST, LMST (GRIT U.)	PPFS - BI GRANO- DIORITE STOCK	ACT-QZ-PR-SCH SKARN IN STEEPLY DIPPING 4 M THICK LENSE; WOLL-QZ-TREM SKARN; QZ-MU-TO VEINS
C	OLIVER CREEK (EPD)	115 P 9,10, 15,16	1) BRECCIA SN, AG 2) SKARN SN, BM (MINOR)	QZIT, SHST (GRIT U.)	PPFS - BI GRANITE PLUG	1) CL (+CT-AG-BM) - MATRIX & TO (+CT-AG-BM) - MATRIX BRECCIAS 2) ACT-CL-PR (+CT) SKARN
D	SUNSHINE CREEK (SP, A)	115 P 15	1) BRECCIA SN, AG 2) BRECCIA AG	QZIT, SHST (GRIT U.)	1,2) PPFS GRANITE STOCK PPQF DYKE	1) QZ MATRIX BRECCIA, TO MATRIX BRECCIA, ABUNDANT FE STAIN 2) SILICA-RICH MATRIX BRECCIA
E	BOULDER CREEK (SNARK, TEE)	115 P 15	1) SKARN (SN?) 2) SKARN SN 3) BRECCIA PB, ZN, AG	QZIT, SHST (GRIT U.)	1) LARGE PPFS GRANITE STOCK 2) SMALL PPFS GRANITE STOCK, PPFS DYKE 3) SMALL PPFS GRANITE STOCK	1) GT-ACT-EP-AZ (+CT?) SKARN 2) ACT-EP-AX-QZ (+GT-PR-PY-CP- CT-SL) SKARN 3) QZ MATRIX BRECCIA (+GL-SL?) ABUNDANT FE AND MN STAIN; ALSO QZ STOCKWORK NEAR MARGIN OF GRANITE STOCK
F	NAHTIN	115 P 15	1) BRECCIA AG 2) VEIN AG 3) SKARN (AG?)	1,2) PPFS GRANITE STOCK 3) LMST, CHRT, SHAL (ROAD (RIVER FM)	PPFS - BI GRANITE STOCK, PPFS SYENITE DYKES	1) TO-ASP (+PY) MATRIX BRECCIA CUTTING QZ VEIN (CENTRAL STOCK AREA) 2) QZ-ASP (+SCOR) VEIN, STEEP DIPPING (MARGIN OF STOCK) 3) DIOP-QZ-CC-ASP (+PY-PR) SKARN
G	LUGDUSH (SPUD)	115 P 10,15	1) SKARN W 2) VEIN PB, AG (FLOAT)	QZIT, SHST, LMST (GRIT U.)	LARGE PPQF - BI GRANITE STOCK	1) DIOP-QZ-CC (+SCH) SKARN, WOLL-QZ SKARN 2) QZ-GL VEIN MATERIAL
H	JABBERWOCK	115 P 15	1) VEIN SN 2) BRECCIA SN, AG 3) VEIN SN	QZIT, SHST (GRIT U.)	PPFS DYKES	1) CT (+KFS) IN NEAR VERTICAL JOINTS 2) TO MATRIX BRECCIA (+CT IN VUGS), TOURMALINITE 3) CT IN VUGGY QZ-LI VEINS
I	RHOSGOBEL	115 P 14	1) SKARN W 2) VEIN W, OR SHEETED VEIN W 3) VEIN AU (+AG)	1) QZIT, SHST, PPFS - BI LMST (GRIT U.) 2) PPFS GRANITE 3) HNPLS	PPFS - BI GRANITE STOCK	1) DIOP-QZ-PLAG-SCH SKARN, WOLL-QZ-PLAG SKARN 2) QZ (+SCH?) VEINS 3) QZ-ASP VEINS
J	PUKELMAN	115 P 14	1) SHEETED VEINS W, MO (ENDOCON- TACT) 2) SHEETED VEINS W (EXOCONTACT) 3) VEIN AU (EXOCONTACT)	1) PPFS GRANITE 2) HNPLS 3) QZIT, SHST (GRIT U.)	PPFS - BI GRANITE STOCK	1) QZ-KFS (+SCH-MO-PY) VEINS 2) QZ-KFS-SCH VEINS, VEINLETS 3) QZ-ASP (+GL) VEINS
K	JOSEPHINE	115 P 14	VEIN AU	QZIT, SHST (GRIT U.)	GRANODIORITE STOCK	QZ-ASP VEINS
L	BARNEY	115 P 14	BRECCIA (SN?)	QZIT, SHST (GRIT U.)	PPQZ DYKE, PPFS - BI GRANITE STOCK	ROCK FLOUR MATRIX BRECCIA, FE STAINED (+CT?) MATRIX; QZ-MU GREISEN VEINS

ABBREVIATIONS:

QZIT	quartzite	PPFO	feldspar-quartz	PY	pyrite	SCH	scHEELITE
SHST	schist		porphyry	PR	pyrrhotite	EP	epidote
LMST	limestone	QZ	quartz	CP	chalcopyrite	AX	axinite
HNPLS	hornfels	TO	tourmaline	MO	molybdenite	WOLL	wollastonite
CHRT	chert	CL	chlorite	LI	limonite	GT	garnet
SHAL	shale	MU	muscovite	GL	galena	PLAG	plagioclase
PPQZ	quartz porphyry	CC	calcite	SL	sphalerite	KFS	K feldspar
PPFS	feldspar porphyry	DIOP	diopside	ASP	arsenopyrite		
PPQF	quartz-feldspar	ACT	actinolite	CT	cassiterite		
	porphyry	BI	biotite	BM	base metals		

wide with euhedrally-terminated cassiterite crystals, and little gangue. Gangue minerals consist of radiating tourmaline aggregates on joint surfaces on JOUMBIRA; and euhedrally terminated K-feldspar crystals on joints, fractures, and in vugs on JABBERWOCK.

A cassiterite-bearing quartz-tourmaline-chlorite-limonite vein occurs at the SHEPPARD (TIN DOME) occurrence, located 20 km north of JOUMBIRA, at Dublin Gulch (Mulligan, 1974). This vein is in the exocontact of a granodiorite stock and is noted to have associated tourmaline-matrix breccias and tourmalinized metasedimentary rocks.

Some tin-bearing veins also occur on the OLIVER CREEK (EPD) property, but most are extensions of breccias. These veins are more gangue rich, with chlorite, or tourmaline gangue.

Tungsten-bearing veins are separate from those with tin, located mainly on the RHOSGOBEL and PUKELMAN properties (at the north end of West Ridge). Sheeted quartz-scheelite (+/- K-feldspar) veins occur in both the endo- and exocontacts of the feldspar porphyry granite stocks. They occur in a vertical to steeply-dipping set of cooling joints which is continuous in the stock and surrounding country rock. The veins are mostly 0.5 to 1.5 cm thick, but reach 7 cm in the main showing, the PUKELMAN occurrence, where the veins cut hornfels. As much as 10% scheelite occurs in the fine grained quartz veins. Veining occurs in the Pukelman stock (west of the occurrence), and in the metasedimentary rocks between the Pukelman and Josephine stock (east of the occurrence). In the Pukelman stock, veining is most dense in the central part. Large flakes of molybdenum and crystals of pyrite occur in some vein material. Similar veining is also present in the central Rhosgobel stock (to the south).

Minor quartz stockwork containing molybdo-scheelite and scheelite also cuts metasedimentary rocks at the SCHEELITE DOME (south of the McQuesten River).

The KALZAS (FLO) tungsten-molybdenum-tin stockwork-vein deposit is located 70 km southeast of Mayo, just north of Big Kalzas Lake. On both peaks of the Kalzas Twins, several types of mineralization overprint each other in rocks of the Grit Unit. Wolframite, molybdenite, and cassiterite mineralization occur in sets of large planar, coarse grained quartz veins. A concentric alteration halo has an outer sericite dominated zone, an inner 'potassic' core and intense tourmalinization throughout the potassic zone and part of the sericite fringe. Intense fracture and quartz-tourmaline veinlet stockworks are present. An underlying pluton is suspected (Lynch, 1985 p. 79). Cassiterite also occurs as euhedrally terminated crystals in gangue-poor veins in a few localities, similar to those at JABBERWOCK.

Breccias

Breccia-vein tin +/- silver occurrences are the OLIVER CREEK (EPD), SUNSHINE CREEK (SP, east of East Ridge), BOULDER CREEK (TEE, southern East Ridge), JABBERWOCK, and SHEPPARD (TIN DOME) properties. These breccias mostly consist of subangular to subrounded fragments of quartzite or vein material (i.e., quartz, tourmaline, or chlorite) in a matrix of crystalline quartz, tourmaline, or chlorite. Cassiterite mainly occurs as grains within the matrix. The breccias are matrix-supported with up to 60% matrix and are thus identified by the matrix material.

At OLIVER CREEK, the main tin- and silver-bearing breccia is chlorite breccia, along with some tourmaline- and rock flour-breccias. The rock flour breccia is a clast-supported breccia with 5-10% matrix made up of cominuted quartzite. Fragments of quartzite are mostly in close to original position (jigsaw texture).

Cassiterite and native silver, along with pyrrhotite, pyrite, chalcopyrite and sphalerite occur in the matrix of these breccias.

The SUNSHINE CREEK and BOULDER CREEK (TEE) properties are mostly quartz breccias with some tourmaline breccia on the former. The quartz breccias are vuggy with euhedrally-terminated quartz matrix and are commonly stained with manganese oxides. Silver values are present at SUNSHINE CREEK. Both the JABBERWOCK and SHEPPARD occurrences have tin-bearing tourmaline breccias. At JABBERWOCK, the breccia contains visible cassiterite in vugs and veins along with K-feldspar.

The breccias mostly occur in the exocontact of small plutons or dykes. Tourmaline-arsenopyrite breccia occurs within a quartz monzonite stock on the MAHTIN property (north part of East

Ridge), and contains some silver, but no tin. All of the breccias are steeply-dipping and vein-like, and are presumably fault controlled. Most are about 1 m wide, but reach 7 m at SUNSHINE CREEK and 15 m at OLIVER CREEK. The lateral extent is up to 250 m on the SUNSHINE CREEK and BOULDER CREEK (TEE), and 1 km at OLIVER CREEK.

Skarns

Several tungsten skarns occur on the margins of McQuesten area plutons, including SCHEELITE DOME, LUGDUSH (on southern West Ridge), RHOSGOBEL, and RAY GULCH (near Dublin Gulch, Lennan, 1985). Scheelite is disseminated in medium- to dark-green diopside-quartz (+/- pyrrhotite) calc-silicate rock interlayered with relatively barren white wollastonite-quartz calc-silicate rock and biotite quartz hornfels. At SCHEELITE DOME, actinolite is present instead of diopside in the dark green layers. Diopside-quartz skarn on the MAHTIN property is adjacent to a feldspar porphyritic granite and contains arsenopyrite, and no scheelite.

Some tin-bearing skarn was noted on the BOULDER CREEK and OLIVER CREEK (EPD) properties. At BOULDER CREEK, actinolite-epidote-axinite (+/- pyrrhotite, pyrite, chalcopyrite) skarn containing cassiterite in vugs occur at one locality (near the TEE claims). Another, tin-bearing garnet-epidote-actinolite-axinite-calcite skarn occurs at another locality on the property (in the southeastern SNARK claims). It is approximately 12 m thick and exposed over 25 m strike length. At OLIVER CREEK, some cassiterite-bearing actinolite-pyrrhotite skarn is intercalated with metasedimentary rocks.

DISCUSSION

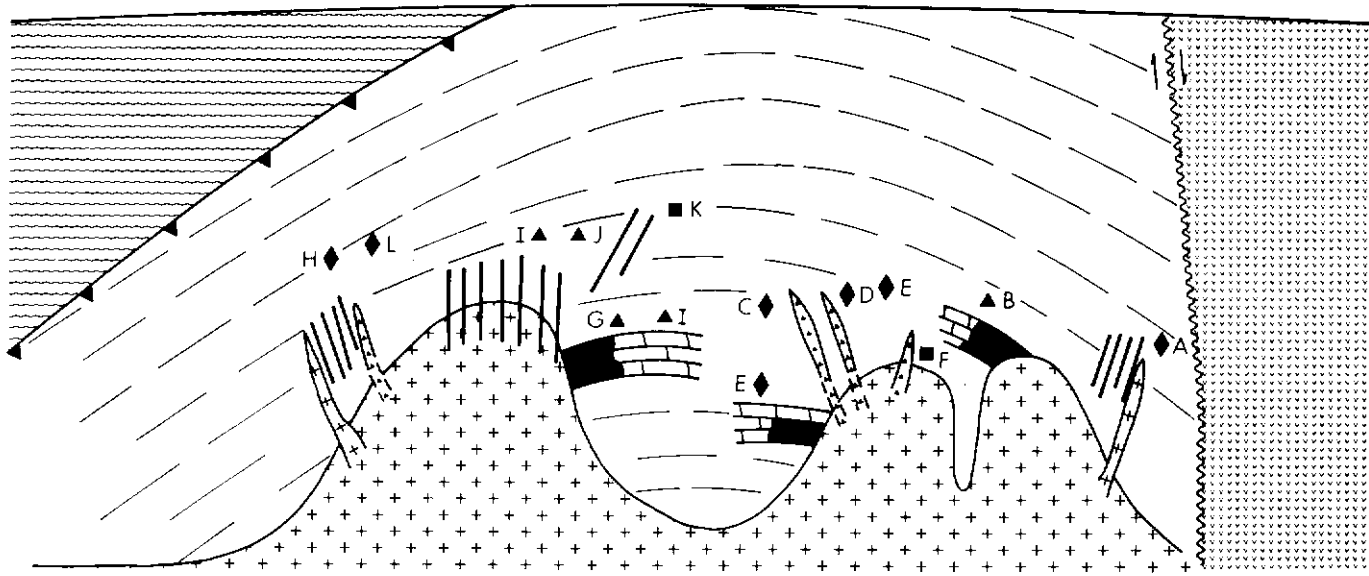
A mock east-west cross section of the McQuesten River area in Figure 3 shows the lithophile occurrences approximate location with respect to the geology. Most occurrences are close to cupolas of the Cretaceous felsic intrusions and are believed to be genetically related to their activity (orthomagmatic model). Cassiterite is mostly in fractures of brittle quartzite, as gangue-poor, or gangue-rich (chlorite, tourmaline, or quartz) veins and/or breccias; and scheelite is mostly in lenses of calc-silicate rock intercalated with the quartzite, and hornfels, and also in sheeted quartz veins in both intrusive cupolas and surrounding hornfels. Thus, aside from proximity to granite cupolas, this mineralization is mainly controlled by fractures in the metasedimentary rocks, joints in both intrusion and surrounding country rock, and location of calc-silicate horizons. The fractures may be either related to emplacement of the intrusion, or pre-intrusive regional patterns. The joints are likely due to cooling of the granite. A structural study of the area would be beneficial to the explorationist.

Zoning appears to only occur on the scale of each intrusive system. For instance, at Mount Haldane quartz-muscovite (+ scheelite) greisen veins occur in the contact zone of the intrusion, and further away (approximately 1 km from the intrusion) cassiterite veins occur in the quartzite. Another example is KALZAS (Lynch, 1985). Tungsten occurs closer to the intrusion than tin. In most cases the intrusion has either tungsten, or tin mineralization associated, but not both. Recent study of the nearby Keno Hill-Galena Hill silver-lead area by Lynch indicates interesting mineral zonation indicating an intrusion at depth (Lynch, pers. comm., 1985).

The McQuesten River area is one of the two major areas of vein and skarn deposits of tin and tungsten in Yukon, along with the Seagull district in southern central Yukon. In both areas, mineralization occurs in Upper Precambrian to Mississippian metasedimentary autochthonous rocks of the ancient North American craton, or in Cretaceous granitoid plutons, intruded after collision of an island arc with ancient North America (Tempelman-Kluit, 1981).

Intrusions in the Seagull area are large concordant batholiths, whereas those in the McQuesten are small discordant stocks, plugs and dykes which were intruded to higher crustal levels.

This difference in size of intrusion accounts for the difference in mineralization styles of the two areas. Large greisen deposits of tin and tungsten, such as that at the East Kempton tin mine in Nova Scotia, would be more likely to occur in the larger plutons of the Seagull area than in the McQuesten. Some greisenized rocks



◆ mineral occurrence - tin ▲ mineral occurrence - tungsten ■ mineral occurrence - gold/silver

[Diamond symbol]	Cretaceous felsic volcanic rocks	[Parallel lines symbol]	foliation	Mineral Occurrences
[Cross-hatch symbol]	Cretaceous felsic intrusive rocks	[Wavy line symbol]	fault	A-JOUMBIRA B-SCHEELITE DOME
[Wavy line symbol]	Ordovician metasedimentary rocks	[Triangle symbol]	thrust fault	C-OLIVER CREEK
[Horizontal line symbol]	Late Proterozoic/Early Cambrian metasedimentary rocks	[Brick pattern symbol]	skarn	D-SUNSHINE CREEK
[Brick pattern symbol]	Late Proterozoic/Early Cambrian marble	[Triangle symbol]	breccia	E-BOULDER CREEK
[Diagonal line symbol]		[Vertical lines symbol]	dyke	F-MAHTIN
				G-LUGDUSH
				H-JABBERWOCK
				I-RHOSGOBEL
				J-PUKELMAN
				K-JOSEPHINE
				L-BARNEY

Figure 3. Model of tin-tungsten mineralization in the McQuesten River area.

do occur in the Surprise Lake Batholith in British Columbia, west of the Seagull area. A difference in stratigraphy in the two areas, i.e. the presence of much thicker calcareous units in the Seagull area gives it a greater potential for extensive skarn development, another economically important mineral deposit type (i.e., Renison Bell tin mine in Australia).

Although there is no known greisen in the McQuesten area, there is some potential in the intrusions underlying tin and tungsten occurrences. There are several sizeable tungsten skarn deposits i.e., RAY GULCH and SCHEELITE DOME, and there are

also several skarn occurrences which have not been thoroughly explored. Another important target for this area are tin veins and breccia of the type mined in southwest England and in Bolivia. Most tin vein occurrences in the McQuesten area have not been extensively explored and a potential may exist in further development of these properties.

Other areas of important potential are thermal aureoles of intrusives which are not exposed at the surface. These may be identified by zones of porphyroblastic hornfels. Fractures, or calcareous lenses in these zones are important targets.

REFERENCES

- BOSTOCK, H.S., 1957. Selected field reports of the Geological Survey of Canada, 1898 to 1933, Yukon Territory; Geol. Surv. Can., Memoir 284.
- BOYLE, R.W., 1965. Geology, geochemistry, and origin of the lead-zinc-silver deposits of the Keno Hill-Galena Hill area, Yukon Territory. Geo. Surv. Can., Bulletin 111, 302 p.
- DEBICKI, R.L., 1983. Yukon placer mining industry 1978-1982; Exploration and Geological Services Division, Yukon, Indian and Northern Affairs Canada, p. 79-80.

- EMOND, D.S., 1985. Geology, mineralogy and petrogenesis of the Oliver Creek tin-bearing breccias, McQuesten River area, Yukon; *Unpublished MSc Thesis*, Carleton University, Ottawa, Ontario.
- FRANZEN, J., 1986. Metal-ratio zonation in the Keno Hill district, central Yukon; *in Yukon Geology, Vol. 1; Exploration and Geological Services Division, Yukon, Indian and Northern Affairs Canada*, p. , this volume.
- FRITZ, W.H., NARBONNE, G.M., and GORDEY, S.P., 1983. Strata and trace fossils near the Precambrian - Cambrian boundary, Mackenzie, Selwyn, and Wernecke Mountains, Yukon and Northwest Territories; *in Current Research, Part B, Geol. Surv. Can., Paper 83-1B*, p. 365-375.
- LENNAN, W.B., 1985. Ray Gulch tungsten skarn deposit, Dublin Gulch area; *Abstracts from papers given at CIM conference, "Mineral Deposits of Northern Cordillera," Dec. 5-7, 1983; in Yukon Exploration and Geology, Dept. Ind. Aff. Nor. Dev., Whitehorse, Yukon*, p. 27-28.
- LYNCH, G.V., 1985. Alteration and zonation in the Kalzas W-Sn-Mo porphyry-vein deposit, 105 M 7, Yukon; *in Yukon Exploration and Geology 1983*, Dept. Ind. Aff. Nor. Dev., Whitehorse, Yukon, p. 79-87.
- LYNCH, G., 1986. Mineral Zoning in the Keno Hill Ag-Pb-Zn mining district, Yukon; *in Yukon Geology, Vol. 1; Exploration and Geological Services Division, Yukon, Indian and Northern Affairs, Canada*, p. , this volume.
- MACLEAN, T.A., 1914. Lode mining in Yukon: an investigation of quartz deposits in the Klondike division; Canada Dept. of Mines, Mines Branch, Publication No. 222.
- MULLIGAN, R., 1974. Geology of Canadian tin occurrences; *Geol. Surv. Can., Economic Geology Report No. 28*, 155 p.
- NOBLE, S.R., 1980. Geology of the EPD tin occurrence, Yukon; *Unpublished BSc Thesis*, University of Toronto, Toronto, Ontario.
- STEVENS, R.D., DELABIO, R.N. and LACHANCE, G.R., 1982a. Age determinations and geological studies, K-Ar isotopic ages, Report 16; *Geol. Surv. Can., Paper 82-2*, 56 p.
- STEVENS, R.D., LACHANCE, G.R. and DELABIO, R.N., 1982b. Age determinations and geological studies, K-Ar isotopic ages, Report 15; *Geol. Surv. Can., Paper 81-2*.
- TEMPELMAN-KLUIT, D.J., 1970. Stratigraphy and structure of the "Keno Hill Quartzite" in Tombstone River-Upper Klondike River map-areas. Yukon Territory (116 B/7, B/8); *Geol. Surv. Can., Bulletin 180*, 102 p.
- TEMPELMAN-KLUIT, D.J., 1981. Geology and mineral deposits of southern Yukon; *in Yukon Geology and Exploration 1979-1980*, Dept. Ind. Aff. Nor. Dev., Whitehorse, Yukon, p. 7-31.
- THOMPSON, R.M., 1945. An occurrence of tin at Dublic Gulch, Yukon; *Economic Geology, Vol. XI*, p. 142.
- WATSON, K., 1986. Silver-lead-zinc deposits of the Keno Hill-Galena Hill area, central Yukon; *in Yukon Geology, Vol. 1; Exploration and Geological Services Division, Yukon, Indian and Northern Affairs Canada*, p. .

PRELIMINARY STRUCTURAL AND KINEMATIC ANALYSIS OF MYLONITIC ROCKS OF THE TESLIN SUTURE ZONE, 105 E, YUKON

V.L. Hansen
Department of Earth and Space Sciences
University of California
Los Angeles, California

HANSEN, V.L., 1986. Preliminary structural and kinematic analysis of mylonitic rocks of the Teslin Suture Zone, 105 E, Yukon; in Yukon Geology, Vol. 1; Exploration and Geological Services Division, Yukon, Indian and Northern Affairs Canada, p. 119-124.

INTRODUCTION

The Teslin suture zone (TSZ), first described by Tempelman-Kluit (1979) forms the fundamental boundary between rocks formed along the ancient western margin of North America and the easternmost allochthonous terrane in northern British Columbia and Yukon. The suture zone is exposed along a north-northwest-trending belt in the Big Salmon Range of the Pelly Mountains within the Laberge map area (105 E), and it is also preserved to the east in klippen within the Quiet Lake (105 F) and Finlayson (105 G) map areas. The TSZ is truncated to the south by younger faults and intrusive rocks, and broadens to the northwest where it merges with the Yukon-Tanana cataclastic terrane in Alaska.

The TSZ comprises variably mylonitized sedimentary and volcanic strata, peridotite, basalt, gabbro, and granodiorite which record upper greenschist to epidote-amphibolite facies metamorphism. Within the TSZ a pervasive, penetrative mylonitic foliation dips steeply and trends north-northwest parallel to the regional TSZ trend, whereas mylonitic foliation preserved in the eastern klippen are subhorizontal, approximately parallel to the basal thrusts (Tempelman-Kluit, 1977, 1978a, 1978b, 1979; Gordey, 1981). TSZ rocks were metamorphosed during synchronous ductile deformation in Late Triassic to mid-Jurassic time and thrust eastward above cratonal sediments during Cretaceous time (Tempelman-Kluit, 1979; Stevens *et al.*, 1982; Metcalfe and Clark, 1983).

An understanding of structural and metamorphic development of the TSZ is of importance to models of early Mesozoic Cordilleran evolution, and is also of economic interest as TSZ rocks appear to be structurally and metamorphically equivalent to rocks of the Klondike area (Ruth Debicki, pers. comm.). Previous structural and petrologic analysis of the TSZ by Erdmer (1981; 1982), and Erdmer and Helmstaedt (1983) provided correlation of three distantly separated portions of the TSZ based on lithology, mylonitic textures, metamorphic grade, and hysteretic metamorphic P-T paths of enclosed eclogite.

The present study is an integrated research project to investigate the structural and metamorphic development of the TSZ within the Laberge map area, eastern half. The goal of this project is to better understand kinematics, P-T conditions, fluid compositions, and timing of deformation of this fundamental boundary. This report summarizes preliminary structural and kinematic interpretations of this portion of the TSZ.

Methods

The TSZ is well exposed along the eastern edge of the Laberge map area, where it is preserved in a 15 km wide vertical zone within the Big Salmon Range of the Pelly Mountains. Geologic mapping and structural analysis, including microstructural analysis, of rocks along three ridge transects perpendicular to the trend of the TSZ form the basis of this report.

Field work consisted of geologic mapping coupled with emphasis on mesoscopic structural data collection and detailed sampling for microscopic kinematic analysis. Samples collected will also be used in later phases of this project for P-T analysis, and fluid inclusion analysis. Approximately two weeks were spent along each of the three east-west-trending ridges approximately 20 km apart: 1) south of Teraktu Creek (TC); 2) north of Dycer Creek (DC); and 3) south of Livingstone Creek (LV) (Fig. 1).

The LV transect crosses the entire width of the TSZ. Due to poor exposure, the TC and DC transects traverse only the eastern three-quarters of the TSZ. The author intends to extend these two transects westward with field work along the Teraktu Creek, Big

Salmon River, and Dycer Creek drainage during the summer of 1985. These transects, parallel to the ridges and perpendicular to the trend of the TSZ, were mapped in reconnaissance in two kilometre-wide strips at a scale of 1:50,000. Within each transect, lithologic units in general are continuous along strike. Lithologic units of the TSZ described by Tempelman-Kluit (1978, 1979) were further subdivided into the following lithologic units. The Nisutlin Allochthonous Assemblage, PPk1, is divided into: 1) chlorite-quartz phyllitic schist; 2) pale green micaceous quartzite; 3) mica-quartz schist; 4) orthoquartzite, and 5) graphitic quartzite. The Anvil Allochthonous Assemblage, CPav and CPAub, is divided into: 1) medium-grained, compositionally layered amphibolite; 2) finely laminated amphibolite; 3) massive, poorly foliated greenstone with possible relict flow breccia and pillow structures; 4) quartz-rich foliated greenstone; 5) fine-grained foliated granodiorite; 6) calc-silicate and white marble; 7) dunite, peridotite, pyroxenite (CPaub); and 8) augen-bearing granodiorite gneiss (Pn of Tempelman-Kluit, 1978). OSQqcl is further divided into: 1) graphitic phyllite; 2) pale green muscovite quartzite; 3) graphitic quartzite; and 4) white marble.

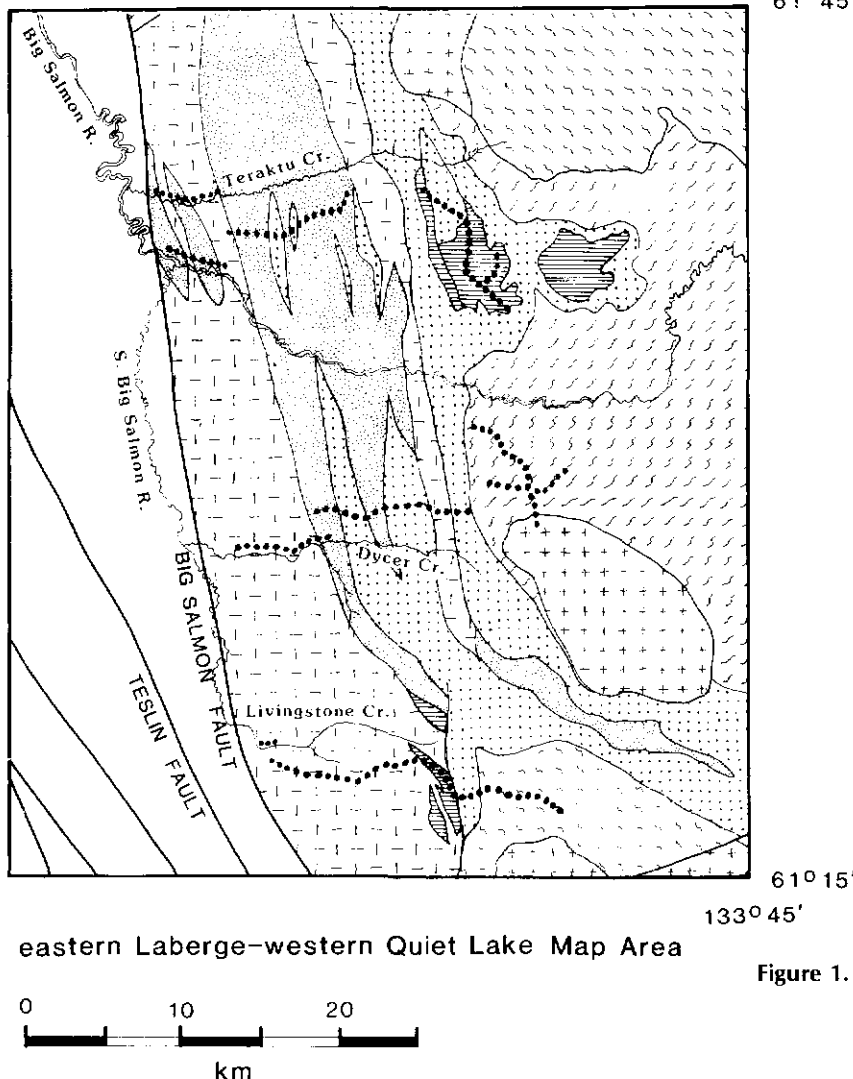
Each lithology is variably mylonitized (usage after Bell and Etheridge, 1973; White, 1976; Sibson, 1977) with a steep south-southwest-dipping foliation and elongation lineation described below. Limiting mineral assemblages indicate middle greenschist to epidote-amphibolite facies metamorphism.

Some 250 sites, at a density of 5-7 stations per km, locate approximately 600 oriented samples. Various rock types were sampled at several stations in order to optimize collateral kinematic and P-T interpretive tools. Petrographic and kinematic data presented in this report stem from preliminary study of over 400 samples.

STRUCTURES

TSZ rocks crop out as flaggy, gneissic to schistose rocks dotting the ridge tops along the three traverses. The flaggy character of these rocks results from a penetrative mylonitic foliation and variably developed elongation lineation. Layers rich in quartz interspersed with layers of mica, feldspar, carbonate, or amphibole define a moderately well-developed, planar, compositional foliation. Within the foliation plane, streaks of quartz, biotite, plagioclase, carbonate, or amphibole define a penetrative mylonitic lineation, Lm. Although Lm is observed in essentially all TSZ rock types, and the orientation of Lm in adjacent lithology is parallel, the character of the lineation is a function of host lithology. Axes of small scale folds, common throughout the TSZ, parallel Lm.

Geologic mapping and structural analysis along the three transects delineate two differently oriented populations of elongation lineations in the north-northwest-trending, steeply-dipping mylonitic foliation. Relationships of these two populations of Lm are best expressed within the LV transect (Fig. 2). In the western portion of the TSZ, Lm plunges moderately to steeply west and is referred to as Lm1. In the eastern portion of the TSZ, Lm plunges gently north-northwest to south-southeast and is here termed Lm2. Fractures are locally present normal to Lm2. Cross-cutting relations in the central portion of the TSZ may indicate that Lm2 locally post-dates Lm1, although no metamorphic or deformational hiatus is recognized. It is unclear at the writing of this report if Lm1 and Lm2 form distinct populations of lineations, or if they represent two end members in a gradual change in orientation from west to east across the TSZ. Continued field work should distinguish which of these two interpretations is correct. The structural characteristics of Lm1 and Lm2 are indistinguishable except for their orientations.

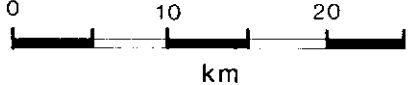


UNITS	
[+ + +]	Kg post-TSZ granites
[]	TR-JR volcanic and related rocks
NISUTLIN ALLOCHTHON	
[]	PMN mu-quartzite, phyllite
[:::]	ODN graphitic quartzite, carbonate, quartz schist
ANVIL ALLOCHTHON	
[---]	CPA amphibolite, metabasalt, diorite gneiss
[]	CPAU dominantly ultramafic rocks
NORTH AMERICAN AUTOCHTHON	
[wavy]	Pns mu-bi granodiorite gneiss
[diagonal hatching]	PICs gt-mica schist, mu-quartzite, marble
.....	transects of this study

Generalized from Tempelman-Kluit 1978, 1984

Figure 1. Generalized geologic map of the Laberge area, eastern half. Mapping and sample transects shown as dotted lines. TC = Teraku Creek DC = Dycer Creek; LV = Livingstone Creek. See text for TSZ lithologic units. Modified from Tempelman-Kluit, 1978b.

eastern Laberge–western Quiet Lake Map Area



The mylonitic fabric of TSZ rocks is dominantly monoclinic, although locally orthorhombic symmetry is observed. This discussion focuses on the monoclinic fabrics which are more pervasive and record more details of the TSZ's structural history. Within the monoclinic fabric, the plane of symmetry is perpendicular to foliation and contains Lm; the 2-fold axis is perpendicular to Lm and parallel to mylonitic foliation (Fig. 3). TSZ fabrics generally consist of: 1) mylonitic foliation; 2) elongation lineation, Lm; and 3) open to isoclinal folds with axes parallel to Lm.

The mylonitic foliation is itself composed of two foliations: a) a penetrative schistosity, S, and b) a spaced, non-penetrative foliation, C (S = "schistosity" and C = "ciséaillement," French for "shear;" after Berthe et al., 1979a, 1979b). S and C planes are best observed in the augen granodiorite gneiss unit. The microstructures of the augen granodiorite are described as an example of the monoclinicity of TSZ fabrics. Layers rich in quartz interspersed with layers of biotite and feldspar define a moderately well-developed, penetrative, planar, compositional mylonitic foliation, S. Within the foliation plane, streaks of quartz, biotite, and plagioclase define a unidirectional penetrative lineation, Lm. Blocky and elongate K-feldspar megacrysts commonly display quartz-filled fractures oriented normal to Lm within the plane of foliation. This relationship, along with observed quartz rodding, and quartz grain and subgrain elongation observed in this section, suggest Lm formed as an extensional lineation. This interpretation is important when evaluating bulk movement direction (see kinematic interpretation below). In sections normal to S and parallel to Lm, a weakly- to moderately-developed, non-penetrative crenulation cleavage-type plane, C, intersects S, defining a fabric asymmetry (Fig. 3). The intersection of S and C is normal to Lm. Aligned and smeared, very fine-grained mica coats

C-planes and marks a second slickenside-type, non-penetrative lineation parallel in trend to Lm. The asymmetry defined by the intersection of S and C planes within the plane of symmetry is extremely useful in interpreting the kinematic development of TSZ fabrics (Berthe et al., 1979a, 1979b; Simpson and Schmid, 1983; Lister and Snoke, 1984). Kinematic interpretations are discussed below.

S and C planes are most easily seen in the granodiorite as a result of its relatively coarse grained nature. Most other TSZ rocks are extremely fine-grained; hence, S and C planes and other developed asymmetries, when present, are distinguished only in thin section. Mylonitic foliation, as mapped in the field, is a combination of these two synchronously developed foliations.

The elongation, or stretching lineation marked most commonly by quartz rodging and mineral alignment, parallels the direction of bulk tectonic transport (Anderson, 1948; Ramsay and Graham, 1970; Lister and Price, 1978; Ramsay, 1980; White et al., 1980). Intersection lineations and crenulation lineations are also locally present within the TSZ rocks. These lineations are generally less well-developed, and exhibit greater variation in orientation from one plane of mylonitic schistosity to the next. Although these lineations may be important in understanding the tectonic development of the TSZ, they are not discussed in this report. Intersection and crenulation lineations result, at least in part, from the interference of small scale folds whose axes parallel mylonitic lineation.

The mylonitic foliation is itself composed of two foliations: a) a penetrative schistosity, S, and b) a spaced, non-penetrative foliation, C (S = "schistosity" and C = "ciséaillement," French for "shear;" after Berthe et al., 1979a, 1979b). S and C planes are best observed in the augen granodiorite gneiss unit. The microstruc-

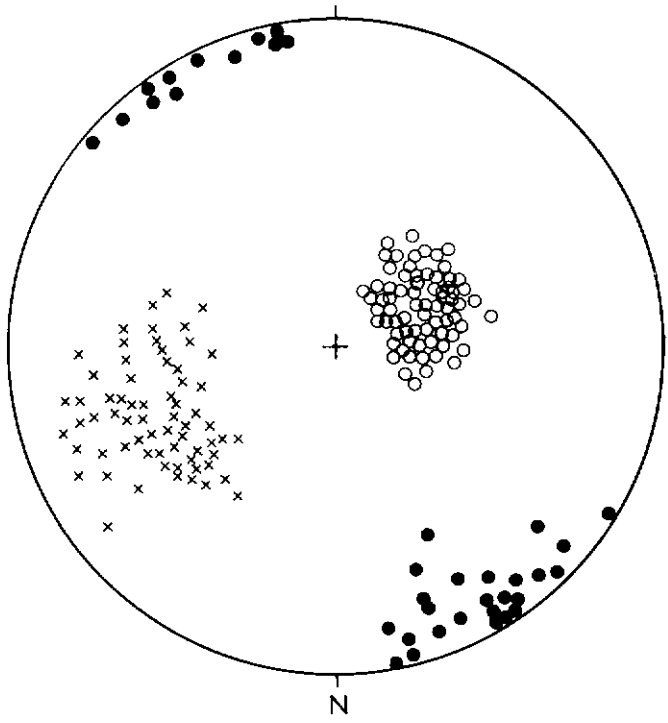


Figure 2. Equal area stereoplot of poles to mylonitic foliation (x), Lm1 (o) and Lm2 (•). Structural data taken from approximately 40 stations along the LV transect.

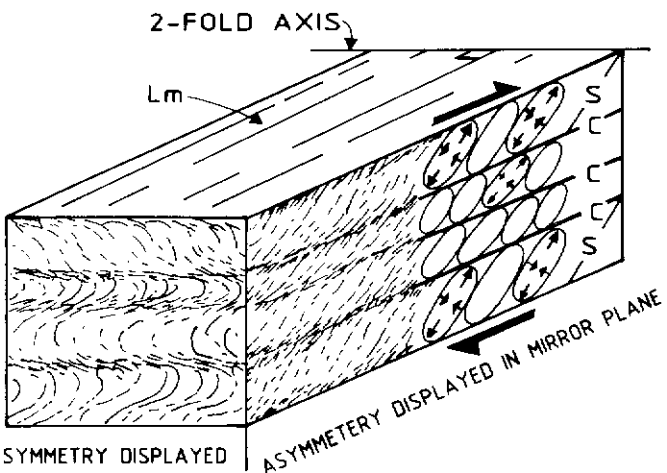


Figure 3. Sketch of mylonitic fabrics in granodiorite gneiss. Plane of symmetry is parallel to Lm and perpendicular to mylonitic foliation; 2-fold axis is normal to Lm. Asymmetric mylonitic fabrics are often composed of two foliations. S planes are planes of penetrative schistosity, composed of numerous quartz subgrains which can be interpreted as tiny qualitative strain ellipses indicating shortening and elongation (arrows). C planes are marked by non-penetrative, spaced cleavage planes dominated by shear mechanisms. The asymmetry described by the relationship of these two surfaces indicates shear direction (Berthe *et al.*, 1978a, 1978b; Simpson and Schmid, 1983; Lister and Snee, 1984).

tures of the augen granodiorite are described as an example of the monoclinicity of TSZ fabrics. Layers rich in quartz interspersed with layers of biotite and feldspar define a moderately well-developed, penetrative, planar, compositional mylonitic foliation, S. Within the foliation plane, streaks of quartz, biotite, and plagioclase define a unidirectional penetrative lineation, Lm. Blocky and elongate K-feldspar megacrysts commonly display

quartz-filled fractures oriented normal to Lm within the plane of foliation. This relationship, along with observed quartz rodding, and quartz grain and subgrain elongation observed in this section, suggest Lm formed as an extensional lineation. This interpretation is important when evaluating bulk movement direction (see kinematic interpretation below). In sections normal to S and parallel to Lm, a weakly- to moderately-developed, non-penetrative crenulation cleavage-type plane, C, intersects S, defining a fabric asymmetry (Fig. 3). The intersection of S and C is normal to Lm. Aligned and smeared, very fine-grained mica coats C-planes and marks a second slickenside-type, non-penetrative lineation parallel in trend to Lm. The asymmetry defined by the intersection of S and C planes within the plane of symmetry is extremely useful in interpreting the kinematic development of TSZ fabrics (Berthe *et al.*, 1979a, 1979b; Simpson and Schmid, 1983; Lister and Snee, 1984). Kinematic interpretations are discussed below.

S and C planes are most easily seen in the granodiorite as a result of its relatively coarse-grained nature. Most other TSZ rocks are extremely fine-grained; hence, S and C planes and other developed asymmetries, when present, are distinguished only in thin section. Mylonitic foliation, as mapped in the field, is a combination of these two synchronously developed foliations.

The elongation, or stretching lineation marked most commonly by quartz rodding and mineral alignment, parallels the direction of bulk tectonic transport (Anderson, 1948; Ramsay and Graham, 1970; Lister and Price, 1978; Ramsay, 1980; White *et al.*, 1980). Intersection lineations and crenulation lineations are also locally present within the TSZ rocks. These lineations are generally less well-developed, and exhibit greater variation in orientation from one plane of mylonitic schistosity to the next. Although these lineations may be important in understanding the tectonic development of the TSZ, they are not discussed in this report. Intersection and crenulation lineations result, at least in part, from the interference of small scale folds whose axes parallel mylonitic lineation.

Minor folds are observed in essentially all rock types which comprise the TSZ. Fold axes parallel Lm; therefore, fold axial profiles are observed in sections cut normal to both mylonitic foliation and lineation. In contrast to the section showing S and C planes described above, these sections display no apparent fabric asymmetry. Although folds within different host lithology vary in their interlimb angle and lengths of their preserved limbs, the folds share three important characteristics: 1) fold axes are parallel to Lm; 2) folds deform mylonitic foliation, yet display axial planar structures coplanar with mylonitic foliation; and 3) spaced foliations, coplanar with fold axial planes and mylonitic foliation, truncate and offset fold limbs with no resultant fold asymmetry. Both folds and mylonitic foliation which display varying degrees of fold limb attenuation, truncation, and offset within different host lithology appear to be the result of refolded and "tectonic kneading" (Fig. 4). For example, granodiorite mylonite gneiss and muscovite quartzite display open style folds with no apparent limb truncation (Fig. 4a). Phyllitic quartzite and graphitic quartzite display multiple refolded folds characterized by attenuated and truncated limbs and apparently thickened fold hinges (Fig. 4c). Amphibolite gneisses contain structures transitional between these two end members; spaced foliation planes parallel to fold axial planes attenuate the long limbs of tight to isoclinal folds, but limbs are rarely truncated along these planes (Fig. 4b).

Parallelism of stretching lineation and minor fold axes is commonly reported from large scale shear zones (Christie, 1963; Eisbacher, 1970; Bell, 1978; Bell and Hammond, 1984), yet mechanisms of fold formation within shear zones are not clearly understood (Bell and Hammond, 1984). Several workers (Bryant and Reed, 1969; Rhodes and Gayer, 1977; Bell, 1978; Williams, 1978) propose that pre-existing, or early-formed folds, rotate into parallelism with elongation lineation with increasing shear deformation. Rotation of folds during shear deformation implies that folds initiate as open folds with axes at an angle to lineation, and become isoclinal folds as they rotate into parallelism with lineation. Minor folds in the TSZ (e.g., in mica quartzite and granodiorite gneiss) are commonly open style folds with axes statistically parallel to Lm (Fig. 5). This relationship indicates that TSZ folds initiated as open folds with axes originally parallel to Lm, and did not rotate into parallelism with continued deformation.

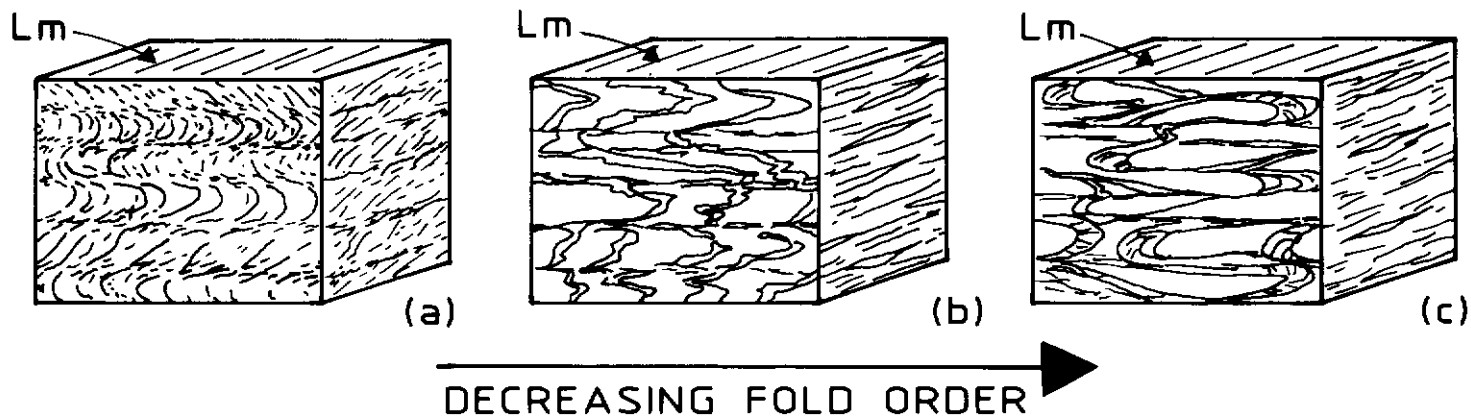


Figure 4 Axial profiles of variably attenuated and “tectonically kneaded” open to isoclinal folds with axes parallel to Lm; (a) granodiorite gneiss and mica quartzite; (b) amphibolite gneiss; and (c) phyllitic quartzite and graphitic quartzite.

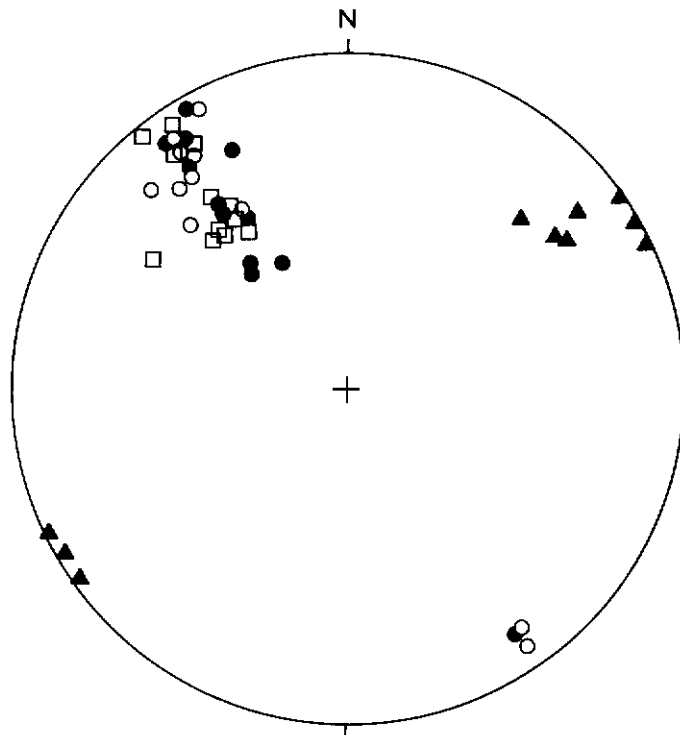


Figure 5 Equal area stereoplot of poles to mylonitic foliation (\blacktriangle); Lm₂ (\bullet); axes of small scale open style folds (\circ); and axes of large scale ($\lambda = 1$ to $1/2$ m) open style folds (\square), from mica quartzite of DC traverse.

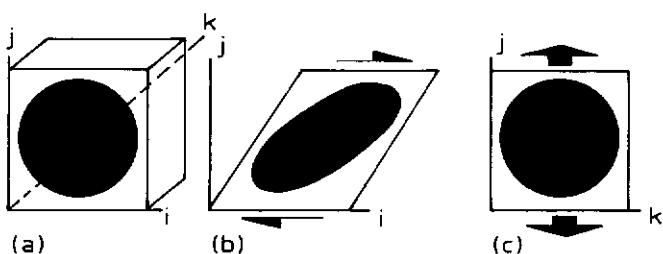


Figure 6 Textural asymmetries develop parallel to bulk movement directions. Consider a cube in ijk coordinates and apply simple shear parallel to i (a). Post-shearing cross-sections ij, parallel to shear direction (b) and jk, normal to shear direction (c) display resultant asymmetry and symmetry respectively. In TSZ rocks, asymmetric textures are expressed in sections cut parallel to Lm, whereas symmetric textures are observed in section cut normal to Lm. Therefore, movement during the formation of TSZ fabrics paralleled Lm.

Models of fold mechanisms in which folds initiate with fold axes parallel to a mylonitic lineation are discussed by Bell and Hammond (1984). Thus, it appears that TSZ folds formed progressively during mylonitization with synchronously developing, multiple generations of mylonitic foliation, and they do not record a later folding event.

The fold styles described above are observed at both mesoscopic and microscopic scales. Field relationships indicate similar fold geometries may be present megascopically within the TSZ. Continued field work will help to clarify these relationships.

In summary, TSZ fabrics are characterized by four structural features: 1) mylonitic foliation; 2) elongation lineation, Lm; 3) minor open to isoclinal folds with axes parallel to Lm; and 4) fractures perpendicular to Lm.

KINEMATICS

Thin sections cut parallel to the plane of fabric symmetry, that is, parallel to Lm and normal to mylonitic foliation, often display asymmetries. The expression of textural asymmetries in sections parallel to Lm supports the conclusion that Lm parallels the bulk movement direction (Fig. 6). Further, textural asymmetries are useful in interpreting the direction of shear during mylonitization (Bouchez et al., 1983; Simpson and Schmid, 1983; Lister and Snoke, 1984). Indicators of shear zone kinematics include: 1) S and C planes; 2) mica and feldspar “fish;” 3) rotated clasts and minerals; and 4) preferred elongation of quartz grains (Fig. 7). Rarely preserved intrafolial folds, with fold axes normal to Lm, when present, are useful kinematic indicators (Ramsay, 1967).

Asymmetric textures described by S and C planes (Fig. 3), mica fish, quartz subgrain elongation, and rotated garnets in sections from the LV and DC traverses, cut normal to mylonitic foliation and parallel to Lm₂ consistently record right-lateral movement parallel to Lm₂. Local intrafolial folds and rotated clasts observed in impure marble units in the field, also indicate right-lateral movement parallel to Lm₂.

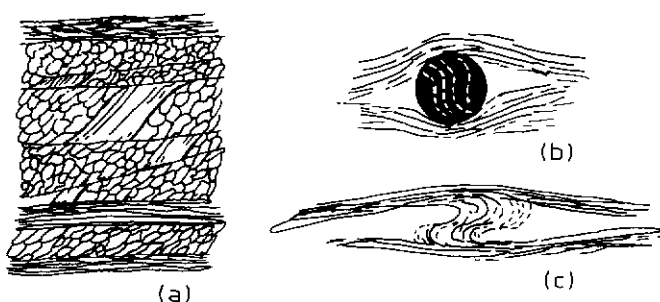


Figure 7 Sketches of microstructural kinematic indicators exhibited in sections cut parallel to Lm; (a) mica “fish”; (b) rotated garnet with inclusion trails; (c) intrafolial fold with fold axis normal to Lm. Each sketch indicates dextral movement.

Kinematic interpretations of sections cut normal to mylonitic foliation and parallel to Lm1 are in preliminary stages. However, research to date indicates dominantly normal movement parallel to Lm1, or west-side-down. The author stresses the preliminary nature of kinematic interpretations of sections parallel to Lm1. Petrofabric analysis of quartz c-axes and calcite c-axes, as well as continued interpretation of textural asymmetries will clarify the kinematic picture.

SUMMARY

The TSZ is a Late Triassic to mid-Jurassic subduction complex and forms the fundamental boundary between rocks deposited along the ancient western margin of North America, and allochthonous terranes to the west. The north-northwest-trending TSZ in the Big Salmon Range includes sedimentary and volcanic strata, basalt, peridotite, and granodiorite metamorphosed to middle greenschist to epidote-amphibolite facies and variably mylonitized. Petrochemical study of co-existing phases now being initiated should allow the assignment of P-T limits attending the recrystallization. Geologic mapping and structural analysis along three 10-15 km transects normal to the trend of the TSZ delineates two populations of stretching lineations, Lm1 and Lm2, in north-northwest-trending, steeply-dipping mylonitic foliation. Lm1, best developed in the western portion of the TSZ, plunges moderately to steeply west. Tight to isoclinal fold axes parallel Lm1. Lm2, best

developed to the east, plunges gently north-northwest and south-southeast. Open to isoclinal fold axes parallel to Lm2, and fractures are locally present normal to Lm2. Folds initiated during mylonitization as open structures with axes parallel to Lm1, and do not record unrelated pre- or post-mylonitic fold events. Crenulation and intersection lineations vary in orientation between schistosity planes in the shear zone. The stretching lineations, Lm1 and Lm2, formed parallel to their bulk movement directions. Kinematic indicators consistently record right-lateral movement parallel to Lm2. Preliminary interpretation of Lm1 kinematics indicate dominantly normal movement parallel to Lm1, or west-side-down.

ACKNOWLEDGEMENTS

This project was inspired by Dirk Tempelman-Kluit who has provided much encouragement and enthusiasm. I would like to thank Jim Morin, Grant Abbott, and Rob McIntyre for their "bush" expertise and hospitality, and a special thanks to Dan Spencer for his assistance and company in the field. This work was supported by the Exploration and Geological Services Division of DIAND, Whitehorse, and a grant from the Department of Earth and Space Sciences, UCLA (Chevron Funds). Many thanks to Ram Alkaly for prolific and careful thin section preparation. John Goodge and W. Gary Ernst greatly improved the manuscript.

REFERENCES

- ANDERSON, M., 1948. On lineation and petrofabric structure, and the shearing movement by which they have been produced; *Geological Society of London Quarterly Journal*, Vol. 104, p. 99-132.
- BELL, T.H. and ETHERIDGE, M.A., 1973. Microstructure of mylonites and their descriptive terminology; *Lithos*, Vol. 6, p. 337-348.
- BELL, T.H. and HAMMOND, R.L., 1984. On the internal geometry of mylonite zones; *Journal of Geology*, Vol. 92, p. 667-686.
- BERTHE, D., CHOUKROUNE, P. and GAPAIS, D., 1979. Orientations préférentielles du quartz et orthogneissification progressive en régime cisailant: L'exemple du cisaillement sud-Américain; *Bulletin de Minéralogie*, Vol. 102, p. 265-272.
- BERTHE, D., CHOUKROUNE, P., and JEGOUZO, P., 1979. Orthogneiss, mylonite and noncoaxial deformation of granite: the example of the South Armorican shear zone; *Journal of Structural Geology*, Vol. 1, p. 31-42.
- BOUCHEZ, J.L., NANTES, LISTER, G.S. and NICOLAS, A., 1983. Fabric asymmetry and shear sense in movement zones; *Geologische Rundschau*, Vol. 72, p. 401-419.
- BRYANT, B. and REEDM, J.C., 1969. Significance of lineation and minor folds near major thrust faults in the southern Appalachians and the British and Norwegian Caledonides; *Geological Magazine*, Vol. 106, p. 412-429.
- CHRISTIE, J.M., 1963. The Moine thrust zone in the Assynt region, Northwest Scotland; *California University Publications of Geological Sciences*, p. 345-439.
- EISBACHER, G.H., 1970. Deformation mechanisms of mylonitic rocks and fractured granites in Cobiquid Mountains, Nova Scotia, Canada; *Geological Society of America Bulletin*, Vol. 81, p. 2009-2020.
- ERDMER, P., 1982. Nature and significance of the metamorphic minerals and structures of cataclastic allochthonous rocks in the White Mountains, Last Peak and Fire Lake areas, Yukon Territory; Unpublished PhD thesis, Queen's University, Kingston, Ontario, 254 p.
- ERDMER, P., 1981. Comparative studies of cataclastic allochthonous rocks in McQuesten, Laberge and Finlayson Lake map areas; in: *Yukon Geology and Exploration 1979-80*. Dept. Ind. Aff. Nor. Dev., Whitehorse, Yukon, p. 60-64.
- ERDMER, P. and HELMSTAEDT, H., 1983. Eclogite from central Yukon: a record of subduction at the western margin of ancient North America; *Canadian Journal of Earth Sciences*, Vol. 20, p. 1389-1408.
- CORDEY, S.P., 1981. Stratigraphy, structure and tectonic evolution of the southern Pelly Mountains in the Indigo Lake Area, Yukon Territory; *Geol. Surv. Can., Bulletin* 318, 44 p.
- LISTER, G.S. and PRICE, G.P., 1978. Fabric development in a quartz-feldspar mylonite; *Tectonophysics*, Vol. 49, p. 37-78.
- METCALFE, P. and CLARK, G.S., 1983. Rb-Sr whole rock age of the Klondike Schist, Yukon Territory; *Canadian Journal of Earth Sciences*, Vol. 20, p. 886-891.
- RAMSAY, J.G., 1967. *Folding and fracturing of rocks*; McGraw Hill Publishing Company, New York, 568 p.
- RAMSAY, J.G., 1980. Shear zone geometry: a review; *Journal of Structural Geology*, Vol. 2, p. 83-99.

- RAMSAY, J.G. and GRAHAM, R.H., 1970. Strain variation in shear belts; *Canadian Journal of Earth Sciences*, Vol. 7, p. 786-813.
- RHODES, S. and GAYER, R.A., 1977. Non-cylindrical folds, linear structures in the X direction of mylonite development during translation of the Caledonian Kalak Nappe Complex of Finnmark; *Geological Magazine*, Vol. 114, p. 329-342.
- SIBSON, R.H., 1977. Fault rocks and fault mechanisms; *Journal of Geological Society of London*, Vol. 133, p. 191-213.
- SIMPSON, C., and SCHMID, S.M., 1984. An evaluation of the sense of movement in sheared rocks; *Geological Society of America Bulletin*, Vol. 94, p. 1281-1288.
- STEVENS, R.D., DELABIO, R.N. and LACHANCE, G.R., 1982. Age determinations and geological studies: K-Ar isotopic ages, report 15; *Geol. Surv. Can., Paper 81-2*, 56 p.
- TEMPELMAN-KLUIT, D.J., 1979. Transported cataclasite, ophiolite and granodiorite in Yukon: evidence of arc-continent collision; *Geol. Surv. Can., Paper 79-14*, 27 p.
- TEMPELMAN-KLUIT, D.J., 1978a. Reconnaissance geology, Laberge map area, Yukon; *Current Research, Part A, Geol. Surv. Can., Paper 78-1A*, p. 61-66.
- TEMPELMAN-KLUIT, D.J., 1978b. Laberge (105 E) map area, Yukon; *Geol. Surv. Can., Open File 578*.
- TEMPELMAN-KLUIT, D.J., 1977. Quiet Lake (105 F) and Finlayson Lake (105 G) map areas, Yukon; *Geol. Surv. Can., Open File 486*.
- WHITE, S.H., BURROWS, S.E., CARRERAS, J., SHAW, N.D. and HUMPHREYS, F.J., 1980. On mylonites in ductile shear zones; *Journal of Structural Geology*, Vol. 2, p. 175-187.
- WHITE, S.H., 1976. The development and significance of mylonites; *25th International Geological Congress, Sydney*, Vol. 1, p. 143.
- WILLIAMS, G.D., 1978. Rotation of contemporary folds into the X direction during overthrust processes in Lakesfjord Finnmark; *Tectonophysics*, Vol. 48, p. 29-40.

PETROTECTONIC STUDY OF THE TESLIN SUTURE ZONE, YUKON: A PROGRESS REPORT

Vicki L. Hansen
Department of Earth and Space Sciences
University of California
Los Angeles, California

HANSEN, V.L., 1986. PetroTECTonic study of the Teslin suture zone, Yukon: a progress report; in Yukon Geology, Vol. 1; Exploration and Geological Services Division, Yukon, Indian and Northern Affairs Canada, p. 125-130.

ABSTRACT

The Teslin suture zone (TSZ) forms the fundamental boundary between rocks deposited along the ancient margin of North America and allochthonous terranes to the west. Both North American and allochthonous rocks were ductilely deformed and concurrently metamorphosed under upper greenschist to amphibolite facies conditions at temperatures of 450-650°C and pressures greater than or equal to 6 kbars, probably during Late Triassic to mid-Jurassic time. North-northwest-striking foliation dips steeply in the western portion of the TSZ, but flattens to the east in North American autochthonous rocks.

The TSZ in the combined eastern Laberge/western Quiet Lake map area is divisible into three distinct elongate structural domains parallel to the NW-trending TSZ. Domains are identified by the distribution of differently oriented stretching lineations, Le1 and Le2, which formed during non-coaxial ductile deformation, and their associated "motion planes." Le1 trends westward and plunges down dip, whereas Le2 trends NNW-SSE and plunges shallowly. Le1 and Le2 are associated with the same mineral assemblages and formed under similar metamorphic conditions. Silicate mineral assemblages record temperatures up to 625°C, and pressures to 8 kbars; carbonate assemblages record temperatures in the range 350-500°C. The difference in temperature suggested by these assemblages may reflect lower temperatures of ductile flow and recrystallization in carbonate rocks.

Elongate lensoidal domains of Le1 are separated from each other by narrower NW-trending zones of Le2, forming a regional-scale anastomosing shear zone. Two western domains of Le1 are comprised chiefly of allochthonous rocks, or rocks of uncertain affinity; however, the eastern domain comprises North American autochthonous rocks, previously considered to be unaffected by TSZ metamorphism and deformation. Macroscopic and microscopic kinematic indicators consistently record right-lateral, or top-to-the-north movement parallel to Le2. Kinematics associated with Le1 are more complex. To the west kinematic indicators record west-side-down (normal) movement parallel to Le1; elsewhere, both reverse and normal movement are recorded. Field relations suggest Le1 began forming earlier than Le2, followed by a period during which both Le1 and Le2 formed, and ended with movement parallel only to Le2. These geometries and movement histories indicate that rocks of the TSZ and structurally associated autochthonous rocks record a history of right-lateral transpression along this portion of the North American margin during Triassic-Jurassic time. Movement consisted of early tectonic shortening at a high angle to the ancient margin, followed by a period of right-lateral translation approximately parallel to the Mesozoic margin of western North America.

INTRODUCTION

The Teslin suture zone (TSZ), initially described by Tempelman-Kluit (1979), forms the fundamental boundary between rocks deposited along the ancient western margin of North America and the eastern-most accreted terrane in northern British Columbia and Yukon. Rocks of the TSZ consist of metamorphosed sedimentary and volcanic strata, peridotite, basalt, gabbro, and granodiorite which were ductilely deformed and concurrently metamorphosed under greenschist to amphibolite facies conditions, probably during Late Triassic to mid-Jurassic time (Tempelman-Kluit, 1979; Metcalfe and Clark, 1983; Stevens et al., 1982). The TSZ probably represents rocks deformed and metamorphosed within the deep-seated portion of the Late Triassic to mid-Jurassic convergent plate margin. It is the purpose of this on-going research to study the structural/metamorphic development of a portion of the TSZ in order to better understand the nature of late Mesozoic plate convergence along this portion of the western North American margin. In this report, the author outlines structures present throughout the TSZ within the eastern Laberge and western Quiet Lake map areas, discusses geometries and kinematics of TSZ deformation, and outlines constraints which structural relations place on models of the tectonic evolution of this ancient western margin.

Data presented in this report summarizes field work from two summer seasons in the Big Salmon Range of the Pelly Mountains, eastern Laberge-western Quiet Lake map area. Field work during the 1985 summer consisted of extending geologic mapping and detailed sampling, begun in 1984, along three transects normal to the trend of the TSZ (Hansen, 1985, 1986a). Mapping along these three transects south of Teraku Creek (TC), north of Dyer and Mendicino Creeks (DC), and south of Livingstone Creek (LV)

(Fig. 1), emphasized mapping of mylonitic elongation lineations (Le) and interpretation of megastructures and microstructures associated with Le. Through mapping the author was able to: 1) document the distribution of two elongation lineations; Le1, generally east-west-trending, and Le2, generally north-south-trending, throughout the TSZ; 2) document the nature of the transition and timing between Le1 and Le2; 3) identify narrow alternating elongate structural domains of Le1 and Le2 parallel to the trend of the TSZ; and 4) provide evidence that rocks of the North American autochthon, previously interpreted to lack evidence of TSZ deformation (Tempelman-Kluit, 1979; Erdmer, 1981, 1985), share the same structural, kinematic and metamorphic signature as TSZ rocks. Data presented and discussed in this report results from detailed field study as well as petrographic analysis and the kinematic interpretation of petrofabrics and micro-textures.

GEOLOGIC SETTING

Yukon comprises autochthonous and allochthonous tectonic elements with distinctive internal stratigraphy. The NW-trending Tintina fault zone separates dominantly autochthonous elements to the northeast from dominantly allochthonous elements to the southwest. The northeastern assemblages include strata deposited on the Paleozoic to Mesozoic North American continental margin. The southwestern tectonic province includes miogeosynclinal rocks deposited in a Paleozoic ocean (Moner, 1977; Moner and Price, 1979) and continental and oceanic terranes of unknown paleogeography. These two distinctive tectonic assemblages collided in Late Triassic to Early Jurassic time and were juxtaposed along the Teslin suture zone.

The TSZ is most simply divided into three assemblages (Tempelman-Kluit, 1979): 1) the Nisutlin allochthon comprises an

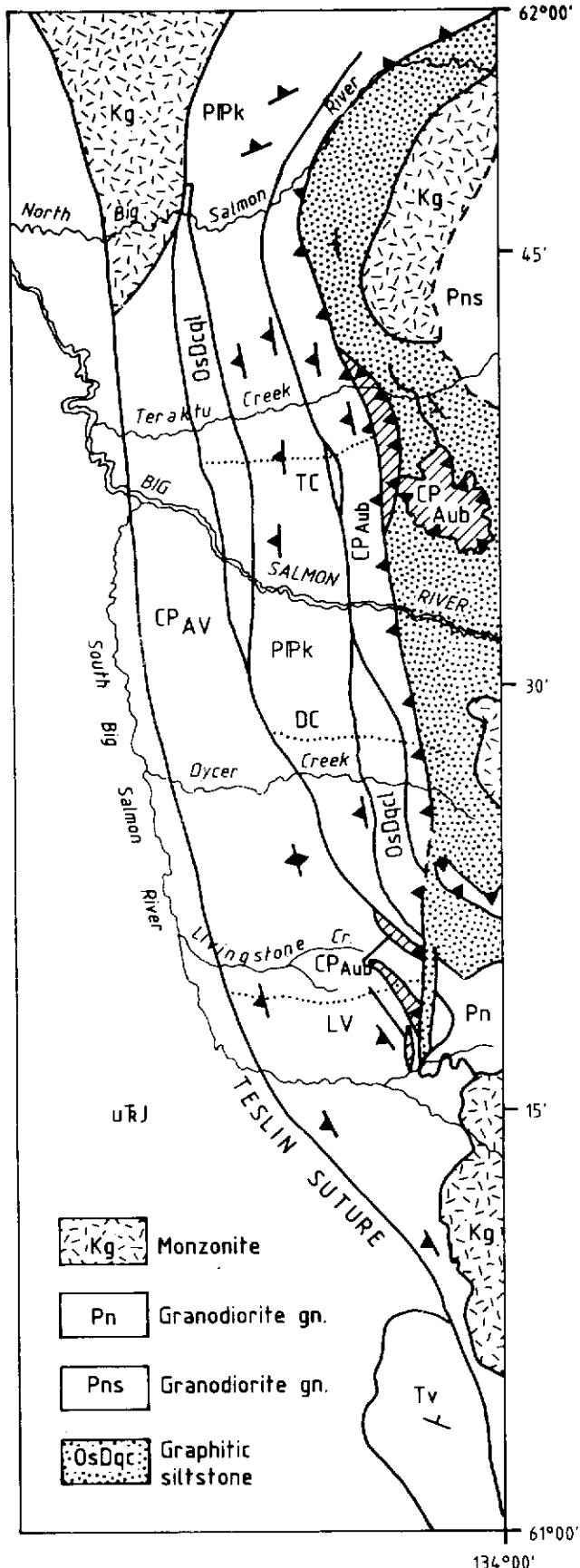


Figure 1. Generalized geologic map of the Teslin suture zone, eastern Laberge-western Quiet Lake map area. Mapping and sampling transects, shown as dotted lines, from north to south are: Teraku Creek, TC; Dycer Creek, DC; and Livingstone Creek, LV.

assemblage of siliceous tectonites derived from sedimentary and volcanic protoliths, and siliceous melange; 2) the Anvil allochthon encompasses an assemblage of sheared ophiolite containing basalt, gabbro and peridotite; and 3) the Simpson allochthon includes mylonitic granitic gneiss. Lithologies within these assemblages have poorly constrained formation ages ranging from late Devonian to mid-Permian (Tempelman-Kluit, 1979; Tempelman-Kluit and Wanless, 1980; Aleinikoff *et al.*, 1981; Mortensen, 1985; Mortensen and Jilson, 1985).

Within the suture zone, in plan, the three allochthonous assemblages or structurally-bound lenses 3-4 km wide and 20-30 km long, elongate parallel to the NNW-trend of the TSZ. The allochthonous assemblages are not chaotically mixed within the suture zone; generally siliceous melange, ophiolite, and granodiorite are exposed successively from northeast to southwest. However, within any one allochthon, lithologies of the other two allochthons may be locally interleaved (Erdmer, 1981, 1985; Erdmer and Helmstaedt, 1983; Hansen, 1985, 1986a; Mortensen, 1985).

TSZ rocks were metamorphosed during synchronous ductile deformation in Late Triassic to mid-Jurassic time (Tempelman-Kluit, 1979; Stevens *et al.*, 1982; Metcalfe and Clark, 1983). These rocks record greenschist- to amphibolite-facies metamorphism (Erdmer, 1981; Hansen, 1986b). Tectonic blocks of eclogite are reported within the Nisutlin siliceous melange assemblage (Tempelman-Kluit, 1970; Erdmer, 1981). Erdmer and Helmstaedt (1983) documented that the basaltic and eclogites record metamorphic pressures to 10 kbars.

Tertiary right-lateral strike-slip deformation characteristic of the North American Cordillera from Mexico to Alaska is localized along the Tintina fault zone to the east and the Denali fault zone to the west. Therefore, the TSZ, although locally offset 450 km by the dextral Tintina fault (Roddick, 1967), does not appear to be internally disrupted by Tertiary-age right-lateral offset within the study area.

Eastern Laberge/Western Quiet Lake Map Area

The geology of the Laberge and Quiet Lake map sheets was first mapped at 1:250,000 in the early 1960's (Bostock and Lees, 1961; Wheeler *et al.*, 1960). Most recent mapping has been completed by Tempelman-Kluit (1977b, 1978a, b), also at 1:250,000 and by Erdmer (1981) at a scale of 1:50,000.

The TSZ is exposed in the eastern half of the Laberge map sheet as a regionally-extensive sub-vertical NNW-trending zone greater than 15 km wide and is preserved in klippen within the Quiet Lake and Finlayson map areas to the east. The TSZ is truncated to the south by faults and intrusive rocks, and it broadens to the northwest where it merges with the "Yukon cataclastic complex" in northern Yukon and Alaska. To the west within the map area the high-angle NNW-trending Big Salmon fault places non-metamorphosed to low-grade volcanic and volcaniclastic sedimentary rocks against high- to moderate-grade rocks of the TSZ (Tempelman-Kluit, 1978b).

METAMORPHIC AND STRUCTURAL RELATIONS OF TSZ

Metamorphic Environment of TSZ

Petrographic investigation to date TSZ metamorphism in the epidote-amphibolite to amphibolite facies is in progress. Mineral assemblages present in TSZ rocks which are useful for P-T estimates include: 1) garnet-biotite; 2) garnet-muscovite; 3) garnet-hornblende; 4) plagioclase-biotite-garnet-muscovite; 5) calcite-dolomite; 6) muscovite composition; 7) plagioclase-amphibole composition; 8) amphibole composition; and 9) coexisting feldspars. Preliminary P-T-ometry constrains metamorphic temperatures at 450-625°C, and pressures greater than or equal to 6 kbars. Coexisting calcite-dolomite mineral pairs (Anovitz and Essene, 1982; Powell *et al.*, 1984) yield values of $T = 450-550^{\circ}\text{C}$, whereas garnet-biotite, garnet-muscovite, and garnet-hornblende mineral pairs (Ferry and Spear, 1978; Graham and Powell, 1984; Green and Hellman, 1982; Hodges and Spear, 1982; Krogh and Raheim, 1978) indicate temperatures of 550-625°C. Carbonate rocks deform ductilely at lower temperatures than silicate rocks (REF); it is possible that the lower apparent temperature of metamorphism recorded by the carbonate rocks records ductile deformation of these rocks to a lower temperature than the silicate rocks. It is also

possible that these temperature differences reveal a metamorphic gradient. Regionally distributed data and more P-T calculations are necessary to substantiate the suggested P-T conditions and place constraints on a tectonic model of TSZ formation. In addition, P-T paths will be studied by examining mineral inclusions in porphyroblasts displaying sieve structures.

Although metamorphic temperatures are quite well constrained in the range 550–625°C for silicate rocks, pressure calculations are less than satisfactory at this time. It is possible that fluid inclusion study will shed light on this problem, by permitting construction of isochores (lines of equal density in P-T space) which, together with temperature data, may further constrain metamorphic pressure.

Structural Environment of TSZ

The TSZ is well-exposed along the eastern edge of the Laberge map sheet where it is preserved in a greater than or equal to 15 km wide belt within the Big Salmon Range. It is bounded to the west by the high-angle, NNW-trending Big Salmon fault. Northward in the Laberge sheet the TSZ broadens to the east, merging with isolated klippen from the south. Within this broad zone rocks of the TSZ are variably ductilely deformed and mylonitized. They crop out as NNW-trending, flaggy, gneissic to schistose rocks dotting the ridge tops throughout the study area. The rocks contain a variably-developed, penetrative mylonitic foliation and lineation (Hansen, 1985, 1986a). Geologic mapping in 1984 delineated two differently oriented elongation lineations, Le1 and Le2, in the steeply-dipping mylonitic foliation. Continued field work in 1985 extended geologic mapping and detailed sample collection along the three transects normal to the TSZ trend. Along the northernmost transect, TC, mapping was extended westward to the Big Salmon fault and eastward to the Dunite klippe area of Erdmer (1981). The central transect, DC, was also extended west to the Big Salmon fault and eastward to the westernmost Quiet Lake area, including rocks of the North American autochthon (Tempelman-Kluit, 1979). The author also revisited the Livingstone transect in order to study details of megascopic structural geometries.

Through mapping and detailed kinematic analysis the author is able to: 1) document the distribution of two distinct elongation lineations, Le1 and Le2, throughout the TSZ; 2) document the nature of the geometric transition and timing relations between Le1 and Le2; 3) identify three NNW-trending structural domains, delineated by the distribution of Le1 and Le2; and 4) provide evidence that rocks of the North American autochthon, previously considered to be unaffected by TSZ deformation and metamorphism (Tempelman-Kluit, 1979; Erdmer, 1981, 1985), bear important structural and metamorphic similarities to TSZ rocks.

Le1 and Le2 are both elongation lineations, as marked by rodded quartz, smeared micas, and aligned minerals, and they formed parallel to the direction of tectonic transport during simple-shear dominated ductile deformation (Hansen, 1985, 1986a). The two lineations are distinguished in the field, in part, by their structural trend. Le1 trends westward and plunges down dip at a high angle to the strike of mylonitic foliation, whereas Le2 trends NNW-SSE and plunges shallowly approximately parallel to the strike of foliation (Hansen, 1985, 1986a).

Other structures geometrically related to Le include 1) small-scale, open to isoclinal folds with axes parallel to Le and axial planes parallel to mylonitic foliation; and 2) mesoscopic fractures perpendicular to Le. These structures are most commonly observed in association with Le2; however, they are also locally preserved with Le1. Folds colinear with Le display no apparent preferred vergence, and they formed synchronously with mylonitization, apparently initiating with fold axes parallel to Le (Hansen, 1985, 1986a). Most importantly, these folds are not useful as kinematic indicators because they formed with their axes parallel to Le.

Valid kinematic indicators must display fabric asymmetry within the motion plane of ductilely deformed rocks. A motion plane is that plane in a sheared rock which contains both the elongation lineation and the pole to foliation (Arthaud, 1969), and it allows us to consider, in three dimensions, the plane in which the movement of a shear zone may be viewed (Fig. 2).

Kinematics associated with Le1 and Le2 were studied in the field and in thin section. Useful kinematic indicators include: 1) S-C fabrics; 2) mica fish; 3) asymmetric quartz strain shadows; 4)

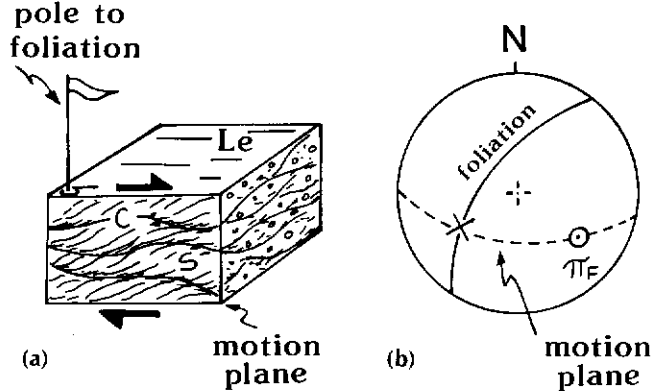


Figure 2. a) S and C planes (Berthe et al., 1979a), b) observed in "motion plane." b) Motion planes as plotted on a stereogram. Note that the motion plane is that plane which contains both Le and the pole to foliation (Arthaud, 1969).

quartz subgrain preferred orientations; 5) preferred orientation to quartz c-axes; and 6) asymmetric vergence of folds with axes normal to Le and axial planes approximately parallel to mylonitic foliation (Berthe et al., 1979a, b; Bouchez et al., 1983; Hanmer, 1982; Lister and Snoke, 1984; Simpson and Schmid, 1984). Megascopic and microscopic kinematic indicators associated with Le2 consistently record right-lateral, or top-to-the-north movement parallel to Le2. However, tectonic movement associated with Le1 is more complex: to the west, kinematic indicators consistently record west-side-down (normal) movement parallel to Le1; elsewhere, both reverse and normal movement are recorded (Fig. 3). It appears that thrust-style, or top-to-the-east, movement is dominant parallel to Le1 further to the east; however, a simple pattern of Le1 kinematics has not yet emerged from the present data. In general, Le1 and Le2 are interpreted to record dip-slip and strike-slip movement, respectively. Le1 and Le2 are associated with the same metamorphic mineral assemblages and formed under similar metamorphic conditions. Therefore it appears that the structural-tectonic environment changed during the formation of Le1 and Le2, although the metamorphic environment remained essentially the same.

Megascopic and microscopic structural relations constrain the relative timing of Le1 and Le2 formation locally. The relative timing between Le1 and Le2 are inferred from: 1) Le1 deformed around folds whose axes are colinear with Le2; 2) rotation of quartz pressure shadows on euhedral pyrite cubes within the plane of the foliation (Fig. 4); 3) the observation that Le2 is locally much more strongly developed than Le1; and 4) strained quartz grains and subgrains associated with Le2 appear to be less annealed than those fabrics associated with Le1. Generally, Le1 can be shown to pre-date Le2 at specific locations where they either occur together, or where Le1 is mapped into regions containing Le2. It is possible that Le1 remained active in one region while Le2 was beginning to form elsewhere. The author interprets the intimate spatial relationship between Le1 and Le2, the similarity in associated metamorphic mineral assemblages, and the similar structural style of Le1 and Le2 to indicate that Le1 and Le2 formed in a similar geologic environment and therefore were probably not separated by a distinct break in time. Le1 probably formed predominantly before Le2, but changes in the regional tectonic regime perhaps led first to a period during which both Le1 and Le2 formed simultaneously, and finally to the cessation of Le1 formation and solely formation of Le2.

The geographic distribution of Le1 and Le2 as mapped in the field outlines distinct structural domains. These domains are most easily illustrated in a diagram of motion planes throughout the study area. A regional plot showing trends of elongation lineations does not distinguish the structural domains because the dip of foliation is near vertical in the west and decreases significantly to the east, and the orientation of the foliation is not considered in such a projection. It is therefore necessary to plot the motion planes associated with Le1 and Le2 in order to consider the three dimensional orientation of the lineations. Stereoplots of poles to motion

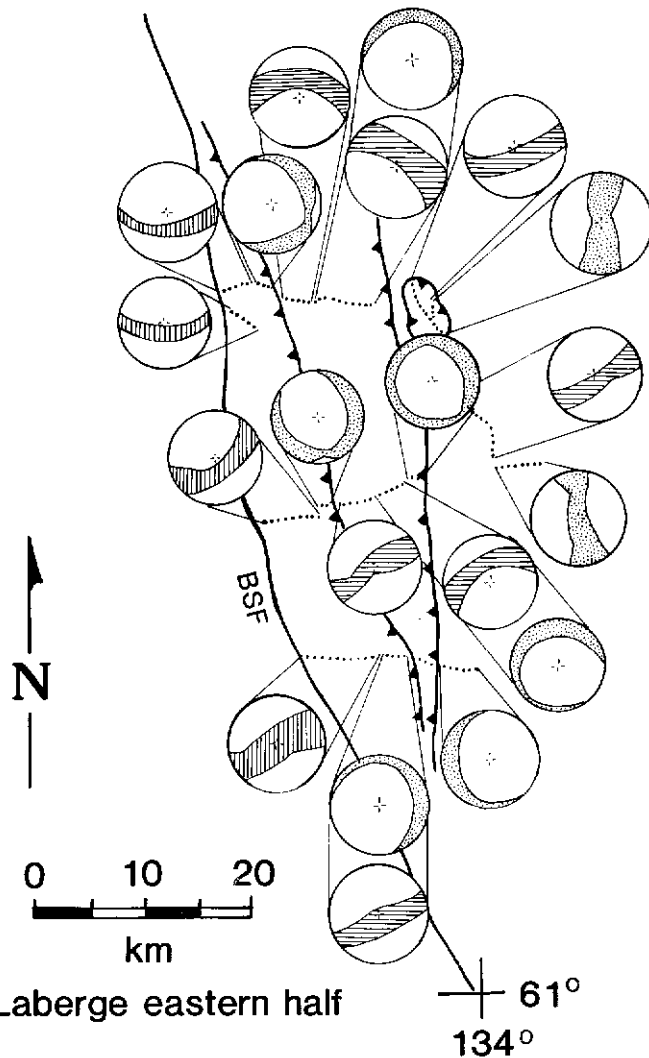


Figure 3. The distribution of Le1 and Le2 and their associated motion planes mark elongate structural domains parallel to the regional trend of the TSZ. Steeply-dipping, east-west-trending motion planes are associated with Le1 (lined pattern); whereas Le2 is associated with gently-dipping horizontal planes or north-south-trending vertical planes (stippled pattern). Pattern girdles on stereoplots represent all motion planes. Horizontally lined pattern indicated normal, or west-side-down movement within the motion planes parallel to Le1; vertically lined pattern indicates either/both normal and thrust-style (top-to-the-east) movement parallel to Le1 within the motion plane; and stippled pattern indicates right-lateral or top-to-the-north movement parallel to Le2 within the motion plane.

planes and Le are plotted in Figure 3.

The domains are delineated by the presence of Le1 or Le2 and the orientation of their associated motion planes (Fig. 3). Motion planes associated with Le1 are steep east-west-striking planes, whereas motion planes associated with Le2 are either subhorizontal, gently-dipping planes, or nearly vertical, north-south-oriented planes depending on the local orientation of foliation. Alternating zones of fabrics dominated by Le1 and Le2 define several lensoidal structural domains elongated parallel to the regional trend of the TSZ. Three NNW-trending zones of Le2 separate domains of Le1 in the west to Le2 in the east vary from gradational to sharp. The domains of Le2 appear to correlate in a general way with lineaments defined by topographic lows. Based on timing relations outlined above, the distribution of Le2, and consistent right-lateral kinematics interpreted from Le2, it appears that the deformation which formed the Le2 fabrics occurred in a regional scale anastomosing shear zone which overprinted older Le1 deformation features and

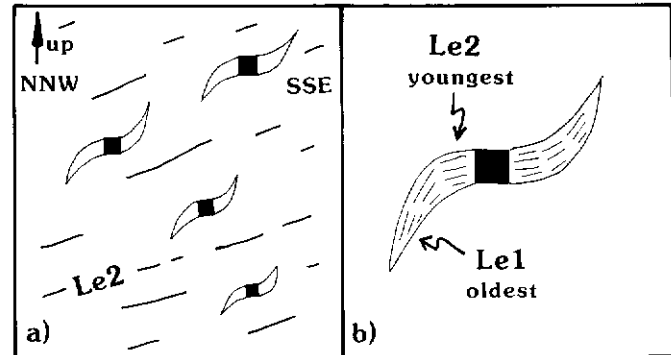


Figure 4. Quartz strain shadows on pyrite looking on to the plane of foliation of a carbonate-rich rock. Tails of strain shadows plunge steeply parallel to Le1; strain shadows closest to the pyrite cube plunge gently parallel to Le2. b) Timing is interpreted from the relative proximity of the quartz fibres to the pyrite cube. The youngest fibres form against the pyrite crystal (Choukroune, 1971). Hence Le2 post-dates Le1.

displaced TSZ rocks right-laterally along the ancient Mesozoic margin (Fig. 5).

Both allochthonous, or "suspect," and autochthonous rocks record Le1 and Le2 structures. The two western domains of Le1 are comprised of chiefly allochthonous rocks, or rocks of uncertain origin; however, the eastern domain comprises rocks which are autochthonous with respect to North America (Tempelman-Kluit, 1979; Erdmer, 1981, 1985), it displays metamorphic foliation and variably developed elongation lineations which are structurally continuous and consistent with TSZ geometries (Fig. 3). Therefore, rocks which are autochthonous with respect to North America have experienced at least a part of the same structural deformation and associated metamorphic history as rocks of the TSZ.

In conclusion, the TSZ forms the fundamental boundary between rocks deposited along the ancient margin of North America and allochthonous terranes to the west. Structurally, this boundary is a transpressional suture affecting both eastern autochthonous rocks and western allochthonous or "suspect" rocks. Rocks within the suture zone were deformed and simultaneously metamorphosed under upper-greenschist to amphibolite facies conditions during a changing structural-tectonic regime. Early collapse of an ocean basin to the west and collision of western allochthonous terranes is recorded by structures associated with Le1. Initial convergence occurred at a high angle to the western continental margin. With continued collision the tectonic regime changed from overall shortening to right-lateral translation approximately parallel to the ancient margin as recorded in the transition from Le1 to Le2.

FUTURE WORK

Rb-Sr whole-rock and mineral dating, to be carried out at the University of British Columbia, should allow the author to place metamorphic and deformation episodes in a quantitative time frame. They may, for instance, enable a chronological distinction of dominantly compressional-age tectonics, Le1, from translation-age tectonics, Le2; or such data may indicate that conclusions with respect to the intimate timing of Le1 and Le2 are incorrect, and in fact that these two lineations may represent distinctly different deformational events. Such time constraints would greatly constrain models of early Mesozoic Cordilleran evolution. Establishment of a quantitative time frame coupled with interpreted P-T constraints may also allow construction of P-T-time paths.

ACKNOWLEDGEMENTS

This project received support from the Exploration and Geological Services Division of the Department of Indian Affairs and Northern Development, Whitehorse, Yukon and National Science Foundation Grant EA-85-07953 to W.G. Ernst and V.L. Hansen. I thank Dan Spencer for field assistance and company in 1984, and thank Heidi Eigel for her undefeatable spirit during the 1985 season. Discussions with P. Choukroune, J.M. Christie, P.

Erdmer, W.G. Ernst, J. Goodge, and B. Hanson have contributed tremendously in the form of discussion to the ideas presented in this paper. Thanks to Ram Alkaly for prolific and careful thin section preparation. John Goodge greatly improved the manuscript.

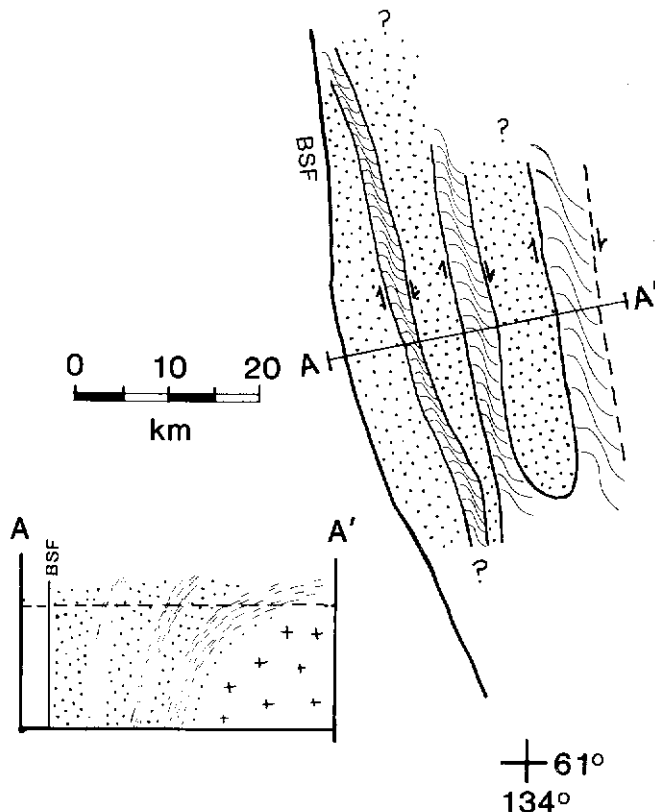


Figure 5. Elongate structural domains are marked by alternating zones of Le1 (dotted pattern) and Le2 (shear pattern). Zones of Le1 record early tectonic shortening overprinted by zones of Le2 which form a regional-scale anastomosing shear zone. Zones of Le2 consistently record right-lateral or top-to-the-north movement parallel to Le2. Cross section displays flattening of foliation to the east and resultant top-to-the-north movement indicated by Le2 kinematic interpretations.

REFERENCES

- ALEINIKOFF, J., DUSEL-BACON, C., FOSTER, H.L., and FUTA, K., 1981. Proterozoic zircon from augen gneiss, Yukon-Tanana Upland, east-central Alaska; *Geology*, Vol. 9, p. 469-473.
- ANOVITZ, L.M. and ESSENE, E.J., 1982. Phase relations in the system $\text{CaCO}_3\text{-MgCO}_3\text{-FeCO}_3$; *Eos*, Vol. 63, p. 464.
- ARTHAUD, F., 1969. Méthode de détermination graphique des directions de recouvrement d'allongement et intermédiaire d'une population de failles; *Société Géologique de France, Bulletin*, Vol. 11, p. 729-737.
- BELL, T.H. and ETHERIDGE, M.A., 1973. Microstructure of mylonites and their descriptive terminology; *Lithos*, Vol. 6, p. 337-348.
- BERTHE, D., CHOUKROUNE, P. and GAPAIS, D., 1979. Orientations préférentielles du quartz et orthogneissification progressive en régime cisailant: l'exemple du cisaillement sud-armoricain; *Bulletin de Minéralogie*, Vol. 102, p. 265-272.
- BERTHE, D., CHOUKROUNE, P. and JEGOUZO, P., 1979. Orthogneiss, mylonite and noncoaxial deformation of granite: the example of the South Armorican shear zone; *Journal of Structural Geology*, Vol. 1, p. 31-42.
- BOSTOCK, H.S. and LESS, E.J., 1961. Laberge map-area, Yukon; *Geol. Surv. Can., Memoir* 217, 31 p.
- BOUCHEZ, J.L., NANTES, LISTER, G.S. and NICOLAS, A., 1983. Fabric asymmetry and shear sense in movement zones; *Geologische Rundschau*, Vol. 72, p. 401-419.
- CHOUKROUNE, P., 1971. Contributions à l'étude des mécanismes de la déformation avec schistosité grâce aux cristallisations syncinétiques dans les "zones abritées" ("pressure shadows"); *Bulletin de la Société Géologique de France*, Vol. 7, p. 257-271.
- ERDMER, P., 1981. Comparative studies of cataclastic allochthonous rocks in McQuesten, Laberge and Finlayson Lake map area; in *Yukon Geology and Exploration 1979-80*, Dept. Ind. Aff. Nor. Dev., Whitehorse, Yukon, p. 60-64.
- ERDMER, P. and HELMSTAEDT, H., 1983. Eclogite from central Yukon: a record of subduction at the western margin of ancient North America; *Canadian Journal of Earth Sciences*, Vol. 20, p. 1389-1408.
- FERRY, J.M. and SPEAR, F.S., 1978. Experimental calibration of the partitioning of Fe and Mg between biotite and garnet; *Contributions to Mineralogy and Petrology*, Vol. 66, p. 113-117.
- GABRIELSE, H., TEMPELMAN-KLUIT, D.J., BLUSSON, S.L. and CAMPBELL, R.B., 1980. Macmillan River, Yukon - District of Mackenzie - Alaska Sheet 105, 115; *Geol. Surv. Can., Map* 1398B, 1:1,000,000 scale.
- GRAHAM, C.M. and POWELL, R., 1984. A garnet-hornblende geothermometer: calibration, testing, and application to the Pelona Schist, southern California; *Journal of Metamorphic Geology*, Vol. 2, p. 13-31.

- GREEN, T.H. and HELLMAN, P.L., 1982. Fe-Mg partitioning between coexisting garnet and phengite at high pressure, and comments on a garnet-phengite geothermometer; *Lithos*, Vol. 15, p. 253-266.
- HANMER, S.K., 1982. Microstructure and geochemistry of plagioclase and microlite in naturally deformed granite; *Journal of Structural Geology*, Vol. 4, p. 197-213.
- HANSEN, V.L., 1986a. Preliminary structural and kinematic analysis of mylonitic rocks of the Teslin suture zone, 105 E, Yukon; in *Yukon Geology 1984-85*, Dept. Ind. Aff. Nor. Dev., Whitehorse, Yukon, this volume.
- HANSEN, V.L., 1986b. Petrotectonic study of the Teslin suture zone, Yukon, Canada; Geological Society of America, Abstracts with Programs, submitted.
- HANSEN, V.L., 1985. Structural analysis of mylonitic rocks in the Teslin suture zone, Yukon; Geological Society of America, Abstracts with Programs, Vol. 17, p. 359.
- HODGES, K.V. and SPEAR, F.S., 1982. Geothermometry, geobarometry and the Al_2SiO_5 triple point at Mt. Mooselauke, New Hampshire; *American Mineralogist*, Vol. 67, p. 1118-1134.
- KROUGH, E.J. and RAHEIM, A., 1978. Temperature and pressure dependence of Fe-Mg partitioning between garnet and phengite, with particular reference to eclogites; *Contributions to Mineralogy and Petrology*, Vol. 66, p. 75-80.
- LISTER, G.S. and SNOKE, A.W., 1984. S-C Mylonites; *Journal of Structural Geology*, Vol. 6, p. 617-638.
- METCALFE, P. and CLARK, G.S., 1983. Rb-Sr whole rock age of the Klondike Schist, Yukon Territory; *Canadian Journal of Earth Sciences*, Vol. 20, p. 886-891.
- MONGER, J.W.H., 1977. Upper Paleozoic rocks of the western Canadian Cordillera and their bearing on Cordilleran evolution; *Canadian Journal of Earth Sciences*, Vol. 14, p. 1832-1859.
- MORTENSEN, J.K., 1985. Field relationships, U-Pb ages, and correlation of meta-igneous rocks in the Klondike District, Yukon-Tanana terrane, west-central Yukon Territory; Geological Society of America, Abstracts with Programs, Vol. 17, p. 37.
- MORTENSEN, J.K. and JILSON, G.A., 1985. Evolution of the Yukon-Tanana terrane: Evidence from south-eastern Yukon Territory; *Geology*, Vol. 13, p. 806-810.
- POWELL, R., CONDLIFFE, D.M. and CONDLIFFE, E., 1984. Calcite-dolomite geothermometry in the system $\text{CaCO}_3\text{-MgCO}_3\text{-FeCO}_3$: an experimental study; *Journal of Metamorphic Geology*, Vol. 2, p. 33-41.
- RODDICK, J.A., 1967. Tintina Trench; *Journal of Geology*, Vol. 75, p. 23-33.
- SIBSON, R.H., 1977. Fault rocks and fault mechanisms; *Journal of Geological Society of London*, Vol. 133, p. 191-213.
- SIMPSON, C., and SCHMID, S.M., 1984. An evaluation of the sense of movement in sheared rocks; *Geological Society of America Bulletin*, Vol. 94, p. 1281-1288.
- STEVENS, R.D., DELABIO, R.N. and LACHANCE, G.R., 1982. Age determination and geological studies: K-Ar isotopic ages, report 15; *Geol. Surv. Can., Paper 81-2*, 56 p.
- TEMPELMAN-KLUIT, D.J., 1979. Transported cataclasite, ophiolite and granodiorite in Yukon: Evidence of arc-continent collision; *Geol. Surv. Can., Paper 79-14*, 27 p.
- TEMPELMAN-KLUIT, D.J., 1978a. Reconnaissance geology, Laberge map area, Yukon; in *Current Research, Part A, Geol. Surv. Can., Paper 78-1A*, p. 61-66.
- TEMPELMAN-KLUIT, D.J., 1978b. Laberge (105 E) map area, Yukon; *Geol. Surv. Can., Open File 578*.
- TEMPELMAN-KLUIT, D.J., 1977. Quiet Lake (105 F) and Finlayson Lake (105 G) map areas, Yukon; *Geol. Surv. Can., Open File 486*.
- TEMPELMAN-KLUIT, D.J., 1970. An occurrence of eclogite near Tintina Trench, Yukon; in *Report of Activities, Part B, Geol. Surv. Can., Paper 70-1B*, p. 19-22.
- TEMPELMAN-KLUIT, D.J., and WANLESS, R.K., 1980. Zircon ages for the Pelly Gneiss and Klotassin granodiorite in western Yukon; *Canadian Journal of Earth Sciences*, Vol. 17, p. 297-306.
- WHEELER, J.O., GREEN, L.H. and RODDICK, J.A., 1960. Finlayson Lake, Yukon Territory; *Geol. Surv. Can., Map 8-1960*.

STRATIGRAPHY AND ECONOMIC POTENTIAL OF PRECAMBRIAN-CAMBRIAN BOUNDARY STRATA, WERNECKE MOUNTAINS, EAST-CENTRAL YUKON

D.T. Osborne, G.M. Narbonne and J. Carrick
Department of Geological Sciences
Queen's University
Kingston, Ontario

OSBORNE, D.T., NARBONNE, G.M. and CARRICK, J., 1986. Stratigraphy and economic potential of Precambrian-Cambrian boundary strata, Werneck Mountains, east-central Yukon; in Yukon Geology, Vol. 1; Exploration and Geological Services Division, Yukon, Indian and Northern Affairs Canada, p. 131-138.

INTRODUCTION

Precambrian-Cambrian boundary strata of the Werneck Mountains east-central Yukon, comprise a succession of alternating carbonate and siliciclastic units (Eisbacher, 1981; Narbonne et al., 1985). To date only minor showings of economic minerals have been found in the siliciclastic units, but significant zinc-lead deposits have been described from carbonate strata (eg. Dawson, 1975; Reeve, 1977). Most of these deposits are hosted by an unnamed Upper Proterozoic dolostone unit (map-unit 11 of Blusson, 1971), or by Lower Cambrian carbonates of the Sekwi Formation.

During the summer of 1984, five composite sections were measured in the Corn Creek/Goz Creek area on the southeastern edge of the Werneck Mountains (Fig. 1). Lithostratigraphic, biostratigraphic and sedimentological studies of the entire Precambrian-Cambrian boundary succession were carried out in order to determine the depositional history and mineral potential. This report will focus on the uppermost Proterozoic (map-unit 11) and lowermost Cambrian (Vampire Formation) units, with only brief description of earlier units.

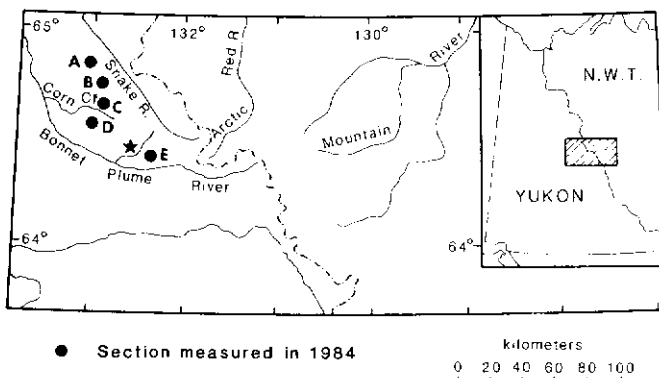


Figure 1. Location map

The study area lies on the extreme southern edge of the Yukon Stable Block (Jeletzky, 1962; Lenz, 1972), a site of predominantly shallow-water sedimentation throughout most of the Late Proterozoic and Early Paleozoic. The uppermost Proterozoic and lowermost Cambrian rocks described in this report occur southwest and south of the Mackenzie and Ogilvie Arches respectively, and were either never deposited, or are no longer preserved north and east of these arches. To the south of the study area, the shallow-water siliciclastics and carbonates pass into the deep-water shales and turbiditic conglomerates of the basinal "Grit Unit" (Gordey, 1980; Aitken, in press).

STRATIGRAPHIC FRAMEWORK

The stratigraphic section at locality D (Fig. 2) is representative of the Upper Proterozoic and Lower Cambrian stratigraphy in the southeastern Werneck Mountains. The uppermost (Cambrian) units have been formally named, but nomenclature in the lower part of the section (Upper Proterozoic) remains informal.

Upper Proterozoic strata comprise alternating units of recessive siltstone and resistant dolostone. The description and correlation of these units has been discussed by Fritz et al. (1983).

1984), Aitken (1984) and Narbonne et al. (1985). The uppermost Proterozoic unit, map-unit 11, is a resistant dolostone recognized by Blusson (1971) in the Sekwi Mountain area and traced north into the Werneck Mountains by Fritz (1982) and Fritz et al. (1983).

The basal Cambrian unit, the Vampire Formation, was first determined by Fritz (1982) for a recessive unit of siltstone and fine sandstone in the Mackenzie Mountains. Fritz et al. (1983) extended the formation name into the Werneck Mountains, and suggested that the Precambrian-Cambrian boundary lay at, or near the base of the Vampire Formation in this area. Aitken (1984) pointed out that the Vampire Formation of the Werneck Mountains exhibits features transitional between the type Vampire Formation and the type Backbone Ranges Formation, but Fritz et al. (1984) defended the continued use of the term "Vampire Formation" in the Werneck Mountains.

UNNAMED DOLOSTONE AND SILSTONE UNITS

These strata comprise the "Sheepbed Carbonate," unnamed dolostone and three unnamed siltstone units (Fig. 2). Very few prospects were observed. Faults and fractures in a thick-bedded quartzarenite in unnamed siltstone unit 2 (Fig. 2) along a small creek 2 km east of section D (Fig. 1) are heavily mineralized with pyrite. Extensive karst breccias occur in the "Sheepbed

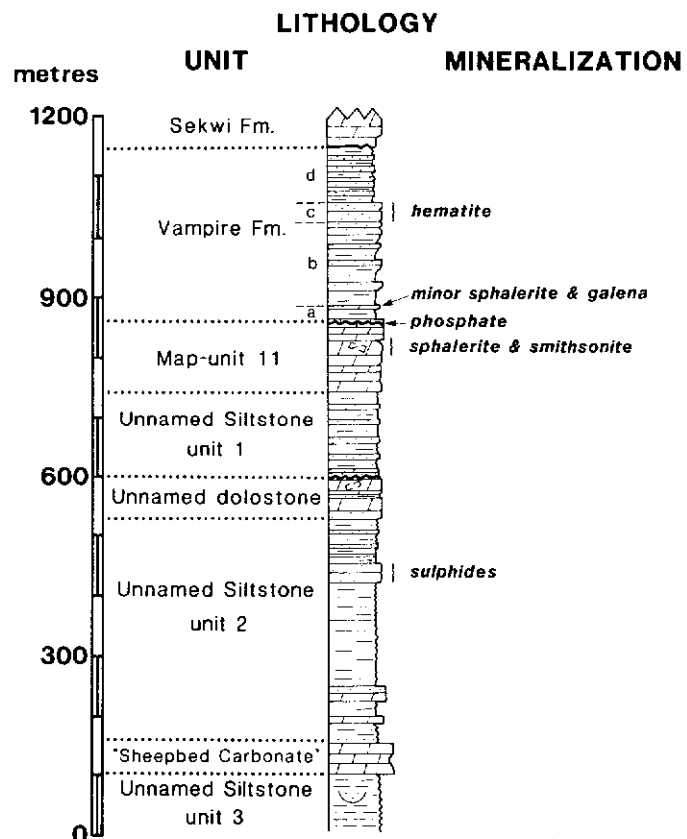


Figure 2. Upper Proterozoic and Lower Cambrian strata at locality D. Lithologic data from Narbonne et al. (1985, Fig. 71.3) and Fritz et al. (1983, Fig. 44.2a).

Carbonate" at locality A (Aitken, 1984) and in the unnamed dolostone unit at localities A and D, but no associated sulphides were noted.

MAP-UNIT 11

Description

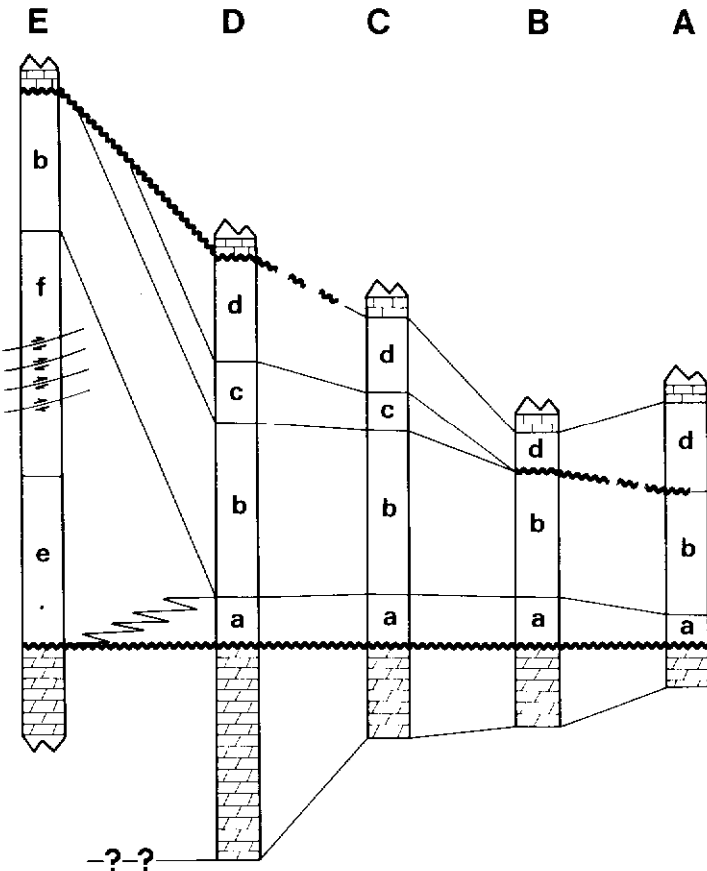
Map-unit 11 consists predominantly of medium- to very thick-bedded dolostone with some siltstone, limestone and dolostone breccia near the top. It is light grey to grey-buff, and weathers with a distinctive orange-pink hue. Extensive dolomitization has obliterated most primary sedimentary structures, but secondary features such as vugs and horizontal stylolites are common. The dolostone is finely to coarsely crystalline with 1-2% quartz, most of it authigenic. Porosity is generally less than 2% and is partially occluded by bitumen. Finely disseminated, intercrystalline pyrite comprises less than 1% of the rock.

Various lines of evidence suggest that the upper surface of map-unit 11 represents a significant disconformity:

- 1) Small shelly fossils (eg. *Protohertzina anabarica*) and Cambrian-type complex burrows (*Phycodes pedum*) occur immediately above the contact in the Wernecke Mountains (Fritz et al., 1983; Nowlan et al., 1985), whereas they occur several hundred metres above the contact in the June Lake area to the southeast (Fritz, 1980; Aitken, 1984).
- 2) The thickness of map-unit 11 decreases northward from 151 m at locality D to 29 m at locality A (Fig. 3). This trend is typical of several disconformities in the area, which progressively bevel older strata onto the Mackenzie and Ogilvie Arches (eg. Aitken, 1982).
- 3) The upper contact of map-unit 11 is extremely sharp and exhibits at least minor relief at most localities.
- 4) Patchy development of phosphatic coatings and breccia-filled, solution-enlarged fractures (Fig. 6) on the upper contact attest to a prolonged period of chemical action on the lithified surface.

South

Sections



5) Dolostone breccias occur near the upper contact of map-unit 11 at localities D and E (Figs. 4, 5). Breccias occur as irregular tabular, pod-shaped and columnar bodies up to 55 m thick. The breccia is composed of pebble- to cobble-sized, predominantly subangular clasts of grey dolostone cemented by dolomite and lesser quartz, sulphides and hematite. Shapes of the breccia bodies (Fig. 4), their consistent association with disconformities (Fig. 4), and the local occurrence of breccia-filled, solution-enlarged fractures (Figs. 4, 6) are indicative of a karstic origin.

This disconformity occurs at the top of map-unit 11 in all sections studied (Fig. 3), and can be traced into the Mackenzie Mountains (Fritz et al., 1984, Fig. 44.2). In addition, two local disconformities (each characterized by erosional relief, phosphatic coatings, and dolostone breccias) occur in the upper part of map-unit 11 at section D (Fig. 4).

Depositional Model

Although primary sedimentary structures are poorly preserved, the presence of planar cross-lamination, scourcs and beds of flat-pebble conglomerate suggest that deposition occurred on a shallow carbonate shelf. The presence of desiccation cracks and karstic erosion surfaces in the upper part of the unit indicates intermittent subaerial exposure. The disconformity at the top of the unit may be related to a global regression that occurred in the lastest Precambrian (cf. Brasier, 1982).

Economic Potential

Fritz et al. (1983) first noted that the Goz zinc deposit is hosted by map-unit 11. At the Goz deposit, ten drill intersections have proven almost 2 million tonnes of zinc in 18% protore with a total potential of 5 million tonnes of 13% zinc or better. Reeve (1977) noted the association of the mineralization with breccia zones within the thick-bedded dolostone. The Goz zinc deposit can be regarded as a Mississippi Valley type deposit, but contains more smithsonite ($ZnCO_3$) and silicified dolostone than is typical of most of this type of deposit (Reeve, 1977).

North

LEGEND

- Sekwi Fm. – Fossiliferous carbonate
- f Vampire Fm. – Siltstone facies
- e Vampire Fm. – Siltstone/Arenite facies
- d Vampire Fm. – Siltstone/Wacke facies
- c Vampire Fm. – Hematitic facies
- b Vampire Fm. – Coarsening upwards facies
- a Vampire Fm. – Shale/Dolostone facies
- Map unit 11 – Blocky dolostone
- Fault – Repeated section

60
30
0
Vertical Scale
in metres

Figure 3. Lithofacies and correlation of map-unit 11 and the Vampire Formation.

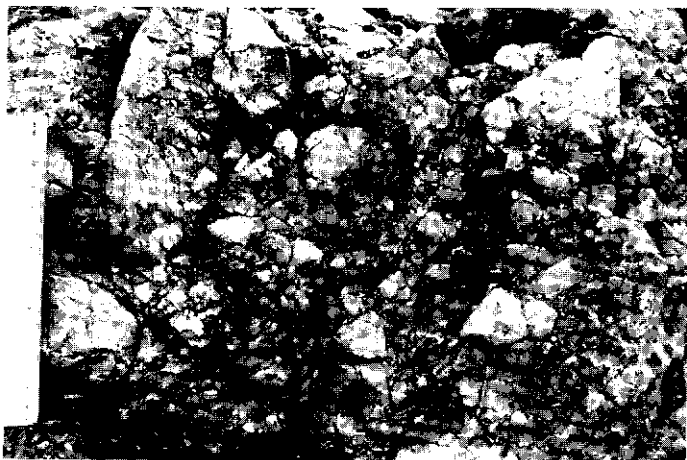


Figure 4. Mineralized dolostone breccia in map-unit 11 at Section E.

Similar mineralized breccias were identified by Fritz et al. (1983) at sections D and E. Investigation in the summer of 1984 allowed us to typify these deposits and to determine a common paragenetic history. Brief examination of the Goz zinc deposit confirmed that it is similar to the deposits at sections D and E, but is considerably more silicified.

At section E, the uppermost 10-55 m of map-unit 11 consists predominantly of well-indurated, dolomite breccia that overlies thick-bedded dolostone with a sharp, but highly irregular contact (Fig. 5a). The thick-bedded dolostone exhibits several high angle, low displacement normal faults, and numerous quartz and galena-filled fractures. Dolomite, quartz, galena, sphalerite and smith-

sonite occur as void-filling cements between clasts in the dolostone breccia.

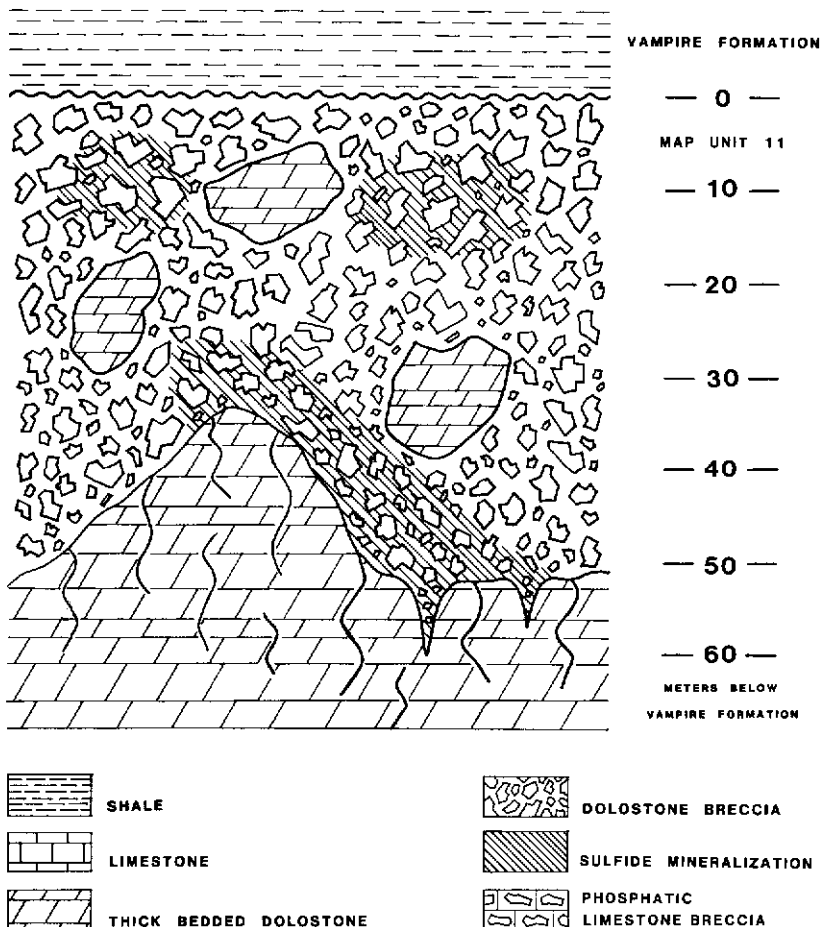
At section D, pod-shaped and columnar breccia bodies 5-20 m deep occur beneath disconformities at two levels in the upper part of map-unit 11 (Fig. 5b). Breccias are poorly indurated, and spaces between clasts are partially cemented by dolomite, quartz and hematite (secondary after pyrite). Quartz-filled fractures occur in both the thick-bedded dolostone and the breccia.

Analyses of thin sections and polished sections from localities D and E and hand samples from the Goz deposit suggest that a common paragenetic sequence typifies these deposits. Differences in the type and abundance of sulphide minerals in the three areas probably reflect local variations in the duration and intensity of particular diagenetic processes. A complete description of the paragenetic history of these deposits will be presented elsewhere, but our major conclusions are summarized below.

Mineralization occurred as part of a complex paragenetic sequence that took place in telogenetic (under influence of meteoric waters) and mesogenetic (deep subsurface) diagenetic environments (terminology after Choquette and Pray, 1970). Early telogenetic processes included dolomitization, karstic dissolution, and cementation by zoned dolomite and (?) calcite. The apparent absence of shale in the breccias of map-unit 11 suggests that at least the upper part of the breccia was cemented prior to the deposition of the overlying Vampire Formation. Following burial, the pores were reopened by dissolution of much of the zoned dolomite and all of the (?) calcite cementing the clasts. Bitumen, quartz, sulphides (galena, sphalerite and pyrite), sparry dolomite and saddle dolomite subsequently migrated and precipitated in the reopened pore spaces (Figs. 7, 8). Later uplift associated with the Laramide Orogeny resulted in fracturing and formation of smithsonite (Fig. 9) in a telogenetic setting (cf. Sangster, 1975).

Despite examination of map-unit 11 at a number of localities

SECTION E



SECTION D

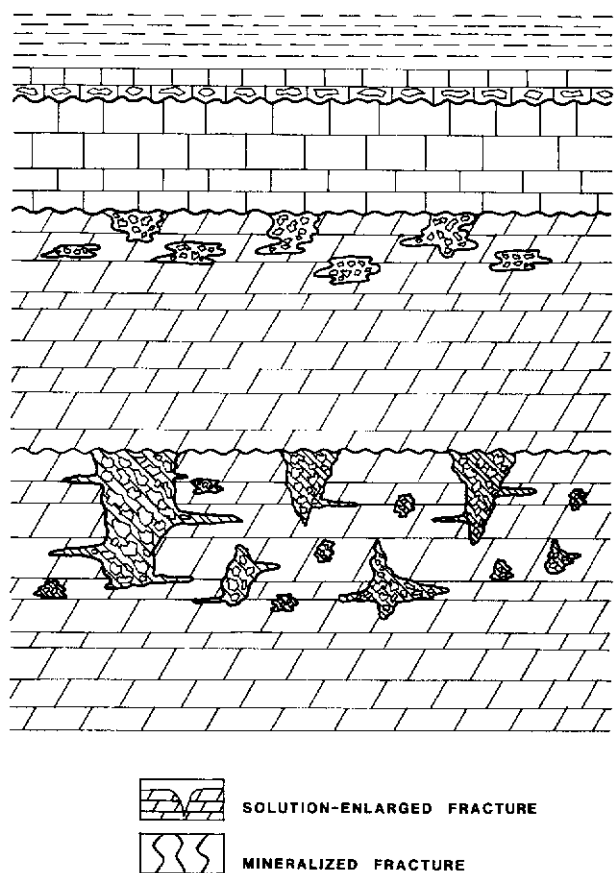


Figure 5. Occurrence of breccias in map-unit 11 and the basal Vampire Formation. 5a — Section E; 5b — Section D.



Figure 6. Breccia-filled, solution enlarged fracture in thick-bedded dolostone of map-unit 11. Locality E.

in the Wernecke Mountains (Fig. 1), lead and zinc mineralization has thus far been observed only in the southernmost sections adjacent to the deeper-water shales. This appears to be related to two factors:

- 1) Most Mississippi Valley type deposits in the Canadian Cordillera are located at or near a platform margin adjacent to a shale basin (Macqueen, 1976), possibly because these shales acted as a source for the metal ions (cf. Jackson and Beales, 1967).
- 2) Although map-unit 11 shows evidence of extensive pre-Vampire erosion in all sections studied (Fig. 3), karstic breccias have thus far been observed only in the southernmost sections.

VAMPIRE FORMATION

Description

In the study area, the Vampire Formation consists predominantly of sandstone, siltstone and shale with subordinate carbonate. The formation ranges in thickness from 150.5 m at section B to 392.1 m at section E, and can be subdivided into six lithofacies (Figs. 3, 10).

The Shale/Dolostone Facies (Facies "a") consists predominantly of recessive, grey-black shales and subordinate, resistant, orange-buff weathering dolostones. This basal Vampire facies disconformably overlies map-unit 11 in sections A, B, C and D. The thin- to medium-bedded dolostones of the facies are typically silty and commonly exhibit relict structures of intraclasts and ooids. Sedimentary structures, including parallel lamination, small-scale planar cross-lamination and hardgrounds are common in the dolostones. A thin- to thick-bedded arenite near the top of the facies exhibits a variety of sedimentary structures including parallel lamination and cross-lamination. Phosphate occurs at the base of the shale/dolostone facies in section D, and is commonly associated with stromatolites and thrombolites. The shale/dolostone facies contains numerous complex Cambrian trace fossils such as *Cruziana*, *Rusophycus* and *Phycodes pedum* (Nowlan et al., 1985); these trace fossils are typical of Seilacher's (1967) *Cruziana* ichnofacies. The presence of flat pebble conglomerates, desiccation cracks and evaporite pseudomorphs in the phosphatic dolomitic limestone suggests periodic emergence of the basal facies. The overlying thrombolite mounds suggest a deepening to a subtidal environment. The intraclasts and ooids of

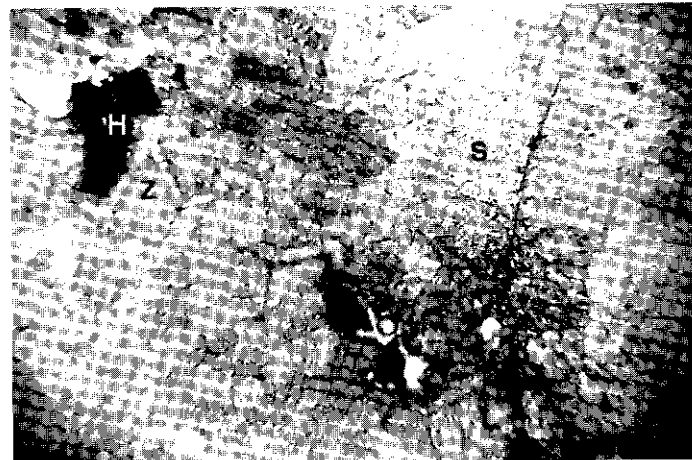


Figure 7. Void fill in dolostone breccia at Section D. Zoned dolomite (Z) shows evidence of partial dissolution. Later cements are hematite (H) and saddle dolomite (S). Hematite occurs as cubic pseudomorphs of pyrite crystals. Field of view is 4 mm.

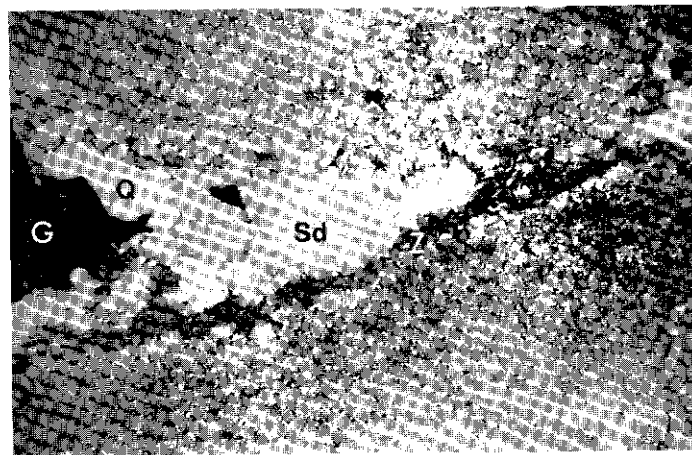


Figure 8. Void fill in dolostone breccia at Section E. Zoned dolomite (Z) shows evidence of partial dissolution. Later cements are quartz (Q), sparry dolomite (Sd) and galena (G). Field of view is 10 mm.

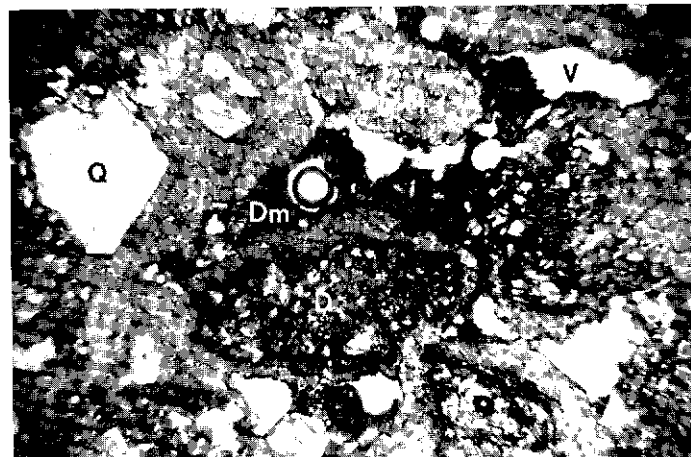


Figure 9. Late telogenetic features in dolostone breccia at Section E. Smithsonite cement (Sm) lines quartz crystals (Q) and remnant corroded dolomite (Dm). Note abundant detrital material (Dm) and secondary porosity (V). Field of view is 4 mm.

the dolostones of the facies suggest energetic conditions, whereas the shales of the facies were probably deposited during calmer periods. These features collectively suggest that, except for the basal transgressive deposits, offshore subtidal conditions prevailed throughout deposition of most of the shale/dolostone facies.

The Coarsening-Upward Facies (Facies "b") consists of arenites, grey siltstones and grey, laminated shales deposited in numerous coarsening-upward cycles 5 to 25 m thick (Fig. 11). The thin- to thick-bedded arenites contain sedimentary structures including parallel lamination, planar cross-lamination, trough cross-lamination, load structures, and hummocky cross-stratification. Graded beds occur rarely in basal portions of the coarsening-upwards facies. Trace fossils are common, and include representatives of the Skolithos and Cruziana ichnofacies of Seilacher (1967). The coarsening-upward cycles of this facies represent shallowing of the depositional environment, with the shales and siltstones deposited under lower energy conditions and the arenites deposited in an energetic environment. The presence of load structures suggests a higher sedimentation rate and sediment instability. Abundant wave-produced structures suggest a wave and/or storm dominated depositional setting, with graded beds most likely representing storm deposits. Deposition probably occurred under predominantly nearshore conditions.

The Hematitic Facies (Facies "c") consists of medium- to thick-bedded, hematite-cemented sublitharenite. This facies is present only in sections C and D, but apparently was removed by erosion at section B and possibly A. Most beds are apparently structureless, with only rare parallel lamination and planar cross-lamination. Simple trace fossils occur very rarely in thin siltstone interbeds. These fossils are indicative of a marine-influenced environment, but further work is necessary to determine the precise depositional setting.

The Siltstone/Wacke Facies (Facies "d") consists of grey-brown siltstones and subordinate, thin- to medium-bedded, grey

matrix-rich arenites and wackes. This facies is present in sections A, B, C and D. The wackes and arenites exhibit a variety of relatively small-scale sedimentary structures including parallel lamination, low angle planar cross-lamination, and symmetric ripple marks. Trace fossils are common; most are typical of the Cruziana ichnofacies (Fig. 12), but representatives of the Skolithos and Zoophycos ichnofacies occur rarely. The dominance of siltstone also suggests deposition under relatively quiet water conditions, possibly in an offshore subtidal environment.

Facies "e" and "f" are present only in section E, and consist mainly of dark grey siltstones (Fig. 3). The Siltstone/Arenite Facies (Facies "e") disconformably overlies map-unit 11 and contains subordinate amounts of very fine-grained, medium-bedded arenites with wavy bedding, parallel lamination and slumps. Trace fossils are mostly facies-crossing forms such as Cochlichnus and Didymaulichnus. The dominance of siltstones and horizontal trace fossils in Facies "e" suggests a relatively low energy environment. Slumps within the siltstone/arenite facies suggest deposition on a slope.

The Siltstone Facies (Facies "f") consists predominantly of resistant, medium- to very thick-bedded, dark grey siltstones (Fig. 13). These siltstones contain few sedimentary structures except for parallel lamination and slumps. Thin, graded beds of sandstone are a minor component of the facies. Trace fossils are extremely rare. The siltstones suggest a relatively low energy depositional environment, whereas the graded beds may represent turbidity current deposits or storm deposits. The presence of numerous slumps suggests sediment instability, perhaps due to rapid sedimentation on a slope.

Depositional Model

The distribution of facies in the Vampire Formation (Fig. 3) indicates that significant differences in depositional environment existed between areas A-D and area E.

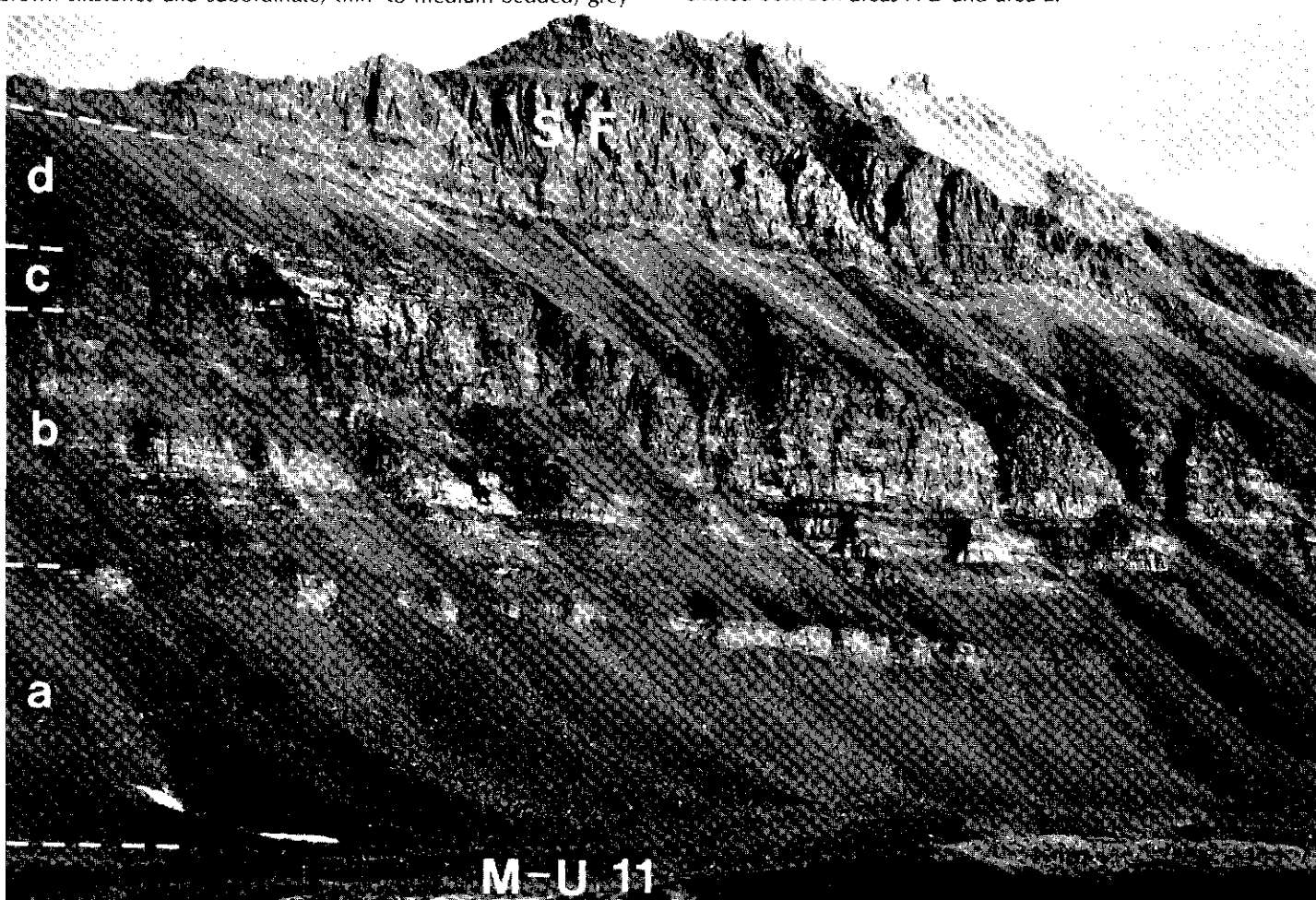


Figure 10. Lithofacies of the Vampire Formation at locality D. M-U 11 = map-unit 11; a = shale/dolostone facies; b = coarsening-upwards facies; c = hematitic facies; d = siltstone/wacke facies; S.F. = Sekwi Formation.



Figure 11. Typical coarsening upwards cycle in the Vampire Formation at locality B. The staff is 1.5 m long.

Areas A-D (Fig. 1) exhibit lithotypes and sedimentary structures typical of shallow shelf environments. This is supported by the trace fossil assemblage, which is dominated by representatives of the typically shallow marine *Skolithos* and *Cruziana* ichnofacies. In contrast, the time-equivalent thick siltstones and minor graded sandstones that characterize the lower two-thirds of section E lack shallow water features. Numerous load structures and slumps suggest rapid deposition on a slope. Trace fossils are rare and low in diversity, a feature typical of Cambrian deep-water environments (Crimes, 1974). This section shoals upward, and is capped by near-shore deposits of the coarsening-upwards facies. These relationships suggest that section E represents a deeper-water equivalent of sections A-D, possibly deposited in a prodelta or upper basin slope environment.

Economic Significance

A phosphatic limestone bed up to one m thick occurs at the base of the Vampire Formation at section D (Figs. 2, 5b). Phosphate occurs sporadically throughout the bed as hardground coatings, small shelly fossils, clasts, and clast coatings (Fig. 14), and locally comprises up to 40% of the bed (average 5%). Phosphate also occurs at the base of section B as thin hardground coatings. The phosphate probably originated as primary phosphate mud and as very early diagenetic replacement of carbonate. Phosphatic beds occur commonly in Precambrian-Cambrian boundary deposits, and are extensively mined in South America, Australia, Africa and Asia (Cook and Shergold, 1984).

Sulphide mineralization occurs sporadically in the basal facies of the Vampire Formation at section D (Fig. 2). Sphalerite, galena, quartz and dolomite occur as vug-fillings in oolitic and intraclastic dolostone. The sulphides are economically insignificant, but may provide some indication of the timing of sulphide mineralization in the Wernecke Mountains.

Detrital hematite grains constitute 1-2% of all facies of the Vampire Formation, but significant accumulations are restricted to the hematitic facies (facies "c") at localities C and D (Fig. 3). The

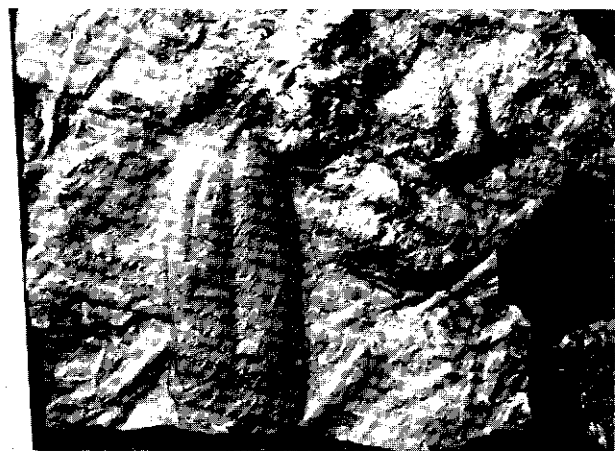


Figure 12. Trilobite trace fossils *Rusophycus* and *Cruziana* on a lower bedding surface in the siltstone/wacke facies of the Vampire Formation, locality D.



Figure 13. Siltstone facies of the Vampire Formation at locality E. Divisions on the staff are in decimeters.

hematitic facies is up to 45 m thick, and contains 30-40% hematite by volume. Poorly developed, centimetre-scale banding of iron-rich and iron-poor layers occur sporadically, but much of the facies is structureless. The hematite is black and aphanocrystalline; it occurs both between grains and as a grain-replacement. The apparent absence of chert and magnetite, the poor development of banding, and the abundance of siliciclastic detritus distinguish these Lower Cambrian deposits from typical Precambrian iron formations, whereas the absence of goethite and oolitic textures distinguishes them from typical Phanerozoic ironstones. The economic potential of the Vampire hematite deposits is enhanced by their proximity to massive iron deposits in the Rapitan Group near the headwaters of the Snake River to the north (cf. Green and Godwin, 1962).

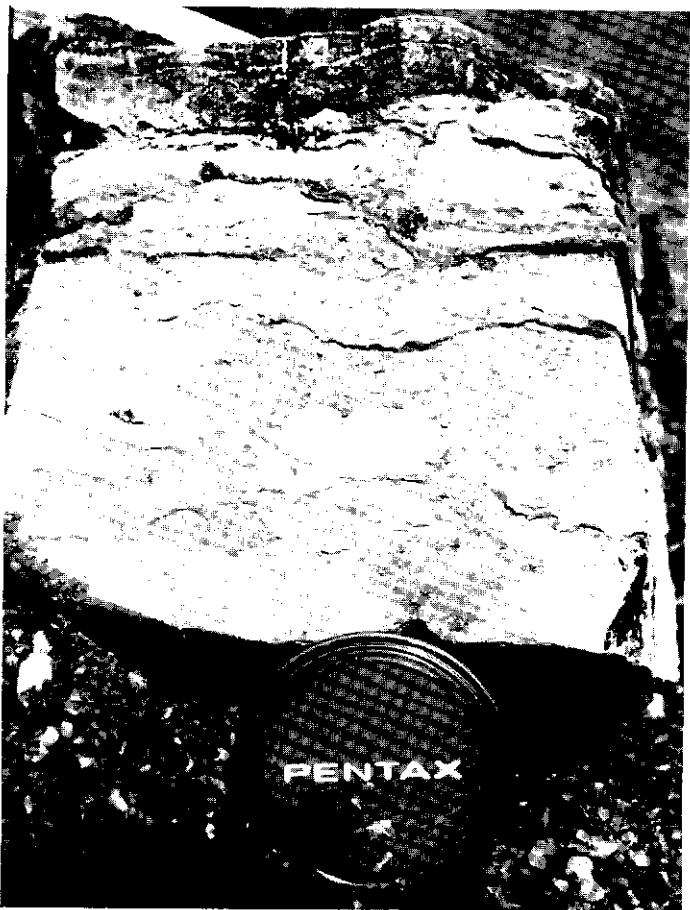


Figure 14. Abundant phosphate in limestone breccia at the base of the Vampire Formation, locality D. Phosphate (black) occurs as small grains, clast-coatings and as a laminated hardground coating (top of photo).

REFERENCES

- AITKEN, J.D., 1982. Precambrian of the Mackenzie Fold Belt — A stratigraphic and tectonic overview; in Hutchinson, R.W. et al., (eds.), *Precambrian Sulphide Deposits*, Geological Association of Canada, Special Paper 25, p. 149-161.
- AITKEN, J.D., 1984. Strata and trace fossils near the Precambrian - Cambrian boundary, Mackenzie, Selwyn and Wernecke Mountains, Yukon and Northwest Territories: Discussion; Geol. Surv. Can., Paper 84-1B, p. 401-407.
- AITKEN, J.D., in press. Uppermost Proterozoic formations in central Mackenzie Mountains, N.W.T.; Geol. Surv. Can., Paper.
- BLUSSON, S.L., 1971. Sekwi Mountain map-area, Yukon Territory and District of Mackenzie; Geol. Surv. Can., Paper 71-22, 17 p.
- BRASIER, M.D., 1982. Sea-level changes, facies changes and the Late Precambrian - Early Cambrian evolutionary explosion; *Precambrian Research*, Vol. 17, p. 105-123.
- CHOQUETTE, P.W. and PRAY, L.C., 1970. Geologic nomenclature and classification of porosity in sedimentary carbonates; American Association of Petroleum Geologists, Bulletin 54, p. 207-250.
- COOK, P.J. and SHERGOLD, J.H., 1984. Phosphorous, phosphorites and skeletal evolution at the Precambrian - Cambrian boundary; *Nature*, Vol. 308, p. 231-236.
- CRIMES, T.P., 1974. Colonisation of the early ocean floor; *Nature*, Vol. 248, p. 328-330.
- DAWSON, K.M., 1975. Carbonate-hosted zinc-lead deposits of the northern Canadian Cordillera; Geol. Surv. Can., Paper 75-1A, p. 239-242.
- EISBACHER, G.H., 1981. Sedimentary tectonics and glacial record in the Windermere Supergroup, Mackenzie Mountains, Northwestern Canada; Geol. Surv. Can., Paper 80-27, 40 p.
- FRITZ, W.H., 1980. International Precambrian - Cambrian Boundary Working Group's 1979 field study to Mackenzie Mountains, Northwest Territories, Canada; Geol. Surv. Can., Paper 80-1A, p. 41-45.
- FRITZ, W.H., 1982. Vampire Formation, a new Upper Precambrian(?) / Lower Cambrian formation, Mackenzie Mountains, Yukon and Northwest Territories; Geol. Surv. Can., Paper 82-1B, p. 83-92.
- FRITZ, W.H., NARBONNE, G.M. and GORDEY, S.P., 1983. Strata and trace fossils near the Precambrian - Cambrian boundary, Mackenzie, Selwyn and Wernecke Mountains, Yukon and Northwest Territories; Geol. Surv. Can., Paper 83-1B, p. 365-375.

- FRITZ, W.H., NARBONNE, G.M. and GORDEY, S.P., 1984. *Strata and trace fossils near the Precambrian - Cambrian boundary, Mackenzie, Selwyn and Wernecke Mountains, Yukon and Northwest Territories: Reply*; Geol. Surv. Can., Paper 84-1B, p. 409-412.
- GORDEY, S.P., 1980. *Stratigraphic cross-section, Selwyn Basin to Mackenzie Platform, Nahanni map area, Yukon Territory and District of Mackenzie*; Geol. Surv. Can., Paper 80-1A, p. 353-355.
- GREEN, L.H., and GODWIN, C.I., 1963. *The mining industry of Yukon Territory and Southwestern District of Mackenzie*; 1962; Geol. Surv. Can., Paper 63-38.
- JACKSON, S.A. and BEALES, F.W., 1967. An aspect of sedimentary basin evolution: the concentration of Mississippi Valley-type ores during the late stages of diagenesis; *Bulletin of Canadian Petroleum Geology*, Vol. 15, p. 393-433.
- JELETZKY, J.A., 1961. *Eastern slope, Richardson Mountains: Cretaceous and Tertiary structural history and regional significance*; in Raasch, G.O. (ed.), *Geology of the Arctic*, Vol. 1, Proceedings, 1st International Symposium on Arctic Geology, Alberta Society of Petroleum Geologists, Calgary, p. 532-583.
- LENZ, A.C., 1972. *Ordovician to Devonian history of northern Yukon and adjacent District of Mackenzie*; *Bulletin of Canadian Petroleum Geology*, Vol. 20, p. 321-361.
- MACQUEEN, R.W., 1976. *Sediments, zinc and lead, Rocky Mountain Belt, Canadian Cordillera*; Geoscience Canada, Vol. 3, p. 71-81.
- NARBONNE, G.M., HOFMANN, H.J., andAITKEN, J.D., 1985. *Precambrian - Cambrian boundary sequence, Wernecke Mountains, Yukon Territory*; Geol. Surv. Can., Paper 85-1A, p. 603-608.
- NOWLAN, G.S., NARBONNE, G.M. and FRITZ, W.H., 1985. *Small shelly fossils and trace fossils near the Precambrian - Cambrian boundary in the Yukon Territory, Canada*; Lethaia, Vol. 18 (in press).
- REEVE, A.F., 1977. *The Goz Creek zinc deposits, Yukon Territory*; in Yukon Territory Mineral Industry Report, 1976, EGS 1977-1, Dept. Ind. Aff. Nor. Dev., Whitehorse, Yukon, p. 6-19.
- SANGSTER, D.F., 1975. *Geology of Canadian lead and zinc deposits*; Geol. Surv. Can., Paper 75-1A, p. 235-237.
- SEILACHER, A., 1967. *Bathymetry of trace fossils*; Marine Geology, Vol. 5, p. 413-428.

BIMODAL PALEOGENE VOLCANICS NEAR TINTINA FAULT, EAST-CENTRAL YUKON, AND THEIR POSSIBLE RELATIONSHIP TO PLACER GOLD (GSC Project No. 800001)

L.E. Jackson* and S.P. Gordey +

*Terrain Sciences Division and +Cordilleran Division

Geological Survey of Canada

Vancouver, British Columbia

(G.S.C. Project Nos. 800001, 820015)

(G.S.C. Contribution 33086)

R.L. Armstrong and J.E. Harakal

Department of Geological Sciences

University of British Columbia

Vancouver, British Columbia

JACKSON, L.E., GORDEY, S.P., ARMSTRONG, R.L. and HARAKAL, J.E., 1986. Bimodal Paleogene volcanics near Tintina Fault, east-central Yukon, and their possible relationship to placer gold; in Yukon Geology, Vol. 1; Exploration and Geological Services Division, Yukon, Indian and Northern Affairs Canada, p. 139-147.

INTRODUCTION

A bimodal volcanic suite of rhyolite intrusions and flows and columnar olivine basalt, basaltic tuff and tuff breccia occurs along and immediately north of the Tintina Fault from near Faro to Tuchitua in east-central Yukon (Fig. 1). This paper reports the results of recent isotopic dating and chemical analyses of these rocks. Preliminary evidence linking volcanics in this area to the regional distribution of placer gold is also discussed.

PREVIOUS WORK

The first reports of volcanic rocks along this belt were made

by Dawson (1888). During a reconnaissance of the Pelly River, he noted discontinuous exposures of "dark brown basalt" from the mouth of the Hoole River to within a few kilometres above the head of Hoole Canyon (p. 122b). He assigned a provisional Miocene age to these flows from analogy to similar rocks in British Columbia (p. 37b). Reconnaissance geologic mapping of this region was achieved by the 1960's (Gabrielse, 1966; Roddick and Green, 1961; Roots et al., 1966; Wheeler et al., 1960a,b) but maps showing most of the volcanic rocks in question at a 1:250,000 or larger scale were not published until the 1970's (Tempelman-Kluit, 1972, 1977). A summary of the pre-Tertiary geology of the area is given by Tempelman-Kluit (1979).

The most striking geological feature of the region is the Tin-

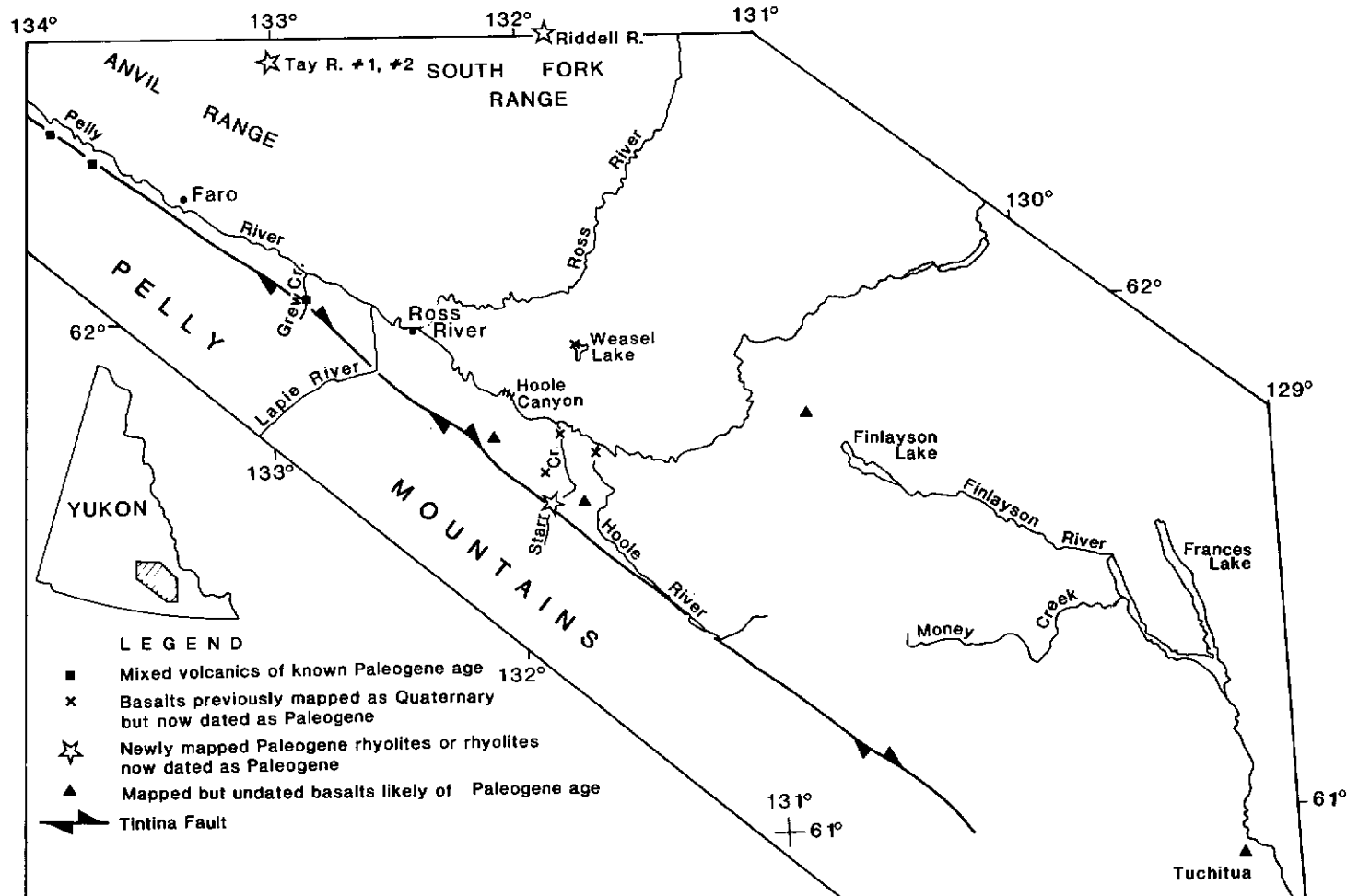


Figure 1. Occurrences of Paleogene volcanics in the upper Pelly and Liard (Frances Lake basin) river basins.

tina Fault, the locus of at least 450 km (Roddick, 1967) and as much as 750 km (Gabrielse, 1985) of dextral strike slip in late Cretaceous to Tertiary time. Tintina Trench, a physiographic feature which follows Tintina Fault is an expression of younger Pliocene normal faulting (Tempelman-Kluit, 1980).

Tempelman-Kluit (1972, 1977) ascribed the volcanic rocks occurring along Tintina Trench and its flanking uplands to three tectonic environments:

- 1) Late Cretaceous to Tertiary intrusions into pre-Cretaceous bedrock, and possibly related felsic flows (e.g. upper Starr Creek rhyolite (Fig. 1),
- 2) Steeply dipping basalts or basaltic tuffs and felsic tuffs occupying fault-bounded panels adjacent and subparallel to Tintina Fault. These were assigned an early Tertiary age based upon their association with Paleocene to Eocene sediments (Kindle, 1946; Hughes and Long, 1979). Paleogene right-lateral slip along Tintina Fault (Roddick, 1967) is thought to be the cause of initial subsidence of small basins through normal faulting, and of subsequent folding of the volcanics and sediments accumulated in them (Hughes and Long, 1979, (e.g. fault-bounded Tertiary strata transected by Grew Creek (Fig. 2)), and
- 3) Flat-lying basalt flows occupying valley floors or with undetermined relations to underlying topography. These occur in a belt between about 10 km and 45 km north of and parallel to the Tintina Fault (Fig. 1). Tempelman-Kluit (1977) assigned them a late Tertiary to Quaternary age (e.g. basalt flows near confluence of Hoole and Pelly rivers shown in Figure 3).

AGE, TECTONIC SETTING AND DESCRIPTION OF NEWLY DATED VOLCANICS

The results of recent fieldwork and geochronometry over the northern part of this belt (Table 1) expands the known areal distribution of rhyolitic volcanics and confirms their age as late Paleocene to Eocene (tectonic environments 1 and 2). Basalt formerly thought Quaternary (tectonic environment 3) is also of Eocene age. The concordance of dates between the mafic and felsic volcanics indicates a single Paleogene bimodal volcanic province. Such bimodal suites are commonly linked to crustal extension and normal faulting (Ewart, 1979), which in this case are presumably related to transcurrent slip along Tintina Fault. That crustal extension was not confined to the locus of faulting is indicated by the occurrence of felsic volcanics well to the northeast (Fig. 1).

Analyses of the basalts (Table 2) shows them to be calc-alkaline to transitional tholeites (Fig. 4). The felsic volcanics (Table 2) are high-K subaluminous rhyolites (Fig. 4).

Felsic Volcanics Northeast of Tintina Fault

Felsic volcanics in close proximity to Tintina Fault were described by Tempelman-Kluit (1972, unit 14) as quartz-feldspar porphyry, ignimbrite and laminated acid crystal tuff. About 28 km northeast of Faro, he also mapped a small circular occurrence of quartz-feldspar porphyry ignimbrite (unit 14a). The age of these volcanics was assumed to be Upper Cretaceous (Tempelman-Kluit, 1972, p. 23) or Tertiary (Tempelman-Kluit, 1972, map 1261A).

Recent field work northeast and east of the area described by Tempelman-Kluit (1972) has outlined two additional felsic volcanic bodies. The smallest (Tay River, Tables 1 and 2) is a semi-circular plug about 400 m in diameter of quartz-feldspar porphyry that intrudes lower Paleozoic sediments. A steep fault of small displacement truncates its southern margin. The rock consists of about 10% phenocrysts of embayed quartz, sanidine, and rare plagioclase in a microfelsitic groundmass. Biotite (2%) occurs as small irregular pleochroic brown grains. The plug is uniform in composition except for a small body of enclosed obsidian. The glass is fresh and contains about 8% phenocrysts of embayed quartz, sanidine and rare plagioclase. Microlites form a trachytoid texture. The body shows a strong sub-horizontal columnar jointing (Fig. 5), the columns being perpendicular to the steeply dipping contacts. Potassium-argon whole rock dates on the porphyry and obsidian are concordant at 54.7 ± 1.8 Ma and 52.3 ± 1.8 Ma respectively.

The second body (Riddell River, Tables 1 and 2) was only briefly examined. It is about 2 km across, and its white weathering colour contrasts markedly with the dark grey to brown weathering mid-Cretaceous (100 Ma) South Fork Volcanics which it intrudes



Figure 2. Basaltic tuff containing fragments of carbonized wood (white mottling) along Grew Creek.

and to which it is unrelated. The rock contains a few percent phenocrysts of quartz, sanidine and rare plagioclase, and about 1% irregular pleochroic brown biotite, in a spherulitic microfelsitic groundmass. Flow-banding is well developed in shades of pink to white. These rocks have yielded a potassium-argon whole rock date of 51.5 ± 1.8 Ma.

The compositional similarity of the above two dated occurrences with felsic volcanics closer to Tintina Fault strongly suggests an Eocene age for the latter. The association of gold with felsic volcanics near Tintina Fault at Grew Creek (T. Garagan, oral presentation, Geoscience Forum, Whitehorse, Yukon, 1985; Duke, 1986) suggests conversely that the two dated bodies may have potential for gold mineralization.

Duke (1986) reports K-Ar dates of 47.0 ± 1.7 Ma to 51.5 ± 1.8 Ma for four samples of sericitized felsic tuff and whole rock basalt from the gold-silver prospect at Grew Creek, confirming the suspected correlation.

Basalts Northeast of Tintina Fault

The dense cover of forest, brush, bog and thick blanket of glacial sediments precludes the tracing of basalt and tuff-breccia unit boundaries or determining their three dimensional geometries. Available exposures of these units suggest they range from extensive flows in the cases of lower Starr Creek and Hoole River localities (Fig. 3) to a volcanic neck at Weasel Lake (Fig. 6), to pillow basalts and pillow tuff breccias of unknown geometries at



Figure 3. Interstratified basalts and fanglomerate (defined by dotted lines) in fault contact (arrowed lines) with Paleozoic schist along Hoole River. A broad gouge and breccia zone is approximately delineated by the dashed lines. The fanglomerate probably derives from a nearby scarp active during volcanism.

Pillow Mountain (informal, see Fig. 1; Fig. 7). Dominant minerals in all of these rocks are plagioclase (An_{48} to An_{60}), augite, and variable amounts of olivine. Textures range from nearly holocrystalline and medium grained with intergranular texture, as at Weasel Lake, to hypocrystalline and fine grained, with intersertal to poikilitic textures in the Hoole River and Starr Creek flows. Pillow basalts and tuff-breccias which crop out on Pillow Mountain (Fig. 1) are holohyaline to hypocrystalline, very fine grained and display glomeroporphyritic to trachytic textures.

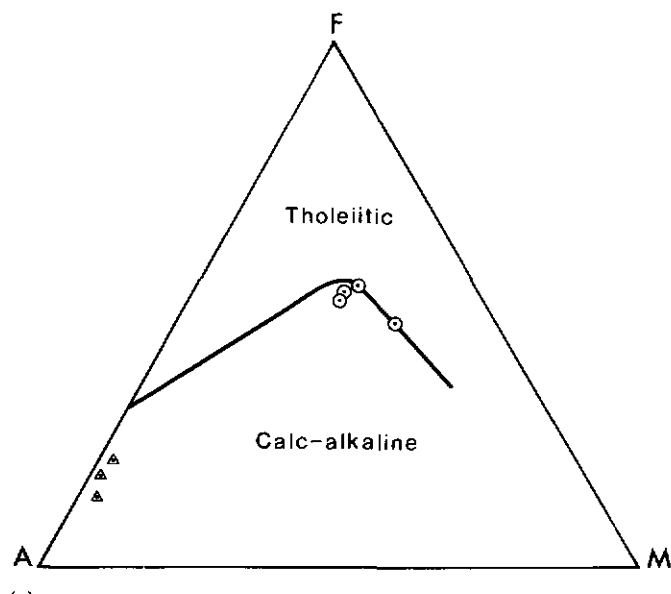
Two circumstances suggest that the newly dated basalts lie in fault controlled basins which have experienced considerable vertical offset. First, Paleogene basalt at a locality along Hoole River, 3 km above its confluence with Pelly River (Fig. 3), is faulted against Paleozoic schist. There, a steeply dipping normal fault is defined by a gouge and breccia zone more than 50 m wide. Two basalt flows are separated by fanglomerate composed of angular fragments of schist. This tongue thins towards the fault, and is identical in texture and composition to modern debris fans which have formed along the south wall of Tintina Trench, thus indicating that a scarp existed at the time the basalts were erupted and that faulting was probably contemporaneous with volcanism. Second, large vertical offsets occur between valley-bottom basalts. The nearly flat-lying flows exposed along the floor of Starr Creek valley lie almost 300 m below thick pillow basalts and pillow basalt tuff breccias (Fig. 7) which cap "Pillow Mountain" about 3 km away. These latter volcanics were likely erupted into or beneath a lake. Such a vertical separation suggests differential erosion since the Eocene of separate adjacent fault-controlled basins or disruption of an originally larger basin.

ASSOCIATION OF PLACER GOLD WITH PALEOGENE VOLCANICS

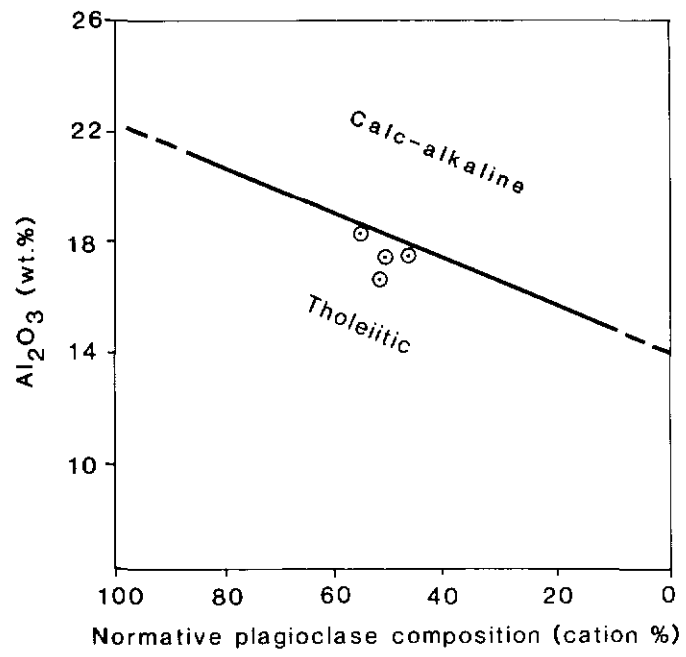
According to Dawson (1889, p. 180b), prospecting for placer gold in the upper Pelly River basin began in 1882. Since then, only prospecting and intermittent minor placer mining has taken place. Origin of the gold has not been determined, but concurrence of the limits of the Paleogene volcanics with the placers and certain surficial geologic features suggests a connection.

Figure 8 shows gold-bearing streams, the distribution of the volcanics, and Quarternary McConnell ice-flow directions. It seems unlikely that placer gold has been transported far from bedrock sources; nearly all of the ice that flowed along the volcanic "belt" originated locally. Flow of the Cordilleran ice sheet paralleled Tintina Fault in this area and the ice divide was close by and transverse to this direction (Fig. 8; Dyke, 1982; Jackson, in press). Furthermore, if gold had been transported by streams draining the Pelly Mountains or areas to the north of the volcanic "belt," it is likely that gold would have been traced northward or southward by prospectors.

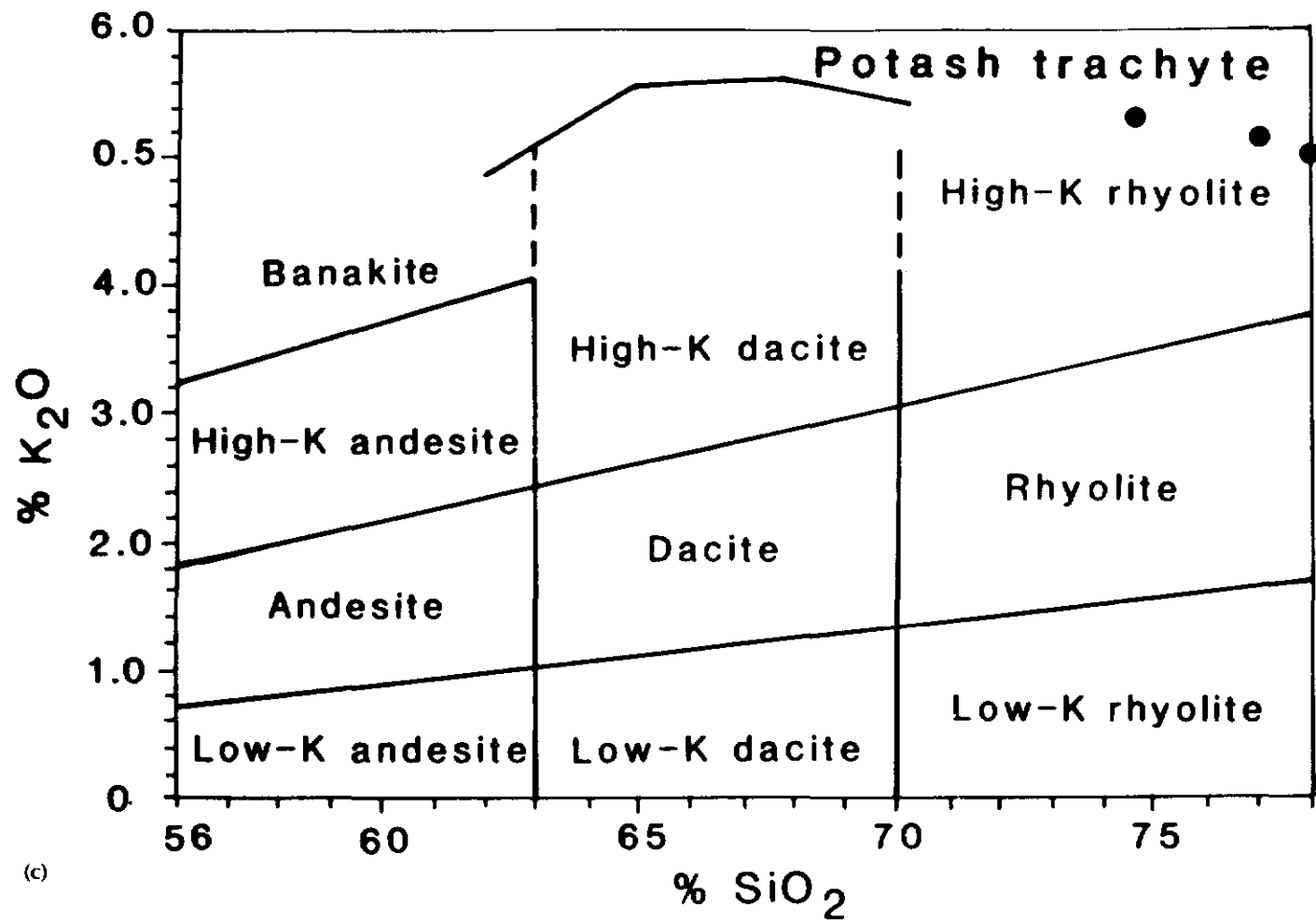
The connection between Paleogene volcanism and the geographical extent of placer gold in this area is more than circumstantial. The recent lode gold discovery at Grew Creek appears to be intimately associated with Paleogene felsic volcanism. (T. Garagan, oral presentation, Geoscience Forum, Whitehorse, Yukon, 1985; Duke, 1986). Hydrothermal systems associated with similar felsic volcanic centers elsewhere in the region, perhaps un-mapped or buried by drift, may be the ultimate source of the placer gold.



(a)



(b)



(c)

Figure 4. Chemistry of Paleogene volcanics. (a) AFM plot (circle - basalt; triangle - rhyolite) and (b) plot of aluminum oxide versus normative plagioclase composition for basalts from Weasel Lake, Starr Creek, Hoole River, and Pillow Mountain. Boundaries from Irvine and Baragar (1971) show basalts to be transitional from tholeiitic to calc-alkaline. The volcanic suite is clearly bimodal. (c) plot of silica versus potash for silicic volcanics from Tay River and Riddell River occurrences (Ewart, 1979) shows them to be high potassic rhyolites.



Figure 5. Columnar jointing in rhyolite at Tay River occurrence. The jointing developed perpendicular to the edge of the body, which is the steep wall away from which the recessive country rock has been eroded.

ACKNOWLEDGEMENTS

The authors gratefully acknowledge the help of Mr. Fred Harris and CANAMAX Resources Inc. for providing the K-Ar date for the upper Starr Creek rhyolite body.



Figure 6. Coarse grained columnar basalt near Weasel Lake. Columns are up to 20 m high.



(a)

Figure 7. (a) An exceptionally large pillow in pillow basalt and (b) pillow basalt tuff breccia, "Pillow Mountain."



(b)

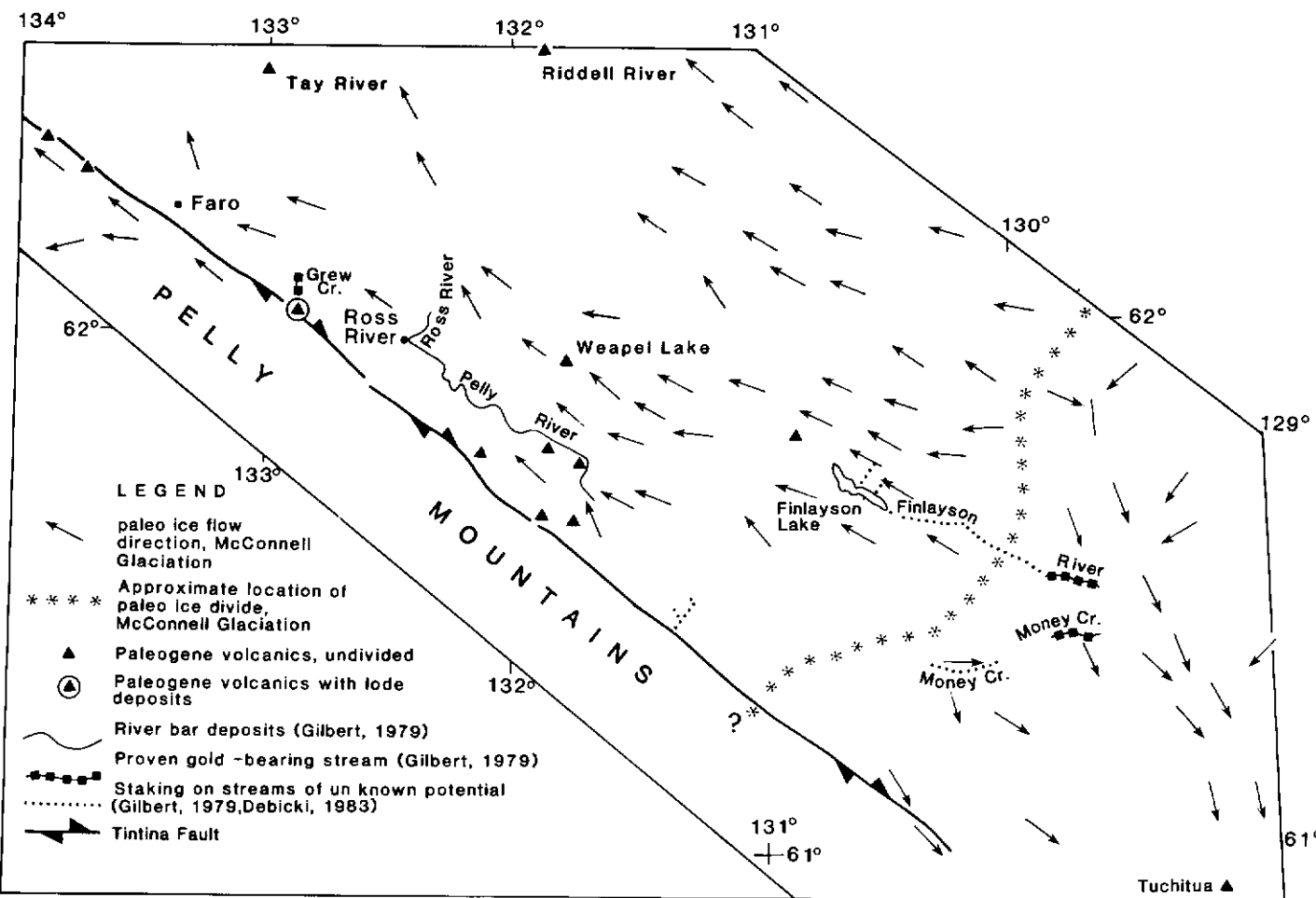


Figure 8. Ice flow patterns during McConnell Glaciation, placer gold occurrences and prospects (accurate to 1985), and known occurrences of volcanic rocks. Pleistocene ice-flow directions rule out a distant gold source and suggest the placer gold may be derived from hydrothermal systems associated with local unmapped or buried felsic Paleogene volcanics.

REFERENCES

- IRVINE, T.N. and BARAGAR, W.R.A., 1971. A guide to the chemical classification of the common volcanic rocks; *Canadian Journal of Earth Sciences*, Vol. 8, p. 523-548.
- DAWSON, G.M., 1888. *The Yukon River and British Columbia; Annual Report, Geological and Natural History Survey of Canada*, Vol. III, Part 1B, p.
- DUKE, J.L., 1986. The geology and alteration of an epithermal gold-silver prospect at Grew Creek, south-central Yukon Territory, BSc thesis, University of British Columbia, Vancouver, 58 p.
- DYKE, A.S., 1982. *Surficial geology of Francis Lake (105 H) Yukon Territory and District of Mackenzie*; Geological Survey of Canada Open File 895.
- EWART, A., 1979. A review of the mineralogy and chemistry of Tertiary-Recent dacitic, latitic, rhyolitic, and related salic volcanic rocks; in Barker, F. (ed.), *Trondhjemites, dacites, and related rocks, Developments in Petrology 6*, Chapter 2, p. 13-121.
- GABRIELSE, H., 1966. Geology, Watson Lake; Geological Survey of Canada Map 19-1966.
- GABRIELSE, H., 1985. Major dextral transcurrent displacements along the Northern Rocky Mountain Trench and related lineaments in north-central British Columbia; *Geological Society of America Bulletin*, Vol. 96, p. 1-14.
- HUGHES, J.D. and LONG, D.G.F., 1979. Geology and coal resource potential of early Tertiary strata along Tintina Trench, Yukon Territory; *Geological Survey of Canada Paper 79-32*, 21 p.
- JACKSON, L.E., In press. Terrain Inventory, Finlayson Lake, (105 G), Yukon Territory; *Geological Survey of Canada Open File Map*.
- KINDLE, E.D., 1946. Geological reconnaissance along the Canol Road, from Teslin River to Macmillan Pass, Yukon; *Geological Survey of Canada Paper 45-21*.
- RODDICK, J.A., 1967. Tintina Trench; *Journal of Geology*, Vol. 75, p. 23-33.

- RODDICK, J.A. and GREEN, L.H., 1961. Geology, Tay River, Yukon Territory; Geological Survey of Canada Map 13-1961.
- ROOTS, E.F., GREEN, L.H., RODDICK, J.A., and BLUSSON, S.L., 1966. Geology, Francis Lake, Yukon Territory and District of Mackenzie; Geological Survey of Canada Map 6-1966.
- TEMPELMAN-KLUIT, D.J., 1972. Geology and origin of the Faro, Vangorda, and Swim concordant zinc-lead deposits central Yukon Territory; Geological Survey of Canada Bulletin 208, 73 p.
- TEMPELMAN-KLUIT, D.J., 1977. Geology of the Quiet Lake (105 F) and Finlayson Lake (105 G) map areas; Geological Survey of Canada Open File Report 486.
- TEMPELMAN-KLUIT, D.J., 1979. Transported cataclasite, ophiolite, and granodiorite in Yukon: evidence of arc-continent collision; Geological Survey of Canada Paper 79-14, 26 p.
- TEMPELMAN-KLUIT, D.J., 1980. Evolution of physiography and drainage in southern Yukon; Canadian Journal of Earth Sciences, Vol. 17, no. 9, p. 1189-1203.
- WHEELER, J.O., GREEN, L.H., and RODDICK, J.A., 1960a. Geology, Quiet Lake, Yukon Territory; Geological Survey of Canada Map 7-1960.
- WHEELER, J.O., GREEN, L.H., and RODDICK, J.A., 1960b. Geology, Finlayson Lake, Yukon Territory; Geological Survey of Canada Map 8-1960.

TABLE 1
WHOLE ROCK K-AR DATES^a

Site Name	Laboratory Name	Latitude N Longitude W	UTM	Lithology	Age (Ma)	Wt % K	Radiogenic Ar (X 10 ⁻⁶ cc/gm)	Atmospheric Ar (%)
L. Starr Creek	LJ0906851	61°45.22' 131°51.38'	Zone 9 349300 6851700	olivine basalt	55.3 ± 2.0	1.10	2.402	5.2
Pillow Mountain	LJ017853	61°42.85' 131°52.65'	Zone 9 347900 6845500	olivine basalt	46.4 ± 2.3	1.23	2.247	84.4
Hoole River	LJ0906853	61°43.64' 131°42.73'	Zone 9 356700 6846600	olivine basalt	55.4 ± 2.0	1.26	2.756	8.5
Weasel Lake	LJ2206854	61°57.18' 131°44.85'	Zone 9 355900 6671800	olivine basalt	48.6 ± 1.7	0.807	1.544	24.5
U. Starr Creek ^a	R5225	61°37.84' 131°54.91'	Zone 9 345500 6836300	feldspar porphyry rhyolite	58.2 ± 2.3	3.806	8.998	19.5
Tay River # 2	GGA-83-35F3	62°30.11' 133°0.40'	Zone 8 602675E 6931475N	obsidian	52.3 ± 1.8	4.22	8.707	7.2
Tay River # 1	GGA-82-47C1	62°30.23' 133°0.07	Zone 8 602950E 6931700N	quartz-feldspar porphyry rhyolite	54.7 ± 1.8	4.26	9.203	2.8
Riddell River	GGA-83-40D	62°32.06' 131°53.07'	Zone 9 351600 6936825	as above	51.5 ± 1.8	4.27	8.672	8.3

^aU. Starr Creek date determined by Geochron Laboratories, Cambridge Mass, U.S.A. Permission from Canamax Resources Inc. to publish this data is gratefully acknowledged. All other dates done at the University of British Columbia, Vancouver, B.C. see appendix for analytical details and decay constants.

TABLE 2
ROCK CHEMISTRY AND NORMATIVE MINERALOGY^a

Sample	2206854	906853	107853	906851	GGA-83-40D	GGA-82-47C1	GGA-83-35F3
Location Lithology	Weasel Lk. basalt	Hoole R. basalt	Pillow Mtn. basalt	L. Starr Cr. basalt	Riddell R. rhyolite	Tay R. #1 rhyolite	Tay R. #2 obsidian
Chemistry (wt. %)							
S _i O ₂	49.08	50.14	49.02	50.37	74.8	75.1	75.3
Al ₂ O ₃	15.41	15.53	14.59	16.03	13.3	11.9	11.6
Fe ₂ O ₃	2.15	4.24	3.54	4.30	1.0	1.0	0.7
FeO	8.40	5.49	7.26	5.56	1.0	0.9	0.9
CaO	8.62	8.68	8.39	8.77	0.89	0.35	0.93
MgO	7.95	4.36	5.09	4.38	0.04	0.12	0.08
Na ₂ O	2.68	3.02	2.43	2.92	3.76	2.00	2.93
K ₂ O	1.01	1.38	1.52	1.25	5.41	5.00	5.15
TiO ₂	1.81	2.33	2.18	2.08	0.07	0.13	0.11
P ₂ O ₅	0.43	0.81	0.69	0.56	0.02	0.04	0.01
MnO	0.16	0.16	0.20	0.14	0.02	0.02	0.03
H ₂ O	1.38	3.18	3.21	2.82	0.6	1.5	3.1
CO ₂					0.1	0.1	0.1
S					0.00	0.00	0.04
TOTALS	99.08	99.32	98.12	99.18	101.01	98.16	100.98
ppm							
Mo	1	1	1	1			
W	10	10	10	10			
Zn	84	109	94	84	120	83	64
Pb	1	1	1	1	63	30	34
Bi	2	2	2	2			
Cd	0.5	0.5	0.5	0.5			
Co	29	22	22	21	3	3	3
Ni	66	40	37	41	7	9	8
Ba	395	710	535	565	10	40	10
Cr	207	159	151	119	6	6	6
V	138	165	141	155	11	3	3
Be	0.5	1.0	0.5	0.5	8.7	6.5	8.4
Cu	37	47	36	42	18	11	10
Ag	0.6	0.2	0.2	0.2	1	1	1
Sr	279	373	318	326			
La					57	62	94
Yb					11	2.8	6.7
Normative mineralogy (wt %)							
Quartz	0.00	5.68	5.19	5.46	29.98	44.76	37.12
Orthoclase	6.11	8.49	9.46	7.67	31.87	30.60	31.08
Albite	23.21	26.59	21.66	25.66	31.72	17.53	27.36
Anorthite	27.66	25.74	25.71	27.97	3.42	1.53	3.42
Clinopyroxene	10.74	10.89	10.87	10.84	0.74	0.00	1.11
Orthopyroxene	19.99	10.28	15.63	11.55	0.64	0.98	0.51
Forsterite	2.83	0.00	0.00	0.00	0.00	0.00	0.00
Fayalite	1.73	0.00	0.00	0.00	0.00	0.00	0.00
Corundum	0.00	0.00	0.00	0.00	0.00	0.00	0.00
Magnetite	3.19	5.78	5.41	5.39	1.45	1.50	1.04
Ilmenite	3.52	4.60	4.36	4.10	0.13	0.26	0.21
Apatite	1.03	1.96	1.69	1.36	0.05	0.10	0.02
Pyrite					0.00	0.00	0.23

^avalues not shown were not determined; see appendix for analytical procedures.

APPENDIX

Analytical techniques for chemical analyses

Analyses on the rhyolites were performed at the Geological Survey of Canada laboratories. Major and minor elements were done by ICP method on 0.5 g of sample fused with lithium methaborate, dissolved in 5% HNO₃ and diluted to 250 ml. S, CO₂, H₂O, and FeO were done by rapid chemical methods. Fe₂O₃ is calculated using Fe₂O₃ = Fe₂O₃T ICP - 1.11134 x FeO (volumetric). Ag and Pb were done by AA. Other trace elements were done by ICP on 1.0 g of sample (acid + fusion of residue) dissolved in 10% HCl and diluted to 100 ml.

Basalt samples were analyzed by Chemex Labs Ltd., North Vancouver, B.C. following similar procedures to those outlined above. Estimates of precision for data sets from both laboratories are available on request.

K-Ar analytical techniques

K is determined in duplicate by atomic absorption using a Techtron AA4 spectrophotometer and Ar by isotope dilution using an AEI MS - 10 mass spectrometer and high purity ³⁸Ar spike. Errors reported are for one standard deviation. The constants used are:

$$K\lambda_e = 0.581 \times 10^{-10} \text{ yr}^{-1}, K\lambda_B = 4.962 \times 10^{-10} \text{ yr}^{-1}$$

$$^{40}\text{K}/\text{K} = 0.01167 \text{ atom percent.}$$

DESCRIPTION OF THE MOUNT SKUKUM VOLCANIC COMPLEX, SOUTHERN YUKON

M.J. Pride

Department of Earth Sciences
University of Manitoba
Winnipeg, Manitoba

PRIDE, M.J., 1986. Description of the Mount Skukum Volcanic Complex southern Yukon; in Yukon Geology, Vol. 1; Exploration and Geological Services Division, Yukon, Indian and Northern Affairs Canada, p. 148-160.

INTRODUCTION

Tectonic Setting

Tectonically, the Yukon is subdivided into two parts: on the northeast, a suite of rocks representing an ancient North American continent (Interior Platform, and Mackenzie and Rocky Mountain Belts), and on the southwest, an allochthonous block accreted to the ancient North American continent (Intermontane Belt, Fig. 1). After accretion of the Intermontane Belt during the Mesozoic (Monger and Price, 1979; Tempelman-Kluit, 1979), a late Cretaceous northeastward subduction of oceanic lithosphere is thought to have been initiated on the southwest side of the newly accreted block. This produced a southwest facing magmatic arc on the newly accreted fragment. This arc is now represented by the Coast Plutonic Belt (Tempelman-Kluit, 1979), which comprises the Kluane schist, a biotite schist of high temperature, low pressure type, intruded and metamorphosed by the Ruby Range Batholith. It is in this belt that the Early Tertiary Mount Skukum Volcanic Complex (MSVC) occurs, along with many other Upper Cretaceous (Grond et al., 1984) and Early Tertiary volcanic complexes (Sloko volcanic province).

DISTRIBUTION OF THE SLOKO VOLCANIC ROCKS

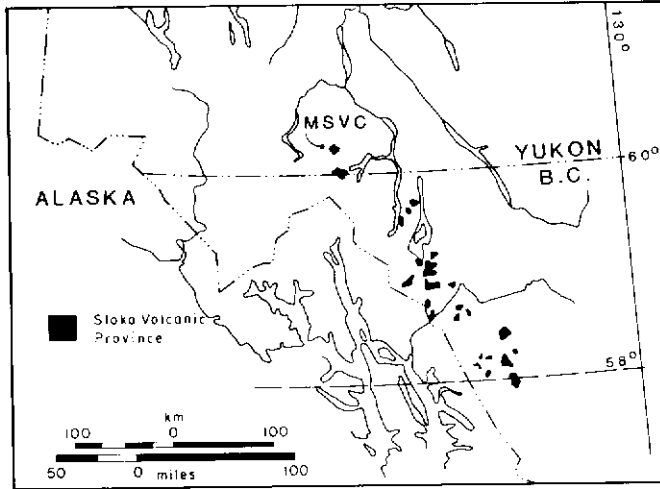


Figure 1. Distribution of Sloko volcanic rocks and location of the Mount Skukum volcanic complex.

The model in which plutonism and volcanism resulted from subduction (Tempelman-Kluit, 1979; Ewing, 1980) has recently been challenged by Gabrielse (1984) who suggests that the emplacement of plutons reflects a regional change in stress. An early stress system producing the characteristic Cordilleran compressional structural trends changed to one producing northwest-striking right lateral strike slip faults and related tensile strain.

Regional Setting

The Mount Skukum Volcanic Complex (MSVC) is about 58 km south-southwest of Whitehorse. It is the northernmost extension of the Sloko volcanic province in western British Columbia, a broad northwest-trending volcanic belt along the northeast margin of the Coast Plutonic Belt (Fig. 1). Rocks of the Sloko volcanic province are preserved as downfaulted blocks and as erosional remnants on higher upland surfaces (Souther, 1967 and 1970). They

comprise an assemblage of intermediate to felsic volcanic rocks and derived sedimentary rocks that lie unconformably on Cretaceous granitic rocks, folded Jurassic rocks and Precambrian (?) metasedimentary rocks.

The MSVC is Paleocene-Eocene in age, and elliptical in plan; it covers an area of about 140 km². It is a downfaulted volcanic block, deposited on Cretaceous granitic rocks of the Ruby Range Batholith and older metasedimentary rocks of the Yukon Group (Fig. 2). At least four volcanic outliers occur within a 16 km radius north and west of the complex, and seem to be associated with the Skukum volcanism. The complex is surrounded peripherally by several high-level rhyolite intrusions, which have recently been dated at 53 ± 1.1 Ma using rubidium-strontium geochronology (Pride and Clark, 1985). The Bennett Lake cauldron complex, studied intensively by Lambert (1974), is about 26 km south of the MSVC.

STRATIGRAPHY

The MSVC (Fig. 3), has a maximum vertical thickness of 850 m. It includes: 1) a downfaulted part of an andesitic stratovolcano which forms the western and southern parts of the complex and comprises the distal and medial facies assemblage of Formations 1 and 2, and the more proximal facies assemblage of Formation 3

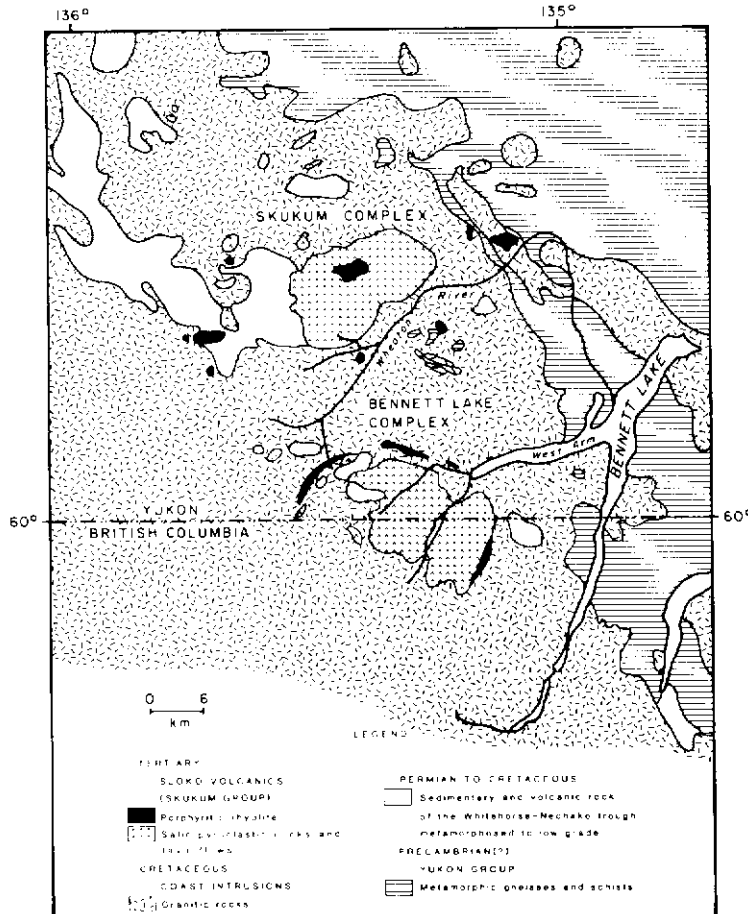
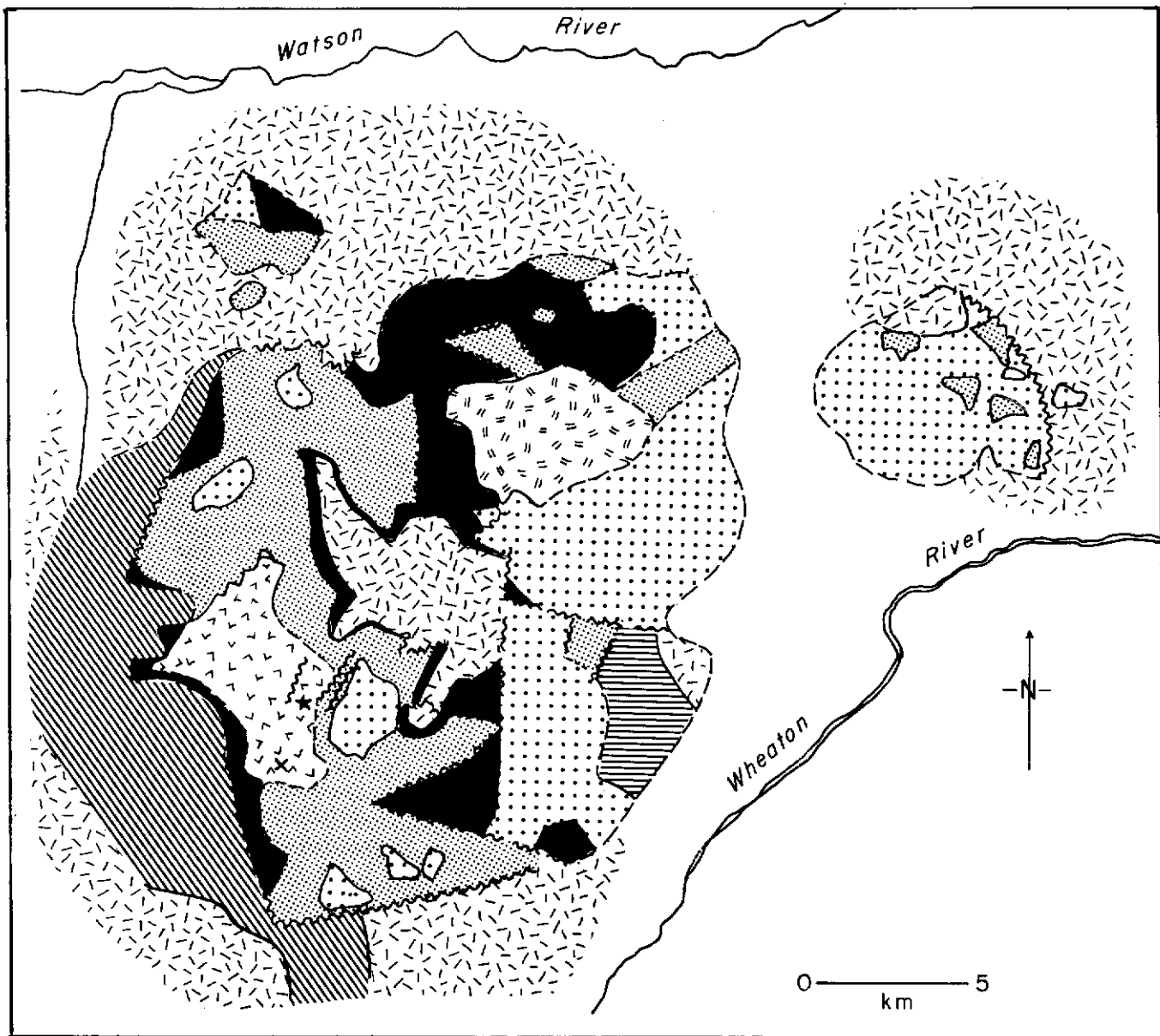


Figure 2. Regional setting of the Mount Skukum volcanic complex.



TERTIARY

- [Diagonal lines] Porphyritic rhyolite
- SLOKO VOLCANICS (SKUKUM GROUP)**
- FORMATION 5**
- [V-shaped pattern] Andesitic breccias and flows
- FORMATION 4**
- [Dotted pattern] Felsic volcanics
- FORMATION 3**
- [Cross-hatched pattern] Interlayered andesitic lava flows and epiclastic rocks with minor pyroclastic rocks
- FORMATIONS 1&2**
- [Solid black] Nonvolcanic coarse alluvial deposits (1), interlayered epiclastic-volcanic sequence (2)

CRETACEOUS

- [Cross-hatched pattern] Coast intrusions
- [Solid black] Granitic rocks
- LOWER JURASSIC & LATER**
- [Horizontal lines] Laberge group
- [Vertical lines] Conglomerate and siltstone
- PRECAMBRIAN AND LATER**
- [Solid black] Yukon group
- [Cross-hatched pattern] Metamorphic gneisses and schists
- X MT SKUKUM
- ★ Approximate mineralized area
- ~~~~~ Faults

Figure 3. Simplified geological map of the Mount Skukum volcanic complex.

(Fig. 3); 2) a small felsic cauldron subsidence structure in the northeast corner of the area represented by the felsic cauldron-fill deposits of Formation 4; 3) an andesitic vent facies environment located in a small area in the midwestern part of the complex and comprising the deposits of Formation 5; and 4) a central quartz-feldspar-phryic rhyolite intrusion along the western boundary of the small felsic cauldron.

The MSVC can be subdivided into four formations based on lithology and major unconformities. The following paragraphs briefly summarize the stratigraphy and interpretation of each of the four formations. More detailed stratigraphic and petrographic information are presented in Table 1.

Formation 1

Outcrops of Formation 1 form many discontinuous exposures that lie unconformably on basement rocks in the west and south parts of the complex. Formation 1 comprises 5 to 100 m thick sequences of coarse alluvial deposits composed entirely of basement fragments. Three facies types can be recognized and coincide reasonably well with Miall's (1978) and Rust's (1978) lithofacies types for coarse alluvial deposits (Figs. 4, 5 a,b,c,d): 1) clast supported boulder to cobble conglomerates, that are sometimes normally graded, imbricated and may contain plant fragments at the base of the beds, equivalent to Miall's (1978) GM lithofacies type; and 3) well sorted sandstones that may be planar crossbedded or massive and may contain plant fossils, equivalent to Miall's Sh and Sp lithofacies type. The stratigraphic section is typical of part of an alluvial plain or braided stream. These deposits can only be distinguished on the basis of extent and paleocurrent data (Rust, 1984), both of which are lacking in the MSVC. However, according to Rust (1984), the presence of debris flow deposits indicates that the sequence is more probably an alluvial fan deposit. Most other exposures of this formation are reasonably thin and usually comprise only one lithofacies type, as opposed to the thick stratigraphic section just described.

Two factors control the deposition of coarse alluvial deposits (Rust, 1984): 1) intracratonic faulting that produces sharp terrestrial relief required for accumulation of the coarse alluvial deposits, and 2) climatic extremes that affect the nature of deposition; e.g., the production of large lithic fragments is maximized on steep slopes and in semi-arid or paraglacial/alpine settings. According to Frakes (1979), and Wolfe and Poors (1982), the climate during late Paleocene and Eocene was subtropical, and therefore intracratonic faulting was probably the controlling factor in the deposition of the coarse alluvial deposits.

Formation 2

Formation 2 is restricted to the west and the south parts of the complex and has a maximum thickness of 300 m. This Formation lies unconformably on basement and conformably on Formation 1. The boundary between Formation 1 and 2 is marked by the presence of volcanic material in Formation 2. Formation 2 was described in Pride (1984) and will only be briefly described in this report.

As a result of more extensive mapping, the members of Formation 2 have been revised to provide a more representative description of the rock types within the entire complex (Table 2). Lithologically, Formation 2 is the most diverse formation in the MSVC consisting of a series of interbedded volcanic and epiclastic deposits that, with the exception of members 4 and 5, have limited lateral extent. The diversity is also reflected by clast type variability. The clast types include essential (glass shards and pumice), accessory (andesite and rhyolite), and accidental fragments (granitic and metasedimentary rocks).

Analysis of structures and lithology indicate the presence of several depositional environments: 1) structures such as channels and crossbedding in moderately-to-well-sorted sandstones and siltstones indicates a fluvial environment (Fig. 6); 2) carbonaceous, laminated to bedded fine sandstone and siltstone, with limited lateral extent and abundant plant fossils suggests swamp deposits; and 3) welded felsic pyroclastic flow deposits (Fig. 7), minor andesitic lava flows and tuffaceous beds containing accretionary lapilli and reasonably intact glass shards and pumice, represent primary volcanic deposits. There is a clear distinction between sedimentary and primary volcanic deposits, but there is a continuum of rock types between these two end members which are not clearly

distinguishable in terms of their environment. A large portion of Formation 2 belongs to this continuum, and the problem of its classification has not yet been resolved. However, the fact that the formation contains a greater proportion of fluvial to primary volcanic deposits, and that the volcanic deposits contain units that are considered more distal suggests that deposition occurred in a medial to distal volcanic facies (Vessel and Davies, 1981). The diversity of lithology may also indicate an interfingering of facies environments from different volcanic centers located at various distances from the MSVC.

Three lines of evidence suggest that faulting occurred prior to and during volcanism: 1) accumulation of coarse alluvial deposits of Formation 1 indicates faulting prior to volcanism; 2) the paleotopographic reconstruction, using a densely-welded flow as a marker horizon, showed that the paleotopography was in part controlled by fault blocks (Pride, 1984); and 3) contemporaneous faults were observed in Formation 2.

The diversity of rock types was probably caused by: 1) committant felsic and andesitic volcanism at different volcanic centers, possibly at various distances away from the MSVC, 2) the effect of volcanism on distally deposited epiclastic rocks; the amount of sediment introduced by volcanic activity would have a major effect on fluvial deposition, and 3) the effect on the deposits of the faulted paleotopography which developed prior to and during the volcanism; this faulting would limit lateral continuity of units and would cause changes in grain size that would not be related to the volcanic center.

Formation 3

Formation 3 represents the upper part of a collapsed strata-volcano and is confined to the west and south parts of the complex. Formations 1 and 2 make up the lower part of this strata-volcano. Formation 3 is a gently-dipping sequence of interlayered lava flows and epiclastic rocks that overlies the interlayered epiclastic volcanic sequence of Formation 2. Large isolated fault blocks and slump blocks of Formation 3 also occur in the eastern part of the complex. The boundary between Formation 2 and 3 is marked by the presence of lava flows in Formation 3 and of a welded pyroclastic flow in Formation 2.

The lava flows are mainly andesitic in composition; they range in thickness from 1 to 10 m, are relatively continuous laterally, and can be traced for about 1 km. The flows occur in very broad shallow channels, indicating deposition on a relatively level topography (Fig. 8). The lava flows are morphologically similar to andesitic lava flows elsewhere (Fig. 9, Macdonald, 1972). The base is generally brecciated, although thin hyaloclastic zones form the base of some flows and others are unbreciated. The flow interior is massive and locally columnar jointed. Vesicularity commonly increases towards the top of the flow, which is usually brecciated; the clasts in the upper breccia are highly vesicular, and void spaces between the vesicular fragments are commonly filled with bedded fine grained pyroclastic and epiclastic material. Distinct changes in phenocryst morphology, type, and abundance occur in the flow sequence indicating a changing magma reservoir.

The epiclastic rocks include laminated to bedded siltstone and sandstone in graded to massive beds that locally contain plant fossils and matrix- to clast-supported conglomerate. These epiclastic rocks mark periods of quiescence. The source area of these epiclastic units was almost exclusively andesite.

Subvertical beds in the lower part of the formation in the west part of the complex that are capped by gently-dipping beds is evidence of an early structural event (Fig. 8). The presence of lava flows suggests a proximal volcanic environment, in which sedimentary rocks derived from an andesitic provenance accumulated during periods of quiescence. The relatively continuous nature of the epiclastic units and lava flows suggest deposition on relatively level topography, after the early collapse event.

Formation 4

The bulk of Formation 4 is a sequence of interlayered, brecciated, flow banded and spherulitic felsic lava flows, pyroclastic rocks that are locally highly altered, and minor felsic epiclastic rocks. These felsic volcanic units form a thick sequence in the northeastern part of the complex which have been downfaulted at least 500 m on the eastern fault contact and about 300 m on the western fault contact. The east and west contacts are well exposed,

TABLE I

Summary of the Stratigraphic and Petrographic Interpretation of the 5 Formations in the MSVC.

FORMATION	THICKNESS MAX (m)	AVERAGE COMPOSITION	DOMINANT ROCK TYPE	MINOR ROCK TYPE	% PYROCLASTICS % LAVA FLOWS % EPICLASTICS	LATERAL CONTINUITY	LOWER CONTACT	FACIES AND DEPOSITIONAL ANALYSIS	ENVIRONMENTAL INDICATORS	COMMENTS		
5	~ 400	Intermediate	Heterolithic breccia, monolithic breccia, lava flows and columnar jointed sills.	Tuff and lapilli-tuff, sandstone.	50 15 35(?)	Moderate to poor	Unconformity	Heterolithic pyroclastic and debris flows with laterally equivalent andesite lava flows. Both are unconformably overlain by ~200 m of coarse monolithic andesitic explosion breccia, debris flows and slump breccias which are, in turn intruded by a series of columnar jointed sills. Sequence represents a vent facies environment.	- Preservation of an ancient crater wall; — extreme propylitic alteration; — poorly bedded monolithic breccia; — ballistic fragments in fine tuffs (possible surge deposit); — coarseness of breccia; numerous intrusions all suggest vent facies environment.	Compared to Fm2, lava flows, intrusions and monolithic breccias are relatively monolithic, and therefore reflect little change in the magma reservoir. Monolithic implies that there is little compositional change throughout the sequence.		
4	500	Felsic	Block, and lapilli tuff, flow banded, spherulitic and brecciated lava flows and intrusions.	Coarse conglomerates and breccias and sandstones.	35 60 5	Moderate	Unconformable	A sequence of felsic pyroclastic flows, lava flows and intrusions confined in a small down-faulted area (~300 m) define a cauldron subsidence structure. Intrusions, and flows lying unconformably on Formation 2 also occur outside the cauldron. Provenance area is strictly volcanic (felsic and altered andesite (?)).	Giant slump blocks on the eastern contact suggest slumping of a caldera wall during subsidence. Abundant flow-banded, spherulitic and brecciated lava flows or intrusions may indicate extensive dome and/or flow development.	Because the Skukum rhyolites in the down-faulted area are poorly exposed and partially eroded, their original form and internal variation were not obtainable. However, the fact that generally viscous rhyolites form domes or short stubby flows (Walker, 1973) limits the interpretation of the Skukum rhyolites to the latter two possibilities. Care should be taken in this interpretation as high alkali content and fluorine in the rhyolites would significantly lower the viscosity of the melt, and would change the morphological sections of the associated flows.		
3	450	Intermediate	Andesitic lava flows, poorly sorted coarse conglomerates and sandstone.	Lapilli-tuff and tuff.	30-65- 60 35	5	Good	Gradational	Interlayered lava flows, debris flows, fluvial sediments and possible cone deposits indicate a proximal volcanic facies environment source area that was largely volcanic (mostly andesite).	Shallow broad channels and relatively continuous flows indicate that deposition took place on a relatively level topography. Subvertical beds in the lower part of the formation indicate an early subsidence event.	The lava flows in this formation show phenocryst size, type, shape and percentage variability throughout the stratigraphic sections. This suggests a changing magma reservoir.	
2	~400	Felsic	Felsic lapilli and block tuffs, and clast and matrix supported coarse conglomerates.	Sandstones, siltstones and tuffs.	~60	—	~40	Poor	Gradational with Fm1 and unconformable with basement	Interlayered volcanic (felsic pyroclastic flows - welded to nonwelded, airfall and surge deposits) and sedimentary (fluvial, lacustrine deposits) clast types indicate concomitant felsic and intermediate volcanism as well as exposed basement in the provenance area.	Structures such as channels and ripples in sandstones and siltstones suggest fluvial deposition; dark black, carbonaceous thinly laminated mudstones with limited lateral extent and abundant plant fossils suggest swamp deposits; the combination of these units suggest medial to distal volcanic environment. Welded to non-welded pyroclastic flows, and accretionary lapilli in thin tuff beds suggest a nearby volcanic center. Some sections show contemporaneous faulting.	It is possible that these deposits were associated with more than one volcanic center which may have been located at various distances away from the MSVC. This hypothesis would explain the variability in lithology and clast type.
1	~100	—	Clast and matrix supported pebble-boulder conglomerates and sandstones.	Mudstones and siltstones.	—	—	100	Poor	Unconformity	Interbedded debris flows, coarse clast-supported conglomerates, and sandstones represent an alluvial fan, proximal braided stream, or proximal alluvial plain depositional environment. Coarse alluvial deposits indicate faulting and uplift. Provenance area is strictly non-volcanic (granitic and metasedimentary).	Debris flows (Gms), normally graded to massive beds, imbricated clast supported coarse conglomerates (Gm) and planar crossbedded and massive sandstone (Sp, Sh) suggest alluvial fan deposit. Plant fossils indicate terrestrial origin (Gms, Gm and Sp, Sh are abbreviations of lithofacies types from Miall (1978)).	

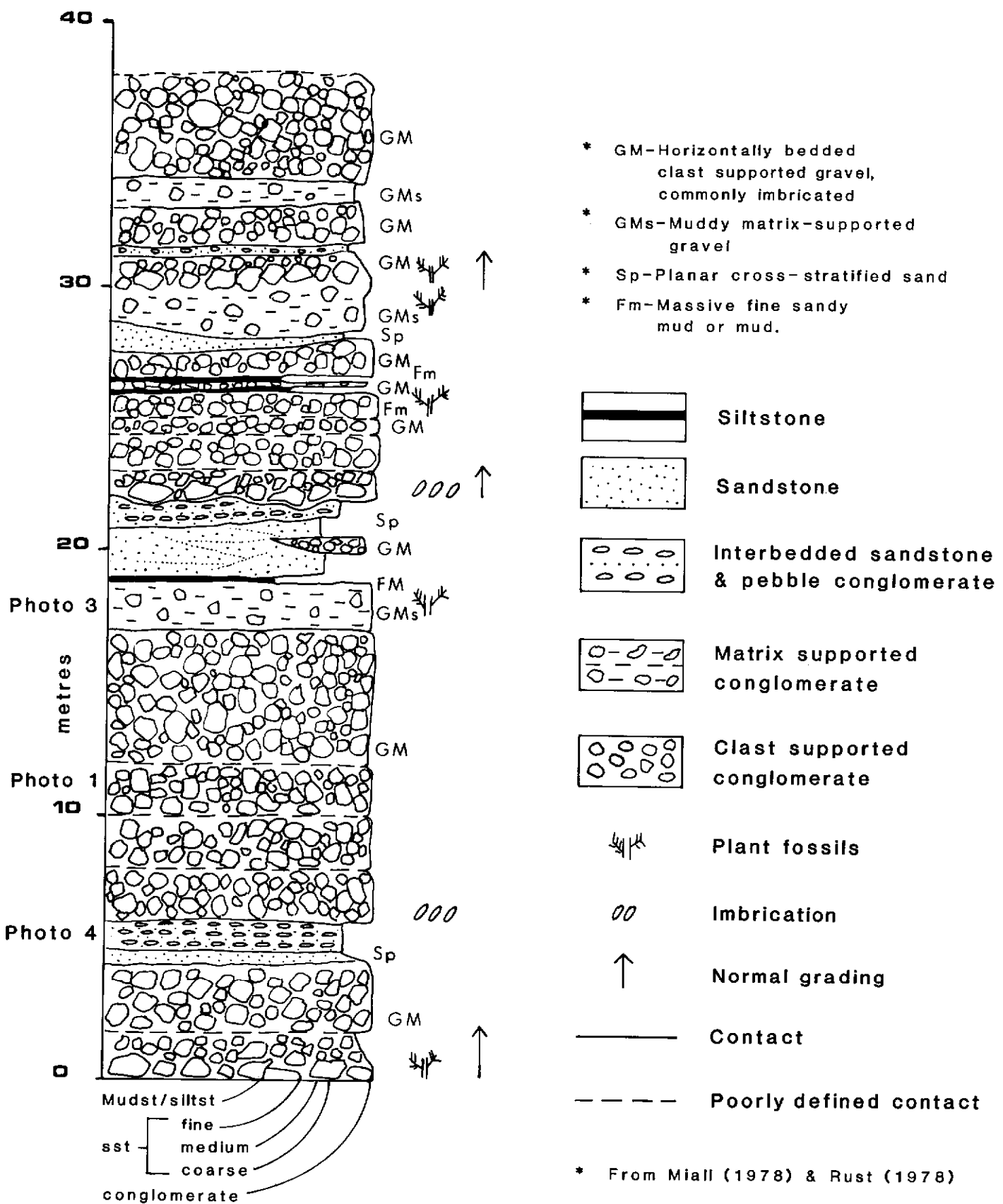


Figure 4. A stratigraphic section of part of Formation 1.

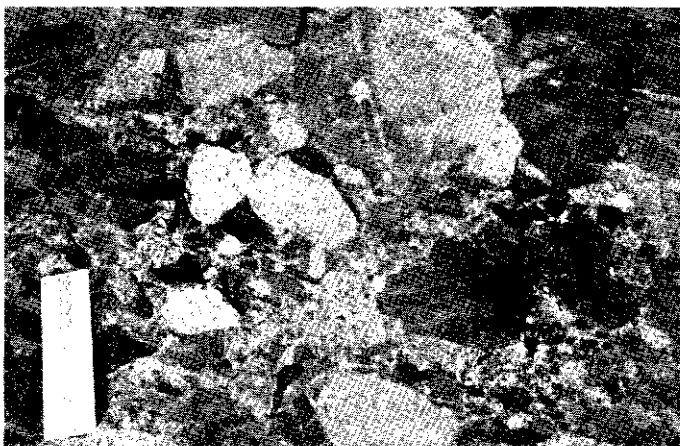


Figure 5. Coarse alluvial clastic rocks:

a) Clast supported conglomerate, from Formation 1, composed entirely of granitic and metasedimentary clasts (scale = 15 cm);



b) Carbonized plant imprints in a sandstone bed, Formation 1;

near vertical faults. Altered felsic volcanic rocks are found along the eastern fault contact and are mixed with giant andesite and conglomerate slump blocks. Steeply east-dipping felsic volcanic units occur in the west half of the downfaulted area (Fig. 10). Other felsic pyroclastic intrusions and flows, and flowbanded, brecciated and spherulitic intrusions and lava flows that occur outside the downfaulted felsic area and lie unconformably on Formation 3 have been correlated with Formation 4.

Most of Formation 4 appears to fill a cauldron subsidence structure. This conclusion is supported by: 1) the occurrence of the bulk of the felsic volcanic rocks in a downfaulted block that has been downdropped at least 300 m; 2) the lithology which is mainly felsic pyroclastic flows, and intrusions that, at one time, may have represented parts of domes, and 3) giant slump blocks that occur along one of the faults suggesting slumping of a caldera wall.

Formation 5

Formation 5 unconformably overlies Formation 1, 2, 3 and 4, within a 4 x 1.5 km area in the west-central part of the complex. It is divisible into three members: a heterolithic breccia, a sequence of andesitic lava flows and minor pyroclastic flows, and monolithic breccias that are spatially associated with columnar-jointed, andesitic intrusions (Fig. 11). The time relationship between flow and heterolithic breccia member is unclear, as they are not found in contact with each other.

Heterolithic breccia is about 120 m thick and is confined to the western half of the area where it unconformably overlies Formations 1, 2, 3, and 4. The breccia is poorly sorted and contains angular to subangular cobble- to pebble-size clasts that are primarily



c) Matrix supported conglomerate, the matrix is carbonaceous and is composed of clay to sand size particles. Clast type includes granite and metasedimentary rocks (Formation 1);



d) Interbedded sandstone and pebble conglomerate (Formation 1).

accessory andesite, although minor essential clasts appear to be present (Fig. 12). The matrix is composed of sand-size particles that are accessory andesite. The breccia forms 5 to 10 m thick beds that probably represent a sequence of debris flows that have accumulated in a reasonably steep-sided valley (Fig. 13).

In the eastern half of the area, the heterolithic breccia is absent, and instead, Formation 3 is overlain by a series of interlayered andesitic lava flows and minor pyroclastic rocks. The lava flows are compositionally distinct from those of Formation 3, and have a high degree of propylitic alteration. Figure 14 shows a sequence of horizontal lava flows in which a crater-like depression developed; the crater was later filled by monolithic breccia.

The heterolithic breccia and flow members are, in turn, overlain by a thick (approximately 200 m) sequence of monolithic breccia composed largely of nonvesicular clasts. The breccia is generally poorly bedded, but differs in clast size, shape, and percentage, from place to place, reflecting different types of deposits - explosion breccia (Fig. 15a), and debris flow breccia (Fig. 15b). The explosion breccia sometimes occurs in single unstratified nongraded beds that do not exceed a few meters in thickness, may be interbedded with debris flow breccias, or a fine-bedded sequence of primary volcanic deposits (surge, airfall, or pyroclastic flow). The explosion breccia is clast supported with subangular to angular clasts. These breccias seem to correspond to those explosion breccias described by Self (1982). The debris flow breccias are typically matrix supported with subrounded to rounded clasts. A complete description of the groundmass characteristics of the breccias is presently underway and therefore a complete interpretation of the breccias is not possible at this time. It seems likely that

TABLE II

Comparison of subdivision of Fm2 used in Pride (1984) to a revised subdivision based on rock types of the entire complex.

SUBDIVISIONS OF Fm2 USED IN PRIDE (1984)	REVISED SUBDIVISION OF FORMATION 2
Members	
7 Planar bedded tuff and conglomerate, reversely graded in part.	These two members are only found locally in the central part of the complex.
6 Interbedded siltstone and sandstone.	
5 Densely to moderately welded felsic pyroclastic flow.	These two members almost always occur together. Member 5 appears to be much more extensive than initially thought.
4 Clast supported conglomerate.	
3 Heterolithic debris and/or pyroclastic flows.	These members are much thicker in the south and have been grouped into one member that is dominantly composed of felsic volcanic and associated epiclastic rocks; heterolithic debris flows, felsic pyroclastic flows, tuffs, sandstone, siltstone and conglomerates and minor lava flows.
2 Interbedded siltstone and sandstone.	
1 Monolithic debris flows.	Equivalent to Formation 1.



Figure 6. Well developed channels in the lower part of Formation 2. These deposits indicate fluvial deposition.



Figure 7. A densely welded flow in Formation 2 indicating a primary volcanic deposit.

the variation in breccias is much larger than the two just mentioned. The breccias have intense propylitic alteration, and in places the matrix is composed of hematite, jasper or a siliceous material. The lower and upper parts of the member contain well-bedded sequences of tuff and lapilli tuff, one of which represents a surge deposit (Fig. 16a,b). This member is intruded by a series of pod-like, columnar-jointed andesitic sills and dykes which vary greatly in size and shape (Figs. 11 and 17).

The great thickness of poorly-bedded coarse-grained breccias, the presence of ballistic fragments in surge deposits, evidence of a crater, and the presence of numerous intrusions support the idea that this formation represents a vent facies environment.

STRUCTURE

The MSVC is a fault bounded, elliptical area of volcanic rock which contains a smaller subsidence structure in its eastern half. The area is downfaulted into Cretaceous and Precambrian basement rocks. There is no clear evidence for cause of the major subsidence of the MSVC, it may have resulted from regional stresses, volcanic activity, volcanic loading, or a combination of all three. It probably was related at least in part to the volcanism. The small felsic cauldron subsidence structure is a volcanic feature and the coincidence of vent facies and subsidence suggest a volcanic origin. However, regional stresses may have contributed also to

subsidence. For example, the accumulation of the non-volcanic, coarse alluvial deposits of Formation 1 suggest that intracratonic faults occurred prior to volcanism. Also, the style of faults is not consistent around the complex: 1) the northern fault is a series of small discontinuous faults that have no consistent trends and are vertical to steeply dipping. The volcanic rocks at the faults are steeply to moderately dipping. 2) The western contact appears to be a moderately-dipping reverse fault. The volcanic rocks are tilted to subvertical at the fault. 3) The southern contact is a straight, continuous vertical fault, that is partly intruded by rhyolite dykes. 4) The eastern contact is sharp and near vertical and marks the wall of the small caldera of Formation 4. It therefore seems likely that downfaulting was not related to single caldera collapse, but rather to a series of different volcanic events, perhaps controlled in part by regional stress.

A NNE-trending fracture system is the dominant, and perhaps the latest structural feature in the MSVC (Fig. 18). It is variably developed throughout the MSVC, controls the trends of some dykes and is the host fracture system for the quartz-calcite precious metal veins near Mt. Skukum.

MINERALIZATION

The star in Figure 2 marks the approximate location of the mineralized area. Economic epigenetic gold veins (V-2) are found

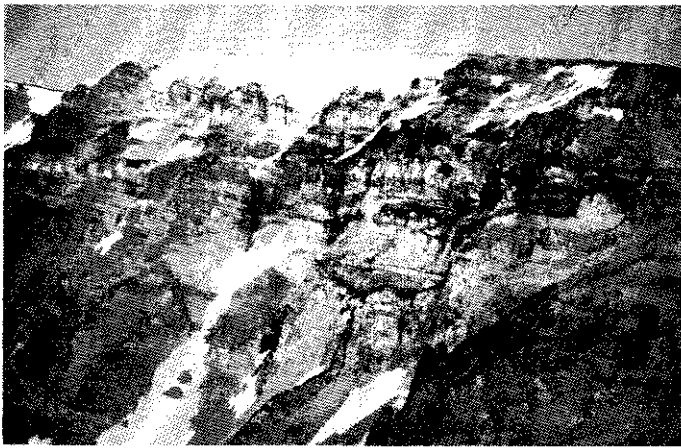


Figure 8. A cliff exposure of Formation 3, located in the mid-western part of the complex. Note the subvertical beds and vertical clastic dykes in the lower part of the section, this suggests an early subsidence event. The upper part of the section comprises a reasonably continuous sequence of interlayered lava flows and epiclastic rocks deposited in broad shallow channels.

in three major subparallel NNE-trending fault zones. The veins consist of quartz and calcite and are unusual in that they contain no sulphides and have poorly developed wall rock alteration. As of February 1984, the average grade was 27 g/t (0.8 oz/ton) gold and 22.63 g/t (0.66 oz/ton) silver, with proven reserves of 149,114 tonnes (164,222 tons). Major features in, and associated with the mineralized area are listed below:

- 1). Two very different vein types are present: 1) early V-1 veins that are restricted to Formation 4, are less than 4 cm wide, are composed of a blue green siliceous material, commonly fill void spaces in breccias, and are not gold bearing, and; 2) late V-2 veins that are restricted almost entirely to the flow member of Formation 5 near Mt. Skukum, are centimetres to metres wide, consist of a medium to coarse grained quartz and calcite assemblage, textures range from massive to brecciated, occur along the NNE-trending fracture system, cross-cut the V-1 veins and are gold bearing. NNE-trending V-2-like veins occur away from Mt. Skukum, but are not gold bearing, are thinner, and may contain gypsum.
- 2). Hematite and jasper veins are concentrated near Mt. Skukum (Fig. 19).
- 3). A pyrite halo occurs around the main mineralized area.
- 4). Andesites in the mineralized zone have a higher degree of propylitic alteration than andesites farther from the mineralized zone.
- 5). Many felsic flows and domes occur near the mineralized area (Fig. 20).
- 6). Faults and brecciated to nonbrecciated dykes are more abundant near the mineralized area (Fig. 20).
- 7). A leached solfatara cap suggests the presence of a hydrothermal vent (Fig. 20).
- 8). The mineralized veins occur in Formation 4, the vent facies environment (Fig. 20).

All these factors suggest that the mineralization was spatially associated with a volcanic vent. The presence of V-1 veins, jasper and hematite, the pyrite halo, the extensive propylitic alteration and the hydrothermal vent, suggests that there may have been several phases of hydrothermal activity, the last of which produced the gold mineralization near Mt. Skukum. Both felsic and andesitic volcanism or even an unknown agent at depth may have been the heat source for the hydrothermal systems.

MODEL FOR THE EVOLUTION OF THE MOUNT SKUKUM VOLCANIC COMPLEX

- 1). Early faulting produced intracratonic uplift, and resulted in deposition of the coarse alluvial deposits of Formation 1.
- 2). Felsic and andesitic volcanism was initiated in the Skukum area and felsic vents may be represented by the peripheral

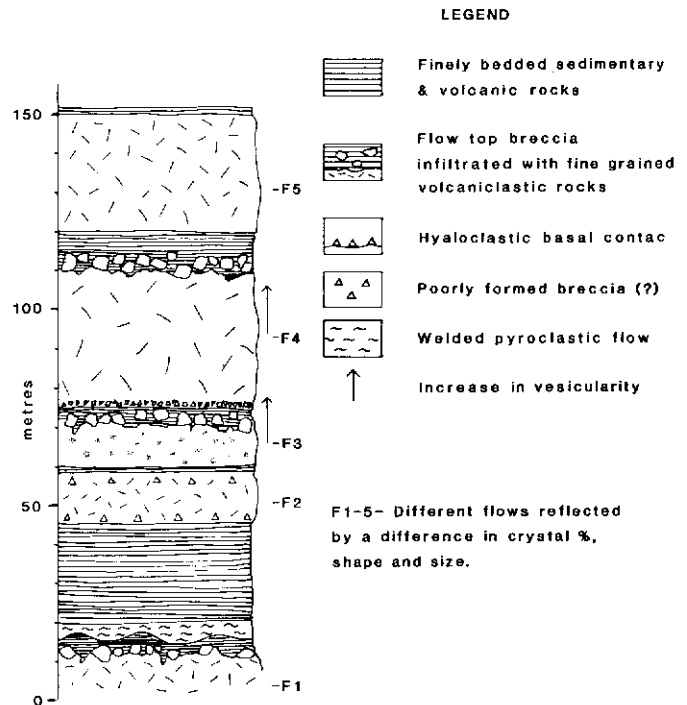


Figure 9. Stratigraphic section of part of Formation 3.



Figure 10. A photograph, looking north at the small felsic cauldron subsidence structure located in the northeast corner of the complex. The felsic beds on the western side of the cauldron dip steeply to the northeast.

- rhyolite plugs. Interfingering of the different facies of individual volcanic centers may have resulted in the distal to medial volcanic deposits of Formation 2. Variability in the clast type indicates that basement was exposed during felsic and andesitic volcanism.
- 3). Faulting continued throughout this time.
 - 4). The topography was gradually infilled by deposition of volcanic units and the densely welded pyroclastic flow of Formation 2 filled most of the remaining depressions.
 - 5). Andesitic lava flows of Formation 3 were erupted intermittently from a nearby vent or vents; periods of quiescence are marked by interbedded epiclastic rocks. Early subsidence in the western part of the complex is defined by the vertical beds in the lower part of the sequence, but the upper sequence which comprises a series of relatively continuous lava flows interbedded with epiclastic rocks was deposited on relatively level topography. The volcanic sequence may have subsided along the southern and western fault contact at any time after the deposition of Formation 3.
 - 6). The deposition of Formation 3 was followed by a period of nondeposition and erosion.

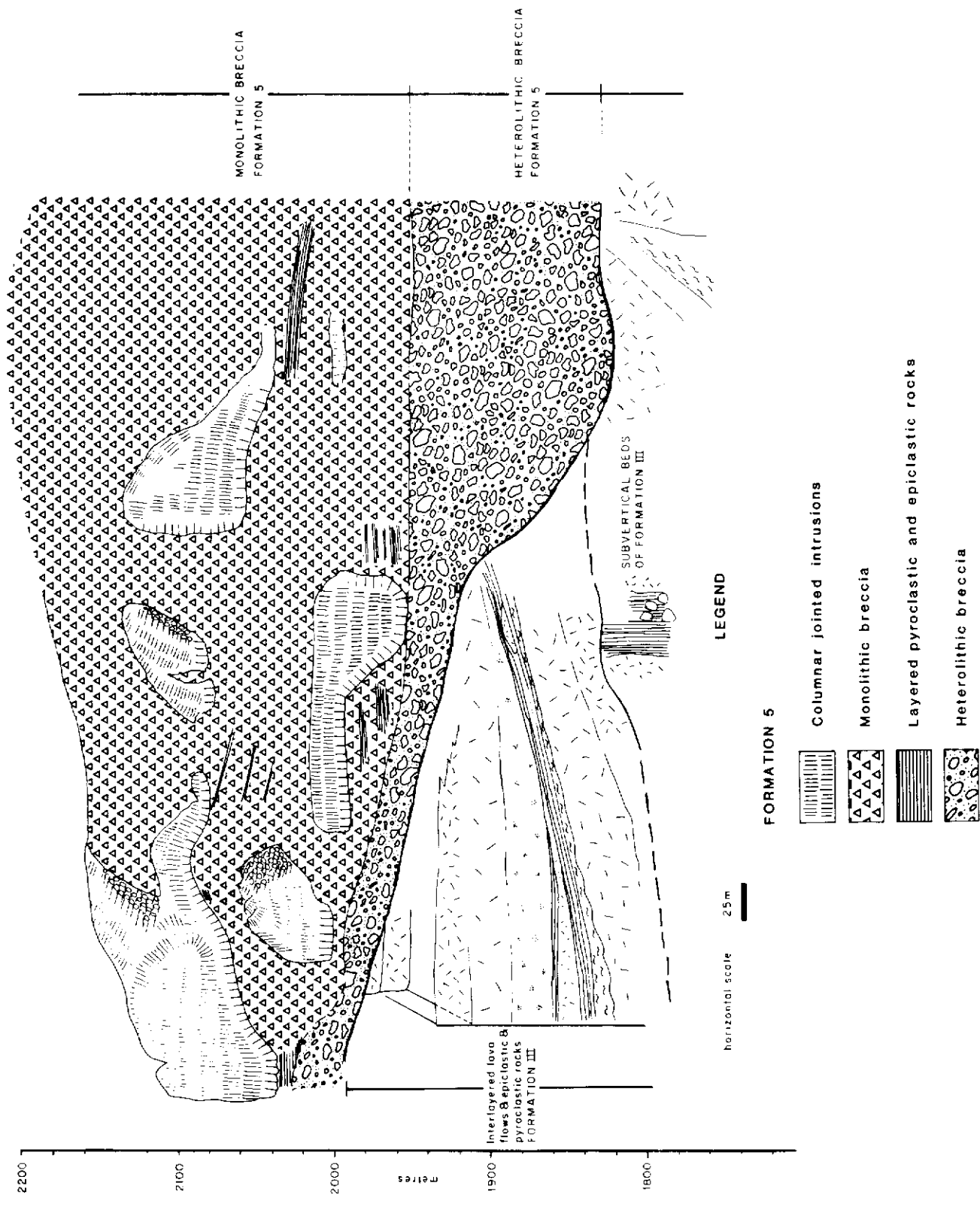


Figure 11. Sketch of a section of two members of Formation 5 northwest of Mt. Skukum.

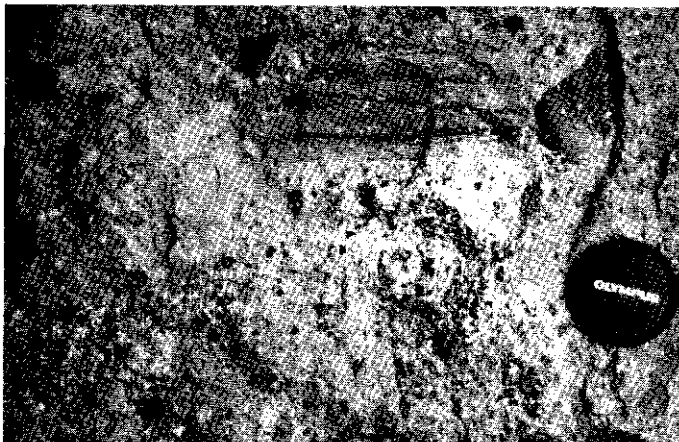


Figure 12. Photograph of a typical heterolithic breccia. The breccia is poorly sorted and contains angular to subangular andesitic clasts which are less than 25 cm in size.

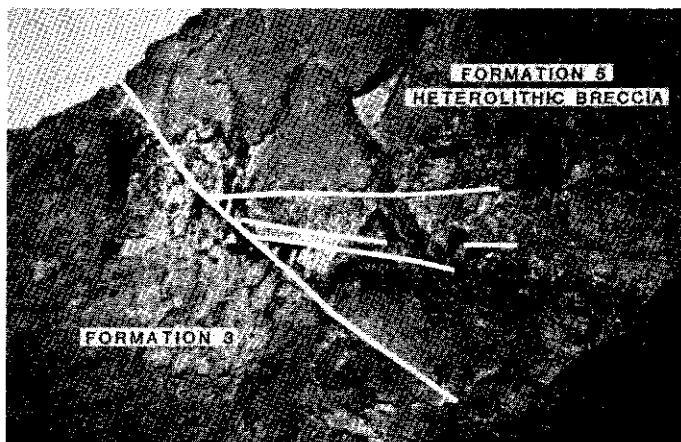


Figure 13. An exposure showing the heterolithic breccia of Formation 5, unconformably overlying Formation 3. The contact marks the outline of a valley which has been filled with a series of beds of heterolithic breccia.

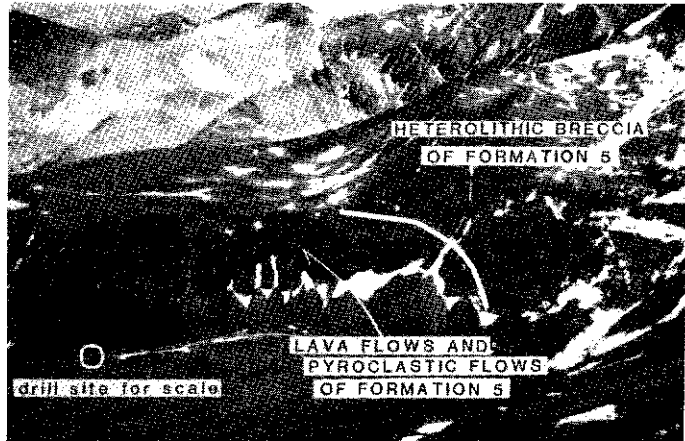


Figure 14. This photograph shows the massive dark bands of near horizontal andesitic lava flows of Formation 5. On the right hand side of the photograph, the lava flows have slumped into a crater-like depression, the crater is now filled with a 200 m thick sequence of poorly bedded monolithic breccia.

- 7). Catastrophic plinian eruptions occurred from a vent that may have been near the central rhyolite plug and resulted in major caldera subsidence in the northeast corner of the complex, and the accumulation of the thick sequence of pyroclastic flows. Other smaller rhyolite intrusions which may represent former vents occur outside the complex.
- 8). After the deposition of Formation 4, there was a period of quiescence, and erosion.
- 9). Faulting or pyroclastic eruptions resulted in the deposition of the heterolithic breccias of Formation 5.
- 10). Compositionally distinct andesites were erupted just north of Mt. Skukum. The eruption began with extrusion of andesitic lavas and minor pyroclastic flows and was followed by catastrophic explosions which produced at least one crater, a thick sequence of poorly bedded monolithic breccias, minor surge, airfall (?), and pyroclastic flow deposits, and andesitic intrusions.
- 11). Intrusion of the central rhyolite plug, and the development of the NNE-trending fracture pattern.
- 12). Hydrothermal systems probably existed at various times throughout volcanism, however, the epigenetic gold veins appear to have been the latest hydrothermal system which was localized in the vent facies environment of Formation 5. Some late felsic dykes crosscut the gold veins.

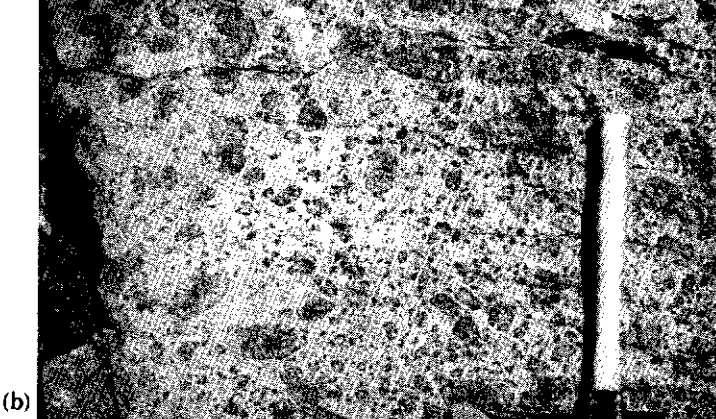
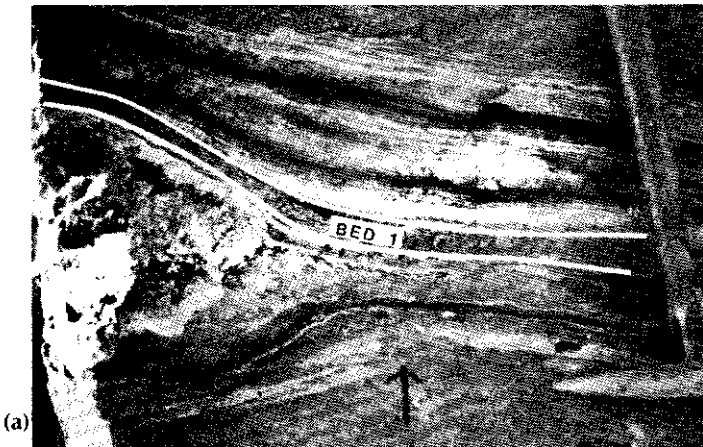


Figure 15. Propylitically altered andesite monolithic breccia from Formation 5. a) This particular exposure has been interpreted as an explosion breccia. b) This exposure may represent a debris flow deposit.

ACKNOWLEDGEMENTS

This project was financially supported by the Exploration and Geological Services Division, Department of Indian Affairs and Northern Development, Whitehorse. I would especially like to thank Dr. L.D. Ayres for reviewing this manuscript.



(a)



(b)

Figure 16. Tuff of Formation 5. a) Photograph of a ballistic fragment of porphyritic andesite which has impacted and truncated the underlying tuff deposits. The sample has subsequently been mantled by a series of tuff beds which, along strike, show small ripple bedforms, suggesting deposition was from a surge. b) The laterally equivalent bedded tuffs of Figure 16a located approximately 5 m along strike.

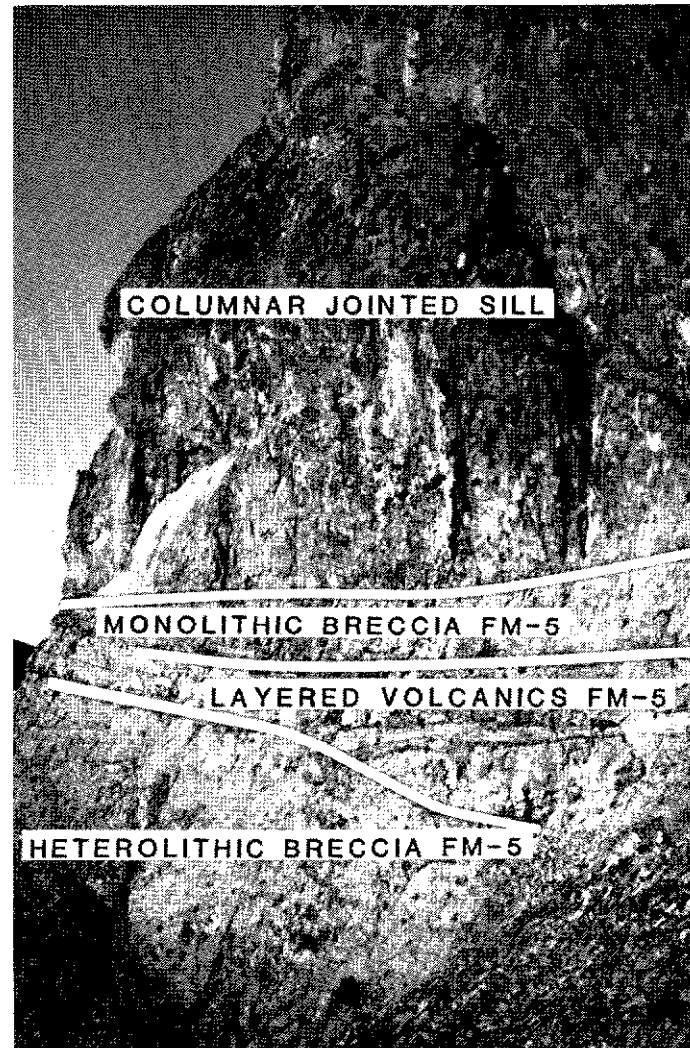


Figure 17. A photograph showing the columnar jointed sill-like intrusions. The basal contact is chilled and irregular and overlies the monolithic breccias. These breccias are in turn underlain by a bedded volcanic sequence and by the heterolithic breccias. (Formation 5).

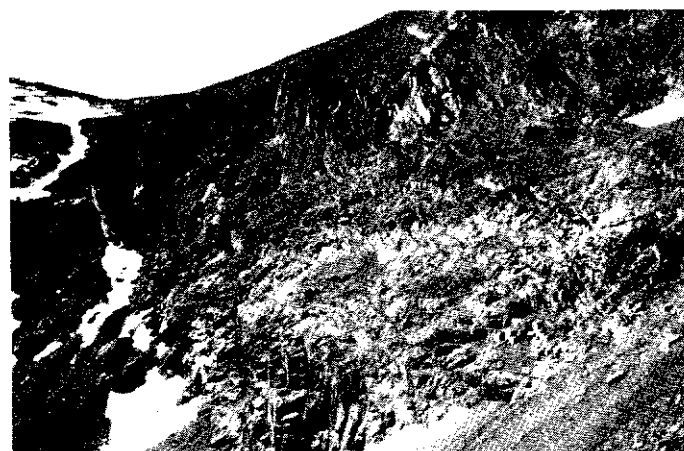


Figure 18. A photograph taken just northwest of Mt. Skukum showing the pervasive NNE-trending fracture pattern.



Figure 19. A photograph of jasper hematite veins in Formation 4.

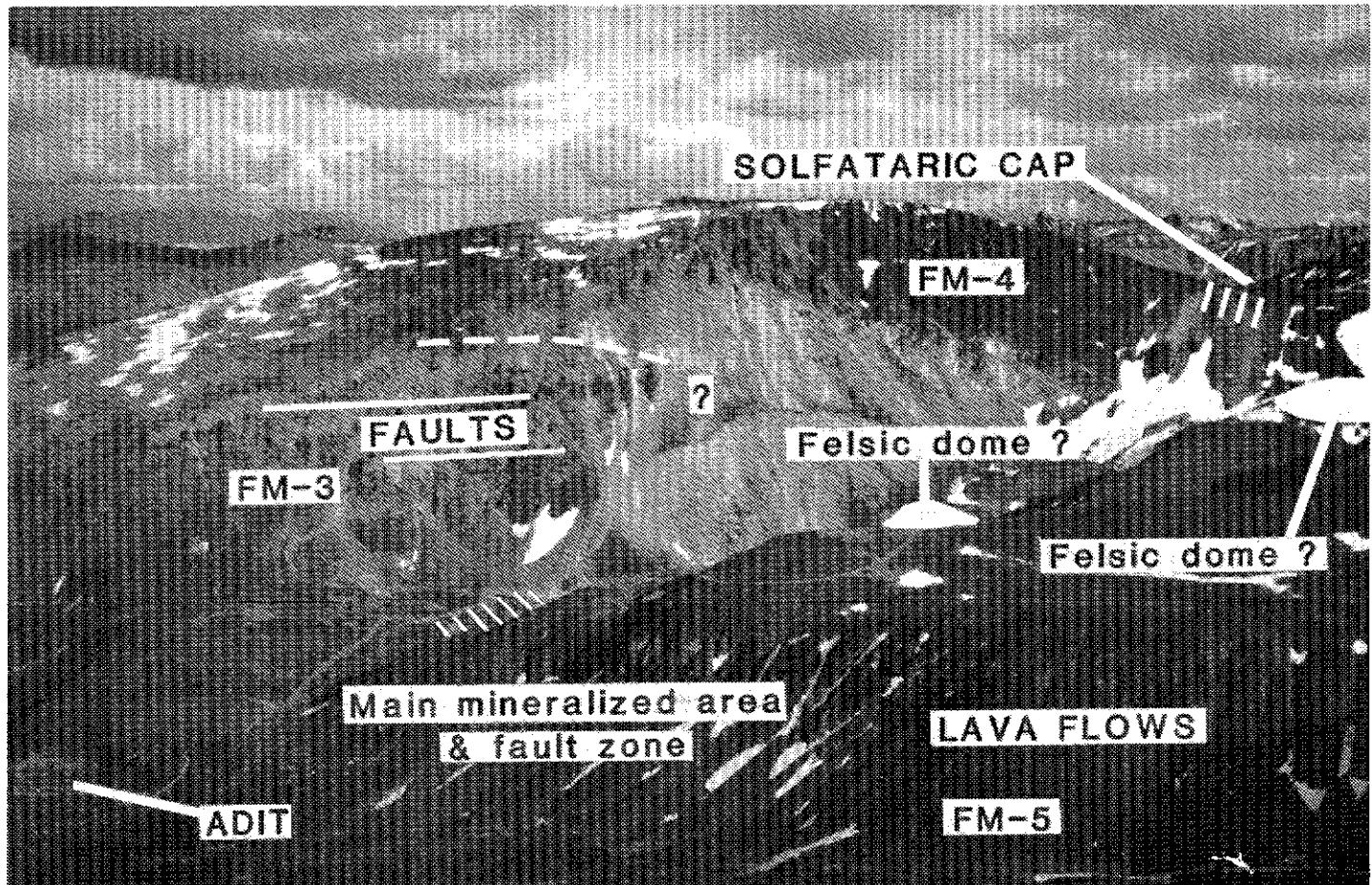


Figure 20. Photograph showing the location of the main mineralized zone, as well as the geology of the area. The photograph shows some features that are associated with the mineralized area: 1) faults and dykes, 2) felsic domes and intrusions, 3) leached solfataric cap, 4) the precious metal veins cut Formation 5. Figure 14 joins Figure 20 on its eastern side.

REFERENCES

- EWING, Thomas E., 1980. Paleogene tectonic evolution of the Pacific Northwest; *Journal of Geology*, Vol. 88, p. 619-638.
- FRAKES, L.A., 1979. *Climates throughout Geologic Time*; Elsevier Scientific Publishing Company, New York, 310 p.
- GABRIELSE, H., 1985. Major dextral transcurrent displacements along the Northern Rocky Mountain Trench and related lineaments in north-central British Columbia; *Geological Society of America, Bulletin* 96, p. 1-14.
- GROND, H.C., CHURCHILL, S.J., ARMSTRONG, R.L., HARAKAL, J.E. and NIXON, C.T., 1984. Late Cretaceous age of the Hutshi, Mount Nansen, and Carmacks groups, southwestern Yukon Territory and northwestern British Columbia; *Canadian Journal of Earth Sciences*, Vol. 21, p. 554-558.
- LAMBERT, M.B., 1974. The Bennett Lake cauldron subsidence complex, British Columbia and Yukon Territory; *Geol. Surv. Can., Bulletin* 227, 213 p.
- MACDONALD, G.A., 1972. *Volcanoes*; Prentice-Hall Inc., 510 p.
- MIALL, A.D., 1978. Lithofacies types and vertical profile models in braided river deposits: a summary; in A.D. Miall, ed., *Fluvial Sedimentology*, Canadian Society of Petroleum Geologists, Memoir 5, p. 807-829.
- MONGER, J.W.H. and PRICE, R.A., 1979. Geodynamic evolution of the Canadian Cordillera: progress and problems; *Canadian Journal of Earth Sciences*, Vol. 16, p. 770-791.
- PRIDE, M.J., 1984. Interlayered sedimentary volcanic sequence, Mt. Skukum volcanic complex; in *Yukon Exploration and Geology 1983*, Dept. Ind. Aff. Nor. Dev., Whitehorse, Yukon, p. 94-104.
- PRIDE, M.J. and CLARK, G., 1985. An Eocene Rb-Sr isochron for rhyolite plugs, Skukum area, Yukon Territory; *Canadian Journal of Earth Sciences* (in press).
- RUST, B.R., 1978. Depositional models for braided alluvium; in A.D. Miall, ed., *Fluvial Sedimentology*, Canadian Society of Petroleum Geologists, Memoir 5, p. 605-625.

- RUST, B.R., 1984. Coarse Alluvial Deposits: in R.G. Walker, ed., *Facies Models*, Geoscience Canada reprint series 1, p. 9-21.
- SELF, S., 1982. Terminology and classifications for pyroclastic deposits in pyroclastic volcanism and deposits of Cenozoic intermediate to felsic volcanic islands with implications for Precambrian greenschist-belt volcanics; in L.D. Ayres, ed., *G.A.S. Short Course Notes*, Vol. 2, University of Manitoba, Winnipeg, Manitoba.
- SOUTHER, J.G., 1967. Acid volcanism and its relationship to the cordillera of British Columbia, Canada; *Bulletin Volcanologique*, Vol. 30, p. 161-176.
- SOUTHER, J.G., 1970. Volcanism and its relationship to recent crustal movements in the Canadian Cordillera; *Canadian Journal of Earth Sciences*, Vol. 7, p. 553-568.
- TEMPELMAN-KLUIT, D.J., 1979. Transported cataclasite, ophiolite and granodiorite in Yukon: evidence of arc-continent collision; *Geol. Surv. Can., Paper 79-14*, 27 p.
- VESSEL, R.R. and DAVIES, P.K., 1981. Nonmarine sedimentation in an active fore-arc basin; in F.G. Ethridge and R.M. Flores, ed., *Recent and Ancient Nonmarine Depositional Environments: Models for Exploration*, Special Publication Society of Economic Paleontologists and Mineralogists, Tulsa, Vol. 31, p. 31-45.
- WALKER, G.P.L., 1973. Lengths of lava flows; *Philosophical Transactions of the Royal Society of London*, Vol. A274, p. 107-118.
- WHEELER, J.O., 1961. Whitehorse map area, Yukon Territory; *Geol. Surv. Can., Memoir 312*, 156 p.
- WOLFE, Jack A. and POORE, Richard, 1982. Tertiary marine and nonmarine climatic trends; in *Studies in Geophysics in Earth History*, National Academy Press, p. 154-158.

ON THE GEOLOGY OF THE TERTIARY WRANGELL LAVAS IN THE ST. CLARE PROVINCE, ST. ELIAS MOUNTAINS, YUKON

Thomas Skulski and Don Francis
Department of Geological Sciences
McGill University
Montreal, Quebec

SKULSKI, T., and FRANCIS, D., 1986. On the geology of the Tertiary Wrangell lavas in the St. Clare Province, St. Elias Mountains, Yukon; in *Yukon Geology, Vol. 1; Exploration and Geological Services Division, Yukon, In-dian and Northern Affairs Canada*, p. 161-170.

ABSTRACT

The Wrangell lavas in the St. Clare province of southwestern Yukon are part of the larger Wrangell volcanic belt that has been active throughout the Late Cenozoic. These lavas have erupted in a transitional tectonic environment that reflects regional transpression along the Queen Charlotte transform-Fairweather-Totschunda Fault System and subduction of the Farallon Plate beneath North America. The volcanic province is composed of subalkaline basalt (31%), basaltic andesite (30%), andesite (21%), dacite (2%) and nepheline normative basalt (16%). The hypersthene normative basalt is (in order of appearance) spinel-olivine-plagioclase ± Fe-Ti oxide ± clinopyroxene phryic, whereas andesite contains plagioclase, Fe-Ti oxide, clinopyroxene, ± orthopyroxene phenocrysts, and dacite and intrusive latite contain phenocrysts of plagioclase, ± clinopyroxene, hornblende, ± biotite, ± sanidine. The nepheline normative rocks, where porphyritic, contain phenocrysts of olivine, plagioclase and hornblende. In the central part of the map area, the lowermost flows are nepheline normative basalt that is interbedded with clastic sediments and is overlain by basaltic andesite, andesite and volcanic conglomerate. This succession is overlain by basalt interbedded with clastic sedimentary rocks and pyroclastic rocks. In the southern part of the map area, alkaline basalt occurs at this stratigraphic level. The uppermost Wrangell lavas are andesitic with minor interbedded volcaniclastic rocks. The hypersthene normative lavas of the St. Clare province are transitional in terms of their $\text{Na}_2\text{O} + \text{K}_2\text{O}/\text{SiO}_2$ ratios between alkaline and subalkaline magma series and in terms of their FeO^*/MgO versus SiO_2 ratios between tholeiitic and calc-alkaline series. Chemical composition of these rocks reflects the unique tectonic setting within which they are found.

INTRODUCTION

The Late Cenozoic Wrangell lavas in southwestern Yukon and Alaska occupy a key position in the tectonic history of the northwestern Cordillera. These volcanic rocks comprise a volcanic belt that erupted along a major tectonic transition in the Cordillera. Toward the southeast, the Pacific-North American plate boundary is the Queen Charlotte Transform Fault (Atwater, 1970; Coney, 1978; Ewing, 1980) which extends northwestward into the continent along the Fairweather-Totschunda Fault System (Fig. 1). In southern Alaska and beneath the Aleutian Arc the plate margin is a subduction zone. In the transition between the Queen Charlotte Fault and the Aleutian trench, the fault-bounded Yakutat block of the North American plate margin (Plafker, 1983), is in the process of accreting with North America. At the leading edge of the Yakutat block a fragment of the Farallon oceanic plate has been subducting beneath the continent throughout the Late Cenozoic (Luhr et al., 1980; Bruns, 1983; Nye, 1983). The Wrangell volcanic belt overlies the Farallon-North American subduction zone in the northwest (Stephens et al., 1983), and a transpressional tectonic zone in the southeast. This paper is a preliminary report of an ongoing PhD study by the first author into the nature of the magmatic and tectonic processes that controlled the evolution of the Wrangell volcanics in the St. Clare province of southwestern Yukon.

This study documents the chemical composition and petrography of Wrangell lavas from selected stratigraphic sections measured within the St. Clare province in southwestern Yukon between Steele, Count and Wolverine Creeks and the Donjek River Valley (longitude $139^{\circ} 45' - 140^{\circ} 35'$ W, latitude $61^{\circ} 15' - 61^{\circ} 35'$ N, Fig. 1). The study summarizes the available geological data on this part of the St. Clare province and attempts to refine the existing stratigraphic nomenclature by describing and correlating measured sections within the volcanic pile. Chemical characteristics of the lavas are related to their macroscopic features and stratigraphic associations with the intention of providing useful mapping criteria.

REGIONAL SETTING

Late Cenozoic volcanic activity in the northwestern Cor-

dilla of Alaska and Canada is confined to two linear volcanic belts. Toward the east, within the Intermontane belt, is the broad Stikine volcanic belt, which is dominantly composed of Quaternary alkaline volcanic rocks (Souther, 1977 (Fig. 1)). Further to the west, within the Insular belt, is a northwesterly-trending volcanic belt known as the Wrangell volcanic belt (Souther, 1977). This volcanic belt is found within the Wrangell Mountains of southeastern Alaska and the St. Elias Mountains and Kluane Range of southwestern Yukon and northern British Columbia (Fig. 1). The Wrangell volcanic belt is comprised of the Wrangell lavas, a stratigraphic unit of formation rank (Mendenhall, 1905; MacKevett, 1970; Souther et al., 1975) which consists mainly of subalkaline Miocene to Recent volcanic and related intrusive rocks (Wrangell Intrusives of Souther et al., 1975).

Within Alaska, the Wrangell lavas range in age from Late Miocene (10 Ma, K-Ar dating — Denton et al., 1969; Nye, 1983) to Recent as evidenced by historic fumarole activity on Mt. Wrangell (Mendenhall, 1905; Nye, 1983). There is a preponderance of Quaternary volcanic products throughout the Wrangell Mountains. The volcanic rocks are calc-alkaline in composition (Richter et al., 1976; Richter et al., 1979; Nye, 1983) and are composed dominantly of andesites (57-63 wt% SiO_2) with lesser amounts of basalt, basaltic andesite, dacite and rhyolite (Nye, 1983). Pyroclastic rocks are subordinate to lavas in the Alaskan part of the Wrangell belt (Richter et al., 1976; MacKevett et al., 1978; Nye, 1983).

In Canada, the Wrangell lavas include those rocks previously called, 'The Tertiary Volcanic Rocks' (McConnell, 1905, 1906; Sharpe, 1943; Bostock, 1952), 'Newer Volcanics' (Cairnes, 1915) and in the Kluane Lake area, 'St. Clare Group' (Muller, 1967; Souther et al., 1975). The lavas in the southwestern part of the Wrangell belt in Canada are of Tertiary age (6 - 16 Ma, K-Ar dating by Souther, (unpublished) in Eisbacher et al., 1977). Souther et al. (1975) subdivided the Wrangell Belt in Canada into three volcanic provinces (Canyon Mountain, St. Clare and Alsek volcanic provinces) based on their distinctive stratigraphic and structural characteristics. These volcanic provinces include various proportions of pyroclastic rocks and sub-aerial lavas of basaltic to rhyolitic composition which are associated with numerous felsic and some mafic intrusives.

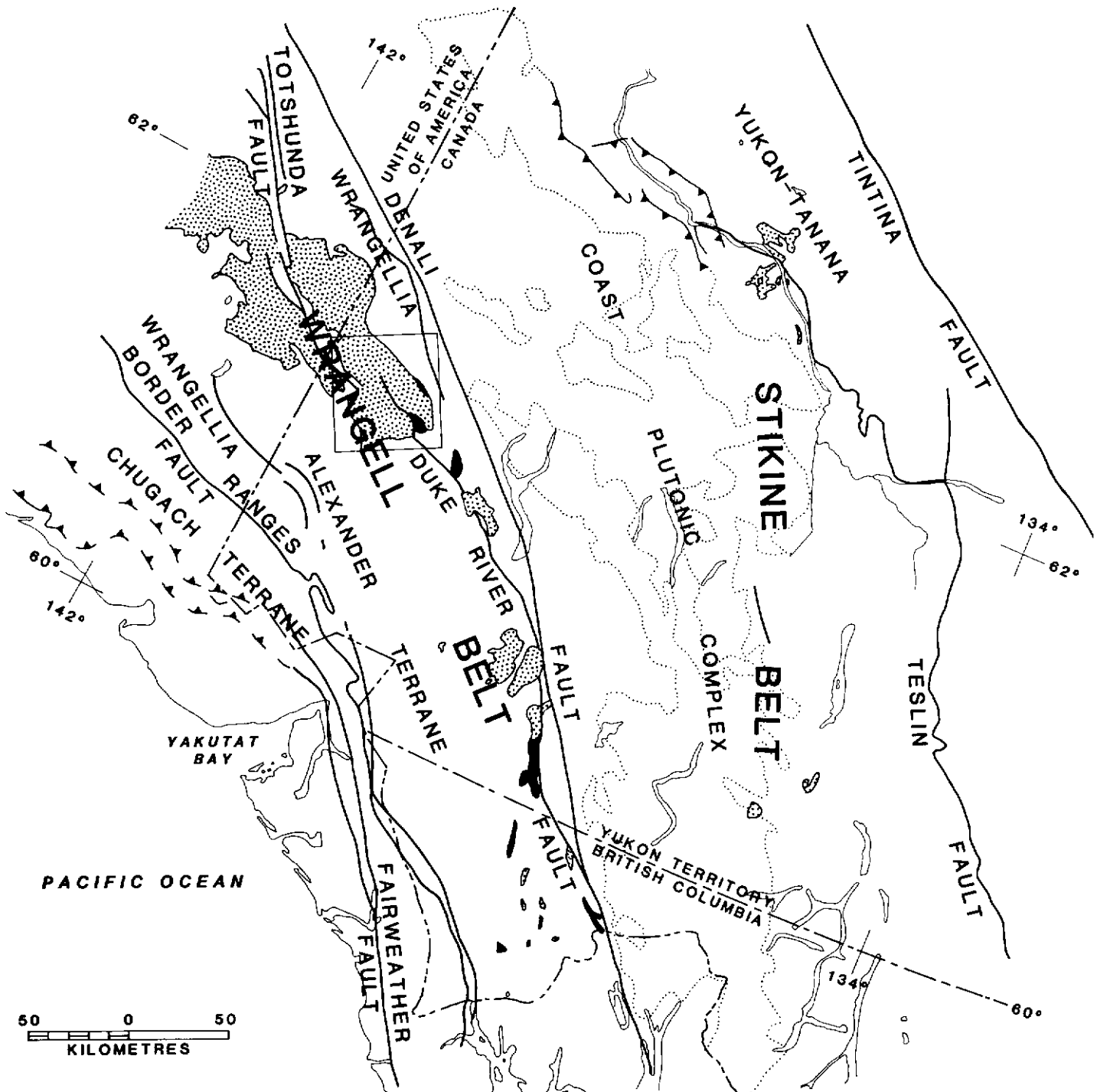


Figure 1. Location Map. The square shows the location of the study area in the St. Clare volcanic province. The dotted pattern represents the Wrangell lavas and the black pattern is the Amphitheater Formation.

PREVIOUS WORK AND GEOLOGICAL SETTING

Previous geological investigations in the study area include those of Sharpe (1943) into the Steele Creek area (Wolf Creek in his report) and Muller (1967) who produced a 1:253,440 scale map of the Kluane Lake area. The area was mapped in the 1970's by J. Souther of the Geological Survey of Canada at a scale of 1:125,000 as part of the St. Elias project, the results of which are found in the Geological Survey open-file map O.F. 829 (S.W. Kluane Lake Map Area, 115G and F (east half), Dodds, 1983).

In the central and northern parts of the map area, lowermost Wrangell lavas conformably overlie, and in places are interbedded with, continental clastic and coal-bearing sedimentary rocks of the Oligocene (?) Amphitheater Formation (cf. Muller, 1967; Eibacher et al., 1977). The Paleozoic and Mesozoic basement to the Tertiary Amphitheater Formation and Wrangell lavas is exposed in the

western and southeastern parts of the map area. Previous workers have shown that these basement rocks consist of two packages of stratigraphically distinct rocks that have been tectonically juxtaposed along the Duke River Fault (Fig. 2) (Muller, 1967; Dodds, 1983). South of the Duke River Fault, the Wrangell lavas unconformably overlie Devonian to Latest Triassic limestones and argillites in the Steele Creek area and Devonian massive to thick-bedded limestone and/or marble in the west near Klutlan Glacier. These rocks comprise a suspect terrane called the Alexander Terrane (Jones et al., 1977; Dodds, 1983). North of the Duke River Fault in the Steele and Cement Creek areas, the basement rocks underlying the Amphitheater Formation are composed of pre-Lower Permian gabbroic intrusive rocks (Dodds, 1983) and younger Latest Pennsylvanian to Lower Permian Skolai Group rocks of the Hasen Creek Formation (siliceous argillite, siltstone and older limestone and minor conglomerate). The Skolai Group rocks are themselves in-

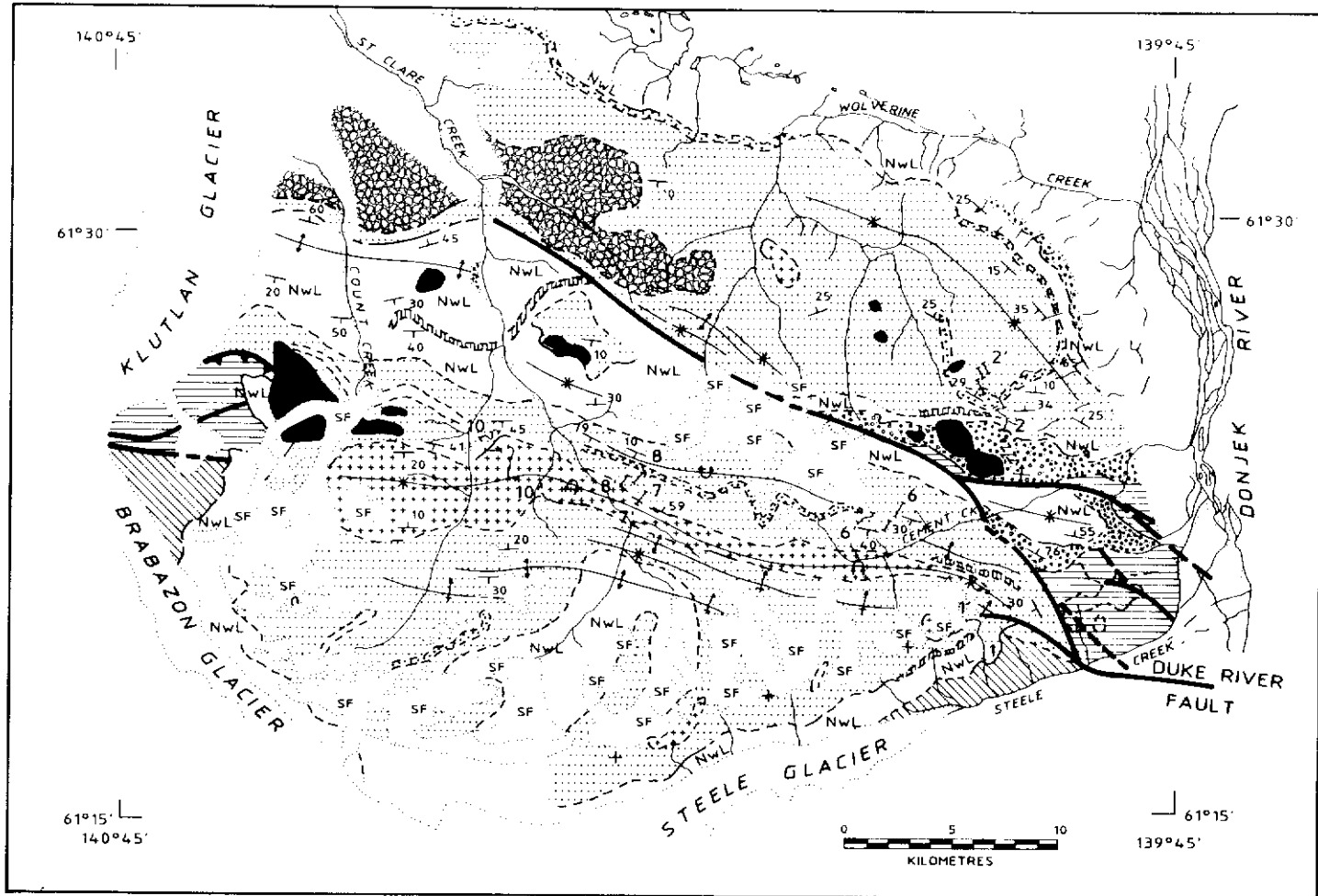
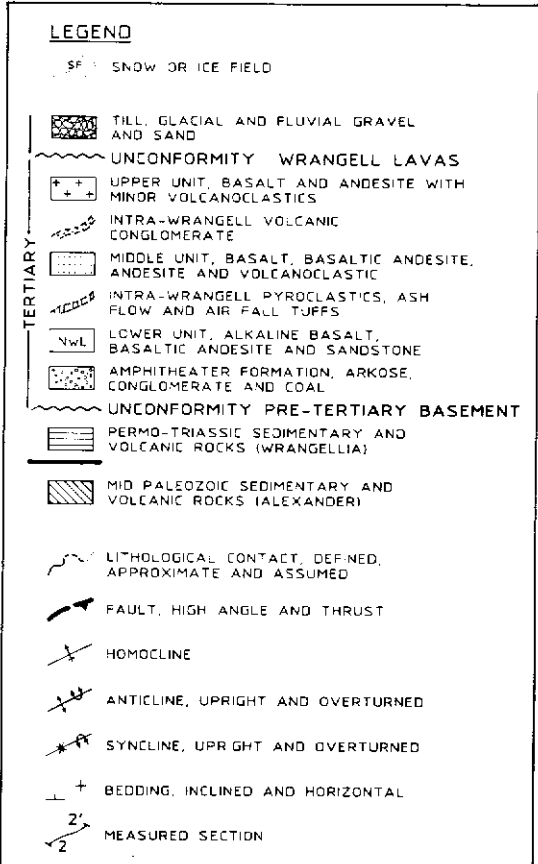


Figure 2. Geology of the Steele Creek Area. Geological map of part of the Wrangell volcanic belt, St. Clare province, St. Elias Mountains in the SW Yukon. Geology modified after Souther et al. (1975) and Muller (1967) and incorporating the results of the present study.

truded by Late Paleozoic to Mesozoic gabbro sills. In the easternmost corner of the map area, the Amphitheater Formation overlies Upper Triassic Chitistone and Nizina Limestones and Nikolai Greenstone. North of Cement Creek, the Amphitheater Formation unconformably overlies Pennsylvanian to Earliest Permian pyroclastic rocks of the Station Creek Formation. In the western part of the map area near Klutlan glacier, the Amphitheater Formation is not present and Wrangell lavas unconformably overlie and in places are in fault contact with the Steele Creek Gabbro Complex. All of these Paleozoic and Mesozoic basement rocks north of the Duke River Fault comprise a suspect terrane known as Wrangellia (Jones et al., 1977; Dodds, 1983).

Throughout Alaska and Yukon, all known contacts between the Wrangellia and Alexander Terranes are faults along which the juxtaposition of dissimilar Triassic sequences suggests post-Triassic docking of these two terranes. Since then, they appear to have comprised a composite terrane which was overlain by the Late Jurassic to Early Cretaceous Gravina and Nutzotin Mountain sequence in the eastern Alaska Range (Coney et al., 1980 and Monger et al., 1982). These terranes are believed to have been accreted to North America by Mid-Cretaceous time and migrated to the north from the Late Cretaceous to Early Tertiary along major strike-slip faults such as the Denali Fault System (Monger, 1984).

The Duke River Fault which separates the Wrangellia and Alexander Terranes in the map area is believed to be part of the Denali Fault System. It was originally mapped as a west-dipping thrust fault that postdated the emplacement of the Wrangell lavas (Muller, 1967). Souther et al. (1975), however, have shown that the main strand of the Duke River Fault cuts only the older Wrangell



lavas in the Steele Creek area. Campbell et al. (1978) have suggested that the age of the principal displacement along the Duke River Fault is early or early Late Cretaceous and pre-Miocene. However, possibly related faults (Cement Creek Fault and unnamed fault, Fig. 2) cut the entire pile of Wrangell lavas between the Duke and Denali-Shakwak faults. Although the sense of displacement along these faults is enigmatic at present, they require that movement continued to Pliocene or younger time (Campbell et al., 1978; Clague, 1979). In addition, Souther et al. (1975) have shown that east of Klutlan glacier (Fig. 2), a young northerly-vergent thrust fault has juxtaposed Latest Pennsylvanian to Lower Permian Hasen Creek Formation rocks on lower Wrangell lavas.

It is clear that the Wrangell lavas were emplaced after most of the principal displacement along the major regional structures. Eibacher et al. (1977) have suggested that the underlying Amphitheater Formation was deposited in small fault-bounded basins during Oligocene time. Paleocurrent data in the Cement Creek area suggest a westerly-directed sediment transport direction and K-Ar ages on detrital biotite in these sedimentary rocks suggests that the source area was east of the Shakwak Valley (Eibacher et al., 1977). Eibacher et al. have suggested that the present outcrop pattern indicates that the width of the valley into which the Amphitheater Formation was deposited must have exceeded 16 km. Furthermore, the present topographic contour interval between 2000 and 3000 m can be taken as the margin of clastic deposition during Amphitheater time, since the Wrangell lavas lie directly on older basement rocks above this elevation. Eibacher et al. conclude that in mid-Tertiary time the St. Elias region was a rolling upland with wide shallow valleys and a temperate climate. Westward flowing drainage deposited blankets of gravel, sand, and coal into a broad valley and later faulting and folding accentuated local relief and triggered rockslides and debris flows (Eibacher et al., 1977). It is within this intermontane setting that large volumes of Miocene Wrangell lavas are believed to have been subsequently erupted.

In Alaska, thick successions of tillite are interbedded with Wrangell lavas of Miocene to Pliocene age (10-3.6 Ma, K-Ar dating — Denton et al., 1969). Similar thick successions of folded tillite unconformably overlie Wrangell lavas in the northwestern part of the map area (Fig. 2), suggesting that in Miocene time the St. Elias Mountains may have attained an elevation sufficiently high to support thick sheets of ice (cf. Eibacher et al., 1977). Continued Neogene uplift of the St. Elias Mountains has resulted in the folding and faulting of the Tertiary Wrangell lavas.

STRUCTURE OF THE WRANGELL LAVAS

The generally excellent exposure afforded by this alpine terrane, and the differential weathering habit of the stratigraphic units permits the tracing of large scale structures for considerable distances on the ground and in aerial photographs.

Souther et al. (1975) have shown that the structural style within the map area (Fig. 2) is highly variable. The trend of the hinge lines of major folds is west-northwest and large scale folds can be traced for distances up to 30 km in the map area. Structural style changes from north to south in terms of the density of folds and the geometry of individual folds. In the southern part of the map area, the Wrangell lavas are flat-lying, whereas a few kilometers toward the north they are folded into a north-dipping homoclinal. Toward the west-northwest, these north-dipping homoclinal structures trend into upright anticlines and then into a tightly folded syncline-anticline pair that is overturned to the south (north-dipping) with dips of approximately 80° in the vicinity of the southeast branch of St. Clare Creek. Further toward the west-northwest in the vicinity of the southwest branch of St. Clare Creek, the syncline becomes upright and open with limbs dipping at 20°. The core of this synclinal structure exposes the youngest stratigraphy in the area.

Souther et al. (1975) pointed out that even in the most intensely folded successions, such as in the St. Clare Creek valley, the internal disruption and deformation of the Wrangell lavas is minimal. Furthermore, the lavas have undergone a minimum of burial metamorphism, with zeolite facies representing the peak metamorphic conditions.

STRATIGRAPHY of the WRANGELL LAVAS

Souther et al. (1975) subdivided the Wrangell lavas in the St. Clare province into three informal units:

(NwL)

A lower unit comprising thick, blocky flows of mainly nonporphyritic basaltic andesite; locally separated by layers of white or light grey clay and coaly siltstone; overlain by a succession of 20 to 40 uniformly thin (0.6 to 1.8 m) closely stacked basaltic andesite flows with no interflow clastic or pyroclastic material.

(NwM)

A middle unit comprising both porphyritic and nonporphyritic basaltic andesite flows and minor pillow lavas, interlayered with a relatively high proportion of felsic ash flows, air fall, and volcanic derived sedimentary deposits including coaly tuff, sandstone and conglomerate.

(NwU)

An upper unit comprising basaltic flows and scoria, volcanic conglomerate, light grey dictytaxitic andesite and olivine basalt (Souther et al., 1975).

In this study, a series of six stratigraphic sections were measured through the volcanic pile of the St. Clare province. Rocks were classified using a two tiered system, first on the basis of SiO₂ weight percent abundance (normalized to 100% volatile free) and second on the presence or absence of nepheline in the norm (calculated assuming Fe₂O₃ = 0.1 Fe total). The arbitrary limits used for the subdivision of the rocks are: basalt (less than 52.0%), basaltic andesite (greater than, or equal to 52.0% and less than 55.0%), andesite (greater than, or equal to 55.0%, and less than 63.0%), dacite (greater than, or equal to 63.0%, and less than 70.0%) and rhyolite (greater than, or equal to 70.0%). A total of 155 whole rock analyses are available from the study area; 31% are basalts, 30% are basaltic andesites, 21% are andesites, 2% are dacites and 16% are nepheline normative basalts. Rocks which were not analysed were classified by comparison with analysed rocks using parameters such as colour, hardness, weathering habit, mineralogy, and abundance of phenocrysts.

PETROGRAPHY OF THE WRANGELL LAVAS

Rocks of basaltic composition in the Wrangell lavas are found as massive flows with vesicle-rich (in places amygdaloidal) oxidized flow tops with smooth or brecciated surfaces. These massive flows range in thickness from less than 5 m (relatively rare) up to 40 m, with most flows around 10 m. Most basalt flows have dark grey to dark green-grey fresh surfaces and brown-grey and brown weathered surfaces. Both porphyritic (the most abundant) and equigranular ophitic basalts are found.

Porphyritic basalts typically contain around 10% phenocrysts (all mineral abundances quoted are based on visual estimates) but can range from 5 to 40%. The phenocrysts are typically small (less than 1.5 mm) but locally plagioclase phenocrysts can range in size up to a few millimetres. The phenocrysts observed are olivine with tiny opaque mineral inclusions (spinel (?)), plagioclase and less commonly clinopyroxene and an opaque phase (Fe-Ti oxide (?)). In rocks with olivine, plagioclase and clinopyroxene phenocrysts, the relative proportion of plagioclase although variable, is typically around 60%, the remainder being typically olivine and minor amounts of clinopyroxene. Olivine almost always shows at least some alteration to goethite, talc or carbonate, which in the least altered grains appears to be concentrated on the margins and in fractures. Plagioclase phenocrysts are commonly zoned and may contain inclusions of olivine. Some rocks contain small glomerocrysts of olivine with laths of plagioclase on their outer margins. Paragenetic sequence of phenocrysts in these rocks is spinel, olivine, plagioclase, an opaque Fe-Ti oxide and clinopyroxene. Groundmass of the porphyritic basalts is commonly intersertal to intergranular and contains microlites of plagioclase (in places trachytic), anhedral granular clinopyroxene, and subhedral to cruciform opaques. Interstitial glass is commonly devitrified to fine, accicular anisotropic mineral(s) (clinopyroxene (?)) that are in turn commonly replaced by carbonate. Carbonate filled amygdalules are less commonly present. The equigranular ophitic basalts range from fine to medium grain size and are composed of euhedral olivine, plagioclase with anhedral clinopyroxene which subophitically encloses plagioclase laths and subhedral

opaque grains. Cores of some plagioclase grains contain olivine inclusions and similarly, some clinopyroxene contains plagioclase inclusions. Some of these rocks are ophimottled with small oikocrysts of clinopyroxene dispersed through the rock that contain plagioclase and olivine chadacrysts. Many of the equigranular ophitic basalts contain interstitial glass.

Basaltic rocks with nepheline in their norms are commonly equigranular and often indistinguishable from the other ophitic basalts. However, the lava flow near the base of Section 2 (Fig. 3) which contains the highest normative nepheline (10.25%) has a trachytic texture and contains phenocrysts of olivine, plagioclase and microphenocrysts of hornblende. The groundmass of this rock is comprised of plagioclase microlites, opaques and biotite.

The basaltic andesite is petrographically similar to the porphyritic basalt and is characterized by clinopyroxene phenocrysts. Size of phenocrysts tends to be larger in the basaltic andesites (up to 3 mm) and the abundance of plagioclase relative to olivine is higher than in the basalts. Only one basaltic andesite flow (Section 1) contains normative nepheline.

Andesite flows are easily identified in the field by their high abundance of plagioclase phenocrysts (up to 45%), the large size of phenocrysts (plagioclase up to 6 mm) and their highly vesicular (or amygdaloidal) nature. Commonly, the andesite flows are thin and have smooth flow tops. Colour of the flows is variable, but is generally grey on the fresh surface and pale grey or grey/brown on weathered surfaces. The andesites have an average phenocryst content of approximately 20% including olivine (rare), plagioclase (85%), opaque (Fe-Ti oxide, less than 5%), clinopyroxene (10%), and orthopyroxene (less than 5%). Paragenetic sequence of phenocrysts is olivine, plagioclase, Fe-Ti oxide (?), clinopyroxene and orthopyroxene. Groundmass is commonly trachytic consisting of microlites of plagioclase with clinopyroxene and opaques. Some andesites at the base of Section 2 contain cognate xenoliths that are plastically deformed and compositionally similar to extrusive rocks in the area.

Dacite occurs as comparatively rare thick flows (up to 100 m in Section 10). The fresh surface is grey and the weathered surface is generally pale-grey/pink or pale-brown. The flows commonly have thick brecciated tops with relatively thin massive portions. Dacites is always porphyritic with phenocryst contents around 25%. Phenocryst phases in order of appearance are plagioclase (75%), an opaque (Fe-Ti oxide (?), less than 5%), clinopyroxene (5%), orthopyroxene (trace), hornblende (20%), biotite (trace, commonly completely oxidized), apatite and zircon (less than 5%). The groundmass contains sanidine laths (?) and quartz.

Although fragmental deposits are subordinate to lavas within the Wrangell lavas, they act as useful marker horizons in the volcanic stratigraphy. Most of the pyroclastic rocks found within the Wrangell lavas are located within the middle unit (NwM). These include welded ash flow deposits such as those found on the northern margin of Wolverine Plateau, felsic air fall deposits, such as those found interbedded with fluvial conglomerates in the St. Clare Creek area and coarse grained matrix and clast supported volcanic conglomerates (NwCG) (Fig. 3). The volcanic conglomerates include both debris flow (lahar) and block and ash flow deposits.

Clastic sedimentary rocks including clast-supported conglomerate, subarkosic sandstone and low-rank coal seams are interbedded with the lower Wrangell lavas. These sedimentary rocks are identical to the underlying Amphitheater Formation. Clast-supported and imbricated conglomerates and cross-bedded sandstones occur within the middle unit (NwM). These rocks contain clasts that are exclusively of intra-Wrangell origin.

There are numerous intrusive bodies related to the Wrangell lavas. Some of these are high level sills or dykes and are petrographically similar to the lavas. A gabbroic sill in Cement Creek (Fig. 3) has a layered stratigraphy and reaches 150 m in thickness. Numerous felsic plugs intrude the Wrangell lavas, some reaching 6 km in width. Most plugs are porphyritic latite with phenocrysts (up to 40%) of sanidine, plagioclase, hornblende and biotite (both of which are generally oxidized). Groundmass of these rocks is fine-grained and contains laths of sanidine and possibly some quartz. Some of the plugs contain cognate xenoliths of surrounding wallrocks. The margins of many of the intrusive plugs are commonly sharp, brecciated and crosscut by thin quartz veins. Pyritization is locally prominent at the margins and within thin quartz veins (2-5 cm) crosscutting the interiors of the large intrusive plugs north

of Cement Creek (Fig. 3). The exposed roof of one of these felsic plugs between the southwestern branch of St. Clare and Count Creeks is bleached and brecciated. Lavas that overlie this intrusive body are also extensively brecciated and bleached white, and all of their opaque minerals have been oxidized. A dense network of andesitic and basaltic dykes (up to 2 m in width) crosscuts the brecciated rocks. Alteration in these dykes is variable, some are heavily oxidized whereas other younger dykes have fresh glassy chill margins. Souther et al. (1975) describe similar intrusive relations and altered wallrocks in the vicinity of Brabazon Glacier.

CHEMICAL STRATIGRAPHY

Wrangell lavas in the St. Clare province straddle the MacDonald (1968) dividing line between alkaline and subalkaline compositions on a total alkalis versus silica diagram (Fig. 4). The nepheline normative rocks quite clearly lie in the alkaline field (Fig. 4). The amount of normative nepheline in the basalts of Section 1 is considerably lower (to 2.7%) than in those of Section 2. In Section 2, nepheline normative basalts occur interbedded with clastic sediments at the base of the section, whereas in Section 1, although a few nepheline normative rocks occur at lower stratigraphic levels, most occur in mid to upper levels in unit NwM (Fig. 3).

Distribution of rock types is generally consistent with the stratigraphy proposed by Souther et al. (1975). In Section 1, basaltic andesite is abundant in the lower unit (NwL), however, many of the flows of the middle unit (NwM) are nepheline normative and subalkaline basalts (Fig. 3). Characteristically, the upper unit (NwU) is rich in basalt. It is clear, however, that Section 1 is considerably thinner than the sections measured to the north. The lower Wrangell lavas in Section 2 are dominated by basaltic andesite but also contain previously unreported nepheline normative basalt. Lower to mid reaches of the middle unit (NwM) in Sections 2, 6 and 7 contain abundant flows of basaltic andesite and andesite, whereas basalt is more important in the upper reaches where flows are interbedded with fragmental rocks (Section 7). Upper parts of the Wrangell stratigraphy (NwU) in Sections 7 and 10 are andesite rich in contrast to the basalt that is characteristic of the upper NwU unit defined by Souther et al. (1975).

It is premature to attempt large scale correlations in the map area due to the large distance between sections and lack of sufficient stratigraphic control. It is clear, however, that the fragmental rocks (volcanic and sedimentary) will play an important role in stratigraphic correlation in this area. The correlation between Sections 8 and 6 are based on their positions relative to the thick volcanic conglomerate that underlies 8 and occurs near the top of 6 (Fig. 3). The occurrence of andesitic lavas relative to this conglomerate is a particularly useful marker between Sections 2, 6 and 8. Correlation between Section 1 and the rest of the area is tenuous at present, because of the probability that this section, which is not underlain by Amphitheater rocks, was topographically high relative to the rest of the area (cf. Eibacher et al., 1977).

CHEMISTRY OF THE WRANGELL LAVAS

The transitional tectonic setting of the Wrangell lavas is reflected in their chemical composition which is not easily classified in terms of type magmatic series. While a distinct group of rocks within the St. Clare province can be classified as alkaline on the basis of $\text{Na}_2\text{O} + \text{K}_2\text{O}/\text{SiO}_2$ ratios and normative nepheline, most lavas are hypersthene normative and transitional in terms of their alkali/silica ratios (Fig. 4). Assigning the hypersthene normative Wrangell lavas in the study area to either the tholeiitic or calc-alkaline magma series is also problematic. Although these lavas lie in the calc-alkaline field of an AFM diagram (Irvine et al., 1971, Fig. 6), they are not clearly discriminated in a plot of FeO^*/MgO versus SiO_2 (Fig. 5), (cf. Miyashiro, 1974). Gill (1982) has observed, however, that many analyses of orogenic andesite (hypersthene normative rocks with SiO_2 of 53 - 63%, K_2O less than (0.145 x SiO_2) and TiO_2 less than 1.75%) considered calc-alkaline on the AFM diagram are tholeiitic using Miyashiro's (1974) criteria. The St. Clare lavas exhibit compositional characteristics which are transitional between alkaline and subalkaline series and tholeiitic and calc-alkaline magma series in terms of their alkali/silica and FeO^*/MgO ratios and normative mineral compositions.

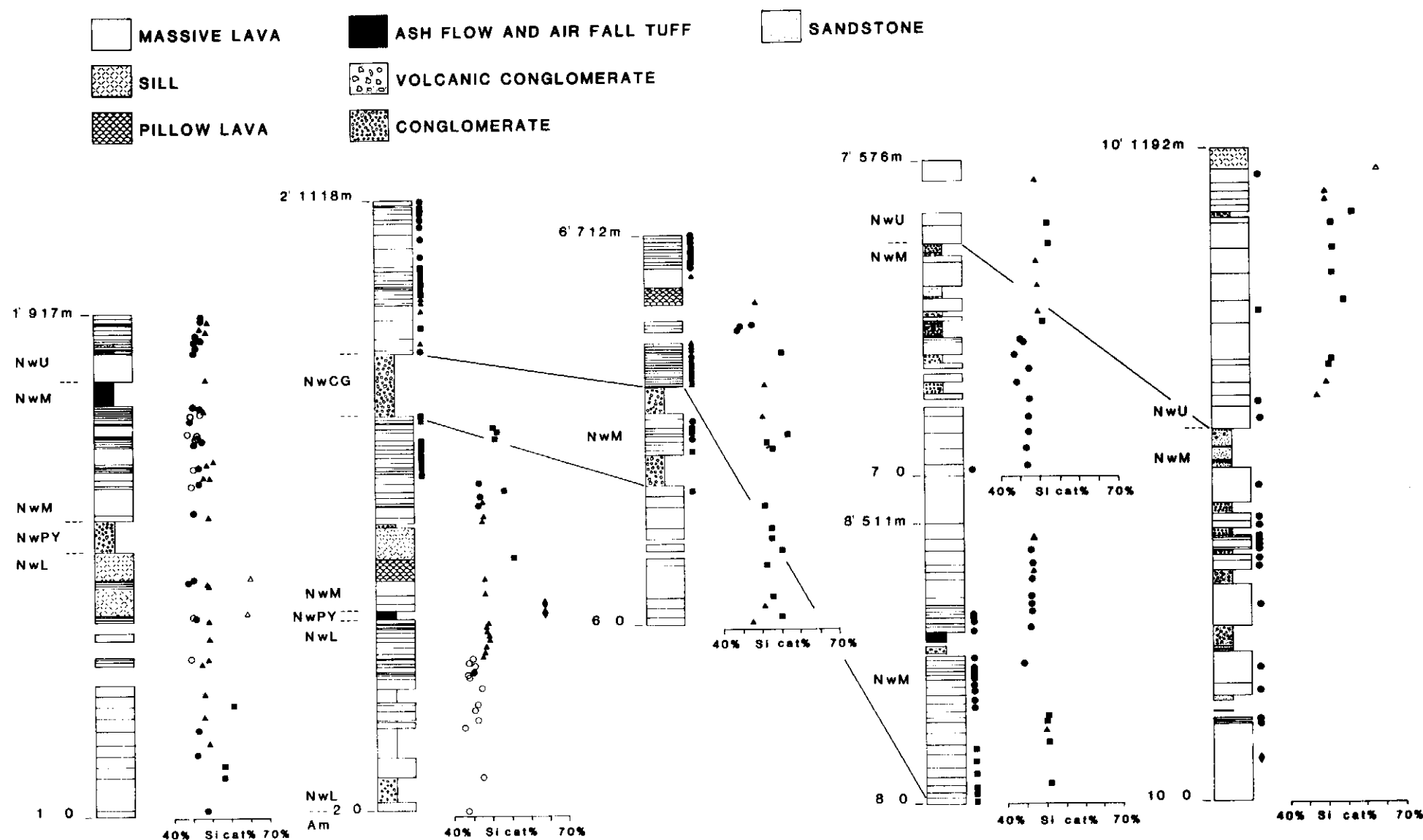


Figure 3. Stratigraphic Sections from the St. Clare Province. Location of measured sections is shown in Fig. 2. The whole rock analyses were made on a Phillips PW1400 x-ray fluorescence unit at McGill University. Open circle symbols represent nepheline normative basalts, dark circles are basalts, black triangles are basaltic andesites, black squares are andesites, black diamonds are dacites and open triangles are intrusive latites.

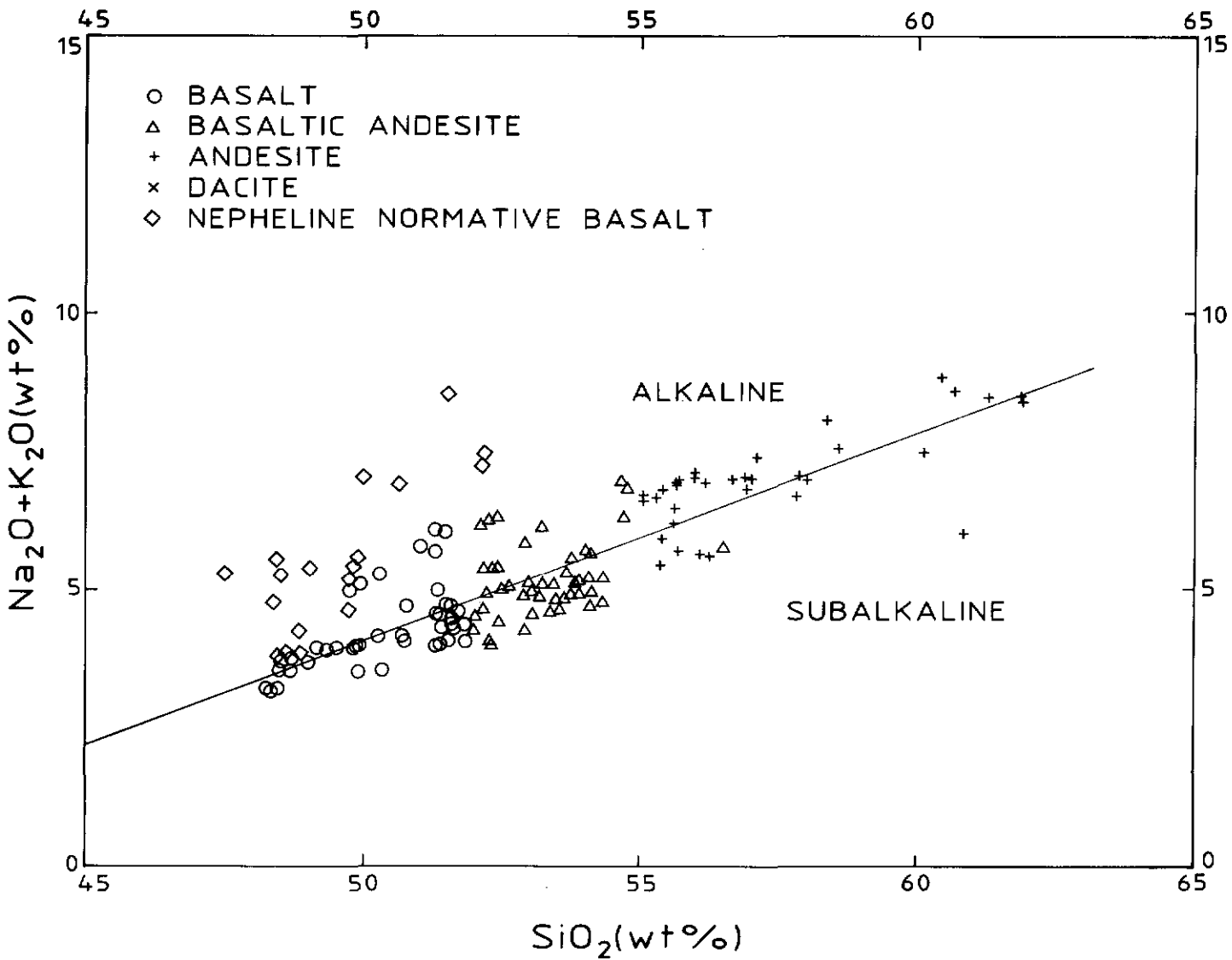


Figure 4. Total Alkalies Versus Silica Diagram. Analyses are presented on a normalized to 100% volatile-free basis. The dividing line is taken from Macdonald (1968) for Hawaiian volcanic rocks.

SUMMARY AND CONCLUSIONS

Approximately 2300 m of Mid-Tertiary Wrangell lavas are preserved in the central part of the St. Clare province in the St. Elias Mountains. The Wrangell lavas conformably overlie, and are in part interbedded with, clastic and coal-bearing continental-derived sedimentary rocks of the Amphitheater Formation, all of which appear to have accumulated in intracontinental fault-bounded basins. The lowermost Wrangell lavas are crosscut by a strike-slip fault, the Duke River Fault, which is part of a large Late Mesozoic to Cenozoic system of dextral transcurrent faults in the northwestern Cordillera. Younger lavas of the St. Clare province, however, overlie this fault. Neogene deformation in this area resulted in the uplift of the St. Elias Mountains and the folding and faulting of the Wrangell lavas. This deformation, however, has been laterally heterogeneous. Over much of the area, the lavas are horizontal or gently folded whereas locally they are crosscut by faults and folded into tight overturned structures.

Wrangell lavas in the St. Clare province are composed of subalkaline basalt, basaltic andesite, andesite, dacite and latite (intrusive) as well as lesser amounts of alkaline basalt. Hypersthene normative basalt and basaltic andesite are (in their relative order of appearance) spinel - olivine - plagioclase \pm Fe-Ti oxide \pm clinopyroxene phryic whereas andesite contains plagioclase, Fe-Ti oxide, clinopyroxene, and late orthopyroxene phenocrysts and dacite and latite contain plagioclase, clinopyroxene, hornblende,

and late biotite and sanidine phenocrysts. The alkaline basalt is commonly equigranular, although the most alkaline flow (10% normative nepheline) contains phenocrysts of olivine, plagioclase and hornblende.

Lowermost Wrangell lavas are composed of alkaline basalt interbedded with clastic sediments in the central part of the map area and hypersthene normative basaltic andesite and basalt in the south. Mid levels of the stratigraphy are composed of basaltic andesite, andesite, and a volcanic conglomerate that can be traced throughout a large part of the map area. These are in turn overlain by a thick succession of subalkaline basalt interbedded with clastic sedimentary rocks and felsic air fall tuff. In the southern part of the map area, alkaline basalt also occurs at this stratigraphic level. The youngest Wrangell lavas are mainly andesite with minor interbedded volcaniclastic rocks.

Mid to Late Cenozoic tectonics of the northwestern Cordillera is transpressional in the vicinity of the Queen Charlotte transform - Fairweather - Totschunda Fault System. Further to the north, the Farallon plate has been subducting beneath the North American plate. The Wrangell volcanic belt overlies the transition zone between these two tectonic regimes. In Alaska, the Wrangell lavas are calc-alkaline and are believed to have erupted over a Benioff Zone. Further to the south in the St. Clare province, the Wrangell lavas contain rocks of both alkaline and subalkaline affinity. The subalkaline rocks cannot be easily categorized as calc-alkaline or tholeiitic, since they share attributes of both series.

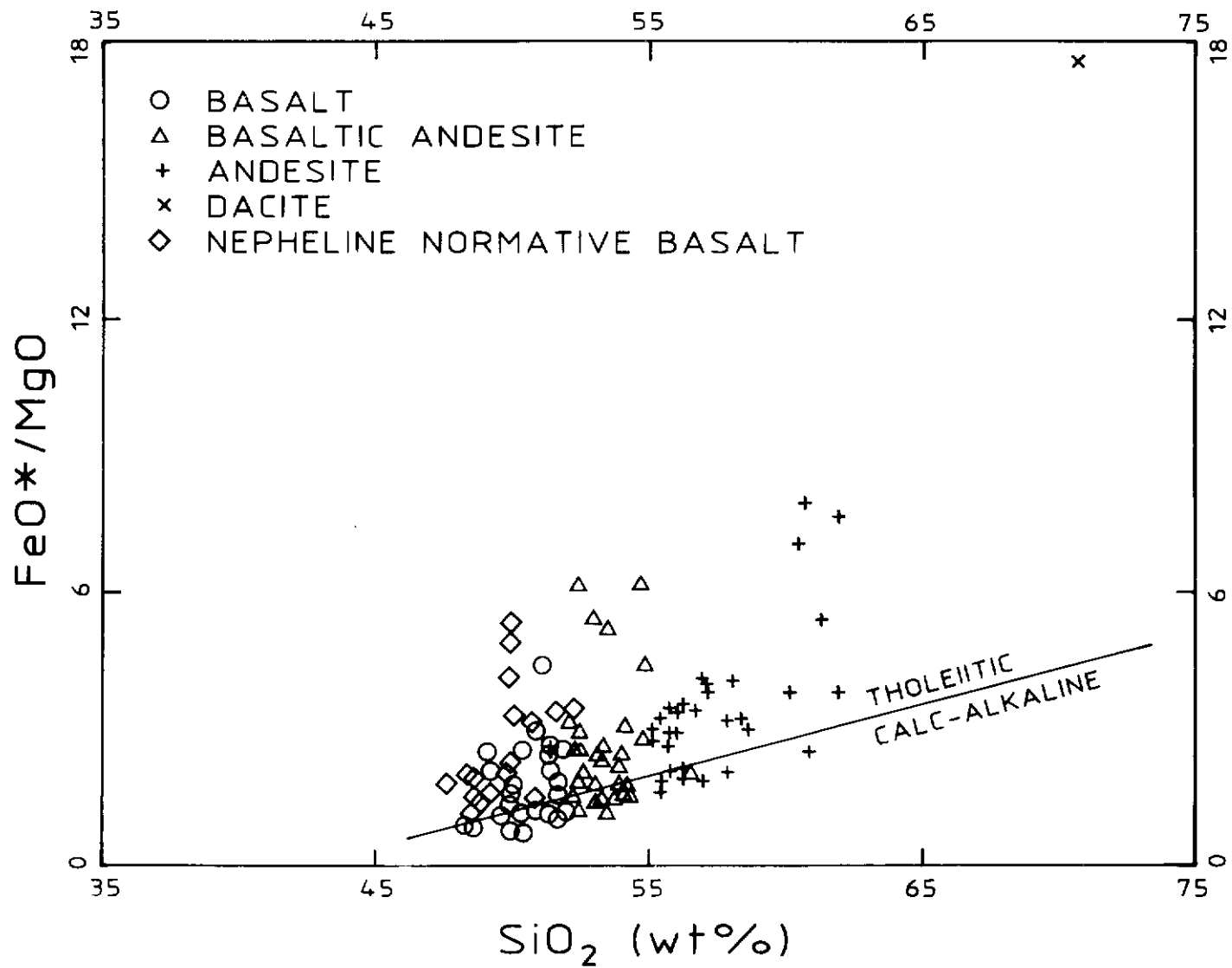


Figure 5. FeO^*/MgO Versus SiO_2 Diagram. Total iron is calculated as FeO and all analyses are normalized to 100% volatile free. The dividing line is taken from Miyashiro (1974).

Future work in this study will concentrate on the relationship between the tectonic setting of these volcanic rocks and the processes which account for their transitional compositional affinities.

ACKNOWLEDGEMENTS

The authors would like to thank John Ludden for his comments on this work and for providing thin sections. T. Skulski is grateful to A. Sasso and D. Heon for assistance in the field and to T. Ahmedali for consultation in laboratory work. The efficient services of the staff at the Arctic Research Institute of North America base at Kluane Lake are gratefully acknowledged. This research was supported by a Northern Supplement NSERC grant to D. Francis and J. Ludden, and from an NSERC operating grant to D. Francis. Field expenses were partly defrayed by a Northern Scientific Training Grant to T. Skulski. Helicopter services were provided courtesy of the Exploration and Geological Services Division, Northern Affairs Program, D.I.A.N.D.

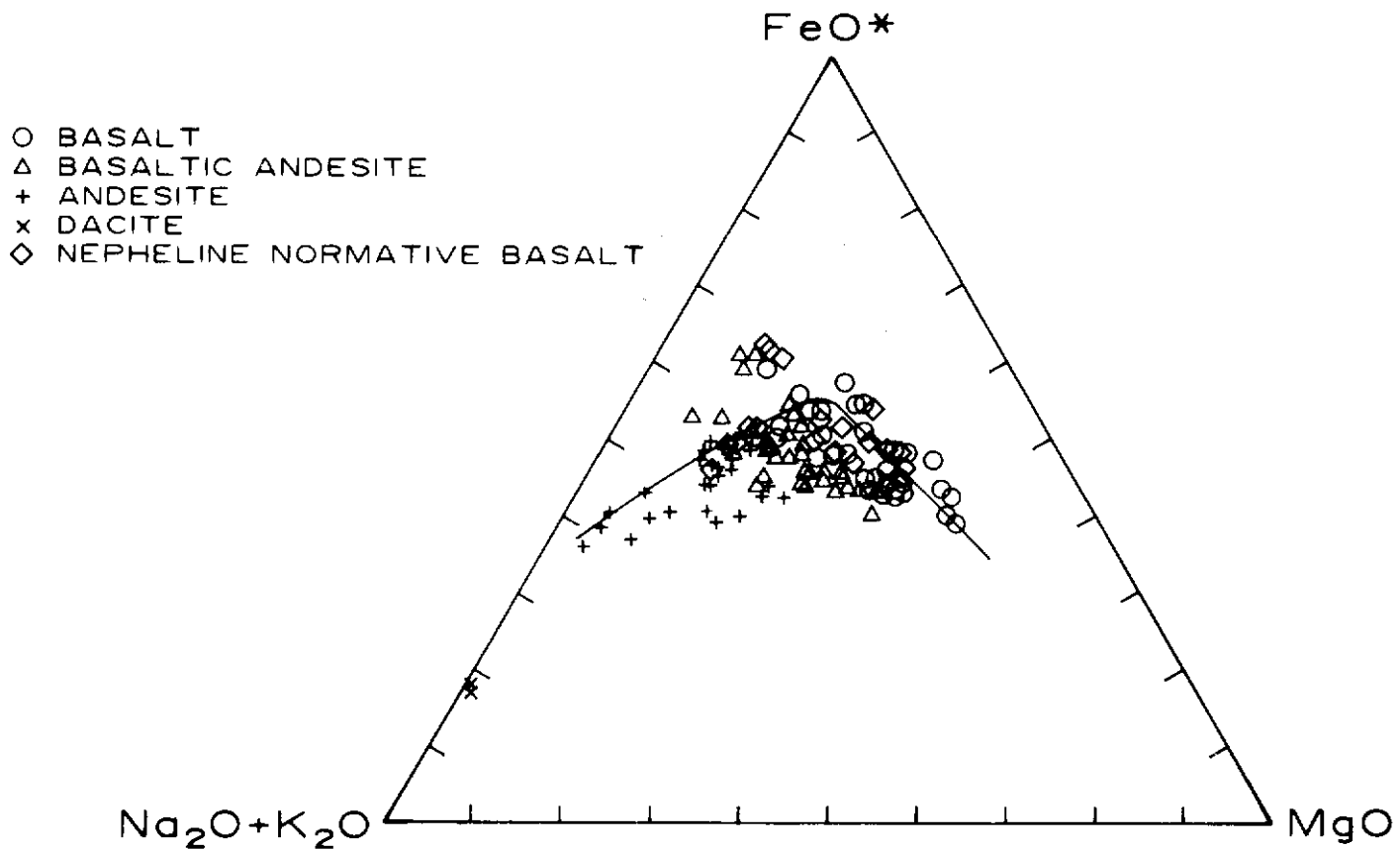


Figure 6. AFM Diagram. The analyses are in weight percent normalized to 100% volatile free. Total iron is calculated as FeO. The subdividing line between tholeiitic (above the curve) and calc-alkaline (below the curve) rocks is taken from Irvine et al. (1971).

REFERENCES

- ATWATER, T., 1970. Implications of plate tectonics for the Cenozoic tectonic evolution of western North America; Geological Society of America Bulletin, Vol. 81, p. 3513-3536.
- BOSTOCK, H.S., 1952. Geology of northwest Shakwak Valley, Yukon Territory; Geological Survey of Canada, Memoir 267.
- BRUNS, T.R., 1983. Model for the origin of the Yakutat block, an accreting terrane in the northern Gulf of Alaska; Geology, Vol. 11, p. 718-721.
- CAIRNES, D.D., 1915. Upper White River district, Yukon; Geological Survey of Canada, Memoir 50, p. 97-102.
- CAMPBELL, R.B., DODDS, C.J., 1978. Operation St. Elias, Yukon Territory; Geological Survey of Canada, Paper 78-1A, p. 35-41.
- CLAGUE, J.J., 1979. The Denali Fault System in southwest Yukon Territory — a geologic hazard?; Geological Survey of Canada, Paper 79-1A, p. 169-178.
- CONEY, P.J., 1978. Mesozoic-Cenozoic Cordilleran plate tectonics; Geological Society of America, Memoir 152, p. 33-50.
- CONEY, P.J., JONES, D.L., MONGER, J.W.H., 1980. Cordilleran suspect terranes; Nature, Vol. 288, p. 329-333.
- DENTON, G.H., ARMSTRONG, R.L., 1969. Miocene-Pliocene glaciations in southern Alaska, American Journal of Science, Vol. 267, p. 1121-1142.
- DODDS, C.J., 1979. Geology southwest Kluane Lake map area (115G and F(E1/2)), Geological Survey of Canada, Open File Map (o.f.829).
- EISBACHER, G.H., HOPKINS, S.L., 1977. Mid-Cenozoic paleogeomorphology and tectonic setting of the St. Elias Mountains, Yukon Territory; Geological Survey of Canada, Paper 77-1B, p. 319-335.
- EWING, T.E., 1980. Paleogene tectonic evolution of the Pacific northwest; The Journal of Geology, Vol. 88, p. 619-638.
- GILL, J., 1981. Orogenic andesites and plate tectonics; Springer-Verlag Berlin, Heidelberg, New York, 390 p.

- IRVINE, T.N., BARAGAR, W.R.A., 1971. A guide to the chemical classification of the common volcanic rocks; *Canadian Journal of Earth Sciences*, Vol. 8, p. 523-548.
- JONES, D.L., SIBERLING, N.J., HILLHOUSE, J., 1977. Wrangellia — a displaced terrane in northwestern North America; *Canadian Journal of Earth Sciences*, Vol. 14, p. 2565-2577.
- LUHR, J.C., PLAFKER, G., 1980. Holocene Pacific - North American plate interaction in southern Alaska: implications for the Yakataga seismic gap; *Geology*, Vol. 8, p. 483-486.
- MCCONNELL, R.G., 1905. The Kluane mining district, southwest Yukon; *Geological Survey of Canada, Annual Report 1904*, Vol. 16, p. 1a-18a.
- MCCONNELL, R.G., 1906. Headwaters of White River Yukon Territory; *Geological Survey of Canada, Summary Report 1905*, p. 19-26.
- MACDONALD, G.A., 1968. Composition and origin of Hawaiian lavas; in: *Studies in Volcanology* (R.R. Coats et al., eds.), *Geological Society of America, Memoir 116*, p. 477-522.
- MACKEVETT, JR., E.M., 1970. Geology of the McCarthy B-4 quadrangle, Alaska; *United States Geological Survey, Bulletin 1333*, 31 p.
- MACKEVETT, JR., E.M., 1978. Geological map of the McCarthy quadrangle, Alaska; *United States Geological Survey, Misc. Inv. map I-1032*, scale 1:250,000.
- MENDENHALL, W.C., 1905. Geology of the Copper River region, Alaska; *United States Geological Survey, Professional Paper 41*, p. 54-62.
- MIYASHIRO, A., 1974. Volcanic rock series in island arcs and active continental margins; *American Journal of Science*, Vol. 274, p. 321-355.
- MONGER, J.W.H., 1984. Cordilleran tectonics: a Canadian perspective; *Bulletin de la Societe Geologique de France*, Vol. 7, p. 255-278.
- MONGER, J.W.H., PRICE, R.A., TEMPELMAN-KLUIT, D.J., 1982. Tectonic accretion and the origin of the two major metamorphic and plutonic welts in the Canadian Cordillera; *Geology*, Vol. 10, p. 70-75.
- MULLER, J.E., 1967. Kluane Lake map-area, Yukon Territory (115G, 115 FE1/2); *Geological Survey of Canada, Memoir 340*, 137 p.
- NYE, C.J., 1983. Petrology and geochemistry of Okmok and Wrangell volcanoes, Alaska; *unpublished PhD thesis, University of California, Santa Cruz*, p. 1-115.
- PLAFKER, G., 1983. The Yakutat block: an actively accreting tectonostratigraphic terrane in southern Alaska; *Geological Society of America abstracts with programs*, Vol. 15, p. 406.
- RICHTER, D.H., SMITH, R.L., 1976. Geologic map of the Nabesna A-5 quadrangle, Alaska; *United States Geological Survey, Map GQ-1292*, scale 1:63,360.
- RICHTER, D.H., SMITH, R.L., YEHLE, L.A., MILLER, T.P., 1979. Geologic map of the Gulkana A-2 quadrangle, Alaska; *United States Geological Survey, Map GQ-1520*, scale 1:63,360.
- SHARPE, R.P., 1943. Geology of the Wolf Creek area, St. Elias Range, Yukon Territory, Canada; *Bulletin of the Geological Society of America*, Vol. 54, p. 625-650.
- SOUTHER, J.G., STANCIU, C., 1975. Operation Saint Elias, Yukon Territory: Tertiary volcanic rocks; *Geological Survey of Canada, Paper 75-1 part A*, p. 63-70.
- SOUTHER, J.G., 1977. Volcanism and tectonic environments in the Canadian Cordillera — a second look; in: *Volcanic Regimes in Canada*, *Geological Association of Canada, Special Paper Number 16*, (W.R.A. Baragar, et al., eds.), p. 3-24.
- STEPHENS, C.D., FOGLEMAN, K.A., LAHR, J.C., PAGE, R.A., 1983. Evidence for a NNE-dipping Benioff zone south of the Wrangell volcanoes, southern Alaska; *EOS*, Vol. 64, p. 263.

SUMMARY OF DGGS INVESTIGATIONS AT LIVENGOOD, ALASKA: GEOLOGY, MINERAL POTENTIAL, AND REGIONAL CORRELATIONS WITH EAST-CENTRAL YUKON

M D. Albanese, T.E. Smith, M.S. Robinson, and T.K. Bundtzen
Division of Geological and Geophysical Surveys
Department of Natural Resources, State of Alaska
Fairbanks, Alaska

ALBANESE, M.D., SMITH, T.E., ROBINSON, M.S. and BUNDTZEN, T.K., 1986. Summary of DGGS investigations at Livengood, Alaska: geology, mineral potential, and regional correlations with east-central Yukon; in Yukon Geology, Vol. 1; Exploration and Geological Services Division, Yukon, Indian and Northern Affairs Canada, p. 171-175.

INFORMATION

As part of a program to reexamine mineral resource potential of Interior Alaska Mining Districts, Alaska Division of Geological and Geophysical Surveys (DGGS) personnel mapped and geochemically sampled approximately 2000 square kilometres in the Livengood B-3, B-4, C-3, and C-4 Quadrangles, Alaska.

According to Alaska Statute 41, the Alaska Division of Geological and Geophysical Surveys (a branch of the Department of Natural Resources within the Alaska State government) is charged with conducting "geological and geophysical surveys to determine the potential of Alaska lands for production of metals, minerals, fuels, and geothermal resources; the locations and supplies of ground water and construction materials; the potential geologic and seismic hazards to buildings, roads, bridges, and other installations and investigations as will advance knowledge of the geology of Alaska."

The results of the DGGS investigation at Livengood, Alaska include bedrock geologic maps (Robinson, 1983; Smith, 1983; Bundtzen, 1983; and Albanese, 1983), a surficial geologic map (Waythomas, 1984), a detailed prospect examination (Allegro, 1984), and analyses of about 2000 stream-sediment, pan-concentrate, and rock samples (Albanese, 1983). The geology and mineral potential of the Livengood area, as well as regional correlations with east-central Yukon are summarized in this report.

GEOLOGIC UNITS

The bedrock geology of the study area is generalized in Figure 1. The rock units generally occur in northeast-trending belts and range from Late Precambrian (?) and Lower Cambrian to Cretaceous. Bedrock units are complexly deformed and outcrop exposure is poor. Contacts, when exposed, are commonly bounded and stratigraphic relationships are difficult to determine.

The oldest rocks comprise an interlayered sequence of maroon and green argillite, black shale and limestone, vitreous quartzite and several types of bimodal quartz sandstone (informally known as the 'Grit Unit' of Chapman and others, 1971). This unit contains *Oldhamia*, a trace fossil of probable Late Precambrian (?) to Early Cambrian age (Churkin and Brabb, 1965). These rocks are bordered on the north and perhaps overlain by a northeast-trending belt of orthoquartzite, chert, maroon or green shale to phyllite, amygdaloidal greenstone, diorite, and gabbro. These younger rocks may represent a sediment-rich facies of the Fossil Creek Volcanics of Middle Ordovician age (Church and Dufree, 1961) which occurs northeast of the map area in the White Mountains (Bundtzen, 1983).

The 'Grit Unit' appears to be in thrust contact with an extensive Chert terrane composed of variegated chert, gray and tan chert, chert conglomerate, quartzite, dolomitic limestone, and minor felsic tuff and greenstone. This unit includes the Livengood Dome Chert of Chapman and others (1980). The age of the chert terrane is believed to be Ordovician to Silurian based primarily on stratigraphic and fossil evidence including graptolites (Chapman and others, 1980), conodonts, brachiopods, and corals (Florence Weber, U.S. Geological Survey, pers. comm., 1982, and Robinson, 1983).

The Chert Terrane is bordered by a Paleozoic clastic and

chert unit consisting of quartzite, maroon and green argillite, lithic sandstone and siltstone, grey chert, limestone, and limestone breccia. This unit may represent a transitional phase between the underlying Ordovician and Silurian Chert terrane and a Devonian clastic sequence which occurs stratigraphically or structurally above the Paleozoic clastics and chert unit.

The Devonian clastic sequence, informally called the Cascaden Ridge Unit (Weber and others, 1985, p. 11) is a turbidic sequence composed of a basal conglomerate containing locally derived rounded chert and pebble clasts in a sandy matrix overlain by a thick section of thinly layered shale, siltstone and sandstone with very minor carbonate layers. Although turbidite features such as flute casts and graded beddings are very rare, debris flows occur near the base of the conglomerate (Weber and others, 1985, p. 22-23). This unit is associated with a wide variety of rock types including volcanic rocks. This complex appears to be tectonically mixed with the clastic rocks (Robinson and others, 1983). Fossil evidence from the Cascaden Ridge unit (primarily gastropods and pelecypods) indicates a Middle Devonian (Eifelian) age and represents a near-shore subtidal or intertidal (?) environment (R. Blodgett, pers. comm., 1982). The upper part of the Tolovana Limestone, exposed as a thrust slice in the Livengood B-3 Quadrangle may represent a shelf-facies equivalent of the Devonian clastic sequence.

The Rampart Group, a heterogenous assemblage of rocks consisting of gabbro, pillow basalt, diorite, chert, conglomerate, sandstone and shale is present in the northern part of the map area. The Rampart Group is considered to be Permian to Triassic based on Permian pelecypods and bryozoans (Brosge and others, 1969) and a recent Upper Triassic radiolarian age date (D. Jones, pers. comm.). In addition to the fossil evidence is a K-Ar age data average of 205 ± 6 m.y. on hornblende from gabbro in the unit (Brosge and others, 1969). The Rampart Group appears to be in fault contact with older rocks to the south (Robinson and others, 1983) and is not considered to be part of the Livengood stratigraphic section.

A thick sequence of clastic Jurassic to Cretaceous flysch unconformably overlies the Grit Unit in the southeastern part of the map area, and the Devonian clastic sequence near Livengood (Robinson and others, 1983). Paleocurrent and point count data collected by Bundtzen (1983) suggest that the Devonian clastic sequence was, in part, the source rock for the Mesozoic flysch.

Felsic to intermediate plutons and dykes of presumed Tertiary to Cretaceous age (Chapman and others, 1971) intrude rocks of both the Mesozoic flysch sequence and the Devonian clastic sequence near Livengood. The intrusions generally range from monzonite to quartz monzonite, with minor syenite phases north of Tolovana Hot Springs Dome. Some appear to be structurally controlled along north-south-trending faults paralleling the Tolovana River Valley.

REGIONAL CORRELATIONS

Chapman and others (1979) proposed correlations between Livengood stratigraphy and stratigraphy in the Charlie River Quadrangle, and suggested right lateral displacement along the Tintina Fault of about 300 km (Fig. 2). The correlation of the Livengood Dome chert (part of terrane) with the Road River Formation extends this correlation from Livengood to the Selwyn Basin in east-central Yukon (Chapman and others, 1979). Addi-

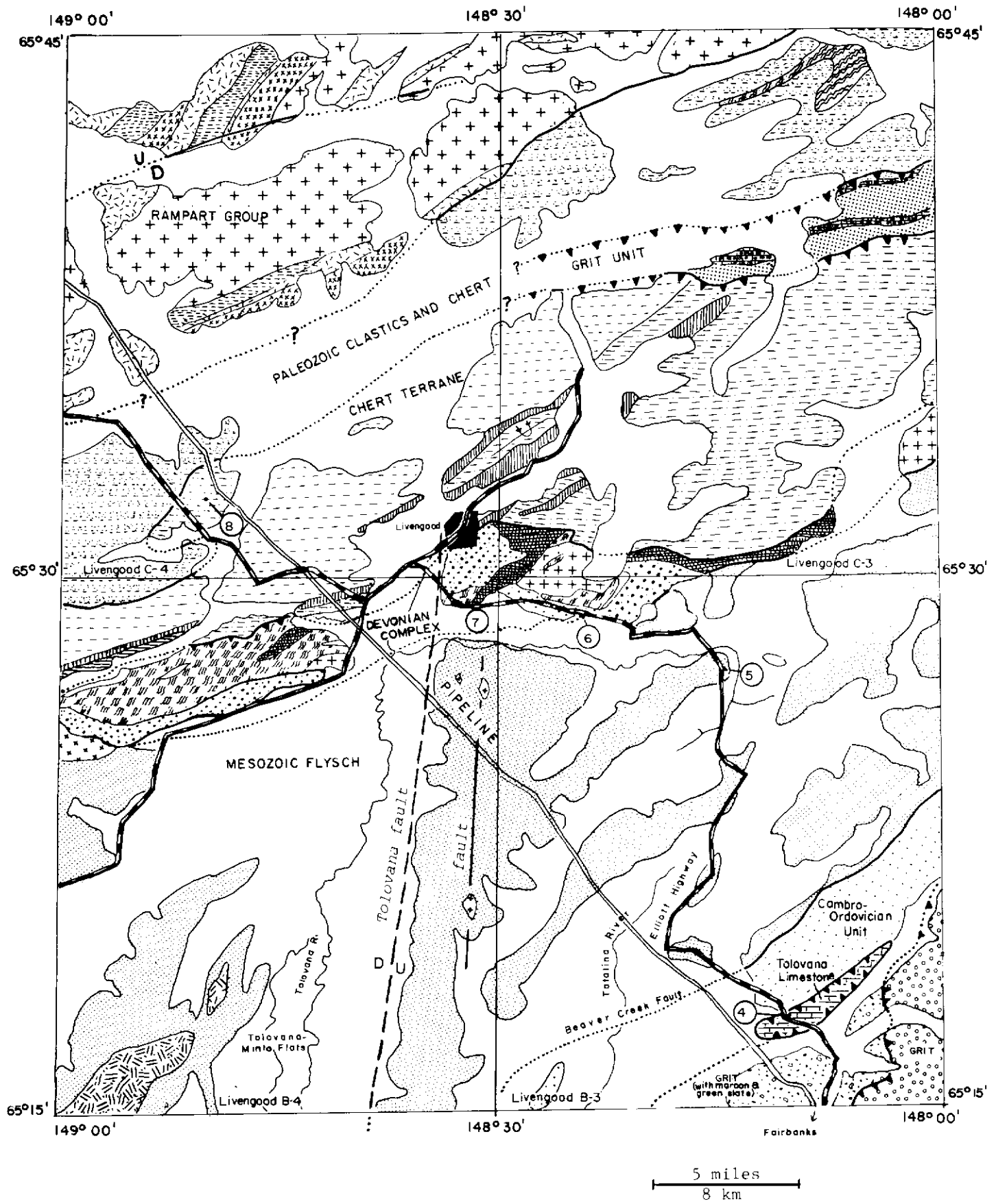
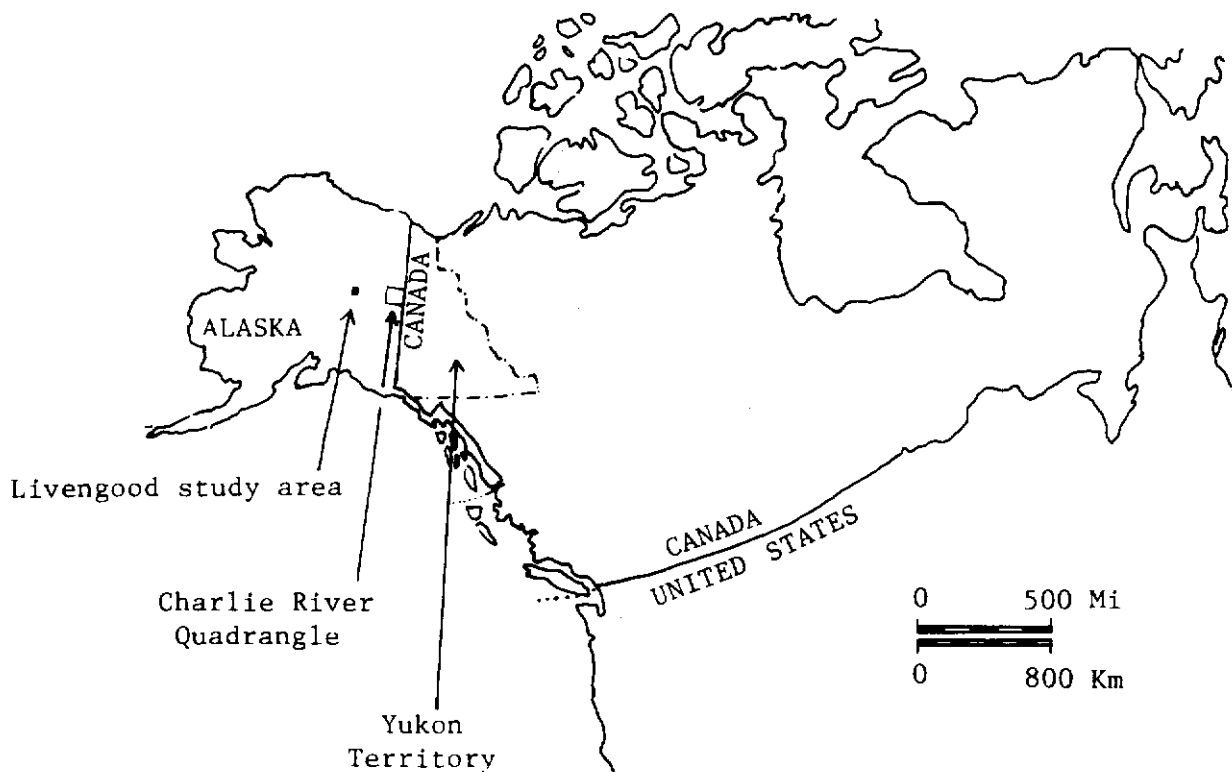


Figure 1. Geology of the Livengood B-3, B-4, C-3 and C-4 Quadrangles, Alaska. Generalized from Albanese, 1983; Bundtzen, 1983; Robinson, 1983; and Smith, 1983 (continued on following page).



EXPLANATION

	Quaternary sediments
Intrusive rocks (Cretaceous-Tertiary)	
Quartz porphyry (small bodies controlled by N-S trending faults)	
Syenite	
Quartz monzonite	
Mesozoic flysch (Jurassic-Cretaceous)	
	Siltstone, sandstone, conglomerate
Rampart Group (Permian-Triassic)	
Basalt, andesite	
Greenstone	
Diorite	
Chert, shale, siltstone	
Tolovana Limestone (Silurian-to-Middle Devonian)	
	Limestone
Devonian clastic rocks (mid-Devonian) and mafic complex	
Sandstone, shale, conglomerate, chert	
Volcanic flows, agglomerate	
Diorite, gabbro, greenstone	
Serpentinized ultramafic mafic rocks	
Paleozoic clastics and chert (Silurian-Devonian)	
Chert, maroon and green slate, sandstone, siltstone, limestone	
Quartzite	
Chert terrane (Ordovician-Silurian)	
Gray and tan chert	
Variegated chert	
Greenstone, mafic volcanic rocks	
Limestone, dolomitic limestone	
Cambro-Ordovician unit	
	Orthoquartzite, mafic igneous rocks, phyllite, limestone, chert, and slate
Grit unit (Precambrian-Cambrian)	
Quartzite, maroon-green slate, chert, sandstone	
Limestone, limestone breccia	
Bimodal quartzite, maroon and green slate	
Bimodal quartzite (grit)	

FIGURE 1 (cont.)

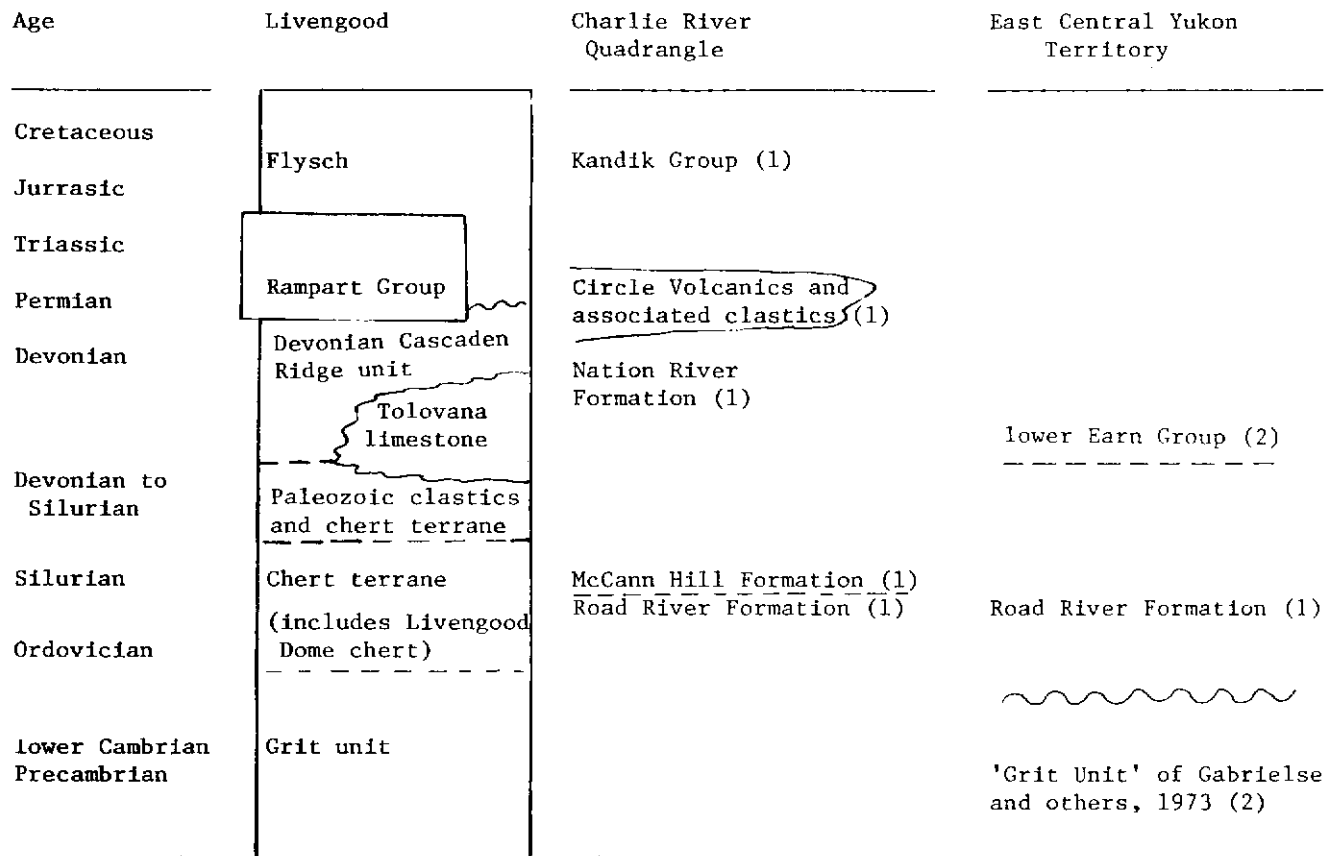


Figure 2. Inferred stratigraphic relationships.

(1) indicates correlation of Champan and others, 1979

(2) indicates correlation of Robinson and others, 1983

tional correlations between Livengood and Yukon stratigraphy have more recently been proposed. A comparison of the restored stratigraphic column of Livengood with Yukon stratigraphy is shown in Figure 2.

The H drynian 'Grit Unit' in east-central Yukon of Gabrielse and others (1973) can be compared to the Livengood grit unit. In east-central Yukon, the Grit Unit consists of gritty quartz arenite, pale brown-slate, and minor limestone overlain by maroon, purple, and green slates with lenses of fine-grained quartz-arenite and brown slate (Gordy, 1978). This lithology is notably similar to the grit unit of Livengood. The east-central Yukon Grit Unit and the Livengood grit are underlain by the Road River Formation and the equivalent Livengood Dome chert of the chert terrane, respectively. In addition to the lithologic and stratigraphic similarities of these two grit units, the age assigned to these units is also similar.

In addition to this correlation, the Lower Earn Group of east-central Yukon which consists of siliceous shale, chert, quartz, sandstone, grit, and chert pebble conglomerate and spans most of the Devonian (Gordy and others, 1982) exhibits lithologic and chronologic similarities to the Cascaden Ridge unit of Livengood. Stratigraphic similarities are also observed as the Lower Earn Group in part, conformably overlies the Road River Formation (Gordy and others, 1982), while the Cascaden Ridge unit overlies the unit that is transitional to the chert terrane. These correlations, first suggested by Robinson and others (1983) have been supported by Tempelman-Kluit (1984) and Hall and others (1984).

MINERAL POTENTIAL

Gold placers in the Livengood area have produced over 10,653,000 grams (375,000 ounces) of gold. There are three types of auriferous or potentially auriferous placer deposits in the Livengood area. These are: 1) gold-bearing fluvial gravels overlain by frozen colluvial silt such as those currently being mined in the

lower Livengood bench on Livengood Creek; 2) poorly preserved, locally derived, potentially auriferous, high-level terrace deposits found along Hess, Fish and Lost Creeks; and 3) gold-bearing alluvial- and colluvial-fan deposits and gravels, such as those on Amy Dome and Money Knob, east of Livengood (Waythomas and others, 1984).

The best exposed lode gold occurrence in the area is the Old Smoky Prospect on Money Knob, 3 km southeast of Livengood. Gold-antimony mineralization occurs in sheared and hydrothermally altered contact zones between Devonian clastics and an intrusive suite composed of biotite monzonite, feldspar porphyry, and felsic dykes. Reported gold values of rock samples from the Old Smoky Prospect range from 0.1 to 29.8 ppm (Allegro, 1984).

Although these altered intrusions and associated vein deposits probably contributed heavily to the placer deposits, their volume at the present erosion surface may not be sufficient to constitute a viable source for all of the placer deposits, suggesting that at least a portion of the lode source for the gold was above the present exposure and has since been removed by erosion.

Other units containing mineral potential include the Chert Terrane which contains stratabound limonitic chert breccia zones with gold concentrations up to 1.3 ppm; the Paleozoic clastics and chert unit which contains zones of layered pyritic massive sulfides in quartzites in the northern part of the map area; the Rampart Group which contains minor copper mineralization in mafic igneous rocks; and the contact zone between the chert terrane and the Cascaden Ridge which contains significant stream-sediment zinc anomalies. It is important to note that these zinc anomalies are hosted within the units that are correlated with the lower and middle Paleozoic units of Yukon which host all of the known shale-hosted stratiform lead-zinc deposits of Yukon and northern British Columbia.

REFERENCES

- ALBANESE, M.D., 1983a. Geochemical reconnaissance of the Livengood B-3, B-4, C-3 and C-4 Quadrangles, Alaska; Summary of data on stream-sediment, pan-concentrate, and rock samples; Alaska Division of Geological and Geophysical Surveys, Fairbanks, Alaska, U.S.A., Report of Investigations 83-1, scale 1:63,360.
- ALBANESE, M.D., 1983b. Bedrock geologic map of the Livengood B-4 Quadrangle, Alaska; Alaska Division of Geological and Geophysical Surveys, Fairbanks, Alaska, U.S.A., Report of Investigations 83-3, scale 1:40,000.
- ALLEGRO, G.L., 1984. Geology of the Old Smoky Prospect, Livengood C-4 Quadrangle, Alaska; Alaska Division of Geological and Geophysical Surveys, Fairbanks, Alaska, U.S.A., Report of Investigations 84-1, 9 p., 1 plate, scale 1:120,000.
- BROSCE, W.P., LANPHERE, M.A., REISER, H.N., and CHAPMAN, R.M., 1969. Probable Permian age of the Rampart Group, central Alaska; U.S. Geological Survey, Bulletin 1294-B, p. B1-B18.
- BUNDTZEN, T.K., 1983. Bedrock Geologic Map of the Livengood B-3 Quadrangle, Alaska; Alaska Division of Geological and Geophysical Surveys, Fairbanks, Alaska, U.S.A., Report of Investigations 83-6, 1 plate, scale 1:40,000.
- CHAPMAN, R.M., WEBER, F.R., and TABER, Bond, 1971. Preliminary geologic map of the Livengood Quadrangle, Alaska; U.S. Geological Survey, Open-file Report 71-66 (483), 2 sheets, scale 1:250,000.
- CHAPMAN, R.M., WEBER, F.R., CHURKIN, Michael Jr., and CARTER, Claire, 1980. The Livengood Dome chert, a new Ordovician formation in central Alaska, and its relevance to displacement on the Tintina Fault; in *Shorter Contributions to Stratigraphy and Structural Geology*, 1979, U.S. Geological Survey, Professional Paper 1126, p. F1-F13.
- CHURCH, R.E., and DURFEE, M.C., 1961. Geology of the Fossil Creek area, White Mountains, Alaska; Unpublished MSc thesis, University of Alaska, Fairbanks, 96 p.
- CHURKIN, Michael Jr., and BRABB, E.E., 1965. Occurrence and significance of *Oldhamia*, a Cambrian trace fossil, in east-central Alaska; U.S. Geological Survey, Professional Paper 525D, p. D120-D124.
- GABRIELSE, H., BLUSSON, S.L., and RODDICK, J.A., 1973. Geology of Flat River, Glacier Lake, and Wrigley Lake map-areas, District of Mackenzie and Yukon Territory; Geol. Surv. Can., Memoir 366, 153 p.
- GORDEY, S.P., 1978. Stratigraphy and structure of the Summit Lake area, Yukon and Northwest Territories; in *Current Research*, Part A, Geol. Surv. Can., Paper 78-1A, p. 43-48.
- GORDEY, S.P., ABBOTT, J.G., ORCHARD, M.J., 1982. Devonian-Mississippian (Earn Group) and younger strata in east-central Yukon; in *Current Research*, Part B, Geol. Surv. Can., Paper 82-1B, p. 93-100.
- HALL, M.H., SMITH, T.E., and WEBER, F.R., 1984. Geologic guide to the Fairbanks-Livengood area, east-central Alaska; A guidebook for the geology of the Yukon-Tanana Uplands; Field trip of the 80th annual meeting of the Cordilleran Section of the Geological Society of America, Anchorage, Alaska, 1984, Unpublished report, 30 p.
- ROBINSON, M.S., 1983. Bedrock geologic map of the Livengood C-4 Quadrangle, Alaska; Alaska Division of Geological and Geophysical Surveys, Fairbanks, Alaska, U.S.A., Report of Investigations 83-4, 1 plate, scale 1:40,000.
- ROBINSON, M.S., SMITH, T.E., BUNDTZEN, T.K., and ALBANESE, M.D., 1982. Geology and metallogeny of the Livengood area, east-central Alaska; A progress report; Presented at the Alaska Miners Association Convention, Anchorage, October, 1982.
- ROBINSON, M.S., SMITH, T.E., BUNDTZEN, T.K., and ALBANESE, M.D., 1983. Geology and metallogeny of the Livengood Area, east-central Alaska; Presented as a poster session at the Alaskan Geological Society Symposium, Anchorage, Alaska, May 1983.
- SMITH, T.E., 1983. Bedrock geologic map of the Livengood C-3 Quadrangle, Alaska; Alaska Division of Geological and Geophysical Surveys, Fairbanks, Alaska, U.S.A., Report of Investigations 83-5, 1 plate, scale 1:40,000.
- TEMPELMAN-KLUIT, D.J., 1984. Counterparts of Alaska's terranes in Yukon; Cordilleran Section of the Geological Association of Canada Symposium, Vancouver, B.C., Canada, February 1984. 4 p.
- WAYTHOMAS, C.F., TEN BRINK, N.W., and RITTER, D.F., 1984. Surficial geology of the Livengood B-3, B-4, C-3 and C-4 Quadrangles, Alaska; Alaska Division of Geological and Geophysical Surveys, Fairbanks, Alaska, U.S.A., Report of Investigations, 84-6.
- WEBER, F.R., SMITH, T.E., HALL, M.H., and FORBES, R.B., 1985. Geologic guide to the Fairbanks-Livengood area, east-central Alaska; Prepared in conjunction with the meeting of the Pacific Section of the American Association of Petroleum Geologists, the Society of Economic Paleontologists and Mineralogists, and the Society of Exploration Geophysicists, May 22-24, 1985, Alaska Geological Society, Anchorage, Alaska, 44 p.